

# UC Santa Cruz

## UC Santa Cruz Electronic Theses and Dissertations

### Title

Chemical Modification of Polyvinyl Chloride: Plasticization and Chemical Degradation

### Permalink

<https://escholarship.org/uc/item/9rm7427s>

### Author

Skelly, Patrick Wayne

### Publication Date

2023

Peer reviewed|Thesis/dissertation

UNIVERSITY OF CALIFORNIA  
SANTA CRUZ

**CHEMICAL MODIFICATION OF POLYVINYL CHLORIDE:  
PLASTICIZATION AND CHEMICAL DEGRADATION**

A dissertation submitted in partial satisfaction  
of the requirements for the degree of

DOCTOR OF PHILOSOPHY

in

CHEMISTRY

by

**Patrick Skelly**

June 2023

The dissertation of Patrick Skelly  
is approved:

---

Professor Rebecca Braslau, advisor

---

Professor John MacMillan, chair

---

Professor Jevgenij Raskatov

---

Peter Biehl  
Vice Provost and Dean of Graduate Studies



## Table of Contents

<b>List of Figures.....</b>	<b>viii</b>
<b>List of Tables .....</b>	<b>x</b>
<b>List of Schemes.....</b>	<b>xi</b>
<b>Abstract.....</b>	<b>xv</b>
<b>Acknowledgements .....</b>	<b>xvii</b>
<b>1 Introduction: Internal Plasticization of PVC .....</b>	<b>1</b>
1.1 Background.....	1
1.2 Plasticizers and Plasticizer Migration.....	2
1.3 Strategies for Avoiding Plasticizer Migration .....	2
1.4 Glass Transition Temperature.....	2
1.5 Covalent Attachment of Plasticizers by Nucleophilic attack.....	3
1.5.1 Covalent Attachment using Sulfide Linkages.....	3
1.5.2 Covalent Attachment using Amine Linkages .....	7
1.5.3 Covalent Attachment using Carboxylate Linkage .....	13
1.5.4 Covalent Attachment using Azide Linkages.....	14
1.5.4.1 Copper-Free 3+2 Thermal Azide-Alkyne Cycloaddition.....	14
1.5.4.2 Copper-Catalyzed 3+2 Azide-Alkyne Cycloaddition.....	21
1.5.5 Comparison of Nucleophilic Substitution Methods.....	25

1.6	Plasticization by Grafting Polymers from PVC.....	26
1.6.1	Cationic Polymerization.....	26
1.6.2	Free Radical Polymerization.....	27
1.6.3	Atom-Transfer Radical Polymerization.....	28
1.7	Conclusion .....	33
1.8	References.....	35
<b>2</b>	<b>Relative Rates of Metal-Free Azide Alkyne Cycloadditions .....</b>	<b>46</b>
2.1	Background.....	46
2.2	Synthesis of electron-poor alkynes .....	48
2.3	Synthesis of a Primary Benzylic Azide .....	51
2.4	Synthesis of Authentic Triazoles for Identification by NMR.....	52
2.5	NOE experiment .....	53
2.6	Competition Experiments Using a Primary Benzylic Azide .....	55
2.7	Competition Experiments Using a Non-benzylic Secondary Azide.....	61
2.8	Time-dependent Competition Experiment.....	62
2.9	DFT Calculations .....	63
2.9.1	Activation Energies.....	64
2.9.2	HOMO-LUMO Gap.....	65
2.9.3	Distortion-Interaction Method .....	67

2.9.4	Wiberg Bond Indices .....	70
2.10	Reaction at Room Temperature .....	73
2.11	Conclusion .....	73
2.12	References.....	75
<b>3</b>	<b>Degradation of Polyvinyl Chloride Using Olefin Metathesis.....</b>	<b>80</b>
3.1	Background.....	80
3.1.1	PVC Waste.....	80
3.1.2	Chemical Upcycling.....	81
3.1.3	Chemical Degradation of PVC .....	82
3.1.4	Degradation of Polymers by Olefin Metathesis.....	83
3.1.5	Precedent for PVC Elimination .....	84
3.1.6	Precedent for Olefin Metathesis on Conjugated Double Bonds .....	85
3.2	Control Reaction: Self Metathesis .....	85
3.3	Complete Elimination of PVC and attempted metathesis.....	86
3.4	Investigations into simultaneous dehydrochlorination and metathesis.....	88
3.5	Optimization of Elimination of PVC .....	90
3.6	Metathesis on Partially Eliminated PVC .....	90
3.7	Elimination Using Allyl Alcohol.....	91
3.8	Metathesis on Allylated DPVC.....	94

3.9	Characterization of DPVC and metathesis products.....	96
3.9.1	Gel Permeation Chromatography .....	96
3.9.2	UV-Vis.....	98
3.9.3	NMR .....	99
3.9.3.1	DOSY NMR .....	104
3.10	Effect of Varying Alkene Partners.....	106
3.11	Effect of Other Conditions.....	108
3.11.1	Temperature and Solvent .....	108
3.11.2	Catalyst .....	109
3.11.3	Oxygen and light.....	109
3.12	Other attempted reactions .....	111
3.13	Conclusion .....	112
3.14	References.....	114
<b>4</b>	<b>Experimental .....</b>	<b>124</b>
4.1	Experimental for Chapter 2.....	124
4.2	Experimental for Chapter 3.....	157
4.3	References.....	167
	<b>Addendum: Contribution to other published works .....</b>	<b>170</b>
	<b>Appendix.....</b>	<b>171</b>

**Bibliography ..... 468**



## List of Figures

Figure 1.1 Phthalates and triazole phthalate mimics .....	15
Figure 2.1 Sources of alkynes used in this chapter .....	48
Figure 2.2 NOESY experiment on triazole 2.8a. Irradiation at proton c leads to enhancement at protons d, e, and g, consistent with the structure of 2.8a shown. The lack of enhancement at proton b helps reject the structure 2.8b. ....	54
Figure 2.3 Expansion of the aromatic region of Figure 2.2 showing enhancement of peak g .....	54
Figure 2.4 Expansion of the upfield region of Figure 2.2 showing lack of enhancement at peak b .....	55
Figure 2.5 Competition experiment between 2.4 and 2.6 at $t = 0$ .....	58
Figure 2.6 Competition experiment between 2.4 and 2.6 at $t = 68$ h.....	59
Figure 2.7 Comparison of azides used in this experiment .....	62
Figure 2.8 Calculated geometries for the starting materials, transition state, and product of the reaction between <i>t</i> -butylbenzyl azide and dimethyl acetylenedicarboxylate ...	64
Figure 2.9 Correlation between the activation energies computed by DFT and the log <sub>10</sub> of the relative rates determined by the competition experiments .....	65
Figure 2.10 HOMO and LUMO of dimethyl acetylenedicarboxylate (2.7) and 4- <i>t</i> -butylbenzyl azide (2.13).....	66
Figure 2.11 Energy of the LUMO plotted against the calculated activation energy. $R^2$ without the phenyl and nitrophenyl points was 0.735 .....	67
Figure 2.12 Distortion energy vs. activation energy .....	69

Figure 2.13 Interaction energy vs. activation energy.....	70
Figure 2.14 Change in bond order vs activation energy. A negative y value represents a loss of conjugation .....	72
Figure 3.1 <sup>1</sup> H NMR spectrum of DPVC3 with peaks labeled .....	93
Figure 3.2 UV-Vis spectra of DPVC1 (solid line) and DPVC2 (dotted line) in THF	98
Figure 3.3 Left: UV-Vis of the metathesis products of DPVC4. The fraction that precipitates in methanol is shown with a dotted line, and the remainder (recovered by evaporation of MeOH) with a solid line. Right: UV-Vis of the metathesis products of DPVC1. The fraction that precipitates in methanol is shown. All UV-Vis spectra were taken in THF. ....	99
Figure 3.4 <sup>1</sup> H NMR Spectra of PVC (top), DPVC4 (middle), and PVC oligomers (produced from DPVC4 with Grubbs 2 and added alkene 3.2) (bottom).....	100
Figure 3.5 <sup>1</sup> H NMR of metathesis product after chromatography .....	101
Figure 3.6 COSY NMR of the metathesis product after chromatography .....	102
Figure 3.7 <sup>1</sup> H NMR of the crude reaction mixture of DPVC3 with DAB and Grubbs catalyst .....	103
Figure 3.8 DOSY NMR of DPVC3 in CDCl <sub>3</sub> .....	105
Figure 3.9 DOSY NMR of the metathesis product of DPVC3 with DAB (crude reaction mixture) in CDCl <sub>3</sub> .....	106

## List of Tables

Table 1.1 Tg values for PVC-g-POEM.....	30
Table 2.1 Results of competition experiments with t-butylbenzyl azide (2.13).....	59
Table 2.2 Results of competition experiments with 3-azido-1-phenylheptane (2.16)	62
Table 2.3 Competition experiment between two alkynes monitored at various time points.....	63
Table 2.4 Activation energies, LUMO energies, and change in bond order .....	71
Table 3.1 Screening of bases that can perform the elimination reaction on PVC .....	89
Table 3.2 Inhibition of olefin metathesis in the presence of base.....	89
Table 3.3 Molecular weights of initial PVC, DPVC1, and metathesis products .....	91
Table 3.4 Metathesis products of DPVC1 through DPVC4 .....	95
Table 3.5 Metathesis products without added alkene .....	96
Table 3.6 Characterization of DPVC .....	97
Table 3.7 Effect of changing olefin partner on the metathesis reaction .....	108
Table 3.8 Effect of temperature and solvent on olefin metathesis reaction.....	108
Table 3.9 Effect of olefin metathesis catalyst on product.....	109
Table 3.10 Effect of removing oxygen and light, and preventing OH substitution..	111

## List of Schemes

Scheme 1.1 Covalent attachment of 2-(2-butoxyethoxy)ethyl thiolate to PVC .....	4
Scheme 1.2 Covalently bonding the 2-ethylhexyl ester of thioglycolic acid to PVC using a sulfide linkage .....	4
Scheme 1.3 Substitution of chlorines on PVC with sodium phenylthiolate .....	5
Scheme 1.4 Modification of PVC using substituted thiophenols .....	6
Scheme 1.5 Substitution with halogenated thiophenols .....	6
Scheme 1.6 Substitution of PVC with three different thiols.....	7
Scheme 1.7 Desired reaction sequence for attachment of PEG to PVC using a urea linker. Crosslinked PVC chains are not shown here, but were observed as side products under prolonged reaction times.....	9
Scheme 1.8 Attachment of a fatty acid ester derived from cooking oil to PVC with an amine tether.....	10
Scheme 1.9 Attachment of lauraldehyde to PVC with an amine tether.....	10
Scheme 1.10 Two methods of using amine linkers to attach dehydroabiatic acid to PVC .....	12
Scheme 1.11 Modification of PVC with diethanolamine, followed by attachment of three different plasticizers.....	13
Scheme 1.12 Pretreatment of PVC with iodide, followed by reaction with carboxylate anion.....	14
Scheme 1.13 Covalent attachment of phthalate mimics onto PVC via thermal azide-alkyne cycloaddition .....	16

Scheme 1.14 Covalent attachment of a tethered DEHP to PVC by thermal azide-alkyne cycloaddition.....	17
Scheme 1.15 Covalent attachment of rotationally labile phthalate mimics with a six-carbon tether to PVC.....	18
Scheme 1.16 Covalent attachment of an internal plasticizer with two tethered triazole phthalate mimics to PVC .....	19
Scheme 1.17 Covalent attachment of polyether propiolic esters to PVC .....	20
Scheme 1.18 Use of glutamic acid as a branched linker to attach four plasticizing R groups per azide anchor point on PVC .....	21
Scheme 1.19 Covalent attachment of cardanol to PVC via CuAAC .....	22
Scheme 1.20 Attachment of citrate plasticizers using a propargyl ether linker.....	23
Scheme 1.21 Covalent attachment of alkyne-terminated monoethyl phthalate derivatives to PVC by CuAAC.....	24
Scheme 1.22 Attachment of two different castor oil derivatives to PVC using a propargyl ether as a linker.....	25
Scheme 1.23 Cationic ring-opening polymerization of THF from a PVC macroinitiator .....	26
Scheme 1.24 Free-radical polymerization of n-butyl methacrylate on PVC .....	27
Scheme 1.25 Graft polymerization of acrylic acid or graft addition of crotonic acid to PVC.....	28
Scheme 1.26 Atom transfer radical polymerization of butyl acrylate on PVC .....	29
Scheme 1.27 ATRP graft polymerization of EHA from PVC.....	29

Scheme 1.28 ATRP graft polymerization of POEM from PVC.....	30
Scheme 1.29 Grafting a poly(ionic liquid) from PVC by ATRP.....	31
Scheme 1.30 Synthesis of PVC-g-PDMA by ATRP.....	31
Scheme 1.31 ARGET-ATRP of butyl acrylate on PVC.....	32
Scheme 1.32 Graft copolymerization of BA and 2EEA from PVC.....	33
Scheme 2.1 Use of electron-poor alkynes in our lab for plasticization of PVC.....	47
Scheme 2.2 Synthesis of <i>N</i> -butylpropiolamide (2.4).....	49
Scheme 2.3 Synthesis of methyl 3-(phenylsulfonyl)-2-propynoate (2.10).....	50
Scheme 2.4 Synthesis of <i>t</i> -butylbenzyl azide.....	52
Scheme 2.5 Preparation of authentic triazoles 2.3a and 2.3b.....	53
Scheme 2.6 General scheme of competition experiments using <i>t</i> -butylbenzyl azide.	56
Scheme 2.7 Synthesis of 3-azido-1-phenylheptane (2.16).....	61
Scheme 2.8 General reaction with atoms labeled. The bond order of bond 4-7 and bond 5-8 were used.....	71
Scheme 2.9 Room-temperature cycloaddition reaction using sulfonyl, ester-substituted alkyne 2.10.....	73
Scheme 3.1 General strategy for PVC degradation by olefin cross metathesis.....	84
Scheme 3.2 Synthesis of allyl acetate.....	85
Scheme 3.3 Self-metathesis of allyl acetate.....	86
Scheme 3.4 Full elimination of PVC and attempted metathesis on the polyacetylene product.....	87
Scheme 3.5 Synthesis of <i>Z</i> -1,4-diacetoxy-2-butene.....	87

Scheme 3.6 Reaction of DAB with the initial catalyst (top) followed by self-metathesis of DAB (bottom).....	88
Scheme 3.7 Model cross-metathesis reaction for base screening.....	89
Scheme 3.8 Partial elimination of PVC.....	90
Scheme 3.9 Olefin metathesis reaction of DPVC1 with added alkene 3.2.....	91
Scheme 3.10 Proposed ring-closing metathesis strategy to introduce the metathesis catalyst onto the internal double bonds of allyl-grafted DPVC.....	92
Scheme 3.11 Dehydrochlorination of PVC using allyl alcohol.....	93
Scheme 3.12 Expected products from the metathesis reaction.....	94
Scheme 3.13 Metathesis reaction of allyl DPVC with added olefin 3.2(Z): for the purposes of comparison throughout this chapter, these are the standard reaction conditions.....	95
Scheme 3.14 Synthesis of Z-1,4-bis-TBSO-2-butene.....	106
Scheme 3.15 Isomerization of the added alkene.....	107
Scheme 3.16 Reaction of bis-TBSO butene with DPVC3 in the presence of benzoquinone.....	107
Scheme 3.17 Elimination of PVC using potassium <i>tert</i> -butoxide.....	110
Scheme 3.18 Olefin metathesis reaction on DPVC5.....	110
Scheme 3.19 Dehydrochlorination and immediate metathesis on PVC shielded from oxygen and light.....	111
Scheme 3.20 Attempted one-pot isomerization/metathesis to form benzene.....	112

## Abstract

# **Chemical Modification of Polyvinyl Chloride: Internal Plasticization and Chemical Degradation**

Patrick Skelly

Polyvinyl Chloride (PVC) is the third most-produced plastic in the world. It is found in construction materials, pipes that contain our drinking water, toys, furniture, clothing, credit cards, medical tubing and blood bags. Because of the sheer quantity of PVC in the world, it is important to make it as safe as possible. Health concerns over additives to PVC can add up over a lifetime of exposure to household products. Environmental concerns over the degradation of PVC also add up with millions of tons entering the waste stream every year.

This dissertation addresses two aspects of chemical modification of PVC with regards to these health and environmental concerns. The first aspect is the internal plasticization of PVC, replacing migratory plasticizers that can enter the body. The second is controlled chemical degradation of PVC, working towards the goal of harvesting PVC waste as a carbon resource.

The first chapter is a review article about internal plasticization: covalently bonding plasticizers to PVC. A comprehensive review of this field was previously lacking. Literature from 1936 to 2021 is reviewed and categorized by method of attachment, either nucleophilic substitution or graft-from polymerization. A perspective is given on the types of structures and syntheses used in successful internal plasticizers.



With the continued goal of internal plasticization, the second chapter is an experimental study of the metal-free azide-alkyne cycloaddition, a reaction well-suited for attaching plasticizers to PVC. To more effectively use this reaction, the effect of different electron-withdrawing groups was studied. A range of alkynes were synthesized and their rates compared by competition experiments. The most reactive alkyne contained a sulfone group and an ester group, and reacted 2100 times faster than the least reactive, containing a phenyl substituent and an ester. Phenyl- and nitrophenyl-substituents surprisingly decreased the reactivity of the alkynes instead of increasing it. DFT calculations of reaction energies, orbital energies, distortion-interaction parameters, and bond indices were performed to help explain the reactivity trends.

The third chapter addresses the chemical degradation of PVC. A method was developed to eliminate chloride from PVC using hydroxide base, and then cleave the all-carbon backbone using olefin metathesis of the newly-created double bonds. Addition of allyl alcohol to the elimination step allows the incorporation of allyl side chains, which more easily attach to the metathesis catalyst and incorporate it into the main chain by a ring-closing metathesis reaction. Over 20x reduction in molecular weight is observed, demonstrating repeated cleavage of the polymer chain. By adding an external alkene to the reaction, a diene with the corresponding substituents is successfully created, indicating some incorporation of PVC carbons into a new chemical product.

## Acknowledgements

Thanks first of all to my advisor Rebecca. You have always been so kind and patient, even when the science isn't working you can give me the motivation to keep on working and figuring out new solutions. Thank you to my committee, John and Jevgenij, you have taught me a lot and pushed me to practice and become a better scientist.

Thanks to Jack and Betsy for lots of help with the NMR. Thanks to Levi and Rachael for help with the UV-Vis and letting me use your instruments. Thanks to Stephen Hauskins for helping me use the hummingbird supercomputer. Thanks to Caitlin Binder for making me practice my teaching and speaking skills.

Thank you to all of my labmates. Longbo, you have taught me and helped me so much, thank you for everything. Thanks to Chad and Wiley for teaching me when I was just getting started in lab. Ana Paula, thank you for all the great music and making lab so much fun. Jira, thank you for all your help in lab, it was very fun to meet you. Chayo, thanks for helping me stay sane in my last few years here. Greg, you were always a great lab neighbor and a pleasure to talk to.

Thanks to my cohort: Victor, Duy, Dorothy, Ariel, John Michael, Brian, Jocelyn, it was great to start grad school with a group of friends like you.

Thanks to all of my friends and family for supporting me and encouraging my interest in science. Thanks to my grandpa Bill Skelly for giving me your handbook of chemistry years ago, proud to be another polymer chemist in the family.

## **1 Introduction: Internal Plasticization of PVC**

This review article was written with contributions from Longbo Li and Rebecca Braslau, and published in Polymer Reviews.<sup>1</sup> Skelly, P. W.; Li, L.; Braslau, R. Internal Plasticization of PVC. *Polym. Rev.* **2022**, *62* (3), 485–528. <https://doi.org/10.1080/15583724.2021.1986066>. My contributions to the review are included here. See the published article for the full review, which contains many more examples of nucleophilic substitution and a section on copolymerization of vinyl chloride with plasticizing monomers, not included here.

### **1.1 Background**

Polyvinyl Chloride (PVC) is one of the most common thermoplastics in the world, making up 17% of the global plastic market<sup>2</sup> amounting to over 44 million metric tons in 2018.<sup>3</sup> Applications range from building materials, toys, credit cards, automotive components and clothing to medical devices. Due to the low cost, optical clarity, and facile sterilization, 40% of plastic medical devices are made of PVC.<sup>4</sup>

PVC as a pure material is a brittle solid. For most applications, it must be mixed with a plasticizer to impart flexibility. Traditionally, plasticizers are mixed with PVC as “external plasticizers,” without covalent attachment. This leads to plasticizer migration, where the plasticizer diffuses out of PVC into adjacent materials for example: into the air, water or other liquids, food, soil or onto the skin of a person who touches a PVC product. Plasticizer migration degrades the properties of the material, contaminates the environment, and exposes people to often harmful plasticizers.<sup>5</sup>

## **1.2 Plasticizers and Plasticizer Migration**

The most commonly used plasticizer is di(2-ethylhexyl)phthalate (DEHP, note: DOP, dioctyl phthalate, is the same as DEHP. DEHP is used throughout, regardless as to which acronym was used in the original literature).<sup>6</sup> The toxicity of DEHP and its subsequent metabolites has been extensively investigated, and has been recently reviewed.<sup>7</sup> Given these toxicity concerns, development of less-toxic small-molecule plasticizers has been an active area of research.<sup>4</sup> Even more attractive are non-migratory plasticizers, as this not only avoids toxicity but also allows the PVC to retain its physical properties over time.

## **1.3 Strategies for Avoiding Plasticizer Migration**

There are several strategies for preventing plasticizer migration. (1) Polymeric plasticizers with high molecular weights have a greatly reduced tendency to migrate. (2) The surface of the PVC material may be crosslinked by radiation or chemical treatment to inhibit plasticizer leaching. (3) The plasticizer may be covalently bound to the PVC polymer chain: “internal plasticization.” Although a few reviews have addressed covalent attachment in the overall context of PVC plasticization,<sup>4,8,9,10</sup> these discussions have been limited to a subset of internal plasticization strategies. This review article was a comprehensive review of internal plasticization.

## **1.4 Glass Transition Temperature**

The glass transition temperature ( $T_g$ ) is the temperature at which a polymer changes from a glassy state to a rubbery state. As a result, materials with lower  $T_g$  values are increasingly flexible. The  $T_g$  of unplasticized PVC is around 81 °C.<sup>11</sup>

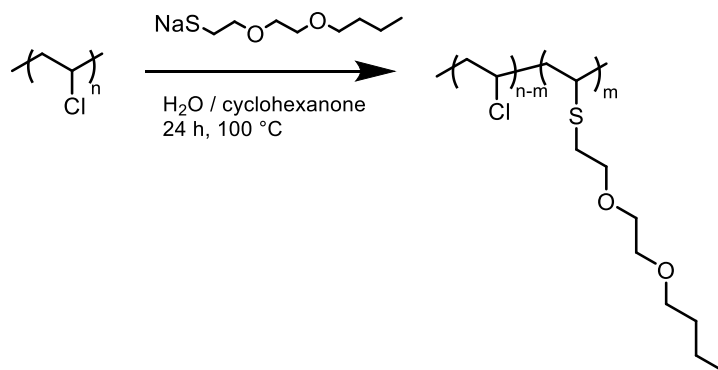
Decreasing  $T_g$  is the main metric for whether a plasticizer is effective, and is often the only metric reported.

In some cases, tensile modulus, tensile strength, and elongation at break are also measured. Tensile modulus is the slope of a stress-strain curve; lower modulus indicates more flexibility as less force is required to deform the material. Tensile strength is the maximum force the material can undergo before breaking; this often decreases as a side effect of plasticization. Elongation at break is the percentage of its original length it has been stretched before breaking; higher values indicate a more flexible material.

## **1.5 Covalent Attachment of Plasticizers by Nucleophilic attack**

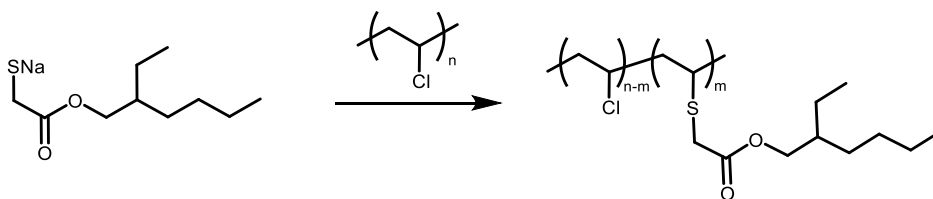
### **1.5.1 Covalent Attachment using Sulfide Linkages**

The first example of internally plasticized PVC by nucleophilic substitution was reported in 1981 by Marian and Levin.<sup>12</sup> Sodium 2-(2'-butoxyethoxy)ethyl thiolate was added to PVC, replacing some of the chloride groups (**Scheme 1.1**).  $T_g$  values were not measured, however, all modified polymers showed a decrease in tensile modulus and tensile strength, and an increase in elongation at break, indicating enhanced flexibility. Increasing the thiol substitution from 10% to 25% (as determined by elemental analysis) further decreased both modulus and tensile strength, and further increased elongation.



**Scheme 1.1** Covalent attachment of 2-(2-butoxyethoxy)ethyl thiolate to PVC

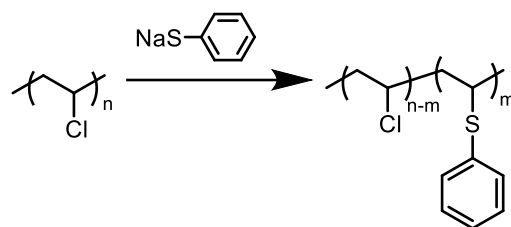
In 1997, del Val et al. performed substitutions with the 2-ethylhexyl ester of thioglycolic acid (**Scheme 1.2**).<sup>13</sup> A  $T_g$  value of 56 °C was observed at 20 wt% of plasticizer. This internal plasticizer was less efficient than a non-bound mixture of PVC and 2-ethylhexyl thioglycolate with the same stoichiometry. This is typically the case, covalently bound plasticizers have less freedom of motion so they plasticize less than a non-bound plasticizer.



**Scheme 1.2** Covalently bonding the 2-ethylhexyl ester of thioglycolic acid to PVC using a sulfide linkage

Millan et al. substituted PVC chlorines with sodium phenylthiolate (**Scheme 1.3**), and measured the resulting  $T_g$  depression in a study of tacticity.<sup>14, 15</sup> This nucleophilic substitution occurs preferentially at isotactic portions of PVC, and converts these segments from a gauche/*trans* mixture to an all-*trans* configuration. This has the effect of straightening the polymer chain, counteracting some of the

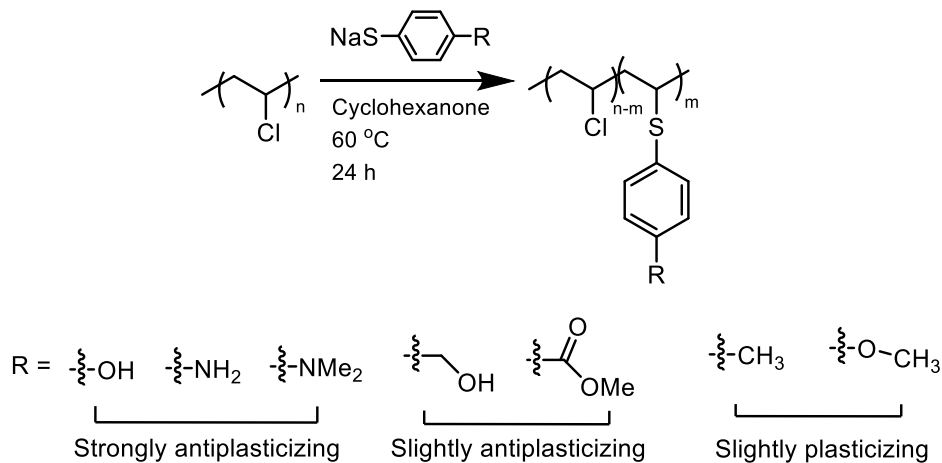
plasticization. Conditions that decreased this selectivity therefore increased plasticization. Running the reaction at higher temperatures (60 vs 25 °C) or in a very polar solvent such as *N*-methylpyrrolidone or hexamethylphosphoramide led to enhanced plasticization.  $T_g$  values ranged from 80 °C for unmodified PVC to 62 °C for PVC with 50% of the chlorine atoms replaced with aryl sulfides under polar conditions. López and Mijangos studied the same reaction; reacting PVC in the melt (160 °C) gave more efficient plasticization than in butanone, tetrahydrofuran (THF), or dimethylmalonate solvents.<sup>16</sup>  $T_g$  values around 60 °C were observed at 55% phenylthiolate substitution.



**Scheme 1.3** Substitution of chlorines on PVC with sodium phenylthiolate

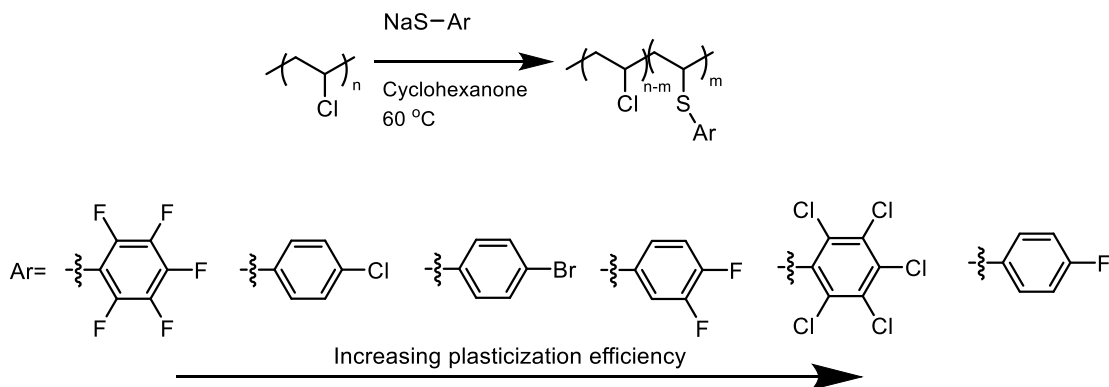
In 2002, the Reinecke group studied similar chlorine atom substitution with thiophenols containing various *para*-substituents (**Scheme 1.4**).<sup>17</sup> Substituents that can participate in hydrogen bonding greatly increased the  $T_g$ , while those that do not hydrogen bond were somewhat plasticizing, lowering the  $T_g$  values to around 70 °C. The density of all modified polymers decreased, indicating a disruption in chain packing. Notably, side reactions including both crosslinking and chloride elimination from PVC were investigated. When a thiol containing an aliphatic amine was used, elimination was observed, however no dehydrochlorination was observed for aromatic

amines. When a thiophenol bearing a carboxylic acid functionality was used, crosslinked polymers were obtained.



**Scheme 1.4** Modification of PVC using substituted thiophenols

The use of halogenated thiophenols was also investigated by the Reinecke group (**Scheme 1.5**).<sup>18</sup>  $T_g$  values ranged from 85 °C for perfluorothiophenol to 54 °C for 4-fluorothiophenol at 55% substitution.

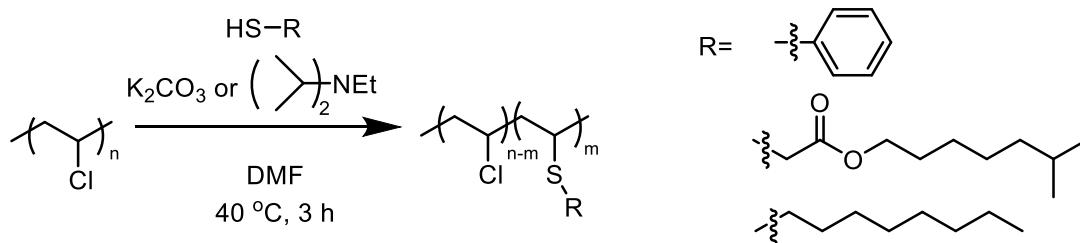


**Scheme 1.5** Substitution with halogenated thiophenols

In 2019 the Yoshioka group performed nucleophilic substitutions on PVC with three different thiols: thiophenol, octanethiol and isooctyl thioglycolate (**Scheme 1.6**).<sup>19</sup> Reaction with octanethiol resulted in nearly as much elimination as substitution,



while thiophenol and isooctyl thioglycolate gave significantly more substitution. Thiophenol was slightly plasticizing, giving a  $T_g$  value of 75 °C at 36% substitution, while octanethiol and isooctylthioglycolate were more effective, both resulting in a  $T_g$  value of 66 °C at only 6% substitution.



**Scheme 1.6** Substitution of PVC with three different thiols

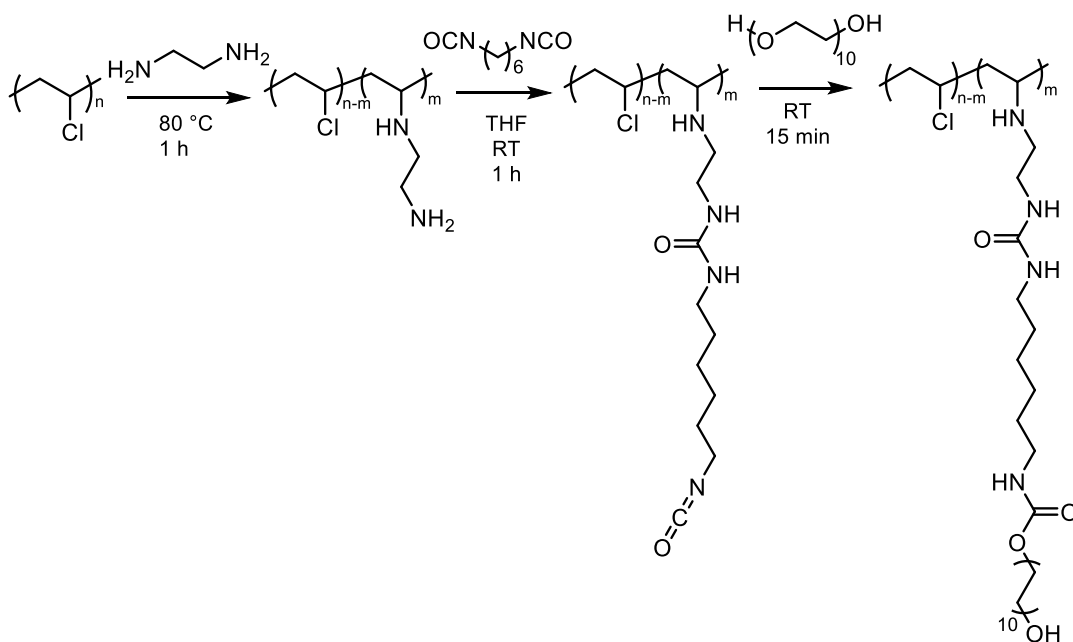
From the sulfide linked plasticizer studies shown here (and more in the review<sup>1</sup>), some patterns are seen. Rigid aromatic rings and hydrogen bond donors or acceptors are antiplasticizing. The most successful plasticizers have relatively long side chains. For a given weight percent plasticizer, larger plasticizers introduce fewer anchor points, which are antiplasticizing tertiary carbons. Increasing miscibility of these side chains helps with plasticization. A drawback of using sulfides as linkages is that sulfides are susceptible to oxidation,<sup>20</sup> which can lead to degradation of the polymer as it ages if these oxidation products undergo further reactions such as elimination. Sulfur compounds often lead to discoloration of the PVC products.

### 1.5.2 Covalent Attachment using Amine Linkages

Amines are good nucleophiles, capable of displacing chlorines on PVC. This strategy has been employed by various research groups to attach plasticizing groups to PVC. One downside of the use of amines is that although they are nucleophiles, they

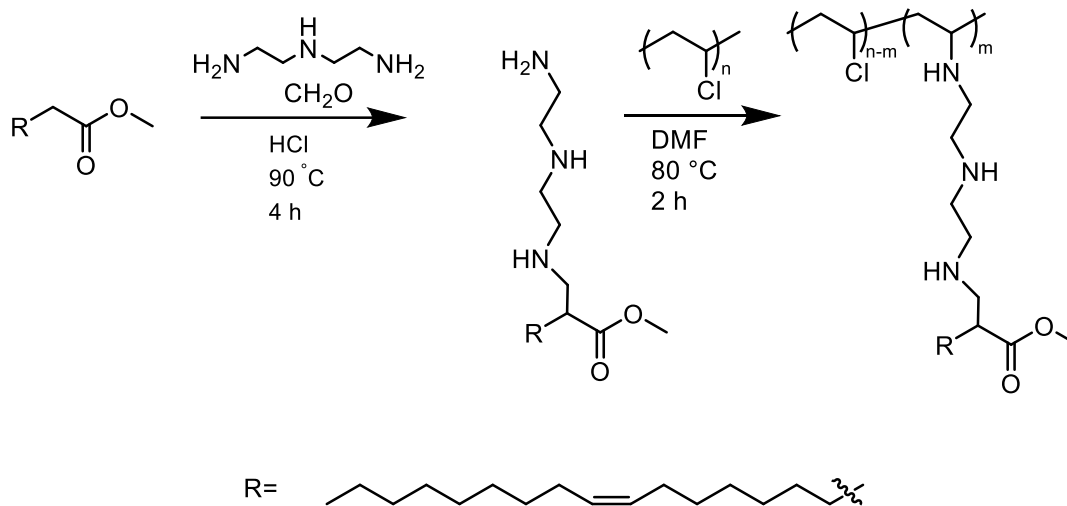
are also good bases, leading to significant amounts of competing elimination. Many of the studies in this section do not address elimination, although it is likely a competing process. In addition, the use of bisamines as nucleophiles can cause cross-linking of PVC as a side reaction; this is addressed by some authors.

In 2005, Jayakrishnan et al. reported attachment of PEG to PVC by a series of reactions.<sup>21</sup> First, PVC was treated with diethylamine, as a nucleophile to displace some of the chlorine atoms. The resulting PVC-amine was then treated with a diisocyanate, which was then allowed to react with hydroxy-terminal PEG (**Scheme 1.7**). Each of these steps has the potential to cause cross-linking: insoluble precipitates were observed when any of the three steps was allowed to run for too long. In an effort to minimize cross-linking, reaction times were kept short so that all products were soluble in THF. The  $T_g$  of the final PVC-*g*-PEG was 25-30 °C.



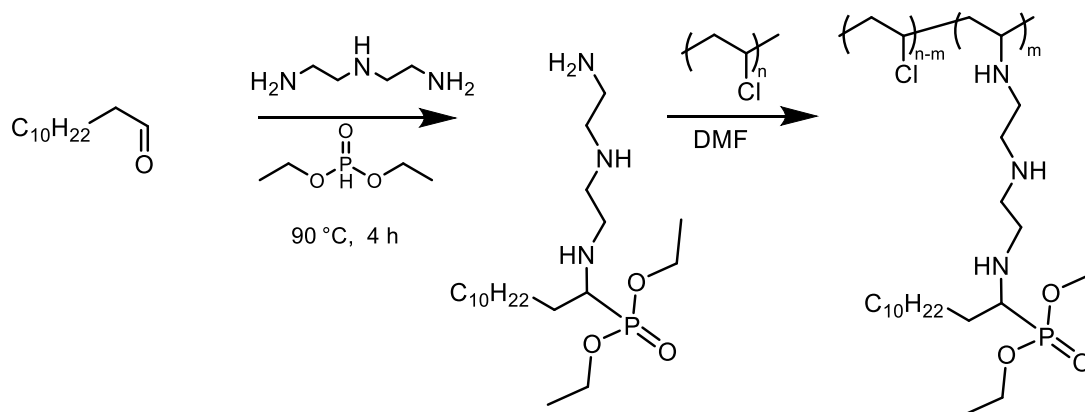
**Scheme 1.7** Desired reaction sequence for attachment of PEG to PVC using a urea linker. Crosslinked PVC chains are not shown here, but were observed as side products under prolonged reaction times

The Zhou group used a Mannich reaction with diethylenetriamine to attach a fatty acid ester to PVC (**Scheme 1.8**).<sup>22</sup> Methanolysis of waste cooking oil provided the long chained methyl ester, making it a sustainably sourced plasticizer. The modified PVC had a  $T_g$  value of 44 °C, and showed lower tensile strength and higher elongation at break than unmodified PVC.



**Scheme 1.8** Attachment of a fatty acid ester derived from cooking oil to PVC with an amine tether

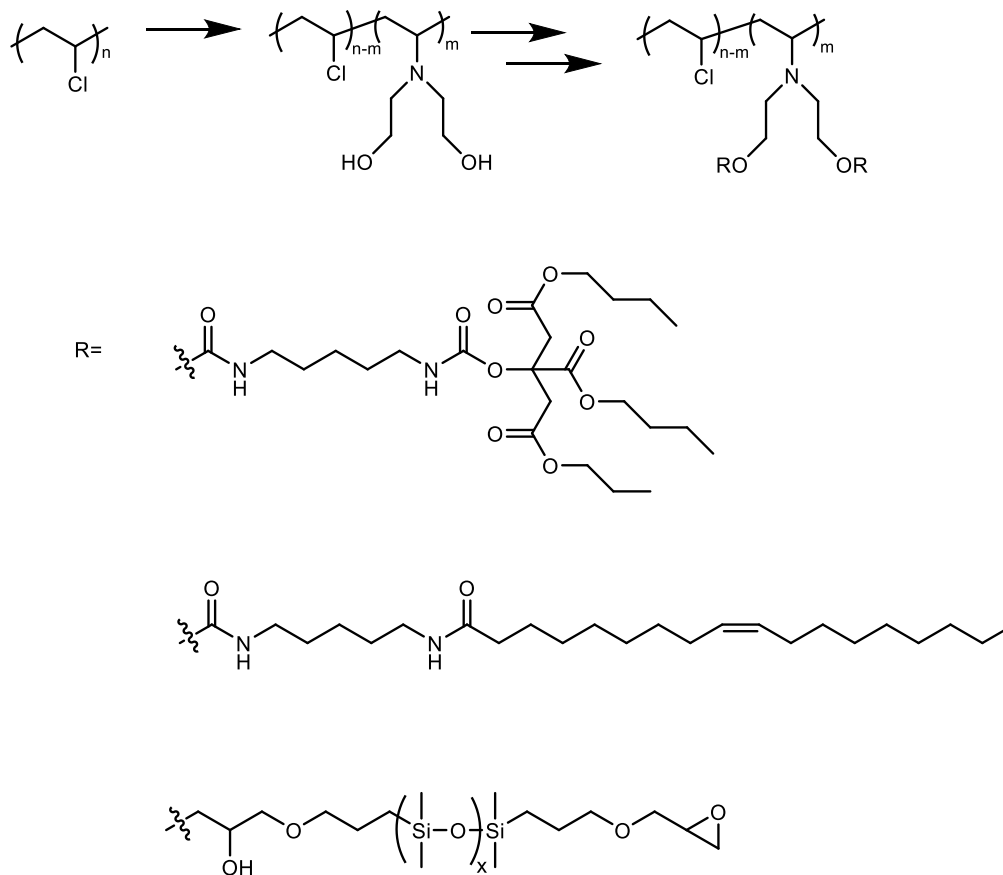
In 2021, Bu *et al.*<sup>23</sup> also employed a Mannich reaction with diethylenetriamine, lauraldehyde and diethyl phosphite in a three component coupling; this material was then attached to PVC via nucleophilic displacement by the remaining primary amine (**Scheme 1.9**).  $T_g$  values as low as 31 °C were measured, along with decreased tensile strength and increased elongation at break.



**Scheme 1.9** Attachment of lauraldehyde to PVC with an amine tether

In 2019, the Zhou group used dehydroabietic acid, a diterpenoid found in coniferous trees, as an internal plasticizer using two different attachment routes.<sup>24</sup> One route used oxalyl chloride to activate the acid, followed by amidification with diethylenetriamine, which was then used as a nucleophile to attack PVC. The other method used epichlorohydrin to install an epoxide on the dehydroabietic acid, which was then opened by triethylenetetramine, followed by attachment to PVC (**Scheme 1.10**). When compared at the same wt%, the epoxide derived material with the triethylenetetramine linker performed slightly better, giving  $T_g$  values 2 to 7 °C lower than with the diethylenetriamine linker. The lowest  $T_g$  value observed was 34 °C for PVC using the triethylenetetramine linker.

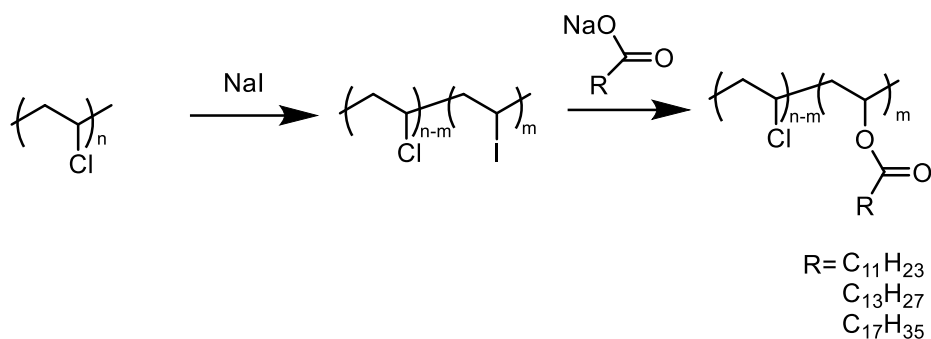




**Scheme 1.11** Modification of PVC with diethanolamine, followed by attachment of three different plasticizers

### 1.5.3 Covalent Attachment using Carboxylate Linkage

In 2013, Liu and Cheng modified PVC using several fatty acids.<sup>26</sup> The PVC was first treated with sodium iodide, exchanging some chlorides for the more reactive iodides. Displacement by sodium carboxylate nucleophiles derived from C12, C14, or C18 fatty acids provided the modified PVC materials (**Scheme 1.12**). The lowest  $T_g$  value observed was 80 °C compared to 90 °C for unmodified PVC. The  $T_g$  values did not consistently decrease with increasing substitution.



**Scheme 1.12** Pretreatment of PVC with iodide, followed by reaction with carboxylate anion

### 1.5.4 Covalent Attachment using Azide Linkages

As a non-basic and excellent nucleophile, azide is able to displace chlorine atoms on PVC without significant competing elimination. The resulting PVC-azide can then take part in azide-alkyne cycloaddition reactions to attach alkyne-functionalized plasticizers to PVC. Two major variants exist: the metal-free thermal azide-alkyne cycloaddition, and the copper-catalyzed azide-alkyne cycloaddition (CuAAC) with terminal alkynes. The thermal reaction is an attractive option as it does not leave any metal residue, which can be difficult to remove from the polymer. However, CuAAC is also commonly used due to the simplicity of the reaction and the ease of appending terminal alkynes onto substrates of interest.

#### 1.5.4.1 Copper-Free 3+2 Thermal Azide-Alkyne Cycloaddition

The thermal azide-alkyne cycloaddition is governed by the HOMO(azide)-LUMO(alkyne) interaction,<sup>27</sup> and is therefore facilitated by the presence of electron withdrawing groups on the alkyne. Studies on the relative rates of this reaction with various alkynes have shown that electron-withdrawing groups, including amides, esters, and sulfones, can significantly enhance reactivity.<sup>28,29</sup> Of these groups, esters and



amides are electron-withdrawing groups while also providing a convenient attachment point for plasticizing side chains. In addition, the triazole products formed by reacting with alkyne diesters resemble the benzene ortho diesters of phthalates such as DEHP, and were thus expected to be good plasticizers (**Figure 1.1**).

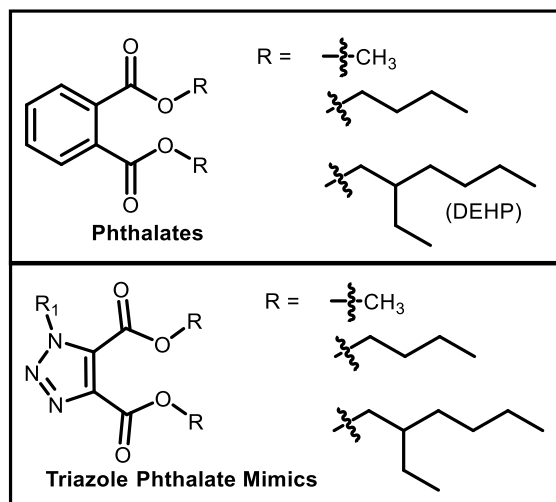
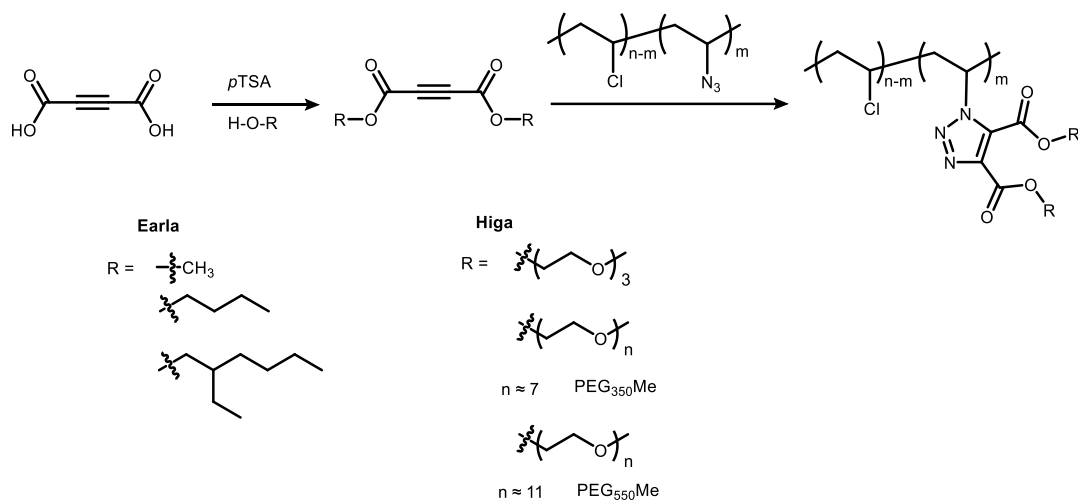


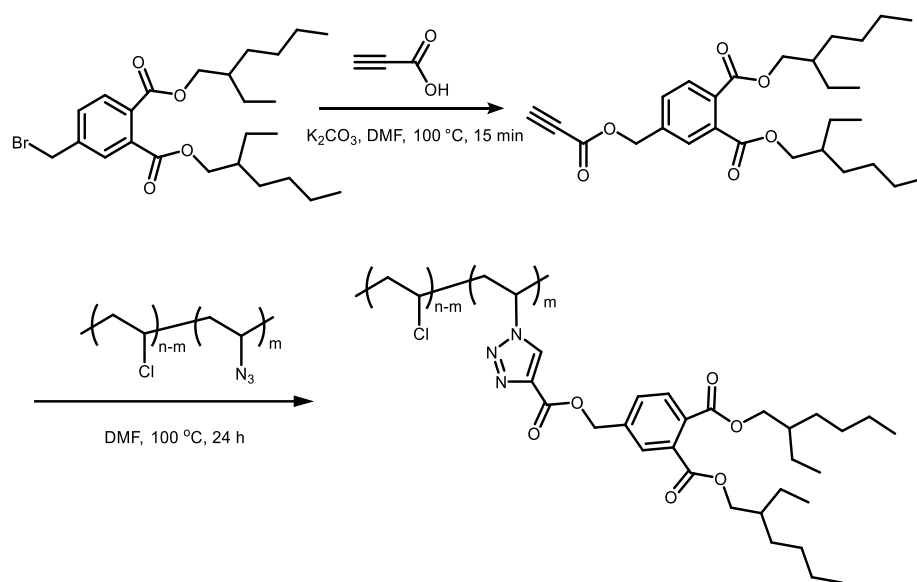
**Figure 1.1** Phthalates and triazole phthalate mimics

In 2014, Earla and Braslau<sup>30</sup> used a thermal azide-alkyne cycloaddition to attach phthalate mimics to PVC (**Scheme 1.13**). In 2018, Higa and Braslau expanded the scope of ester substituents to polyethylene glycol methyl ethers.<sup>11</sup> The lowest  $T_g$  obtained was  $-29\text{ }^\circ\text{C}$  for the phthalate mimic with the longest polyethylene glycol side chain (PEG<sub>550</sub>Me) at 15 mol% substitution. Interestingly, the phthalate mimic with the shortest side chains (R=Me) had an increased  $T_g$  of  $96\text{ }^\circ\text{C}$ , compared to  $81\text{ }^\circ\text{C}$  for unplasticized PVC. This indicates that the triazole ring itself is antiplasticizing likely due to its rigidity, but longer side chains counteract this effect for net plasticization.



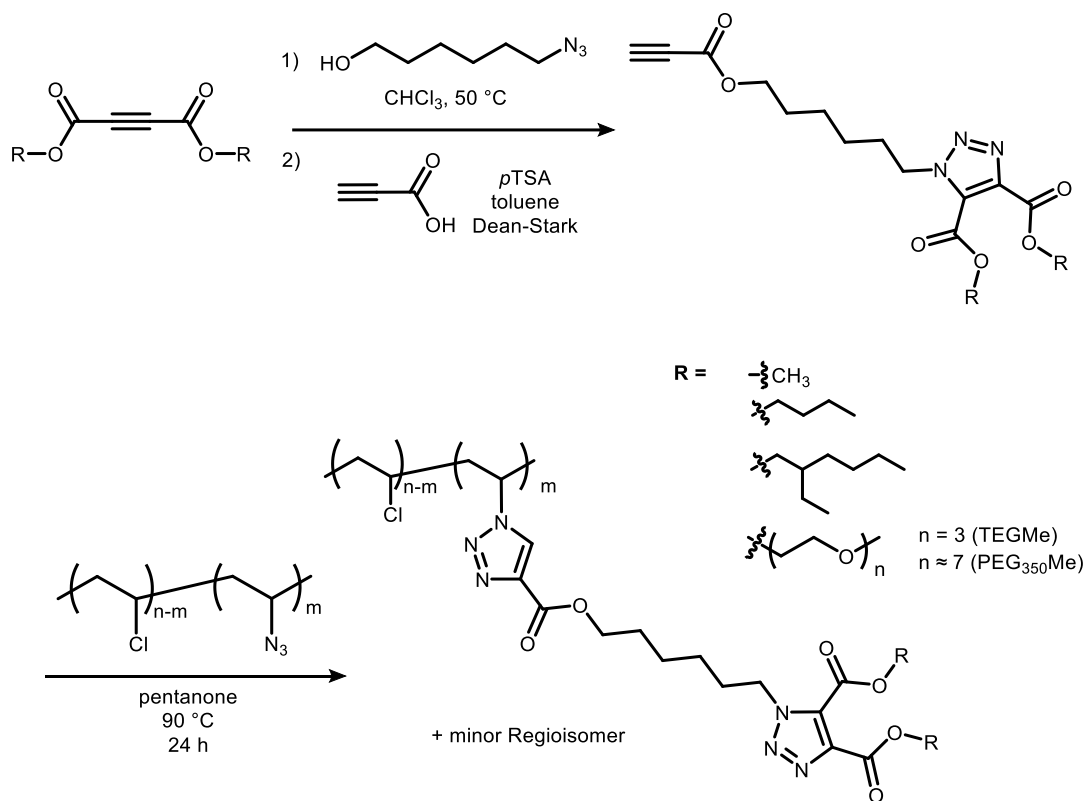
**Scheme 1.13** Covalent attachment of phthalate mimics onto PVC via thermal azide-alkyne cycloaddition

In 2017, Earla and Braslau used an alkyne with a single ester as a linker to attach a DEHP derivative to PVC-azide using thermal addition (**Scheme 1.14**).<sup>31</sup> Spacing the DEHP moiety farther from the PVC backbone (compared to the phthalate mimic in **Scheme 1.13**) was expected to increase the rotational freedom of the aromatic group, enhancing the plasticization. PVC substituted with 15 mol% of covalently linked DEHP resulted in a material with a  $T_g$  of 60 °C.



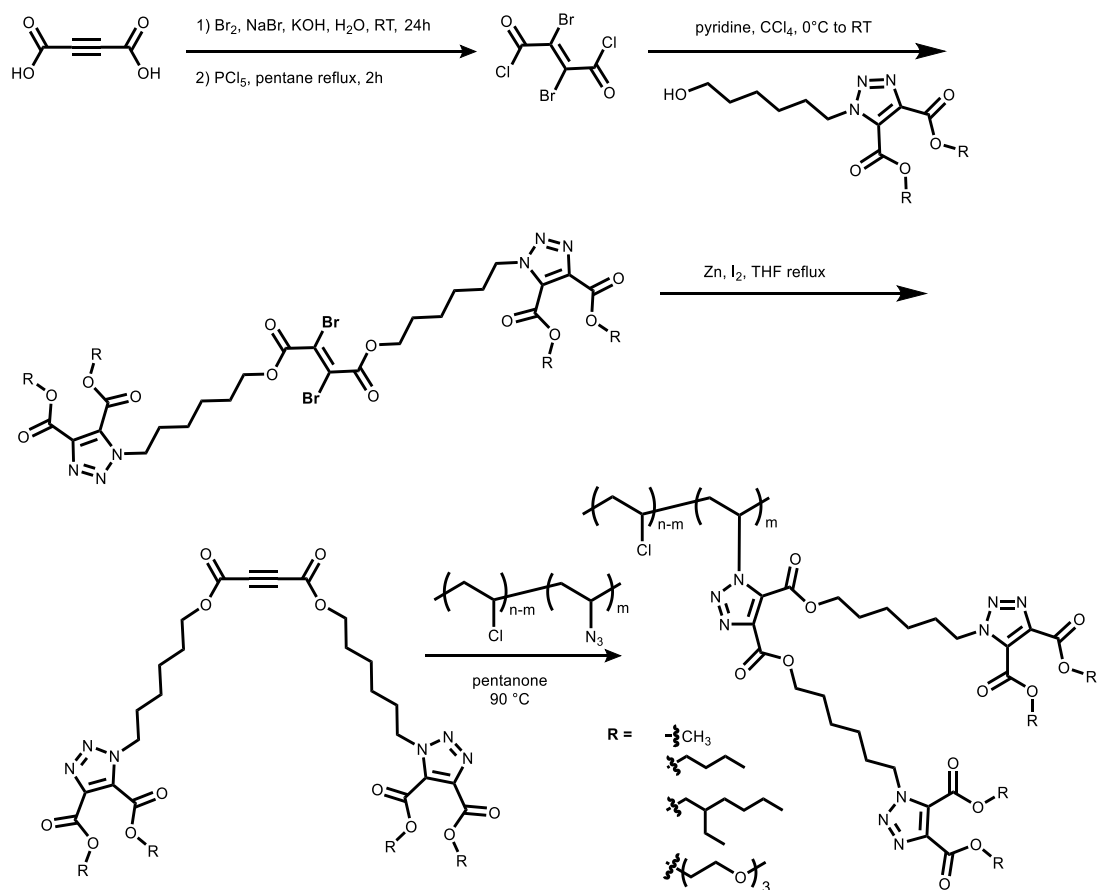
**Scheme 1.14** Covalent attachment of a tethered DEHP to PVC by thermal azide-alkyne cycloaddition

In 2018, Higa and Braslau further explored this class of triazole plasticizers, this time with phthalate mimics attached by a six-carbon linker to a propargyl ester. **(Scheme 1.15)**.<sup>11</sup> The  $T_g$  values for internal plasticization with this six-carbon linker are lower than the analogous PVC samples where the triazole diester is directly attached to the PVC chain. The lowest  $T_g$  obtained in this series is  $18\text{ }^\circ\text{C}$ , where R = triethylene glycol methyl ether (TEGMe) at 15 mol% substitution.



**Scheme 1.15** Covalent attachment of rotationally labile phthalate mimics with a six-carbon tether to PVC

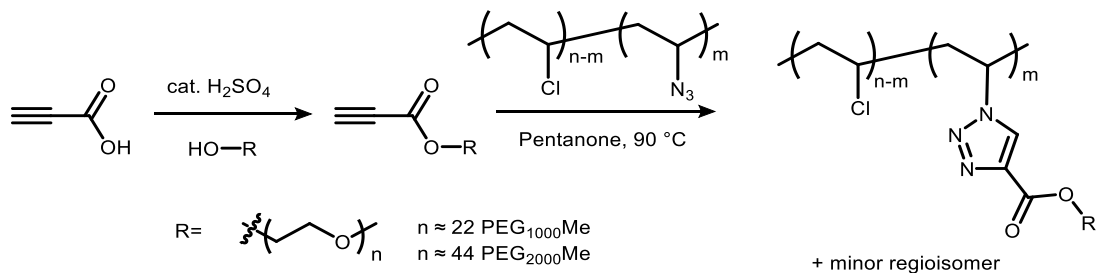
Larger plasticizers with a triazole bearing two additional triazoles were also explored (**Scheme 1.16**). The lowest  $T_g$  value is  $-17^\circ\text{C}$  for the sample bearing two TEGMe polyether esters.



**Scheme 1.16** Covalent attachment of an internal plasticizer with two tethered triazole phthalate mimics to PVC

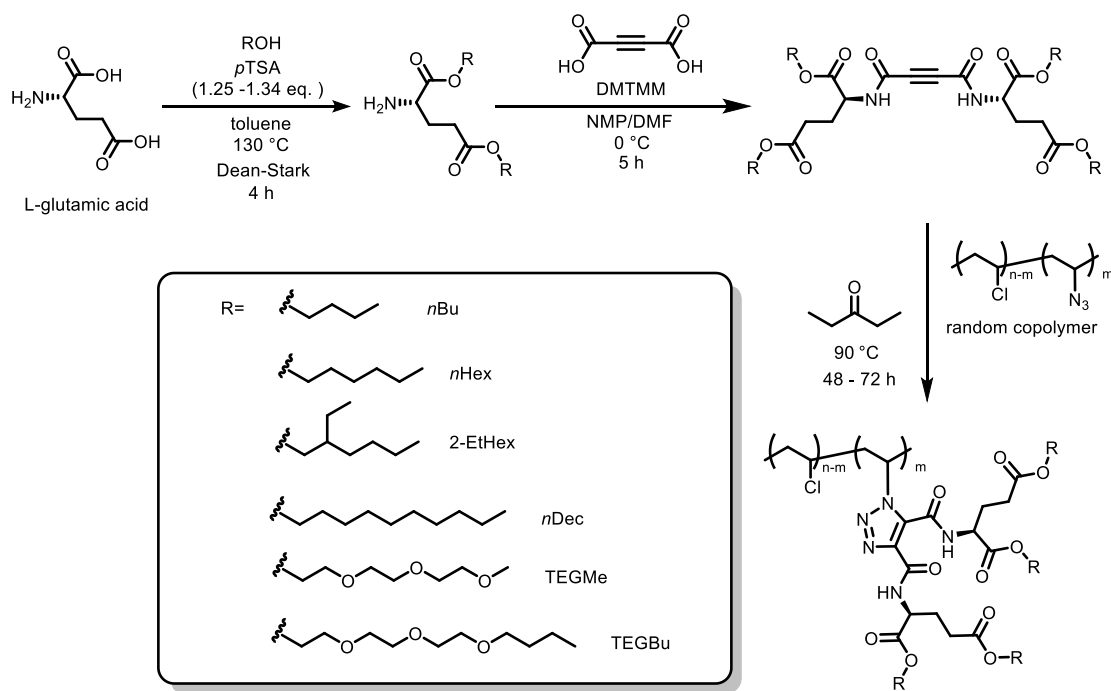
Unfortunately, this system required multistep synthesis, including protection of the diester alkyne as a dibromofumarate. The much simpler and cost efficient alternative using PEG esters directly attached to propiolic acid (**Scheme 1.17**) provided a better approach. PEG chain propargyl esters proved to be the simplest to synthesize,

while also being the most effective plasticizers: a  $T_g$  value of  $-42\text{ }^\circ\text{C}$  was obtained with PEG<sub>2000</sub>Me at 15 mol% azidation.



**Scheme 1.17** Covalent attachment of polyether propiolic esters to PVC

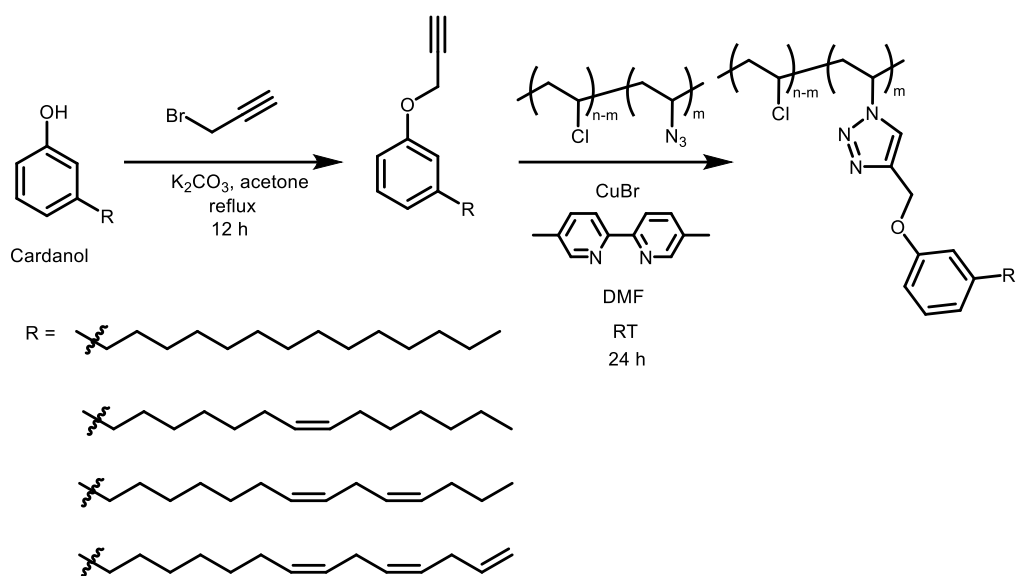
In 2019, Li and Braslau used thermal azide-alkyne cycloadditions to attach branched plasticizers to PVC.<sup>32</sup> Alkynes activated by two electron-withdrawing amides were selected, to enhance reactivity in the dipolar cycloaddition. Each amide contained a branched glutamate linker to provide attachment of four plasticizing chains per azide anchor point on PVC (**Scheme 1.18**). These chains were varied to include alkyl and polyether moieties. Plasticization efficiency increased with chain length, and polyethers were more effective plasticizers than the corresponding alkyl esters.  $T_g$  values as low as  $-1\text{ }^\circ\text{C}$  at 12 mol% substitution were obtained.



**Scheme 1.18** Use of glutamic acid as a branched linker to attach four plasticizing R groups per azide anchor point on PVC

#### 1.5.4.2 Copper-Catalyzed 3+2 Azide-Alkyne Cycloaddition

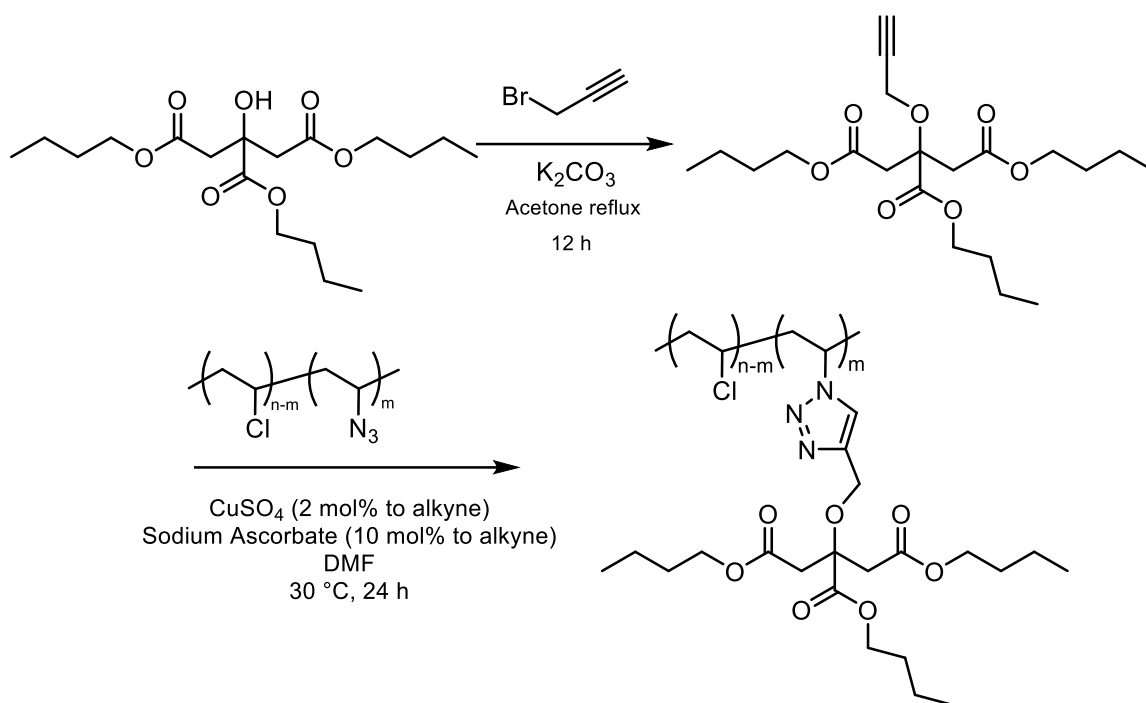
The Zhou group used propargyl bromide to attach a terminal alkyne to cardanol, a byproduct of cashew agriculture, then used a copper-catalyzed reaction to attach it to PVC-azide (**Scheme 1.19**).<sup>33</sup> They observed a  $T_g$  value of 42 °C, and proposed that the cardanol groups added more movement to the PVC chain, thereby increasing free volume. Two equivalents of copper (relative to alkyne) were used for the CuAAC reaction.



**Scheme 1.19** Covalent attachment of cardanol to PVC via CuAAC

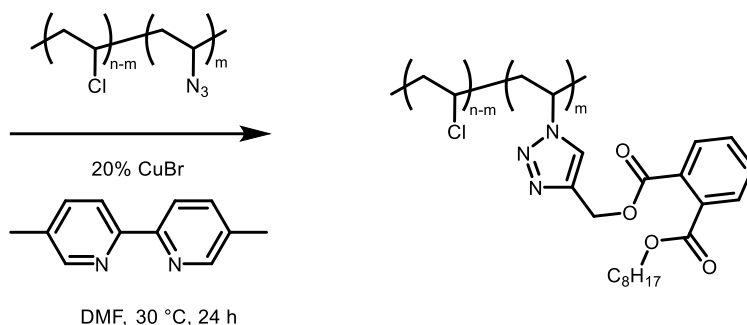
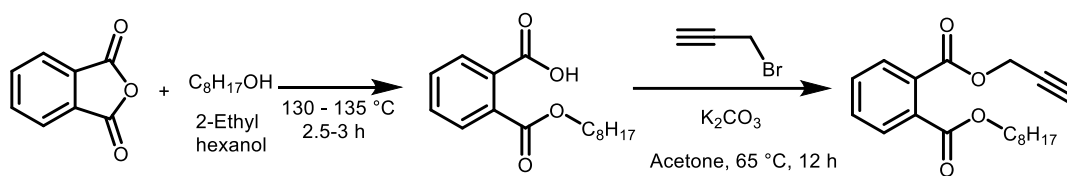
Also using propargyl bromide, Najafi and Abdollahi prepared the propargyl ether of tributyl citrate and attached it to PVC-azide (**Scheme 1.20**).<sup>25</sup> A  $T_g$  of 53 °C was observed. Notably, only 2 mol% of copper was needed for the azide-alkyne cycloaddition step in the presence of ascorbate.





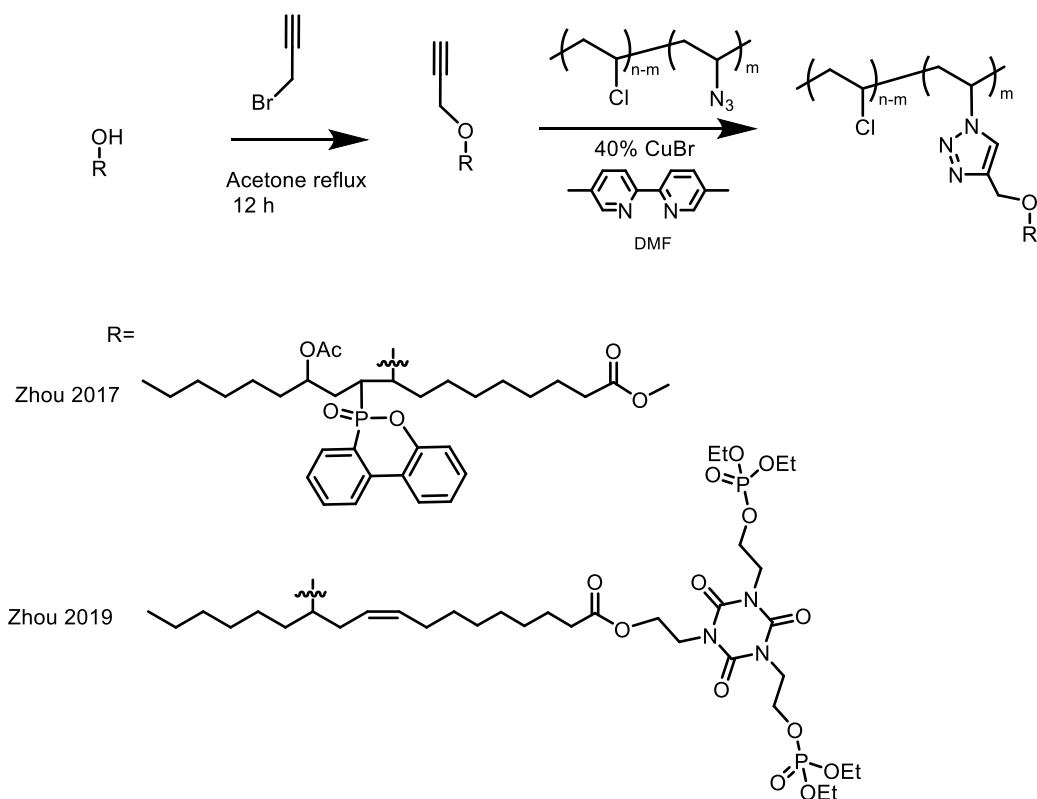
**Scheme 1.20** Attachment of citrate plasticizers using a propargyl ether linker

In 2017, the Zhou group<sup>34</sup> covalently attached mono-2-ethylhexyl phthalate derivatives to PVC to achieve a  $T_g$  value of 66 °C (**Scheme 1.21**). The TGA data showed that this modified PVC was less stable than unmodified PVC.



**Scheme 1.21** Covalent attachment of alkyne-terminated mono-octyl phthalate derivatives to PVC by CuAAC

In 2017 and 2019, the Zhou group used propargyl bromide as a linker to attach two different castor oil derivatives to PVC (**Scheme 1.22**). When castor oil containing a phosphaphenanthrene group was attached to PVC, a  $T_g$  value of 46 °C was observed.<sup>35</sup> Similarly, a castor oil derivative containing a cyanurate group and two phosphate groups was grafted to PVC, giving a  $T_g$  value of 51 °C.<sup>36</sup> The plasticized PVC showed decreased tensile strength and increased elongation at break, and also showed fire-retardant properties as measured by the limiting oxygen index.



**Scheme 1.22** Attachment of two different castor oil derivatives to PVC using a propargyl ether as a linker

### 1.5.5 Comparison of Nucleophilic Substitution Methods

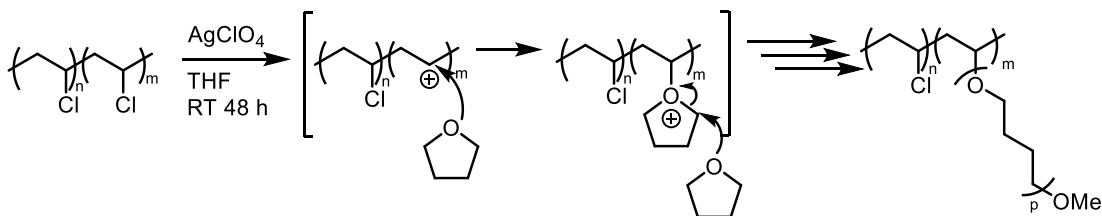
The strategy of nucleophilic substitution of chlorine atoms on the PVC chain as an attachment point for plasticizing species has been investigated using sulfur, nitrogen and carboxylate nucleophiles. Thiols are excellent nucleophiles and poor bases, providing good  $\text{S}_{\text{N}}2$  substitution, but the long-term oxidation derivatives may pose problems as these hybrid materials age. Amine nucleophiles are also good bases, suffering from competing HCl elimination reactions. In the case of bisamines, cross-linking is another competing process. Azides are excellent nucleophiles, but industry

is understandably reticent to adopt azidization of PVC on a large scale, due to concerns of the explosive nature of the azide reagent, reaction waste, and possible small molecule azides formed as side products. The use of copper-mediated azide alkyne cycloaddition leaves behind residual copper; this is not acceptable for biomedical and electronic applications. Ultimately, multi-step synthesis to build up or attach plasticizers is not practical for industry that can simply compound PVC with a small molecule plasticizer. Strategies to replace external plasticizers with internal plasticizers need to be inexpensive and ideally one-step in order to be industrially viable.

## 1.6 Plasticization by Grafting Polymers from PVC

### 1.6.1 Cationic Polymerization

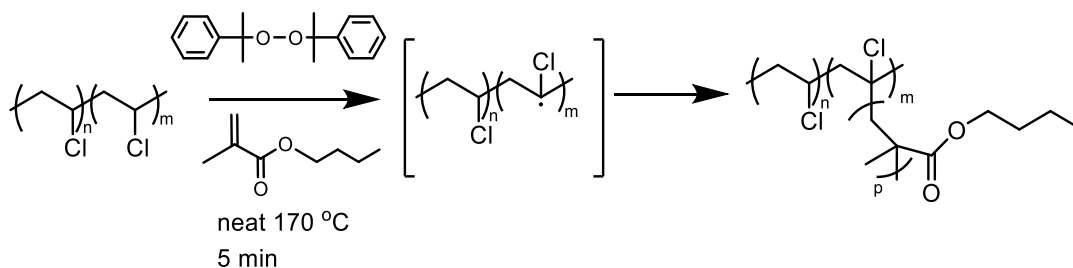
In 1981 Marian and Levin<sup>12</sup> used silver perchlorate as a Lewis acid to produce carbocations from the secondary chlorides of PVC. These carbocations were used to initiate a ring-opening polymerization of THF (**Scheme 1.23**). Although the  $T_g$  was not measured, the modified polymer showed a lower tensile strength and higher elongation at break than neat PVC, which indicates plasticization. The authors noted the cost of the silver salts as a potential drawback to this method.



**Scheme 1.23** Cationic ring-opening polymerization of THF from a PVC macroinitiator

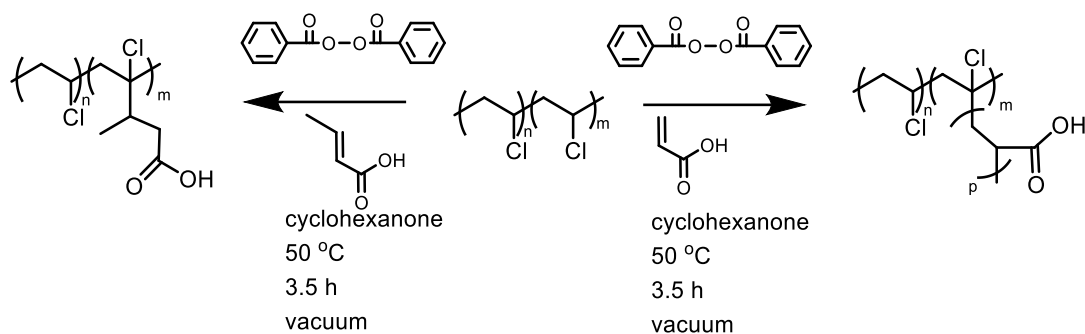
## 1.6.2 Free Radical Polymerization

Alkoxy radicals abstract hydrogen atoms from PVC to produce carbon radicals, which then initiate radical polymerizations with available monomer. In 2004, Maiti and Choudhary<sup>37</sup> performed a free-radical polymerization on PVC at 170 °C using dicumyl peroxide as a radical source and butyl methacrylate as monomer (**Scheme 1.24**). The  $T_g$  of the modified polymer was 61 °C. Interestingly, the same reaction in the absence of peroxide generated a polymer with roughly the same degree of grafting, and a similar  $T_g$  of 63 °C. It is possible that defect sites in the PVC have weak C-Cl bonds that can homolyze at the high reaction temperature, thus acting as initiators in the absence of an external radical source.



**Scheme 1.24** Free-radical polymerization of n-butyl methacrylate on PVC

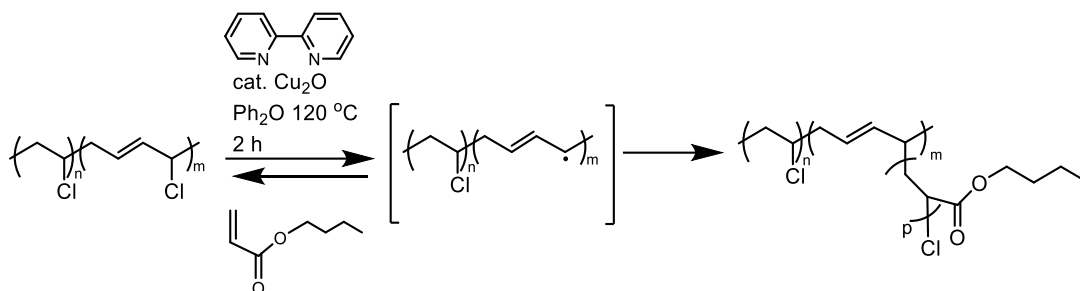
In 2017 the Odelius group used free radical chemistry to modify PVC with acrylic acid and crotonic acid.<sup>38</sup> Acrylic acid (AA) undergoes polymerization, giving PVC-g-PAA copolymers, while under the same conditions crotonic acid (CA) undergoes radical addition, adding just a single crotonic acid unit per graft site (**Scheme 1.25**). At 10 wt% internal plasticizer, the  $T_g$  values of PVC-g-PAA and PVC-g-CA were 71 °C and 75 °C respectively.



**Scheme 1.25** Graft polymerization of acrylic acid or graft addition of crotonic acid to PVC

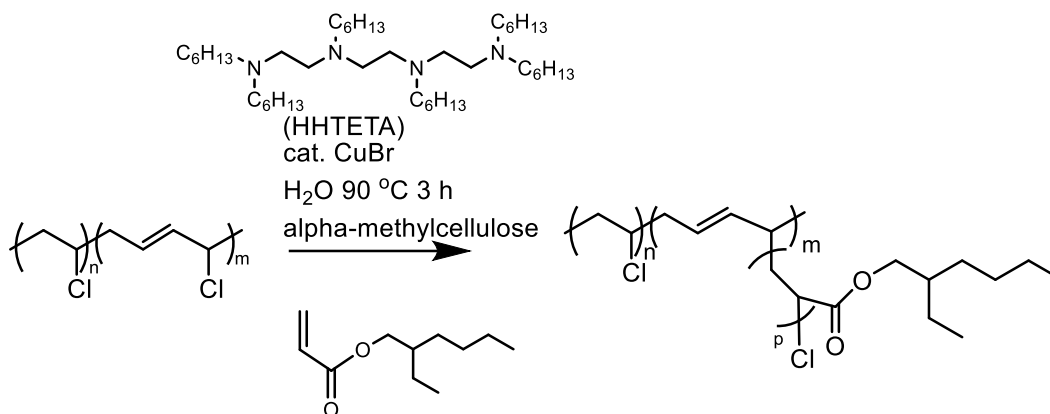
### 1.6.3 Atom-Transfer Radical Polymerization

Atom transfer radical polymerization (ATRP) is a technique that has become very popular because it combines the wide functional group tolerance of radical polymerizations with levels of molecular weight control and end group fidelity similar to those seen in ionic polymerizations. Although ATRP was applied to PVC-co-poly(vinyl chloroacetate) by Matyjaszewski,<sup>39</sup> the first example of ATRP directly on PVC was in 2001 when Percec studied the inherent reactivity of the different types of chlorines in PVC.<sup>40</sup> Through a series of model reactions, it was determined that the secondary chlorides of PVC do not act as ATRP initiators. However, PVC includes tertiary and allylic chlorides as defect sites along the backbone. The allylic chlorides in particular, and to a lesser extent the tertiary chlorides, are capable of initiating ATRP. After determining this, the authors performed several graft polymerizations on PVC with different monomers (**Scheme 1.26**). Poly methyl methacrylate and poly 4-chlorostyrene side chains were found to be antiplasticizing, but grafting poly *n*-butyl acrylate from PVC decreased the  $T_g$  value to  $-4$  °C.



**Scheme 1.26** Atom transfer radical polymerization of butyl acrylate on PVC

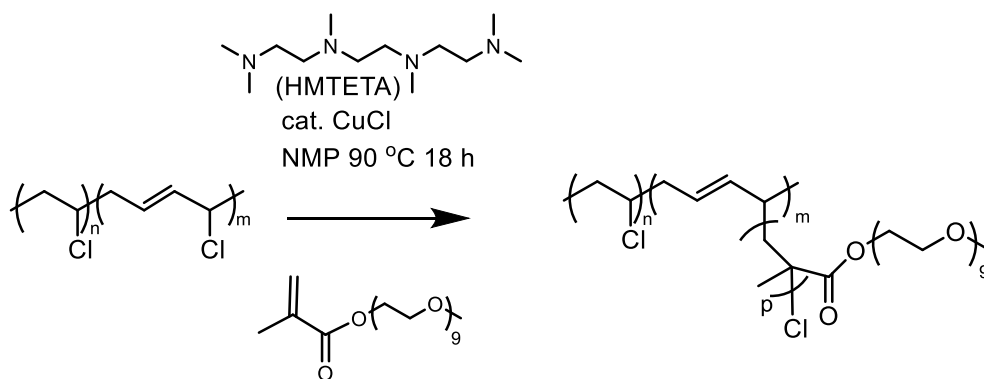
In two studies, Bicak et al. grafted ethylhexyl acrylate (EHA) from the defect sites of PVC (**Scheme 1.27**). The polymerization was done first in dichlorobenzene,<sup>41</sup> then adapted to work in a water suspension for a more cost effective and greener synthesis.<sup>42</sup> A hydrophobic ligand was used to ensure the copper stayed in the organic phase. The  $T_g$  value of the modified polymer was 58 °C.



**Scheme 1.27** ATRP graft polymerization of EHA from PVC

Several studies by both the Hong group<sup>43,44</sup> and the Kim group<sup>45,46,47,48</sup> have grafted polyoxyethylene methacrylate (POEM) from PVC defect sites. In all cases the polymerizations were done at 90 °C in *N*-methylpyrrolidinone (NMP) with catalytic CuCl and hexamethyltriethylenetetramine (HMTETA) as the ligand (**Scheme 1.28**). In all but one of these cases, two separate  $T_g$  values were seen, indicating phase separation.

The  $T_g$  values are given in **Table 1.1**, with the lower  $T_g$  corresponding to the POEM phase and the higher  $T_g$  corresponding to the PVC phase. In one example<sup>48</sup> a single  $T_g$  value was observed but phase separation was still seen by TEM, so the second  $T_g$  may have simply not been visible due to the relatively small amount of PVC in the final material.



**Scheme 1.28** ATRP graft polymerization of POEM from PVC

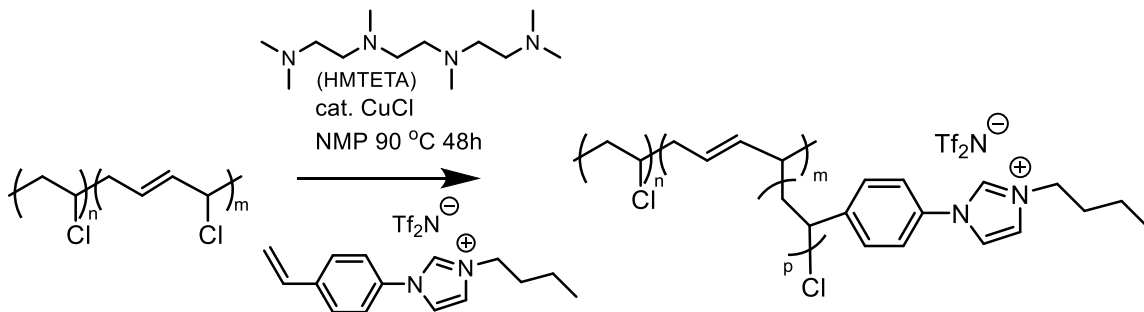
**Table 1.1**  $T_g$  values for PVC-g-POEM

Source	$T_{g1}$ ( $^\circ\text{C}$ )	$T_{g2}$ ( $^\circ\text{C}$ )
[43]	-68	32
[44]	-67	34
[45]	-57	30
[46]	-58	70
[47]	-62	96
[48]	-59	–

In another study by the Kim group,<sup>49</sup> ionic liquid polymers were grafted from PVC (**Scheme 1.29**). This also led to phase separation, with two  $T_g$  values: 55  $^\circ\text{C}$  and

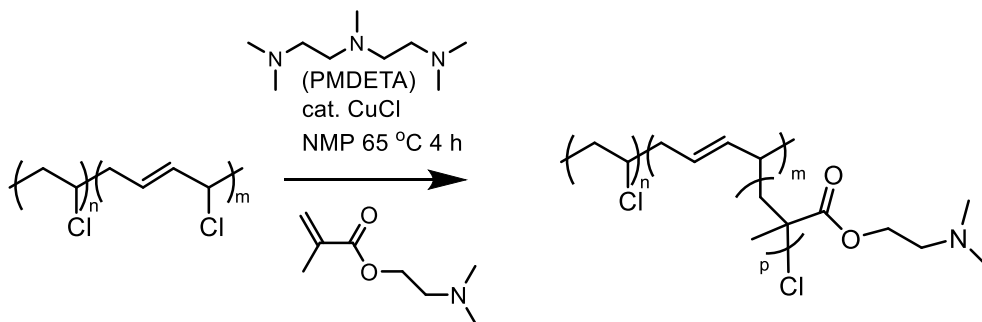


88°C. The graft copolymer with 65 % ionic liquid by weight showed higher elongation at break and lower tensile strength and modulus than pure PVC.



**Scheme 1.29** Grafting a poly(ionic liquid) from PVC by ATRP

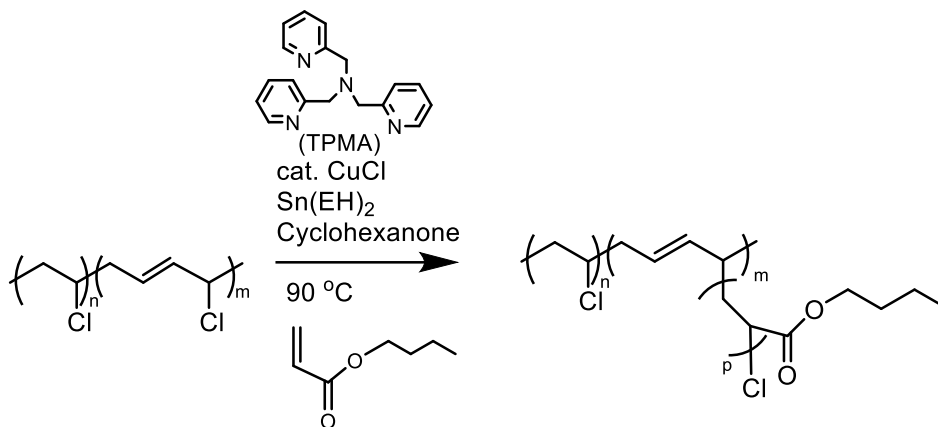
Poly(*N,N*-dimethylaminoethyl methacrylate) has also been explored as a plasticizing side chain (**Scheme 1.30**).<sup>50</sup> After grafting, the  $T_g$  value decreased to 58 °C for polymers with 57% of internal plasticizer by weight. The graft polymerization was carried out at the relatively low temperature of 65 °C, due to the higher reactivity of methacrylate compared to acrylate monomers.<sup>51</sup>



**Scheme 1.30** Synthesis of PVC-g-PDMA by ATRP

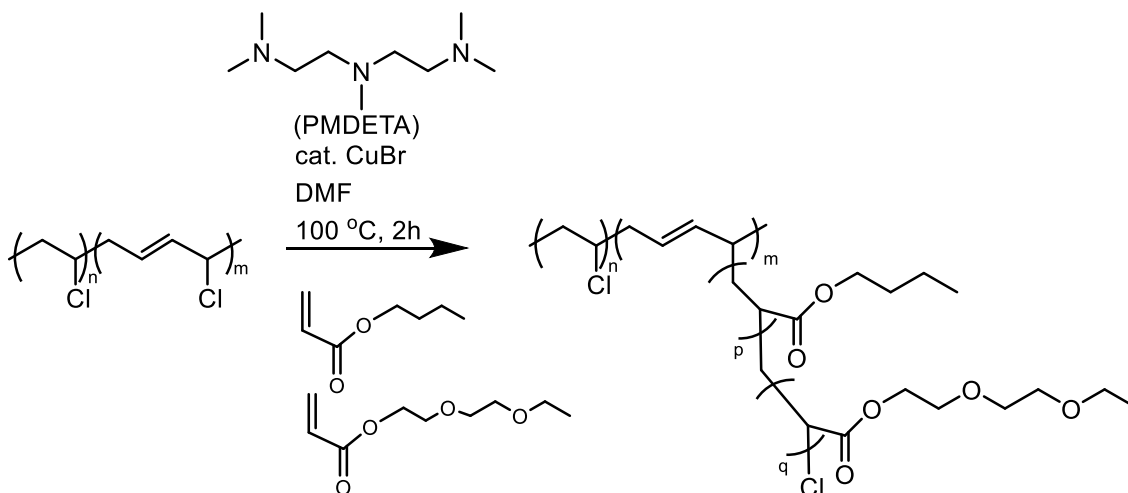
In 2014, Liu and Bao<sup>52</sup> used Activators ReGenerated by Electron Transfer (ARGET) ATRP to graft polybutyl acrylate from a specially prepared PVC with an increased number of allylic defect sites (**Scheme 1.31**). Copper chloride and tris(pyridylmethyl)amine (TPMA) ligand were used, along with diethylhexyl tin

(Sn(EH)<sub>2</sub>) which acts as a reducing agent to regenerate the active Cu<sup>I</sup> species. This allows the reaction to be run with only 0.1 mol% copper, although the potential for tin residues becomes a concern with 5 mol% tin being used. The T<sub>g</sub> of the resulting PVC-g-PBA was 8 °C.



**Scheme 1.31** ARGET-ATRP of butyl acrylate on PVC

In two studies in 2021, Li and Braslau used ATRP to grow copolymers of butyl acrylate and 2-(2-ethoxyethoxy)ethyl acrylate (2EEA) as grafts from a PVC backbone: PVC-g-(PBA-co-P2EEA) (**Scheme 2.10**).<sup>53,54</sup> The ratio of BA to 2EEA was varied; all resulting polymers had T<sub>g</sub> values below 0 °C, with the lowest being -50 °C, and each had a single T<sub>g</sub> value, indicating the lack of phase separation. The process was scaled up from 2g to 14g with similar results observed at both scales. In the second study, they varied the ratio of plasticizer to PVC, allowing them to tune the T<sub>g</sub> value anywhere between 54 °C and -54 °C.



**Scheme 1.32** Graft copolymerization of BA and 2EEA from PVC

In contrast to the plasticizing side chains discussed above, many monomers have been found to produce *antiplasticizing* side chains when grafted from PVC. These monomers include ethyl acrylate,<sup>55</sup> methyl methacrylate,<sup>40,56</sup> *tert*-butyl methacrylate,<sup>57</sup> hydroxyethyl methacrylate,<sup>58</sup> 3-sulfopropyl methacrylate,<sup>59</sup> styrene,<sup>60</sup> ,<sup>61</sup> 4-chlorostyrene,<sup>40</sup> and 4-vinyl pyridine.<sup>62</sup> Methods for adding these graft copolymers include traditional free radical polymerization,<sup>55</sup> ATRP,<sup>40,56,57,58,59,60,62</sup> and nitroxide-mediated polymerization.<sup>61</sup>

## 1.7 Conclusion

From these studies it can be concluded that mimicking the structure of DEHP is not necessary for internal plasticization. As an external plasticizer, DEHP's miscibility with PVC is what makes it so effective, however internal plasticizers are covalently attached to the PVC backbone, and cannot phase separate unless very large. Therefore, a larger variety of structures are available. Those most similar to DEHP can in fact be antiplasticizing due to the rigidity of the aromatic ring. The most successful

plasticizers have long alkyl or polyether chains; the attachment point, being a tertiary carbon, is antiplasticizing, so it must be counteracted by a long flexible chain.

As PVC is produced on the megaton scale, keeping costs down is essential for any plasticizer to be adopted. Internal plasticizers that use agricultural byproducts as their starting materials can help with affordability, as can plasticizers that reduce the need of other additives like stabilizers and flame retardants. Synthetic simplicity is also a factor in cost. Longer synthetic sequences to produce a specific structure will not be as attractive as reactions that plasticize PVC in a single step. With this in mind, graft polymerizations using the PVC as an initiator appear to be a good option. Polymerization can create a large plasticizing side chain and reach very low  $T_g$  values in a single step.

## 1.8 References

<sup>1</sup> Skelly, P. W.; Li, L.; Braslau, R. Internal Plasticization of PVC. *Polym. Rev.* **2022**, *62* (3), 485–528. <https://doi.org/10.1080/15583724.2021.1986066>.

<sup>2</sup> IHS Markit. Population Growth and Materials Demand Study Prepared for: American Chemistry Council  
<https://www.americanchemistry.com/content/download/8057/file/Population-Growth-and-Materials-Demand-Study-IHS-Markit.pdf> (Accessed April 2023).

<sup>3</sup> Statista. PVC Production Worldwide in 2018 and 2025. <https://www.statista.com/statistics/720296/global-polyvinyl-chloride-market-size-in-tons/#:~:text=Global%20PVC%20production%20volume%202018%20%26%202025&text=The%20total%20global%20production%20volume,to%2044.3%20million%20metric%20tons>, (Accessed April 2023).

<sup>4</sup> Chiellini, F.; Ferri, M.; Morelli, A.; Dipaola, L.; Latini, G. Perspectives on Alternatives to Phthalate Plasticized Poly(Vinyl Chloride) in Medical Devices Applications. *Prog. Polym. Sci.* **2013**, *38* (7), 1067–1088. <https://doi.org/10.1016/j.progpolymsci.2013.03.001>.

<sup>5</sup> Bui, T. T.; Giovanoulis, G.; Cousins, A. P.; Magnér, J.; Cousins, I. T.; de Wit, C. A. Human Exposure, Hazard and Risk of Alternative Plasticizers to Phthalate Esters. *Sci. Total Environ.* **2016**, *541* (Supplement C), 451–467. <https://doi.org/10.1016/j.scitotenv.2015.09.036>.

- <sup>6</sup> IHS Markit. Plasticizers <https://Ihsmarkit.com/Products/Plasticizers-Chemical-Economics-Handbook.Html>, (Accessed April 2023)
- <sup>7</sup> Rowdhwal, S. S. S.; Chen, J. Toxic Effects of Di-2-Ethylhexyl Phthalate: An Overview. *Biomed Res. Int.* **2018**, *2018* (Figure 1). <https://doi.org/10.1155/2018/1750368>.
- <sup>8</sup> Ma, Y.; Liao, S.; Li, Q.; Guan, Q.; Jia, P.; Zhou, Y. Physical and Chemical Modifications of Poly(Vinyl Chloride) Materials to Prevent Plasticizer Migration - Still on the Run. *React. Funct. Polym.* **2020**, *147* (December 2019), 104458. <https://doi.org/10.1016/j.reactfunctpolym.2019.104458>
- <sup>9</sup> Bodaghi, A. An Overview on the Recent Developments in Reactive Plasticizers in Polymers. *Polym. Adv. Technol.* **2020**, *31* (3), 355–367. <https://doi.org/10.1002/pat.4790>.
- <sup>10</sup> Czogała, J.; Pankalla, E.; Turczyn, R. Recent Attempts in the Design of Efficient PVC Plasticizers with Reduced Migration. *Materials (Basel)*. **2021**, *14* (4), 844. <https://doi.org/10.3390/ma14040844>.
- <sup>11</sup> Higa, C. M.; Tek, A. T.; Wojtecki, R. J.; Braslau, R. Nonmigratory Internal Plasticization of Poly(Vinyl Chloride) via Pendant Triazoles Bearing Alkyl or Polyether Esters. *J. Polym. Sci. Part A Polym. Chem.* **2018**, *56* (21), 2397–2411. <https://doi.org/10.1002/pola.29205>.

<sup>12</sup> Marian, S.; Levin, G. Modification of Polyvinylchloride in Solution or Suspension by Nucleophilic Substitution. *J. Appl. Polym. Sci.* **1981**, *26*, 3295–3304. <https://doi.org/10.1002/app.1981.070261009>.

<sup>13</sup> Elicegui, A.; del Val, J. J.; Bellenger, V.; J, V. A Study of Plasticization Effects in Poly (Vinyl Chloride). **1997**, *38* (7), 1647–1657. [https://doi.org/10.1016/S0032-3861\(96\)00671-4](https://doi.org/10.1016/S0032-3861(96)00671-4).

<sup>14</sup> Guarrotxena, N.; Martinez, J. M.; Gomez-Elvira, J. M.; Millan, J. Solvent Dependence of Stereoselective Substitution Reaction on Poly(Vinyl Chloride). A Useful Tool to Investigate the Tacticity Effect on Tg. *Eur. Polym. J.* **1993**, *29* (5), 685–688. [https://doi.org/10.1016/0014-3057\(93\)90129-4](https://doi.org/10.1016/0014-3057(93)90129-4).

<sup>15</sup> Guarrotxena, N.; Martinez, G.; Gomez-Elvira, J. M.; Millan, J. L. Effect of Some Tacticity-Depending Local Chain Conformations on the Behaviour of Poly(Vinyl Chloride). Changes of Glass Transition Temperature through Stereoselective Substitution in Solution. *Macromol. Rapid Commun.* **1994**, *15*, 189–196. <https://doi.org/10.1002/marc.1994.030150302>.

<sup>16</sup> Lopez, D.; Mijangos, C. Effect of Solvent on Glass Transition Temperature in Chemically Modified Polyvinyl Chloride (PVC). *Colloid Polym. Sci.* **1994**, *272*, 159–167. <https://doi.org/10.1007/BF00658842>.

<sup>17</sup> Herrero, M.; Tiemblo, P.; Reyes-Labarta, J.; Mijangos, C.; Reinecke, H. PVC Modification with New Functional Groups. Influence of Hydrogen Bonds on

Reactivity, Stiffness and Specific Volume. *Polymer (Guildf)*. **2002**, *43*, 2631–2636.

[https://doi.org/10.1016/S0032-3861\(02\)00064-2](https://doi.org/10.1016/S0032-3861(02)00064-2).

<sup>18</sup> Navarro, R.; Bierbrauer, K.; Mijangos, C.; Goiti, E.; Reinecke, H. Modification of Poly (Vinyl Chloride) with New Aromatic Thiol Compounds. Synthesis and Characterization. *Polym. Degrad. Stab.* **2008**, *93*, 585–591.

<https://doi.org/10.1016/j.polymdegradstab.2008.01.015>.

<sup>19</sup> Lu, L.; Kumagai, S.; Kameda, T.; Luo, L.; Yoshioka, T. Degradation of PVC Waste into a Flexible Polymer by Chemical Modification Using DINP Moieties. *RSC Adv.* **2019**, *9* (49), 28870–28875. <https://doi.org/10.1039/c9ra05081g>.

<sup>20</sup> Barnard, D.; Bateman, L.; Cunneen, J. I. *Oxidation of Organic Sulfides*; Pergamon Press Inc., **1961**. <https://doi.org/10.1016/b978-1-4831-9982-5.50024-5>.

<sup>21</sup> Balakrishnan, B.; Kumar, D. S.; Yoshida, Y.; Jayakrishnan, A. Chemical Modification of Poly (Vinyl Chloride) Resin Using Poly (Ethylene Glycol) to Improve Blood Compatibility. *Biomaterials* **2005**, *26*, 3495–3502. <https://doi.org/10.1016/j.biomaterials.2004.09.032>.

<sup>22</sup> Jia, P.; Zhang, M.; Hu, L.; Song, F.; Feng, G.; Zhou, Y. A Strategy for Nonmigrating Plasticized PVC Modified with Mannich Base of Waste Cooking Oil Methyl Ester. *Sci. Rep.* **2018**, *8* (1589). <https://doi.org/10.1038/s41598-018-19958-y>.

<sup>23</sup> Wang, M.; Kong, X.; Song, X.; Chen, Y.; Bu, Q. Construction of Enhanced Self-Plasticized PVC via Grafting with a Bio-Derived Mannich Base . *New J. Chem.* **2021**, 3441–3447. <https://doi.org/10.1039/d0nj05714b>.



- <sup>24</sup> Jia, P.; Ma, Y.; Song, F.; Hu, Y.; Zhang, C.; Zhou, Y. Toxic Phthalate-Free and Highly Plasticized Polyvinyl Chloride Materials from Non-Timber Forest Resources in Plantation. *React. Funct. Polym.* **2019**, *144*, 104363. <https://doi.org/10.1016/j.reactfunctpolym.2019.104363>.
- <sup>25</sup> Najafi, V.; Abdollahi, H. Internally Plasticized PVC by Four Different Green Plasticizer Compounds. *Eur. Polym. J.* **2020**, *128* (109620). <https://doi.org/10.1016/j.eurpolymj.2020.109620>.
- <sup>26</sup> Liu, Y.; Cheng, P. Structure and Thermal Properties of PVC Grafted with Crystallizable Side Chains. *Hecheng Shuzhi Ji Suliao/China Synth. Resin Plast.* **2013**, *30* (2), 67–70.
- <sup>27</sup> Ess, D. H.; Houk, K. N. Theory of 1,3-Dipolar Cycloadditions: Distortion/Interaction and Frontier Molecular Orbital Models. *J. Am. Chem. Soc.* **2008**, *130* (31), 10187–10198. <https://doi.org/10.1021/ja800009z>.
- <sup>28</sup> Pascoal, M.; Brook, M. A.; Gonzaga, F.; Zepeda-Velazquez, L. Thermally Controlled Silicone Functionalization Using Selective Huisgen Reactions. *Eur. Polym. J.* **2015**, *69* (Supplement C), 429–437. <https://doi.org/10.1016/j.eurpolymj.2015.06.026>.
- <sup>29</sup> Skelly, P. W.; Sae-Jew, J.; Kitos Vasconcelos, A. P.; Tasnim, J.; Li, L.; Raskatov, J. A.; Braslau, R. Relative Rates of Metal-Free Azide–Alkyne Cycloadditions: Tunability over 3 Orders of Magnitude. *J. Org. Chem.* **2019**, *84* (21), 13615–13623. <https://doi.org/10.1021/acs.joc.9b01887>.

- <sup>30</sup> Earla, A.; Braslau, R. Covalently Linked Plasticizers: Triazole Analogues of Phthalate Plasticizers Prepared by Mild Copper-Free “Click” Reactions with Azide-Functionalized PVC. *Macromol. Rapid Commun.* **2014**, *35* (6), 666–671. <https://doi.org/10.1002/marc.201300865>.
- <sup>31</sup> Earla, A.; Li, L.; Costanzo, P.; Braslau, R. Phthalate Plasticizers Covalently Linked to PVC via Copper-Free or Copper Catalyzed Azide-Alkyne Cycloadditions. *Polymer (Guildf)*. **2017**, *109*, 1–12. <https://doi.org/10.1016/j.polymer.2016.12.014>.
- <sup>32</sup> Li, L.; Tek, A. T.; Wojtecki, R. J.; Braslau, R. Internal Plasticization of Poly(Vinyl) Chloride Using Glutamic Acid as a Branched Linker to Incorporate Four Plasticizers per Anchor Point. *J. Polym. Sci. Part A Polym. Chem.* **2019**, *57* (17), 1821–1835. <https://doi.org/10.1002/pola.29455>.
- <sup>33</sup> Jia, P.; Zhang, M.; Hu, L.; Wang, R.; Sun, C.; Zhou, Y. Cardanol Groups Grafted on Poly(Vinyl Chloride)-Synthesis, Performance and Plasticization Mechanism. *Polymers (Basel)*. **2017**, *9* (621), 1–12. <https://doi.org/10.3390/polym9110621>.
- <sup>34</sup> Jia, P.; Wang, R.; Hu, L.; Zhang, M.; Zhou, Y. Self-Plasticization of PVC via Click Reaction of a Monoctyl Phthalate Derivative. *Polish J. Chem. Technol.* **2017**, *19* (3), 16–19. <https://doi.org/10.1515/pjct-2017-0042>.
- <sup>35</sup> Jia, P.; Hu, L.; Zhang, M.; Feng, G.; Zhou, Y. Phosphorus Containing Castor Oil Based Derivatives: Potential Non-Migratory Flame Retardant Plasticizer. *Eur. Polym. J.* **2017**, *87*, 209–220. <https://doi.org/10.1016/j.eurpolymj.2016.12.023>.

- <sup>36</sup> Jia, P.; Ma, Y.; Zhang, M.; Hu, L.; Li, Q.; Yang, X.; Zhou, Y. Flexible PVC Materials Grafted with Castor Oil Derivative Containing Synergistic Flame Retardant Groups of Nitrogen and Phosphorus. *Sci. Rep.* **2019**, *9* (1766), 1–8. <https://doi.org/10.1038/s41598-018-38407-4>.
- <sup>37</sup> Maiti, A. K.; Choudhary, M. S. Melt Grafting of *N*-Butyl Methacrylate onto Poly(Vinyl Chloride): Synthesis and Characterization. *J. Appl. Polym. Sci.* **2004**, *92* (4), 2442–2449. <https://doi.org/10.1002/app.20234>.
- <sup>38</sup> Salazar Avalos, A.; Hakkarainen, M.; Odelius, K. Superiorly Plasticized PVC/PBSA Blends through Crotonic and Acrylic Acid Functionalization of PVC. *Polymers (Basel)*. **2017**, *9* (12), 84. <https://doi.org/10.3390/polym9030084>.
- <sup>39</sup> Paik, H. J.; Gaynor, S. G.; Matyjaszewski, K. Synthesis and Characterization of Graft Copolymers of Poly(Vinyl Chloride) with Styrene and (Meth)Acrylates by Atom Transfer Radical Polymerization. *Macromol. Rapid Commun.* **1998**, *19* (1), 47–52. [https://doi.org/10.1002/\(SICI\)1521-3927\(19980101\)19:1<47::AID-MARC47>3.0.CO;2-Q](https://doi.org/10.1002/(SICI)1521-3927(19980101)19:1<47::AID-MARC47>3.0.CO;2-Q).
- <sup>40</sup> Percec, V.; Asgarzadeh, F. Metal-Catalyzed Living Radical Graft Copolymerization of Olefins Initiated from the Structural Defects of Poly(Vinyl Chloride). *J. Polym. Sci. Part A Polym. Chem.* **2001**, *39* (7), 1120–1135. [https://doi.org/10.1002/1099-0518\(20010401\)39:7<1120::AID-POLA1089>3.0.CO;2-Z](https://doi.org/10.1002/1099-0518(20010401)39:7<1120::AID-POLA1089>3.0.CO;2-Z).
- <sup>41</sup> Bicak, N.; Ozlem, M. Graft Copolymerization of Butyl Acrylate and 2-Ethyl Hexyl Acrylate from Labile Chlorines of Poly(Vinyl Chloride) by Atom Transfer Radical

Polymerization. *J. Polym. Sci. Part A Polym. Chem.* **2003**, *41* (21), 3457–3462.  
<https://doi.org/10.1002/pola.10944>.

<sup>42</sup> Bicak, N.; Karagoz, B.; Emre, D. Atom Transfer Graft Copolymerization of 2-Ethyl Hexylacrylate from Labile Chlorines of Poly(Vinyl Chloride) in an Aqueous Suspension. *J. Polym. Sci. Part A Polym. Chem.* **2006**, *44* (6), 1900–1907.  
<https://doi.org/10.1002/pola.21298>.

<sup>43</sup> Ahn, S. H.; Seo, J. A.; Kim, J. H.; Ko, Y.; Hong, S. U. Synthesis and Gas Permeation Properties of Amphiphilic Graft Copolymer Membranes. *J. Memb. Sci.* **2009**, *345* (1–2), 128–133. <https://doi.org/10.1016/j.memsci.2009.08.037>.

<sup>44</sup> Ahn, S. H.; Park, J. T.; Kim, J. H.; Ko, Y.; Hong, S. U. Nanocomposite Membranes Consisting of Poly(Vinyl Chloride) Graft Copolymer and Surface-Modified Silica Nanoparticles. *Macromol. Res.* **2011**, *19* (11), 1195–1201.  
<https://doi.org/10.1007/s13233-011-1116-1>.

<sup>45</sup> Koh, J. H.; Lee, K. J.; Seo, J. A.; Kim, J. H. Amphiphilic Polymer Electrolytes Consisting of PVC-g-POEM Comb-Like Copolymer and LiCF<sub>3</sub>SO<sub>3</sub>. *J. Polym. Sci. Part B Polym. Phys.* **2009**, *47* (15), 1443–1451. <https://doi.org/10.1002/polb.21745>.

<sup>46</sup> Roh, D. K.; Park, J. T.; Ahn, S. H.; Ahn, H.; Ryu, D. Y.; Kim, J. H. Amphiphilic Poly(Vinyl Chloride)-g-Poly(Oxyethylene Methacrylate) Graft Polymer Electrolytes: Interactions, Nanostructures and Applications to Dye-Sensitized Solar Cells. *Electrochim. Acta* **2010**, *55* (17), 4976–4981.  
<https://doi.org/10.1016/j.electacta.2010.03.106>.

- <sup>47</sup> Chi, W. S.; Kim, S. J.; Lee, S. J.; Bae, Y. S.; Kim, J. H. Enhanced Performance of Mixed-Matrix Membranes through a Graft Copolymer-Directed Interface and Interaction Tuning Approach. *ChemSusChem* **2015**, *8* (4), 650–658. <https://doi.org/10.1002/cssc.201402677>.
- <sup>48</sup> Seo, J. A.; Koh, J. K.; Koh, J. H.; Kim, J. H. Preparation and Characterization of Plasticized Poly(Vinyl Chloride)-*g*-Poly(Oxyethylene Methacrylate) Graft Copolymer Electrolyte Membranes. *Membr. J.* **2011**, *21* (3), 222–228. [https://doi.org/10.14579/membrane\\_journal.2011.21.3.222](https://doi.org/10.14579/membrane_journal.2011.21.3.222).
- <sup>49</sup> Chi, W. S.; Hong, S. U.; Jung, B.; Kang, S. W.; Kang, Y. S.; Kim, J. H. Synthesis, Structure and Gas Permeation of Polymerized Ionic Liquid Graft Copolymer Membranes. *J. Memb. Sci.* **2013**, *443*, 54–61. <https://doi.org/10.1016/j.memsci.2013.04.049>.
- <sup>50</sup> Fang, L.; Wang, N.; Zhou, M.; Zhu, B.; Zhu, L.; John, A. E. Poly(N,N-Dimethylaminoethyl Methacrylate) Grafted Poly(Vinyl Chloride)s Synthesized via ATRP Process and Their Membranes for Dye Separation. *Chinese J. Polym. Sci.* **2015**, *33* (11), 1491–1502. <https://doi.org/10.1007/s10118-015-1701-4>.
- <sup>51</sup> Matyjaszewski, K. Atom Transfer Radical Polymerization (ATRP): Current Status and Future Perspectives. *Macromolecules* **2012**, *45* (10), 4015–4039. <https://doi.org/10.1021/ma3001719>.
- <sup>52</sup> Liu, K.; Bao, Y. Synthesis of Poly(Vinyl Chloride)- Butyl Acrylate Graft Copolymer by ARGET ATRP Method. *CIESC J.* **2014**, *65* (8).

<sup>53</sup> Li, L.; Schneider, Y.; Hoeglund, A. B.; Braslau, R. Internal Plasticization of Poly(Vinyl Chloride) by Grafting Acrylate Copolymers via Copper-Mediated Atom Transfer Radical Polymerization. *J. Appl. Polym. Sci.* **2021**, *138* (31), 1–11. <https://doi.org/10.1002/app.50747>.

<sup>54</sup> Li, L.; Schneider, Y.; Hoeglund, A. B.; Braslau, R. Advances in Internal Plasticization of PVC: Copper-Mediated Atom-Transfer Radical Polymerization from PVC Defect Sites To Form Acrylate Graft Copolymers. *Synlett* **2021**, No. Scheme 1, 497–501. <https://doi.org/10.1055/s-0037-1610764>.

<sup>55</sup> Toma, M. A.; Najim, T. S.; Abdulhameed, Q. F. Synthesis and Characterization of Poly (Vinyl Chloride)-Graft-Poly (Ethyl Acrylate) and Its Membrane. *Al-Mustansiriyah J. Sci.* **2016**, *27* (1), 15–20.

<sup>56</sup> Coşkun, M.; Seven, P. Synthesis, Characterization and Investigation of Dielectric Properties of Two-Armed Graft Copolymers Prepared with Methyl Methacrylate and Styrene onto PVC Using Atom Transfer Radical Polymerization. *React. Funct. Polym.* **2011**, *71* (4), 395–401. <https://doi.org/10.1016/j.reactfunctpolym.2010.12.012>.

<sup>57</sup> Coşkun, M.; Barim, G.; Demirelli, K. A Grafting Study on Partially Dehydrochlorinated Poly(Vinyl Chloride) by Atom Transfer Radical Polymerization. *J. Macromol. Sci. Part A Pure Appl. Chem.* **2007**, *44* (5), 475–481. <https://doi.org/10.1080/10601320701229068>.

<sup>58</sup> Lanzalaco, S.; Galia, A.; Lazzano, F.; Mauro, R. R.; Scialdone, O. Utilization of Poly(Vinylchloride) and Poly(Vinylidene fluoride) as Macroinitiators for ATRP

Polymerization of Hydroxyethyl Methacrylate: Electroanalytical and Graft-Copolymerization Studies. *J. Polym. Sci. Part A Polym. Chem.* **2015**, *53* (21), 2524–2536. <https://doi.org/10.1002/pola.27717>.

<sup>59</sup> Patel, R.; Chi, W. S.; Ahn, S. H.; Park, C. H.; Lee, H. K.; Kim, J. H. Synthesis of Poly(Vinyl Chloride)-g-Poly(3-Sulfopropyl Methacrylate) Graft Copolymers and Their Use in Pressure Retarded Osmosis (PRO) Membranes. *Chem. Eng. J.* **2014**, *247*, 1–8. <https://doi.org/10.1016/j.cej.2014.02.106>.

<sup>60</sup> Abbasian, M.; Entezami, A. A. Metal-Catalyzed Living Radical Graft Copolymerization of Styrene Initiated from Arylated Poly(Vinyl Chloride). *Iran. Polym. J. (English Ed.)* **2006**, *15* (5), 395–404.

<sup>61</sup> Abbasian, M.; Entezami, A. A. Nitroxide Mediated Living Radical Polymerization of Styrene onto Poly (Vinyl Chloride). *Polym. Adv. Technol.* **2007**, *18* (4), 306–312. <https://doi.org/10.1002/pat.886>.

<sup>62</sup> Koh, J. H.; Seo, J. A.; Koh, J. K.; Kim, J. H. Self-Assembled Structures of Hydrogen-Bonded Poly(Vinyl Chloride-g-4-Vinyl Pyridine) Graft Copolymers. *Nanotechnology* **2010**, *21* (35). <https://doi.org/10.1088/0957-4484/21/35/355604>.

## 2 Relative Rates of Metal-Free Azide Alkyne Cycloadditions

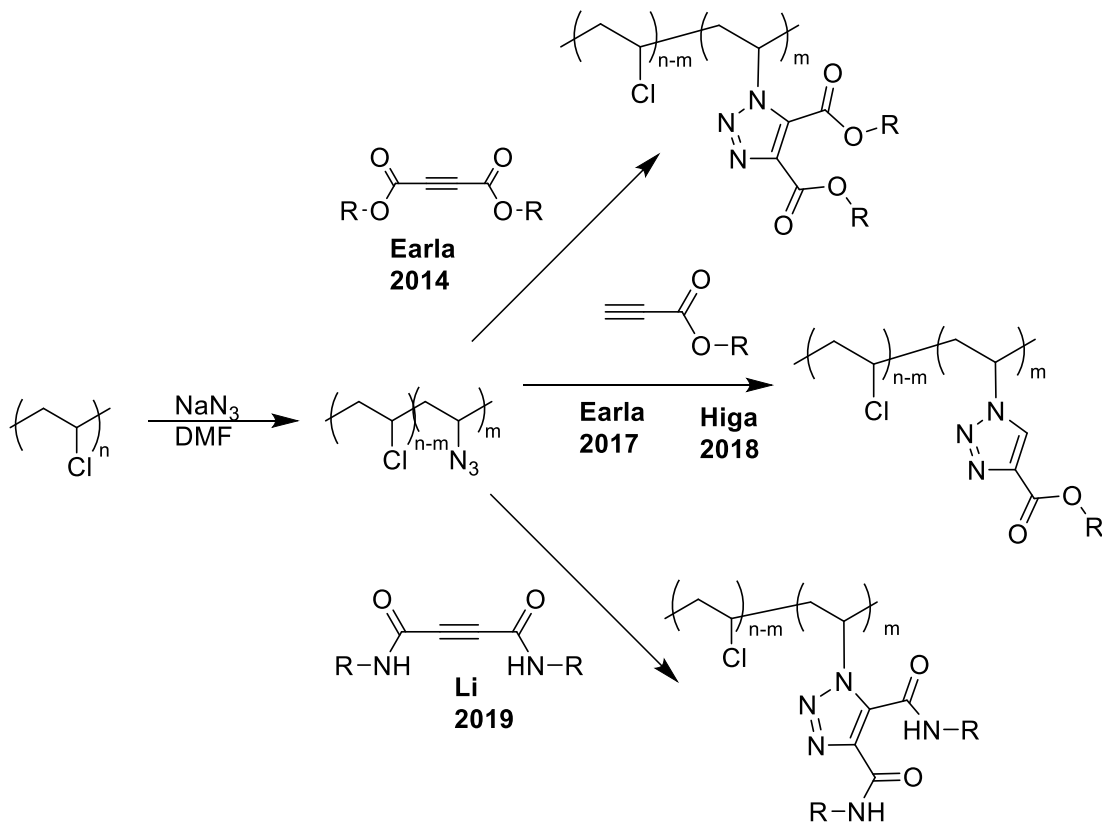
This paper was published.<sup>1</sup> Skelly, P. W.; Sae-Jew, J.; Kitos Vasconcelos, A. P.; Tasnim, J.; Li, L.; Raskatov, J. A.; Braslau, R. Relative Rates of Metal-Free Azide-Alkyne Cycloadditions: Tunability over 3 Orders of Magnitude. *J. Org. Chem.* **2019**, *84*, 13615–13623. <https://doi.org/10.1021/acs.joc.9b01887>. I was primarily responsible for the paper. Longbo Li and Jerin Tasnim synthesized several of the starting alkynes and Longbo helped synthesize the secondary azide. Jirapon Sae-Jew and Ana Paula Kitos Vasconcelos were undergraduate students under my guidance who helped me perform many of the competition experiments.

### 2.1 Background

Our lab has used the metal-free azide-alkyne cycloaddition reaction in several different instances to attach plasticizing groups to the PVC backbone.<sup>2,3,4,5</sup> The non-basic nucleophilicity of the azide anion helps prevent competing elimination of PVC. The ability to perform the cycloaddition reaction without metal is important if we are to replace the plasticizers used in medical-grade PVC, where metal contamination is not tolerated. A project by another student in the lab, Jerin Tasnim, aimed to modify the surface of PVC medical tubing. Treating the surface without degrading or dissolving the PVC requires mild reaction conditions in addition to the metal-free requirement. In order to perform this reaction in the absence of metal, alkynes containing electron-withdrawing groups must be used. Previous projects used alkyne esters,<sup>2,3</sup> alkyne diesters<sup>3,4</sup>, and alkyne diamides<sup>5</sup> (**Scheme 2.1**) We wanted to quantify



the effect that these electron-withdrawing different groups have in order to inform the future design of plasticizers and other functionalizations that could be applied to PVC.



**Scheme 2.1** Use of electron-poor alkynes in our lab for plasticization of PVC

In addition to applications to PVC, this metal-free reaction is used in other areas such as polymer functionalization,<sup>6</sup> crosslinking to form hydrogels,<sup>7</sup> synthesis of conjugated polymers,<sup>8</sup> and DNA tagging and immobilization.<sup>9</sup> Bioconjugation methods tend to employ strained cyclooctynes due to their greater reactivity and selectivity.<sup>10</sup> However, expanding the suite of available electron-deficient alkynes could allow linear electron-poor alkynes to compete with the more synthetically challenging cyclooctynes in bioconjugation. Further understanding the role of electron withdrawing groups in this reaction could benefit these applications.

## 2.2 Synthesis of electron-poor alkynes

Several electron-poor alkynes were already in use by our lab. To investigate a spectrum of reactivities, several more were synthesized.

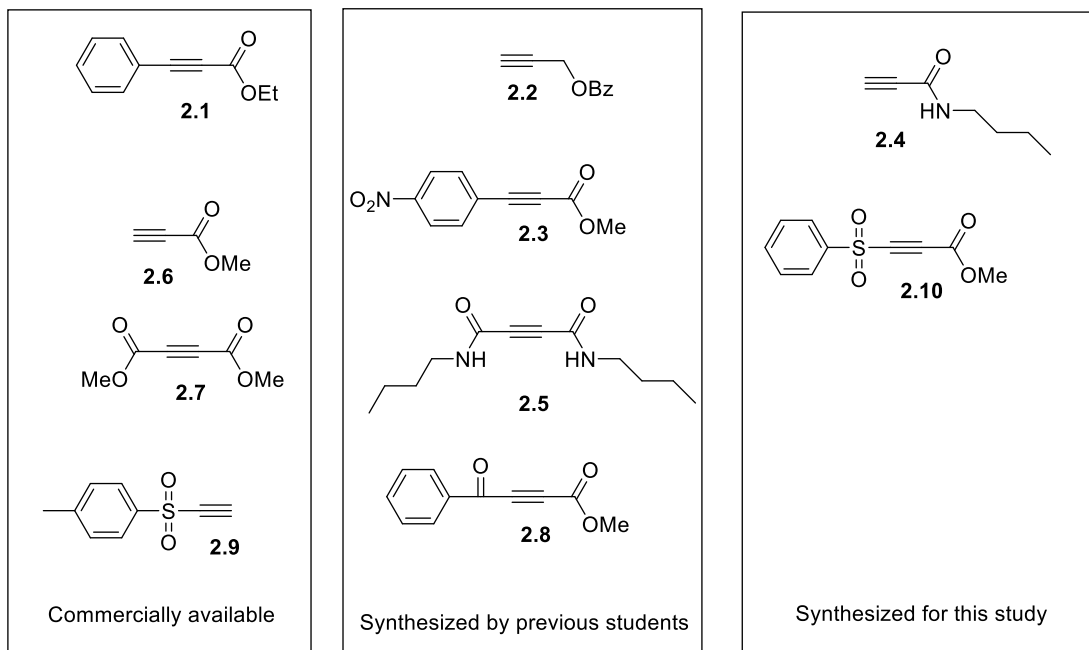
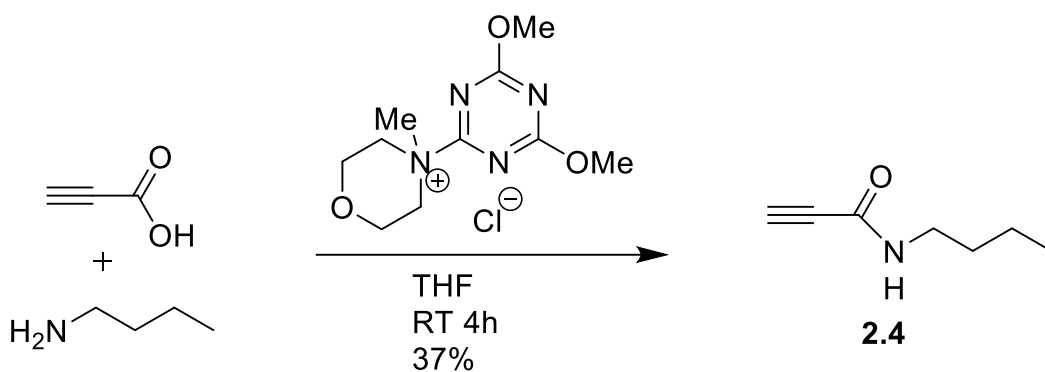


**Figure 2.1** Sources of alkynes used in this chapter

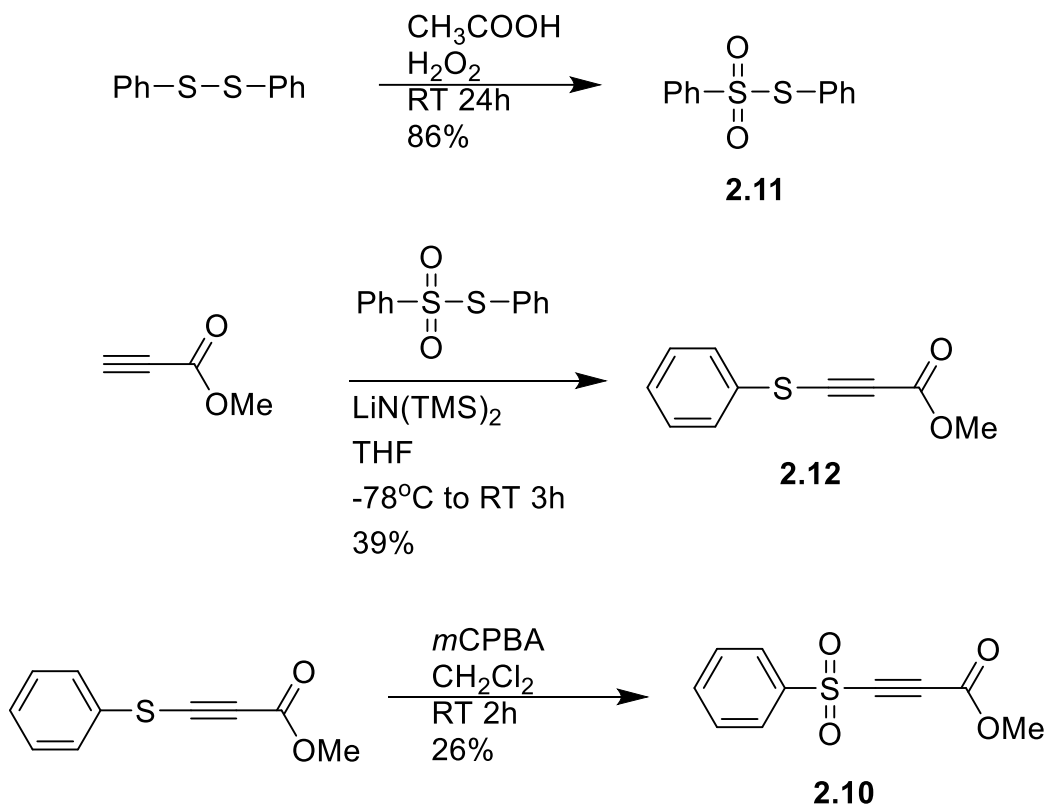
*N*-butylpropiolamide was synthesized using the coupling reagent 4-(4,6-dimethoxy-1,3,5-triazin-2-yl)-4-methylmorpholinium chloride (DMTMM) (**Scheme 2.2**).<sup>11</sup>



**Scheme 2.2** Synthesis of *N*-butylpropiolamide (**2.4**)

The sulfone-bearing alkyne was synthesized using the procedure of Takeda.<sup>12</sup> First, diphenyl disulfone was oxidized with hydrogen peroxide and acetic acid to form diphenyl thiosulfate **2.11** (**Scheme 2.3**). The structure was confirmed by <sup>13</sup>C NMR. Next, methyl propiolate was deprotonated using lithium bis-(trimethylsilyl)-amide, and

diphenyl thiosulfate was added, producing the thioether-substituted alkyne **2.12**. This was oxidized using *m*-CPBA to produce the sulfone **2.10**.



**Scheme 2.3** Synthesis of methyl 3-(phenylsulfonyl)-2-propynoate (**2.10**)

Alkynes bearing other electron-withdrawing groups were considered, but ultimately decided against. Nitroalkynes tend to be explosive.<sup>13</sup> Alkynes with two sulfone substituents decompose within hours at room temperature.<sup>14</sup> Nitrile-substituted alkynes may undergo competing tetrazole formation from a reaction between the azide and the nitrile instead of the alkyne.<sup>15</sup> The synthesis of trifluoromethylalkynes requires expensive reagents.<sup>16</sup> Ynammonium salts<sup>17,18</sup> remain an interesting option due to the

electron-withdrawing nature of the ammonium group,<sup>19</sup> but were ultimately not investigated in this study.

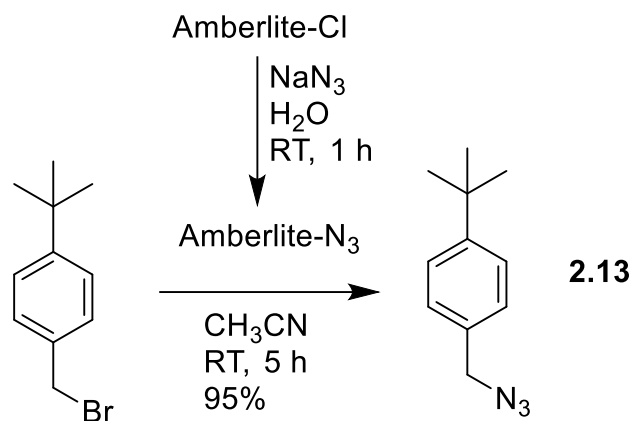
### 2.3 Synthesis of a Primary Benzylic Azide

Tert-butylbenzyl azide was selected as the azide partner for competition experiments for three reasons. First, it can be synthesized in one step from the corresponding bromide. Second, it satisfies the safety requirements for small organic azides: to prevent the compounds from being explosive, the number of carbons and oxygens must exceed three times the number of nitrogens (**Equation 2.1**).<sup>20</sup>

$$\frac{N_C + N_O}{N_N} \geq 3 \quad \text{Equation 2.1}$$

Where  $N_C$ ,  $N_O$ , and  $N_N$  are the number of carbon, oxygen and nitrogen atoms respectively in the molecule. For *t*-butylbenzyl azide,  $N_C=11$ ,  $N_O=0$ , and  $N_N=3$ , giving a value of  $3.66 \geq 3$ . Third, the phenyl ring allows it to absorb UV light, facilitating detection on TLC and column chromatography.

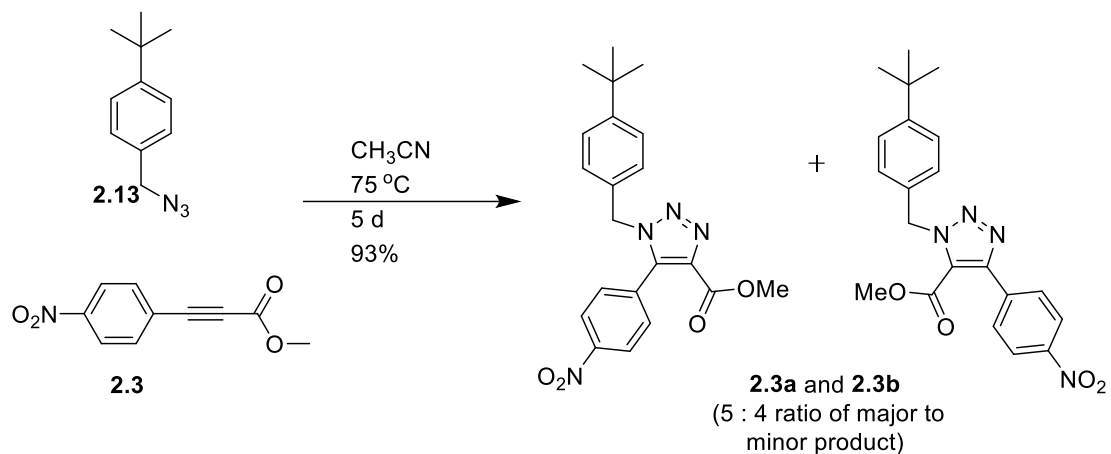
*T*-butylbenzyl azide **2.13** was synthesized using the procedure of Li.<sup>5</sup> First, amberlite IRA-400 was charged with azide using sodium azide in water. This resin allows the azidation step to occur in organic solvent and excess azide to be filtered off easily.<sup>21</sup> Then the charged amberlite was added to *t*-butylbenzyl bromide in acetonitrile to produce the azide. NMR Spectra for the azide match the literature.<sup>22</sup>



**Scheme 2.4** Synthesis of *t*-butylbenzyl azide

#### 2.4 Synthesis of Authentic Triazoles for Identification by NMR

Authentic triazoles were prepared by combining the corresponding alkyne with a slight excess of **2.13** in CH<sub>3</sub>CN at 75 °C until the disappearance of the alkyne by TLC (1 h to 14 d, depending on the reactivity of the alkyne). The two regioisomers formed were separated by column chromatography except in the cases of **2.2** and **2.4** which produced inseparable mixtures of isomers. In general, the triazole product of alkyne **2.1** is designated as **2.1a**, with the other regioisomer **2.1b** when applicable. All triazoles were characterized by <sup>1</sup>H NMR, <sup>13</sup>C NMR and DEPT 135, IR, and HRMS.



**Scheme 2.5** Preparation of authentic triazoles **2.3a** and **2.3b**

### 2.5 NOE experiment

To determine the regiochemistry, **2.8a** was investigated by a 1D-NOE experiment (**Figure 2.2**). The molecule was irradiated at the benzylic position (c), which should cause through-space enhancement of the ester peak (b) if it were structure **2.8b**, and enhancement of the aromatic peaks (g) near the ketone if it were structure **2.8a**. Enhancement at g and lack of enhancement at the b confirmed structure **2.8a**. Because the regioselectivity of the reaction was not the focus of this paper, it was decided it was not worth the cost to repeat this experiment on all remaining triazoles.

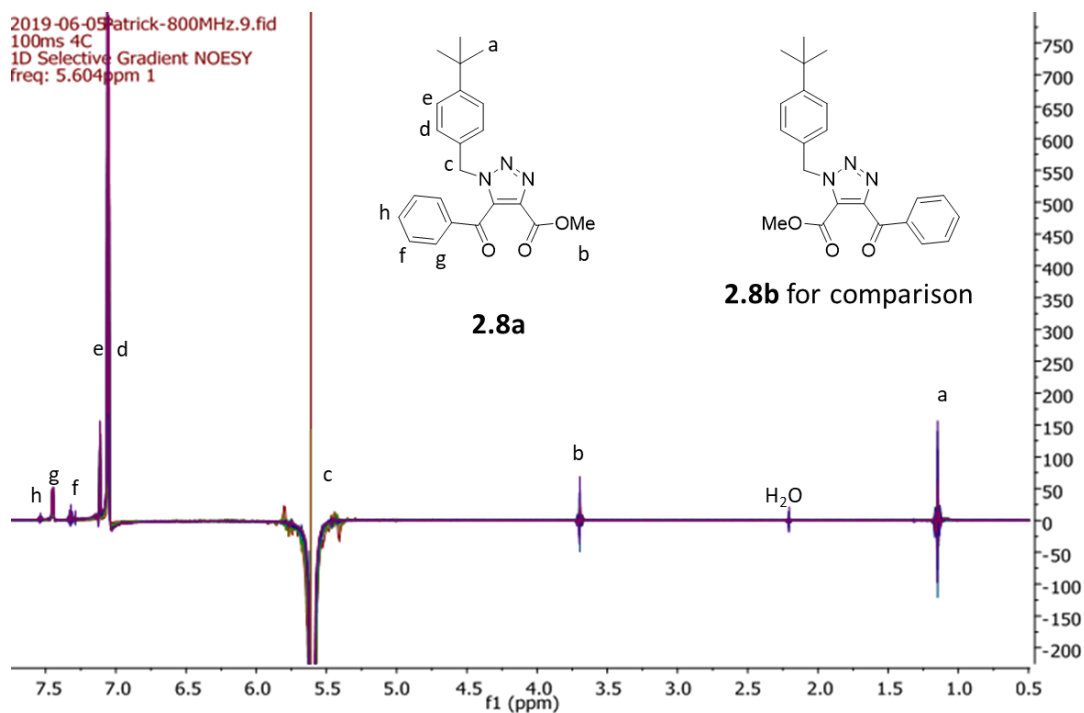


**Figure 2.2** NOESY experiment on triazole **2.8a**. Irradiation at proton c leads to enhancement at protons d, e, and g, consistent with the structure of **2.8a** shown. The lack of enhancement at proton b helps reject the structure **2.8b**.

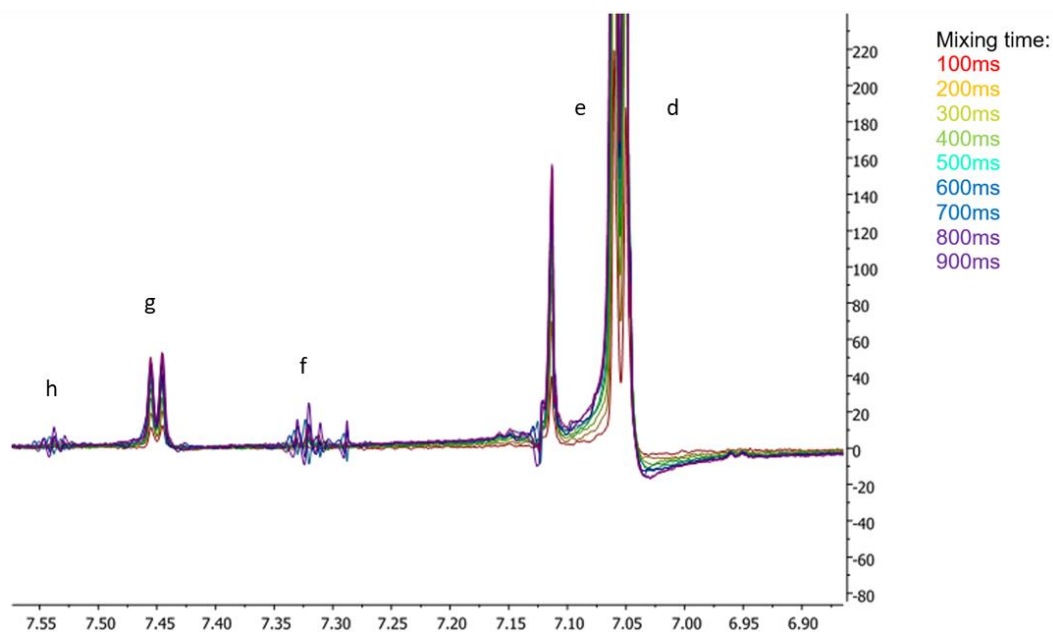


**Figure 2.3** Expansion of the aromatic region of **Figure 2.2** showing enhancement of peak g



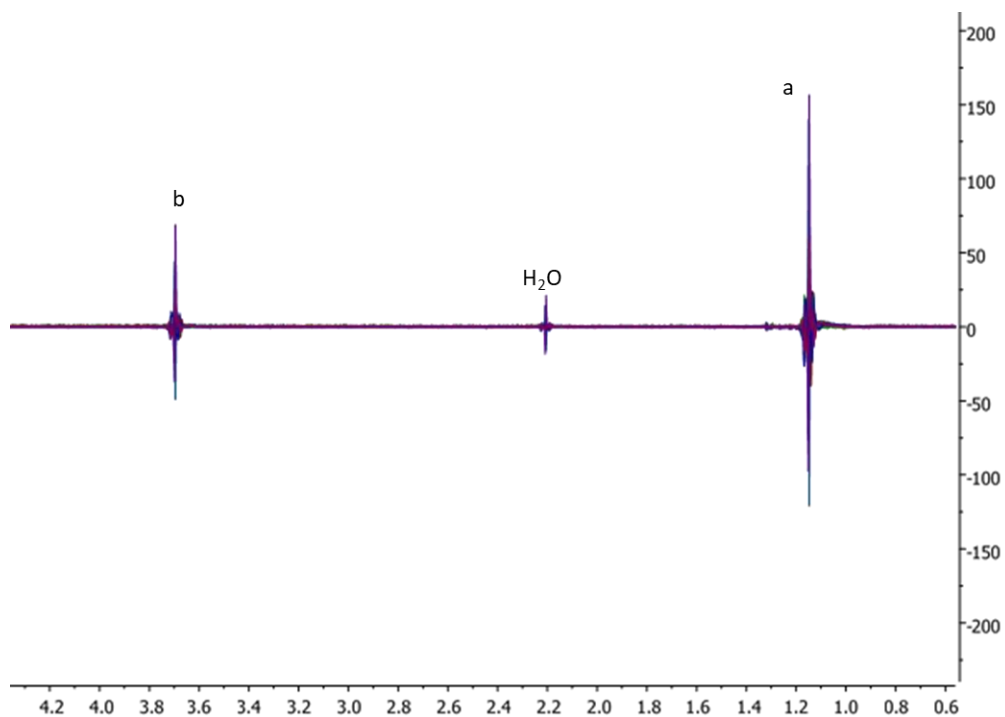
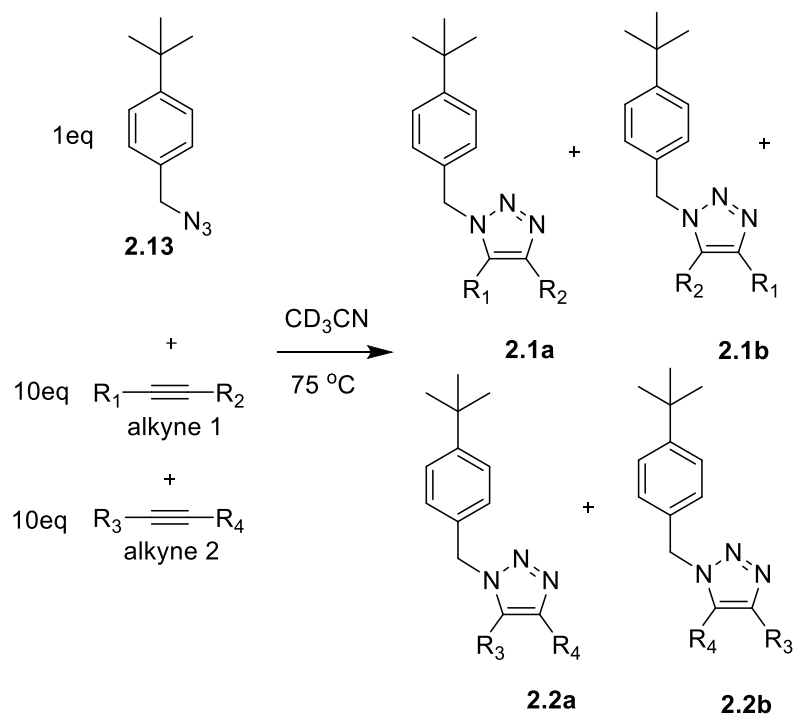


**Figure 2.4** Expansion of the upfield region of **Figure 2.2** showing lack of enhancement at peak b

## 2.6 Competition Experiments Using a Primary Benzylic Azide

To compare the relative rates of the cycloaddition reaction, alkynes with similar expected rates were selected pairwise and heated to 75 °C in CD<sub>3</sub>CN in an NMR tube with a limiting amount of 4-*t*-butylbenzyl azide. CD<sub>3</sub>CN was chosen for its higher boiling point compared to CDCl<sub>3</sub>, allowing for higher reaction temperatures. These pairings had to be changed a few times because the actual rates were not as expected.



**Scheme 2.6** General scheme of competition experiments using *t*-butylbenzyl azide

The metal-free azide-alkyne cycloaddition follows the second-order kinetics shown in **Equation 2.2**. The ratio of product formation for two competing alkynes is then shown in **Equation 2.3**.

$$\frac{d[\mathbf{1}]}{dt} = k_1[\mathbf{A1}][\mathbf{1}] \quad \text{Equation 2.2}$$

$$\frac{\frac{d[\mathbf{T1}]}{dt}}{\frac{d[\mathbf{T2}]}{dt}} = \frac{k_1[\mathbf{A1}][\mathbf{1}]}{k_2[\mathbf{A1}][\mathbf{2}]} \quad \text{Equation 2.3}$$

Where **A1** is *t*-butylbenzyl azide **2.13**, **1** and **2** are two different alkynes, and **T1** and **T2** are the two triazole products formed from those alkynes. In cases where one alkyne can produce two regioisomers, [**T1**] is defined as [**T1a**] + [**T1b**].

A 1 : 10 : 10 ratio of azide : alkyne 1 : alkyne 2 was chosen to create pseudo-first order conditions. This allows us to substitute the concentrations of alkynes with their initial concentrations (**Equation 2.4**). The ratio of rates is then constant, which allows us to use **Equation 2.5**.

$$\frac{\frac{d[\mathbf{T1}]}{dt}}{\frac{d[\mathbf{T2}]}{dt}} = \frac{k_1[\mathbf{A1}][\mathbf{1}]_0}{k_2[\mathbf{A1}][\mathbf{2}]_0} \quad \text{Equation 2.4}$$

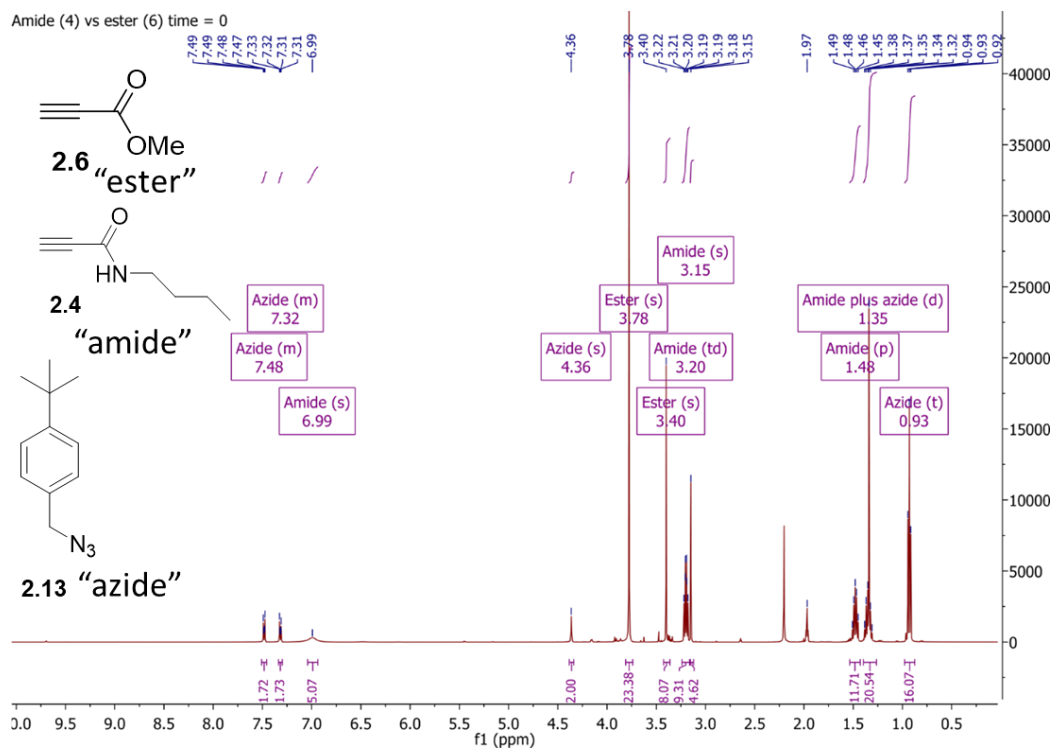
$$\frac{[\mathbf{T1}]_{final}}{[\mathbf{T2}]_{final}} = \frac{k_1[\mathbf{1}]_0}{k_2[\mathbf{2}]_0} \quad \text{Equation 2.5}$$

Although efforts were made to keep the initial molar ratio to 1 : 10 : 10, the NMR at t=0 often revealed a different starting ratio due to errors in weighing the reactants out. This was corrected for by dividing the ratio of final products by the initial ratio of starting materials to get the ratio of rates (**Equation 2.6**).

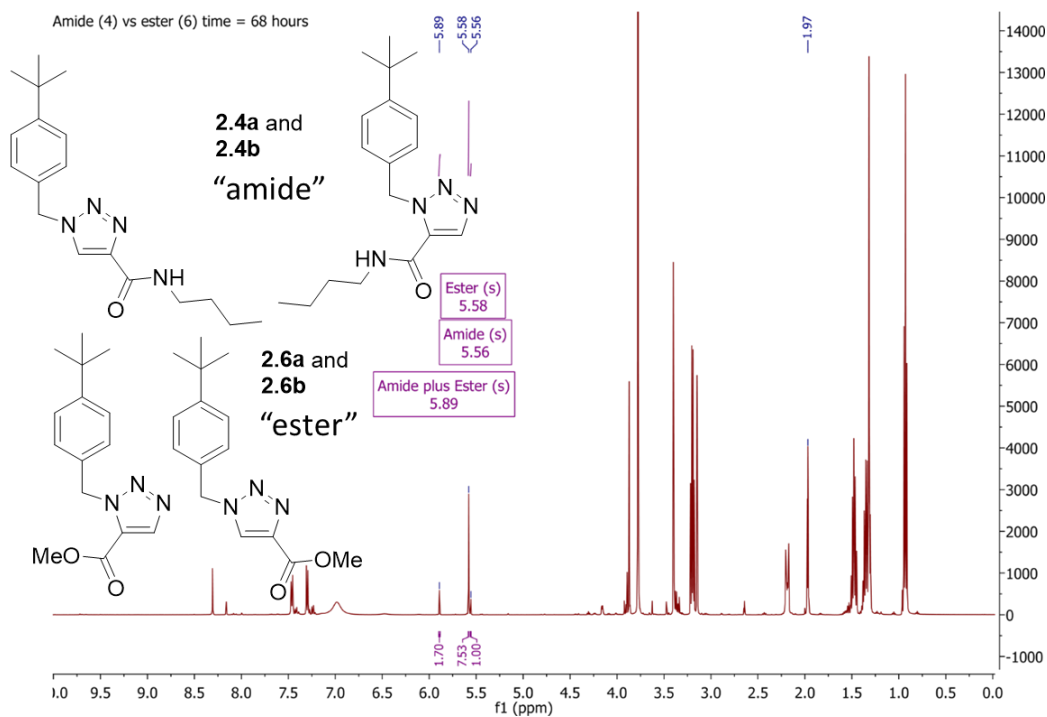
$$\frac{k_1}{k_2} = \frac{[\mathbf{T1}]_{final}}{[\mathbf{T2}]_{final}} \times \frac{[\mathbf{2}]_0}{[\mathbf{1}]_0} \quad \text{Equation 2.6}$$

An example competition experiment is shown in **Figure 2.5** and **Figure 2.6**. The initial ratio of azide : ester : amide was 1.0 : 7.8 : 4.7, based on integrations of azide  $\text{CH}_2\text{Ar}$  ( $\delta = 4.36$ ,  $I = 2.00$ ), ester  $\text{OCH}_3$  ( $\delta = 3.78$ ,  $I = 23.38$ ), and amide  $\text{CH}_2\text{NH}$  ( $\delta = 3.23$ ,  $I = 9.31$ ). The ratio of products was ester : diamide 5.9 : 1.0, based on integrations of the benzylic protons of **T4a** ( $\delta = 5.56$ ,  $I = 1.00$ ), **T6a** plus **T4b** ( $\delta = 5.89$ ,  $I = 1.70$ , overlap), and **T6b** ( $\delta = 5.58$ ,  $I = 5.89$ ). Overlap was resolved by assuming the ratio of **T6b** : **T6a** 1 : 0.16 and **T4a** : **T4b** 0.43, which was consistently found in other

competitions involving **4** or **6** After dividing by the initial concentrations, the rate ratio was ester : diamide 3.5 : 1.0.



**Figure 2.5** Competition experiment between **2.4** and **2.6** at  $t = 0$

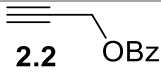
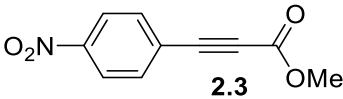
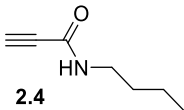
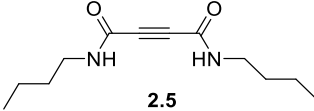
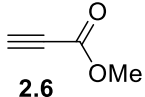
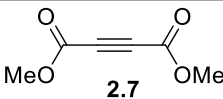
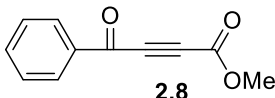
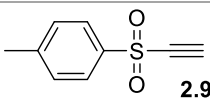
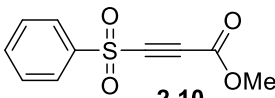


**Figure 2.6** Competition experiment between **2.4** and **2.6** at  $t = 68$  h

Each competition experiment was done in duplicate, and the average of the product ratios, corrected for initial ratios, was used to construct the relative rate scale shown in **Table 2.1**. The relative rate of alkyne **2.1** is defined as 1.0. Other rates were found by sequentially multiplying: for example, amide **2.4** reacted 6.3x faster than benzoyl **2.2**, which reacted 1.4x faster than **2.1**, giving amide **2.4** a relative rate of  $6.3 \times 1.4 = 8.8$ .

**Table 2.1** Results of competition experiments with t-butylbenzyl azide (**2.13**)

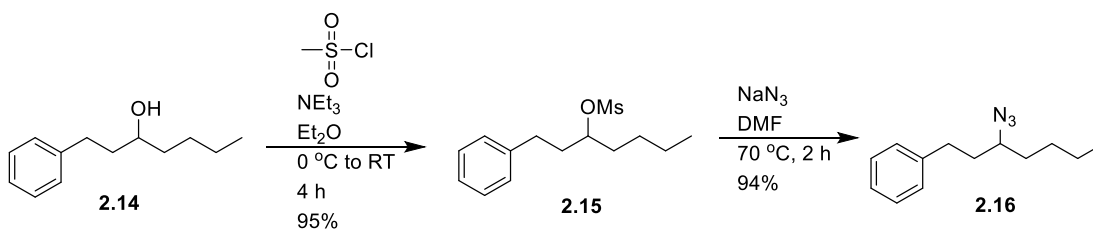
Alkyne	Relative rate
<p><b>2.1</b></p>	1.0

 <p style="text-align: center;"><b>2.2</b></p>	1.4
 <p style="text-align: center;"><b>2.3</b></p>	3.7
 <p style="text-align: center;"><b>2.4</b></p>	8.8
 <p style="text-align: center;"><b>2.5</b></p>	15
 <p style="text-align: center;"><b>2.6</b></p>	25
 <p style="text-align: center;"><b>2.7</b></p>	130
 <p style="text-align: center;"><b>2.8</b></p>	150
 <p style="text-align: center;"><b>2.9</b></p>	340
 <p style="text-align: center;"><b>2.10</b></p>	2100

Most of the results were consistent with the expected trend: stronger electron-withdrawing groups lead to more reactive alkynes, but with notable exceptions. The two alkynes that did not match expectations were the aryl-substituted alkynes **2.1** and **2.3**. Although the nitrophenyl group in **2.3** is expected to be electron-withdrawing, it did not outcompete the mono-ester **2.6**, which has a hydrogen in place of the nitrophenyl group. The low reactivity of the phenyl-substituted alkyne **2.1** was the most surprising: the phenyl ring seems to overwhelm the electron-withdrawing effect of the ester, making it slower than the completely unactivated alkyne **2.2**.

## 2.7 Competition Experiments Using a Non-benzylic Secondary Azide

To investigate azide scope, selected alkynes were also reacted with a secondary alkyl azide, 3-azido-1-phenylheptane. This azide was prepared using a modified procedure of Earla.<sup>4</sup> First, the corresponding alcohol **2.14** was mesylated using methanesulfonyl chloride and triethylamine in diethyl ether (**Scheme 2.7**). The mesylate **2.15** was then added to sodium azide in DMF at 70 °C to create the azide **2.16**.



**Scheme 2.7** Synthesis of 3-azido-1-phenylheptane (**2.16**)

Authentic triazoles were prepared for four of the alkynes studied, covering a range from the fastest (**2.10**) to the third-slowest (**2.3**). Three pairs of alkynes out of those four were used in three competition experiments with the new azide. The relative rates are similar to those found with *t*-butylbenzyl azide (**Table 2.2**), indicating general applicability of the results to other azides.

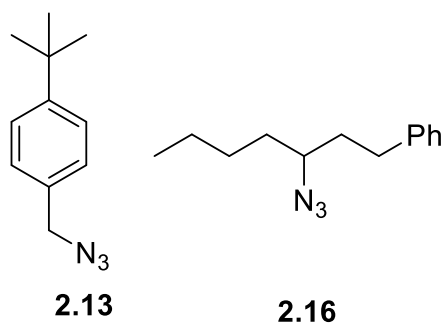


**Figure 2.7** Comparison of azides used in this experiment

**Table 2.2** Results of competition experiments with 3-azido-1-phenylheptane (**2.16**)

Alkyne pair	Ratio with 1° benzylic azide <b>2.13</b>	Ratio with 2° alkyl azide <b>2.16</b>
<b>2.6 vs 2.3</b>	6.8 : 1.0	7.9 : 1.0
<b>2.7 vs 2.6</b>	5.2 : 1.0	5.6 : 1.0
<b>2.10 vs 2.7</b>	16.3 : 1	24.4 : 1.0

[a] Unsymmetrical alkynes form two regioisomeric products **a** and **b**; for simplicity, the overall relative rates are defined by the sum of both regioisomers formed from each alkyne.

## 2.8 Time-dependent Competition Experiment

The competition reaction between nitrophenyl alkyne **2.3** and acetylene diamide **2.5** was monitored over time, confirming that the product ratio did not change



as a function of conversion. Based on this result, all other product ratios were measured after all of the azide had been consumed.

**Table 2.3** Competition experiment between two alkynes monitored at various time points

Time (h)	% azide consumed	Ratio of products
0.5	8.6	5.0 : 1.0
2	29	4.8 : 1.0
15	93	4.8 : 1.0
42	100	4.8 : 1.0

## 2.9 DFT Calculations

In order to better understand these results, the starting materials, transition states, and products of each reaction with t-butylbenzyl azide were modeled using the B3LYP functional and the 6-31G\* basis set in Gaussian 09.<sup>23</sup>

Ground state geometry optimizations were performed. Energy minima were confirmed by lack of imaginary frequencies. Geometry scans were then performed bringing the two C atoms of the alkyne closer to the N atoms of the azide; the highest energy of this scan was used as a starting point to find the transition state. Transition states were confirmed as having one imaginary frequency. Energies were corrected for zero-point energies. The solvent was simulated using the polarizable continuum model (acetonitrile,  $\epsilon = 35.688$ ). An example of the calculated geometries is shown in **Figure 2.8**.

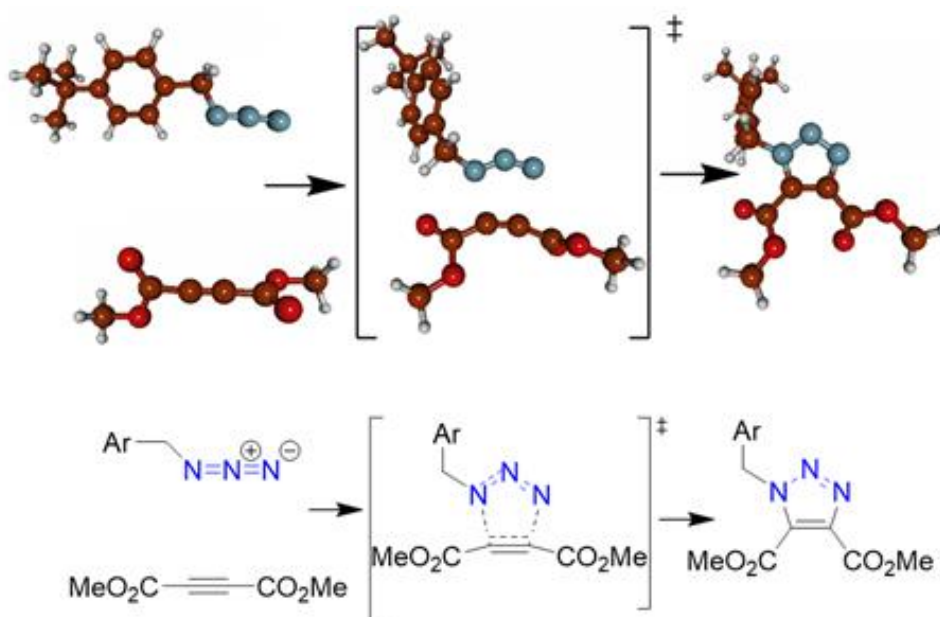


**Figure 2.8** Calculated geometries for the starting materials, transition state, and product of the reaction between *t*-butylbenzyl azide and dimethyl acetylenedicarboxylate

### 2.9.1 Activation Energies

The calculated activation energies for each reaction show a good correlation with the log of the relative rates determined experimentally. This gave us confidence that the computational level used is accurate enough that we can use it to get other insights into the reaction.

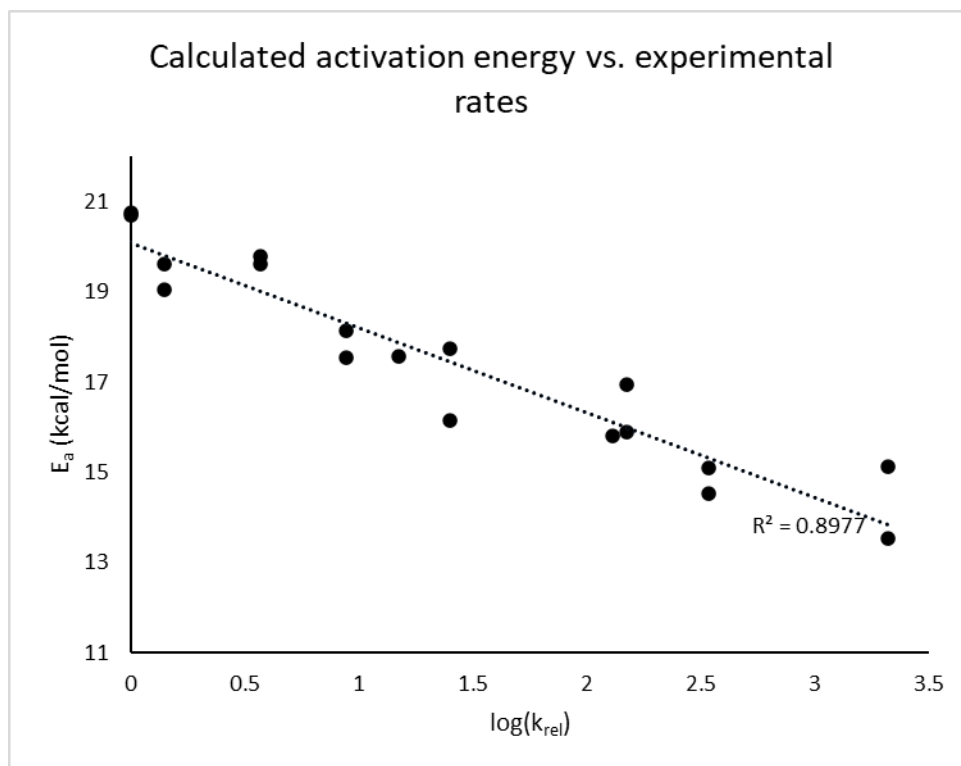


**Figure 2.9** Correlation between the activation energies computed by DFT and the log<sub>10</sub> of the relative rates determined by the competition experiments

### 2.9.2 HOMO-LUMO Gap

The Highest Occupied Molecular Orbital (HOMO) and Lowest Unoccupied Molecular Orbital (LUMO) were calculated for the azide and each alkyne. This reaction is governed by the interaction between the HOMO of the azide and the LUMO of the alkyne.<sup>6,24</sup> Calculated energies were consistent with this; in all cases, the HOMO (azide) - LUMO (alkyne) gap was smaller than the HOMO (alkyne) - LUMO (azide) gap ( **Figure 2.10**).

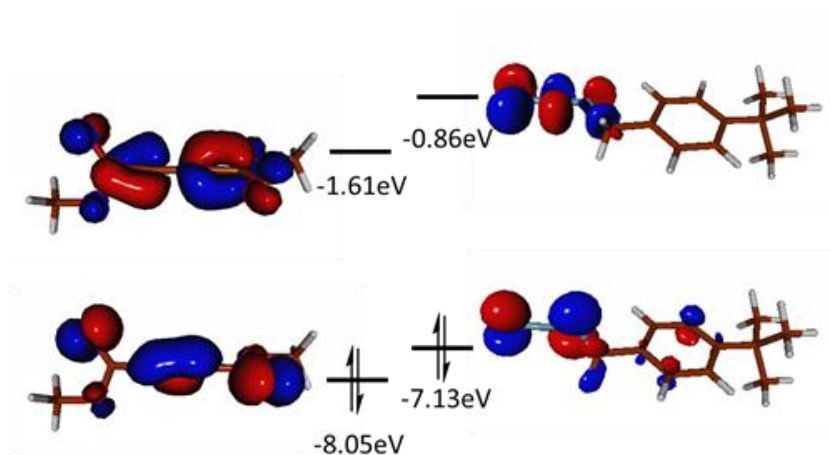


**Figure 2.10** HOMO and LUMO of dimethyl acetylenedicarboxylate (**2.7**) and 4-t-butylbenzyl azide (**2.13**)

It was expected that the size of this energy gap would explain the relative rates of the reaction. A correlation was observed, with the notable exception of the phenyl- and nitrophenyl-substituted alkynes, which were calculated to have a low LUMO but reacted quite slowly.

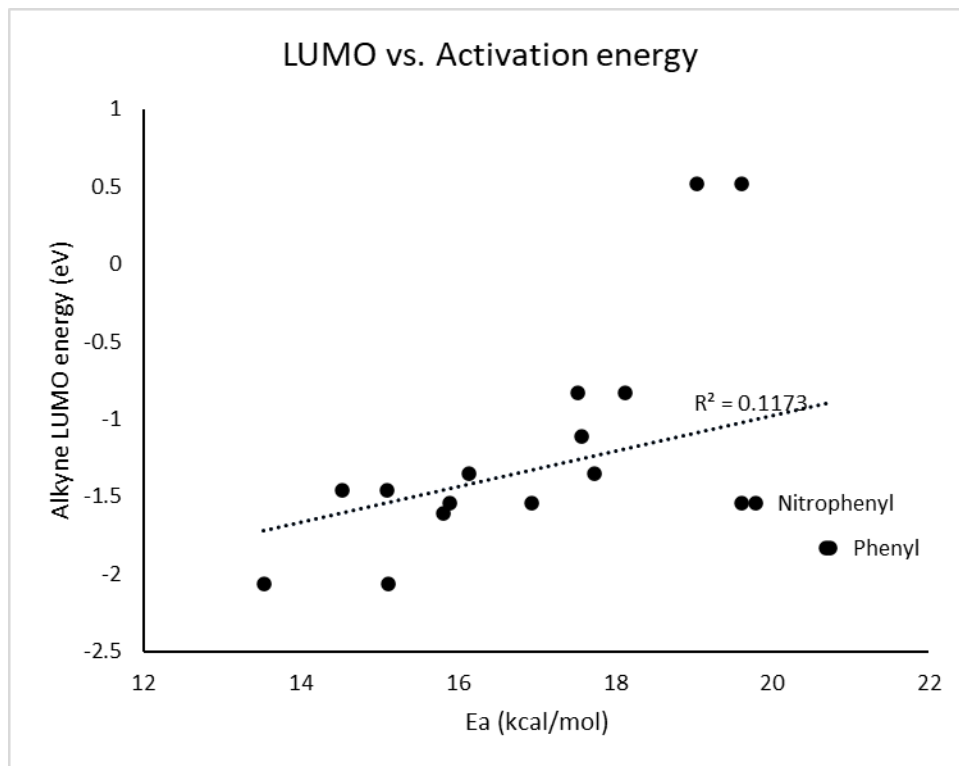


**Figure 2.11** Energy of the LUMO plotted against the calculated activation energy.  $R^2$  without the phenyl and nitrophenyl points was 0.735

### 2.9.3 Distortion-Interaction Method

The distortion-interaction model separates the transition state energy into the energetic penalty of deforming each reactant into its transition state conformation (distortion energy), and the stabilization of that geometry caused by the two reagents' proximity (interaction energy).<sup>25</sup> This is not quite the same as separating sterics from electronics: for example a bond breaking contributes to distortion energy despite having little to do with sterics.<sup>26</sup>

The distortion energy of each reaction was calculated using a single-point calculation of each alkyne and each azide frozen in its transition state geometry. The interaction energy is the difference between the distortion energy and the transition state energy. The interaction energy of each reaction was roughly the same (**Figure 2.12**), while the distortion energy increased with a slope of about one vs the activation energy (**Figure 2.13**), similar to results found for other 1,3-dipolar cycloaddition reactions.<sup>25</sup> This means that the difference in reactivity across the different alkynes depends on the geometries the reactants are forced to adopt at the transition state. Note that this includes the distortion of both the alkyne and the azide. Although this method doesn't directly reveal the role of sterics, it is likely that sterics are a factor given the high reactivity of monosubstituted alkynes **2.4** and **2.6**.

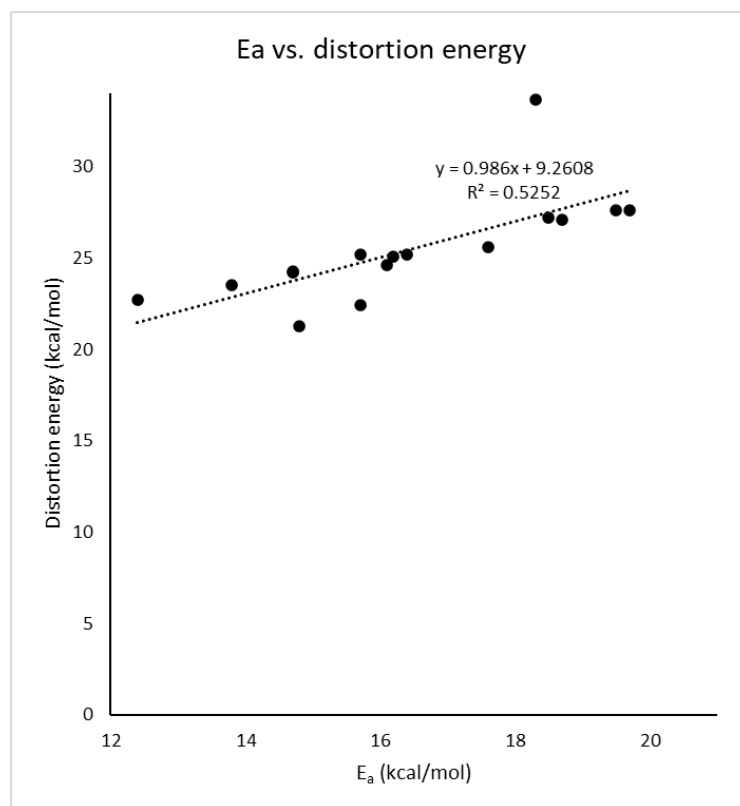


**Figure 2.12** Distortion energy vs. activation energy

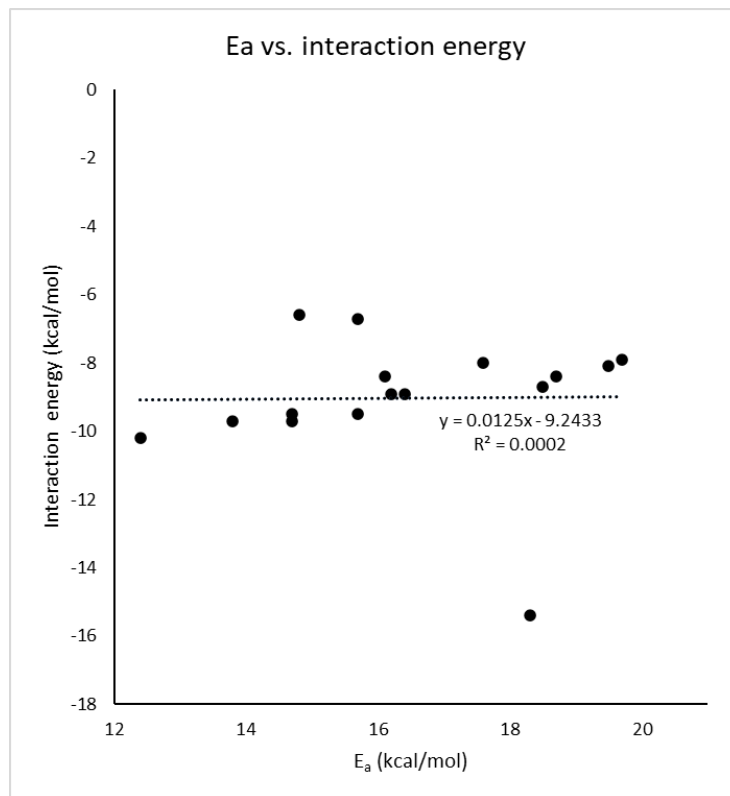


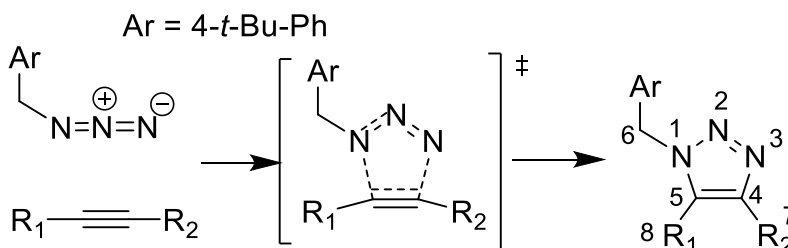
**Figure 2.13** Interaction energy vs. activation energy

#### 2.9.4 Wiberg Bond Indices

The Wiberg Bond Index<sup>27</sup> is a measure of the bond order between two atoms. A single bond would have a value of one; a conjugated double bond would have a value between one and two, depending on how much double bond character it has. It was hypothesized that the aryl-substituted alkynes had conjugation between the alkyne and the phenyl ring, but were forced out of conjugation at the transition state, causing an energetic penalty. This would be consistent with the results of Hosoya,<sup>28</sup> who found that phenyl azide is less reactive than a 2,6-disubstituted phenyl azide that cannot



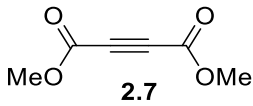
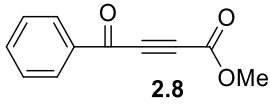
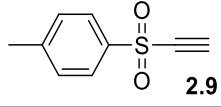
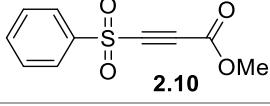
participate in aryl-azide resonance due to steric interactions. If so, the order of bond 5-8 and bond 4-6 (**Scheme 2.8**) would be greater than one in the starting material and decrease at the transition state. This was found to be the case. A decrease in bond order was also seen in other alkynes, but to a lesser extent. More reactive alkynes tended to have a smaller decrease in bond order, as shown in **Table 2.4** and **Figure 2.14**.



**Scheme 2.8** General reaction with atoms labeled. The bond order of bond 4-7 and bond 5-8 were used.

**Table 2.4** Activation energies, LUMO energies, and change in bond order

Alkyne	$E_a^{[a]}$ (kcal/mol)	Alkyne LUMO (eV)	Change in bond order <sup>[a,b]</sup>
 <b>2.1</b>	20.7	-1.83	-0.049
	20.7		-0.026
 <b>2.2</b>	19.6	0.52	-0.025
	19.0		-0.033
 <b>2.3</b>	19.6	-1.54	-0.039
	19.8		-0.034
 <b>2.4</b>	17.5	-0.83	-0.017
	18.1		-0.032
 <b>2.5</b>	17.6	-1.11	-0.025
 <b>2.6</b>	16.1	-1.35	+0.006
	17.7		-0.026

 2.7	15.8	-1.61	+0.004
 2.8	16.9	-1.54	-0.008
	15.9		+0.018
 2.9	14.5	-1.46	-0.001
	15.1		-0.019
 2.10	13.5	-2.06	+0.004
	15.1		-0.010

[a] Two energies and two bond orders are shown for unsymmetrical alkynes, referring to the two regioisomers formed. [b] Bond order is the sum of bonds between atoms 4-7 and 5-8, change in bond order is measured from the starting material to the transition state.

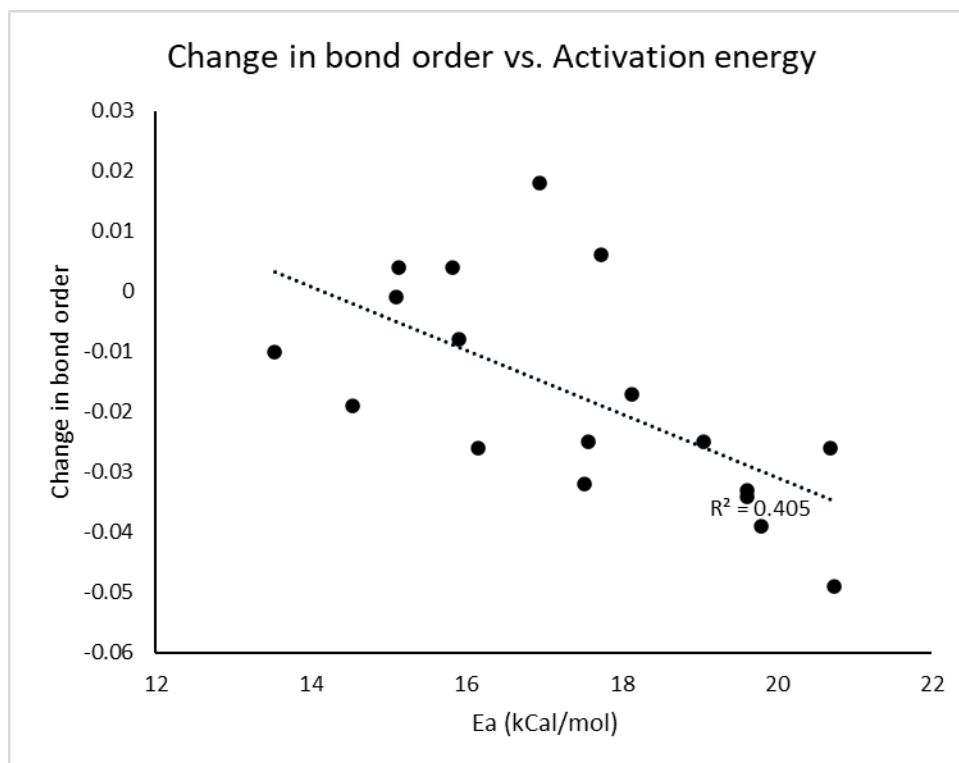
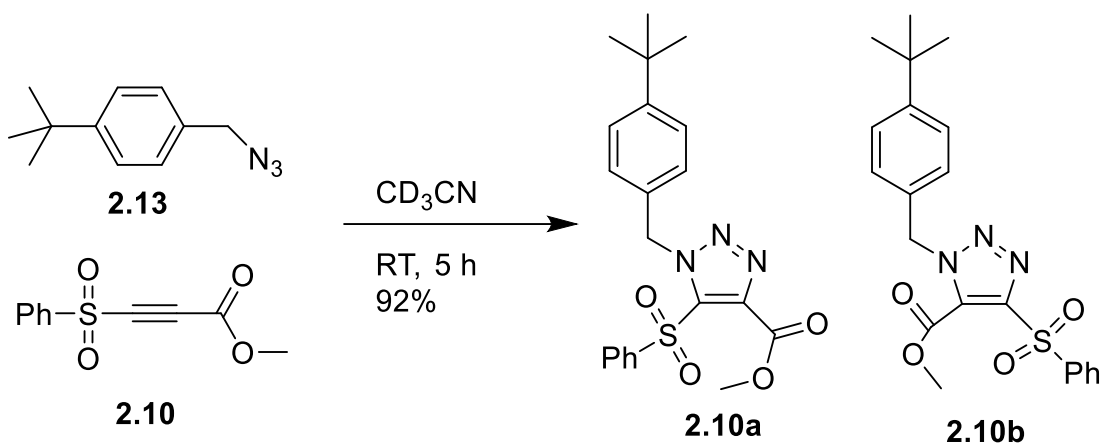


**Figure 2.14** Change in bond order vs activation energy. A negative y value represents a loss of conjugation

The change in bond order on its own is not a strong predictor of reactivity, but the aryl substituted alkynes are no longer anomalous. The change in bond order provides an explanation for the low reactivity of aryl substituted alkynes. The phenyl ring is conjugated to the alkyne at the ground state, but must lose conjugation due to the geometry of the transition state, where they can no longer act as electron-withdrawing groups.

## 2.10 Reaction at Room Temperature

Pleasingly, the sulfonyl, ester-substituted alkyne **2.10** reacts considerably faster than the commonly used diester alkyne **2.7**. As the cycloaddition with sulfonyl alkyne **2.10** is rapid, it was examined in a room temperature reaction with 4-*t*-butylbenzyl azide, reaching 92% completion in 5 hours (**Scheme 2.9**).



**Scheme 2.9** Room-temperature cycloaddition reaction using sulfonyl, ester-substituted alkyne **2.10**

## 2.11 Conclusion

Alkynes with various substituents were compared to determine their relative rates in reacting with a model azide to form a triazole ring. Electron-withdrawing

groups were found to enhance the rate of the metal-free azide-alkyne cycloaddition. However, aryl-substituted alkynes react slower than expected, probably due to a loss of conjugation at the transition state. DFT calculations support this explanation. The reactivity of ketone, ester substituted alkyne **2.8** did not differ much from that of the more commonly utilized diester **7**, but the sulfonyl, ester-substituted alkyne **2.10** reacts 16 times faster than the diester and 1500 times faster than unactivated alkyne **2.2**. Derivatives of this sulfonyl, ester alkyne may find large applicability for ligation under very mild conditions. These findings should also lead to the rational design of other highly reactive alkynes for the metal-free azide-alkyne cycloaddition.

For example, in our lab's work with plasticizers, alkynes with a single plasticizing side chain (similar in structure to monoester **2.6**) can be produced in a single step, while alkynes with two ester functionalities (similar to diester **2.7**) require a longer synthesis with protecting groups.<sup>3</sup> Knowing that the reactivity difference between these two is only five-fold allows us to more confidently choose the simpler mono-ester. The knowledge that the nitrophenyl group decreases reactivity allowed it to be ruled out as an activator when designing alkynes to react at mild conditions.

## 2.12 References

<sup>1</sup> Skelly, P. W.; Sae-Jew, J.; Kitos Vasconcelos, A. P.; Tasnim, J.; Li, L.; Raskatov, J. A.; Braslau, R. Relative Rates of Metal-Free Azide-Alkyne Cycloadditions: Tunability over 3 Orders of Magnitude. *J. Org. Chem.* **2019**, *84*, 13615–13623. <https://doi.org/10.1021/acs.joc.9b01887>.

<sup>2</sup> Earla, A.; Li, L.; Costanzo, P.; Braslau, R. Phthalate Plasticizers Covalently Linked to PVC via Copper-Free or Copper Catalyzed Azide-Alkyne Cycloadditions. *Polymer (Guildf)*. **2017**, *109*, 1–12. <https://doi.org/10.1016/j.polymer.2016.12.014>.

<sup>3</sup> Higa, C. M.; Tek, A. T.; Wojtecki, R. J.; Braslau, R. Nonmigratory Internal Plasticization of Poly(Vinyl Chloride) via Pendant Triazoles Bearing Alkyl or Polyether Esters. *J. Polym. Sci. Part A Polym. Chem.* **2018**, *56* (21), 2397–2411. <https://doi.org/10.1002/pola.29205>.

<sup>4</sup> Earla, A.; Braslau, R. Covalently Linked Plasticizers: Triazole Analogues of Phthalate Plasticizers Prepared by Mild Copper-Free “Click” Reactions with Azide-Functionalized PVC. *Macromol. Rapid Commun.* **2014**, *35* (6), 666–671. <https://doi.org/10.1002/marc.201300865>.

<sup>5</sup> Li, L.; Tek, A. T.; Wojtecki, R. J.; Braslau, R. Internal Plasticization of Poly(Vinyl Chloride) Using Glutamic Acid as a Branched Linker to Incorporate Four Plasticizers per Anchor Point. *J. Polym. Sci. Part A Polym. Chem.* **2019**, *57* (17), 1821–1835. <https://doi.org/10.1002/pola.29455>.

- <sup>6</sup> Pascoal, M.; Brook, M. A.; Gonzaga, F.; Zepeda-Velazquez, L. Thermally Controlled Silicone Functionalization Using Selective Huisgen Reactions. *Eur. Polym. J.* **2015**, *69*, 429–437. <https://doi.org/10.1016/j.eurpolymj.2015.06.026>.
- <sup>7</sup> Clark, M.; Kiser, P. In Situ Crosslinked Hydrogels Formed Using Cu(I)-Free Huisgen Cycloaddition Reaction. *Polym. Int.* **2009**, *58* (10), 1190–1195. <https://doi.org/10.1002/pi.2650>.
- <sup>8</sup> Qin, A.; Lam, J. W. Y.; Tang, B. Z. Click Polymerization. *Chem. Soc. Rev.* **2010**, *39* (7), 2522–2544. <https://doi.org/10.1039/b909064a>.
- <sup>9</sup> Li, Z.; Seo, T. S.; Ju, J. 1,3-Dipolar Cycloaddition of Azides with Electron-Deficient Alkynes under Mild Condition in Water. *Tetrahedron Lett.* **2004**, *45* (15), 3143–3146. <https://doi.org/10.1016/j.tetlet.2004.02.089>.
- <sup>10</sup> Jewett, J. C.; Bertozzi, C. R. Cu-Free Click Cycloaddition Reactions in Chemical Biology. *Chemical Society Reviews.* **2010**, pp 1272–1279. <https://doi.org/10.1039/b901970g>.
- <sup>11</sup> Heyl, D.; Fessner, W. D. Facile Direct Synthesis of Acetylenedicarboxamides. *Synth.* **2014**, *46* (11), 1463–1468. <https://doi.org/10.1055/s-0033-1341101>.
- <sup>12</sup> Okumura, S.; Takeda, Y.; Kiyokawa, K.; Minakata, S. Hypervalent Iodine(III)-Induced Oxidative [4+2] Annulation of o-Phenylenediamines and Electron-Deficient Alkynes: Direct Synthesis of Quinoxalines from Alkyne Substrates under Metal-Free Conditions. *Chem. Commun.* **2013**, *49* (81), 9266–9268. <https://doi.org/10.1039/c3cc45469j>.

- <sup>13</sup> Eaton, P. E.; Steele, I.; Gilardi, R. Nitroacetylene: HC≡CNO<sub>2</sub>. *Synthesis (Stuttg)*. **2002**, No. 14, 2013–2018. <https://doi.org/10.1055/s-2002-34387>.
- <sup>14</sup> Pasquato, L.; De Lucchi, O.; Krotz, L. Bis(Arylsulphonyl)Acetylenes. *Tetrahedron Lett.* **1991**, 32 (19), 2177–2178. [https://doi.org/10.1016/S0040-4039\(00\)71269-X](https://doi.org/10.1016/S0040-4039(00)71269-X).
- <sup>15</sup> Tsarevsky, N. V.; Bernaerts, K. V.; Dufour, B.; Du Prez, F. E.; Matyjaszewski, K. Well-Defined (Co)Polymers with 5-Vinyltetrazole Units via Combination of Atom Transfer Radical (Co)Polymerization of Acrylonitrile and “Click Chemistry”-Type Postpolymerization Modification. *Macromolecules* **2004**, 37 (25), 9308–9313. <https://doi.org/10.1021/ma048207q>.
- <sup>16</sup> Gao, P.; Song, X. R.; Liu, X. Y.; Liang, Y. M. Recent Developments in the Trifluoromethylation of Alkynes. *Chem. - A Eur. J.* **2015**, 21 (21), 7649–7661. <https://doi.org/10.1002/chem.201406432>.
- <sup>17</sup> Tikhomirov, D. A.; Shubina, Y. V.; Ereemeev, A. V. Ynaziradines. Methods of Synthesis of a New Type of Ynamines. *Chem. Heterocycl. Compd.* **1984**, 20, 1231–1235. <https://doi.org/10.1007/BF00505713>.
- <sup>18</sup> Tanaka, R.; Miller, S. I. Nucleophilic Substitution at an Acetylenic Carbon. Kinetics of the Reaction between Bromoacetylene and Triethylamine in Dimethylformamide. *J. Org. Chem.* **1971**, 36 (25), 3856–3861. <https://doi.org/10.1021/jo00824a003>.
- <sup>19</sup> Hansch, C.; Leo, A.; Taft, R. W. A Survey of Hammett Substituent Constants and Resonance and Field Parameters. *Chem. Rev.* **1991**, 91 (2), 165–195. <https://doi.org/10.1021/cr00002a004>.

<sup>20</sup> Bräse, S.; Gil, C.; Knepper, K.; Zimmermann, V. Organic Azides: An Exploding Diversity of a Unique Class of Compounds. *Angew. Chem. Int. Ed.* 2005, 44 (33), 5188–5240. <https://doi.org/10.1002/anie.200400657>.

<sup>21</sup> Hassner, A.; Stern, M. Synthesis of Alkyl Azides with a Polymeric Reagent. *Angew. Chem. Int. Ed. Engl.* 1986, 25 (5), 478–479. <https://doi.org/10.1002/anie.198604781>

<sup>22</sup> Huy, P. H.; Filbrich, I. A General Catalytic Method for Highly Cost- and Atom-Efficient Nucleophilic Substitutions. *Chem. - A Eur. J.* **2018**, 24 (29), 7410–7416. <https://doi.org/10.1002/chem.201800588>.

<sup>23</sup> Frisch, M. J.; Trucks, G. W.; Schlegel, H. B.; Scuseria, G. E.; Robb, M. A.; Cheeseman, J. R.; Scalmani, G.; Barone, V.; Mennucci, B.; Petersson, G. A.; Nakatsuji, H.; Caricato, M.; Li, X.; Hratchian, H. P.; Izmaylov, A. F.; Bloino, J.; Zheng, G.; Sonnenberg, J. L.; Hada, M.; Ehara, M.; Toyota, K.; Fukuda, R.; Hasegawa, J.; Ishida, M.; Nakajima, T.; Honda, Y.; Kitao, O.; Nakai, H.; Vreven, T.; Montgomery, J. A., Jr.; Peralta, J. E.; Ogliaro, F.; Bearpark, M.; Heyd, J. J.; Brothers, E.; Kudin, K. N.; Staroverov, V. N.; Kobayashi, R.; Normand, J.; Raghavachari, K.; Rendell, A.; Burant, J. C.; Iyengar, S. S.; Tomasi, J.; Cossi, M.; Rega, N.; Millam, J. M.; Klene, M.; Knox, J. E.; Cross, J. B.; Bakken, V.; Adamo, C.; Jaramillo, J.; Gomperts, R.; Stratmann, R. E.; Yazyev, O.; Austin, A. J.; Cammi, R.; Pomelli, C.; Ochterski, J. W.; Martin, R. L.; Morokuma, K.; Zakrzewski, V. G.; Voth, G. A.; Salvador, P.; Dannenberg, J. J.; Dapprich, S.; Daniels, A. D.; Farkas, O.; Foresman, J. B.; Ortiz, J. V.; Cioslowski, J.; Fox, D. J.. Gaussian 09, revision A.02; Gaussian, Inc.: Wallingford, CT, 2009



- <sup>24</sup> Qin, A.; Jim, C. K. W.; Lu, W.; Lam, J. W. Y.; Häussler, M.; Dong, Y.; Sung, H. H. Y.; Williams, I. D.; Wong, G. K. L.; Tang, B. Z. Click Polymerization: Facile Synthesis of Functional Poly(Aroyltriazole)s by Metal-Free, Regioselective 1,3-Dipolar Polycycloaddition. *Macromolecules* **2007**, *40* (7), 2308–2317. <https://doi.org/10.1021/ma062859s>.
- <sup>25</sup> Ess, D. H.; Houk, K. N. Theory of 1,3-Dipolar Cycloadditions: Distortion/Interaction and Frontier Molecular Orbital Models. *J. Am. Chem. Soc.* **2008**, *130* (31), 10187–10198. <https://doi.org/10.1021/ja800009z>.
- <sup>26</sup> Bickelhaupt, F. M.; Houk, K. N. Analyzing Reaction Rates with the Distortion/Interaction-Activation Strain Model. *Angew. Chemie - Int. Ed.* **2017**, *56* (34), 10070–10086. <https://doi.org/10.1002/anie.201701486>.
- <sup>27</sup> Wiberg, K. B. Application of the Pople-Santry-Segal CNDO Method to the Cyclopropylcarbinyl and Cyclobutyl Cation and to Bicyclobutane. *Tetrahedron* **1968**, *24* (3), 1083–1096. [https://doi.org/10.1016/0040-4020\(68\)88057-3](https://doi.org/10.1016/0040-4020(68)88057-3).
- <sup>28</sup> Yoshida, S.; Shiraishi, A.; Kanno, K.; Matsushita, T.; Johmoto, K.; Uekusa, H.; Hosoya, T. Enhanced Clickability of Doubly Sterically-Hindered Aryl Azides. *Sci. Rep.* **2011**, *1*, 4–7. <https://doi.org/10.1038/srep00082>.

### 3 Degradation of Polyvinyl Chloride Using Olefin Metathesis

Although internal plasticization of PVC has been a focus of our lab, increasing concerns about plastic waste have prompted us to turn our attention towards the study of chemical recycling and upcycling. Turning plastic waste into a chemical feedstock will be an important tool in transitioning to a sustainable overall economy. This paper is our lab's first foray into the realm of chemical upcycling.

This paper has been published.<sup>1</sup> Skelly, P. W.; Fuentes Chang, C.; Braslau, R. Degradation of Polyvinyl Chloride by Sequential Dehydrochlorination and Olefin Metathesis. *Chempluschem* **2023**, *88* (e202300184). <https://doi.org/10.1002/cplu.202300184>.

#### 3.1 Background

##### 3.1.1 PVC Waste

An estimated 1 billion tons of PVC has been produced since 1960, over half of which is still in use.<sup>2</sup> In the coming years, PVC waste generation will see a large increase as long-lived products such as window frames and pipes come to the end of their usable lifetimes and enter the waste stream.<sup>3</sup>

Making productive use of PVC waste is a challenge. Mechanical recycling is difficult because different PVC products each contain different blends of plasticizers, stabilizers, and other additives; combining these additives leads to diminished mechanical properties.<sup>3,4,5</sup> Meanwhile, incineration of PVC is an issue because it produces corrosive HCl and toxic chlorinated dioxins, a class of persistent organic pollutants.<sup>3</sup> Changing regulations also present an issue: harmful plasticizers such as

diethylhexylphthalate (DEHP) still present in legacy PVC products are now banned in newly made (or newly recycled) PVC in the EU.<sup>6</sup> In the US, DEHP is restricted in childcare articles and food packaging.<sup>7</sup> Vinyloop®, a plant designed to recycle PVC from mixed waste by selective dissolution/precipitation, was shut down in 2018 due to its inability to remove phthalates.<sup>8,9</sup> Lead stabilizers found in legacy PVC products are similarly banned in new products, complicating attempts at PVC recycling.<sup>5,10</sup>

### **3.1.2 Chemical Upcycling**

Chemical recycling and upcycling of polymers is a growing field of interest with the goal of creating a circular economy. Breaking down a polymer into monomer or other useful small molecules allows purification of the products and avoids the downcycling phenomenon seen in mechanical recycling. Polymers with labile ester or amide bonds in their backbone are more amenable to this treatment than polymers with an all-carbon backbone. For instance, polyethylene terephthalate and polyurethane can both be depolymerized by hydrolysis, alcoholysis, or aminolysis; the monomers or short oligomers obtained can be repolymerized to form the original polymer or other high-performance polymers.<sup>11, 12</sup> Polymers with all-carbon backbones are more challenging to controllably cleave, but many methods have been developed to break down polyethylene, polypropylene, and polystyrene into light hydrocarbon fuels, benzene derivatives, or H<sub>2</sub> gas. However, even small amounts of PVC can contaminate these reactions and deactivate the catalyst, requiring PVC to be carefully removed first.<sup>11,12</sup>

### 3.1.3 Chemical Degradation of PVC

Chemical upcycling of PVC is underdeveloped compared to that of other polymers, despite the fact that it is the third-most produced plastic in the world.<sup>2</sup> Most PVC degradation procedures explored have been carried out at high temperatures (200-900 °C) and focus on pyrolysis to small hydrocarbons or oxidation to carboxylic acids.<sup>3,13,14</sup> Pyrolysis of PVC is complicated by the release of HCl, which corrodes equipment and deactivates catalysts. Solutions to this include pre-treatment with base, or pyrolysis in the presence of base or bio-waste. In some cases, products are a mixture of acetone, benzene, and other aromatics. In other cases, alkanes or syngas (CO and H<sub>2</sub>) are produced.<sup>13,14</sup>

Oxidation of PVC has been performed using oxygen in water,<sup>15</sup> using hydrogen peroxide and a palladium catalyst,<sup>16</sup> or using electrooxidation.<sup>17</sup> Extensive oxidation leads to formation of carbon dioxide; small carboxylic acids such as oxalic acid are formed along the way. The Yoshioka group has focused on maximizing the ratio of oxalic acid to CO<sub>2</sub> produced. Oxidation of PVC in oxygen and aqueous NaOH at 250 °C yields up to 30% oxalic acid from rigid PVC waste,<sup>18</sup> as well as from flexible PVC waste containing DEHP plasticizer.<sup>19</sup> The Yanagisawa group used a two-step process wherein PVC was first dehydrochlorinated in KOH/PEG/THF, then treated by aqueous O<sub>2</sub> oxidation. They found that by decreasing the temperature to 100 °C, little to no CO<sub>2</sub> was produced and the majority of the carbon in PVC was converted into formic, maleic, fumaric, and other carboxylic acids.<sup>20</sup>

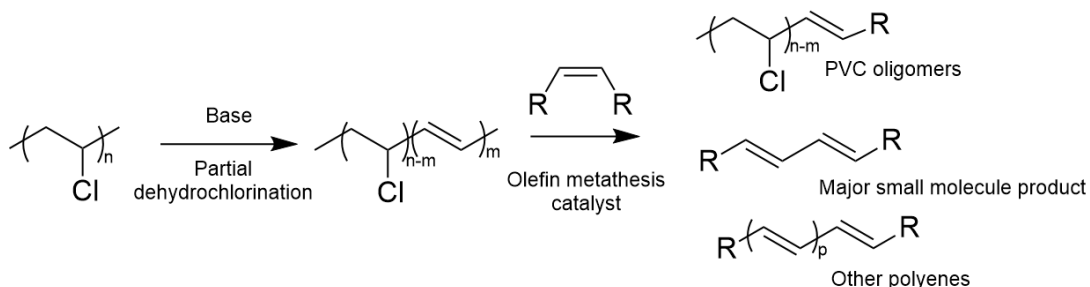
In 2003, Partenheimer developed an aqueous O<sub>2</sub> oxidation of PVC in the presence of a vanadium and bromide catalyst to produce a 38% yield of succinic acid.<sup>21</sup> In a study by the Xiu group, oxidation at 300 °C with a limited amount of oxygen was used to selectively form benzaldehyde and acetophenone as the major oil products, although the total yield was not reported.<sup>22</sup> Aside from harvesting the carbon, waste PVC can also be used as a chloride source to trap heavy metals,<sup>23</sup> or as a hydrogen donor to upconvert CO<sub>2</sub> into formic acid.<sup>24</sup>

### **3.1.4 Degradation of Polymers by Olefin Metathesis**

There remains a need for new approaches to chemically break down PVC. Expanding the toolbox of reactions that can controllably degrade PVC will allow a wider range of products to be made, and bring the world closer to the goal of harvesting plastic waste as a resource. Olefin metathesis is a promising method for polymer breakdown because it cleaves carbon-carbon double bonds, which can be readily introduced into the PVC backbone. Olefin metathesis has been used to degrade polybutadiene,<sup>25,26</sup> natural rubber,<sup>27,28,29</sup> and styrene-butadiene-styrene (SBS) rubber.<sup>30</sup> In particular, the Wagener group was able to depolymerize polybutadiene to almost exclusively monomer rather than oligomers using Grubbs 2 catalyst and copper iodide.<sup>31</sup> Abu Omar et al. broke down polyethylene into oligomers in a three-step process. First polyethylene was brominated, then elimination of HBr produced carbon-carbon double bonds, which were then cleaved by olefin cross metathesis with ethylene.<sup>32</sup> In 2016, Huang et al. paired iridium pincer catalysts with a Re<sub>2</sub>O<sub>7</sub>/γ-Al<sub>2</sub>O<sub>3</sub> metathesis catalyst to perform a one-pot dehydrogenation/olefin

metathesis/rehydrogenation sequence, breaking down polyethylene into low-molecular-weight alkanes.<sup>33</sup> In 2021, Beckham et al. performed a similar one-pot reaction using SnPt/ $\gamma$ -Al<sub>2</sub>O<sub>3</sub> as the (de)hydrogenation catalyst and Re<sub>2</sub>O<sub>7</sub>/ $\gamma$ -Al<sub>2</sub>O<sub>3</sub> as the metathesis catalyst.<sup>34</sup>

We envisaged a method of chemically degrading PVC in two steps (**Scheme 3.1**). First, elimination of HCl by addition of base will create carbon-carbon double bonds, while sequestering the chloride as a salt. Subsequent olefin metathesis with an added alkene will cleave the double bonds, resulting in scission of the all-carbon polymer backbone.



**Scheme 3.1** General strategy for PVC degradation by olefin cross metathesis

### 3.1.5 Precedent for PVC Elimination

Elimination of HCl from PVC has been extensively explored, ranging from partial elimination<sup>35</sup> to full elimination forming polyacetylene.<sup>36,37</sup> Elimination likely begins at defect sites such as allylic chlorides. Once the first elimination reaction occurs, the neighboring chloride becomes allylic, making it the most likely to react next. This “zipper” reaction leads to long stretches of conjugated alkenes between regions of unreacted PVC.<sup>38</sup> The use of hydroxide for the initial dehydrochlorination step has the

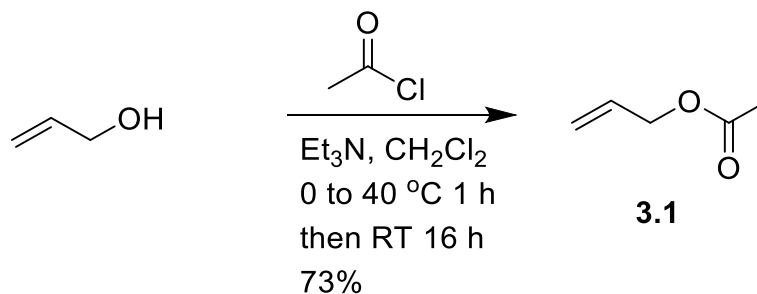
added benefit of hydrolyzing harmful phthalate esters present in flexible PVC waste into the safer phthalic acid,<sup>19</sup> making this an appealing strategy.

### 3.1.6 Precedent for Olefin Metathesis on Conjugated Double Bonds

Conjugated double bonds are less reactive towards olefin metathesis catalysts than isolated double bonds,<sup>39</sup> however there is precedent for olefin metathesis on conjugated polymers,<sup>40</sup> including polyacetylene,<sup>41,42,43</sup> which closely resembles the conjugated stretches of alkenes in dehydrochlorinated PVC.

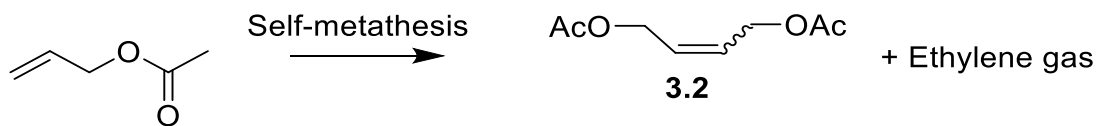
### 3.2 Control Reaction: Self Metathesis

Allyl acetate (**3.1**) was chosen as the alkene partner to undergo cross-metathesis with dehydrochlorinated PVC. Allyl acetate was synthesized from allyl alcohol and acetyl chloride (**Scheme 3.2**).<sup>44</sup>



**Scheme 3.2** Synthesis of allyl acetate

During metathesis, this compound reacts with itself to form the homodimer **3.2** (**Scheme 3.3**). This reaction acts as an internal control: the homodimerization is expected to be faster than cross-metathesis with a less activated alkene, such as a conjugated one.<sup>45</sup> If the homodimer does not form, there may be something inhibiting the catalyst or metathesis is not happening under these conditions.

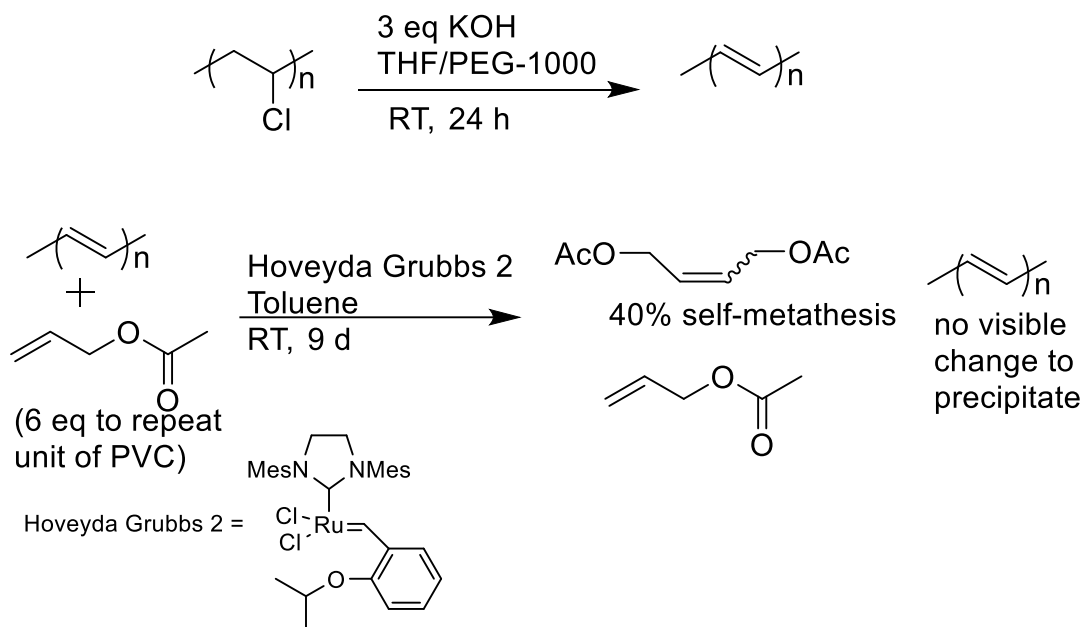


**Scheme 3.3** Self-metathesis of allyl acetate

### 3.3 Complete Elimination of PVC and attempted metathesis

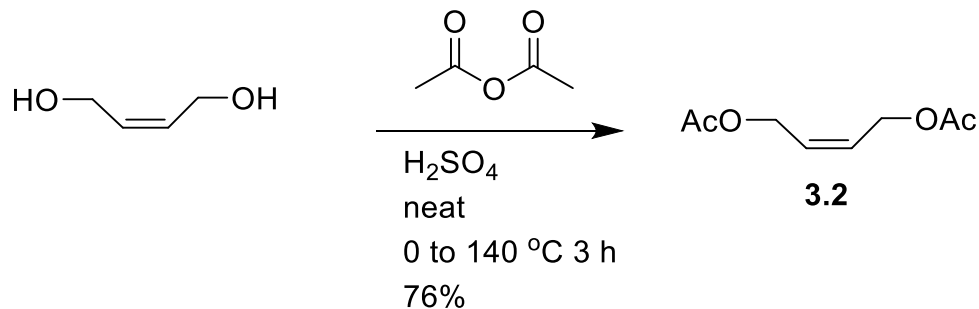
Treatment of PVC with an excess of KOH in a THF/PEG-1000 solvent mixture produced fully eliminated PVC (polyacetylene) as a black precipitate, as reported in the literature (**Scheme 3.4**, top).<sup>37</sup> Polyacetylene is famously insoluble,<sup>46</sup> so a metathesis reaction was attempted on a suspension of polyacetylene powder in toluene, based on literature reports that some metathesis reactions can happen on solid polyacetylene.<sup>47</sup> When polyacetylene was stirred with the Hoveyda-Grubbs 2 catalyst and cross-metathesis partner **3.1** (**Scheme 3.4**, bottom), some self-metathesis to **3.2** was seen, but no other products seen on NMR. If any cross-metathesis did occur, it did not cleave the chains sufficiently to produce soluble products: the black precipitate appeared unchanged over the course of the reaction.





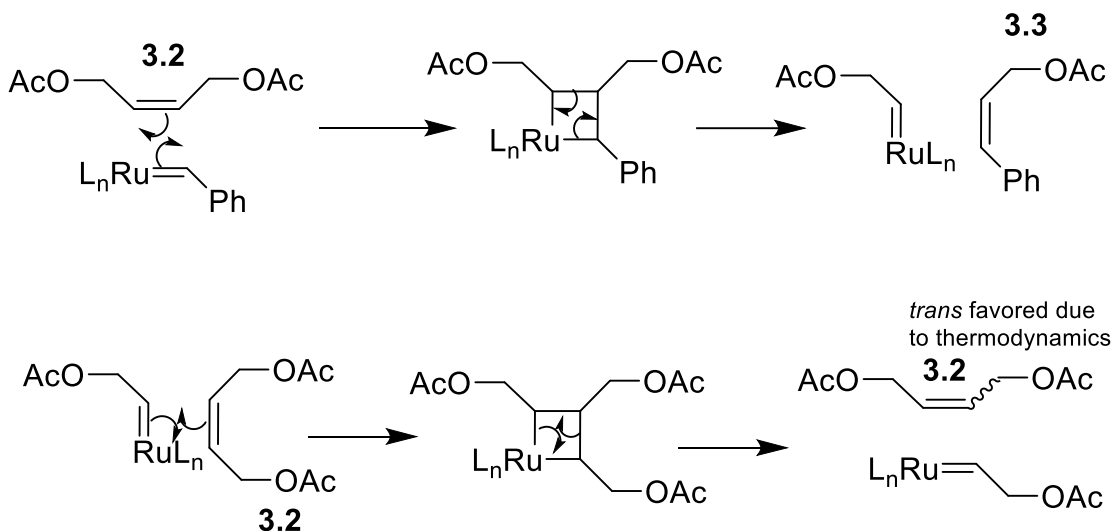
**Scheme 3.4** Full elimination of PVC and attempted metathesis on the polyacetylene product

Because of the volatility of allyl acetate (b.p. 103 °C), determination of the amount of starting material left over may be biased by evaporation. In addition, some sources from the literature avoid terminal alkenes due to the formation of  $\text{Ru}=\text{CH}_2$  species which can decompose.<sup>48</sup> For these reasons, *Z*-1,4-diacetoxy-2-butene (DAB) was synthesized for use as a partner alkene. *Z*-1,4-Diacetoxy-2-butene was synthesized from the corresponding diol with acetic anhydride (**Scheme 3.5**).<sup>49</sup>



**Scheme 3.5** Synthesis of *Z*-1,4-diacetoxy-2-butene

During the metathesis reaction, the *Z*-isomer can undergo self-metathesis to the more stable *E*-isomer (**Scheme 3.6**), again providing an internal control reaction. *Z*-1,4-Diacetoxy-2-butene was used as the partner for metathesis reactions going forward.

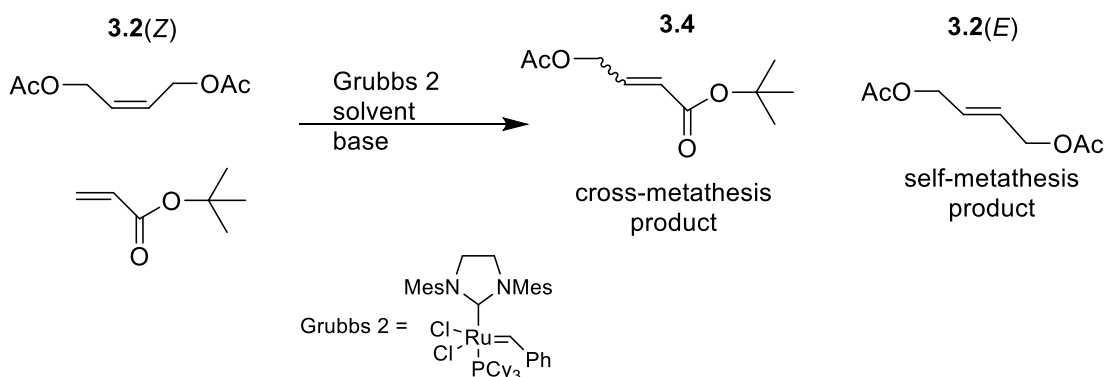


**Scheme 3.6** Reaction of DAB with the initial catalyst (top) followed by self-metathesis of DAB (bottom)

### 3.4 Investigations into simultaneous dehydrochlorination and metathesis

Another proposed strategy involved simultaneous dehydrochlorination and metathesis. This would avoid the issue of insolubility, as the alkenes could be cleaved before they grow long enough to precipitate. In order to test the feasibility of a simultaneous reaction, the compatibility of several bases with the Grubbs catalyst was investigated. A model cross-metathesis reaction was used, with *tert*-butyl acrylate acting as a less-reactive alkene,<sup>45</sup> to simulate the low reactivity of the conjugated double bonds in dehydrochlorinated PVC (**Scheme 3.7**). Several bases were screened for their ability to eliminate HCl from PVC, as measured by the stark color change seen when even a few percent of chlorines are eliminated from PVC (**Table 3.1**). The two

successful bases were screened in the cross-metathesis reaction and both were found to strongly inhibit reactivity (**Table 3.2**). Based on these results, we decided to instead focus on the stepwise elimination and metathesis route, with the possibility of looking at the simultaneous route again later, at which time a more exhaustive screening of bases and conditions could be performed.



**Scheme 3.7** Model cross-metathesis reaction for base screening

**Table 3.1** Screening of bases that can perform the elimination reaction on PVC

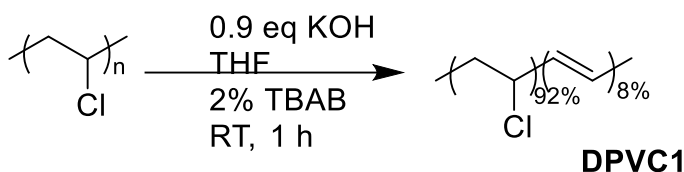
Base	Eliminates HCl from PVC?
KOtBu (1eq in THF, RT)	Yes
Pyridine (1 eq in THF, reflux)	No
Pyridine (neat, reflux)	Yes
2,6-Lutidine (neat, 60 °C)	No
Triethylamine (10eq in THF, 60 °C)	No

**Table 3.2** Inhibition of olefin metathesis in the presence of base

Solvent	Base	Cross-metathesis	Self-metathesis
THF	-	8%	72%
DCM	-	49%	92%
DCM	KOtBu	0%	0%
THF	Pyridine	0%	16%
Pyridine	Pyridine	0%	16%

### 3.5 Optimization of Elimination of PVC

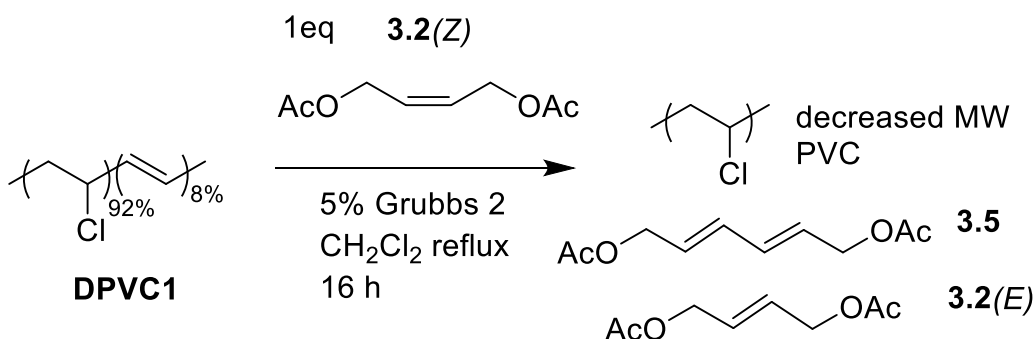
The course of the elimination reaction is influenced by the solvent, the amount of base used, and the presence or absence of competing nucleophiles. Decreasing the amount of base used led to partially dehydrochlorinated PVC (DPVC) that was fully soluble in THF. Using 0.02eq tetrabutylammonium bromide (TBAB) and 0.9eq KOH in THF, DPVC up to 8% was formed (**DPVC1**) (**Scheme 3.8**).  $^1\text{H}$  NMR spectra are in agreement with the literature for similar levels of dehydrochlorination.<sup>35</sup>



**Scheme 3.8** Partial elimination of PVC

### 3.6 Metathesis on Partially Eliminated PVC

DPVC1 was treated with Grubbs catalyst and added olefin **3.2**, with the expected reaction products shown in **Scheme 3.9**. One equivalent of **3.2** and 0.05 equivalents of catalyst were used relative to the number of double bonds in the DPVC. The self-metathesis product, **3.2E** was observed, indicating the catalyst was active. The expected diene **3.5** was present in low enough quantities to go unnoticed, but after later experiments was seen to be present in trace amounts in this experiment.



**Scheme 3.9** Olefin metathesis reaction of DPVC1 with added alkene **3.2**

To determine if the molecular weight decreased, unmodified PVC, DPVC1, and the metathesis product were compared using Gel Permeation Chromatography (GPC). The molecular weight did decrease, which provided an important proof of concept that the backbone of the PVC was being cleaved (**Table 3.3**). However, the molecular weight decrease was modest, indicating that the double bonds in the backbone may not be as accessible to the metathesis catalyst as we had hoped.

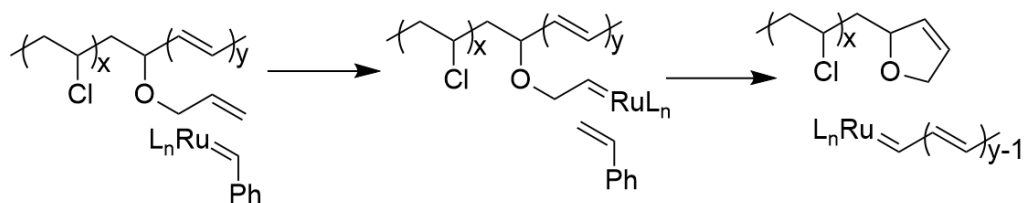
**Table 3.3** Molecular weights of initial PVC, DPVC1, and metathesis products

Sample	MW
PVC	65 ± 3
DPVC1	44 ± 6
Metathesis product of DPVC1, DAB and Grubbs 2	15.0

### 3.7 Elimination Using Allyl Alcohol

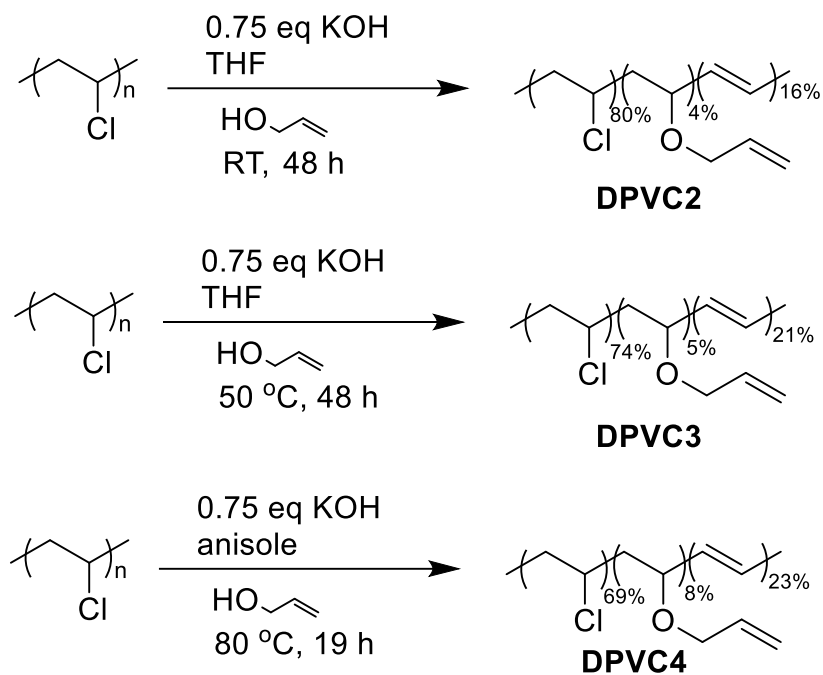
Given the low reactivity of the internal conjugated double bonds of DPVC1, another strategy was proposed. In this strategy, allyl ethers containing highly reactive terminal alkenes grafted to the PVC could react quickly with the metathesis catalyst and then undergo an intramolecular ring-closing metathesis reaction similar to that seen

in polybutadiene at the 1,2 residues,<sup>25,44</sup> cleaving the chain and providing the catalyst access to the internal double bonds of the polymer (**Scheme 3.10**).



**Scheme 3.10** Proposed ring-closing metathesis strategy to introduce the metathesis catalyst onto the internal double bonds of allyl-grafted DPVC

To this end, elimination was performed with KOH in 2:1 THF/allyl alcohol as a solvent. The allyl oxide generated in situ can act as both a base and a nucleophile (**Scheme 3.11**). To vary the ratio of substitution to elimination, reactions were done at three temperatures: room temperature (~20 °C) (**DPVC2**), 50 °C (**DPVC3**), and 80 °C (using anisole instead of THF) (**DPVC4**).



**Scheme 3.11** Dehydrochlorination of PVC using allyl alcohol

The percent elimination and substitution were calculated using **Equation 3.1** and **Equation 3.2** respectively, using the peak integrations from the  $^1\text{H}$  NMR of each DPVC sample (one example shown in **Figure 3.1**).

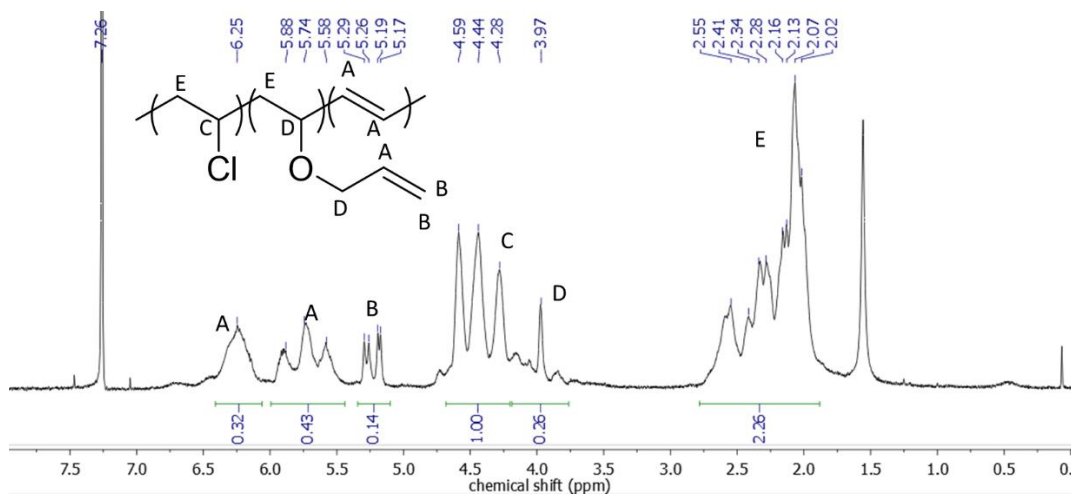


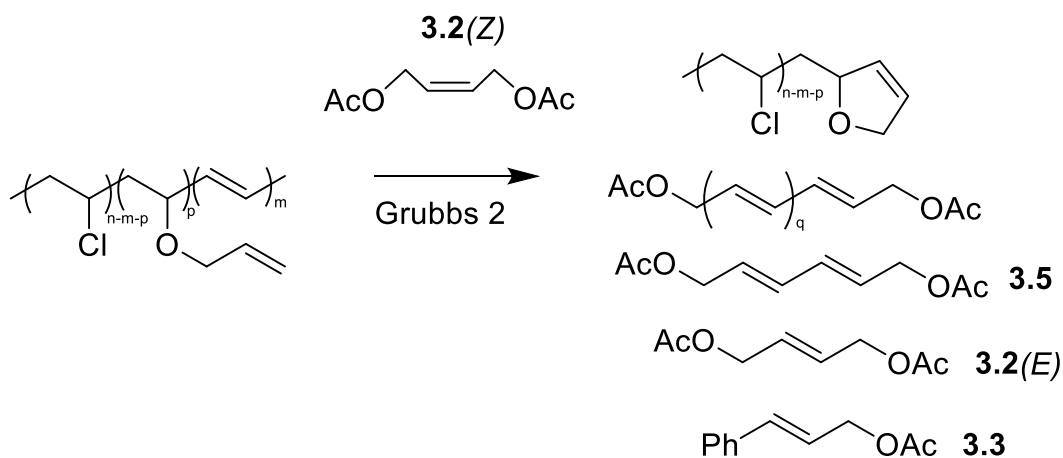
**Figure 3.1**  $^1\text{H}$  NMR spectrum of DPVC3 with peaks labeled

$$\% \text{ elimination} = \frac{A - \frac{B}{2}}{A - \frac{B}{2} + E} \quad \text{Equation 3.1}$$

$$\% \text{ substitution} = \frac{B}{A - \frac{B}{2} + E} \quad \text{Equation 3.2}$$

### 3.8 Metathesis on Allylated DPVC

Olefin metathesis was performed using *Z*-1,4-diacetoxy-2-butene (**3.2**), DPVCx and Grubbs 2 catalyst in refluxing dichloromethane (DCM). After olefin metathesis at many double bond sites, the expected products are PVC oligomers (from the non-eliminated segments) and a statistical mixture of different-length polyenes (**Scheme 3.12**). Using an excess of added olefin (**3.2**), and assuming extensive cross-metathesis, the largest fraction of polyenes are expected to be diene **3.5**.



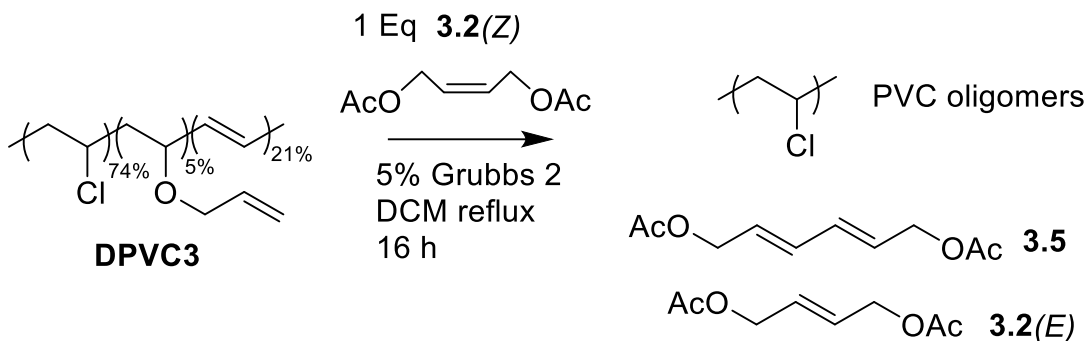
**Scheme 3.12** Expected products from the metathesis reaction

Although none of the allylDPVC samples are fully soluble in the solvents used, the metathesis reaction proceeds on the partially dissolved material, and gives a product



that is fully soluble. The increase in solubility is likely due to a shortening of the polymer chains, as corroborated by GPC.

"Standard Conditions"



**Scheme 3.13** Metathesis reaction of allyl DPVC with added olefin **3.2(Z)**: for the purposes of comparison throughout this chapter, these are the standard reaction conditions

DPVC2 through DPVC4 show a much greater MW decrease upon metathesis than DPVC1 (**Table 3.4**), indicating that the allyl ether pendants successfully facilitate cleavage of the polymer backbone.

**Table 3.4** Metathesis products of DPVC1 through DPVC4

Condition	MW of oligomers <sup>a</sup> (kDa)	Diene formed? <sup>b</sup>
DPVC1	15.0	Yes
DPVC2	3.5 ± 0.8	Yes
(standard conditions) DPVC3	3.0 ± 1.3	Yes
DPVC4	2.7 ± 0.5	Yes

<sup>a</sup>Determined by GPC vs polystyrene standards.  $\pm$  values are from duplicate reactions.

<sup>b</sup>Determined by <sup>1</sup>H NMR of reaction mixture.

Carrying out the metathesis reaction in the absence of an added olefin partner (**Table 3.5**) gives roughly the same molecular weights as in the presence of an added olefin, which implies that the ring closing metathesis reaction shown in **Scheme 3.10** is the major driver of MW decrease. Another control without the metathesis catalyst gave no MW decrease, indicating that metathesis is the mechanism, rather than oxidative cleavage or some other reaction.

**Table 3.5** Metathesis products without added alkene

Condition	MW of oligomers <sup>a</sup> (kDa)	Diene formed? <sup>b</sup>
DPVC3 with no added alkene	1.9 $\pm$ 0.4	N/A

<sup>a</sup>Determined by GPC vs polystyrene standards.  $\pm$  values are from duplicate reactions.

<sup>b</sup>Determined by <sup>1</sup>H NMR of reaction mixture.

### 3.9 Characterization of DPVC and metathesis products

#### 3.9.1 Gel Permeation Chromatography

GPC was run on all the DPVC samples (**Table 3.6**) and on the metathesis products (**Tables 3.4-5** and **3.7-10** throughout chapter). Retention time increases with increasing diffusion coefficient, which is inversely proportional to molecular weight, but also depends on the coiling behavior of the polymer in solution. A more rigid

polymer would have a higher apparent molecular weight. For calibration, a ladder of five polystyrene standards was run with each set of samples and an exponential fit was used to calculate the molecular weight relative to the standards.

**Table 3.6** Characterization of DPVC

	MW <sup>a</sup> (kDa)
PVC	65 ± 3
DPVC1	44 ± 6
DPVC2 <sup>d</sup>	29 ± 5
DPVC3 <sup>d</sup>	12 ± 2
DPVC4 <sup>d</sup>	14 ± 1

<sup>a</sup>Determined by GPC vs linear polystyrene standards. ± values are from duplicate GPC runs. <sup>d</sup>Not fully soluble in CDCl<sub>3</sub> or THF, insoluble portion was filtered before GPC and UV-Vis.

Note: the molecular weight of the PVC as purchased is 22kDa, compared to the 65kDa measured using GPC with polystyrene reference standards, indicating that these standards do not behave the same as PVC in solution. However, they can still be used to give a general idea of the differences in molecular weights between samples.

The lower apparent molecular weights for DPVC2 through DPVC4 may be due in part to insolubility of high MW fractions after extensive elimination; insoluble portions were removed by filtration before GPC analysis.

The metathesis products, shown in tables later in the chapter, were always fully soluble and did not need to be filtered before GPC analysis. This means the MW difference between DPVC and the metathesis products may be even larger than

reported here, as the DPVC values are artificially low but the metathesis product values are not.

### 3.9.2 UV-Vis

A distinct color change was observed during the elimination reaction, with the PVC turning from colorless to orange to brown to black. This indicates the presence of increasingly conjugated double bonds.<sup>50</sup> To further study this conjugation, and what happens to it after metathesis, UV-Vis spectra were recorded of DPVC and the metathesis products.

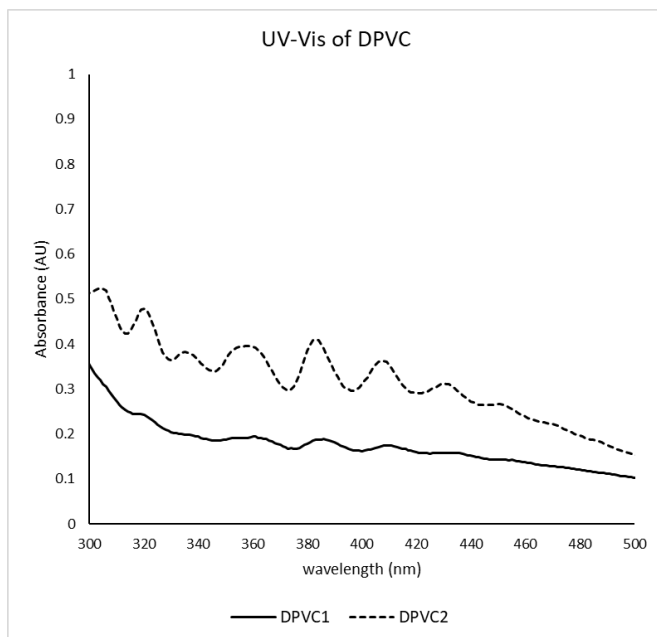


**Figure 3.2** UV-Vis spectra of DPVC1 (solid line) and DPVC2 (dotted line) in THF

The UV-Vis spectra of DPVC1-4 (**Figure 3.2**) are similar to those from previous reports of DPVC<sup>50</sup> and polyacetylene.<sup>41</sup> All exhibit long conjugated regions due to the zipper reaction. Peaks at 305, 321, and 336 nm correspond to conjugation

lengths as low as 4 double bonds, while the highest distinguishable peak at 452 nm corresponds to a conjugation length of 11-13 double bonds.<sup>50</sup>

The oligomers from the allyl DPVC (DPVC2-4) show no distinguishable peaks on UV-Vis, indicating the long conjugated stretches are no longer present. However, the oligomers made from DPVC1 (lacking allyl pendants) still have several peaks, indicating unreacted conjugated double bonds (**Figure 3.3**). The methanol-soluble fraction shows only slight peaks at 320 and 353 nm, indicating no polyenes greater than five double bonds are present.<sup>50</sup>

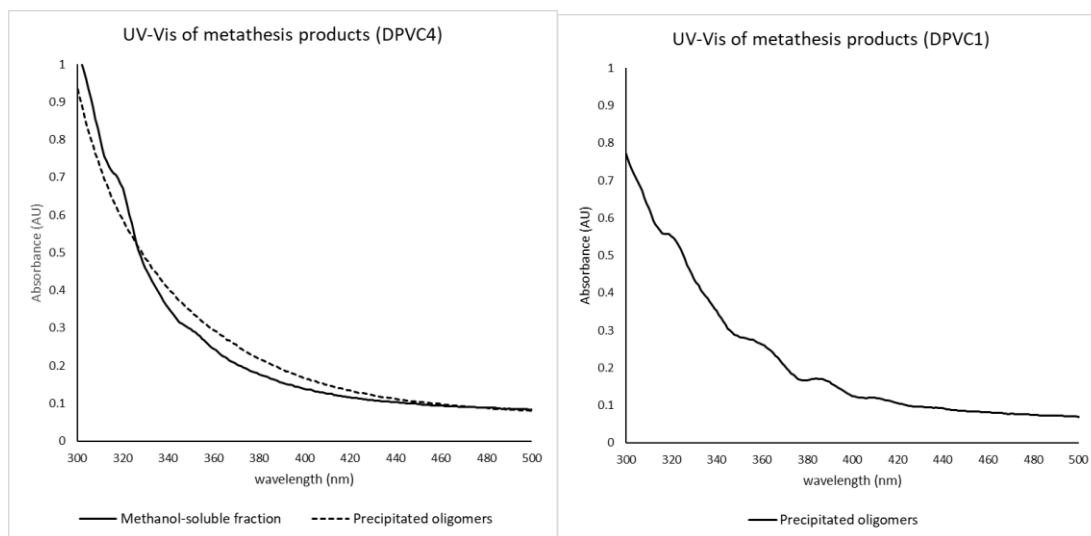


**Figure 3.3** Left: UV-Vis of the metathesis products of DPVC4. The fraction that precipitates in methanol is shown with a dotted line, and the remainder (recovered by evaporation of MeOH) with a solid line. Right: UV-Vis of the metathesis products of DPVC1. The fraction that precipitates in methanol is shown. All UV-Vis spectra were taken in THF.

### 3.9.3 NMR

NMR was used to characterize the dehydrochlorinated PVC as well as the products of the metathesis reactions. The crude product was a mixture of compounds shown in **Figure 3.7**. This could be precipitated into methanol; the spectrum of the

precipitate is shown in **Figure 3.4**, with PVC and DPVC for comparison. The precipitate is largely PVC, with some alkene peaks remaining that did not react. The terminal alkene peaks at 5.20 and 5.30 corresponding to the allyl ethers are almost entirely consumed.

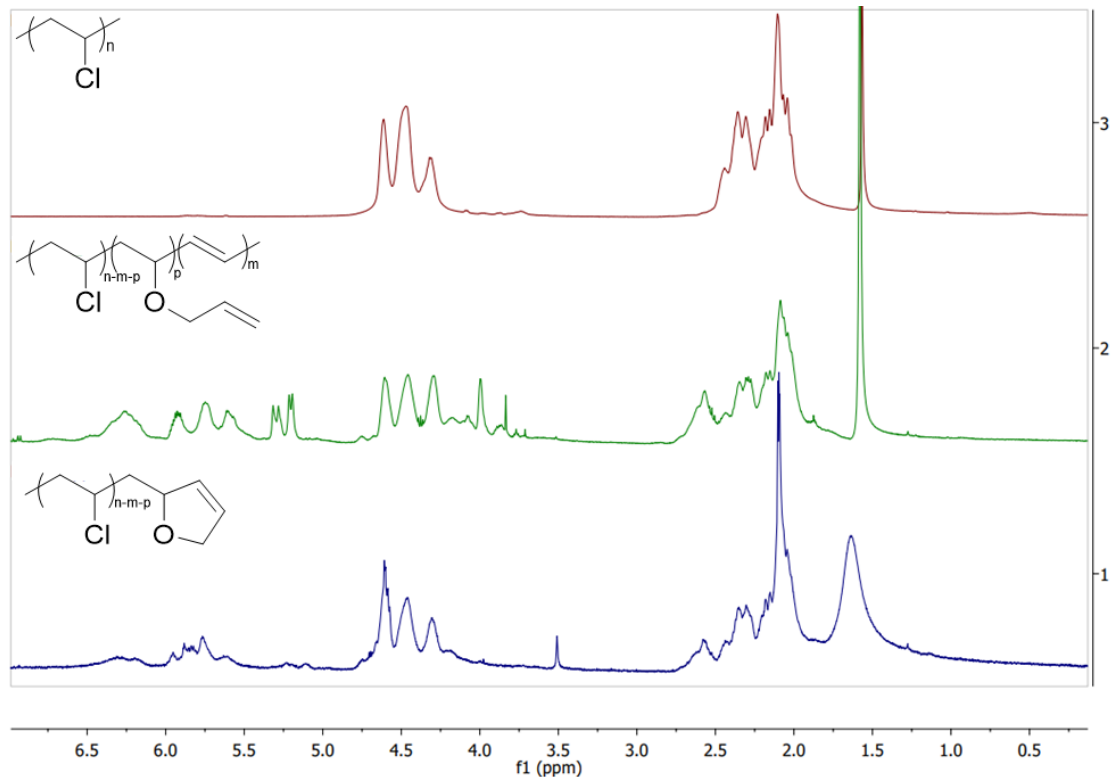


**Figure 3.4**  $^1\text{H}$  NMR Spectra of PVC (top), DPVC4 (middle), and PVC oligomers (produced from DPVC4 with Grubbs 2 and added alkene **3.2**) (bottom)

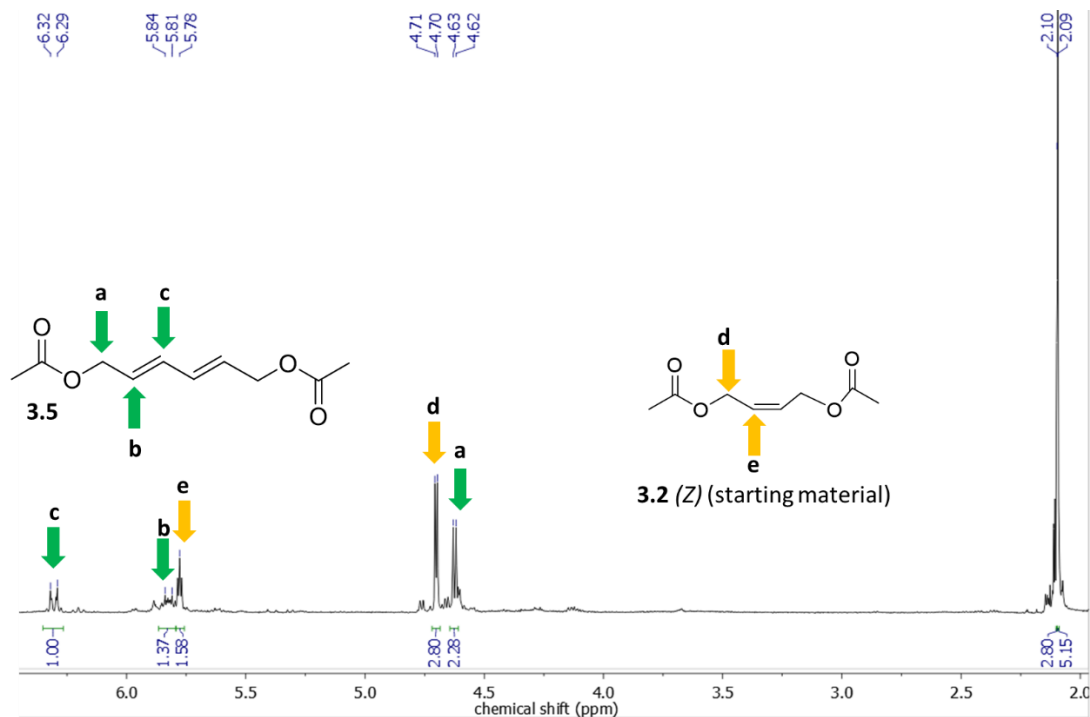


**Figure 3.5**  $^1\text{H}$  NMR of metathesis product after chromatography

The methanol-soluble fraction was then subjected to column chromatography. The expected major small-molecule product of the metathesis reaction, 1,6-diacetoxy-2,4-hexadiene (**3.5**) (**Figure 3.5** peaks a, b, and c), could be partially isolated from the reaction mixture, but coeluted with the starting material *cis*-1,4-diacetoxy-2-butene (**3.2**) (peaks d and e). Peaks a, b, and c are consistent with the literature values for this compound.<sup>51,52</sup> The COSY spectrum (**Figure 3.6**) shows the expected correlations between a&b and b&c. High-resolution mass spectrometry shows the diene:  $[\text{C}_{10}\text{H}_{14}\text{O}_4\text{Na}]^+$  ( $\text{M}+\text{Na}$ )<sup>+</sup> calcd. 221.0785, obs. 221.0781

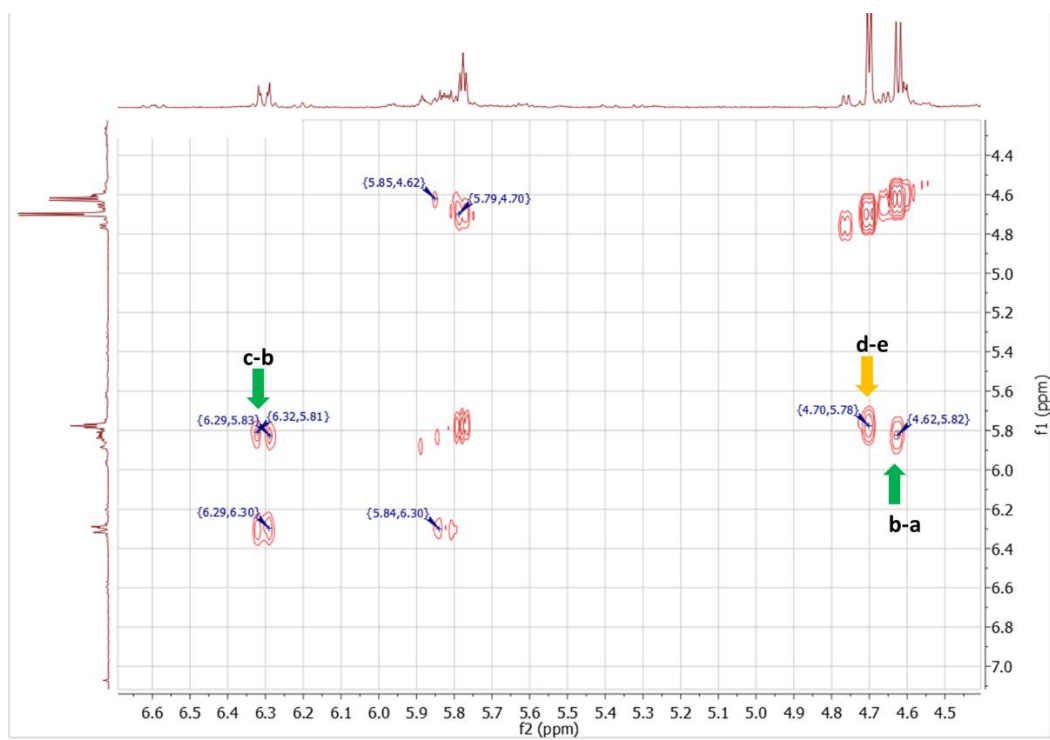


**Figure 3.6** COSY NMR of the metathesis product after chromatography



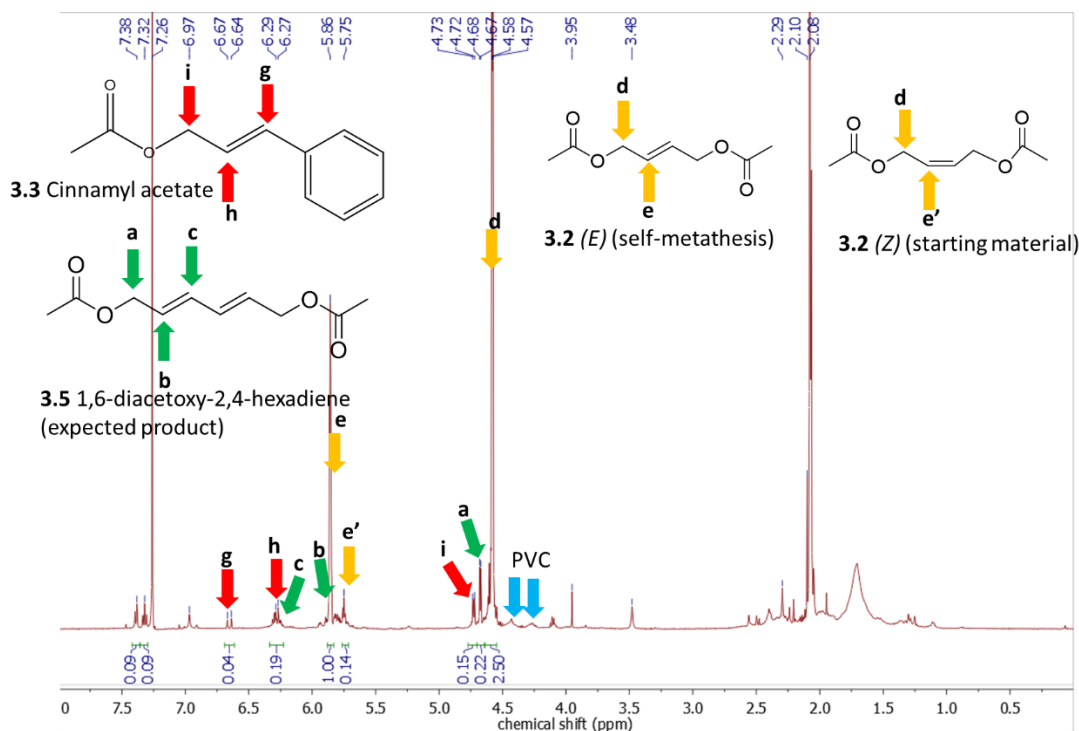


**Figure 3.7**  $^1\text{H}$  NMR of the crude reaction mixture of DPVC3 with DAB and Grubbs catalyst

The crude reaction mixture was used to determine the conversion of double bonds in DPVC into diene product. Peaks a and b of the diene product overlap with the starting material. Peak c is the most distinctive, but still overlaps with peak h from cinnamyl acetate **3.3**. Since h should integrate to the same as g, one can subtract g (0.04) from h+c (0.19) to get an integration of 0.15 for c. The conversion of starting material is estimated as  $c/(c+e+e') = 0.15/(0.15+1.00+0.14) = 12\%$ . This reaction was done with 1 eq of **3.2** per internal double bond of DPVC. Increasing the equivalents of **3.2** did not increase the conversion.

### 3.9.3.1 DOSY NMR

In order to further look at the molecular weight changes, Diffusion Ordered Spectroscopy (DOSY) NMR was performed on one of the allyl DPVC samples (**Figure 3.8**) and the metathesis products of that allylDPVC with DAB (**Figure 3.9**). The x-axis shows  $^1\text{H}$  NMR chemical shifts and the y-axis shows diffusion coefficients, which depend directly on hydrodynamic radius, which correlates to molecular weight. Note that GPC also measures diffusion coefficients. If a MW measured by GPC is off due to the way the sample coils in solution, the MW measured by DOSY will be equally off. For this reason, we decided to run DOSY qualitatively rather than running standards. It can, however, give us information that GPC cannot. **Figure 3.8** shows that the allyl pendants, internal alkenes, and unreacted chloride repeat units all show up at the same diffusion coefficient, indicating that they are all present on the same polymer chain. No corrections were made for viscosity which likely differs between the samples, the diffusion scale is approximate.

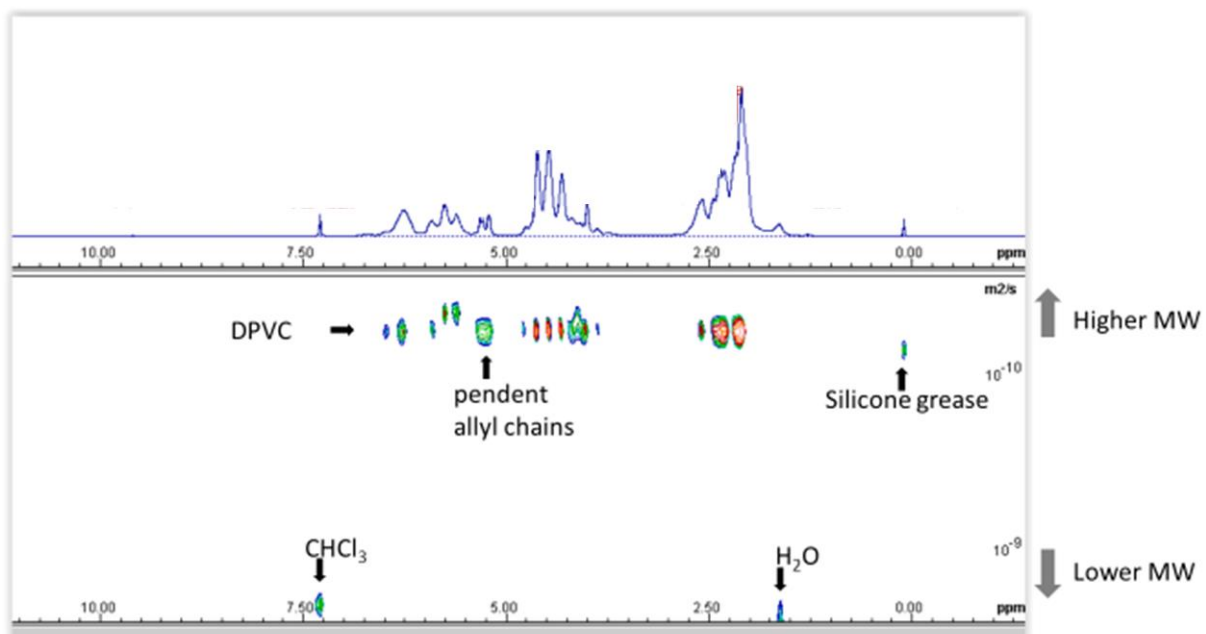


**Figure 3.8** DOSY NMR of DPVC3 in  $\text{CDCl}_3$

DOSY NMR of the metathesis products shows that a variety of molecular weights are present, all of which are smaller than the original polymer, indicating that extensive chain scission has occurred.

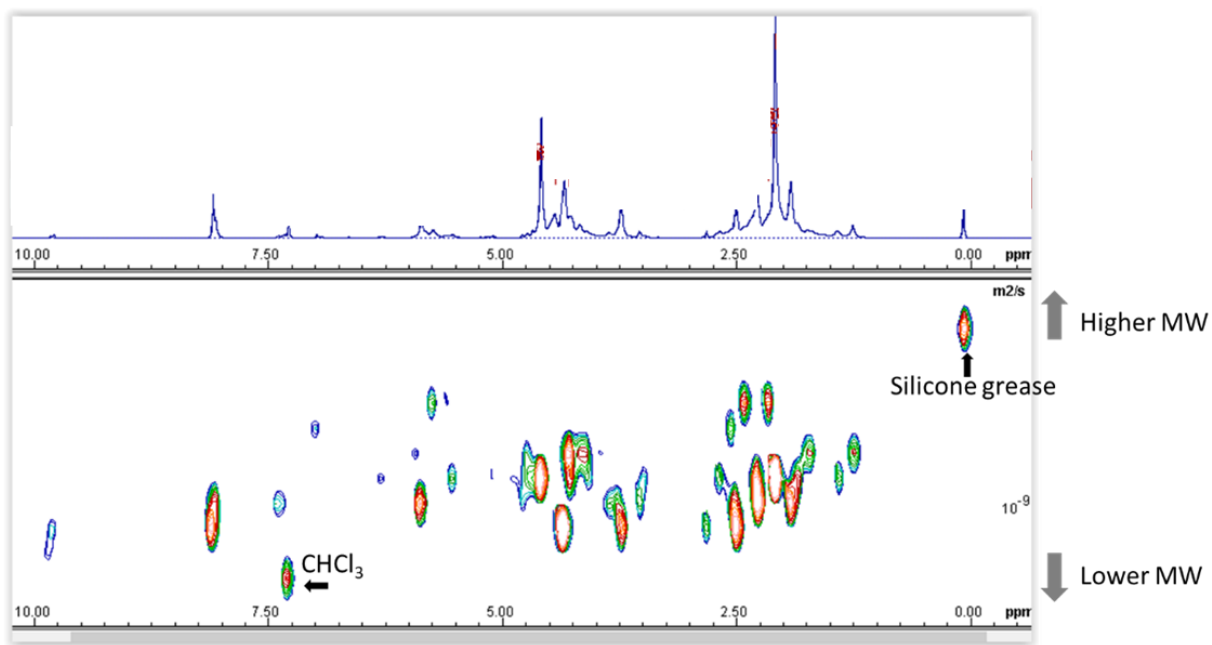
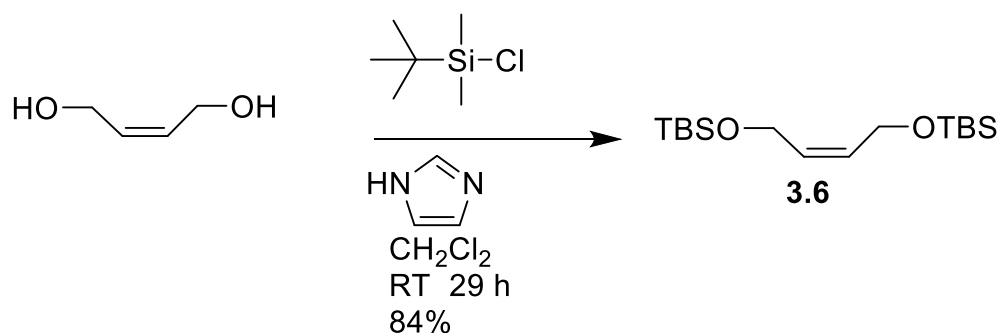


**Figure 3.9** DOSY NMR of the metathesis product of DPVC3 with DAB (crude reaction mixture) in CDCl<sub>3</sub>

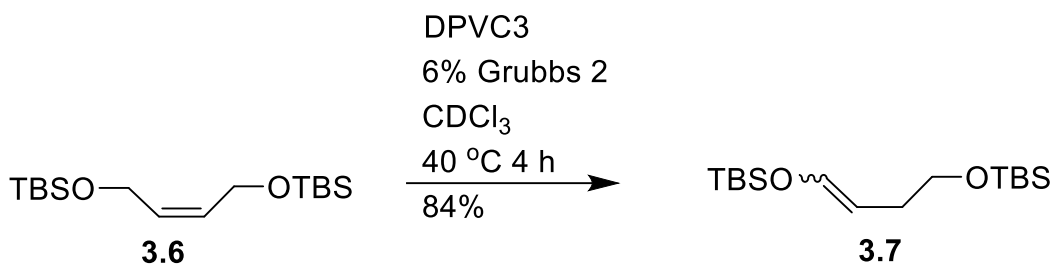
### 3.10 Effect of Varying Alkene Partners

To see if other added alkenes could provide a more successful reaction than bis-acetate **3.2**, reactions were attempted with other alkenes. Electron-rich alkenes are expected to be among the most reactive alkenes for metathesis,<sup>45</sup> so another protected diol was synthesized, using TBS-Cl and imidazole to add two TBSO groups to butenediol (**Scheme 3.14**).<sup>53</sup>



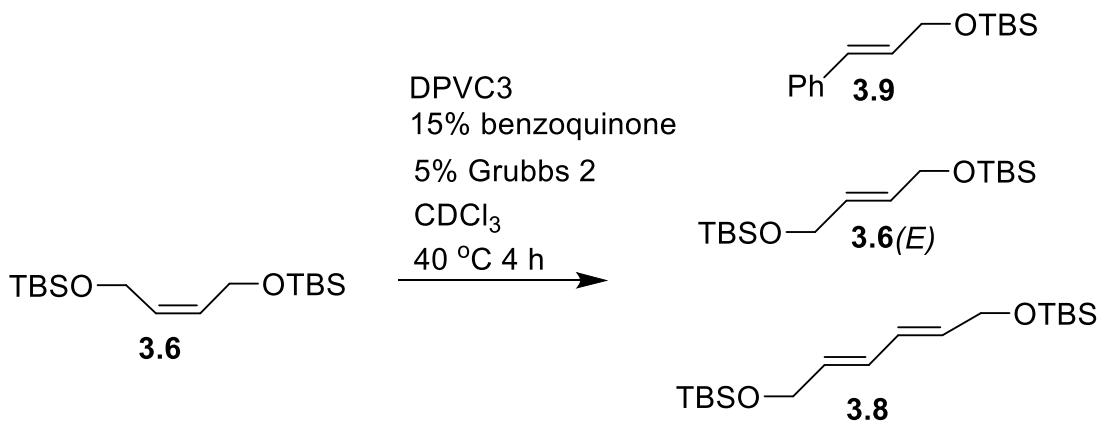
**Scheme 3.14** Synthesis of Z-1,4-bis-TBSO-2-butene

Initial attempts at olefin metathesis using **3.6** and DPVC3 led to quantitative isomerization to **3.7** as seen in **Scheme 3.15**. This has been reported in the literature as happening via a ruthenium hydride intermediate formed from the Grubbs catalyst.<sup>54</sup> Since **3.7** is a vinyl ether, it quenches the catalyst preventing any further metathesis reactions.



**Scheme 3.15** Isomerization of the added alkene

The addition of benzoquinone can inhibit this ruthenium hydride species from forming,<sup>54</sup> so the metathesis reaction was rerun with added benzoquinone (**Scheme 3.16**). This time, no double bond migration was seen, and self-metathesis to the *trans* alkene was observed, along with **3.9** formed from initial reaction with the catalyst. However, if any of the expected diene **3.8** formed, its peaks were overshadowed by the other species on <sup>1</sup>H NMR,<sup>55</sup> so must have been present in less than 10%, at best offering no improvement over the bis-acetate **3.2**.



**Scheme 3.16** Reaction of bis-TBSO butene with DPVC3 in the presence of benzoquinone

Two electronically-neutral alkenes, *trans*-stilbene and 1-hexene, and one electron-poor alkene, butyl acrylate, were each separately attempted in the metathesis reaction with DPVC3. In none of the three cases was the expected diene product observed. The low reactivity of the conjugated double bonds in DPVC likely requires a reactive, electron-rich alkene in order to react.

**Table 3.7** Effect of changing olefin partner on the metathesis reaction

Condition	MW of oligomers <sup>a</sup> (kDa)	Diene formed? <sup>b</sup>
(standard conditions) DAB	3.0 ± 1.3	Yes
Bis-TBSO butene	Not measured	No
Trans-stilbene	2.8	No
1-hexene	2.3	No
Butyl acrylate	5.4	No

<sup>a</sup>Determined by GPC vs. polystyrene standards. ± Values are from duplicate reactions.

Values without ± are from one reaction. <sup>b</sup>Determined by <sup>1</sup>H NMR of reaction mixture.

### 3.11 Effect of Other Conditions

#### 3.11.1 Temperature and Solvent

**Table 3.8** Effect of temperature and solvent on olefin metathesis reaction

Condition	MW of oligomers <sup>a</sup> (kDa)	Diene formed? <sup>b</sup>
(standard conditions) DCM reflux	3.0 ± 1.3	Yes
1,2-dichloroethane, 55 °C	1.9 ± 0.2	Yes
CHCl <sub>3</sub> , 55 °C	1.8 ± 0.3	Yes

<sup>a</sup>Determined by GPC vs. polystyrene standards. ± Values are from duplicate reactions.

Values without ± are from one reaction. <sup>b</sup>Determined by <sup>1</sup>H NMR of reaction mixture.

Previous investigations by Tuba showed temperatures higher than 40 °C led to more effective metathesis on conjugated alkenes.<sup>39</sup> However, raising the temperature from 40 to 55 °C in either 1,2-dichloroethane (DCE) or CHCl<sub>3</sub> gave similar results to refluxing DCM.

### 3.11.2 Catalyst

**Table 3.9** Effect of olefin metathesis catalyst on product

Condition	MW of oligomers <sup>a</sup> (kDa)	Diene formed? <sup>b</sup>
(standard conditions) 5% Grubbs 2	3.0 ± 1.3	Yes
5% Hoveyda Grubbs 2	4.6	Yes
5% Grubbs 3	7.2	No
1% Grubbs 2	10.8	No

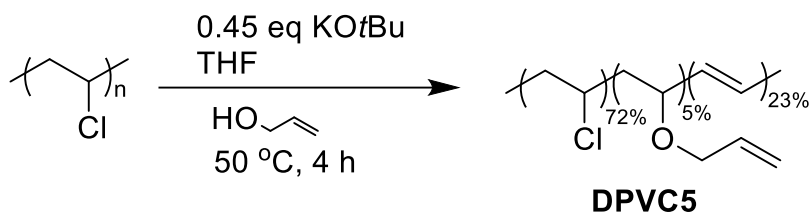
<sup>a</sup>Determined by GPC vs. polystyrene standards. ± Values are from duplicate reactions.

Values without ± are from one reaction. <sup>b</sup>Determined by <sup>1</sup>H NMR of reaction mixture.

The Grubbs 3 and Hoveyda Grubbs 2 catalysts proved less effective than Grubbs 2. Decreasing the catalyst loading of Grubbs 2 from 5% to 1% gave worse results.

### 3.11.3 Oxygen and light

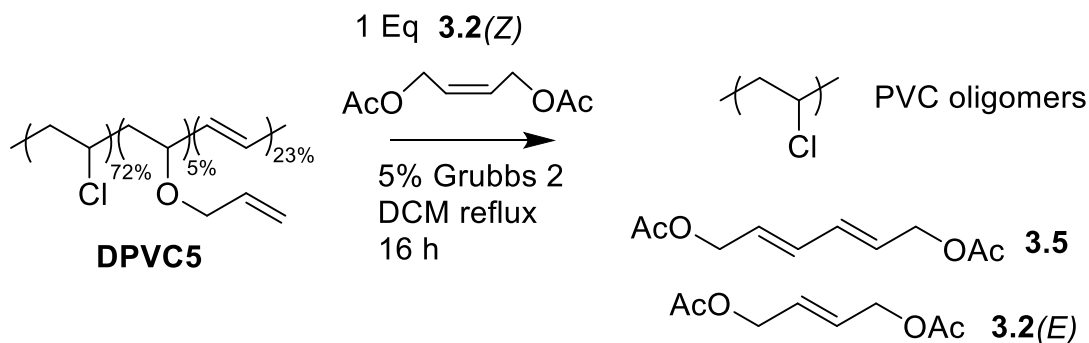
It is possible that competing S<sub>N</sub>2 by hydroxide could introduce OH groups on the polymer backbone, interrupting the double bonds without providing a reactive site. To avoid this possibility, a separate elimination was performed using potassium *tert*-butoxide as the base in anhydrous THF/allyl alcohol (**DPVC5**).



**Scheme 3.17** Elimination of PVC using potassium *tert*-butoxide

DPVC5 was characterized by GPC, NMR, and UV-vis. The NMR spectrum appeared quite similar to DPVC3, giving the composition shown in **Scheme 3.17**. UV-vis showed the same conjugation length of 4-13 double bonds as the other allylDPVC samples. GPC revealed a molecular weight of  $10.9 \pm 0.2$  kDa, which is likely artificially low due to the removal of precipitates by filtration.

DPVC5 was exposed to the standard metathesis reaction conditions, with added alkene **3.2** and Grubbs 2 catalyst (**Scheme 3.18**). Similar to DPVC3, a small amount of **3.5** was produced, and similar molecular weight oligomers were formed (**Table 3.10**).

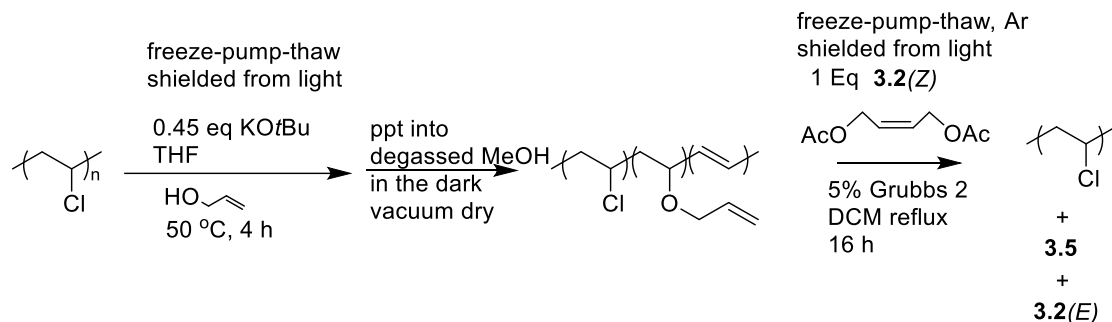


**Scheme 3.18** Olefin metathesis reaction on DPVC5

Polyacetylene is sensitive to oxygen, degrading into a mixture of products. Oxidation of the polyacetylene segments may contribute to the low amount of diene **3.5** formed. To avoid possible oxidative degradation, metathesis was performed on a fresh DPVC sample in the dark under argon atmosphere (freeze-pump-thaw),



immediately after the elimination reaction (**Scheme 3.19**). Similar amounts of diene **3.5** and similar molecular weights for the PVC oligomers were observed compared to the standard conditions (**Table 3.10**).



**Scheme 3.19** Dehydrochlorination and immediate metathesis on PVC shielded from oxygen and light

**Table 3.10** Effect of removing oxygen and light, and preventing OH substitution

Condition	MW of oligomers <sup>a</sup> (kDa)	Diene formed? <sup>b</sup>
(standard conditions) DPVC3, degassed by bubbling N <sub>2</sub>	3.0 ± 1.3	Yes
DPVC5, degassed by bubbling N <sub>2</sub>	3.8	Yes
Freshly prepared DPVC5, freeze-pump-thaw, shielded from light	3.0	Yes

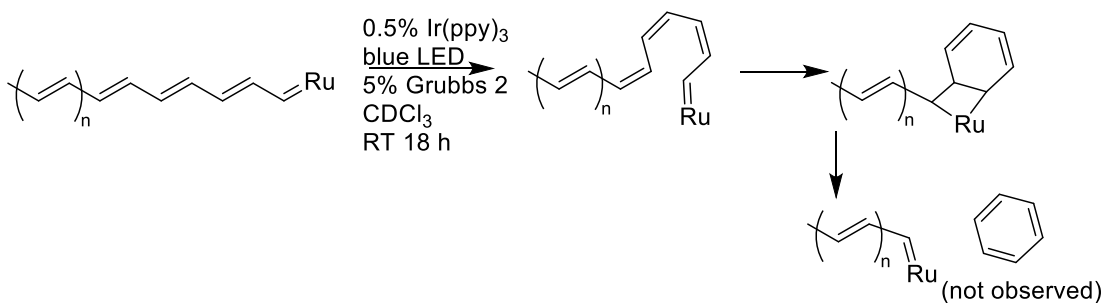
<sup>a</sup>Determined by GPC vs. polystyrene standards. ± Values are from duplicate reactions.

Values without ± are from one reaction. <sup>b</sup>Determined by <sup>1</sup>H NMR of reaction mixture.

### 3.12 Other attempted reactions

Multiple authors<sup>41,42,56</sup> have observed benzene formation from backbiting during metathesis of polyacetylene. However, benzene was not detected in our experiments by crude NMR, or in reactions in an NMR tube specifically looking for

benzene. This may be explained by the fact *cis* double bonds are required for benzene formation, while dehydrochlorinated PVC likely contains *trans* double bonds. The Ir(ppy)<sub>3</sub> catalyst was shown in the literature to isomerize some conjugated double bonds from *trans* to *cis*.<sup>57</sup> Attempts to combine Ir(ppy)<sub>3</sub> with Grubbs 2 and DPVC in one pot under blue light did not produce benzene under unoptimized conditions.



**Scheme 3.20** Attempted one-pot isomerization/metathesis to form benzene

Because the oligomers obtained are predominately PVC, they should be able to undergo a second partial elimination, followed by a second metathesis step to break them down further. Attempts to perform elimination on the oligomers using the same conditions used for PVC were unsuccessful. Resulting products after the second elimination were either too fully eliminated, forming polyacetylene, or difficult to isolate by precipitation, due to their lower molecular weight and due to the small amount of material used. A scale-up of the metathesis reaction would be needed, followed by a new optimization of the elimination reaction.

### 3.13 Conclusion

We have successfully demonstrated that elimination of HCl followed by olefin cross metathesis with an added alkene effectively cleaves the all-carbon backbone of

PVC to create much lower molecular weight oligomers. Using 1,4-diacetoxy-2-butene as an added olefin, the expected diene product was produced, providing a proof of concept for harvesting carbon from PVC. Given the paucity of upcycling options for PVC, the third-largest commodity plastic, this work provides an entry for the use of olefin metathesis to create new products from PVC waste.

### 3.14 References

- <sup>1</sup> Skelly, P. W.; Fuentes Chang, C.; Braslau, R. Degradation of Polyvinyl Chloride by Sequential Dehydrochlorination and Olefin Metathesis. *Chempluschem* **2023**, *88* (e202300184). <https://doi.org/10.1002/cplu.202300184>.
- <sup>2</sup> Geyer, R.; Jambeck, J. R.; Law, K. L. Production, Use, and Fate of All Plastics Ever Made. *Sci. Adv.* **2017**, *3* (7), 25–29. <https://doi.org/10.1126/sciadv.1700782>.
- <sup>3</sup> Sadat-Shojai, M.; Bakhshandeh, G. R. Recycling of PVC Wastes. *Polym. Degrad. Stab.* **2011**, *96* (4), 404–415. <https://doi.org/10.1016/j.polymdegradstab.2010.12.001>.
- <sup>4</sup> Braun, D. Recycling of PVC. *Prog. Polym. Sci.* **2002**, *27* (10), 2171–2195. [https://doi.org/10.1016/S0079-6700\(02\)00036-9](https://doi.org/10.1016/S0079-6700(02)00036-9).
- <sup>5</sup> Lewandowski, K.; Skórczewska, K. A Brief Review of Poly(Vinyl Chloride) (PVC) Recycling. *Polymers (Basel)*. **2022**, *14* (15), 3035. <https://doi.org/10.3390/polym14153035>.
- <sup>6</sup> Timeline on European Regulations on DEHP [https://pvcmed.org/wp-content/uploads/2020/08/DEHP\\_Timeline\\_5.pdf](https://pvcmed.org/wp-content/uploads/2020/08/DEHP_Timeline_5.pdf), accessed Oct 10, 2022.
- <sup>7</sup> CPSC Prohibits Certain Phthalates in Children’s Toys and Child Care Products <https://www.cpsc.gov/Newsroom/News-Releases/2018/CPSC-Prohibits-Certain-Phthalates-in-Childrens-Toys-and-Child-Care-Products>, accessed Dec 16, 2022.
- <sup>8</sup> Sherwood, J. Closed-loop recycling of polymers using solvents; remaking plastics for a circular economy *Johnson Matthey Technol. Rev.*, **2020**, *64*, 4-15. <https://doi.org/10.1595/205651319X15574756736831>

<sup>9</sup> Vinyloop

[https://www.plasteurope.com/news/Closure\\_of\\_operation\\_in\\_Italy\\_Phthalates\\_issue\\_und%20er\\_REACH\\_brings\\_do\\_t240095/](https://www.plasteurope.com/news/Closure_of_operation_in_Italy_Phthalates_issue_und%20er_REACH_brings_do_t240095/), accessed Oct 10, 2022.

<sup>10</sup> Impact of lead restrictions on the recycling of PVC [https://vinylplus.eu/wp-content/uploads/2021/06/2013\\_07\\_13-impact\\_lead-restrictions\\_pvc\\_recycling-tauw.pdf](https://vinylplus.eu/wp-content/uploads/2021/06/2013_07_13-impact_lead-restrictions_pvc_recycling-tauw.pdf), accessed Dec 16, 2022.

<sup>11</sup> Martin, A. J.; Mondelli, C.; Jaydev, S. D.; Perez Ramirez, J. Catalytic Processing of Plastic Waste on the Rise. *Chem* **2021**, *7* (6), 1487–1533. <https://doi.org/10.1016/j.chempr.2020.12.006>.

<sup>12</sup> Hou, Q.; Zhen, M.; Qian, H.; Nie, Y.; Bai, X.; Xia, T. Upcycling and Catalytic Degradation of Plastic Wastes. *Cell Reports Phys. Sci.* **2021**, *2* (8), 1–30. <https://doi.org/10.1016/j.xcrp.2021.100514>.

<sup>13</sup> Zakharyan, E. M.; Petrukhina, N. N.; Maksimov, A. L. Pathways of Chemical Recycling of Polyvinyl Chloride: Part 1. *Russ. J. Appl. Chem.* **2020**, *93* (9), 1271–1313. <https://doi.org/10.1134/S1070427220090013>.

<sup>14</sup> Zakharyan, E. M.; Petrukhina, N. N.; Dzhubarov, E. G.; Maksimov, A. L. Pathways of Chemical Recycling of Polyvinyl Chloride. Part 2. *Russ. J. Appl. Chem.* **2020**, *93* (10), 1445–1490. <https://doi.org/10.1134/S1070427220100018>.

<sup>15</sup> Sorensen, E.; Bjerre, A. B. Combined Wet Oxidation and Alkaline Hydrolysis of Polyvinylchloride. *Waste Manag.* **1992**, *12*, 349–354. [https://doi.org/10.1016/0956-053X\(92\)90037-J](https://doi.org/10.1016/0956-053X(92)90037-J).

- <sup>16</sup> Lv, B.; Zhao, G.; Li, D.; Liang, C. Dechlorination and Oxidation for Waste Poly (Vinylidene Chloride) by Hydrothermal Catalytic Oxidation on Pd / AC Catalyst. *Polym. Degrad. Stab.* **2009**, *94*, 1047–1052. <https://doi.org/10.1016/j.polymdegradstab.2009.04.004>.
- <sup>17</sup> Miao, F.; Liu, Y.; Gao, M.; Yu, X.; Xiao, P.; Wang, M.; Wang, S.; Wang, X. Degradation of Polyvinyl Chloride Microplastics via an Electro-Fenton-like System with a TiO<sub>2</sub>/Graphite Cathode. *J. Hazard. Mater.* **2020**, *399* (May), 1–9. <https://doi.org/10.1016/j.jhazmat.2020.123023>.
- <sup>18</sup> Yoshioka, T.; Furukawa, K.; Okuwaki, A. Chemical Recycling of Rigid-PVC by Oxygen Oxidation in NaOH Solutions at Elevated Temperatures. *Polym. Degrad. Stab.* **2000**, *67*, 285–290. [https://doi.org/10.1016/S0141-3910\(99\)00128-7](https://doi.org/10.1016/S0141-3910(99)00128-7).
- <sup>19</sup> Yoshioka, T.; Furukawa, K.; Sato, T.; Okuwaki, A. Chemical Recycling of Flexible PVC by Oxygen Oxidation in NaOH Solutions at Elevated Temperatures. *J. Appl. Polym. Sci.* **1998**, *70*, 129–135. [https://doi.org/10.1002/\(SICI\)1097-4628\(19981003\)70:1%3C129::AID-APP13%3E3.0.CO;2-2](https://doi.org/10.1002/(SICI)1097-4628(19981003)70:1%3C129::AID-APP13%3E3.0.CO;2-2).
- <sup>20</sup> Okuda, K.; Yanagisawa, K.; Moritaka, S.; Onda, A. Solubilization of Dechlorinated Poly (Vinyl Chloride) in Water by Wet Oxidation. *Polym. Degrad. Stab.* **2003**, *79*, 105–110. [https://doi.org/10.1016/S0141-3910\(02\)00262-8](https://doi.org/10.1016/S0141-3910(02)00262-8).

- <sup>21</sup> Partenheimer, W. Valuable Oxygenates by Aerobic Oxidation of Polymers Using Metal / Bromide Homogeneous Catalysts. *Catal. Today* **2003**, *81*, 117–135. [https://doi.org/10.1016/S0920-5861\(03\)00124-X](https://doi.org/10.1016/S0920-5861(03)00124-X).
- <sup>22</sup> Qi, Y.; He, J.; Xiu, F. R.; Nie, W.; Chen, M. Partial Oxidation Treatment of Waste Polyvinyl Chloride in Critical Water: Preparation of Benzaldehyde/Acetophenone and Dechlorination. *J. Clean. Prod.* **2018**, *196*, 331–339. <https://doi.org/10.1016/j.jclepro.2018.06.074>.
- <sup>23</sup> Kurashima, K.; Kumagai, S.; Kameda, T.; Saito, Y.; Yoshioka, T. Heavy Metal Removal from Municipal Solid Waste Fly Ash through Chloride Volatilization Using Poly (Vinyl Chloride) as Chlorinating Agent. *J. Mater. Cycles Waste Manag.* **2020**, *22* (4), 1270–1283. <https://doi.org/10.1007/s10163-020-01021-6>.
- <sup>24</sup> Lu, L.; Zhong, H.; Wang, T.; Wu, J.; Jin, F.; Yoshioka, T. A New Strategy for CO<sub>2</sub> Utilization with Waste Plastics: Conversion of Hydrogen Carbonate into Formate Using Polyvinyl Chloride in Water. *Green Chem.* **2020**, *22* (2), 352–358. <https://doi.org/10.1039/c9gc02484k>.
- <sup>25</sup> Watson, M. D.; Wagener, K. B. Acyclic Diene Metathesis (ADMET) Depolymerization: Ethenolysis of 1,4-Polybutadiene Using a Ruthenium Complex. *J. Polym. Sci. Part A Polym. Chem.* **1999**, *37* (12), 1857–1861. [https://doi.org/10.1002/\(SICI\)1099-0518\(19990615\)37:12<1857::AID-POLA15>3.0.CO;2-C](https://doi.org/10.1002/(SICI)1099-0518(19990615)37:12<1857::AID-POLA15>3.0.CO;2-C).

- <sup>26</sup> Smith, R. F.; Boothroyd, S. C.; Thompson, R. L.; Khosravi, E. A Facile Route for Rubber Breakdown via Cross Metathesis Reactions. *Green Chem.* **2016**, *18* (11), 3448–3455. <https://doi.org/10.1039/c5gc03075g>.
- <sup>27</sup> Solanky, S. S.; Campistrone, I.; Laguerre, A.; Pilard, J. F. Metathetic Selective Degradation of Polyisoprene: Low-Molecular-Weight Telechelic Oligomer Obtained from Both Synthetic and Natural Rubber. *Macromol. Chem. Phys.* **2005**, *206* (10), 1057–1063. <https://doi.org/10.1002/macp.200400416>.
- <sup>28</sup> Gutiérrez, S.; Tlenkopatchev, M. A. Metathesis of Renewable Products: Degradation of Natural Rubber via Cross-Metathesis with  $\beta$ -Pinene Using Ru-Alkylidene Catalysts. *Polym. Bull.* **2011**, *66* (8), 1029–1038. <https://doi.org/10.1007/s00289-010-0330-x>.
- <sup>29</sup> Ouardad, S.; Peruch, F. Metathetic Degradation of Trans-1,4-Polyisoprene with Ruthenium Catalysts. *Polym. Degrad. Stab.* **2014**, *99* (1), 249–253. <https://doi.org/10.1016/j.polymdegradstab.2013.10.022>.
- <sup>30</sup> Martínez, A.; Gutiérrez, S.; Tlenkopatchev, M. A. Citrus Oils as Chain Transfer Agents in the Cross-Metathesis Degradation of Polybutadiene in Block Copolymers Using Ru-Alkylidene Catalysts. *Nat. Sci.* **2013**, *05* (07), 857–864. <https://doi.org/10.4236/ns.2013.57103>.
- <sup>31</sup> Schulz, M. D.; Ford, R. R.; Wagener, K. B. Insertion Metathesis Depolymerization. *Polym. Chem.* **2013**, *4* (13), 3656–3658. <https://doi.org/10.1039/c3py00531c>.
- <sup>32</sup> Zeng, M.; Lee, Y. H.; Strong, G.; Lapointe, A. M.; Kocen, A. L.; Qu, Z.; Coates, G. W.; Scott, S. L.; Abu-Omar, M. M. Chemical Upcycling of Polyethylene to Value-



Added  $\alpha,\omega$ -Divinyl-Functionalized Oligomers. *ACS Sustain. Chem. Eng.* **2021**, *9* (41), 13926–13936. <https://doi.org/10.1021/acssuschemeng.1c05272>.

<sup>33</sup> Jia, X.; Qin, C.; Friedberger, T.; Guan, Z.; Huang, Z. Efficient and Selective Degradation of Polyethylenes into Liquid Fuels and Waxes under Mild Conditions. *Sci. Adv.* **2016**, *2* (6), 1–8. <https://doi.org/10.1126/sciadv.1501591>.

<sup>34</sup> Ellis, L. D.; Orski, S. V.; Kenlaw, G. A.; Norman, A. G.; Beers, K. L.; Román-Leshkov, Y.; Beckham, G. T. Tandem Heterogeneous Catalysis for Polyethylene Depolymerization via an Olefin-Intermediate Process. *ACS Sustain. Chem. Eng.* **2021**, *9* (2), 623–628. <https://doi.org/10.1021/acssuschemeng.0c07612>.

<sup>35</sup> Khunsriya, P.; Wootthikanokkhan, J.; Seeponkai, N.; Luangchaisri, C. Preparation of Dehydrochlorinated Poly (Vinyl Chloride) (DHPVC) and DHPVC Nanofibres : Effects of Reaction Time on Conductivity , Electrospinnability , and Fibre Morphology. *Polym. Polym. Compos.* **2014**, *22* (7), 581–591. <https://doi.org/10.1177/096739111402200701>.

<sup>36</sup> Glas, D.; Hulsbosch, J.; Dubois, P.; Binnemans, K.; Vos, D. E. De. End-of-Life Treatment of Poly (Vinyl Chloride) and Chlorinated Polyethylene by Dehydrochlorination in Ionic Liquids. **2014**, 610–617. <https://doi.org/10.1002/cssc.201300970>.

- <sup>37</sup> Guo, L.; Shi, G.; Liang, Y. Poly (Ethylene Glycol) s Catalyzed Homogeneous Dehydrochlorination of Poly (Vinyl Chloride) with Potassium Hydroxide. *Polymer (Guildf)*. **2001**, *42*, 5581–5587. [https://doi.org/10.1016/S0032-3861\(01\)00037-4](https://doi.org/10.1016/S0032-3861(01)00037-4).
- <sup>38</sup> Park, E. J.; Park, B. C.; Kim, Y. J.; Canlier, A.; Hwang, T. S. Elimination and Substitution Compete During Amination of Poly(Vinyl Chloride) with Ethylenediamine: XPS Analysis and Approach of Active Site Index. *Macromol. Res.* **2018**, *26* (10), 913–923. <https://doi.org/10.1007/s13233-018-6123-z>.
- <sup>39</sup> Balla, Á.; Al-Hashimi, M.; Hlil, A.; Bazzi, H. S.; Tuba, R. Ruthenium-Catalyzed Metathesis of Conjugated Polyenes. *ChemCatChem* **2016**, *8* (18), 2865–2875. <https://doi.org/10.1002/cctc.201600479>
- <sup>40</sup> Bunz, U. H. F.; Mäker, D.; Porz, M. Alkene Metathesis - A Tool for the Synthesis of Conjugated Polymers. *Macromol. Rapid Commun.* **2012**, *33* (10), 886–910. <https://doi.org/10.1002/marc.201200001>.
- <sup>41</sup> Scherman, O. A.; Rutenberg, I. M.; Grubbs, R. H. Direct Synthesis of Soluble, End-Functionalized Polyenes and Polyacetylene Block Copolymers. *J. Am. Chem. Soc.* **2003**, *125* (28), 8515–8522. <https://doi.org/10.1021/ja0301166>
- <sup>42</sup> Shin, S.; Yoon, K. Y.; Choi, T. L. Simple Preparation of Various Nanostructures via in Situ Nanoparticlization of Polyacetylene Blocklike Copolymers by One-Shot Polymerization. *Macromolecules* **2015**, *48* (5), 1390–1397. <https://doi.org/10.1021/ma502530x>.

- <sup>43</sup> Yoon, K. Y.; Lee, I. H.; Kim, K. O.; Jang, J.; Lee, E.; Choi, T. L. One-Pot in Situ Fabrication of Stable Nanocaterpillars Directly from Polyacetylene Diblock Copolymers Synthesized by Mild Ring-Opening Metathesis Polymerization. *J. Am. Chem. Soc.* **2012**, *134* (35), 14291–14294. <https://doi.org/10.1021/ja305150c>.
- <sup>44</sup> Francová, D.; Kickelbick, G. Synthesis of Methacrylate-Functionalized Phosphonates and Phosphates with Long Alkyl-Chain Spacers and Their Self-Aggregation in Aqueous Solutions. *Monatshefte für Chemie* **2009**, *140* (4), 413–422. <https://doi.org/10.1007/s00706-008-0045-y>.
- <sup>45</sup> Chatterjee, A. K.; Choi, T. L.; Sanders, D. P.; Grubbs, R. H. A General Model for Selectivity in Olefin Cross Metathesis. *J. Am. Chem. Soc.* **2003**, *125* (37), 11360–11370. <https://doi.org/10.1021/ja0214882>.
- <sup>46</sup> Saxman, A. M.; Liepins, R.; Aldissi, M. Polyacetylene: Its Synthesis, Doping and Structure. *Prog. Polym. Sci.* **1985**, *11* (1–2), 57–89. [https://doi.org/10.1016/0079-6700\(85\)90008-5](https://doi.org/10.1016/0079-6700(85)90008-5).
- <sup>47</sup> Bolton, S. L.; Schuehler, D. E.; Niu, X.; Gopal, L.; Sponsler, M. B. Olefin Metathesis for Metal Incorporation: Preparation of Conjugated Ruthenium-Containing Complexes and Polymers. *J. Organomet. Chem.* **2006**, *691* (24–25), 5298–5306. <https://doi.org/10.1016/j.jorganchem.2006.08.085>.

- <sup>48</sup> Hong, S. H.; Day, M. W.; Grubbs, R. H. Decomposition of a Key Intermediate in Ruthenium-Catalyzed Olefin Metathesis Reactions. *J. Am. Chem. Soc.* **2004**, *126* (24), 7414–7415. <https://doi.org/10.1021/ja0488380>.
- <sup>49</sup> von Czapiewski, M.; Kreye, O.; Mutlu, H.; Meier, M. A. R. Cross-Metathesis versus Palladium-Catalyzed C-H Activation: Acetoxy Ester Functionalization of Unsaturated Fatty Acid Methyl Esters. *Eur. J. Lipid Sci. Technol.* **2013**, *115* (1), 76–85. <https://doi.org/10.1002/ejlt.201200196>.
- <sup>50</sup> Bengough, W. I.; Varma, I. K. The Thermal Degradation of Polyvinylchloride in Solution - IV Changes in Absorption Spectra During Degradation. *Eur. Polym. J.* **1966**, *2*, 61–77. [https://doi.org/10.1016/0014-3057\(66\)90061-9](https://doi.org/10.1016/0014-3057(66)90061-9).
- <sup>51</sup> Boone, M.A. and Hembre, R.T., Eastman Chemical Co, **2015**. *Low-pressure synthesis of cyclohexanedimethanol and derivatives*. U.S. Patent 9,115,155.
- <sup>52</sup> Turczel, G.; Kovács, E.; Csizmadia, E.; Nagy, T.; Tóth, I.; Tuba, R. One-Pot Synthesis of 1,3-Butadiene and 1,6-Hexanediol Derivatives from Cyclopentadiene (CPD) via Tandem Olefin Metathesis Reactions. *ChemCatChem* **2018**, *10* (21), 4884–4891. <https://doi.org/10.1002/cctc.201801088>.
- <sup>53</sup> Dow, M.; Marchetti, F.; Abrahams, K. A.; Vaz, L.; Besra, G. S.; Warriner, S.; Nelson, A. Modular Synthesis of Diverse Natural Product-Like Macrocycles: Discovery of Hits with Antimycobacterial Activity. *Chem. - A Eur. J.* **2017**, *23* (30), 7207–7211. <https://doi.org/10.1002/chem.201701150>.

- <sup>54</sup> Hong, S. H.; Sanders, D. P.; Lee, C. W.; Grubbs, R. H. Prevention of Undesirable Isomerization during Olefin Metathesis. *J. Am. Chem. Soc.* **2005**, *127* (49), 17160–17161. <https://doi.org/10.1021/ja052939w>.
- <sup>55</sup> Krasovskiy, A.; Tishkov, A.; Del Amo, V.; Mayr, H.; Knochel, P. Transition-Metal-Free Homocoupling of Organomagnesium Compounds. *Angew. Chemie - Int. Ed.* **2006**, *45* (30), 5010–5014. <https://doi.org/10.1002/anie.200600772>.
- <sup>56</sup> Klavetter, F. L.; Grubbs, R. H. Polycyclooctatetraene (Polyacetylene): Synthesis and Properties. *J. Am. Chem. Soc.* **1988**, *110* (23), 7807–7813. <https://doi.org/10.1021/ja00231a036>.
- <sup>57</sup> Singh, K.; Staig, S. J.; Weaver, J. D. Facile Synthesis of Z -Alkenes via Uphill Catalysis. *J. Am. Chem. Soc.* **2014**, *136* (14), 5275–5278. <https://doi.org/10.1021/ja5019749>.

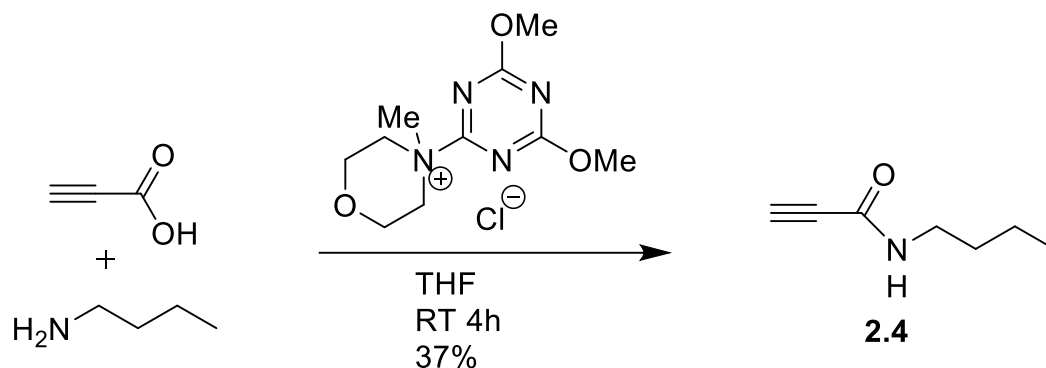
## **4 Experimental**

### **4.1 Experimental for Chapter 2**

#### **Materials and General Methods**

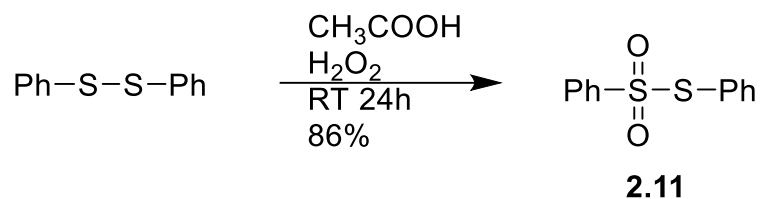
All reagents and solvents were used as received unless otherwise noted. Dry tetrahydrofuran (THF) was obtained by distillation over sodium and benzophenone. Dry CH<sub>2</sub>Cl<sub>2</sub> was obtained by distillation over CaH<sub>2</sub>. Nuclear Magnetic Resonance (NMR) spectra were recorded on a Bruker Avance III HD 4 channel 500 MHz Oxford Magnet NMR spectrometer with Automation. NOE experiments were recorded on a Bruker Avance III HD 800 MHz NMR Spectrometer with cryoprobe at 4 °C. FTIR spectra were taken in CDCl<sub>3</sub> and recorded with a Perkin Elmer Spectrum One spectrometer in NaCl microsolution cells. HRMS was recorded with a Thermo Scientific LTQ - Orbitrap Velos Pro Mass Spectrometer. Calculations were performed using the B3LYP functional and the 6-31G\* basis set using the Gaussian09 suite of software. Transition states were confirmed to have 1 negative frequency and energy minima were confirmed to have no negative frequencies. Energies were corrected for zero-point energies. Solvent was simulated using the polarizable continuum model (acetonitrile,  $\epsilon = 35.688$ ).

#### **Preparation of *N*-butylpropiolamide (2.4)**



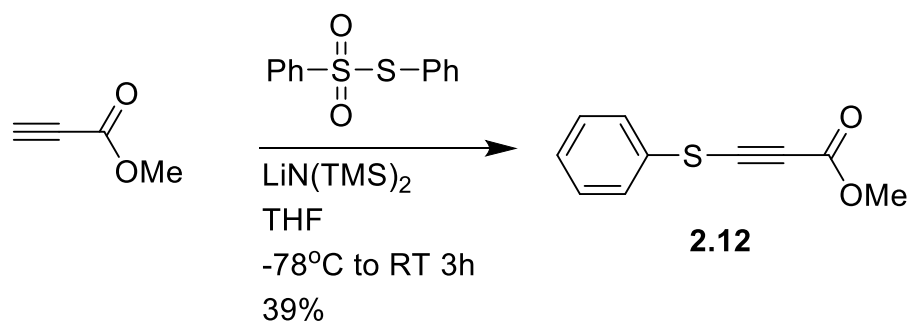
In a modified procedure of Kunishima,<sup>1</sup> a mixture of propiolic acid (140.1 mg, 2.000 mmol) and butylamine (160.9 mg, 2.199 mmol) in THF (10 mL) was stirred at room temperature for 10 min. 4-(4,6-Dimethoxy-1,3,5-triazin-2-yl)-4-methylmorpholinium chloride (DMTMM) (608.8 mg, 2.2 mmol) was added to the mixture and stirred at room temperature overnight. The next day, the reaction mixture was poured into water and extracted with diethyl ether (3 x 10mL). The combined organic phase was washed successively with saturated sodium carbonate (10 mL), water (10 mL), 1 M HCl (10 mL), water (10 mL), brine (10 mL) and dried over MgSO<sub>4</sub>. The crude product was purified by silica gel column using 3:2 hexanes:ethyl acetate to give 91.8 mg (36.7%) of *N*-butylpropiolamide as a colorless liquid. *R*<sub>f</sub> = 0.50 (3:2 hexanes:ethyl acetate, KMnO<sub>4</sub>); <sup>1</sup>H NMR (500 MHz, CDCl<sub>3</sub>): δ = 5.89 (bs, 1H), 3.33 (td, *J* = 7.2, 5.9 Hz, 2H), 2.79 (s, 1H), 1.54 (p, *J* = 7.4 Hz, 2H), 1.39 (h, *J* = 7.4 Hz, 2H), 0.95 (t, *J* = 7.3 Hz, 3H) ppm; <sup>13</sup>C{<sup>1</sup>H} and DEPT NMR (126 MHz, CDCl<sub>3</sub>): δ = 152.18 (C), 79.2 (apparent CH due to long-range coupling), 72.9 (CH), 39.6 (CH<sub>2</sub>), 31.2 (CH<sub>2</sub>), 20.0 (CH<sub>2</sub>), 13.6 (CH<sub>3</sub>) ppm; IR (NaCl, CDCl<sub>3</sub>): ν = 3437, 3302, 2114, 1659 cm<sup>-1</sup>; HRMS (ESI): *m/z* calcd for C<sub>7</sub>H<sub>12</sub>NO [M+H]<sup>+</sup> 126.0913, found 126.0924.

### Preparation of diphenyl thiosulfate (2.11)<sup>2</sup>



Following a modified procedure from Takeda,<sup>2</sup> diphenyl disulfide (3.70 g, 16.9 mmol) was dissolved in 27 mL of glacial acetic acid. Hydrogen peroxide (30% in water, 3.5 mL, 34 mmol) was added dropwise. The mixture was stirred for 24 h, diluted with water (50 mL), extracted with chloroform (2 x 50 mL), and washed with saturated sodium bicarbonate (50 mL). The organic layer was dried over sodium sulfate, and concentrated under vacuum to give the crude product. Purification by column chromatography (0 to 40% ethyl acetate in hexanes) gave the product as brown crystals: 3.68 g (86.9% yield). <sup>13</sup>C{<sup>1</sup>H} NMR (126 MHz, CDCl<sub>3</sub>): δ = 142.9, 136.6, 133.7, 131.45, 129.5, 128.9, 127.8, 127.5 ppm.

#### Preparation of methyl 3-(phenylsulfanyl)-2propynoate (2.12)<sup>2</sup>

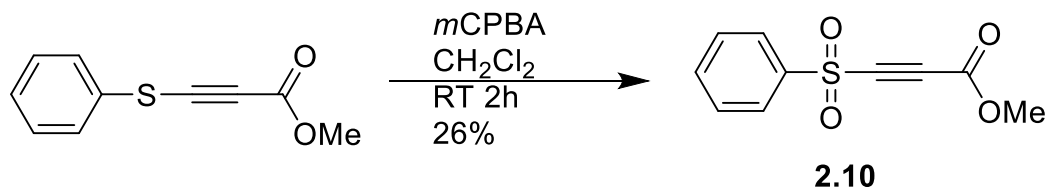


Following the procedure of Takeda,<sup>2</sup> methyl propiolate (0.93 mL, 10.5 mmol) was dissolved in 20 mL of dry THF at -78 °C. Lithium bis(trimethylsilyl)amide (1.3 M in THF, 8 mL, 10.5 mmol) was added and stirred for 30 min. Diphenyl thiosulfate (2.553



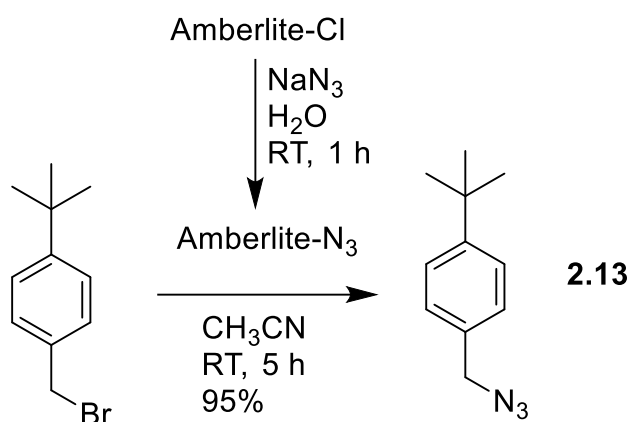
g, 10.20 mmol) in 20 mL dry THF was added dropwise. The mixture was warmed to room temperature and stirred for 2 h, then quenched with water (30 mL), and extracted with diethyl ether (2x 30 mL). The organic layer was dried over sodium sulfate and concentrated under vacuum to give the crude product which was purified by silica gel column chromatography to give a yellow oil: 784 mg, 39.9% yield.  $R_f = 0.76$  (1:4 ethyl acetate:hexanes, UV and  $\text{KMnO}_4$ ).  $^1\text{H NMR}$  (500 MHz,  $\text{CDCl}_3$ ):  $\delta = 7.50$  (d,  $J = 7.6$  Hz, 2H), 7.42 (t,  $J = 7.7$  Hz, 2H), 7.34 (t,  $J = 6.5$  Hz, 1H), 3.84 (s, 3H) ppm.

#### Preparation of Methyl 3-(phenylsulfonyl)-2-propynoate (2.10)<sup>2</sup>



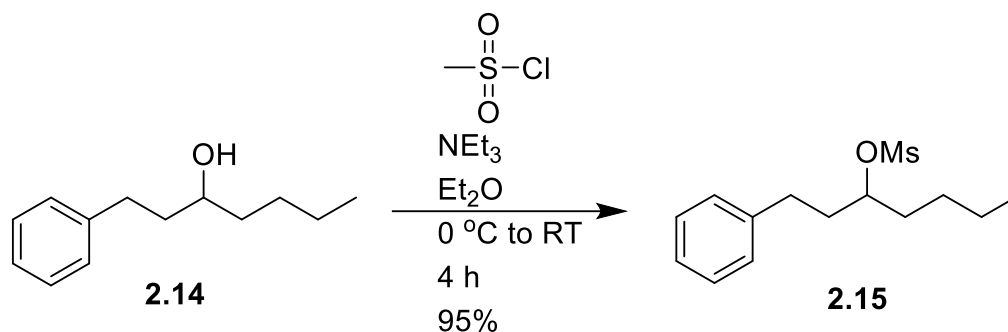
Following the procedure of Takeda,<sup>2</sup> methyl 3-(phenylsulfonyl)-2-propynoate (600 mg, 3.12 mmol) was dissolved in 20 mL of  $\text{CH}_2\text{Cl}_2$ . *m*CPBA (3.0 g, 55% by weight, 9.6 mmol) dissolved in 40 mL of  $\text{CH}_2\text{Cl}_2$  was added. The solution was stirred for 2 h, then quenched with solid  $\text{NaHSO}_3$  (2 g), washed with saturated aqueous  $\text{NaHCO}_3$  (2 x 20 mL), and extracted with  $\text{CH}_2\text{Cl}_2$  (2 x 10 mL). The crude product was purified by silica gel column chromatography (ethyl acetate/hexanes) to give 180.8 mg of a yellow oil, 25.8% yield.  $R_f = 0.37$  (1:4 ethyl acetate:hexanes, UV and  $\text{KMnO}_4$ );  $^1\text{H NMR}$  (500 MHz,  $\text{CDCl}_3$ ):  $\delta = 8.04$  (d,  $J = 7.1$  Hz, 2H), 7.77 (t,  $J = 7.5$  Hz, 1H), 7.65 (t,  $J = 7.9$  Hz, 2H), 3.84 ppm (s, 3H) ppm.

### Preparation of 4-*t*-butylbenzyl azide (2.13).<sup>3</sup>



NaN<sub>3</sub> (15 g, 230.73 mmol) was dissolved in 80 mL of water, then stirred with 40 g of Amberlite<sup>®</sup> IRA-400 for 1 h. The resulting beads were filtered, washed with water (80 mL) and EtOH (50 mL) to give charged Amberlite-N<sub>3</sub>. 4-*t*-Butylbenzyl bromide (4.02 g, 17.7 mmol) and Amberlite-N<sub>3</sub> (40 g) were combined in CH<sub>3</sub>CN (60 mL) and stirred for 5 h at room temperature. The reaction was monitored by TLC. Mixture was filtered, the filtrate was concentrated under vacuum, dissolved in Et<sub>2</sub>O, dried over MgSO<sub>4</sub> and concentrated under vacuum, yielding 3.178 g of slightly yellow liquid (94.9% yield). R<sub>f</sub> = 0.85 (4:1 hexanes/ethyl acetate UV); <sup>1</sup>H NMR (500 MHz, CDCl<sub>3</sub>): δ = 7.44 (d, *J* = 8.0 Hz, 1H), 7.28 (d, *J* = 8.1 Hz, 1H), 4.34 (s, 1H), 1.36 (s, 4H) ppm.

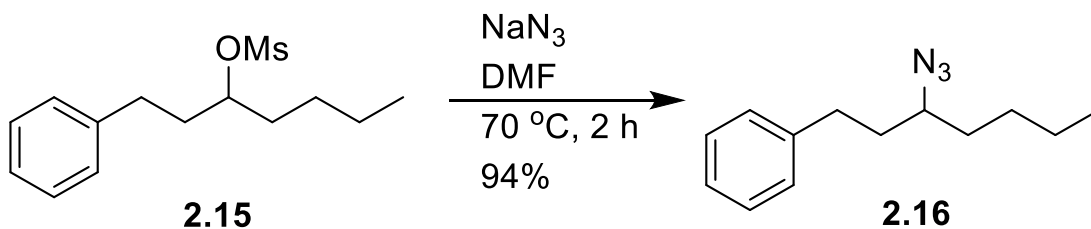
### Preparation of 1-Phenylheptan-3-yl methanesulfonate (2.15)



To a solution of 3-hydroxy-1-phenylheptane (633 mg, 3.29 mmol) and NEt<sub>3</sub> (0.55 mL, 4.0 mmol) in Et<sub>2</sub>O (5 mL) at 0 °C was dropwise added methanesulfonyl chloride (0.30 mL, 3.9 mmol). The reaction mixture was warmed to room temperature and stirred for 4 h. The reaction mixture was diluted with brine (20 mL) and extracted with Et<sub>2</sub>O (3x 20 mL). The combined organic layers were dried over MgSO<sub>4</sub> and concentrated under vacuum to give 906 mg (94.6%) of the product as a colorless liquid.

R<sub>f</sub> = 0.53 (4:1 hexanes:ethyl acetate, UV); <sup>1</sup>H NMR (500 MHz, CDCl<sub>3</sub>): δ = 7.32 (t, *J* = 7.5 Hz, 2H), 7.23 (m, 3H), 4.79 (tt, *J* = 4.1, 9.2 Hz, 1H), 3.02 (s, 3H), 2.75 (m, 2H), 2.04 (m, 2H), 1.78 (m, 2H), 1.38 (m, 2H), 0.94 (t, *J* = 7.0 Hz, 3H) ppm; <sup>13</sup>C{<sup>1</sup>H} and DEPT NMR (126 MHz, CDCl<sub>3</sub>): δ = 140.9(C), 128.53(CH), 128.33(CH), 126.15(CH), 83.41(CH<sub>3</sub>), 38.74(CH), 36.14(CH<sub>2</sub>), 34.22(CH<sub>2</sub>), 31.30(CH<sub>2</sub>), 27.01(CH<sub>2</sub>), 22.46(CH<sub>2</sub>), 13.90 (CH<sub>3</sub>) ppm; IR (NaCl, CDCl<sub>3</sub>): ν = 1353, 1333, 1174 cm<sup>-1</sup>; HRMS (ESI): *m/z* calcd for C<sub>14</sub>H<sub>22</sub>SO<sub>3</sub>Na [M+Na]<sup>+</sup> 293.1182, found 293.1177.

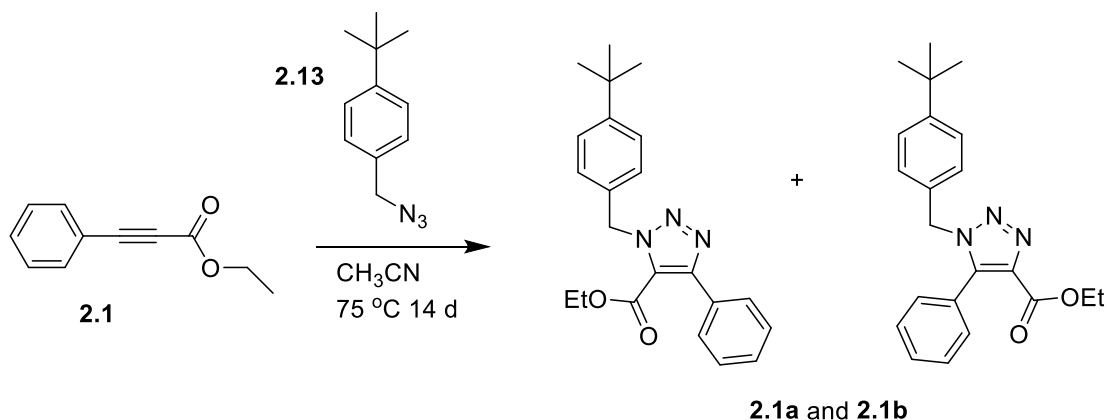
#### Preparation of 3-azido-1-phenylheptane (2.16)<sup>4</sup>



In a modified procedure of Earla,<sup>4</sup> to a solution of 1-phenylheptan-3-yl methanesulfonate (291 mg, 1.00 mmol) in DMF (5 mL) under nitrogen was added NaN<sub>3</sub> (196.0 mg, 3.015 mmol). The mixture was heated to 70 °C and stirred for 2 h. The reaction was cooled to room temperature, brine (15 mL) was added, and the product was extracted with Et<sub>2</sub>O (3x 15 mL). The combined organic extracts were washed with brine (3x 30 mL), dried over MgSO<sub>4</sub>, and concentrated under vacuum to give 204 mg (93.8%) of the product as a colorless liquid. <sup>1</sup>H NMR (500 MHz, CDCl<sub>3</sub>): δ=7.32 (t, *J* = 7.2 Hz, 2H), 7.23 (t, *J* = 7.2 Hz, 1H), 7.22 (d, *J* = 7.2 Hz, 2H), 3.27 (tt, *J* = 7.2, 5.4 Hz, 1H), 2.82 (m, 1H), 2.71 (m, 1H), 1.85 (m, 2H), 1.58 (m, 2H), 1.45 (m, 1H), 1.36 (m, 3H), 0.94 (t, *J* = 7.1 Hz, 3H) ppm.

### Preparation of Authentic Triazoles

**Ethyl 1-(4-*t*-butylbenzyl)-5-phenyl-1,2,3-triazole-4-carboxylate and Ethyl 1-(4-*t*-butylbenzyl)-4-phenyl-1,2,3-triazole-5-carboxylate, 2.1a and 2.1b**



Ethyl phenylpropiolate (188.5 mg, 1.082 mmol) and 4-*t*-butylbenzyl azide (306.5 mg, 1.619 mmol) were combined in 2 mL of CH<sub>3</sub>CN and heated to 75 °C for 14 days. The product was purified by silica gel column chromatography (5% to 40% ethyl acetate in hexanes) to give 293.3 mg (74.58%) of the two regioisomeric triazole products, separable: 185.4 mg of **2.1a** as a clear oil, and 111.9 mg of **2.1b** as a white powder.

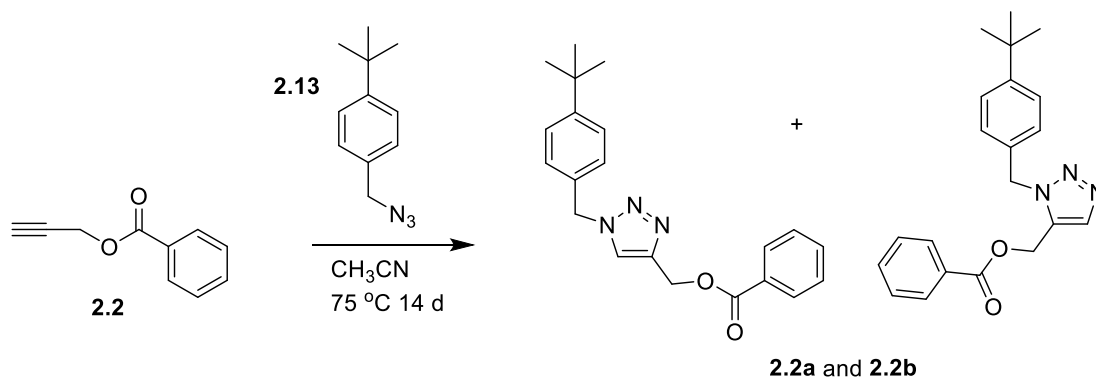
**2.1a** (regioisomer not identified):

Clear liquid.  $R_f = 0.67$  (4:1 hexanes:ethyl acetate, UV); <sup>1</sup>H NMR (500 MHz, CDCl<sub>3</sub>):  $\delta = 7.78 - 7.68$  (m, 2H), 7.47 – 7.42 (m, 3H), 7.38 (d,  $J = 8.4$  Hz, 2H), 7.31 (d,  $J = 8.1$  Hz, 2H), 5.93 (s, 2H), 4.29 (q,  $J = 7.2$  Hz, 2H), 1.32 (s, 9H), 1.20 (t,  $J = 7.1$  Hz, 3H) ppm; <sup>13</sup>C{<sup>1</sup>H} and DEPT NMR (126 MHz, CDCl<sub>3</sub>):  $\delta = 159.2$ (C), 151.4(C), 150.4(C), 132.2(C), 130.4(C), 129.4(CH), 128.9(CH), 127.9(CH), 127.8(CH), 125.7(CH), 124.1(C), 61.8(CH<sub>2</sub>), 53.8(CH<sub>2</sub>), 34.6(C), 31.3(CH<sub>3</sub>), 13.7 (CH<sub>3</sub>) ppm; IR (NaCl, CDCl<sub>3</sub>)  $\nu = 1720$  cm<sup>-1</sup>; HRMS (ESI):  $m/z$  calcd for C<sub>22</sub>H<sub>26</sub>N<sub>3</sub>O<sub>2</sub> [M+H]<sup>+</sup> 364.2020, found 364.2047.

**2.1b** (regioisomer not identified):

White powder.  $R_f = 0.29$  (4:1 hexanes:ethyl acetate, UV); m.p. 70-71 °C;  $^1\text{H NMR}$  (500 MHz,  $\text{CDCl}_3$ ):  $\delta = 7.52$  (t,  $J = 7.4$  Hz, 1H), 7.46 (t,  $J = 7.3$  Hz, 2H), 7.28 (d,  $J = 8.3$  Hz, 2H), 7.24 (d,  $J = 6.9$  Hz, 2H), 6.97 (d,  $J = 8.2$  Hz, 2H), 5.41 (s, 2H), 4.31 (q,  $J = 7.1$  Hz, 2H), 1.29 (s, 9H), 1.27 (t,  $J = 7.2$  Hz, 3H) ppm;  $^{13}\text{C}\{^1\text{H}\}$  and DEPT NMR (126 MHz,  $\text{CDCl}_3$ ):  $\delta = 161.0(\text{C})$ , 151.5(C), 141.2(C), 137.1(C), 131.6(C), 130.0(CH), 129.9(CH), 128.5(CH), 127.4(CH), 126.1(C), 125.7(CH), 60.9(CH<sub>2</sub>), 51.9(CH<sub>2</sub>), 34.6(C), 31.2(CH<sub>3</sub>), 14.1 (CH<sub>3</sub>) ppm; IR (NaCl,  $\text{CDCl}_3$ ):  $\nu = 1725$   $\text{cm}^{-1}$ ; HRMS (ESI):  $m/z$  calcd for  $\text{C}_{22}\text{H}_{26}\text{N}_3\text{O}_2$   $[\text{M}+\text{H}]^+$  364.2020, found 364.2012.

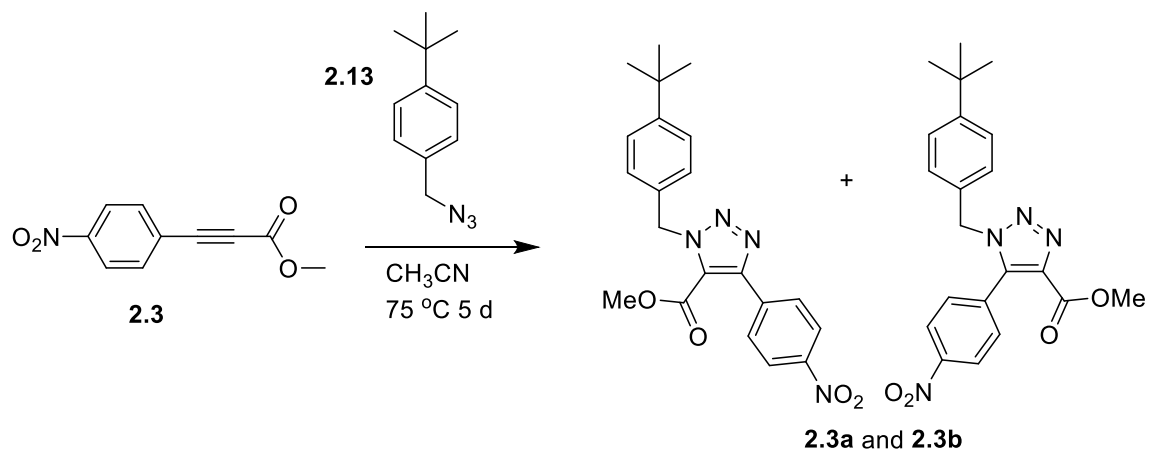
**1-(4-*t*-butylbenzyl)-1,2,3-triazol-4-ylmethyl benzoate and 1-(4-*t*-butylbenzyl)-1,2,3-triazol-5-ylmethyl benzoate, 2.2a and 2.2b**



Propargyl benzoate (24.0 mg, 0.149 mmol) and 4-*t*-butylbenzyl azide (41.4 mg, 0.219 mmol) were combined in 2 mL of  $\text{CH}_3\text{CN}$  and heated to  $75^\circ\text{C}$  for 14 days. Attempts to separate the two regioisomers by column chromatography were unsuccessful, providing 11.49 mg (22.1% yield) of the mixture (6.8 : 1 ratio by  $^1\text{H NMR}$ ) as a white powder.  $R_f = 0.27, 0.21$  (4:1 hexanes:ethyl acetate, UV);  $^1\text{H NMR}$  of major isomer (500 MHz,  $\text{CDCl}_3$ ):  $\delta = 8.05$  (dd,  $J = 7.8, 1.5$  Hz, 2H), 7.63 (s, 1H), 7.57 (t,  $J = 7.5$  Hz, 1H),

7.45 (t,  $J = 7.8$  Hz, 2H), 7.42 (d,  $J = 8.4$  Hz, 2H), 7.25 (d,  $J = 8.2$  Hz, 2H), 5.51 (s, 2H), 5.47 (s, 2H), 1.33 (s, 9H), ppm;  $^1\text{H}$  NMR of minor isomer (500 MHz,  $\text{CDCl}_3$ ):  $\delta = 7.93$  (d,  $J = 7.0$  Hz 2H), 7.84 (s, 1H), 7.34 (d,  $J = 8.2$  Hz, 2H), 7.16 (d,  $J = 8.1$  Hz, 2H), 5.68 (s, 2H), 5.31 (s, 2H), 1.28 (s, 9H) ppm;  $^{13}\text{C}\{^1\text{H}\}$  and DEPT NMR of major isomer (126 MHz,  $\text{CDCl}_3$ ):  $\delta = 166.4(\text{C})$ , 152.0(C), 143.3 (C), 133.2(CH), 131.3(C), 129.77(C), 129.75(CH), 128.4(CH), 128.0(CH), 126.1(CH), 123.8(CH), 58.1 ( $\text{CH}_2$ ), 54.0( $\text{CH}_2$ ), 34.7(C), 31.3( $\text{CH}_3$ ), ppm;  $^{13}\text{C}\{^1\text{H}\}$  and DEPT NMR of minor isomer (126 MHz,  $\text{CDCl}_3$ ):  $\delta = 165.7(\text{C})$ , 151.6(C), 143.3 (C), 133.6(CH), 131.4(C), 129.70(CH), 129.0(C), 128.5(CH), 127.1(CH), 126.0(CH), 123.8 (C), 52.2( $\text{CH}_2$ ), 54.1( $\text{CH}_2$ ), 34.6(C), 31.2( $\text{CH}_3$ ) ppm; IR (NaCl,  $\text{CDCl}_3$ ):  $\nu = 1719\text{ cm}^{-1}$ ; HRMS (ESI):  $m/z$  calcd for  $\text{C}_{21}\text{H}_{24}\text{N}_3\text{O}_2$  (M+H) 350.1863, found 350.1889.

**Methyl 1-(4-*t*-butylbenzyl)-5-(4-nitrophenyl)-1,2,3-triazole-4-carboxylate and Methyl 1-(4-*t*-butylbenzyl)-4-(4-nitrophenyl)-1,2,3-triazole-5-carboxylate 2.3a and 2.3b**



A solution of methyl (4-nitrophenyl)propiolate (26.7 mg, 0.13 mmol) and *t*-butylbenzyl azide (36.0 mg, 0.19 mmol) dissolved in 2.0 mL CH<sub>3</sub>CN was heated to 75 °C. TLC was checked at 120 h (5 days) and indicated that the reaction was done. The mixture was purified by column chromatography (19:1 to 4:1 hexanes:ethyl acetate) to afford 46.3 mg (0.093 mmol, 93%) of triazole product, separable: (20.8 mg of **2.3a**, 25.5 mg of **2.3b**).

**2.3a** (regioisomer not identified):

Brown crystals, R<sub>f</sub> = 0.43 (4:1 hexanes:ethyl acetate, UV); m.p. 132-136 °C; <sup>1</sup>H NMR (500 MHz, CDCl<sub>3</sub>): δ = 8.31 (d, *J* = 8.6 Hz, 2H), 7.95 (d, *J* = 8.6 Hz, 2H), 7.40 (d, *J* = 8.3 Hz, 2H), 7.32 (d, *J* = 8.2 Hz, 2H), 5.94 (s, 2H), 3.86 (s, 3H), 1.32 (s, 9H) ppm; <sup>13</sup>C{<sup>1</sup>H} and DEPT NMR (126 MHz, CDCl<sub>3</sub>): δ = 159.0(C), 151.8(C), 148.3(C), 148.0(C), 136.7(C), 131.7(C), 130.2(CH), 127.8(CH), 125.8(CH), 124.7(C), 123.3(CH), 54.2(CH<sub>2</sub>), 52.6(CH<sub>3</sub>), 34.6(C), 31.3(CH<sub>3</sub>) ppm; IR (NaCl, CDCl<sub>3</sub>): ν = 1731, 1524, 1348 cm<sup>-1</sup>; HRMS (ESI): m/z calcd for C<sub>21</sub>H<sub>23</sub>N<sub>4</sub>O<sub>4</sub> [M+H]<sup>+</sup> 395.1715, found 395.1706.

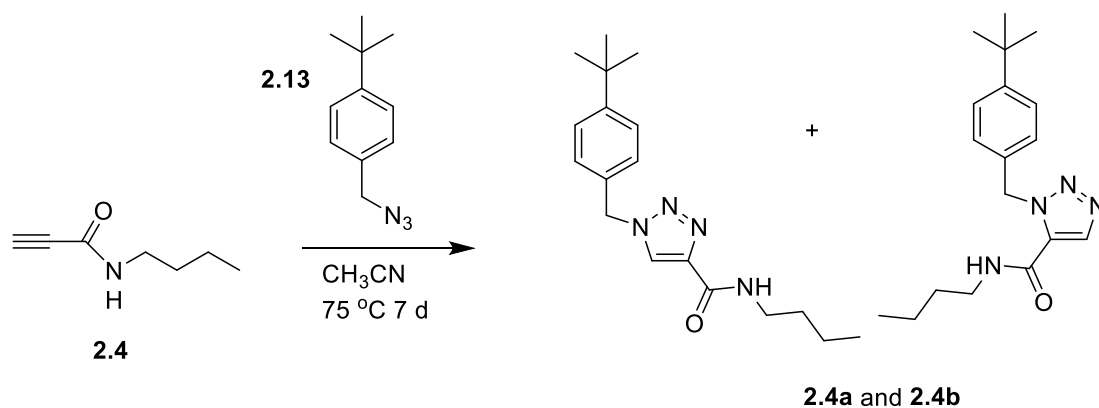
**2.3b** (regioisomer not identified):

Yellow crystals. R<sub>f</sub> = 0.12 (4:1 hexanes:ethyl acetate, UV); m.p. 147-148 °C; <sup>1</sup>H NMR (500 MHz, CDCl<sub>3</sub>): δ = 8.30 (d, *J* = 8.6 Hz, 2H), 7.40 (d, *J* = 8.6 Hz, 2H), 7.29 (d, *J* = 8.8 Hz, 2H), 6.93 (d, *J* = 8.0 Hz, 2H), 5.45 (s, 2H), 3.87 (s, 3H), 1.30 (s, 9H) ppm; <sup>13</sup>C{<sup>1</sup>H} and DEPT NMR (126 MHz, CDCl<sub>3</sub>): δ = 161.0(C), 152.1(C), 148.7(C), 139.1(C), 137.4(C), 132.6(C), 131.1(CH), 130.9(C), 127.3(CH), 126.0(CH), 123.6(CH), 52.5(CH<sub>2</sub>), 52.2(CH<sub>3</sub>), 34.6(C), 31.2 (CH<sub>3</sub>) ppm; IR (NaCl, CDCl<sub>3</sub>): ν =



1730, 1528, 1350  $\text{cm}^{-1}$ ; HRMS (ESI):  $m/z$  calcd for  $\text{C}_{21}\text{H}_{23}\text{N}_4\text{O}_4$   $[\text{M}+\text{H}]^+$  395.1715, found 395.1704.

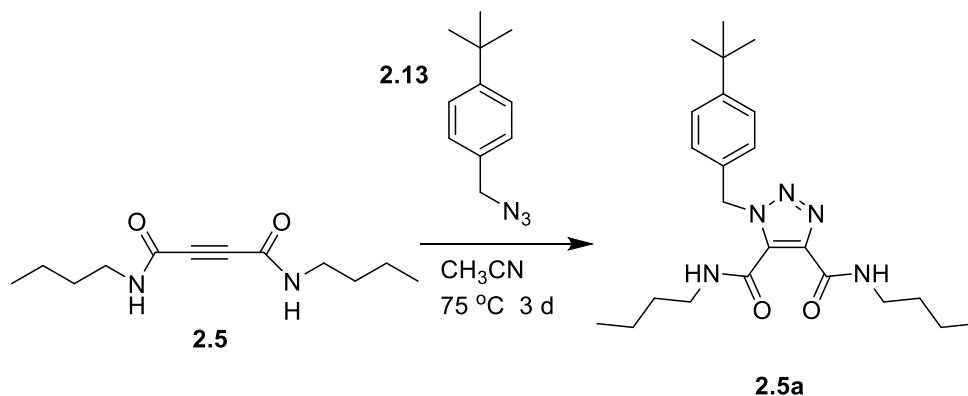
***N*-butyl 1-(4-*t*-butylbenzyl)-1,2,3-triazole-4-carboxamide and *N*-butyl 1-(4-*t*-butylbenzyl)-1,2,3-triazole-5-carboxamide, 2.4a and 2.4b**



solution of *n*-butyl propiolamide (20.0 mg, 0.160 mmol) and *t*-butylbenzyl azide (45.4 mg, 0.240 mmol) dissolved in 2.0 mL of  $\text{CHCl}_3$  was heated to  $75^\circ\text{C}$ . The reaction was monitored by TLC. After 168 h (7 days), the reaction was complete. Attempts to separate the two regioisomers by column chromatography were unsuccessful, providing 44.0 mg (0.139 mmol, 86.8%) of the triazole mixture (2.2 : 1 ratio of isomers by  $^1\text{H}$ NMR) as a brown liquid.  $R_f = 0.07, 0.21$  ( $\text{CH}_2\text{Cl}_2$ , UV);  $^1\text{H}$  NMR of major isomer (500 MHz,  $\text{CDCl}_3$ ):  $\delta = 7.41$  (d,  $J = 8.0$  Hz, 2H), 7.24 (d,  $J = 8.0$  Hz, 2H), 5.52 (s, 2H), 3.44 (q,  $J = 6.7$  Hz, 2H), 1.60 (p,  $J = 7.3$  Hz, 2H), 1.42 (h,  $J = 6.9$  Hz, 3H), 1.33 (s, 9H), 0.95 ppm (t,  $J = 7.3$  Hz, 3H);  $^1\text{H}$  NMR of minor isomer (500 MHz,  $\text{CDCl}_3$ ):  $\delta = 7.33$  (d,  $J = 2.2$  Hz, 2H), 5.91 (s, 2H), 3.39 (q,  $J = 6.8$  Hz, 2H), 1.52 (q,  $J = 7.5$  Hz, 2H), 1.29 (s, 9H), 0.93 ppm (t,  $J = 7.4$  Hz, 3H);  $^{13}\text{C}\{^1\text{H}\}$  and DEPT NMR of major isomer (126

MHz, CDCl<sub>3</sub>):  $\delta$  = 160.0(C), 152.3(C), 143.7(C), 132.4(C), 130.7(C), 128.2(CH), 126.2(CH), 54.2(CH<sub>2</sub>), 38.9(CH<sub>2</sub>), 34.7(C), 31.6(CH<sub>2</sub>), 31.23(CH), 20.05(CH<sub>2</sub>), 13.72(CH<sub>3</sub>) ppm; <sup>13</sup>C{<sup>1</sup>H} and DEPT NMR of minor isomer (126 MHz, CDCl<sub>3</sub>):  $\delta$  = 158.0(C), 151.3(C), 133.4(C), 133.3(C), 128.1(CH), 125.6(CH), 125.2(CH), 52.7(CH<sub>2</sub>), 39.5(CH<sub>2</sub>), 34.5(C), 31.4(CH<sub>2</sub>), 31.25(CH), 20.0(CH<sub>2</sub>), 13.70 (CH<sub>3</sub>); IR (NaCl, CDCl<sub>3</sub>):  $\nu$  = 3419, 1664 cm<sup>-1</sup>; HRMS (ESI): m/z calcd for C<sub>18</sub>H<sub>27</sub>N<sub>4</sub>O [M+H]<sup>+</sup> 315.2179, found 315.2209.

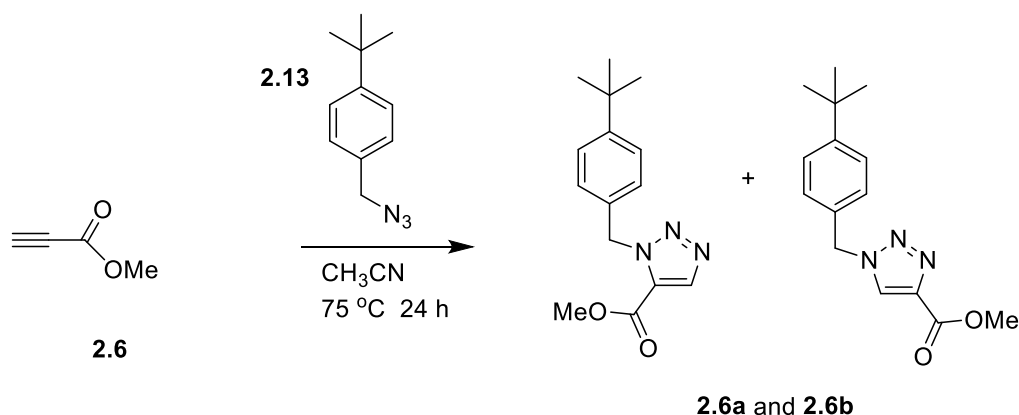
***N,N'*-Bis-(*n*-butyl) 1-(4-*t*-butylbenzyl)-1,2,3-triazole-4,5-dicarboxamide, 2.5a**



Bis-(*n*-butyl)-acetylenediamide (26.9 mg, 0.120 mmol) and *t*-butylbenzyl azide (34.1 mg, 0.180 mmol) were combined in 2 mL of CH<sub>3</sub>CN and heated to 75 °C. TLC was checked at 72 h and indicated that the reaction was complete. The mixture was purified by column chromatography (19:1 to 4:1 hexanes:ethyl acetate) to give 38.6 mg (0.0933 mmol, 77.8 %) of the title compound as white crystals. R<sub>f</sub> = 0.35 (9:1 hexanes:ethyl acetate, UV); m.p. 76-78 °C; <sup>1</sup>H NMR (500 MHz, CDCl<sub>3</sub>):  $\delta$  = 7.37 (d, *J* = 8.0 Hz, 2H), 7.35 (d, *J* = 8.0 Hz, 2H), 6.15 (s, 2H), 3.48 (q, *J* = 6.8 Hz, 2H), 3.42 (td, *J* = 7.2, 5.4

Hz, 2H), 1.64 (p,  $J = 7.1$  Hz, 2H), 1.63 (p,  $J = 7.1$  Hz, 2H), 1.45 (h,  $J = 7.5$  Hz, 2H), 1.40 (h,  $J = 7.5$  Hz, 2H) 1.30 (s, 9H), 0.98 (t,  $J = 7.4$  Hz, 3H), 0.96 (t,  $J = 7.4$  Hz, 3H) ppm;  $^{13}\text{C}\{^1\text{H}\}$  and DEPT NMR (126 MHz,  $\text{CDCl}_3$ ):  $\delta = 161.5(\text{C})$ ,  $156.6(\text{C})$ ,  $151.2(\text{C})$ ,  $138.7(\text{C})$ ,  $132.5(\text{C})$ ,  $130.8(\text{C})$ ,  $128.2(\text{CH})$ ,  $125.6(\text{CH})$ ,  $53.9(\text{CH}_2)$ ,  $39.4(\text{CH}_2)$ ,  $39.3(\text{CH}_2)$ ,  $34.5(\text{C})$ ,  $31.4(\text{CH}_2)$ ,  $31.3(\text{CH}_3)$ ,  $31.2(\text{CH}_2)$ ,  $20.2(\text{CH}_2)$ ,  $20.1(\text{CH}_2)$ ,  $13.8(\text{CH}_3)$ ,  $13.7(\text{CH}_3)$  ppm; IR (NaCl,  $\text{CDCl}_3$ ):  $\nu = 3409$ ,  $3221$ ,  $1672$ ,  $1649\text{ cm}^{-1}$ ; HRMS (ESI):  $m/z$  calcd for  $\text{C}_{23}\text{H}_{36}\text{N}_5\text{O}_2$   $[\text{M}+\text{H}]^+$  414.2865, found 414.2855.

**Methyl 1-(4-*t*-butylbenzyl)-1,2,3-triazole-4-carboxylate and methyl 1-(4-*t*-butylbenzyl)-1,2,3-triazole-5-carboxylate, 2.6a and 2.6b**



A solution of methyl propiolate (15.6 mg, 0.186 mmol) and *t*-butylbenzyl azide (49.4 mg, 0.261 mmol) dissolved in 2.0 mL of  $\text{CH}_3\text{CN}$  was heated to  $75^\circ\text{C}$ . TLC was checked at 24 h and indicated that the reaction was done. The mixture was purified by column chromatography (0% to 60% ethyl acetate in hexanes) to afford 25.4 mg (0.0929 mmol, 50.0%) total of two regioisomers, consisting of 5.5 mg of **2.6a**, and 19.9 mg of **2.6b**.

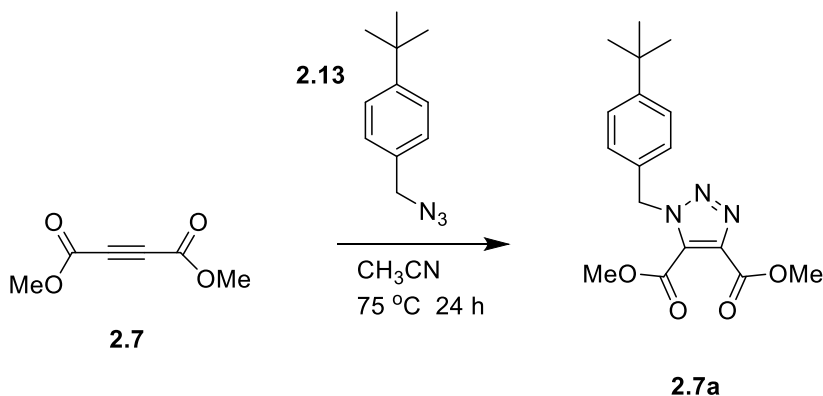
**2.6a** (regioisomer not identified):

Yellow liquid  $R_f = 0.36$  (4:1 hexanes:ethyl acetate, UV);  $^1\text{H NMR}$  (500 MHz,  $\text{CDCl}_3$ ):  $\delta = 8.15$  (s, 1H), 7.37 (d,  $J = 8.3$  Hz, 2H), 7.31 (d,  $J = 8.4$  Hz, 2H), 5.91 (s, 2H), 3.92 (s, 3H), 1.31 (s, 9H) ppm;  $^{13}\text{C}\{^1\text{H}\}$  and DEPT NMR (126 MHz,  $\text{CDCl}_3$ ):  $\delta = 158.9(\text{C})$ , 151.5(C), 131.9(C), 127.9(CH), 125.7(CH), 53.1( $\text{CH}_2$ ), 52.4( $\text{CH}_3$ ), 34.6(C), 31.3 ( $\text{CH}_3$ ) ppm; IR (NaCl,  $\text{CDCl}_3$ ):  $\nu = 1727\text{ cm}^{-1}$ ; HRMS (ESI):  $m/z$  calcd for  $\text{C}_{15}\text{H}_{20}\text{N}_3\text{O}_2$  (M+H) 274.1550, found 274.1578

**2.6b** (regioisomer not identified):

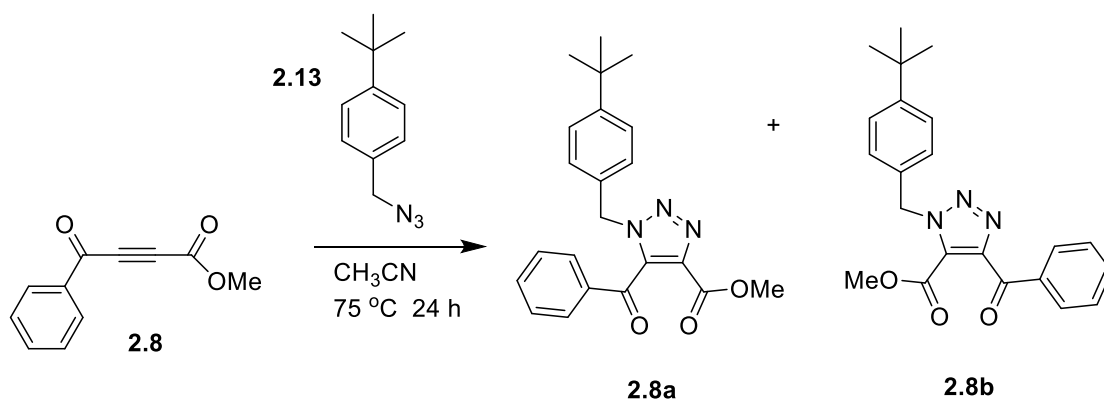
White crystals,  $R_f = 0.12$  (4:1 hexanes:ethyl acetate, UV); m.p. 120-121 °C;  $^1\text{H NMR}$  (500 MHz,  $\text{CDCl}_3$ ):  $\delta = 7.98$  (s, 1H), 7.43 (d,  $J = 8.4$  Hz, 2H), 7.25 (d,  $J = 8.3$  Hz, 2H), 5.56 (s, 2H), 3.94 (s, 3H), 1.34 (s, 9H) ppm;  $^{13}\text{C}\{^1\text{H}\}$  and DEPT NMR (126 MHz,  $\text{CDCl}_3$ ):  $\delta = 161.2(\text{C})$ , 152.4(C), 140.2(C), 130.6(C), 128.2(CH), 127.3(CH), 126.3(CH), 54.2( $\text{CH}_2$ ), 52.2( $\text{CH}_3$ ), 34.7(C), 31.2 ( $\text{CH}_3$ ) ppm; IR (NaCl,  $\text{CDCl}_3$ ):  $\nu = 1731\text{ cm}^{-1}$ ; HRMS (ESI):  $m/z$  calcd for  $\text{C}_{15}\text{H}_{20}\text{N}_3\text{O}_2$  (M+H) 274.1550, found 274.1576.

### Dimethyl 1-(4-*t*-butylbenzyl)-1,2,3-triazole-4,5-dicarboxylate, 2.7a



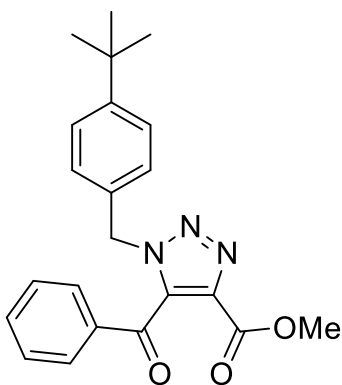
A solution of dimethyl acetylenedicarboxylate (21.1 mg, 0.15 mmol) and *t*-butylbenzyl azide (42.5 mg, 0.22 mmol) dissolved in 2.0 mL of CH<sub>3</sub>CN was heated to 75 °C. TLC was checked at 24 h and indicated that the reaction was done. The mixture was purified by column chromatography (10% to 70% ethyl acetate in hexanes) to afford 50.4 mg (0.15 mmol, 100%) of the title compound as a brown liquid. *R*<sub>f</sub> = 0.29 (4:1 hexanes:ethyl acetate, UV); <sup>1</sup>H NMR (500 MHz, CDCl<sub>3</sub>): δ = 7.36 (d, *J* = 8.0 Hz, 2H), 7.22 (d, *J* = 8.1 Hz, 2H), 5.78 (s, 2H), 3.96 (s, 3H), 3.89 (s, 3H), 1.30 ppm (s, 9H) ppm; <sup>13</sup>C{<sup>1</sup>H} and DEPT NMR (126 MHz, CDCl<sub>3</sub>) δ = 160.5(C), 158.9(C), 152.0(C), 140.1(C), 130.9(C), 129.8(C), 127.9(CH), 125.9(CH), 53.7(CH<sub>2</sub>), 53.3(CH<sub>3</sub>), 52.7(CH<sub>3</sub>), 34.6(C), 31.2 (CH<sub>3</sub>) ppm; IR (NaCl, CDCl<sub>3</sub>): ν = 1735 cm<sup>-1</sup>; HRMS (ESI): *m/z* calcd for C<sub>17</sub>H<sub>22</sub>N<sub>3</sub>O<sub>4</sub> [M+H]<sup>+</sup> 332.1605, found 332.1599.

**Methyl 1-(4-*t*-butylbenzyl)-5-phenyloxomethyl-1,2,3-triazole-4-carboxylate (2.8a) and Methyl 1-(4-*t*-butylbenzyl)-4-phenyloxomethyl-1,2,3-triazole-5-carboxylate (2.8b)**



A solution of methyl 4-oxo-4-phenyl-2-butynoate (26.0 mg, 0.138 mmol) and *t*-butylbenzyl azide (39.0 mg, 0.206 mmol) dissolved in 2.0 mL of CH<sub>3</sub>CN was heated to 75°C. TLC was checked at 24 h and showed that the reaction was done. The mixture was purified by column chromatography (10% to 40% ethyl acetate in hexanes) afforded 45.0 mg (0.125 mmol, 90.6%) total of product, which were separable: 22.0mg of **2.8a**, and 23.0 mg of **2.8b** as white solids.

**Regioisomer 2.8a:**

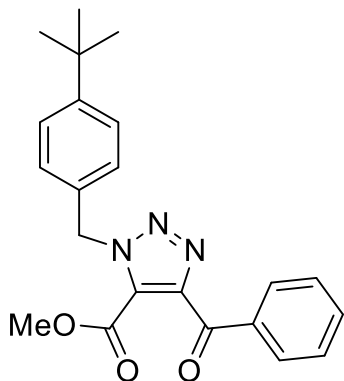


**2.8a**

White crystals,  $R_f = 0.31$  (4:1 hexanes:ethyl acetate, UV); m.p. 100-102 °C; <sup>1</sup>H NMR (500 MHz, CDCl<sub>3</sub>):  $\delta = 7.54$  (t,  $J = 7.4$  Hz, 1H), 7.46 (d,  $J = 8.5$  Hz, 2H), 7.32 (t,  $J = 7.7$  Hz, 2H), 7.13 (d,  $J = 8.1$  Hz, 2H), 7.06 (d,  $J = 8.1$  Hz, 2H), 5.60 (s, 2H), 3.69 (d,  $J = 0.7$  Hz, 3H), 1.16ppm (s, 9H); irradiation at 5.60 ppm results in NOE enhancement of signal at 7.46 ppm, but none at 3.69 ppm; <sup>13</sup>C{<sup>1</sup>H} and DEPT NMR (126 MHz, CDCl<sub>3</sub>):  $\delta = 186.7$ (C), 160.2(C), 152.0(C), 138.8(C), 137.1(C), 135.8(C), 134.5(CH), 130.3(C), 129.1(CH), 128.52(CH), 128.51(CH), 125.7(CH), 53.3(CH<sub>2</sub>), 52.2(CH<sub>3</sub>),

34.5(C), 31.1 (CH<sub>3</sub>) ppm; IR (NaCl, CDCl<sub>3</sub>):  $\nu = 1732, 1671 \text{ cm}^{-1}$ ; HRMS (ESI):  $m/z$  calcd for C<sub>22</sub>H<sub>24</sub>N<sub>3</sub>O<sub>3</sub> [M+H]<sup>+</sup> 378.1812, found 378.1802.

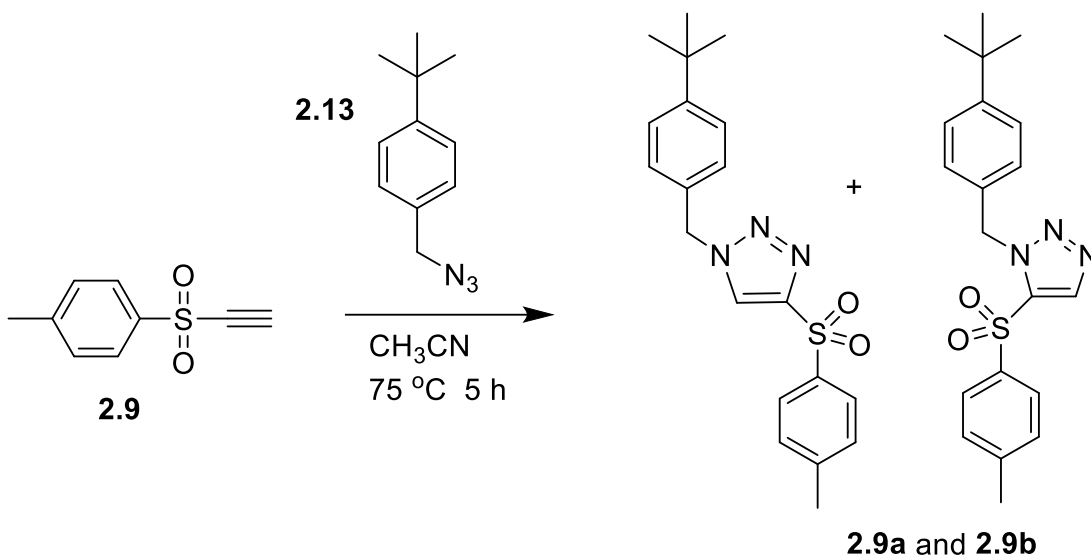
**Regioisomer 2.8b:**



**2.8b**

White crystals,  $R_f = 0.43$  (4:1 hexanes:ethyl acetate, UV); m.p. 99-105 °C; <sup>1</sup>H NMR (500 MHz, CDCl<sub>3</sub>):  $\delta = 8.08$  (dd,  $J = 8.3, 1.4$  Hz, 2H), 7.64 (t,  $J = 7.4$  Hz, 1H), 7.52 (t,  $J = 7.8$  Hz, 2H), 7.40 (d,  $J = 8.4$  Hz, 2H), 7.33 (d,  $J = 8.3$  Hz, 2H), 5.88 (s, 2H), 3.78 (s, 3H), 1.33 (s, 9H) ppm; <sup>13</sup>C {<sup>1</sup>H} and DEPT NMR (126 MHz, CDCl<sub>3</sub>):  $\delta = 186.6$ (C), 159.0(C), 151.9(C), 147.6(C), 136.3(C), 133.8(CH), 131.1(C), 130.4(CH), 128.8(CH), 128.5(C), 128.1(CH), 125.9(CH), 53.5(CH<sub>2</sub>), 53.0(CH<sub>3</sub>), 34.6(C), 31.3 (CH<sub>3</sub>) ppm; IR (NaCl, CDCl<sub>3</sub>):  $\nu = 1735, 1673 \text{ cm}^{-1}$ ; HRMS (ESI):  $m/z$  calcd for C<sub>22</sub>H<sub>24</sub>N<sub>3</sub>O<sub>3</sub> [M+H]<sup>+</sup> 378.1812, found 378.1806.

**1-(4-*t*-Butylbenzyl)-4-(4-methylphenylsulfonyl)-1,2,3-triazole** and **1-(4-*t*-butylbenzyl)-5-(4-methylphenylsulfonyl)-1,2,3-triazole, 2.9a and 2.9b**



Ethynyl *p*-tolylsulfone (24.8 mg, 0.138 mmol) and *t*-butylbenzyl azide (38.1 mg, 0.201 mmol) were dissolved in 2 mL of CH<sub>3</sub>CN and heated to 75 °C for 5 h. The mixture was cooled to 0 °C to produce 25.3 mg of **2.9b** as a white precipitate, then 6.8 mg of **2.9a** as a white solid was isolated by silica gel column chromatography (0% to 40% ethyl acetate in hexanes) to give 32.0 mg (63.0%) of total product.

**2.9a** (regioisomer not identified):

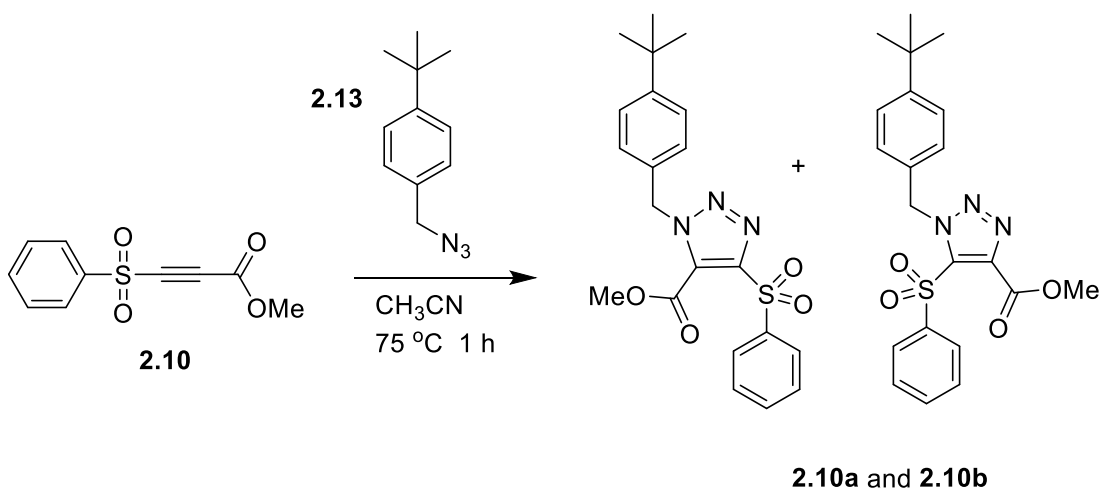
White solid. *R*<sub>f</sub> = 0.26 (4:1 hexanes:ethyl acetate, UV); m.p. 152-154 °C; <sup>1</sup>H NMR (500 MHz, CDCl<sub>3</sub>): δ = 8.11 (s, 1H), 7.53 (d, *J* = 8.4 Hz, 2H), 7.27 (d, *J* = 8.2 Hz, 2H), 7.16 (d, *J* = 8.2 Hz, 2H), 7.05 (d, *J* = 8.4 Hz, 2H), 5.82 (s, 2H), 2.39 (s, 3H), 1.31 (s, 9H) ppm; <sup>13</sup>C{<sup>1</sup>H} and DEPT NMR (126 MHz, CDCl<sub>3</sub>): δ = 151.6(C), 145.5(C), 137.7(CH), 137.3(C), 136.5(C), 130.8(C), 129.9(CH), 127.6(CH), 127.4(CH), 125.6(CH), 52.9(CH<sub>2</sub>), 34.6(C), 31.3(CH<sub>3</sub>), 21.7(CH<sub>3</sub>) ppm; IR (NaCl, CDCl<sub>3</sub>): ν = 1339, 1148 cm<sup>-1</sup>; HRMS (ESI): *m/z* calcd for C<sub>20</sub>H<sub>24</sub>N<sub>3</sub>SO<sub>2</sub> [M+H]<sup>+</sup> 370.1579, found 370.1573.

**2.9b** (regioisomer not identified):



White solid.  $R_f = 0.15$  (4:1 hexanes:ethyl acetate, UV); m.p. 252-255 °C;  $^1\text{H NMR}$  (500 MHz,  $\text{CDCl}_3$ ):  $\delta = 7.97$  (d,  $J = 8.4$  Hz, 2H), 7.95 (s, 1H), 7.45 (d,  $J = 8.2$  Hz, 2H), 7.35 (d,  $J = 8.2$  Hz, 2H), 7.25 (d,  $J = 8.4$  Hz, 2H), 5.51 (s, 2H), 2.44 (s, 3H), 1.35 (s, 9H) ppm;  $^{13}\text{C}\{^1\text{H}\}$  and DEPT NMR (126 MHz,  $\text{CDCl}_3$ ):  $\delta = 152.8(\text{C})$ , 149.5(C), 145.0(C), 137.1(C), 129.9(CH), 129.8(C), 128.4(CH), 128.2(CH), 126.4(CH), 125.4(CH), 54.6( $\text{CH}_2$ ), 34.8(C), 31.2( $\text{CH}_3$ ), 21.7( $\text{CH}_3$ ) ppm; IR (NaCl,  $\text{CDCl}_3$ ):  $\nu = 1331, 1158 \text{ cm}^{-1}$ ; HRMS (ESI):  $m/z$  calcd for  $\text{C}_{20}\text{H}_{24}\text{N}_3\text{SO}_2$   $[\text{M}+\text{H}]^+$  370.1579, found 370.1577.

**Methyl 1-(4-*t*-butylbenzyl)-5-phenylsulfonyl-1,2,3-triazole-4-carboxylate and Methyl 1-(4-*t*-butylbenzyl)-4-phenylsulfonyl-1,2,3-triazole-5-carboxylate, 2.10a and 2.10b**



Methyl 3-(phenylsulfonyl)-2-propynoate (28.1 mg, 0.12 mmol) and *t*-butylbenzyl azide (34.3 mg, 0.181 mmol) were dissolved in 2 mL of  $\text{CH}_3\text{CN}$  and heated to 75 °C for 1 h. The mixture was purified by silica gel column chromatography (5% to 40% ethyl acetate in hexanes), 19.2 mg (37.0%) (5.5 mg of **2.10a**, 13.7 mg of **2.10b**)

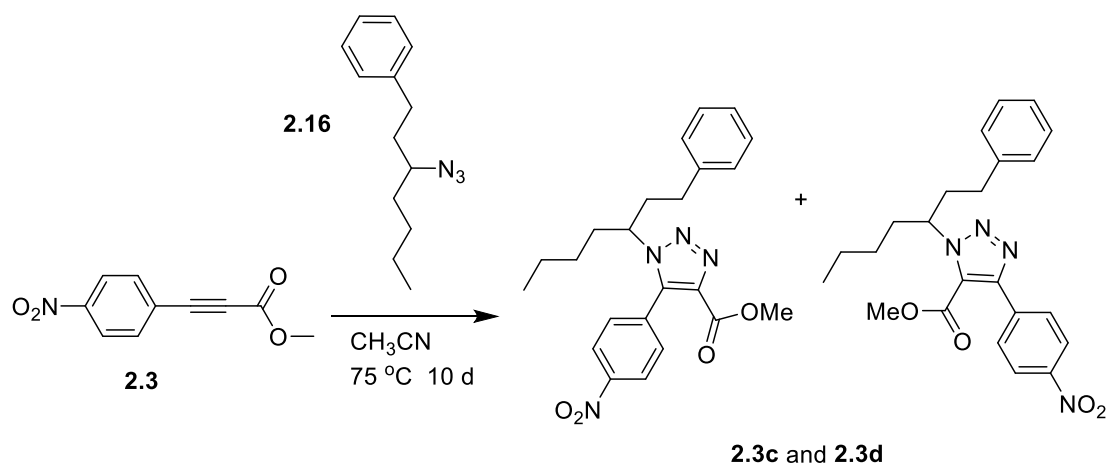
**2.10a** (regioisomer not identified):

Colorless crystals.  $R_f = 0.14$  (4:1 hexanes:ethyl acetate, UV); m.p. 99-113 °C;  $^1\text{H}$  NMR (500 MHz,  $\text{CDCl}_3$ ):  $\delta = 7.59$  (d,  $J = 7.1$  Hz, 2H), 7.54 (t,  $J = 7.4$  Hz, 1H), 7.36 (d,  $J = 8.4$  Hz, 2H), 7.31 (t,  $J = 8.3$  Hz, 2H), 7.19 (d,  $J = 8.2$  Hz, 2H), 6.09 (s, 2H), 3.96 (s, 3H), 1.35 (s, 9H) ppm;  $^{13}\text{C}\{^1\text{H}\}$  and DEPT NMR (126 MHz,  $\text{CDCl}_3$ ):  $\delta = 159.5(\text{C})$ , 152.1(C), 140.5(C), 139.0(C), 137.4(C), 134.5(CH), 131.1(C), 128.8(CH), 128.5(CH), 127.7(CH), 125.9(CH), 54.5(CH<sub>2</sub>), 52.9(CH), 34.7(C), 31.4 (CH<sub>3</sub>) ppm; IR (NaCl,  $\text{CDCl}_3$ ):  $\nu = 1742, 1350, 1172$  cm<sup>-1</sup>; HRMS (ESI): m/z calcd for C<sub>21</sub>H<sub>24</sub>N<sub>3</sub>SO<sub>4</sub> [M+H]<sup>+</sup> 414.1482, found 414.1518.

**2.10b** (regioisomer not identified):

Colorless viscous liquid.  $R_f = 0.17$  (4:1 hexanes:ethyl acetate, UV);  $^1\text{H}$  NMR (500 MHz,  $\text{CDCl}_3$ ):  $\delta = 8.09$  (d,  $J = 7.4$  Hz, 2H), 7.70 (t,  $J = 7.4$  Hz, 1H), 7.60 (t,  $J = 7.8$  Hz, 2H), 7.37 (d,  $J = 8.4$  Hz, 2H), 7.26 (d,  $J = 8.4$  Hz, 2H), 5.80 (s, 2H), 3.99 (s, 3H), 1.31 (s, 9H) ppm;  $^{13}\text{C}\{^1\text{H}\}$  and DEPT NMR (126 MHz,  $\text{CDCl}_3$ ):  $\delta = 157.6(\text{C})$ , 152.2(C), 149.4(C), 139.4(C), 134.2(CH), 130.4(C), 129.1(CH), 128.9(CH), 128.2(CH), 127.6(C), 125.9(CH), 54.2(CH<sub>2</sub>), 53.5(CH), 34.7(C), 31.2 (CH<sub>3</sub>) ppm; IR (NaCl,  $\text{CDCl}_3$ ):  $\nu = 1740, 1330, 1163$  cm<sup>-1</sup>; HRMS (ESI): m/z calcd for C<sub>21</sub>H<sub>24</sub>N<sub>3</sub>SO<sub>4</sub> [M+H]<sup>+</sup> 414.1482, found 414.1521.

**Methyl 1-(1-phenylheptan-3-yl)-5-(4-nitrophenyl)-1,2,3-triazole-4-carboxylate and methyl 1-(1-phenylheptan-3-yl)-4-(4-nitrophenyl)-1,2,3-triazole-5-carboxylate, 2.3c and 2.3d**



Methyl 4-nitrophenylpropiolate (26.8 mg, 0.131 mmol) and 3-azido-1-phenylheptane (41.2 mg, 0.190 mmol) were dissolved in 2 mL of CH<sub>3</sub>CN and heated to 75 °C for 10 days. The mixture was purified by silica gel column chromatography (0% to 40% ethyl acetate in hexanes) to give 35.1 mg (63.4%) of total product, 12.9 mg of **2.3c**, 22.2 mg of **2.3d** as colorless liquids.

**2.3c** (regioisomer not identified)

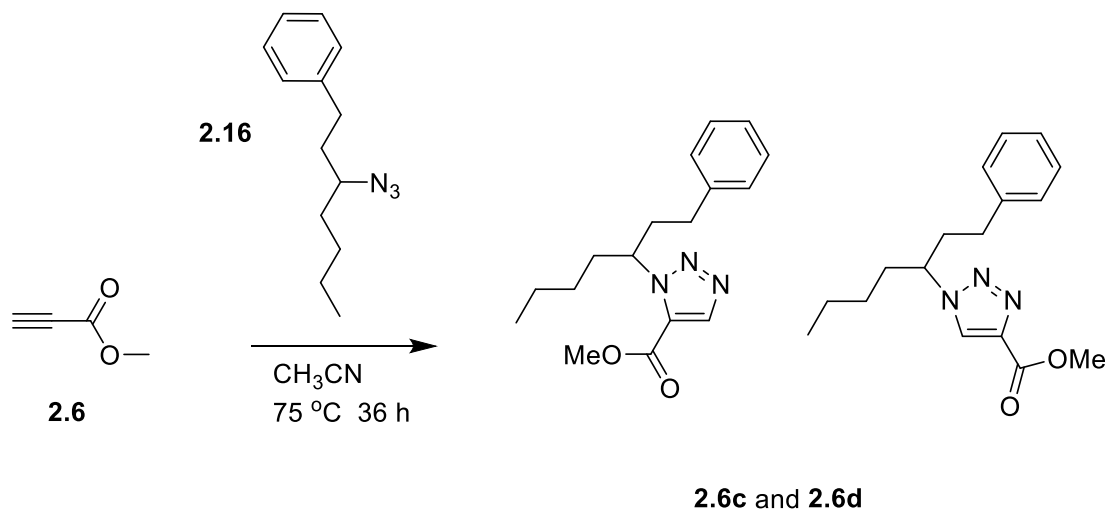
Colorless liquid.  $R_f = 0.48$  (4:1 hexanes:ethyl acetate, UV); <sup>1</sup>H NMR (500 MHz, CDCl<sub>3</sub>):  $\delta = 8.33$  (d,  $J = 8.8$  Hz, 2H), 7.94 (d,  $J = 8.8$  Hz, 2H), 7.27 (t,  $J = 7.3$  Hz, 2H), 7.20 (t,  $J = 7.3$  Hz, 1H), 7.11 (d,  $J = 7.3$  Hz, 2H), 5.20 (tt,  $J = 9.5, 4.9$  Hz, 1H), 3.83 (s, 3H), 2.61 (m, 1H), 2.56 (m, 2H), 2.31 (m, 1H), 2.20 (m, 1H), 1.99 (m, 1H), 1.31 (m, 3H), 1.12 (m, 1H), 0.88 (t,  $J = 7.1$  Hz, 3H) ppm; <sup>13</sup>C{<sup>1</sup>H} and DEPT NMR (126 MHz, CDCl<sub>3</sub>):  $\delta = 159.5$ (C), 147.9(C), 147.2(C), 140.4(C), 136.9(C), 130.1(CH), 128.5(CH), 128.3(CH), 126.2(CH), 126.0(C), 123.3(CH), 61.6(CH), 52.6(CH<sub>3</sub>), 36.5(CH<sub>2</sub>), 35.6(CH<sub>2</sub>), 32.2(CH<sub>2</sub>), 28.0(CH<sub>2</sub>), 22.3(CH<sub>2</sub>), 13.9(CH<sub>3</sub>) ppm; IR (NaCl, CDCl<sub>3</sub>):  $\nu =$

1728, 1524, 1349  $\text{cm}^{-1}$ ; HRMS (ESI):  $m/z$  calcd for  $\text{C}_{23}\text{H}_{27}\text{N}_4\text{O}_4$   $[\text{M}+\text{H}]^+$  423.2027, found 423.2016.

**2.3d** (regioisomer not identified)

Colorless liquid.  $R_f = 0.30$  (4:1 hexanes:ethyl acetate, UV);  $^1\text{H}$  NMR (500 MHz,  $\text{CDCl}_3$ ):  $\delta = 8.26$  (d,  $J = 8.7$  Hz, 2H), 7.32 (d,  $J = 8.7$  Hz, 2H), 7.28 – 7.21 (m, 3H), 7.04 (d,  $J = 6.8$  Hz, 2H), 4.08 (tt,  $J = 9.4, 5.3$  Hz, 1H), 3.87 (s, 3H), 2.49 (m, 3H), 2.32 (m, 1H), 2.11 (m, 1H), 1.91 (m, 1H), 1.18 (m, 2H), 1.03 (m, 2H) 0.83 (t,  $J = 7.3$  Hz, 1H) ppm;  $^{13}\text{C}\{^1\text{H}\}$  and DEPT NMR (126 MHz,  $\text{CDCl}_3$ ):  $\delta = 161.2(\text{C})$ , 148.6(C), 139.8(C), 132.8(C), 131.1(CH), 128.7(CH), 128.2(CH), 126.5(CH), 123.7(CH), 59.4(CH), 52.2(CH<sub>3</sub>), 36.4(CH<sub>2</sub>), 35.0(CH<sub>2</sub>), 31.9(CH<sub>2</sub>), 28.1(CH<sub>2</sub>), 22.2(CH<sub>2</sub>), 13.7(CH<sub>3</sub>) ppm; IR (NaCl,  $\text{CDCl}_3$ ):  $\nu = 1728, 1528, 1350$   $\text{cm}^{-1}$ ; HRMS (ESI):  $m/z$  calcd for  $\text{C}_{23}\text{H}_{27}\text{N}_4\text{O}_4$   $[\text{M}+\text{H}]^+$  423.2027, found 423.2014.

**Methyl 1-(1-phenylheptan-3-yl)-1,2,3-triazole-4-carboxylate and methyl 1-(1-phenylheptan-3-yl)-1,2,3-triazole-5-carboxylate, 2.6c and 2.6d**



Methyl propiolate (21.8 mg, 0.259 mmol) and 3-azido-1-phenylheptane (36.3 mg, 0.167 mmol) were dissolved in 2 mL of CH<sub>3</sub>CN and heated to 75 °C for 36 h. The mixture was purified by silica gel column chromatography (0% to 40% ethyl acetate in hexanes) to give 26.3 mg (52.2%) of total product: 4.2 mg of **2.6c**, 22.1 mg of **2.6d** as colorless liquids.

**2.6c** (regioisomer not identified)

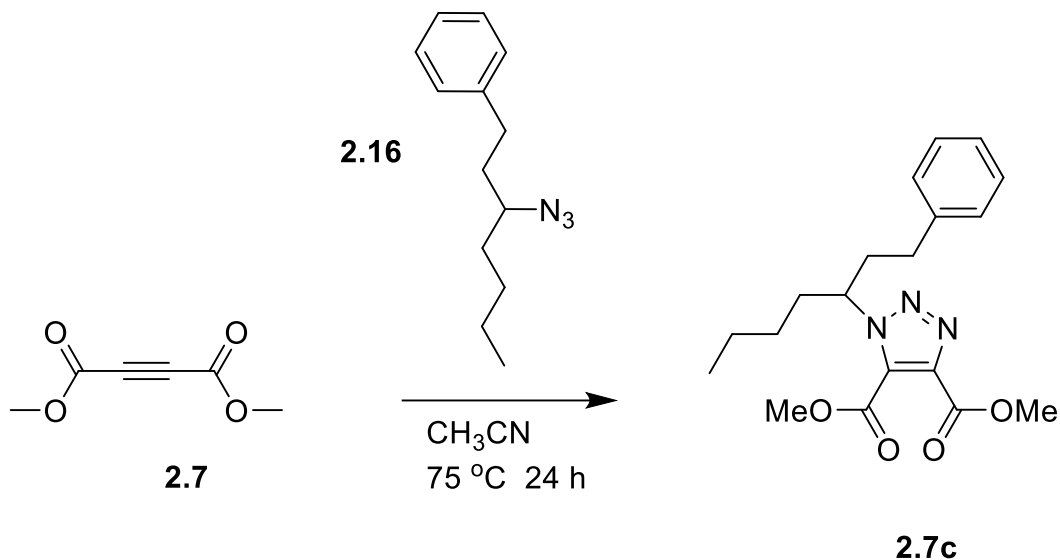
Colorless liquid. *R<sub>f</sub>* = 0.50 (4:1 hexanes:ethyl acetate, UV); <sup>1</sup>H NMR (500 MHz, CDCl<sub>3</sub>): δ = 8.15 (s, 1H), 7.26 (t, *J* = 7.4 Hz, 2H), 7.19 (t, *J* = 7.4 Hz, 1H), 7.08 (d, *J* = 7.4 Hz, 2H), 5.38 (tt, *J* = 9.5, 4.8 Hz, 1H), 3.91 (s, 3H), 2.49 (m, 3H), 2.24 (m, 1H), 2.15 (m, 1H), 1.94 (m, 1H), 1.29 (m, 2H), 1.24 (m, 1H), 1.03 (m, 1H) 0.85 (t, *J* = 7.2 Hz, 3H) ppm; <sup>13</sup>C{<sup>1</sup>H} and DEPT NMR (126 MHz, CDCl<sub>3</sub>): δ = 159.1(C), 140.7(C), 137.7(CH), 128.4(CH), 128.3(CH), 126.1(CH), 60.7(CH), 52.3(CH<sub>3</sub>), 36.8(CH<sub>2</sub>), 35.5(CH<sub>2</sub>), 32.2(CH<sub>2</sub>), 27.9(CH<sub>2</sub>), 22.3(CH<sub>2</sub>), 13.8(CH<sub>3</sub>) ppm; IR (NaCl, CDCl<sub>3</sub>): ν = 1735 cm<sup>-1</sup>; HRMS (ESI): *m/z* calcd for C<sub>17</sub>H<sub>24</sub>N<sub>3</sub>O<sub>2</sub> [M+H]<sup>+</sup> 302.1858, found 302.1857.

**2.6d** (regioisomer not identified)

Colorless liquid. *R<sub>f</sub>* = 0.24 (4:1 hexanes:ethyl acetate, UV); <sup>1</sup>H NMR (500 MHz, CDCl<sub>3</sub>): δ = 8.05 (s, 1H), 7.28 (t, *J* = 7.3 Hz, 2H), 7.21 (t, *J* = 7.3 Hz, 1H), 7.10 (d, *J* = 7.3 Hz, 2H), 4.53 (tt, *J* = 9.6, 5.0 Hz, 1H), 3.98 (s, 3H), 2.47 (m, 2H), 2.30 (m, 1H), 2.23 (m, 1H), 1.91 (m, 2H), 1.28 (m, 2H), 1.19 (m, 1H), 1.02 (m, 1H), 0.84 (t, *J* = 7.2 Hz, 3H) ppm; <sup>13</sup>C{<sup>1</sup>H} and DEPT NMR (126 MHz, CDCl<sub>3</sub>): δ = 161.3(C), 140.0(C), 128.6(CH), 128.3(CH), 126.3(CH), 126.2(CH), 62.1(CH), 52.2(CH<sub>3</sub>), 37.0(CH<sub>2</sub>),

35.4(CH<sub>2</sub>), 32.0(CH<sub>2</sub>), 27.9(CH<sub>2</sub>), 22.1(CH<sub>2</sub>), 13.8(CH<sub>3</sub>) ppm; IR (NaCl, CDCl<sub>3</sub>):  $\nu$  = 1725 cm<sup>-1</sup>; HRMS (ESI):  $m/z$  calcd for C<sub>17</sub>H<sub>24</sub>N<sub>3</sub>O<sub>2</sub> [M+H]<sup>+</sup> 302.1858, found 302.1859.

**Dimethyl 1-(1-phenylheptan-3-yl)-1,2,3-triazole-4,5-dicarboxylate,**



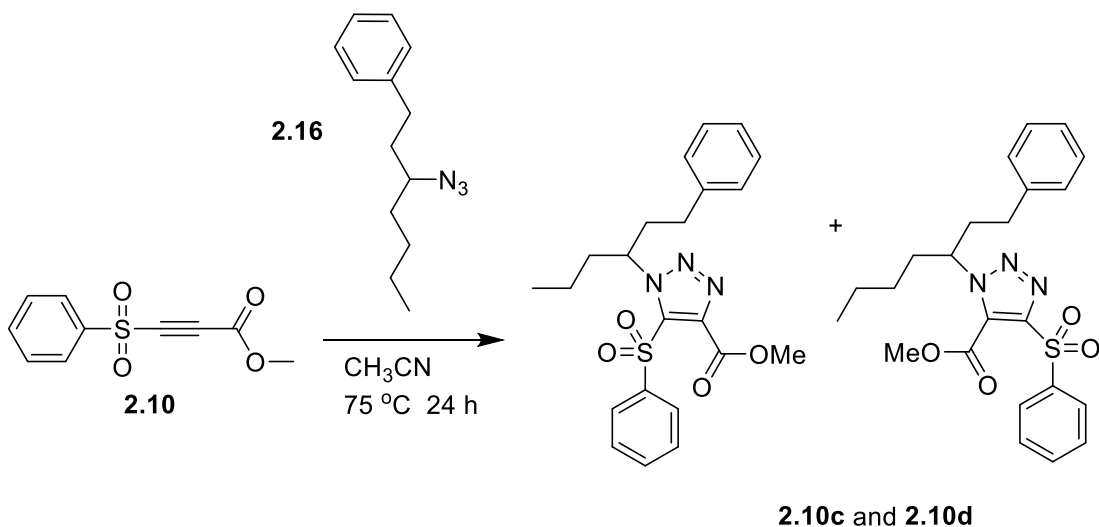
Dimethyl acetylenedicarboxylate (30.2 mg, 0.213 mmol) and 3-azido-1-phenylheptane (30.4 mg, 0.140 mmol) were dissolved in 2 mL of CH<sub>3</sub>CN and heated to 75 °C for 24 h. The mixture was purified by silica gel column chromatography (0% to 40% ethyl acetate in hexanes) to give 42.8 mg (85.2%) of **2.7c** as a colorless liquid.

**2.7c**

Colorless liquid.  $R_f$  = 0.33 (4:1 hexanes:ethyl acetate, UV); <sup>1</sup>H NMR (500 MHz, CDCl<sub>3</sub>):  $\delta$  = 7.26 (t,  $J$  = 7.4 Hz, 2H), 7.19 (t,  $J$  = 7.4 Hz, 1H), 7.08 (d,  $J$  = 7.4 Hz, 2H), 4.75 (tt,  $J$  = 9.6, 4.9 Hz, 1H), 3.98 (s, 3H), 3.94 (s, 3H), 2.53 (m, 1H), 2.47 (m, 2H), 2.22 (m, 1H), 2.11 (m, 1H), 1.91 (m, 1H), 1.26 (m, 2H), 1.21 (m, 1H), 1.04 (m, 1H), 0.84 (t,  $J$  = 7.2 Hz, 3H) ppm; <sup>13</sup>C{<sup>1</sup>H} and DEPT NMR (126 MHz, CDCl<sub>3</sub>):  $\delta$  =

160.6(C), 159.4(C), 140.2(C), 138.9(C), 131.6(C), 128.5(CH), 128.3(CH), 126.2(CH), 61.8(CH), 53.4(CH<sub>3</sub>), 52.6(CH<sub>3</sub>), 36.5(CH<sub>2</sub>), 35.2(CH<sub>2</sub>), 32.0(CH<sub>2</sub>), 27.8(CH<sub>2</sub>), 22.1(CH<sub>2</sub>), 13.8(CH<sub>3</sub>) ppm; IR (NaCl, CDCl<sub>3</sub>):  $\nu = 1737 \text{ cm}^{-1}$ ; HRMS (ESI):  $m/z$  calcd for C<sub>19</sub>H<sub>26</sub>N<sub>3</sub>O<sub>4</sub> [M+H]<sup>+</sup> 360.1913, found 360.1925.

**Methyl 1-(1-phenylheptan-3-yl)-4-phenylsulfonyl-1,2,3-triazole-5-carboxylate and methyl 1-(1-phenylheptan-3-yl)-5-phenylsulfonyl-1,2,3-triazole-4-carboxylate, 2.10c and 2.10d**

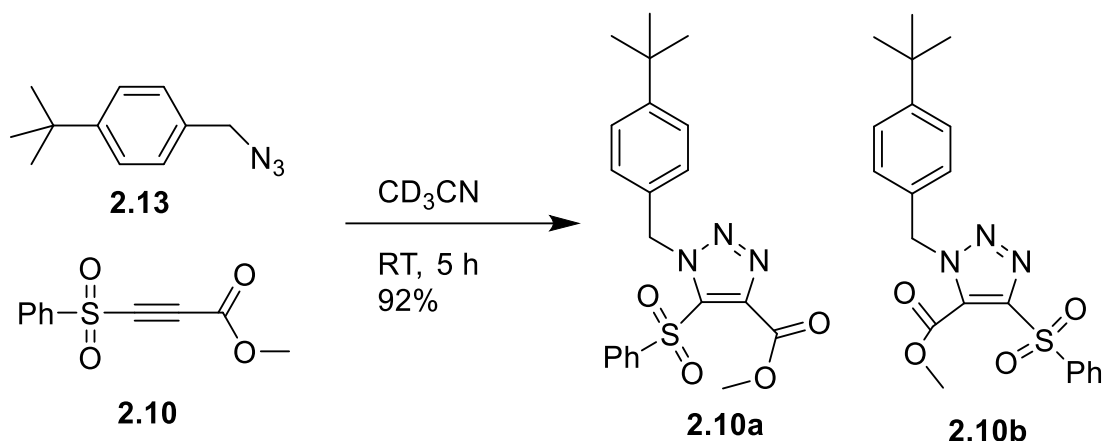


Methyl phenylsulfonylpropiolate (32.3 mg, 0.144 mmol) and 3-azido-1-phenylheptane (49.4 mg, 0.227 mmol) were dissolved in 2 mL of CH<sub>3</sub>CN and heated to 75 °C for 5h. Attempts to separate the regioisomers by column chromatography were unsuccessful, but produced 27.8 mg (43.6%) of total product as a colorless liquid (2.2 : 1 ratio of isomers by <sup>1</sup>HNMR).  $R_f = 0.43, 0.38$  (4:1 hexanes:ethyl acetate, UV); <sup>1</sup>H NMR of major regioisomer (500 MHz, CDCl<sub>3</sub>):  $\delta = 8.13$  (d,  $J = 7.7$  Hz, 2H), 7.70 (t,  $J = 7.7$  Hz,

1H), 7.62 (t,  $J = 7.7$  Hz, 2H), 7.22 (t,  $J = 7.3$  Hz, 2H), 7.17 (t,  $J = 7.3$  Hz, 1H), 7.02 (d,  $J = 7.3$  Hz, 2H), 4.91 (tt,  $J = 9.3, 5.0$  Hz, 1H), 3.98 (s, 1H), 2.46 (m, 3H), 2.26 (m, 1H), 2.06 (m, 1H), 1.93 (m, 1H), 1.23 (m, 3H), 1.01 (m, 1H), 0.84 (t,  $J = 7.1$  Hz, 3H) ppm;  $^1\text{H}$  NMR of minor regioisomer (500 MHz,  $\text{CDCl}_3$ ):  $\delta = 8.13$  (d,  $J = 7.8$  Hz, 2H), 7.70 (t,  $J = 7.8$  Hz, 1H), 7.61 (t,  $J = 7.8$  Hz, 2H), 7.29 (t,  $J = 7.4$  Hz, 2H), 7.22 (t,  $J = 7.4$  Hz, 1H), 7.10 (d,  $J = 7.4$  Hz, 2H), 5.30 (tt,  $J = 8.3, 5.1$  Hz, 1H), 4.01 (s, 3H), 2.46 (m, 2H), 2.26 (m, 2H), 2.06 (m, 1H), 1.93 (m, 1H), 1.23 (m, 2H), 1.09 (m, 1H), 0.90 (m, 1H), 0.80 (t,  $J = 7.3$  Hz, 3H) ppm;  $^{13}\text{C}\{^1\text{H}\}$  and DEPT NMR of major regioisomer (126 MHz,  $\text{CDCl}_3$ ):  $\delta = 157.9(\text{C}), 148.3(\text{C}), 139.9(\text{C}), 139.66(\text{C}), 134.1(\text{CH}), 129.1(\text{CH}), 128.7(\text{CH}), 128.50(\text{CH}), 128.17(\text{CH}), 126.26(\text{CH}), 62.3(\text{CH}), 53.6(\text{CH}_3), 36.1(\text{CH}_2), 35.3(\text{CH}_2), 32.0(\text{CH}_2), 27.8(\text{CH}_2), 22.2(\text{CH}_2), 13.74(\text{CH}_3)$  ppm;  $^{13}\text{C}\{^1\text{H}\}$  and DEPT NMR of minor regioisomer (126 MHz,  $\text{CDCl}_3$ ):  $\delta = 160.3(\text{C}), 140.3(\text{C}), 139.61(\text{C}), 137.7(\text{C}), 134.9(\text{CH}), 129.5(\text{CH}), 129.3(\text{C}), 128.52(\text{CH}), 128.4(\text{CH}), 128.23(\text{CH}), 126.24(\text{CH}), 62.7(\text{CH}), 53.2(\text{CH}_3), 37.2(\text{CH}_2), 35.4(\text{CH}_2), 32.1(\text{CH}_2), 27.9(\text{CH}_2), 22.3(\text{CH}_2), 13.77(\text{CH}_3)$  ppm; IR (NaCl,  $\text{CDCl}_3$ ):  $\nu = 1741, 1334, 1163$   $\text{cm}^{-1}$ ; HRMS (ESI):  $m/z$  calcd for  $\text{C}_{23}\text{H}_{28}\text{N}_3\text{SO}_4$   $[\text{M}+\text{H}]^+$  442.1795, found 442.1780.

### Room temperature cycloaddition





Methyl 3-(phenylsulfonyl)-2-propynoate (41.7 mg, 0.186 mmol) and *t*-butylbenzyl azide (31.4 mg, 0.166 mmol) were combined in 0.6 mL CD<sub>3</sub>CN at room temperature. At time zero, the azide : alkyne ratio was 1.0 : 0.68 based on integrations of azide CH<sub>2</sub>Ar ( $\delta = 4.36$ , I = 2.00), sulfone OCH<sub>3</sub> ( $\delta = 3.82$ , I = 2.04). After 5 hours, 92% of the alkyne had been converted to triazole, based on integrations of **2.10a** OCH<sub>3</sub> ( $\delta = 3.93$ , I = 1.90), **2.10b** OCH<sub>3</sub> ( $\delta = 3.91$ , I = 1.40), and **2.10** OCH<sub>3</sub> ( $\delta = 3.82$ , I = 0.29).

**Competition Experiments with *t*-butylbenzyl azide:** A representative procedure for the competition experiments is as follows.

#### Amide (2.4) vs Nitroaryl (2.3)

*N*-butyl propiolamide (23 mg, 0.18 mmol), methyl 4-nitrophenylpropiolate (37 mg, 0.18 mmol), and 4-*t*-butylbenzyl azide (3.4 mg, 0.018 mmol) were combined in 0.60 mL of CD<sub>3</sub>CN in an NMR tube. NMR of the initial solution revealed a ratio of azide : amide : nitro of 1 : 8.3 : 9.9, based on integrations of azide CH<sub>2</sub>Ar ( $\delta = 4.35$ , I = 2.00), amide CH<sub>2</sub>NH ( $\delta = 3.19$ , I = 17.98), amide CCH ( $\delta = 3.16$ , I = 6.84), and nitro OCH<sub>3</sub> ( $\delta = 3.84$ , I = 29.81). The reaction mixture was heated to 75 °C in an oil bath. After 5

days, NMR confirmed all of the azide had been consumed. The ratio of products was amide : nitro 2.2 : 1.0, based on integrations of the benzylic protons of **2.4a** ( $\delta = 5.55$ ,  $I = 3.80$ ), **2.4b** ( $\delta = 5.88$ ,  $I = 1.70$ ), **2.3b** ( $\delta = 5.46$ ,  $I = 1.54$ ), and **2.3a** ( $\delta = 5.91$ ,  $I = 1.00$ ).

#### **Amide (2.4) vs Benzoyl (2.2)**

The initial ratio of azide : amide : benzoyl was 1.0 : 8.7 : 13.1, based on integrations of  $\text{CH}_2\text{Ar}$  ( $\delta = 4.35$ ,  $I = 2.00$ ), amide  $\text{CH}_2\text{NH}$  plus amide  $\text{CCH}$  (overlapping,  $\delta = 3.19$ ,  $I = 26.18$ ), and benzoyl  $\text{OCH}_2$  ( $\delta = 4.94$ ,  $I = 26.23$ ). The ratio of products was amide : benzoyl 4.7:1, based on integrations of the benzylic protons of **2.2b** ( $\delta = 5.66$ ,  $I = 0.24$ ,  $\delta = 5.39$ ,  $I = 0.27$ ) **2.2a** ( $\delta = 5.54$ ,  $I = 0.55$ ,  $\delta = 5.42$ ,  $I = 0.44$ ), **2.4b** ( $\delta = 5.90$ ,  $I = 1.00$ ), and **2.4a** ( $\delta = 5.56$ ,  $I = 2.52$ ).

#### **Ester (2.6) vs Diamide (2.5)**

The initial ratio of azide : ester : diamide was 1.0 : 14.6 : 12.4, based on integrations of azide  $\text{CH}_2\text{Ar}$  ( $\delta = 4.36$ ,  $I = 2.00$ ), ester  $\text{OCH}_3$  ( $\delta = 3.78$ ,  $I = 43.84$ ), and diamide  $\text{CH}_2\text{NH}$  ( $\delta = 3.23$ ,  $I = 49.40$ ). The ratio of products was ester : diamide 2.2 : 1.0, based on integrations of the benzylic protons of **2.5a** ( $\delta = 6.09$ ,  $I = 1.00$ ), **2.6a** ( $\delta = 5.89$ ,  $I = 0.31$ ), and **2.6b** ( $\delta = 5.58$ ,  $I = 1.90$ ).

#### **Ketone (2.8) vs Diester (2.7)**

The initial ratio of azide : ketone : diester was 1.0 : 12.5 : 12.4, based on integrations of azide  $\text{CH}_2\text{Ar}$  ( $\delta = 4.36$ ,  $I = 2.00$ ), ketone  $\text{OCH}_3$  ( $\delta = 3.89$ ,  $I = 37.54$ ), and diester  $\text{OCH}_3$  ( $\delta = 3.84$ ,  $I = 74.66$ ). The ratio of products was ketone : diester 1.1 : 1.0, based

on integrations of the benzylic protons of **2.7a** ( $\delta = 5.73$ ,  $I = 1.32$ ), **2.8b** ( $\delta = 5.86$ ,  $I = 1.00$ ), and **2.8a** ( $\delta = 5.57$ ,  $I = 0.46$ ).

#### **Diester (2.7) vs Ester (2.6)**

The initial ratio of azide : diester : ester was 1.0 : 11.6 : 9.0, based on integrations of azide  $\text{CH}_2\text{Ar}$  ( $\delta = 4.36$ ,  $I = 2.00$ ), diester  $\text{OCH}_3$  ( $\delta = 3.84$ ,  $I = 69.88$ ), and ester  $\text{OCH}_3$  ( $\delta = 3.78$ ,  $I = 27.00$ ). The ratio of products was diester : ester 6.4 : 1.0, based on integrations of the benzylic protons of **2.6a** ( $\delta = 5.89$ ,  $I = 0.16$ ), **2.6b** ( $\delta = 5.58$ ,  $I = 1.00$ ), and **2.7a** ( $\delta = 5.73$ ,  $I = 7.42$ ).

#### **Ketone (2.8) vs Ester (2.6)**

The initial ratio of azide : ketone : ester was 1.0 : 11.7 : 20.3, based on integrations of azide  $\text{CH}_2\text{Ar}$  ( $\delta = 4.36$ ,  $I = 2.00$ ), ketone  $\text{OCH}_3$  ( $\delta = 3.89$ ,  $I = 35.23$ ), and ester  $\text{OCH}_3$  ( $\delta = 3.78$ ,  $I = 60.95$ ). The ratio of products was ketone : ester 2.7 : 1.0, based on integrations of the benzylic protons of **2.6a** ( $\delta = 5.88$ ,  $I = 0.09$ ), **2.6b** ( $\delta = 5.58$ ,  $I = 0.43$ ), **2.8b** ( $\delta = 5.86$ ,  $I = 1.00$ ), and **2.8a** ( $\delta = 5.57$ ,  $I = 0.41$  overlap).

#### **Sulfone Ester (2.10) vs Diester (2.7)**

The initial ratio of azide : sulfone : diester was 1.0 : 11.1 : 11.1, based on integrations of azide  $\text{CH}_2\text{Ar}$  ( $\delta = 4.36$ ,  $I = 2.00$ ), sulfone  $\text{OCH}_3$  ( $\delta = 3.89$ ,  $I = 33.18$ ), and diester  $\text{OCH}_3$  ( $\delta = 3.78$ ,  $I = 66.35$ ). The ratio of products was sulfone : diester 17.2 : 1.0, based on integrations of the benzylic protons of **2.7a** ( $\delta = 5.74$ ,  $I = 0.13$ ), **2.10b** ( $\delta = 5.74$ ,  $I = 1.22$ ), and **2.10a** ( $\delta = 6.03$ ,  $I = 1.00$ ).

#### **Diamide (2.5) vs Nitroaryl (2.4)**

The initial ratio of azide : diamide : nitro was 1.0 : 12.7 : 13.3, based on integrations of azide  $\text{CH}_2\text{Ar}$  ( $\delta = 4.35$ ,  $I = 2.00$ ), diamide  $\text{CH}_2\text{NH}$  ( $\delta = 3.22$ ,  $I = 50.75$ ), and nitro  $\text{OCH}_3$  ( $\delta = 3.85$ ,  $I = 39.97$ ). The ratio of products was diamide : nitro 4.3 : 1.0, based on integrations of the benzylic protons of **2.3a** ( $\delta = 5.91$ ,  $I = 0.09$ ), **2.3b** ( $\delta = 5.47$ ,  $I = 0.14$ ), and **2.5a** ( $\delta = 6.08$ ,  $I = 1.00$ ).

#### **Benzoyl (2.2) vs Phenyl (2.1)**

The initial ratio of azide : benzoyl : phenyl was 1.0 : 7.8 : 9.5, based on integrations of azide  $\text{CH}_2\text{Ar}$  ( $\delta = 4.36$ ,  $I = 2.00$ ), benzoyl  $\text{OCH}_2$  ( $\delta = 4.94$ ,  $I = 15.59$ ), and phenyl  $\text{OCH}_2$  ( $\delta = 4.28$ ,  $I = 18.90$ ). The ratio of products was benzoyl : phenyl 1.2 : 1.0, based on integrations of the benzylic protons of **2.1a** ( $\delta = 5.89$ ,  $I = 0.25$ ), **2.1b** ( $\delta = 5.42$ ,  $I = 0.50$ , overlap), **2.2b** ( $\delta = 5.66$ ,  $I = 0.28$ ,  $\delta = 5.39$ ,  $I = 0.31$ ), and **2.2a** ( $\delta = 5.53$ ,  $I = 0.59$ ,  $\delta = 5.42$ ,  $I = 0.60$ , overlap).

#### **Sulfone (2.9) vs Ester (2.6)**

The initial ratio of azide : sulfone : ester was 1.0 : 10.1 : 10.1, based on integrations of azide  $\text{CH}_2\text{Ar}$  ( $\delta = 4.36$ ,  $I = 2.00$ ), sulfone  $\text{CCH}$  ( $\delta = 4.12$ ,  $I = 10.12$ ), and ester  $\text{CCH}$  ( $\delta = 3.40$ ,  $I = 10.05$ ). The ratio of products of sulfone : ester was 10.6 : 1.0, based on integrations of the benzylic protons of **2.9a** ( $\delta = 5.79$ ,  $I = 1.64$ ), **2.9b** ( $\delta = 5.55$ ,  $I = 10.07$ ), **2.6a** ( $\delta = 5.89$ ,  $I = 0.10$ ), and **2.6b** ( $\delta = 5.58$ ,  $I = 1.00$ ).

#### **Sulfone (2.9) vs Diester (2.7)**

The initial ratio of azide : sulfone : diester was 1 : 8.2 : 8.2, based on integrations of azide  $\text{CH}_2\text{Ar}$  ( $\delta = 4.36$ ,  $I = 2.00$ ), sulfone  $\text{CCH}$  ( $\delta = 4.12$ ,  $I = 8.19$ ), and diester  $\text{OCH}_3$  ( $\delta = 3.84$ ,  $I = 49.05$ ). The ratio of products of sulfone : diester was 2.6 : 1.0, based on

integrations of the benzylic protons of **2.9a** ( $\delta = 5.79$ ,  $I = 0.33$ ), **2.9b** ( $\delta = 5.55$ ,  $I = 2.29$ ), and **2.7a** ( $\delta = 5.73$ ,  $I = 1.00$ ).

### **Competition Experiments with 3-azido-1-phenylheptane:**

#### **Ester (2.6) vs Nitro (2.3)**

The initial ratio of azide : ester : nitro was 1 : 9.5 : 10.2, based on integrations of azide  $\text{CHN}_3$  ( $\delta = 3.33$ ,  $I = 1.00$ ), ester  $\text{OCH}_3$  ( $\delta = 3.77$ ,  $I = 28.58$ ), and nitro  $\text{OCH}_3$  ( $\delta = 3.85$ ,  $I = 30.68$ ). The ratio of products of ester : nitro was 7.4 : 1.0, based on integrations of the protons alpha to the triazole of **2.3c** ( $\delta = 5.20$ ,  $I = 1.00$ ), **2.3d** ( $\delta = 4.10$ ,  $I = 1.24$ ), **2.6c** ( $\delta = 5.33$ ,  $I = 2.36$ ), and **2.6d** ( $\delta = 4.58$ ,  $I = 14.17$ ).

#### **Diester (2.7) vs Ester (2.6)**

The initial ratio of azide : diester : ester was 1 : 6.1 : 7.0, based on integrations of azide  $\text{CHN}_3$  ( $\delta = 3.34$ ,  $I = 1.00$ ), ester  $\text{OCH}_3$  ( $\delta = 3.77$ ,  $I = 20.91$ ), and diester  $\text{OCH}_3$  ( $\delta = 3.84$ ,  $I = 36.66$ ). The ratio of products of diester : ester was 4.9 : 1.0, based on integrations of the protons alpha to the triazole of **2.6c** ( $\delta = 5.33$ ,  $I = 0.14$ ), **2.6d** ( $\delta = 4.58$ ,  $I = 1.00$ ), and **2.7c** ( $\delta = 4.72$ ,  $I = 5.55$ ).

#### **Sulfone Ester (2.10) vs Diester (2.7)**

The initial ratio of azide : sulfone ester : diester was 1 : 7.6 : 9.7, based on integrations of azide  $\text{CHN}_3$  ( $\delta = 3.33$ ,  $I = 1.00$ ), sulfone ester  $\text{OCH}_3$  ( $\delta = 3.82$ ,  $I = 22.67$ ), and diester  $\text{OCH}_3$  ( $\delta = 3.84$ ,  $I = 58.14$ ). The ratio of products of sulfone ester : diester was 19.0 : 1.0, based on integrations of the protons alpha to the triazole of **2.10c** ( $\delta = 5.17$ ,  $I = 6.76$ ), **2.10d** ( $\delta = 4.80$ ,  $I = 12.25$ ), and **2.7c** ( $\delta = 4.72$ ,  $I = 1.00$ ).

### Time-based competition

Methyl 4-nitrophenylpropiolate (16.5 mg, 0.0804 mmol), bis-*N*-butyl acetylenediamide (20.2 mg, 0.0901 mmol), and 4-*t*-butylbenzyl azide (1.7 mg, 0.0090 mmol) were combined in 0.60 mL of CD<sub>3</sub>CN. NMR of the initial solution revealed a ratio of azide : diamide:nitro of 1.0 : 9.1 : 9.6, based on integrations of azide CH<sub>2</sub>Ar ( $\delta$  = 4.36, I = 2.00), diamide CH<sub>2</sub>NH ( $\delta$  = 3.23, I = 18.19), and nitro OCH<sub>3</sub> ( $\delta$  = 3.85, I = 14.40). The reaction mixture was heated to 75 °C in an oil bath.

After 30 min, 8.6% of the azide had been consumed, and the product ratio was diamide : nitro 5.0 : 1.0, based on integrations of the benzylic protons of azide ( $\delta$  = 4.35 , I = 12.76), **2.5a** ( $\delta$  = 6.08, I = 1.00), **2.3a** ( $\delta$  = 5.91, I = 0.08), and **2.3b** ( $\delta$  = 5.47, I = 0.12).

After 2 h, 29% of the azide had been consumed, and the product ratio was diamide : nitro 4.8 : 1.0, based on integrations of the benzylic protons of azide ( $\delta$  = 4.35 , I = 3.00), **2.5a** ( $\delta$  = 6.08, I = 1.00), **2.3a** ( $\delta$  = 5.91, I = 0.09), and **2.3b** ( $\delta$  = 5.47, I = 0.12).

After 15 h, 93% of the azide had been consumed, and the product ratio was diamide : nitro 4.8 : 1.0, based on integrations of the benzylic protons of azide ( $\delta$  = 4.35 , I = 0.09), **2.5a** ( $\delta$  = 6.08, I = 1.00), **2.3a** ( $\delta$  = 5.91, I = 0.09), and **2.3b** ( $\delta$  = 5.47, I = 0.12).

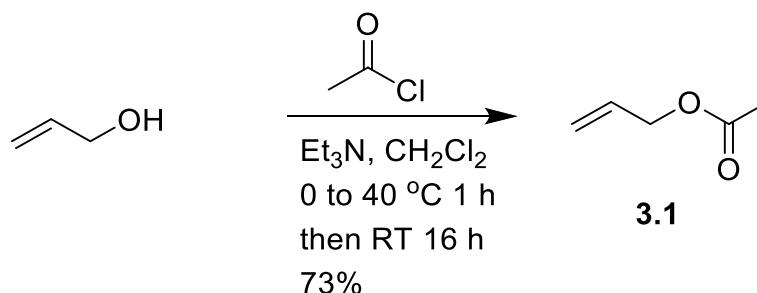
After 42 h, no azide starting material was detected, and the product ratio was diamide : nitro 4.8 : 1.0, based on integrations of the benzylic protons of **2.5a** ( $\delta$  = 6.08, I = 1.00), **2.3a** ( $\delta$  = 5.91, I = 0.09), and **2.3b** ( $\delta$  = 5.47, I = 0.12).

## 4.2 Experimental for Chapter 3

PVC ( $M_n= 22\text{kDa}$ ,  $M_w= 43\text{kDa}$ , Aldrich) was purified by dissolving in THF and precipitation in methanol three times. Anhydrous THF was dried using a PureSolv-EN purification system. All other reagents were used as received.

Nuclear Magnetic Resonance (NMR) spectra were recorded on a Bruker Avance III HD four channel 500 MHz Oxford Magnet NMR spectrometer with automation. High Resolution Mass Spectrometry (HRMS) was recorded with a Thermo Scientific LTQ-Orbitrap Velos Pro mass spectrometer. UV-Vis measurements were taken on a Shimadzu UV-2700 UV-Vis Spectrophotometer with samples dissolved in THF. Gel Permeation Chromatography (GPC) measurements were performed in THF using two Agilent PLgel 5 $\mu\text{m}$  Mixed-D columns, and a Waters 2410 refractive index detector, using linear polystyrene standards. IR was performed using a Perkin-Elmer Spectrum Two FT-IR with ATR.

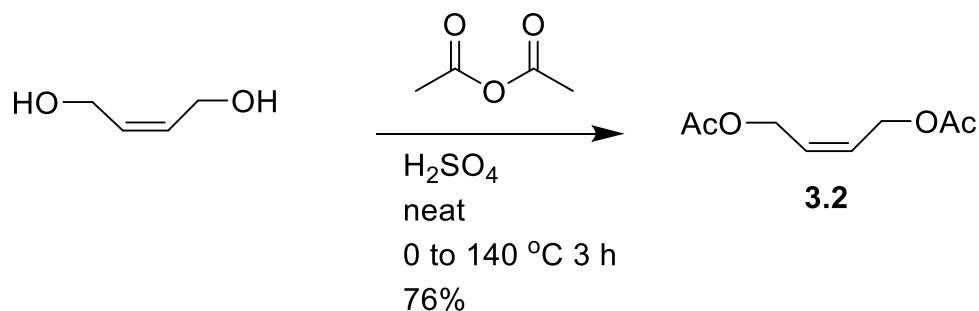
### Synthesis of Allyl Acetate (3.1)<sup>5</sup>



Following the procedure of Francova,<sup>5</sup> in a flame-dried 3-neck round bottom flask, allyl alcohol (7.0 mL, 103 mmol) and triethylamine (19.6 mL, 140 mmol) in anhydrous dichloromethane (60 mL) were cooled to 0 °C in an ice bath. Acetyl chloride (10 mL, 140 mmol) was dissolved in anhydrous dichloromethane (30 mL)

and added to the allyl alcohol solution dropwise by addition funnel. Resulting solution was brought to reflux for 1 h, then stirred at room temperature for 16 h. Solution was washed with 5% NaHCO<sub>3</sub> (100 mL), saturated NaHCO<sub>3</sub> (100 mL), and water (100 mL), then dried over MgSO<sub>4</sub>, filtered, and concentrated by rotary evaporator to produce a light yellow liquid (7.55 g, 73%). <sup>1</sup>H NMR (500 MHz, Chloroform-d) δ 5.92 (ddt, J = 17.0, 10.5, 5.8 Hz, 1H), 5.31 (dq, J = 17.3, 1.5 Hz, 1H), 5.23 (dq, J = 10.4, 1.2 Hz, 1H), 4.57 (dt, J = 5.7, 1.3 Hz, 3H), 2.08 (s, 3H).

#### Synthesis of **Z-1,4-Diacetoxy-2-butene (3.2)**<sup>6</sup>

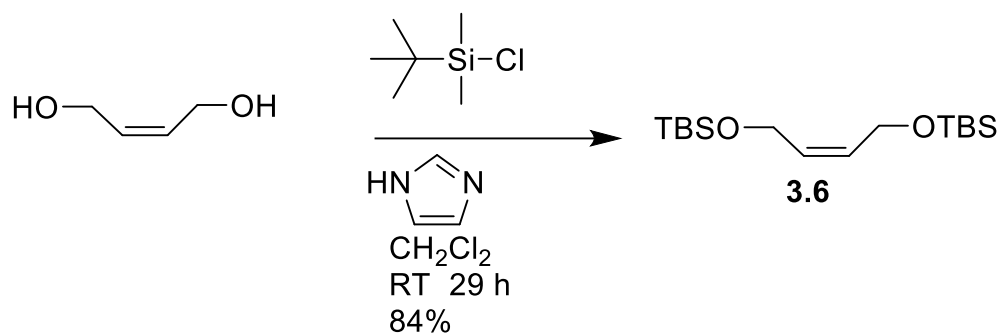


Following the procedure of von Czapiewski,<sup>6</sup> in an ice bath, sulfuric acid (6 drops) was added to acetic anhydride (18.6 mL, 195 mmol). Z-2-buten-1,4-diol (6.6 mL, 82 mmol) was added dropwise. The reaction mixture was stirred at 140 °C for 3 h. The reaction mixture was cooled to RT, then 50 mL water and 30 mL ethyl acetate were added. The organic layer was washed with 30 mL water then 2 x 20 mL saturated NaHCO<sub>3</sub>, dried over sodium sulfate and concentrated in vacuo (10.69 g, 76% yield).

<sup>1</sup>H NMR (500 MHz, Chloroform-d) δ 5.75 (t, J = 4.2 Hz, 2H), 4.67 (d, J = 4.4 Hz, 4H), 2.06 (s, 6H).

#### Synthesis of **Bis-TBSO-2-butene (3.6)**<sup>7</sup>

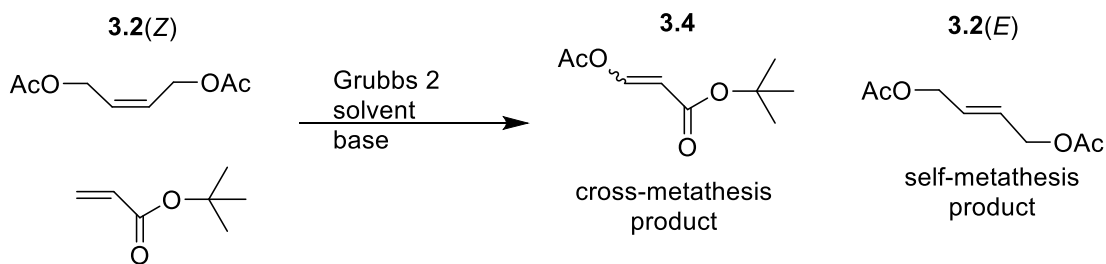




Following the procedure of Dow,<sup>7</sup> imidazole (1.58 g, 23.2 mmol) and TBS-Cl (3.57 g, 23.8 mmol) were dissolved in anhydrous dichloromethane (10 mL) and stirred for 10 min. 1,4-diacetoxy-2-butene was dissolved in anhydrous dichloromethane (10 mL) and added. Resulting cloudy white mixture was stirred at room temperature for 29 h. Mixture was filtered through silica, rinsed with dichloromethane, and concentrated by rotary evaporator. 2.99g, 84%.

<sup>1</sup>H NMR (500 MHz, Chloroform-*d*)  $\delta$  5.55 (t,  $J = 3.4$  Hz, 2H), 4.23 (d,  $J = 4.1$  Hz, 4H), 0.90 (s, 18H), 0.07 (s, 12H).

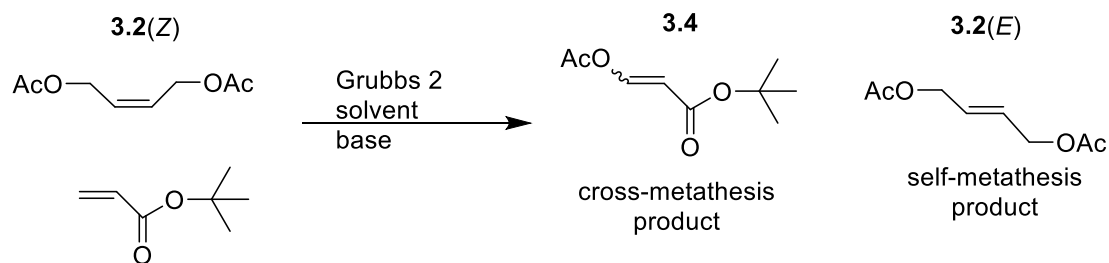
#### Cross Metathesis control reaction in THF



*Z*-1,4-diacetoxy-2-butene (173 mg, 1.00 mmol) and *t*-butyl acrylate (145  $\mu$ L, 1.00 mmol) were dissolved in THF (5 mL) in a round bottom flask. Grubbs II catalyst (18 mg, 0.021 mmol) was added. Solution was stirred at 60  $^{\circ}$ C for 24 h. Crude <sup>1</sup>H NMR was measured without evaporation of solvent. The cross metathesis product **3.4** was

identified by  $^1\text{H}$  NMR and compared to the literature spectrum.<sup>8</sup> Three peaks were used to confirm the product (6.83 (dt,  $J = 15.7, 4.8$  Hz, 1H), 5.96 (dt,  $J = 15.8, 1.9$  Hz, 1H), 4.73 (dd,  $J = 4.9, 1.8$  Hz, 2H)). The integration of these peaks compared to *t*-butyl acrylate (6.31 (dd,  $J = 17.3, 1.5$  Hz, 1H), 6.05 (dd,  $J = 17.3, 10.3$  Hz, 1H), 5.73 (dd,  $J = 10.4, 1.5$  Hz, 1H)) revealed 8% conversion. Of the leftover 1,4-diacetoxybutene, 75% is *trans* (5.87 (dt,  $J = 3.0, 1.6$  Hz, 2H)) and 25% is *cis* (5.79 (t,  $J = 2.4$  Hz, 2H)), indicating self-metathesis.

### Cross Metathesis control reaction in DCM



Z-1,4-diacetoxy-2-butene (178 mg, 1.03 mmol) and *t*-butyl acrylate (145  $\mu\text{L}$ , 1.00 mmol) were dissolved in DCM (5 mL) in a round bottom flask. Grubbs II catalyst (18 mg, 0.021 mmol) was added. Solution was refluxed for 24 h. Crude  $^1\text{H}$  NMR was measured without evaporation of solvent. The integration of **3.4** peaks compared to *t*-butyl acrylate revealed 49% conversion. Of the leftover 1,4-diacetoxy-2-butene, 92% is *trans* and 8% is *cis*, indicating self-metathesis.

### Cross Metathesis in the presence of base

#### Potassium *tert*-butoxide

Z-1,4-bis-TBSO-2-butene (156 mg, 0.49 mmol) and *t*-butyl acrylate (74  $\mu\text{L}$ , 0.51 mmol) were dissolved in DCM (3 mL) in a round bottom flask. Potassium *t*-butoxide

(59 mg, 0.53 mmol) was added. Grubbs II catalyst (9.2 mg, 0.011 mmol) was added. Solution was stirred at room temperature for 21 h. Crude  $^1\text{H}$  NMR was measured without evaporation of solvent. No cross-metathesis or self-metathesis products were seen.

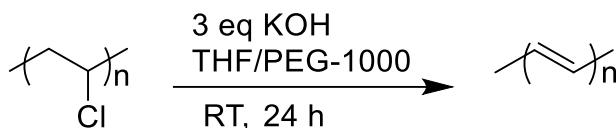
### Pyridine in THF

Z-1,4-diacetoxy-2-butene (178 mg, 1.03 mmol) and *t*-butyl acrylate (145  $\mu\text{L}$ , 1.00 mmol) were dissolved in THF (5 mL) in a round bottom flask. Pyridine (80  $\mu\text{L}$ , 1.0 mmol) was added. Grubbs II catalyst (19 mg, 0.022 mmol) was added. Solution was refluxed for 24 h. Crude  $^1\text{H}$  NMR was measured without evaporation of solvent. No cross-metathesis product is visible. Of the leftover starting material, 16% is *trans* and 84% is *cis*, indicating that self-metathesis is largely inhibited.

### Pyridine as solvent

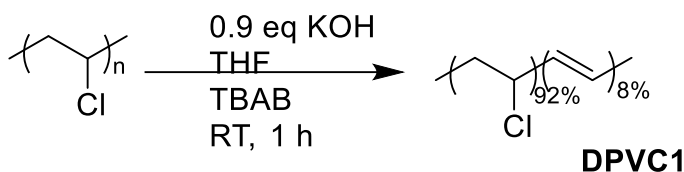
Z-1,4-diacetoxy-2-butene (173 mg, 1.00 mmol) and *t*-butyl acrylate (145  $\mu\text{L}$ , 1.00 mmol) were dissolved in pyridine (5 mL, 50 mmol) in a round bottom flask. Grubbs II catalyst (18 mg, 0.021 mmol) was added. Solution was refluxed for 24 h. Crude  $^1\text{H}$  NMR was measured without evaporation of solvent. No cross-metathesis product is visible. Of the leftover starting material, 16% is *trans* and 84% is *cis*, indicating that self-metathesis is largely inhibited.

### Full elimination of PVC to polyacetylene<sup>9</sup>



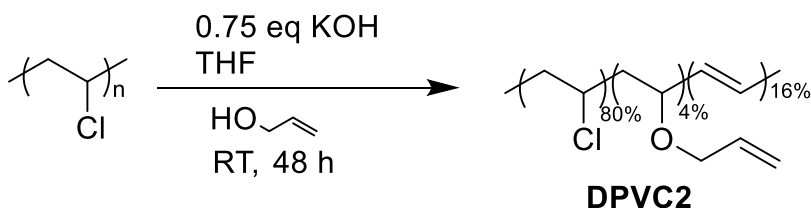
Following the procedure of Guo,<sup>9</sup> PVC (0.10 g, 1.6 mmol) was dried at 60 °C under vacuum then dissolved in 100mL of THF. PEG-1000 (12.08 g, 12.08 mmol) was dried at 60 °C under vacuum. KOH (0.30 g, 5.3 mmol) was dissolved in the PEG-1000, which was then added dropwise to the PVC solution and stirred at RT for 1h. 20 mL of 1:1 MeOH/THF was added. Mixture was vacuum filtered, rinsed with MeOH and water to produce a black powder (0.02 g, 50% yield).

### Partial elimination of PVC (DPVC1)



PVC (1.01 g, 16.2 mmol repeat unit) and tetrabutylammonium bromide (0.10 g, 0.31 mmol) were dissolved in 100 mL of THF. KOH pellets (0.8 g, 14 mmol) were crushed then added. The reaction mixture was stirred at room temperature for 1 h. The reaction mixture was precipitated into methanol, filtered, dissolved in THF, and precipitated into methanol again to produce a brown solid (0.80 g, 83% yield).

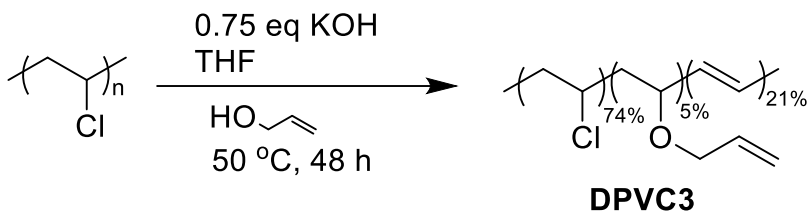
### Elimination of PVC with allyl alcohol at RT (DPVC2)



PVC (0.97 g, 15.5 mmol of repeat unit) was dissolved in 20 mL of THF and 10 mL (150 mmol) of allyl alcohol. KOH pellets (0.64 g, 11.4 mmol) were crushed then added.

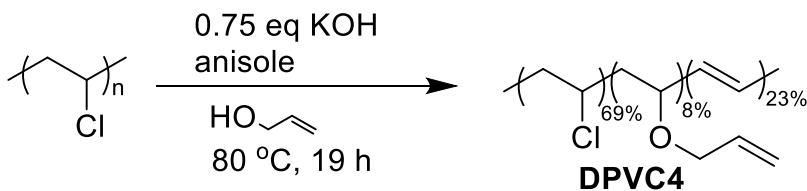
The reaction mixture was stirred at RT (~20 °C) for 48 h. The mixture was concentrated by rotary evaporator then precipitated into methanol, producing a dark brown solid (915 mg, 102% yield).

#### Elimination of PVC with allyl alcohol at 50 °C (DPVC3)



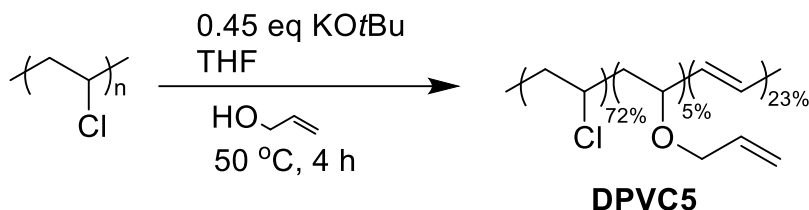
PVC (3.00 g, 48.0 mmol of repeat unit) was dissolved in 60 mL of THF and 30 mL (440 mmol) of allyl alcohol. KOH pellets (1.97 g, 35.1 mmol) were crushed then added. The reaction mixture was stirred at 50 °C for 48 h. The mixture was concentrated by rotary evaporator then precipitated into methanol, producing a dark brown solid (2.74 g, 102% yield).

#### Elimination of PVC with allyl alcohol at 80 °C (DPVC4)



PVC (0.99 g, 15.8 mmol of repeat unit) was dissolved in 20 mL of THF and 10 mL (150 mmol) of allyl alcohol. KOH pellets (0.66 g, 11.8 mmol) were crushed then added. The reaction mixture was stirred at 80 °C for 19 h. The mixture was concentrated by rotary evaporator then precipitated into methanol, producing a dark brown solid (709 mg, 80.4% yield).

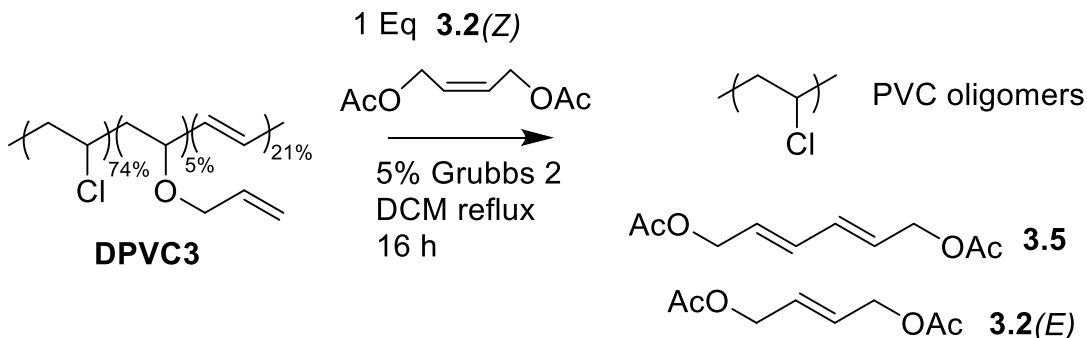
## Elimination of PVC with allyl alcohol and *t*-butoxide (DPVC5)



A flame-dried flask was charged with potassium *t*-butoxide (833.4 mg, 7.426 mmol) and dried under vacuum. Allyl alcohol (10 mL, 150 mmol) was added. In a separate flask, PVC (1.01 g, 16.2 mmol of repeat unit) was dissolved in 20 mL of anhydrous THF. The PVC solution was added to the *t*BuOK solution by syringe. The mixture was stirred at 50 °C for 4 h. The mixture was concentrated by rotary evaporator then precipitated into methanol, producing a dark brown solid (962.2 mg, 111% yield).

## General procedure for olefin metathesis

"Standard Conditions"



DPVC3 (199.1 mg, 0.748 mmol of internal double bonds) was added to 20 mL DCE, which dissolved some of the polymer but left large amounts solid. *Z*-1,4-Diacetoxy-2-butene (127.1 mg, 0.738 mmol) and Grubbs 2 (33.4 mg, 0.0393 mmol) were added.

The mixture was stirred at 55 °C for 16 h, resulting in a homogenous brown solution. The reaction mixture was concentrated by rotary evaporator, redissolved in a minimum amount of THF, and precipitated into methanol. The precipitate was filtered and rinsed with methanol. The filtrate was concentrated by rotary evaporator, then subjected to column chromatography (ethyl acetate 0 to 40% in hexanes). 1,6-Diacetoxy-2,4-hexadiene (**2.5**) coeluted with *Z*-1,4-diacetoxy-2-butene. <sup>1</sup>H NMR of **2.5** matches the literature.<sup>10,11</sup> <sup>1</sup>H NMR (500 MHz, Chloroform-*d*) δ 6.28 (d, *J* = 14.6 Hz, 1H), 5.80 (ddd, *J* = 12.3, 9.7, 6.6 Hz, 2H), 4.60 (d, *J* = 6.0 Hz, 2H), 2.07 (s, 6H). HRMS: [C<sub>10</sub>H<sub>14</sub>O<sub>4</sub>Na]<sup>+</sup> (M+Na)<sup>+</sup> calcd. 221.0785, obs. 221.0781.

#### **Olefin metathesis without an added alkene**

DPVC3 (49.0 mg, 0.202 mmol of internal double bonds) was added to 4 mL DCM, which dissolved some of the polymer but left large amounts solid. Grubbs 2 (8.4 mg, 0.0099 mmol) were added. The mixture was degassed by bubbling argon, and stirred at 40 °C for 17 h, resulting in a homogenous brown solution. The reaction mixture was concentrated by rotary evaporator, redissolved in a minimum amount of THF, and precipitated into methanol. The precipitate was filtered and rinsed with methanol, then characterized by GPC and NMR.

#### **Olefin Metathesis with DPVC and 1,4-bis-TBSO-butene**

The diene product (1,6-bis-TBSO-2,4-hexadiene) would be expected at 6.14 and 5.55 and 4.27, but is not seen.<sup>12</sup>

### **Olefin Metathesis with DPVC and trans-stilbene**

On the  $^1\text{H}$  NMR the diene (1,4-diphenyl-1,3-butadiene) would be expected at 6.54-6.74 and 6.95-7.02 but is not seen.<sup>13</sup>

### **Olefin Metathesis with DPVC and 1-hexene**

On the  $^1\text{H}$  NMR the 1-hexene starting material is visible at 4.93, 5.00, and 5.81. The diene product (5,7-dodecadiene) would be expected at 5.56 and 6.00 but is not seen.<sup>14</sup>

### **Olefin Metathesis with DPVC and butyl acrylate**

On the  $^1\text{H}$  NMR butyl acrylate starting material is present at 5.81, 6.12, and 6.39. The diene product (dibutyl muconate) would be expected at 7.32-7.26 and 6.21-6.12, but was not seen.<sup>15</sup>



### 4.3 References

- <sup>1</sup> Kunishima, M.; Kawachi, C.; Morita, J.; Terao, K.; Iwasaki, F.; Tani, S. 4-(4,6-Dimethoxy-1,3,5-Triazin-2-Yl)-4-Methylmorpholinium Chloride: An Efficient Condensing Agent Leading to the Formation of Amides and Esters. *Tetrahedron* **1999**, *55* (46), 13159–13170. [https://doi.org/10.1016/S0040-4020\(99\)00809-1](https://doi.org/10.1016/S0040-4020(99)00809-1).
- <sup>2</sup> Okumura, S.; Takeda, Y.; Kiyokawa, K.; Minakata, S. Hypervalent Iodine(III)-Induced Oxidative [4+2] Annulation of o-Phenylenediamines and Electron-Deficient Alkynes: Direct Synthesis of Quinoxalines from Alkyne Substrates under Metal-Free Conditions. *Chem. Commun.* **2013**, *49* (81), 9266–9268. <https://doi.org/10.1039/c3cc45469j>.
- <sup>3</sup> Huy, P. H.; Filbrich, I. A General Catalytic Method for Highly Cost- and Atom-Efficient Nucleophilic Substitutions. *Chem. - A Eur. J.* **2018**, *24* (29), 7410–7416. <https://doi.org/10.1002/chem.201800588>.
- <sup>4</sup> Earla, A.; Braslau, R. Covalently Linked Plasticizers: Triazole Analogues of Phthalate Plasticizers Prepared by Mild Copper-Free “Click” Reactions with Azide-Functionalized PVC. *Macromol. Rapid Commun.* **2014**, *35* (6), 666–671. <https://doi.org/10.1002/marc.201300865>.
- <sup>5</sup> Francová, D.; Kickelbick, G. Synthesis of Methacrylate-Functionalized Phosphonates and Phosphates with Long Alkyl-Chain Spacers and Their Self-Aggregation in Aqueous Solutions. *Monatshefte fur Chemie* **2009**, *140* (4), 413–422. <https://doi.org/10.1007/s00706-008-0045-y>.

<sup>6</sup> von Czapiewski, M.; Kreye, O.; Mutlu, H.; Meier, M. A. R. Cross-Metathesis versus Palladium-Catalyzed C-H Activation: Acetoxy Ester Functionalization of Unsaturated Fatty Acid Methyl Esters. *Eur. J. Lipid Sci. Technol.* **2013**, *115* (1), 76–85. <https://doi.org/10.1002/ejlt.201200196>.

<sup>7</sup> Dow, M.; Marchetti, F.; Abrahams, K. A.; Vaz, L.; Besra, G. S.; Warriner, S.; Nelson, A. Modular Synthesis of Diverse Natural Product-Like Macrocycles: Discovery of Hits with Antimycobacterial Activity. *Chem. - A Eur. J.* **2017**, *23* (30), 7207–7211. <https://doi.org/10.1002/chem.201701150>.

<sup>8</sup> Anderson, N. A.; Campbell, I. B.; Fallon, B. J.; Lynn, S. M.; Macdonald, S. J. F.; Pritchard, J. M.; Procopiou, P. A.; Sollis, S. L.; Thorp, L. R. Synthesis and Determination of Absolute Configuration of a Non-Peptidic Av $\beta$ 6 Integrin Antagonist for the Treatment of Idiopathic Pulmonary Fibrosis. *Org. Biomol. Chem.* **2016**, *14* (25), 5992–6009. <https://doi.org/10.1039/c6ob00496b>.

<sup>9</sup> Guo, L.; Shi, G.; Liang, Y. Poly (Ethylene Glycol) s Catalyzed Homogeneous Dehydrochlorination of Poly (Vinyl Chloride) with Potassium Hydroxide. *Polymer (Guildf)*. **2001**, *42*, 5581–5587. [https://doi.org/10.1016/S0032-3861\(01\)00037-4](https://doi.org/10.1016/S0032-3861(01)00037-4).

<sup>10</sup> Boone, M.A. and Hembre, R.T., Eastman Chemical Co, **2015**. *Low-pressure synthesis of cyclohexanedimethanol and derivatives*. U.S. Patent 9,115,155.

<sup>11</sup> Turczel, G.; Kovács, E.; Csizmadia, E.; Nagy, T.; Tóth, I.; Tuba, R. One-Pot Synthesis of 1,3-Butadiene and 1,6-Hexanediol Derivatives from Cyclopentadiene

(CPD) via Tandem Olefin Metathesis Reactions. *ChemCatChem* **2018**, *10* (21), 4884–4891. <https://doi.org/10.1002/cctc.201801088>.

<sup>12</sup> Krasovskiy, A.; Tishkov, A.; Del Amo, V.; Mayr, H.; Knochel, P. Transition-Metal-Free Homocoupling of Organomagnesium Compounds. *Angew. Chemie - Int. Ed.* **2006**, *45* (30), 5010–5014. <https://doi.org/10.1002/anie.200600772>.

<sup>13</sup> Zhang, H. P.; Dai, Y. Z.; Zhou, X.; Yu, H. Efficient Pyrimidone-Promoted Palladium-Catalyzed Suzuki-Miyaura Cross-Coupling Reaction. *Synlett* **2012**, *23* (8), 1221–1224. <https://doi.org/10.1055/s-0031-1290885>.

<sup>14</sup> Conn, C.; Lloyd-Jones, D.; Kannangara, G. S. K.; Baker, A. T. Reductive Coupling of Alkynes by Oxobis(Diethyldithiocarbamate)Molybdenum(IV)-Sodium Borohydride. *J. Organomet. Chem.* **1999**, *585* (1), 134–140. [https://doi.org/10.1016/S0022-328X\(99\)00205-3](https://doi.org/10.1016/S0022-328X(99)00205-3).

<sup>15</sup> Shin, N.; Kwon, S.; Moon, S.; Hong, C. H.; Kim, Y. G. Ionic Liquid-Mediated Deoxydehydration Reactions: Green Synthetic Process for Bio-Based Adipic Acid. *Tetrahedron* **2017**, *73* (32), 4758–4765. <https://doi.org/10.1016/j.tet.2017.06.053>.

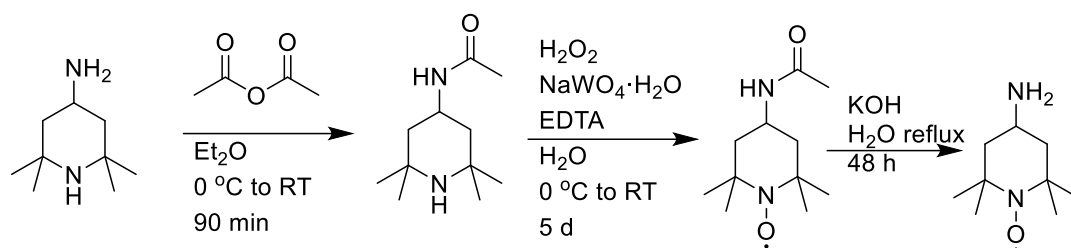
### Addendum: Contribution to other published works

Schultz-Simonton, W.; Skelly, P.; Chakraborty, I.; Mascharak, P.; Braslau, R.

Synthesis, Structure, and Fluorescence Behavior of Profluorescent 8-Amino

BODIPY Nitroxides. *European J. Org. Chem.* **2019**, 2019 (7).

<https://doi.org/10.1002/ejoc.201801758>.

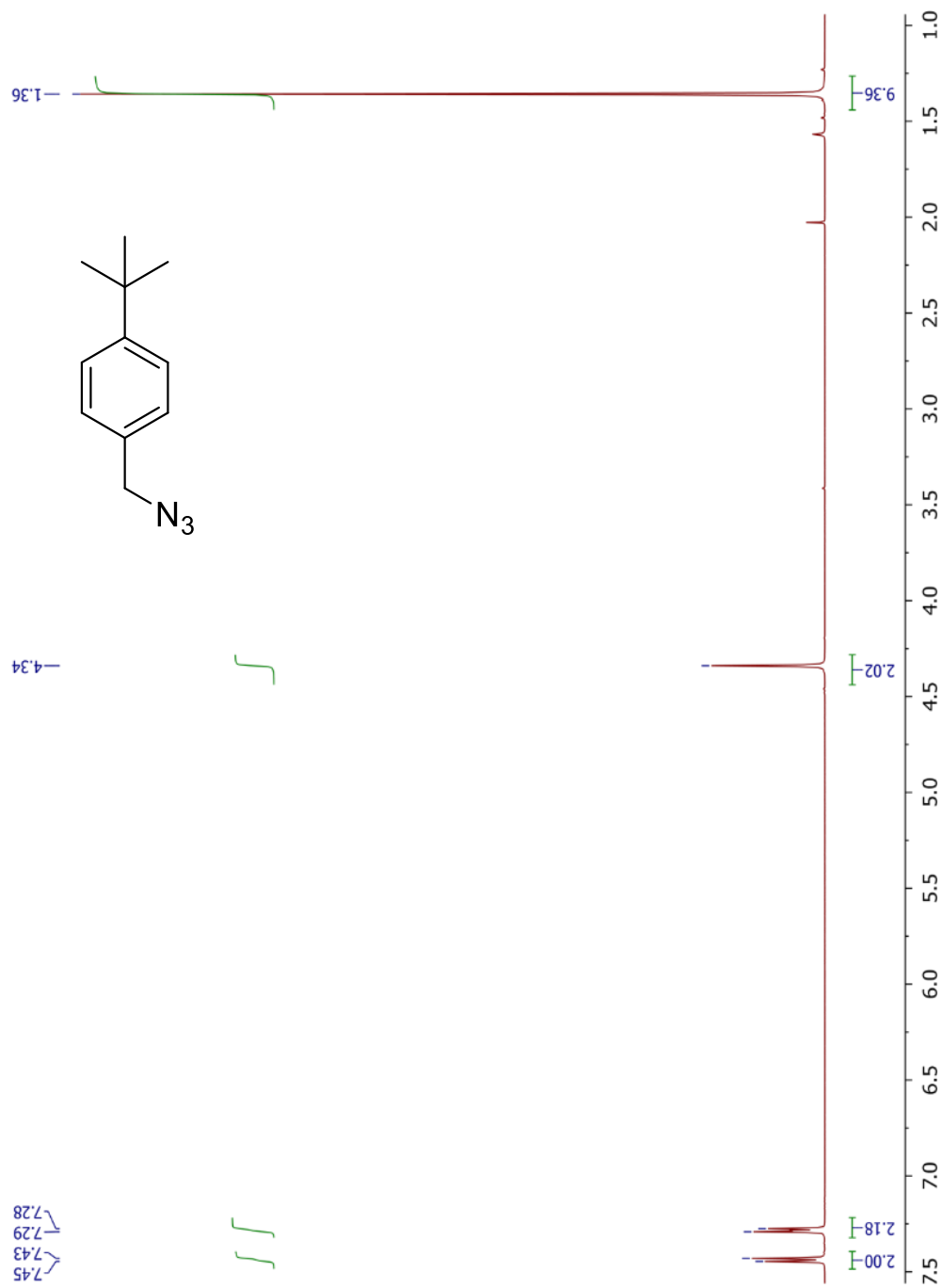


I synthesized 4-amino TEMPO, a precursor compound for the profluorescent nitroxides, and assisted in collecting UV-vis and fluorescence measurements.

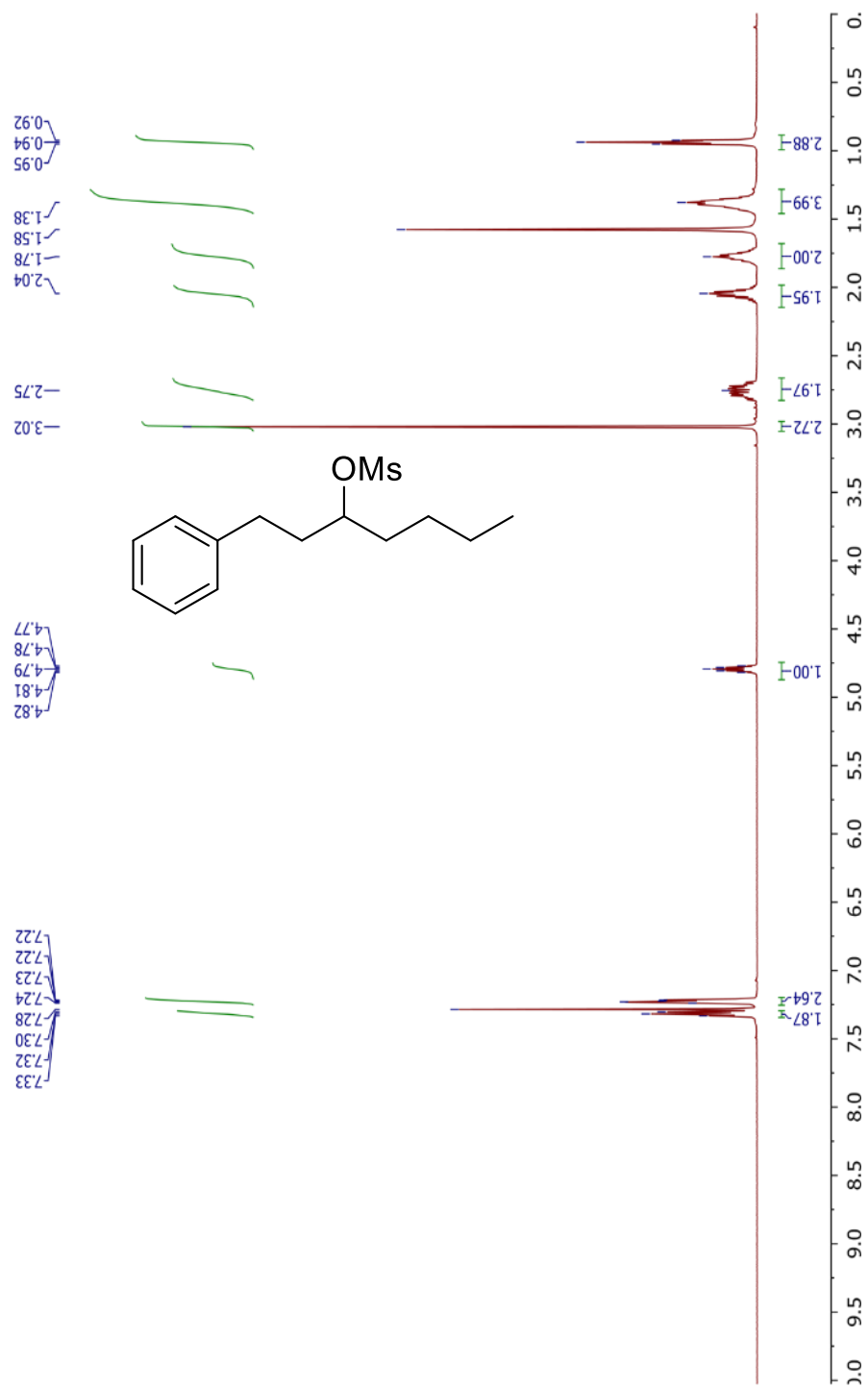
## Appendix

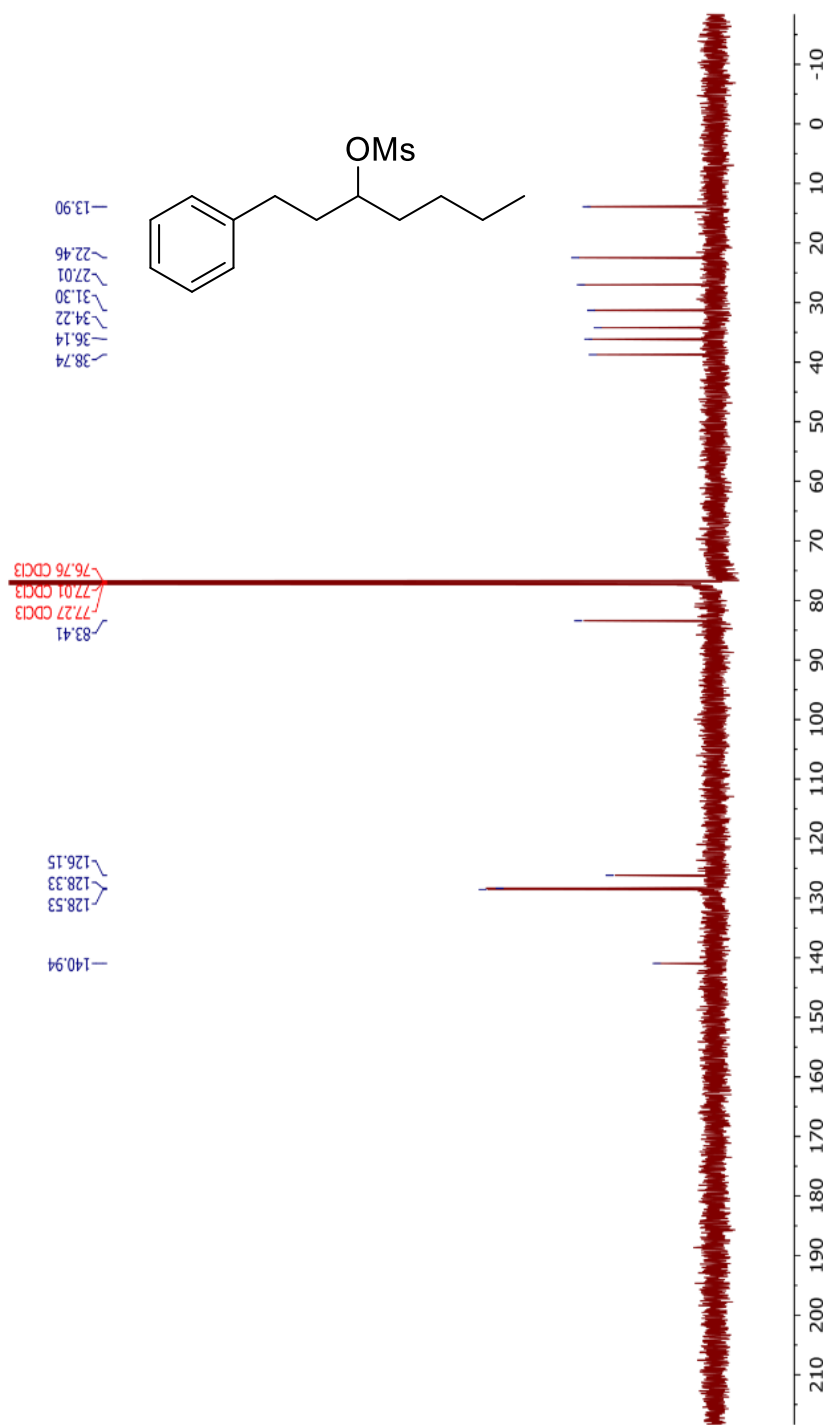
### NMR Spectra of Authentic Compounds from Chapter 2

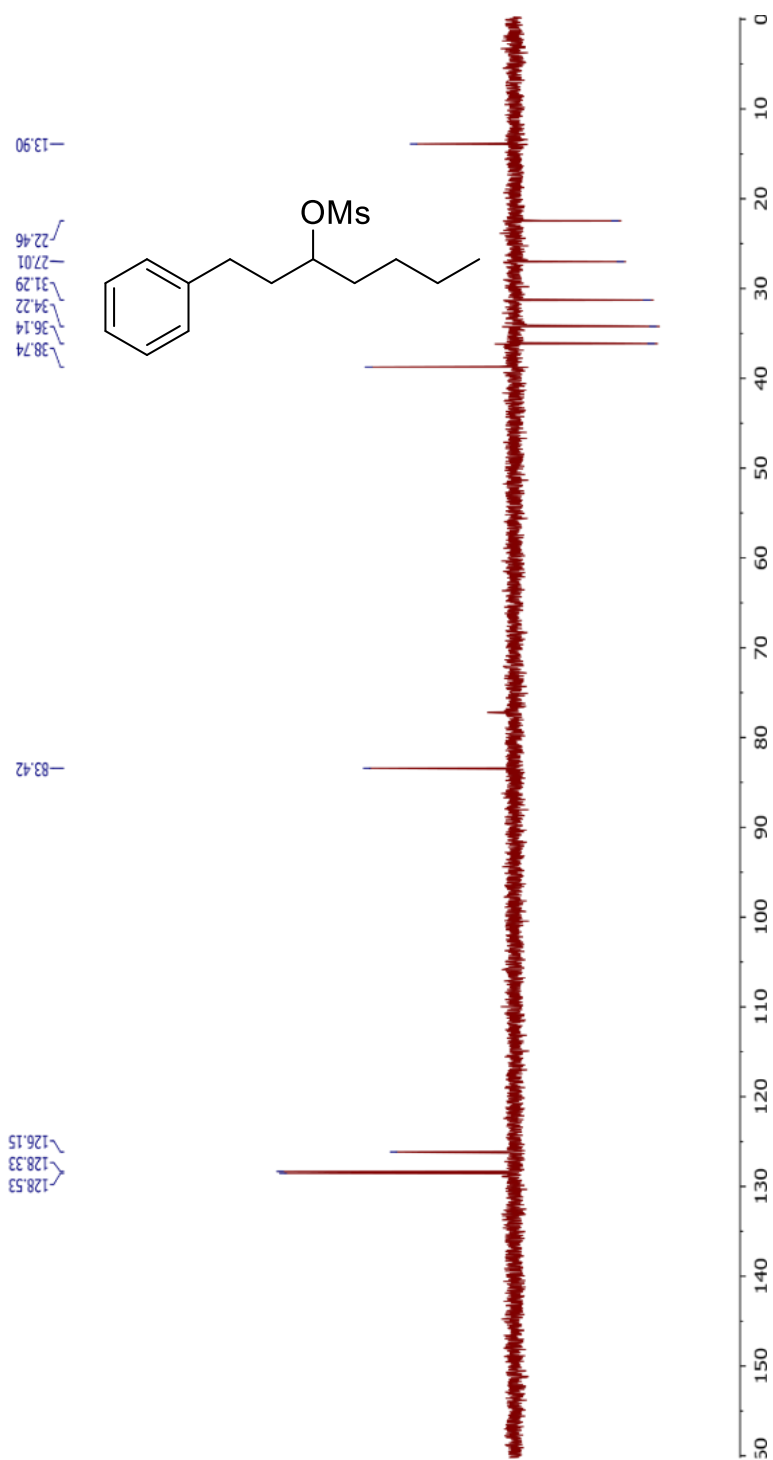
#### 4-*t*-butylbenzyl azide **2.13**



1-Phenylheptan-3-yl methanesulfonate **2.15**

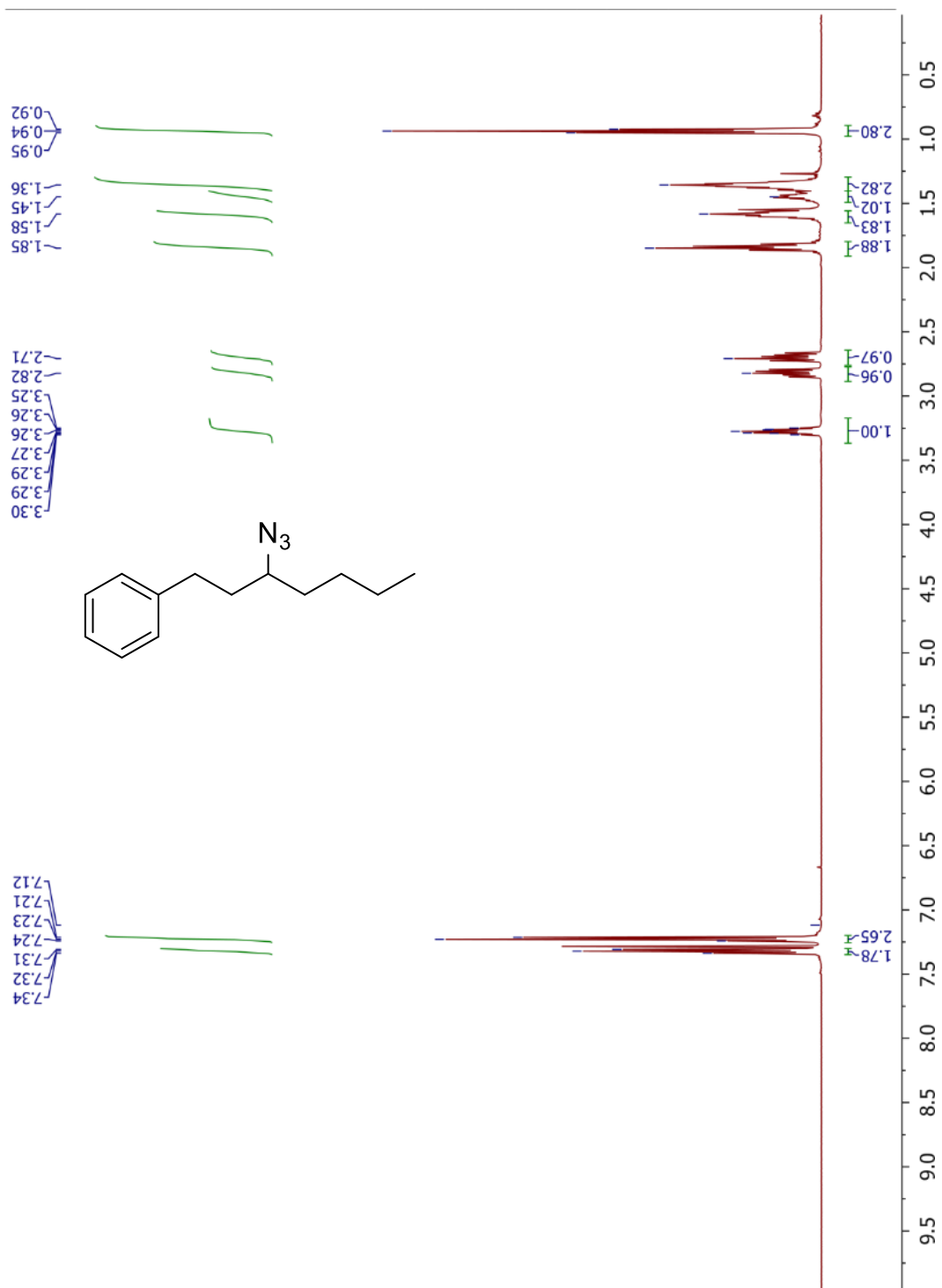




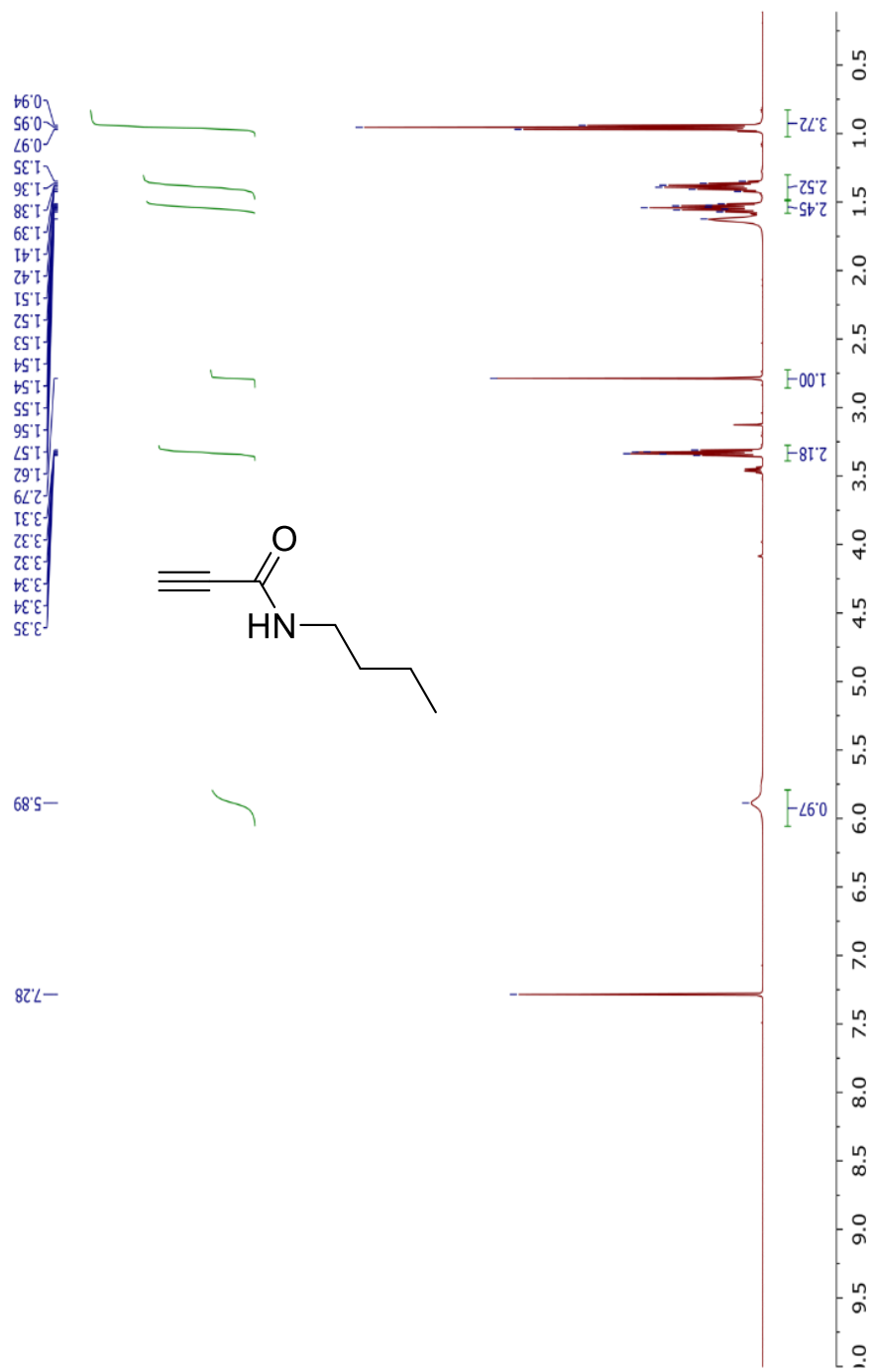


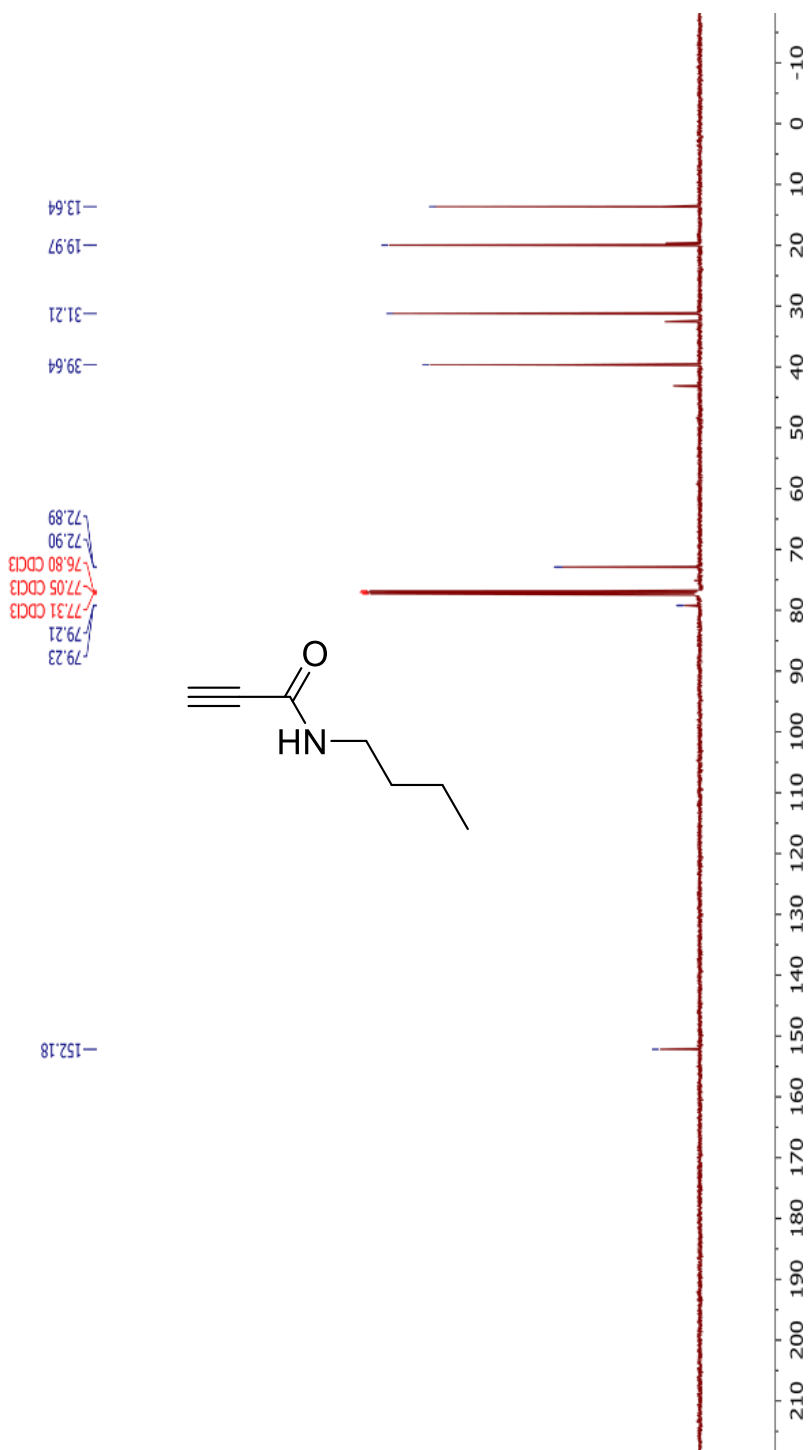


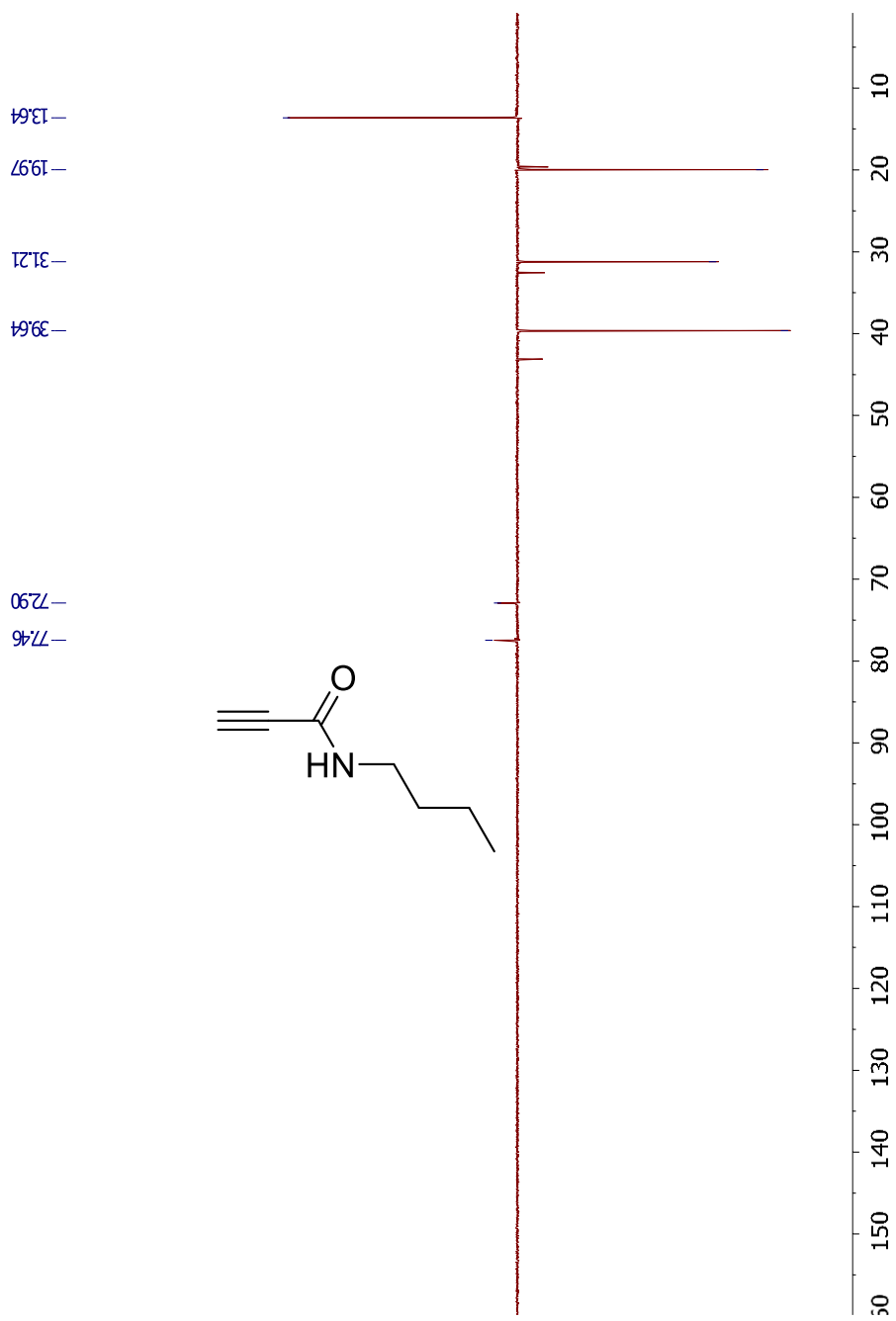
### 3-Azido-1-phenylheptane **2.16**



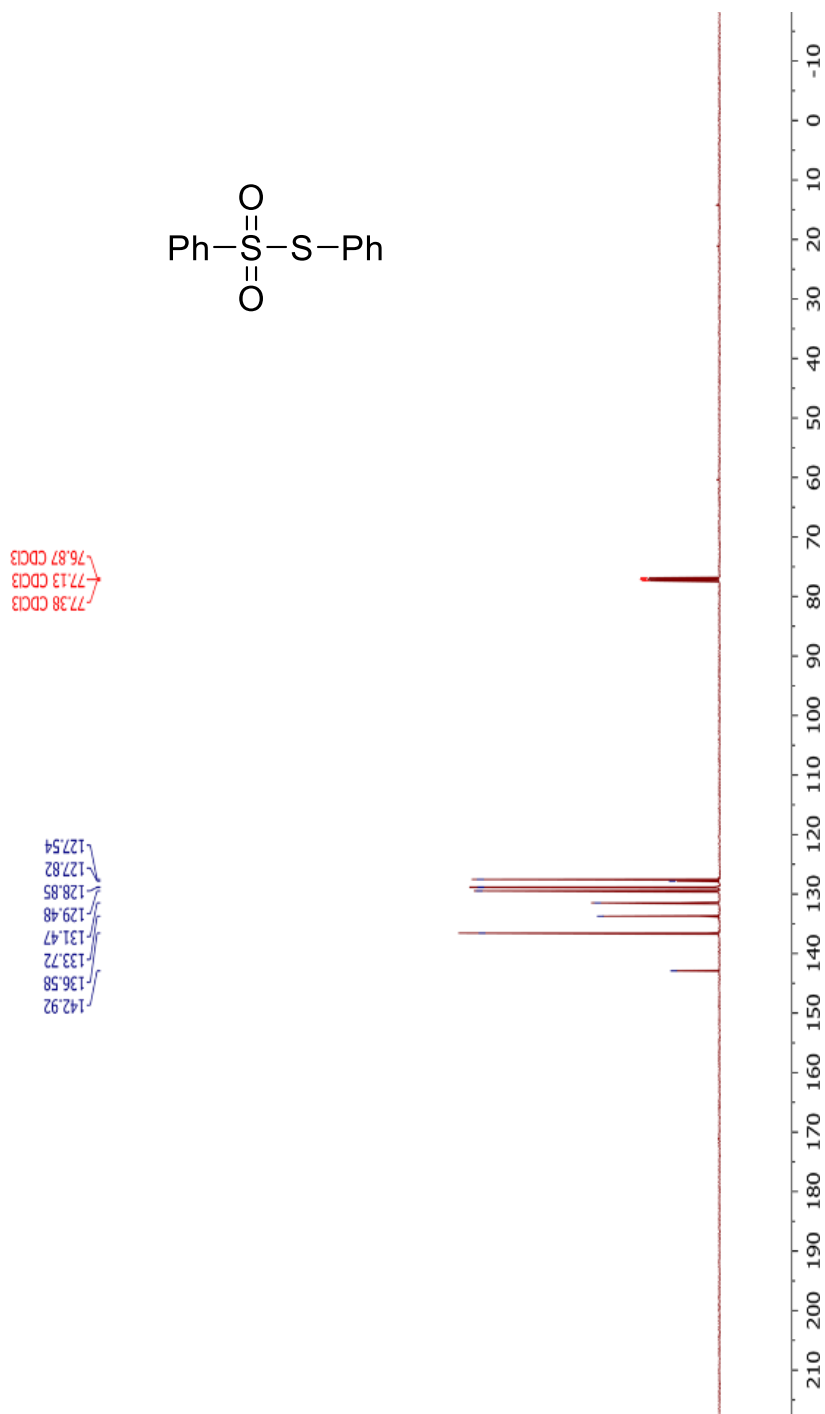
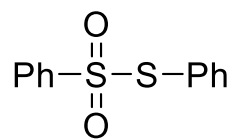
N-butyl propiolamide **2.4**



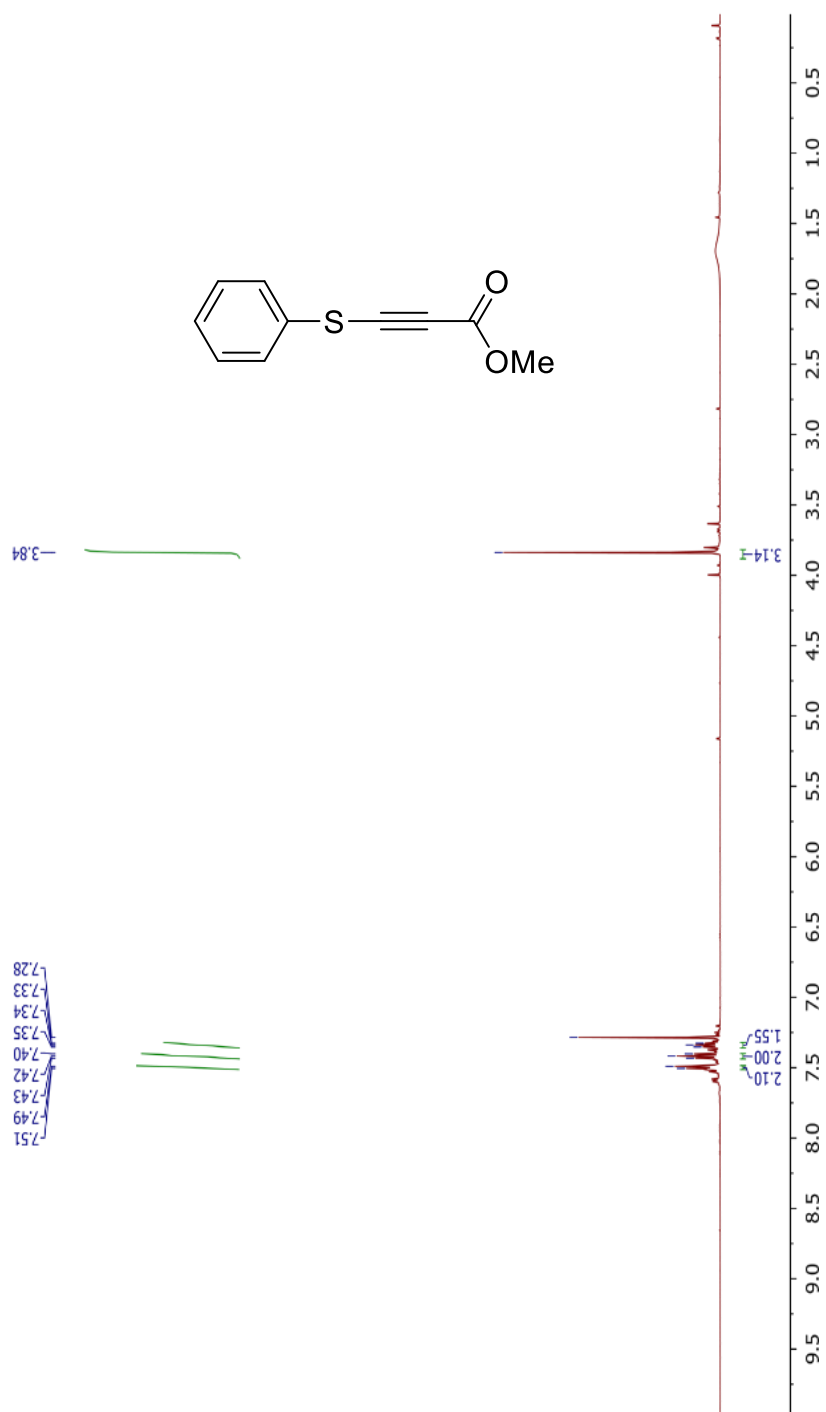




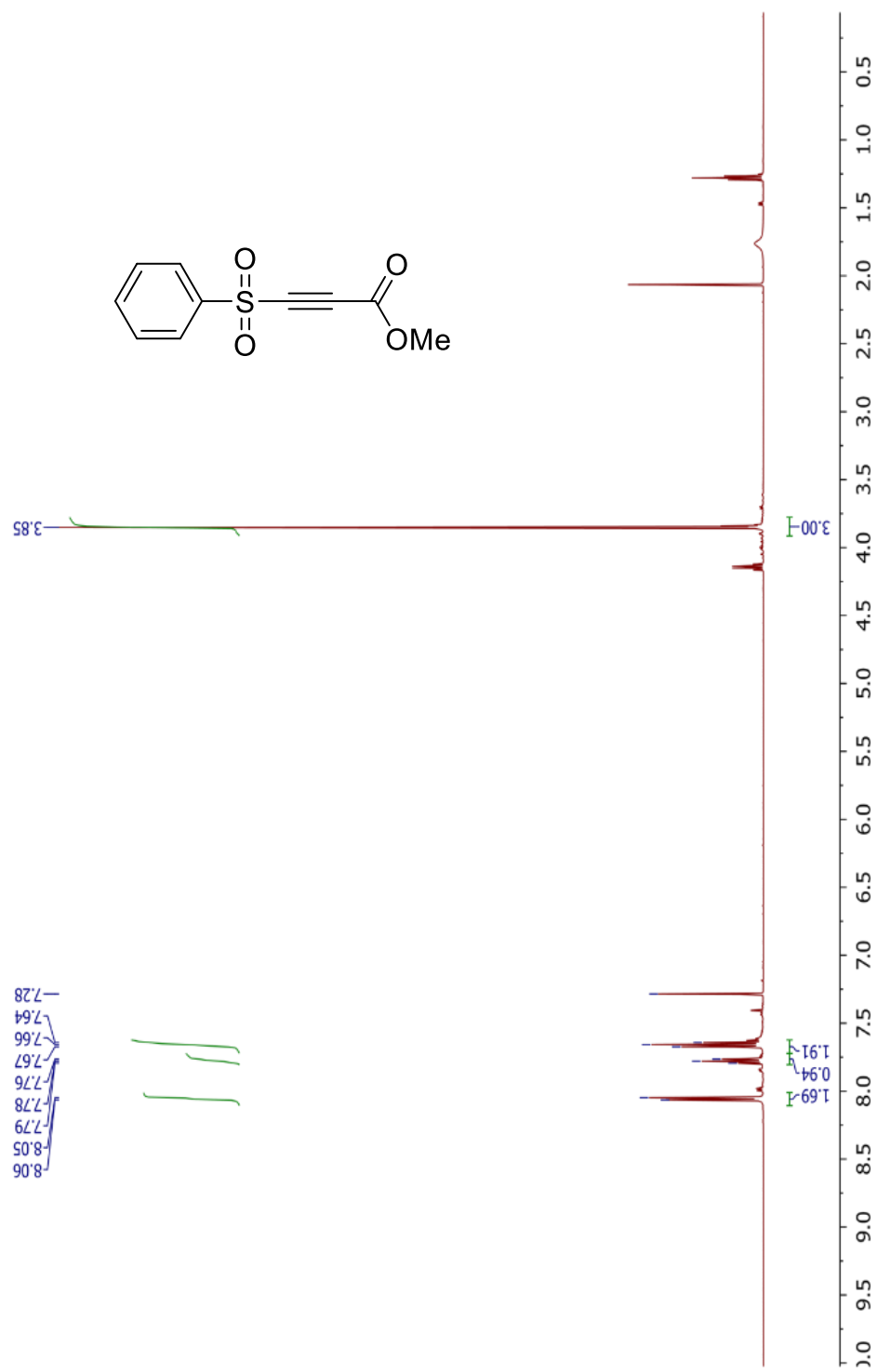
Diphenyl thiosulfate **2.11**



Methyl 3-(phenylsulfanyl)-2-propynate

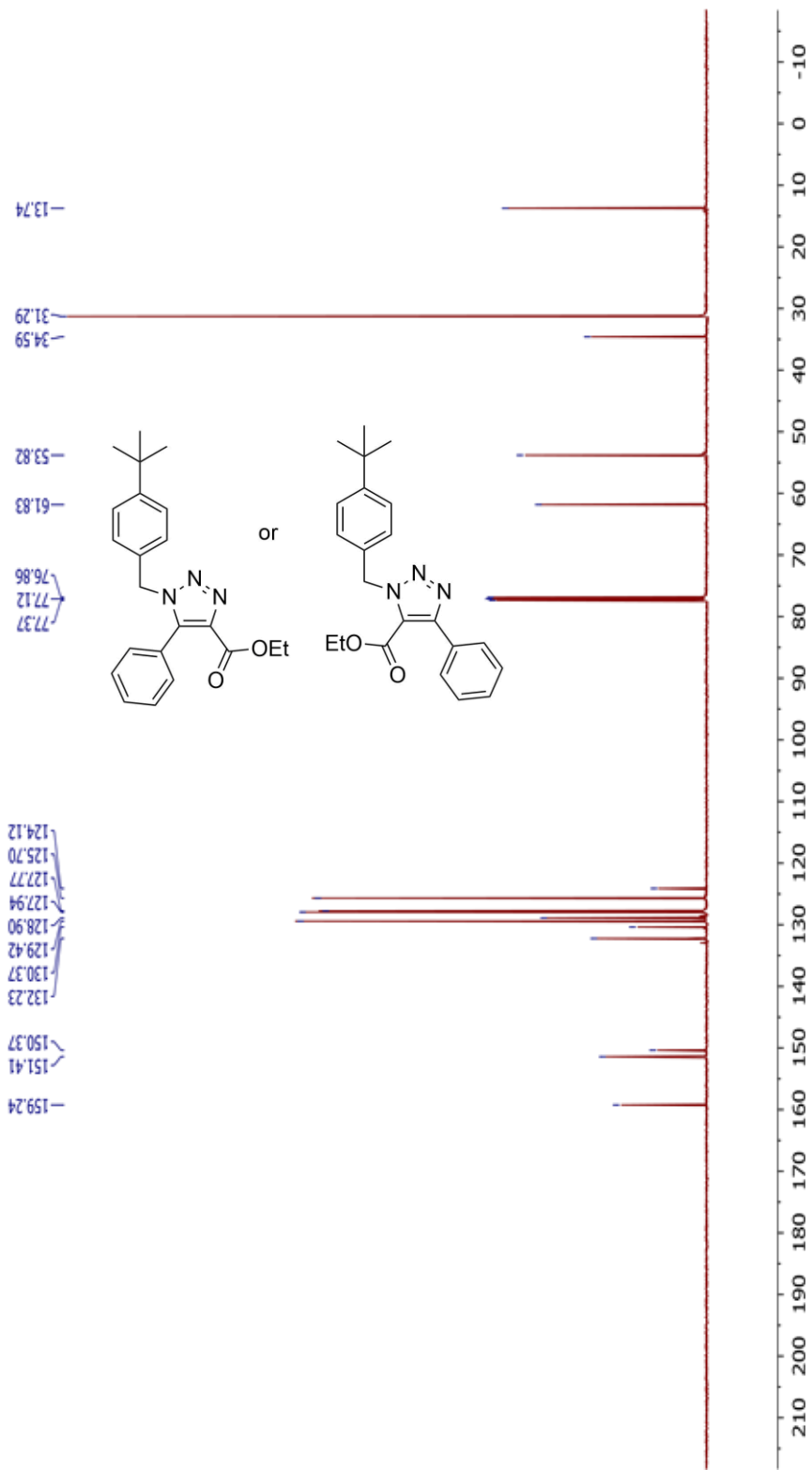


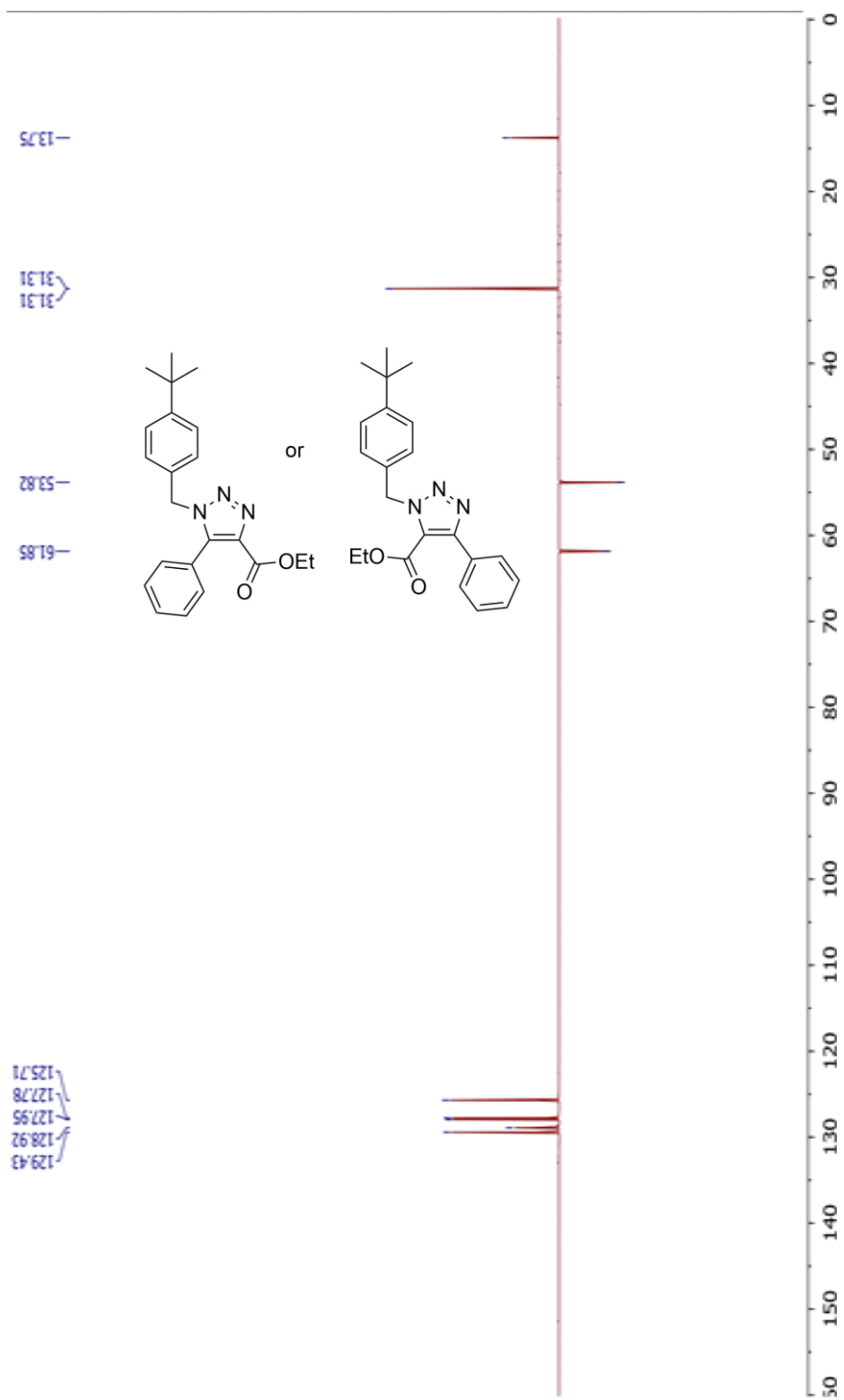
Methyl 3-(phenylsulfonyl)-2-propynate **2.10**



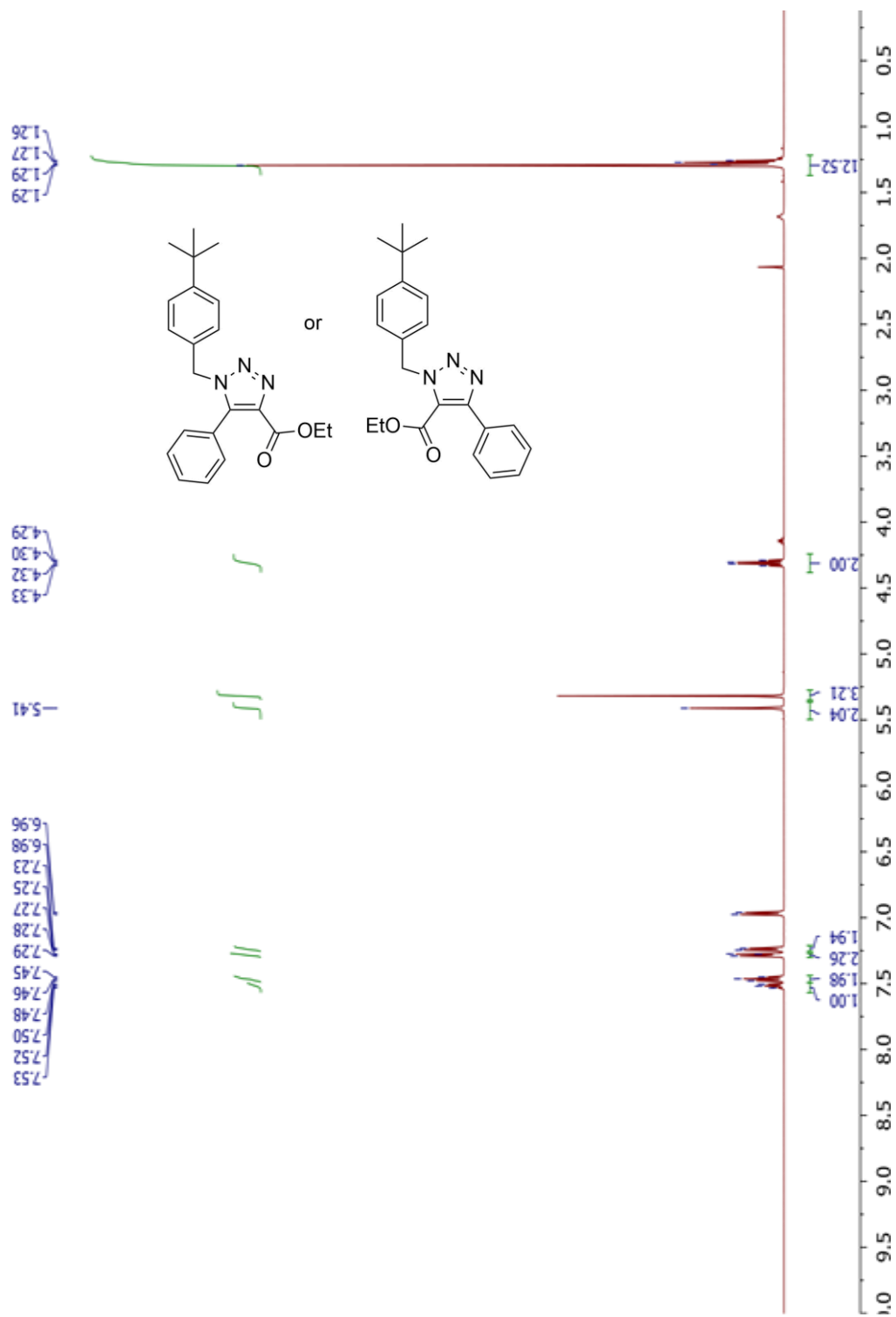


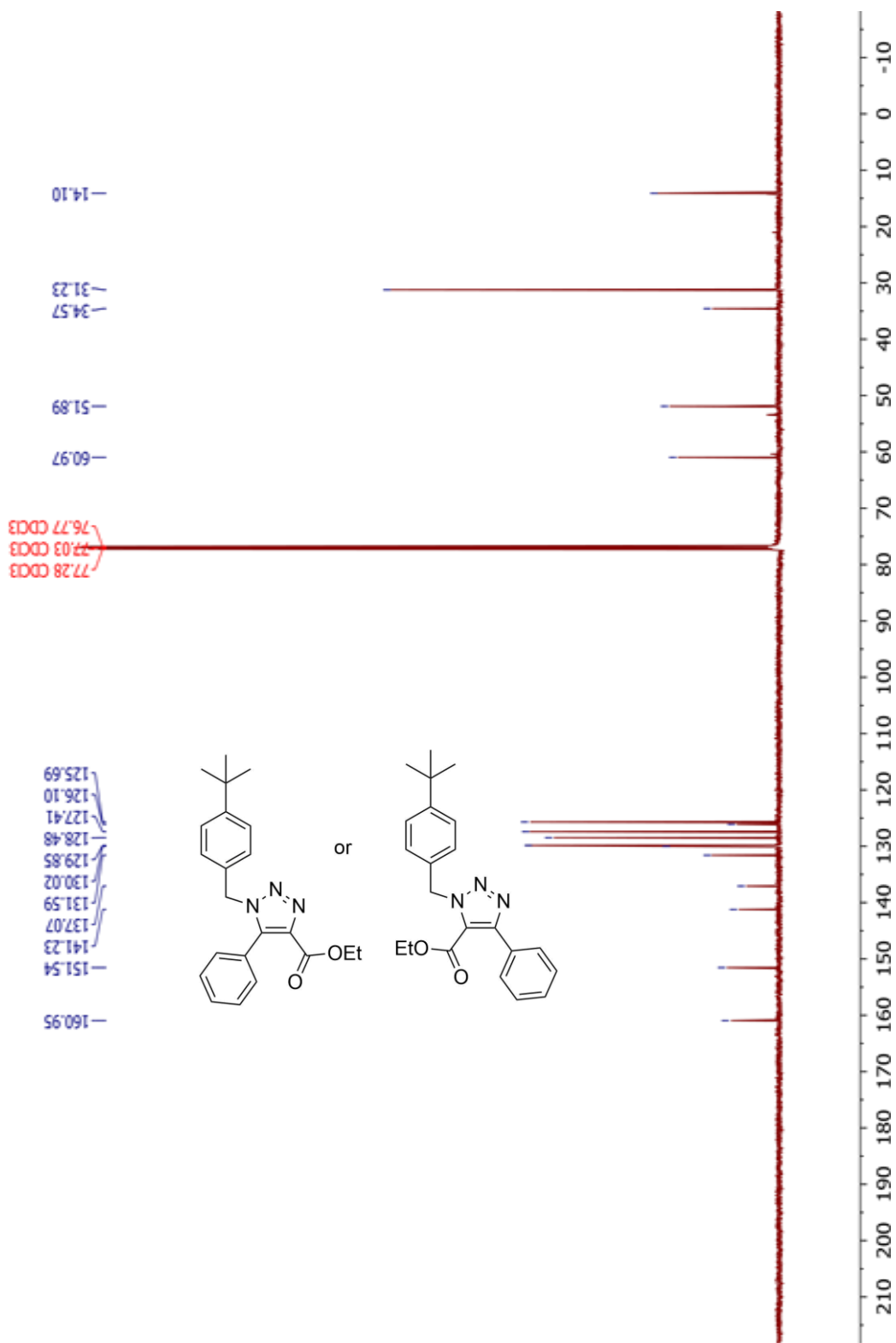


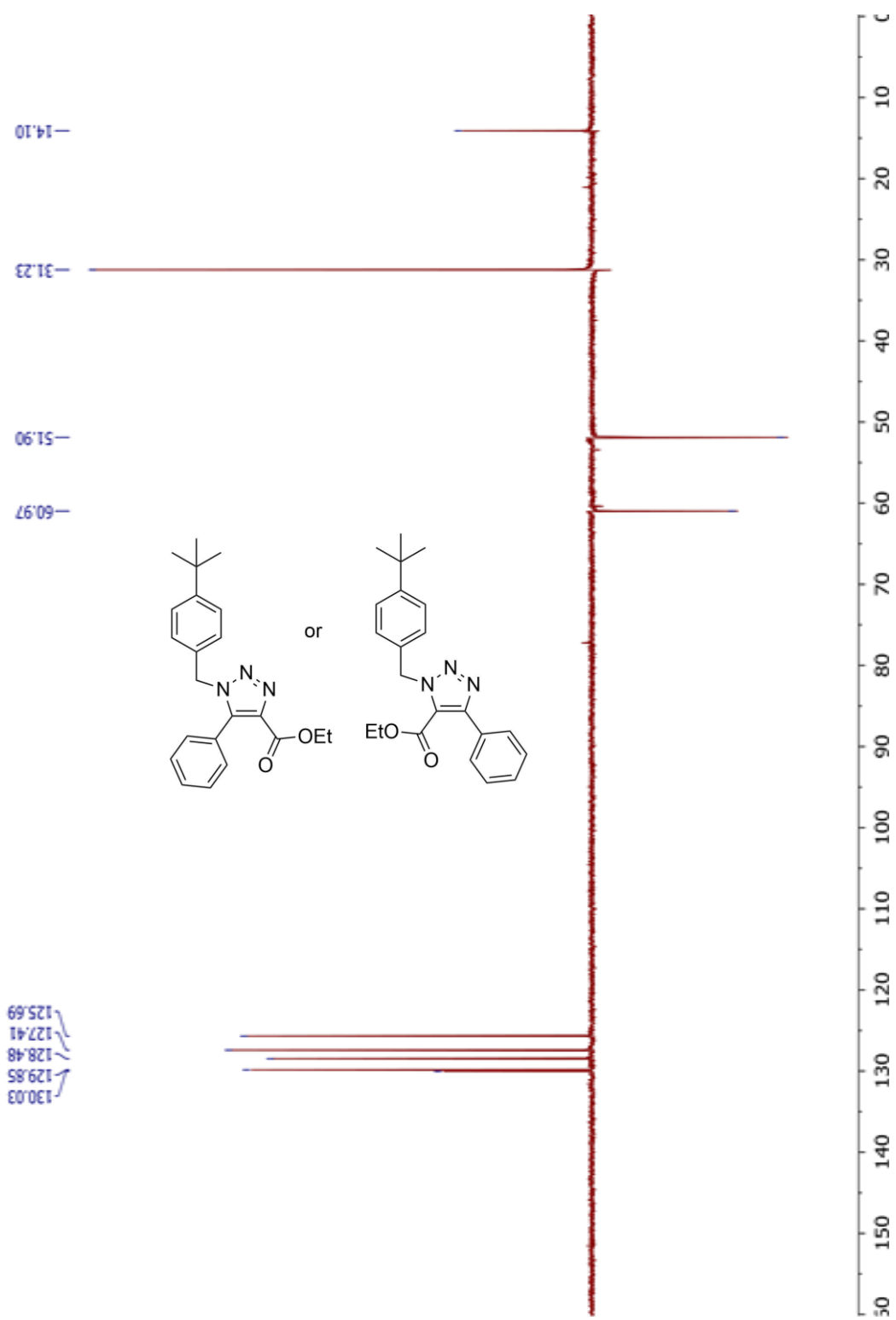




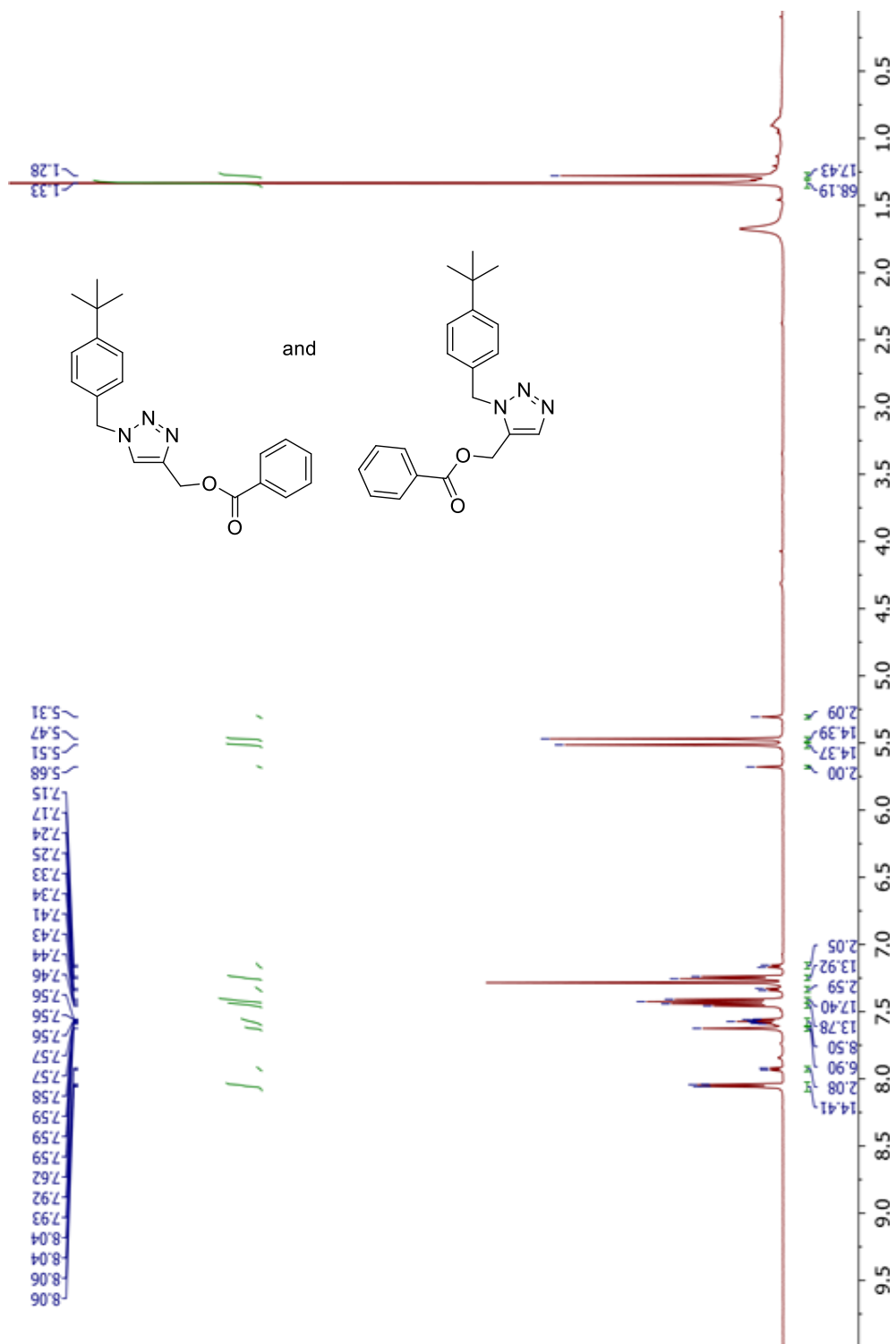
Triazole **2.1b** (regioisomer not identified)

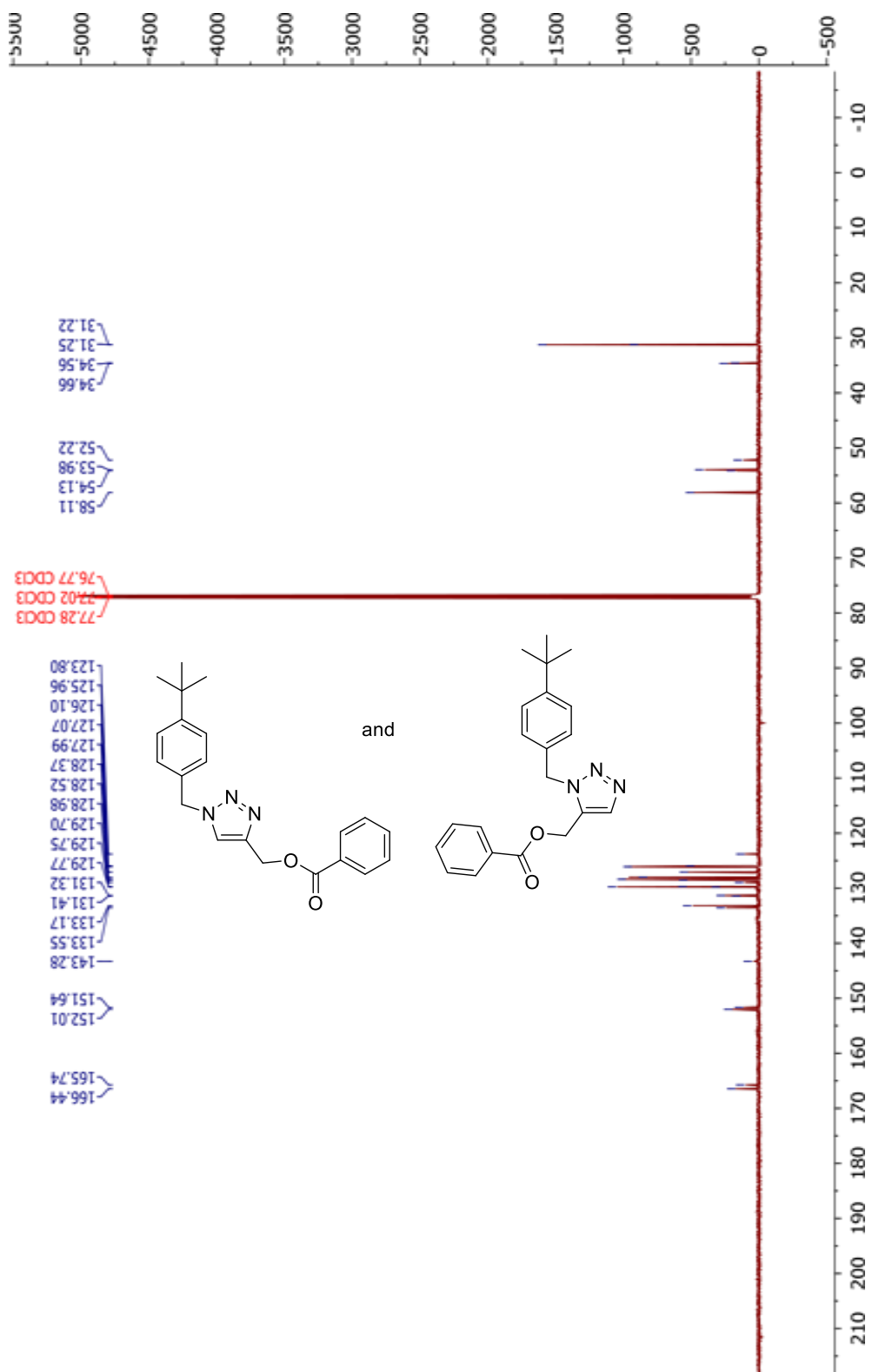


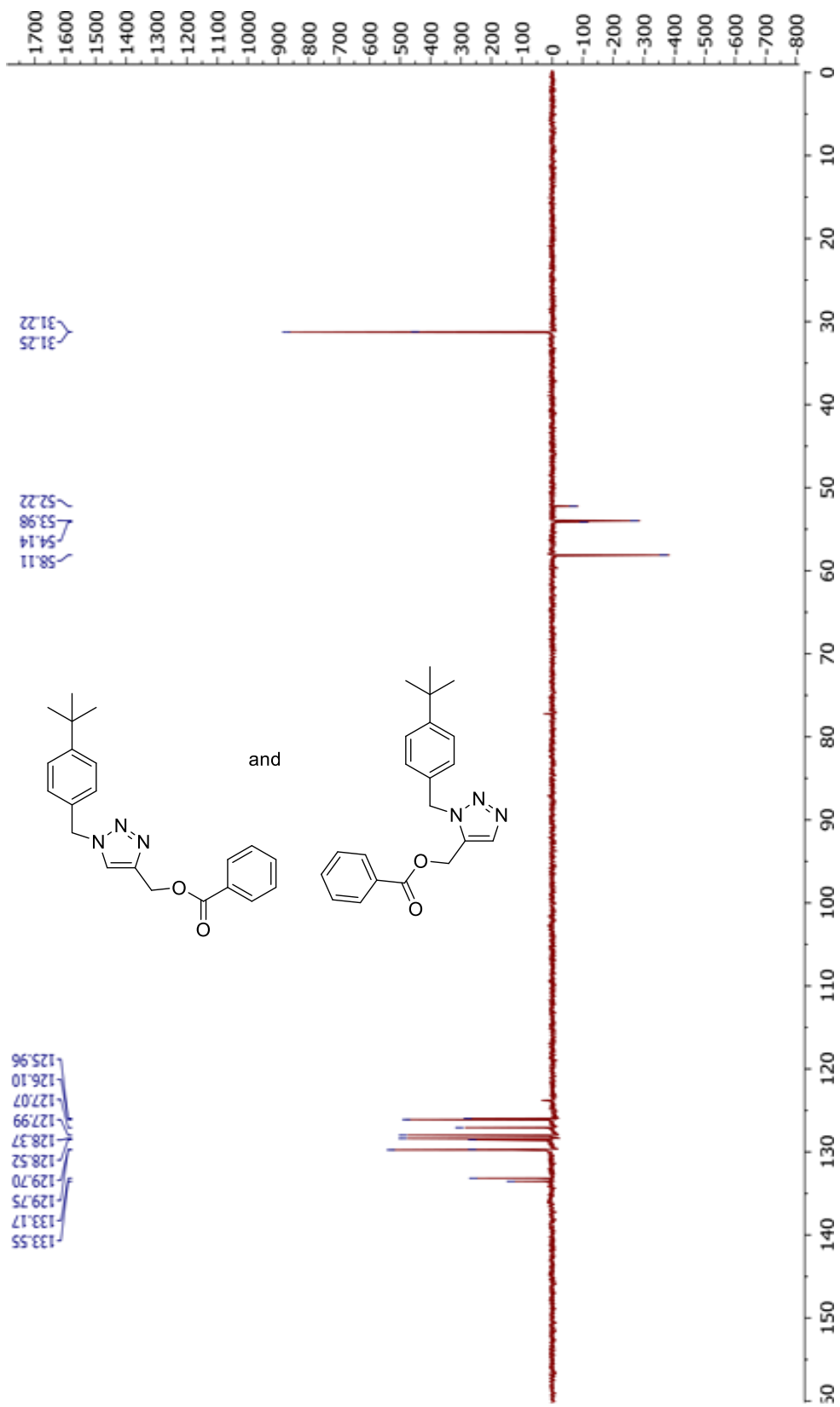




Triazoles **2.2a** and **2.2b** (regioisomers not separated)

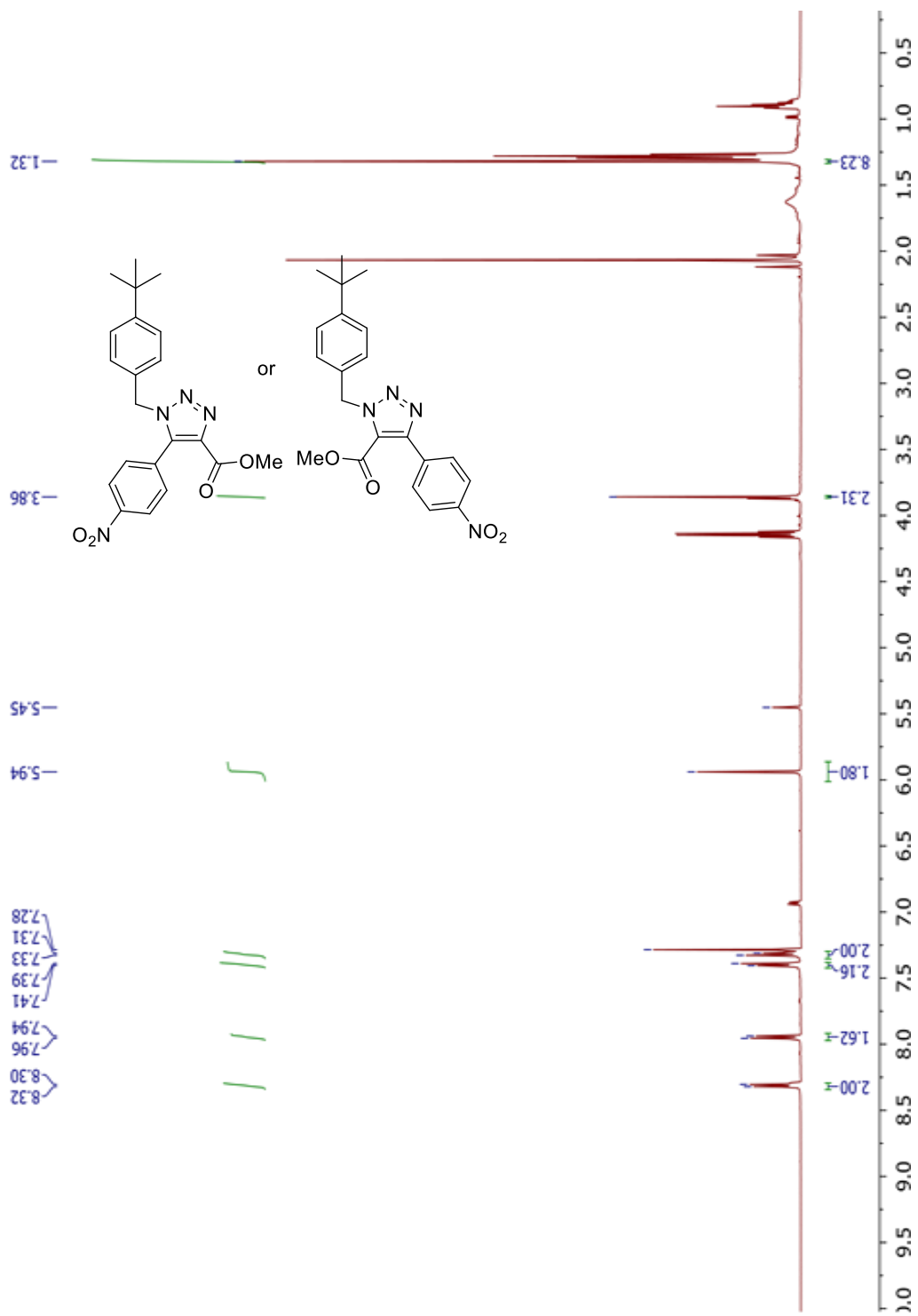


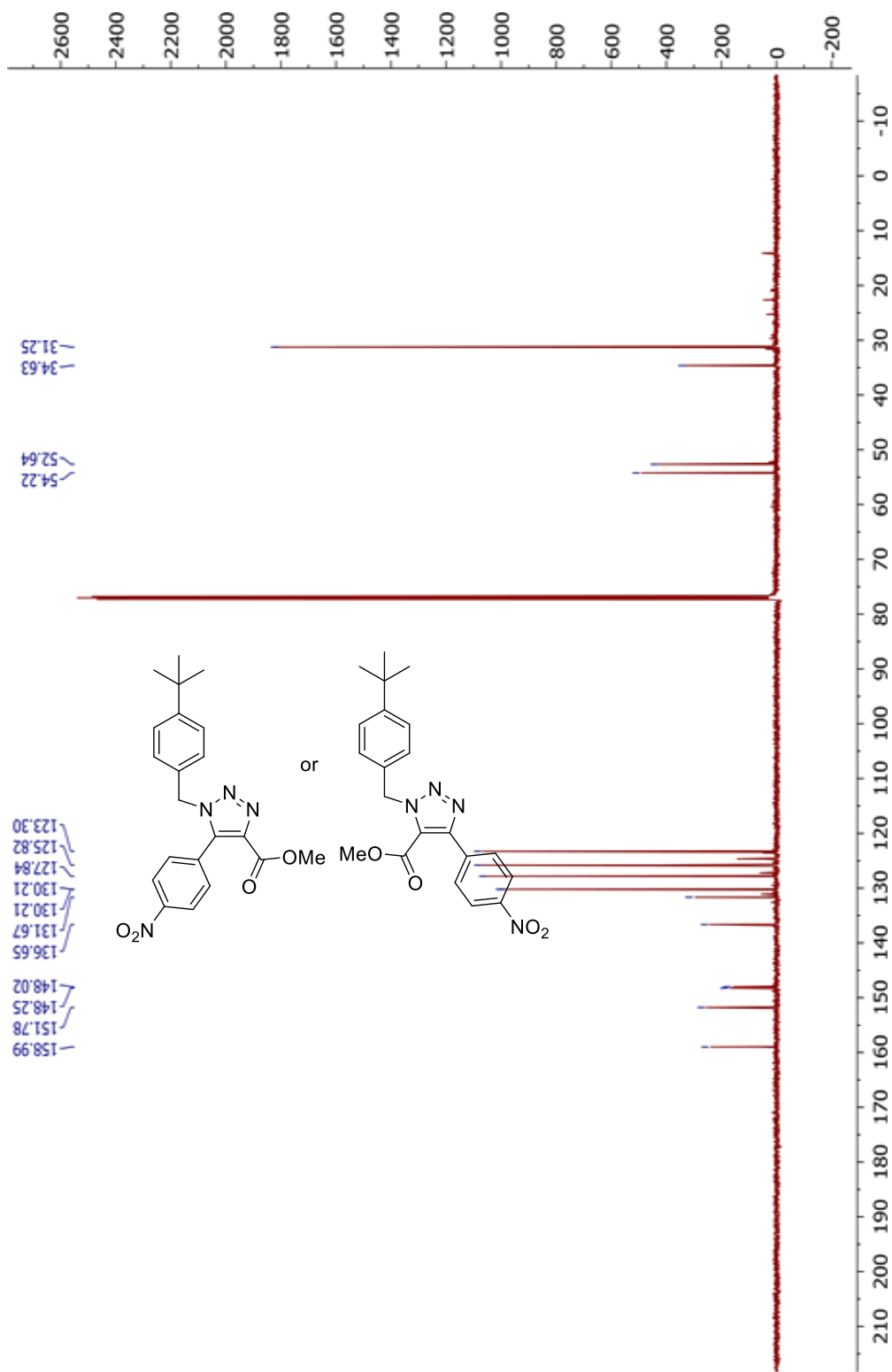


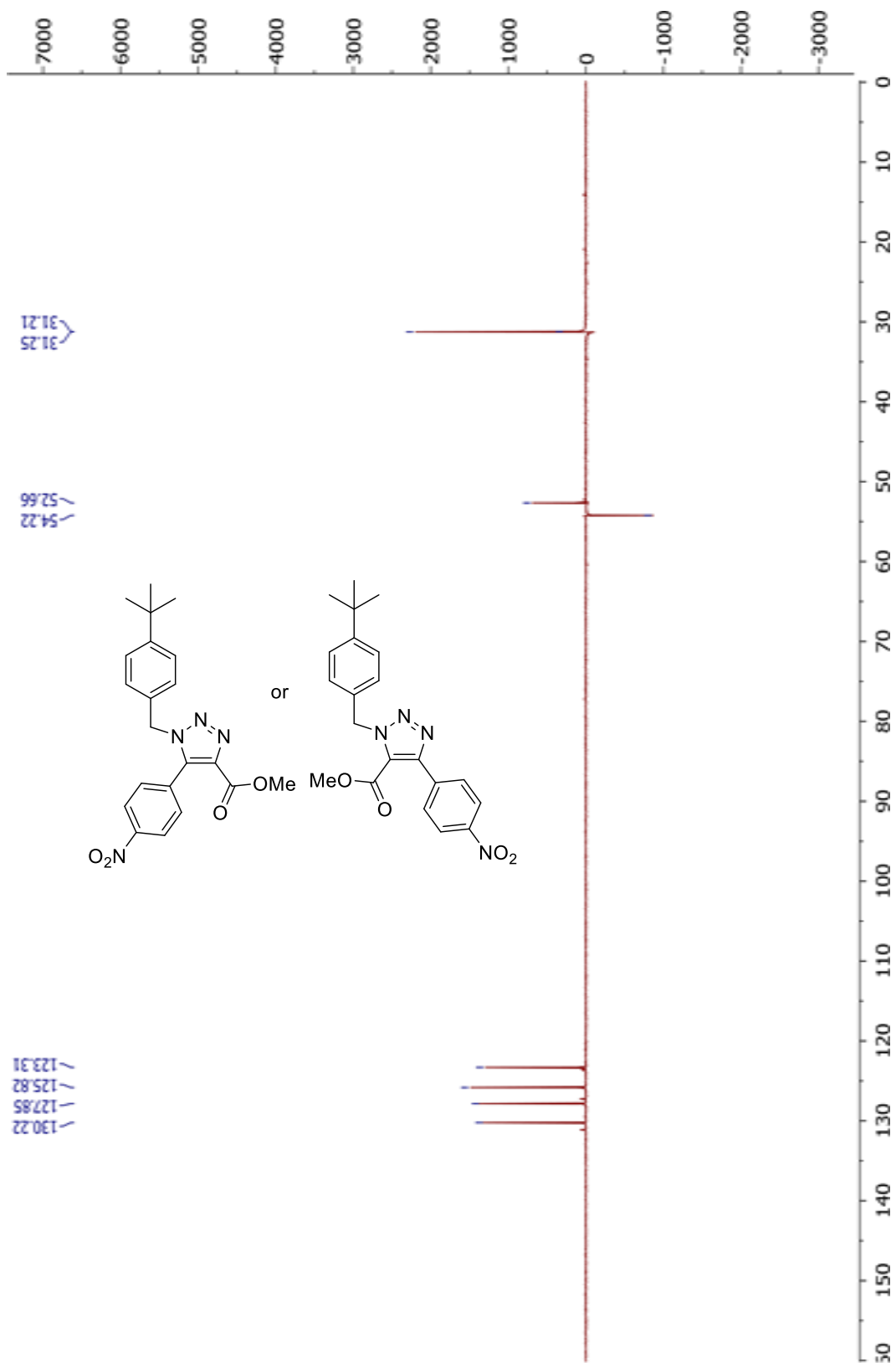




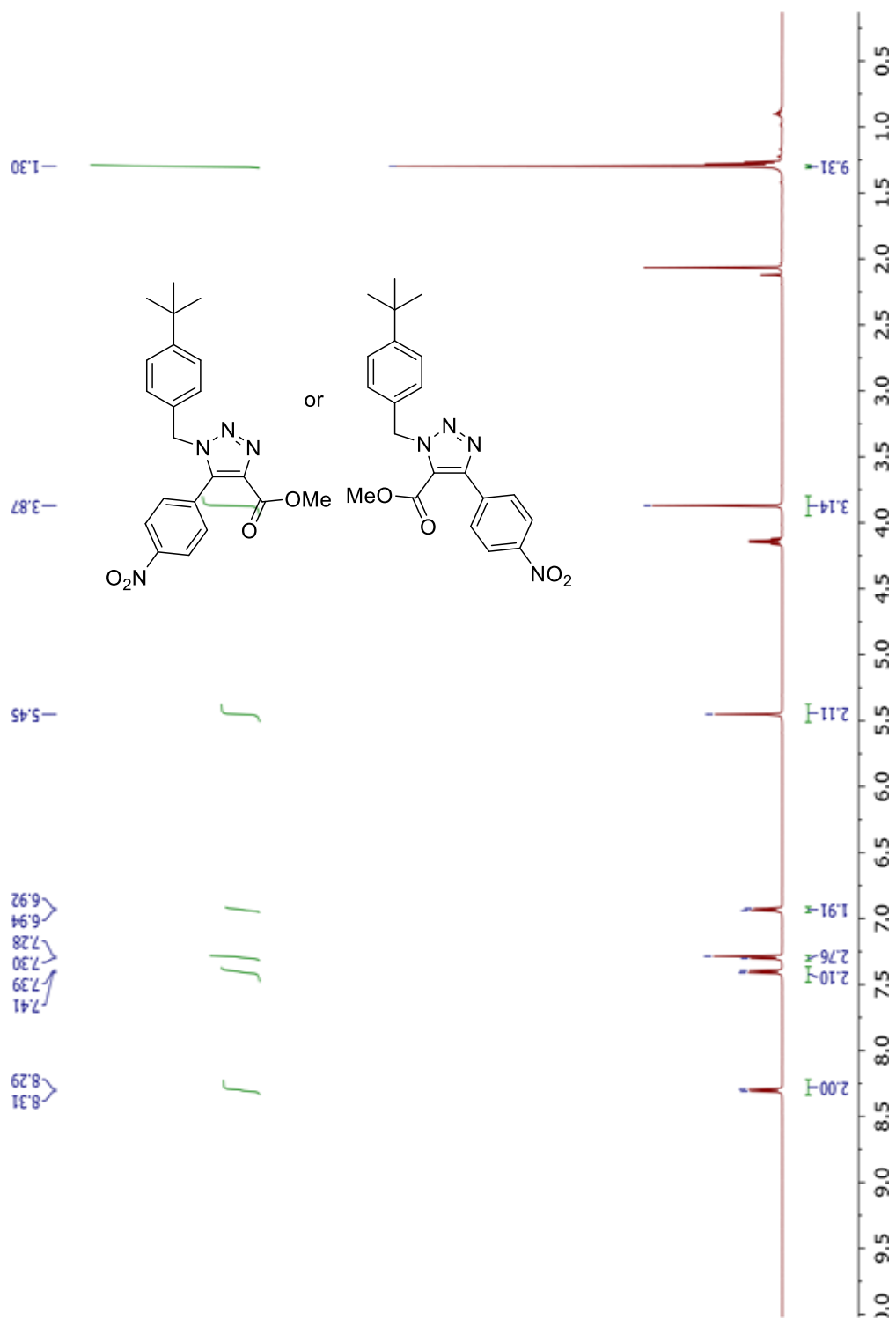
Triazole **2.3a** (regioisomer not identified)

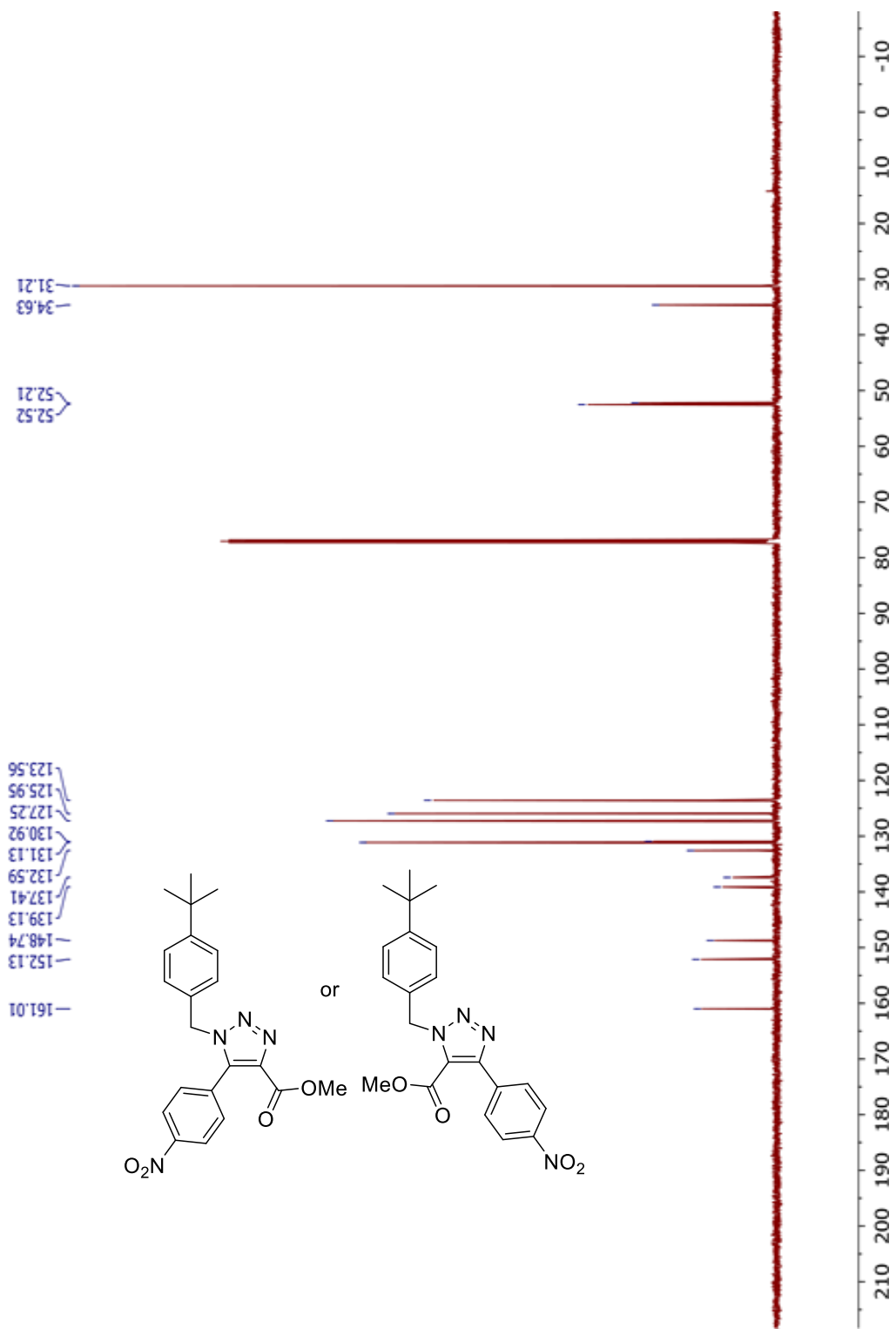


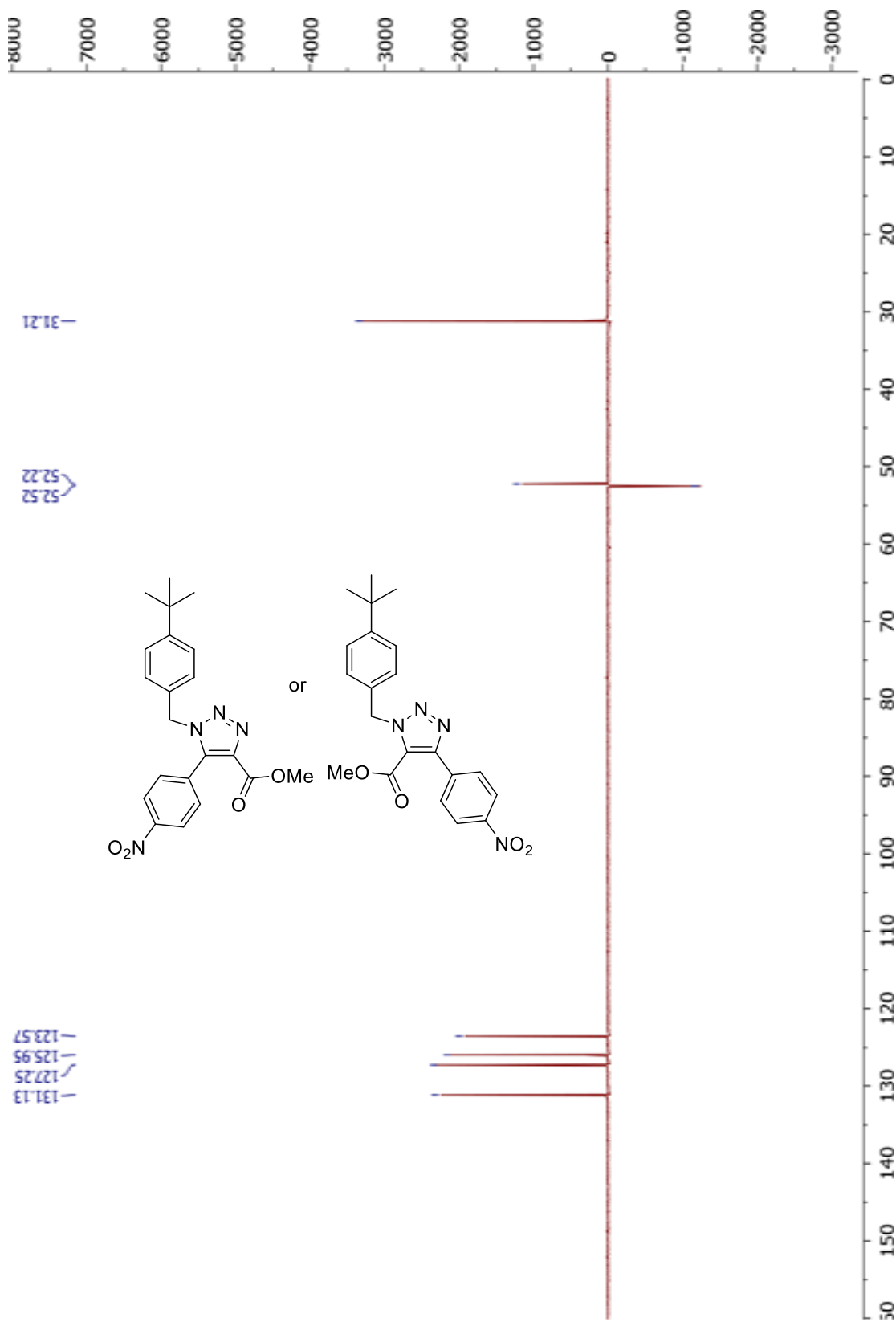




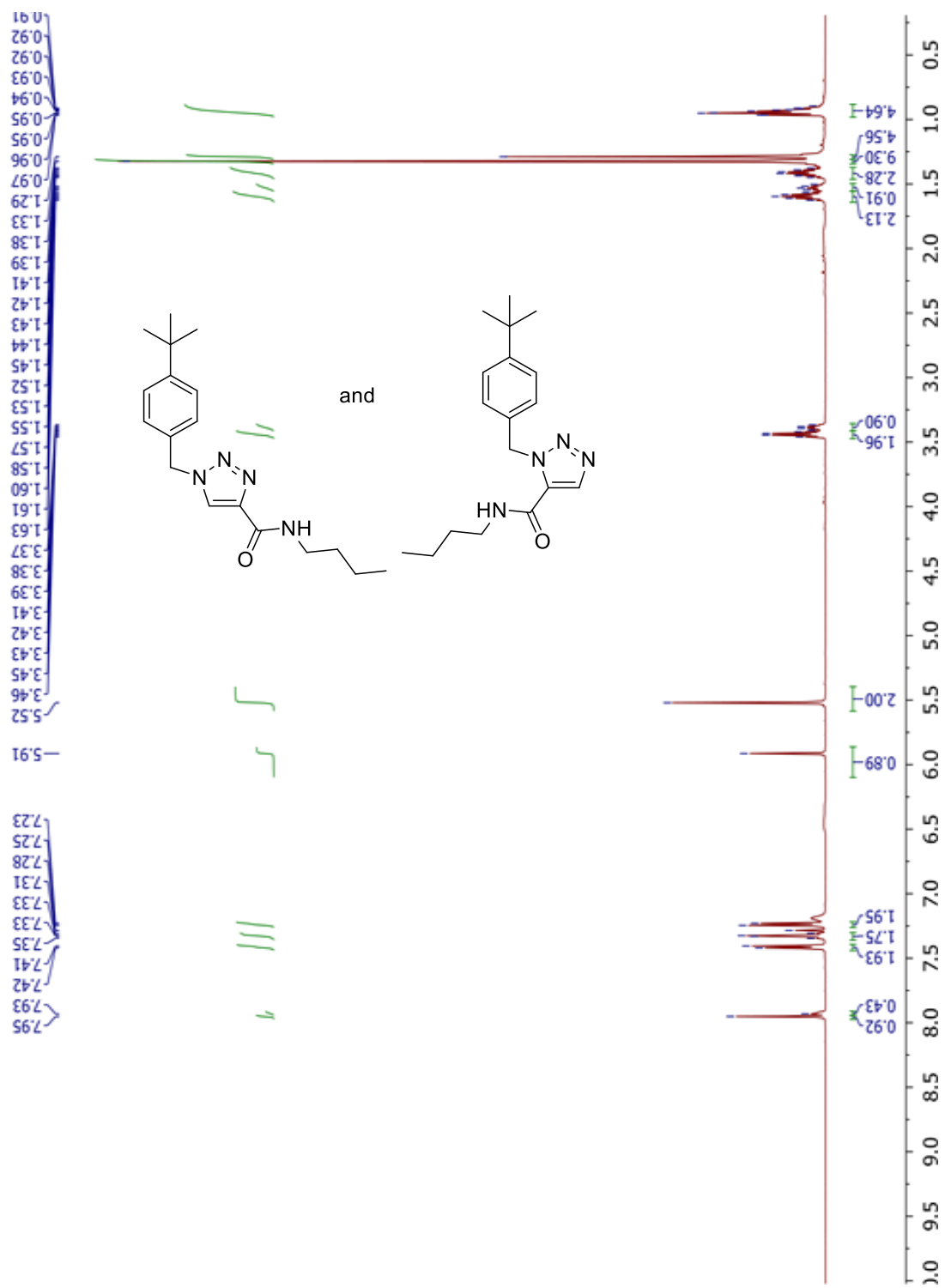
Triazole **2.3b** (regioisomer not identified)

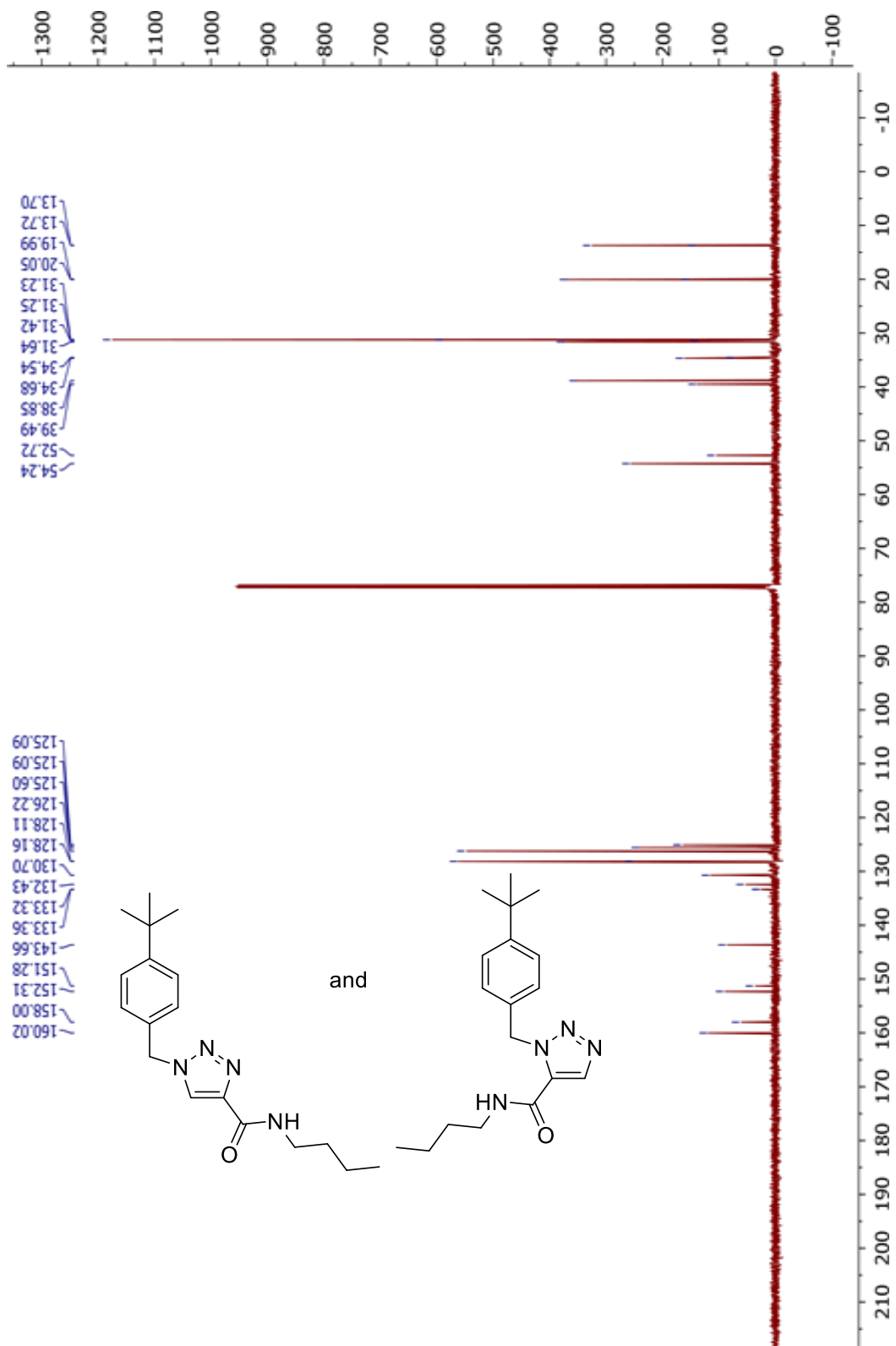




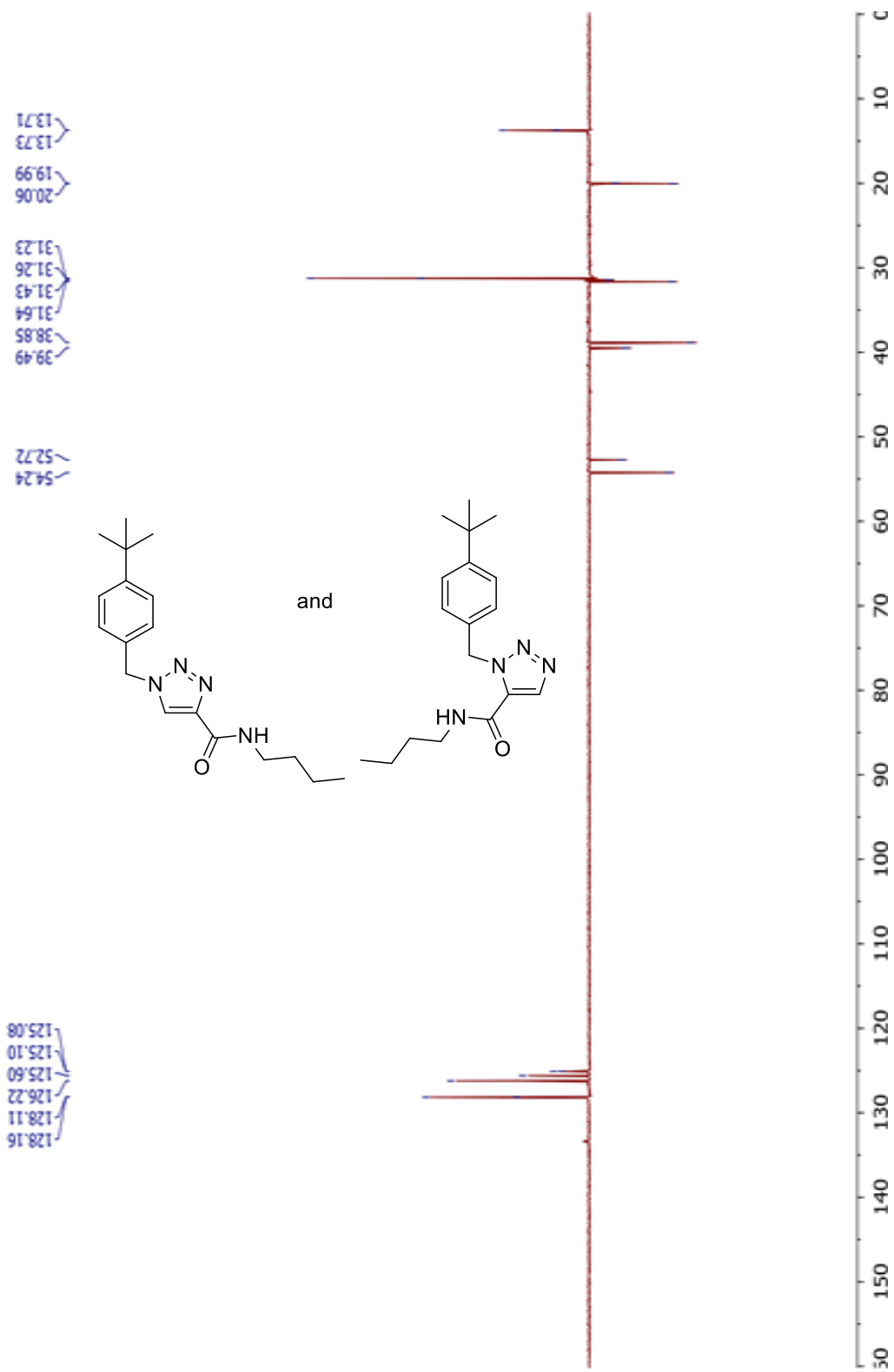


Trizoles **2.4a** and **2.4b** (regioisomers not separated)

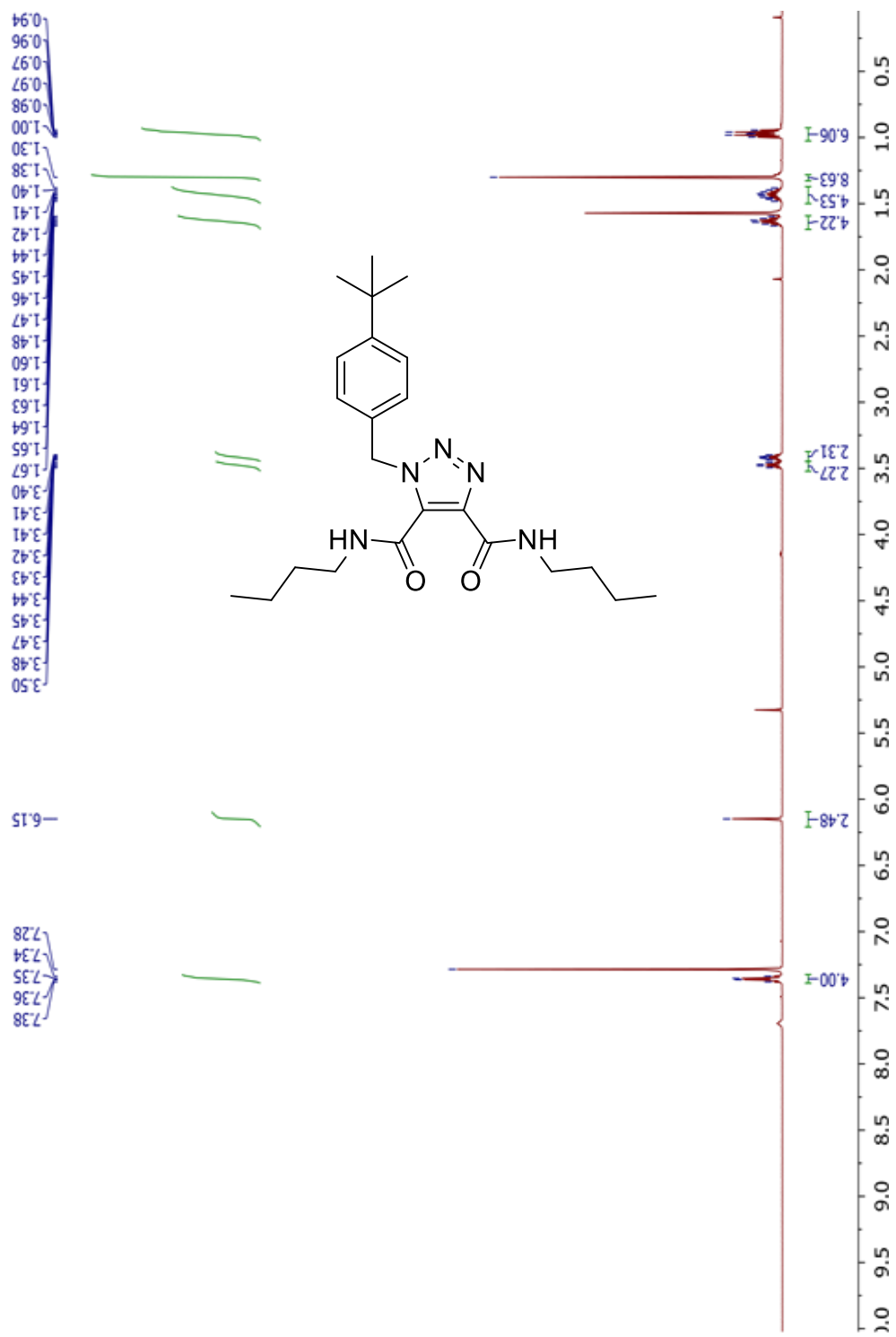


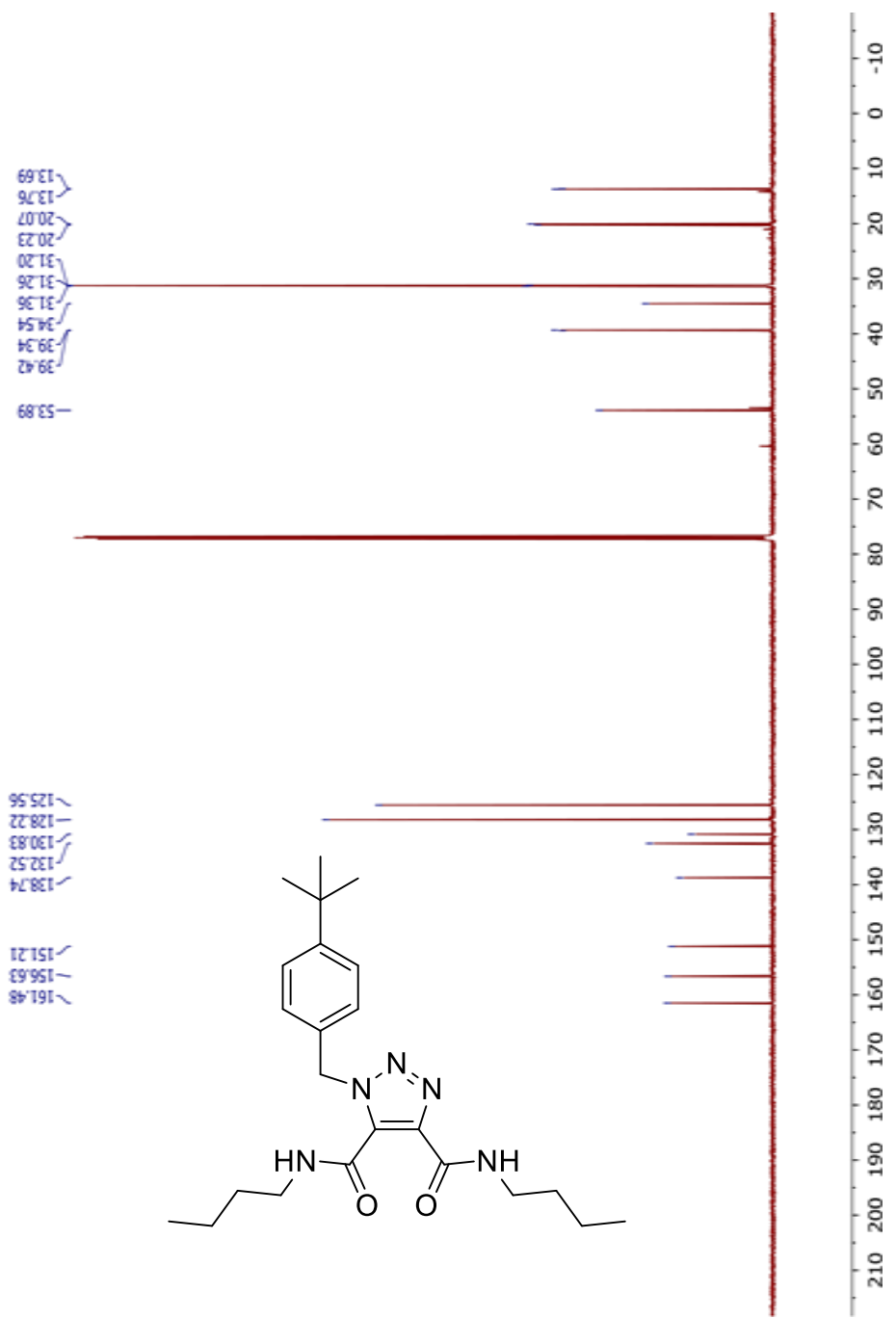


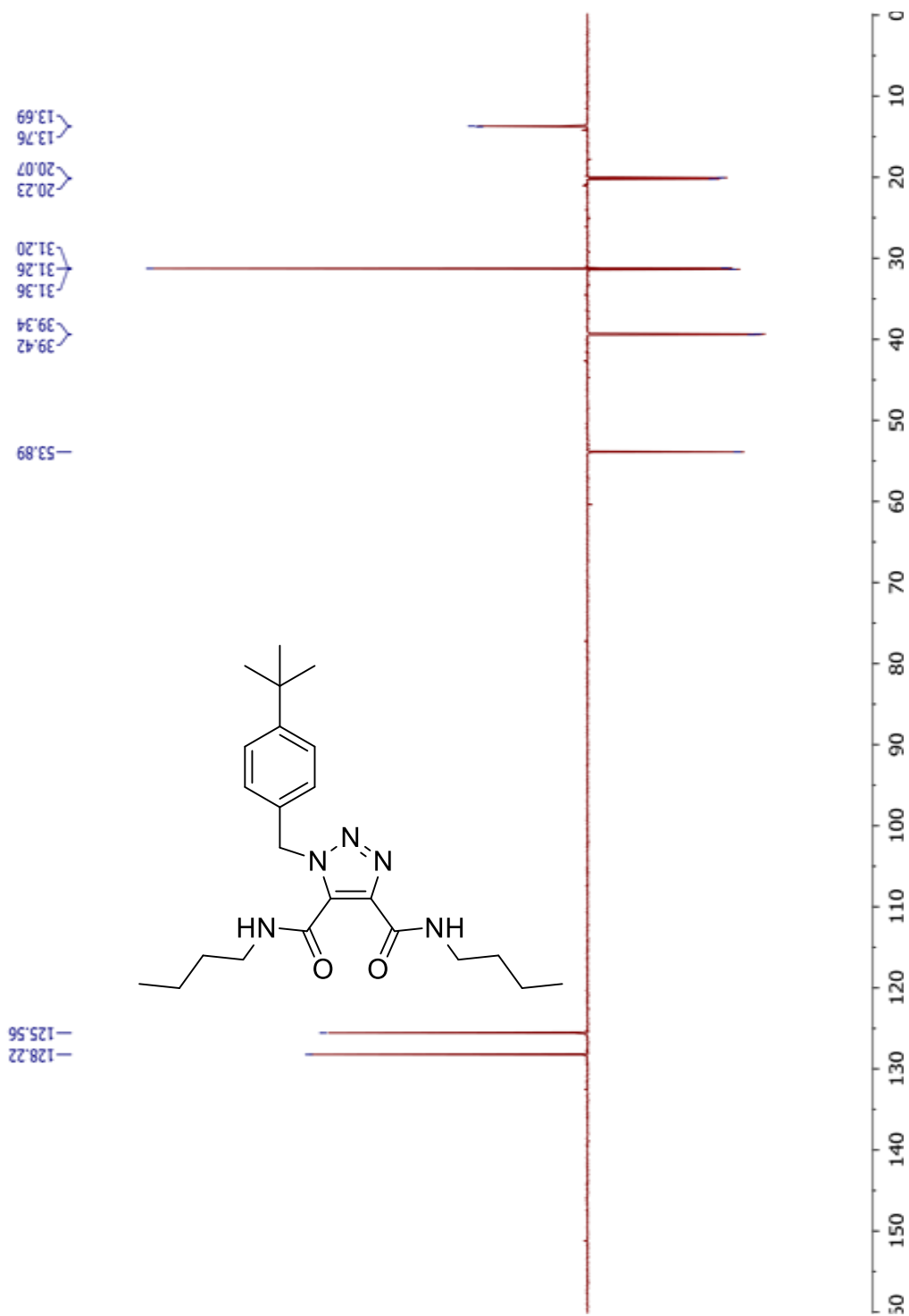




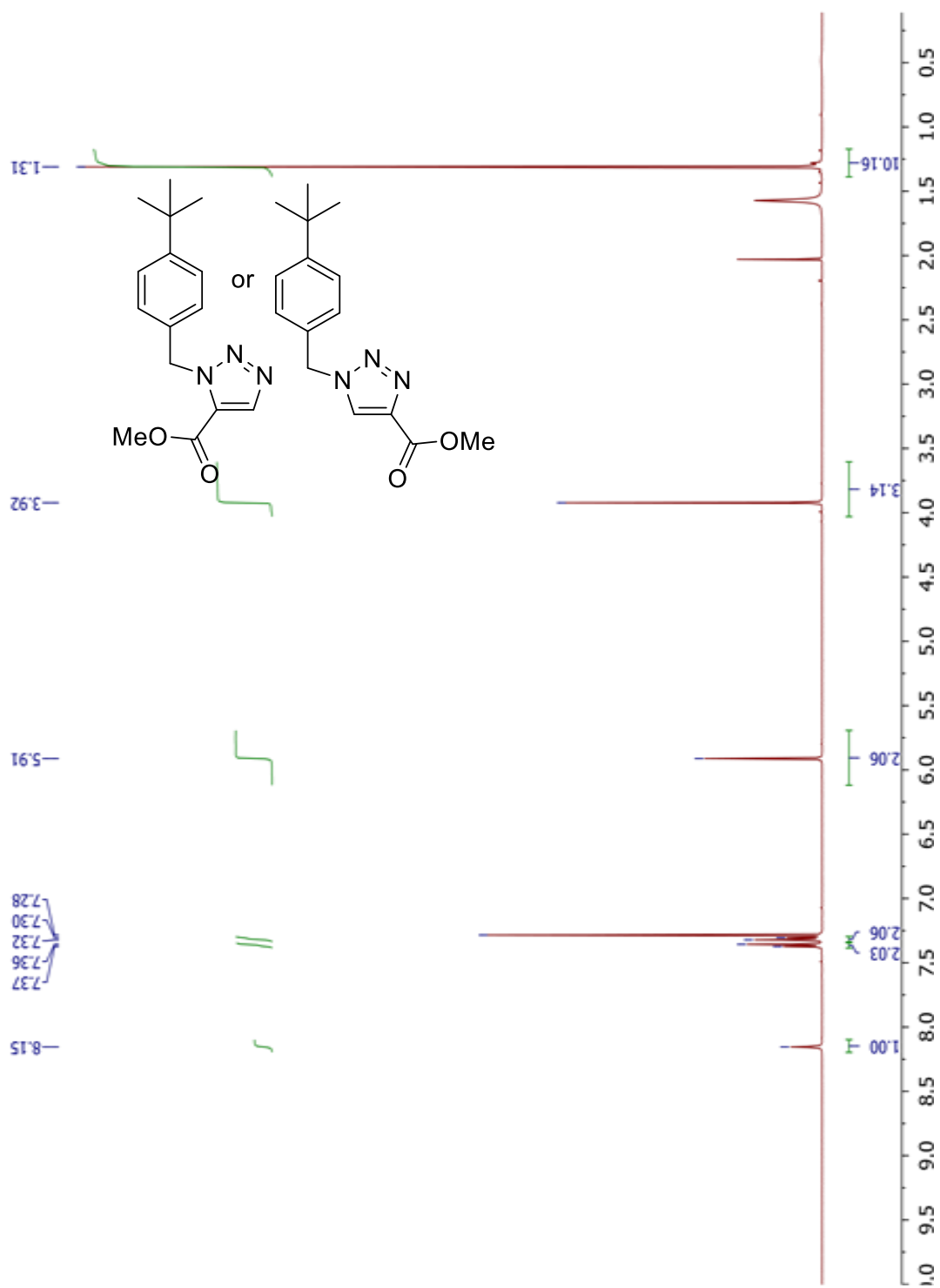
# Triazole 2.5a



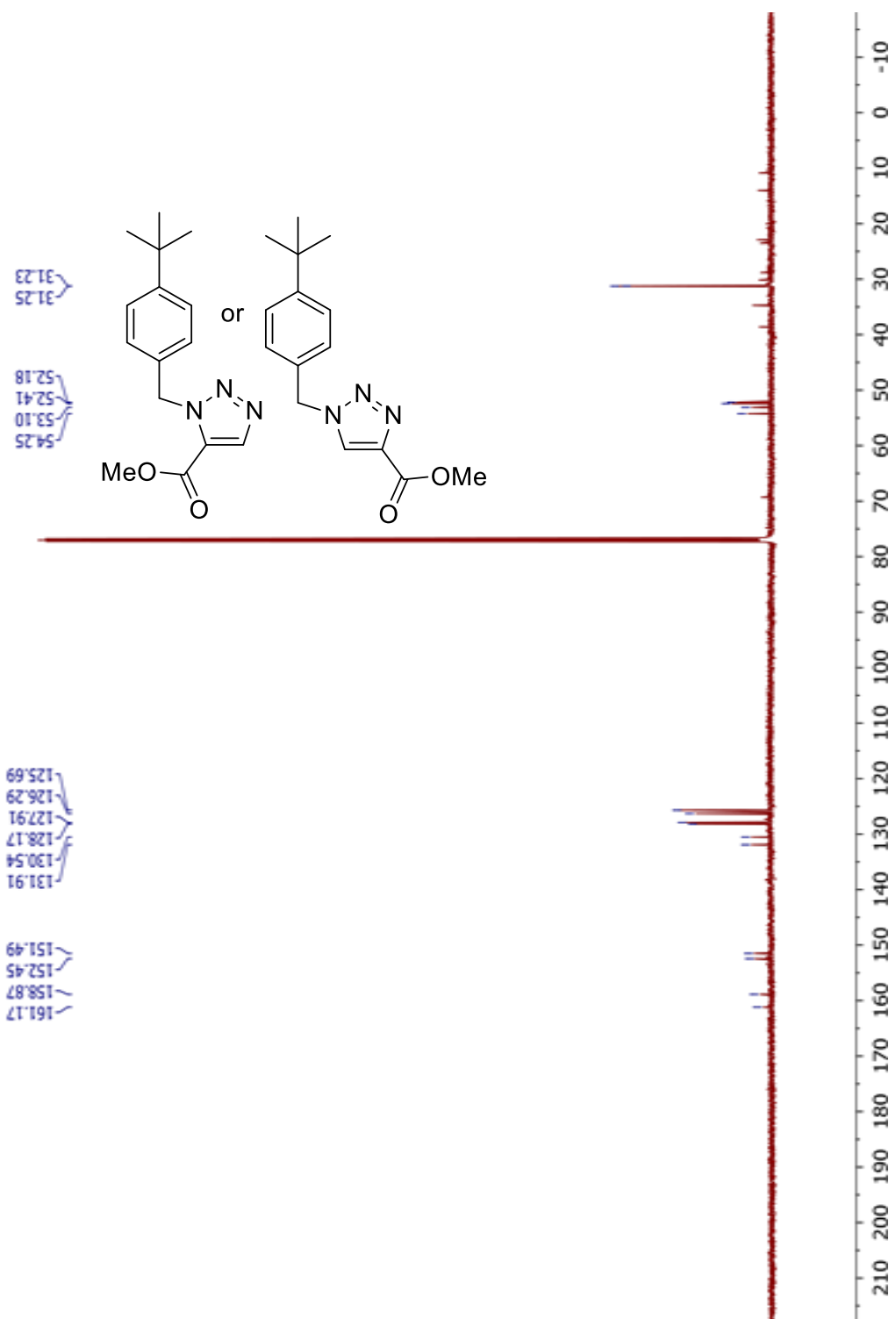


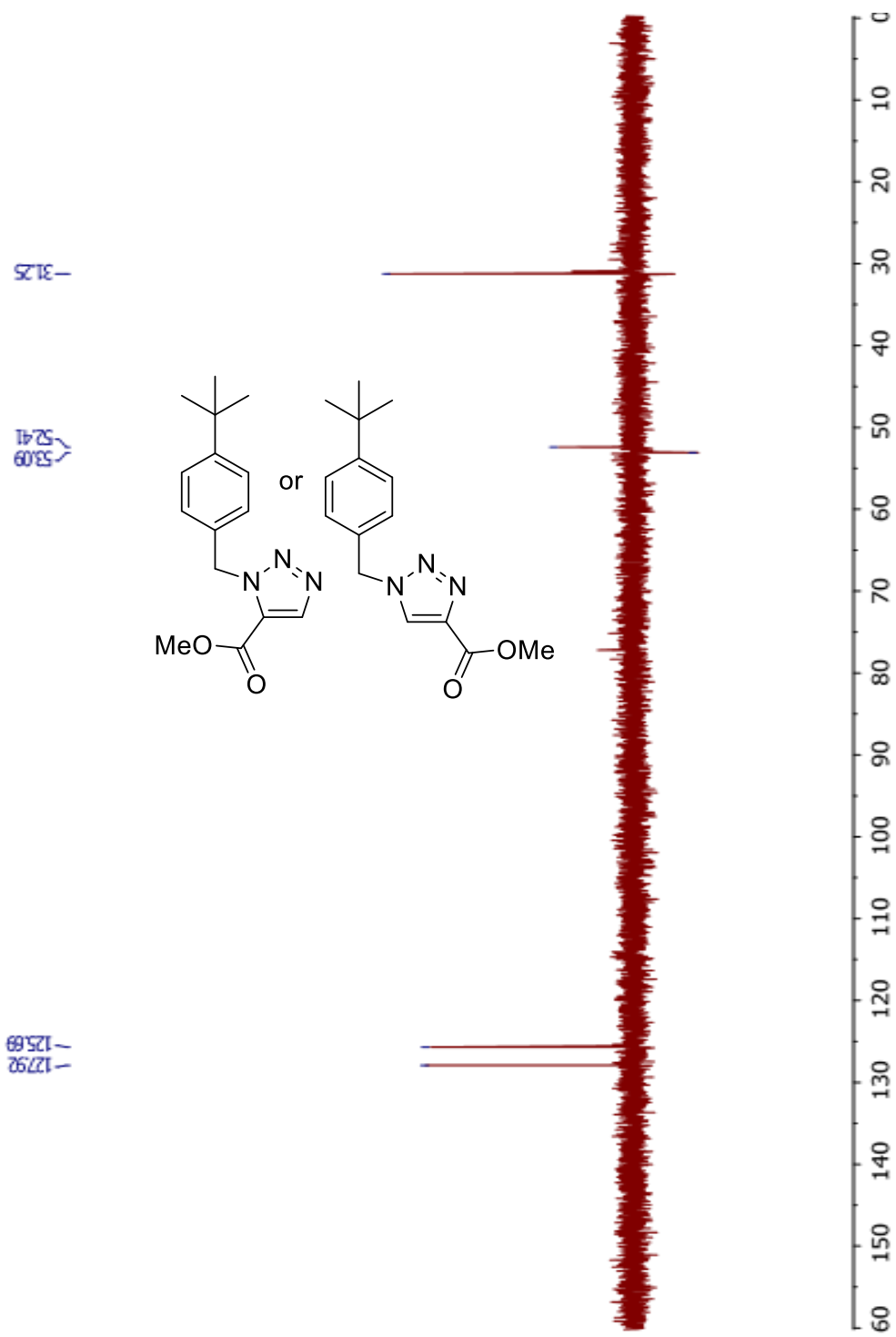


Triazole **2.6a** (regioisomer not identified)

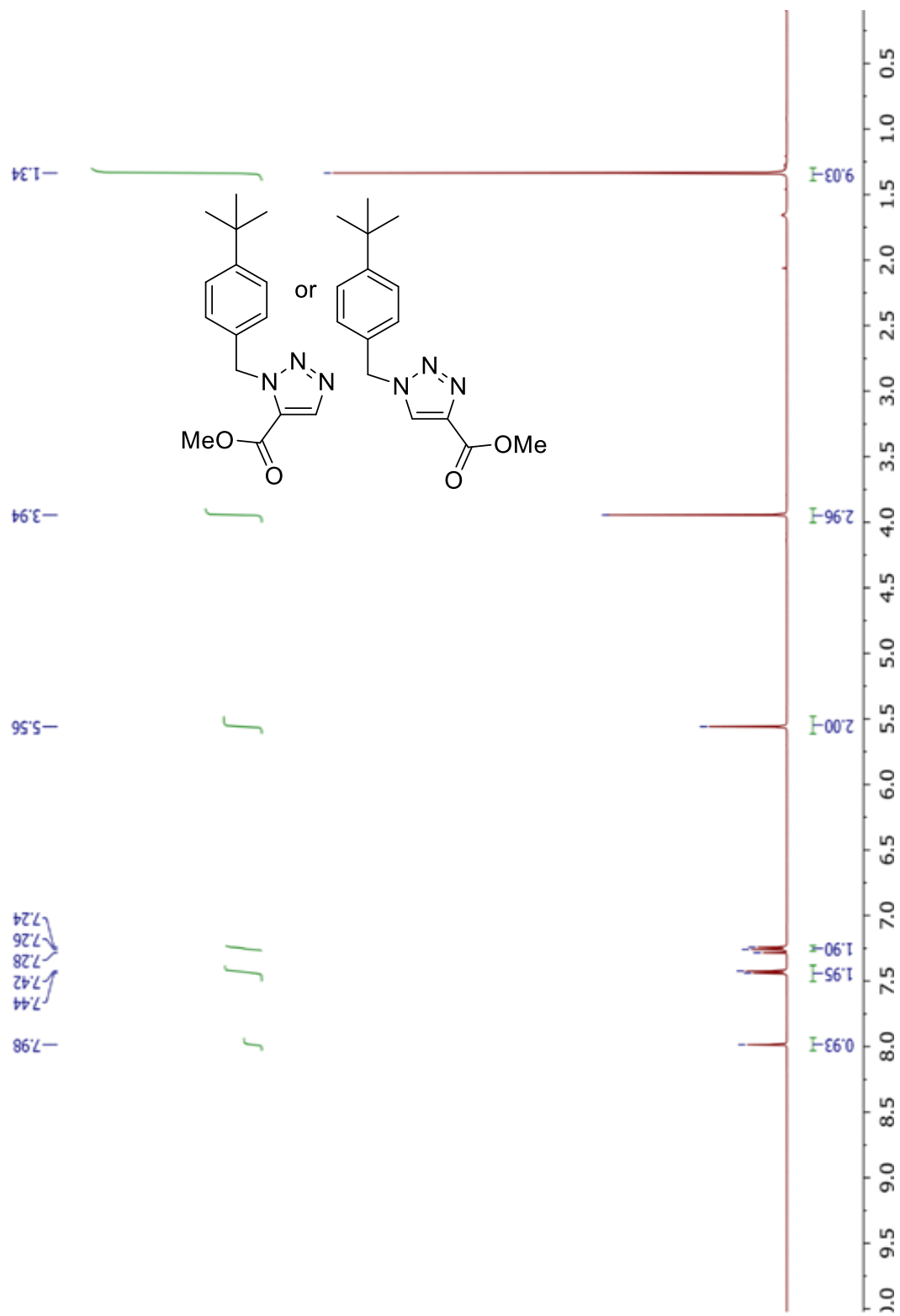


$^{13}\text{C}$ NMR is a mixture with **T6b**

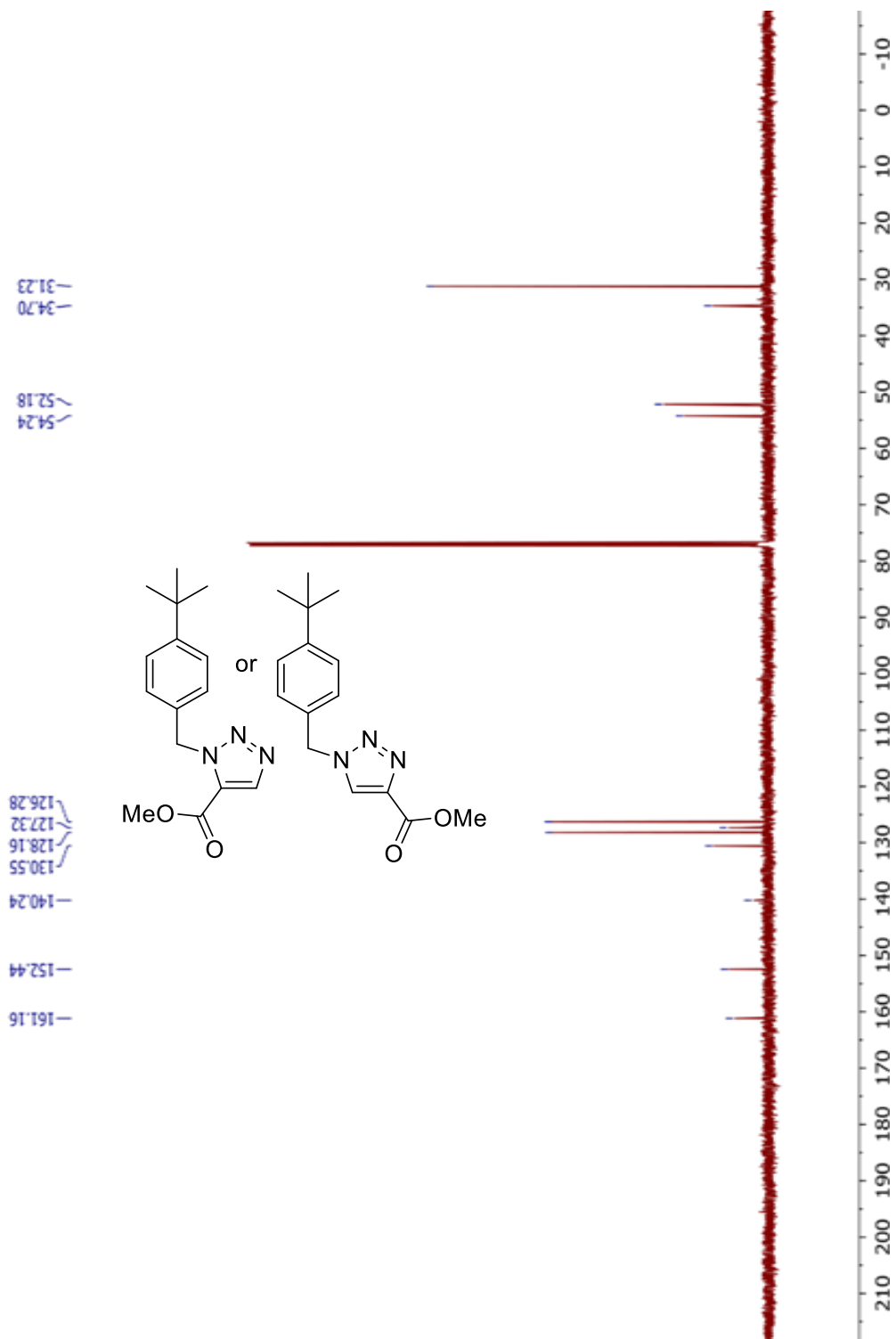


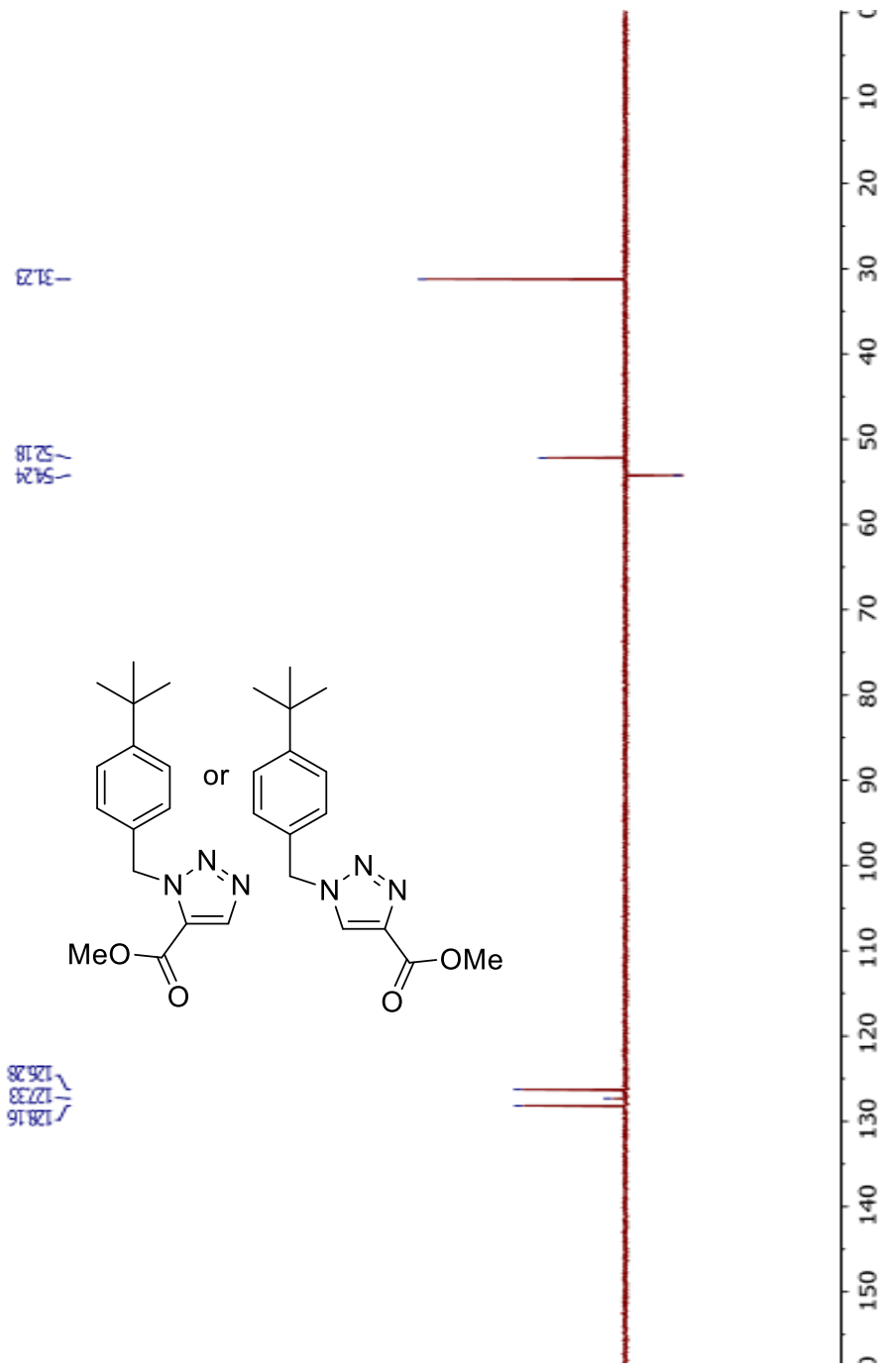


Triazole **2.6b** (regioisomer not identified)

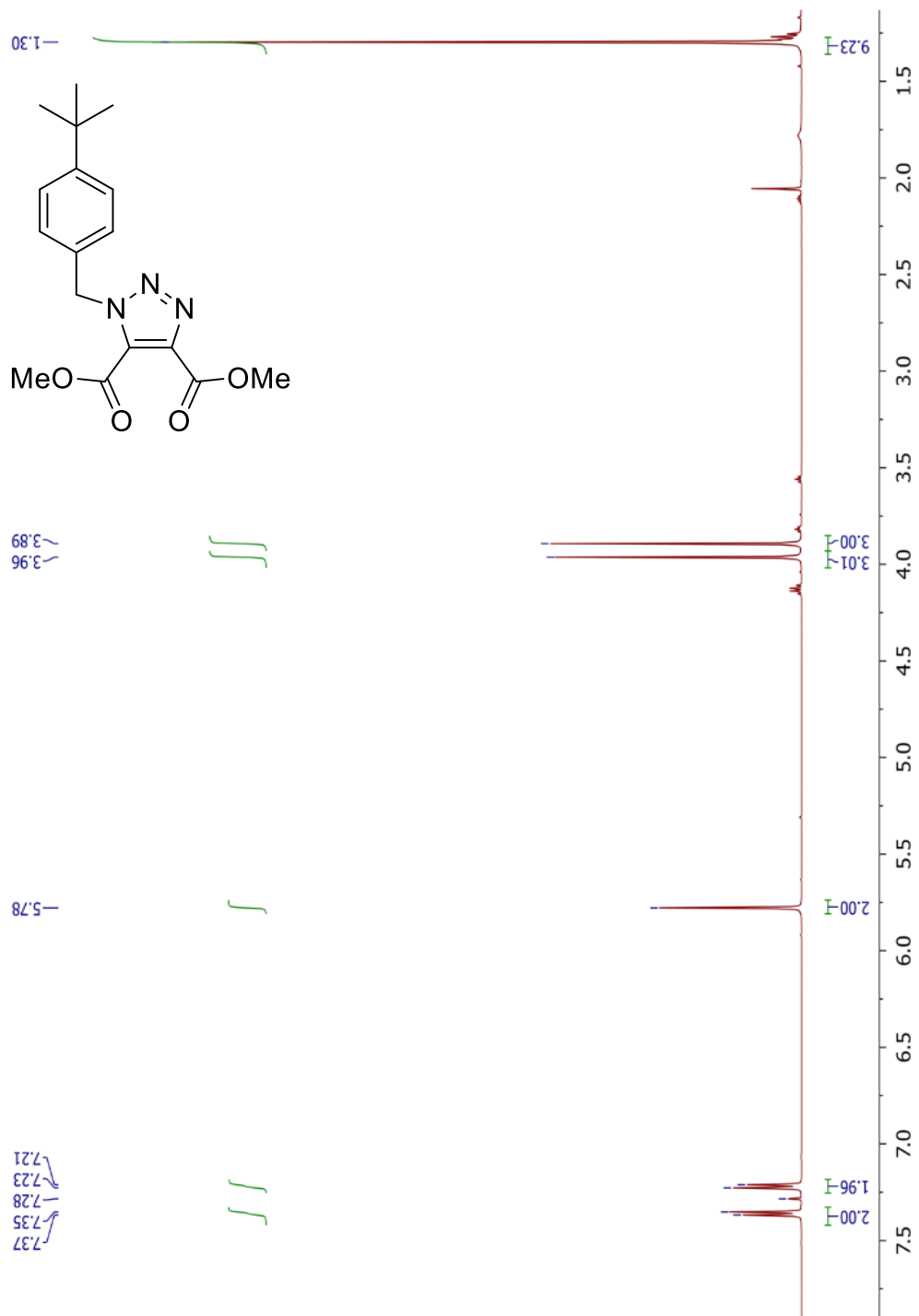


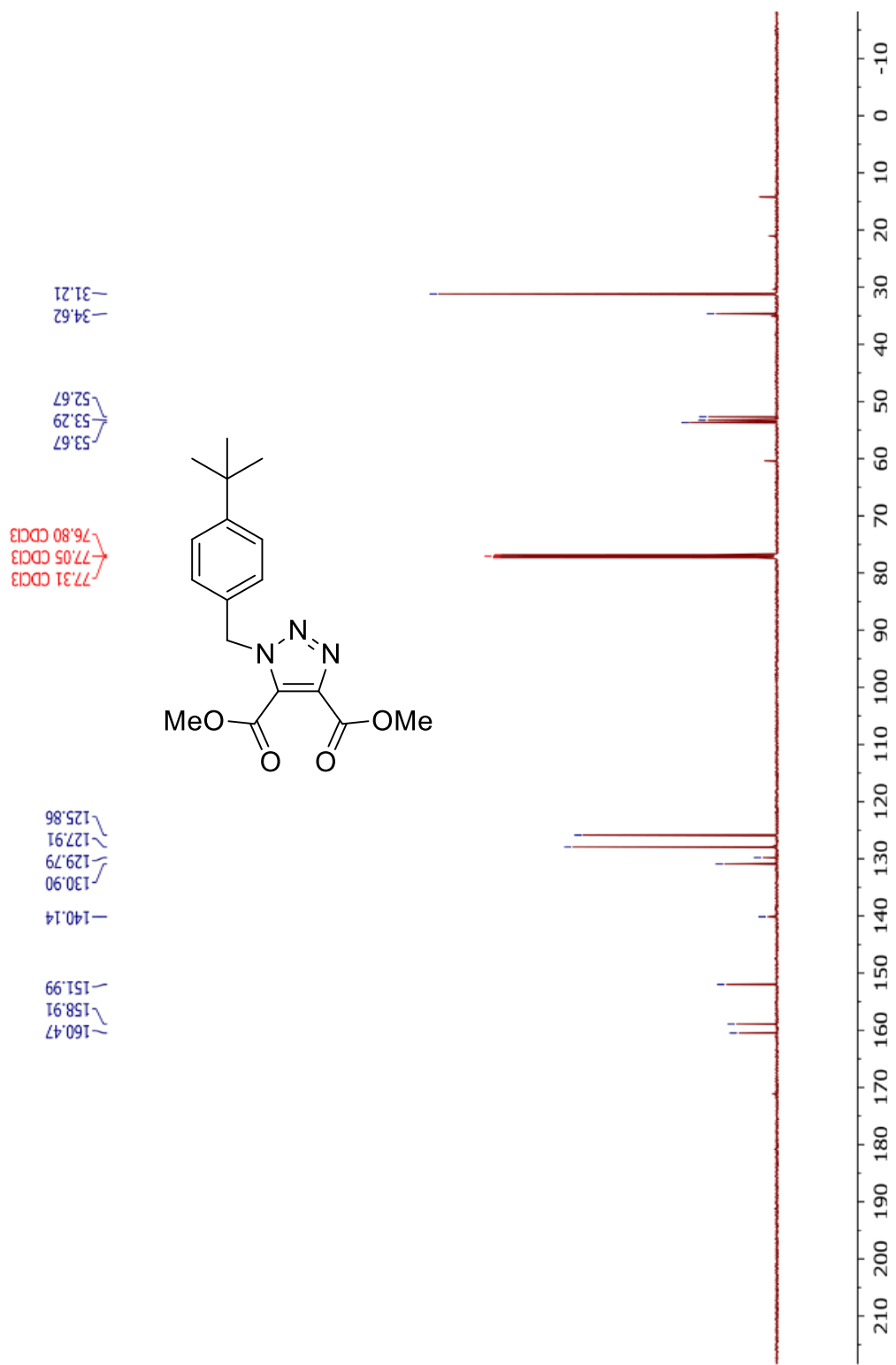


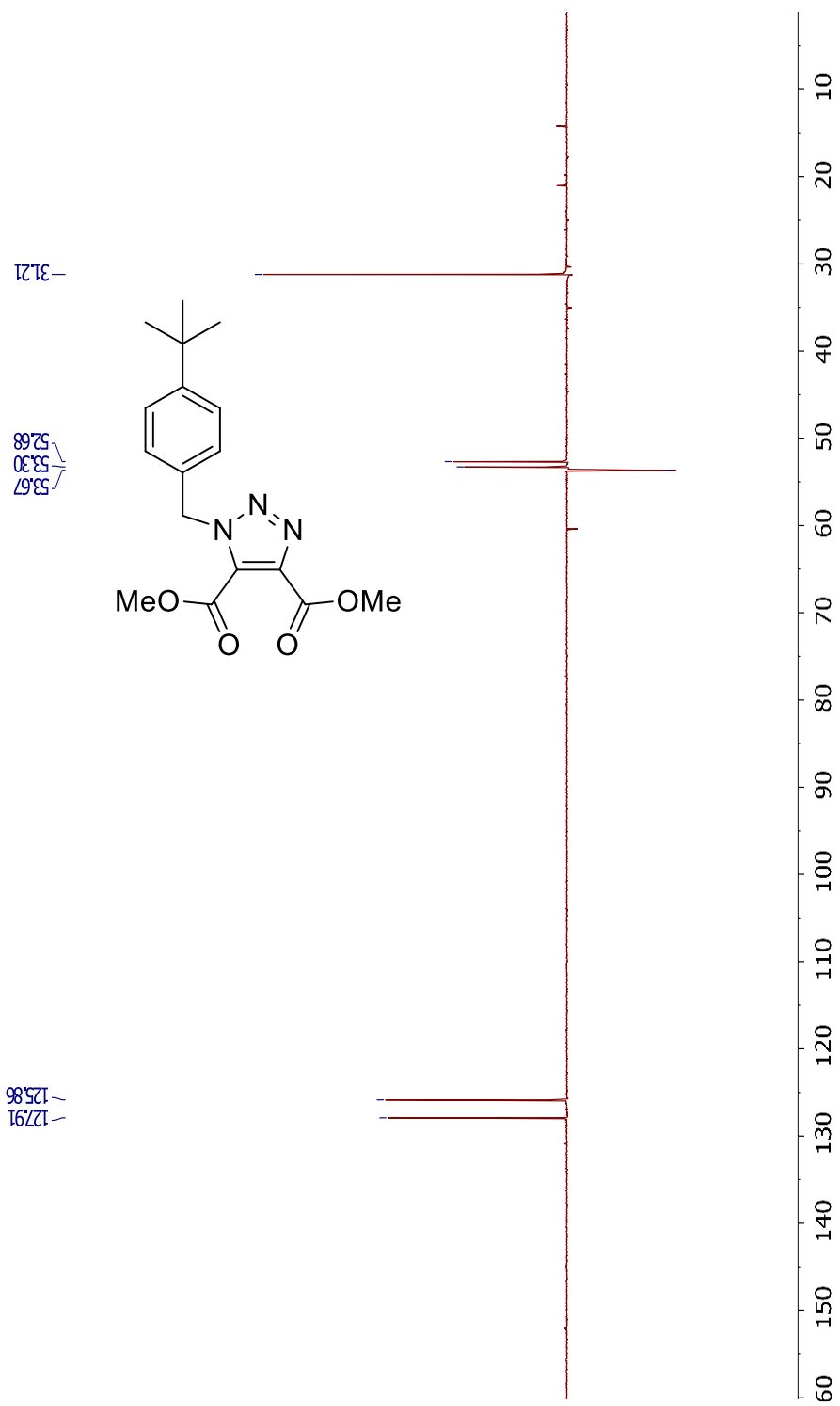




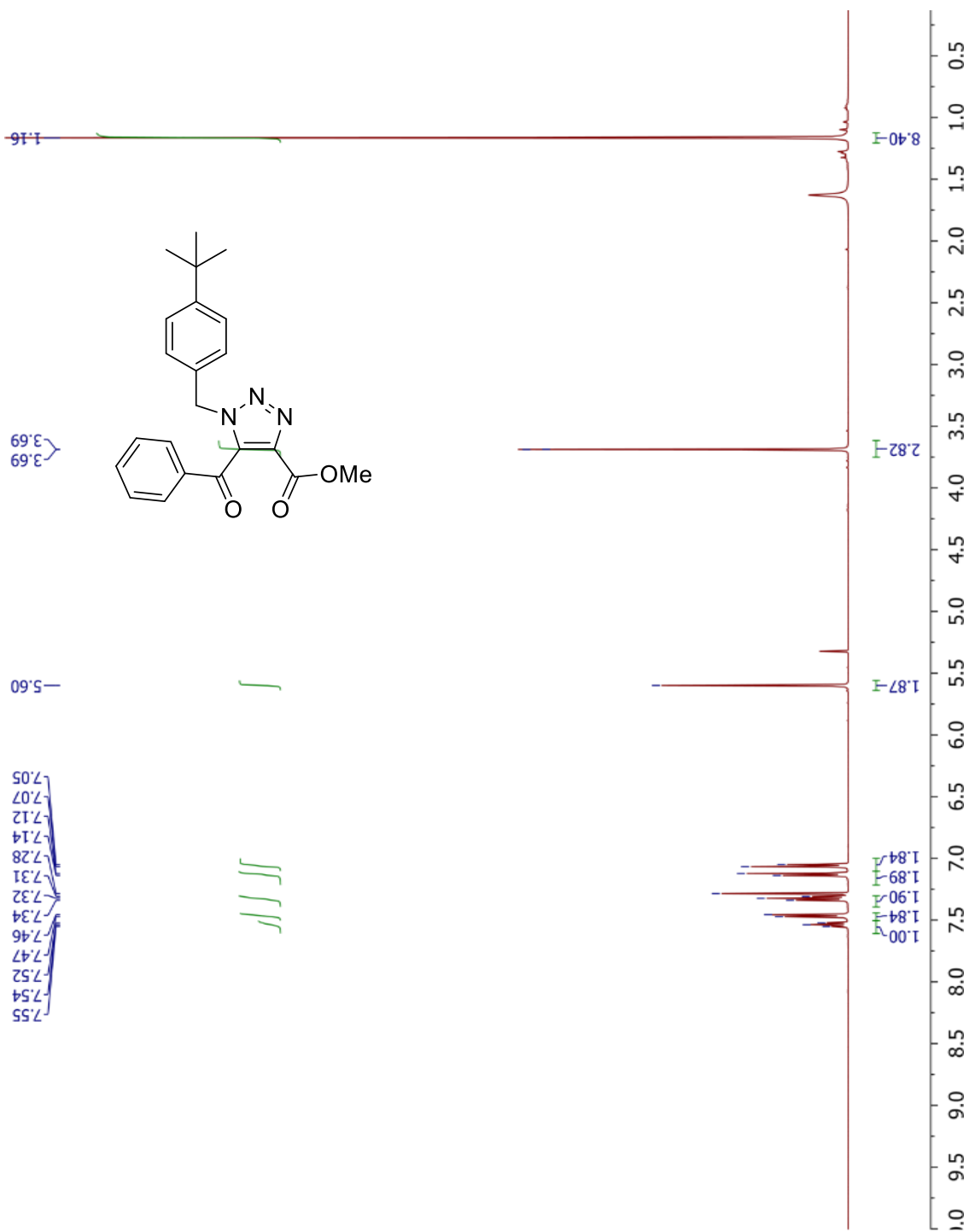
# Triazole 2.7a

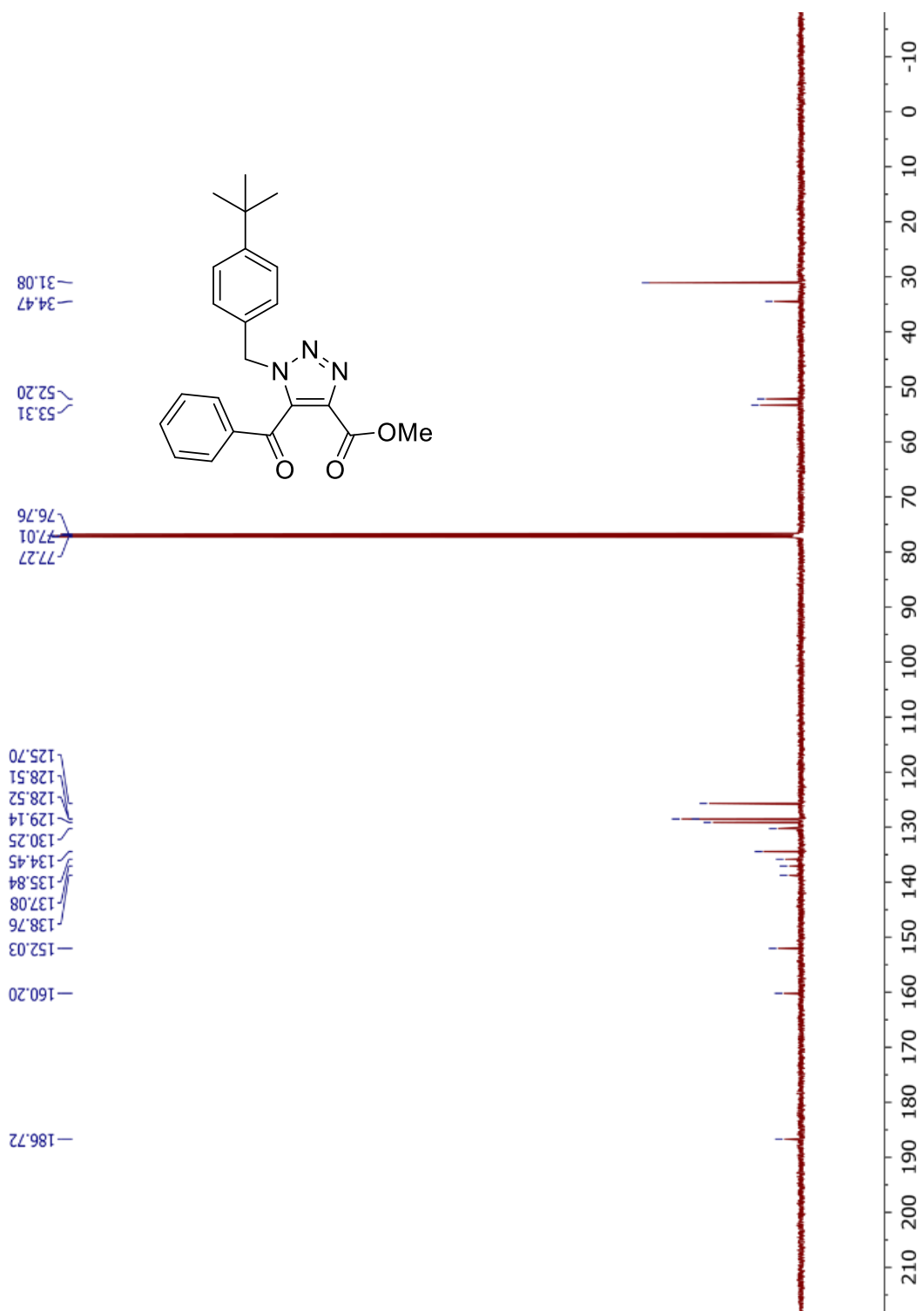


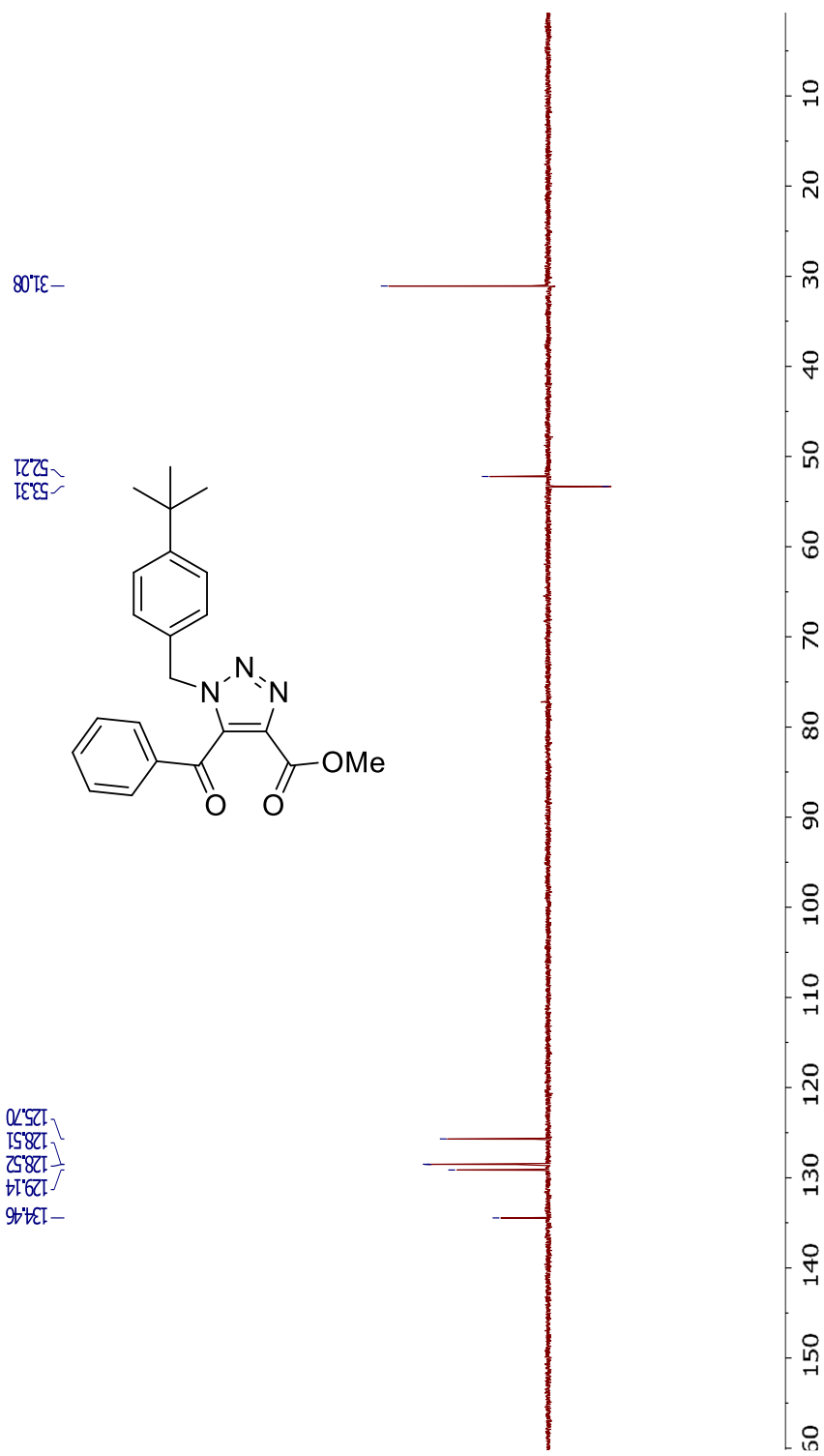




Triazole 2.8a

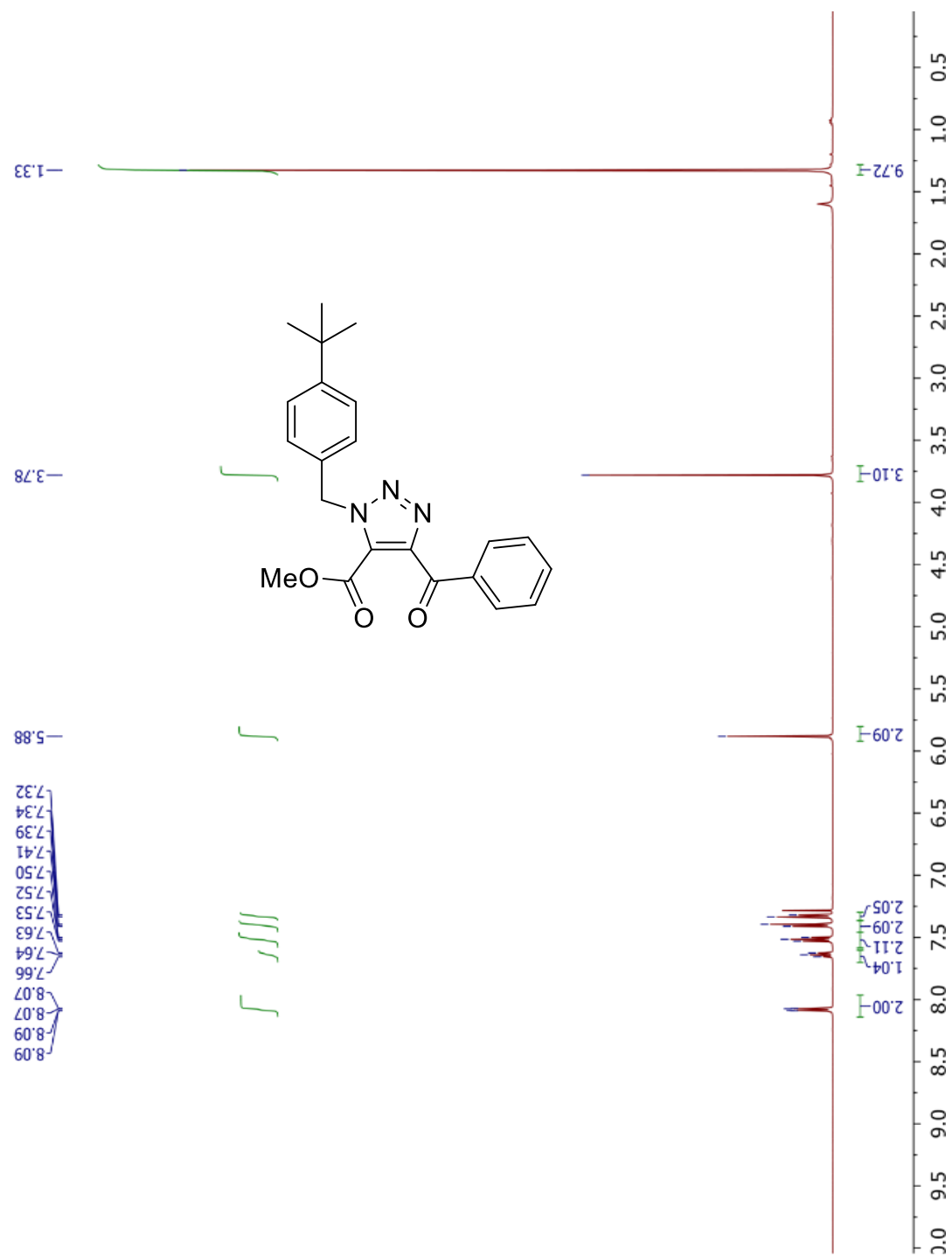


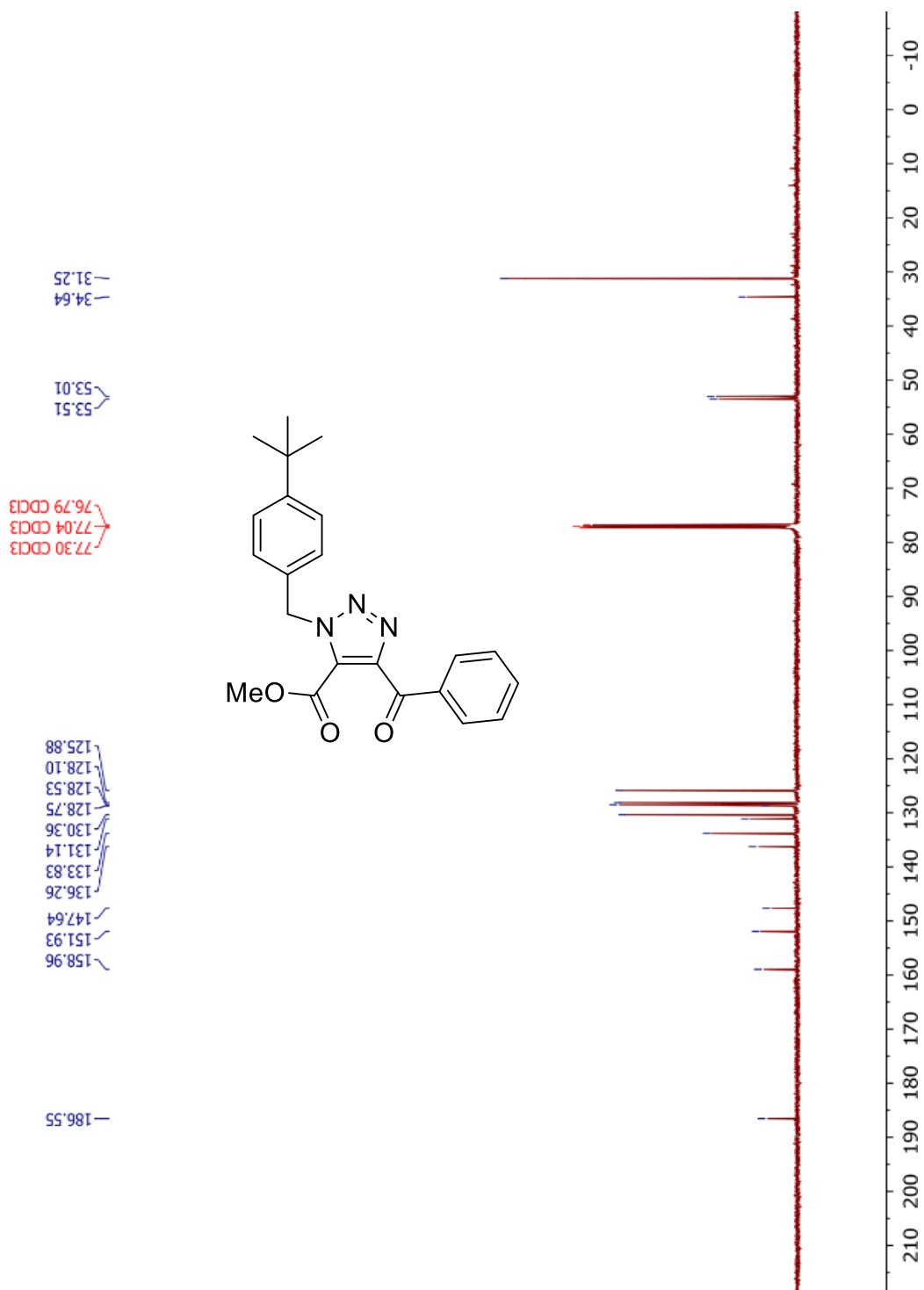


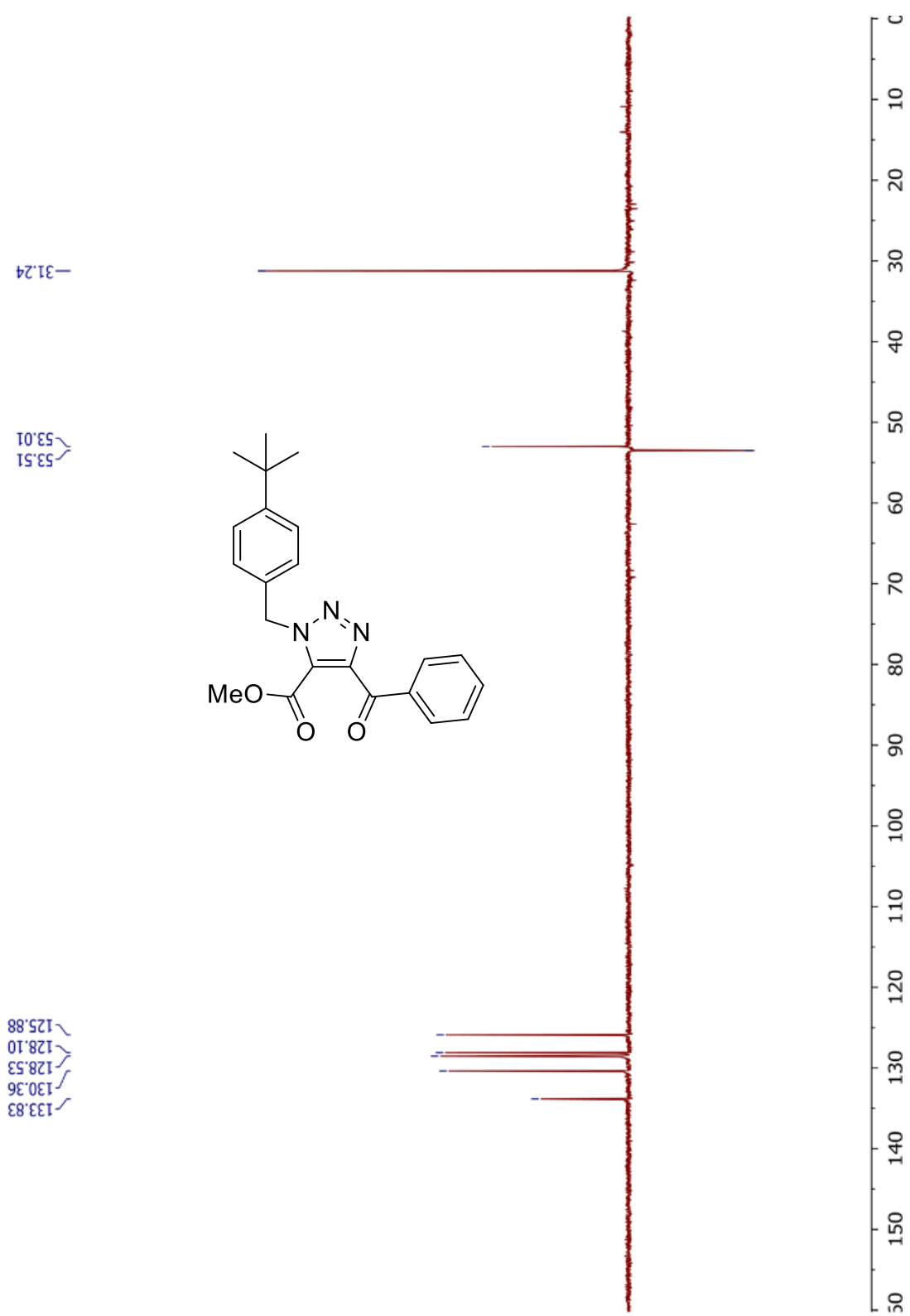




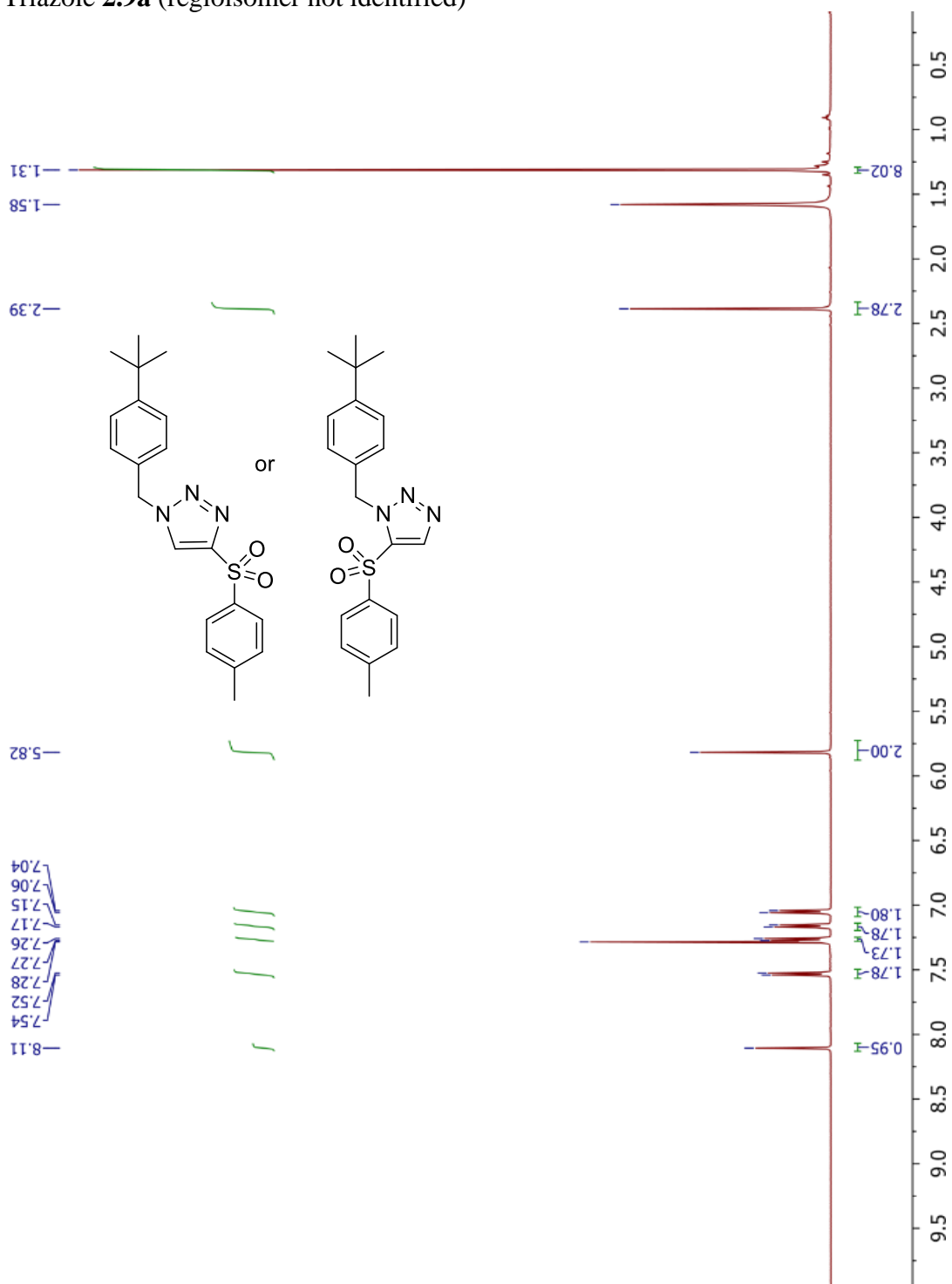
Triazole **2.8b**

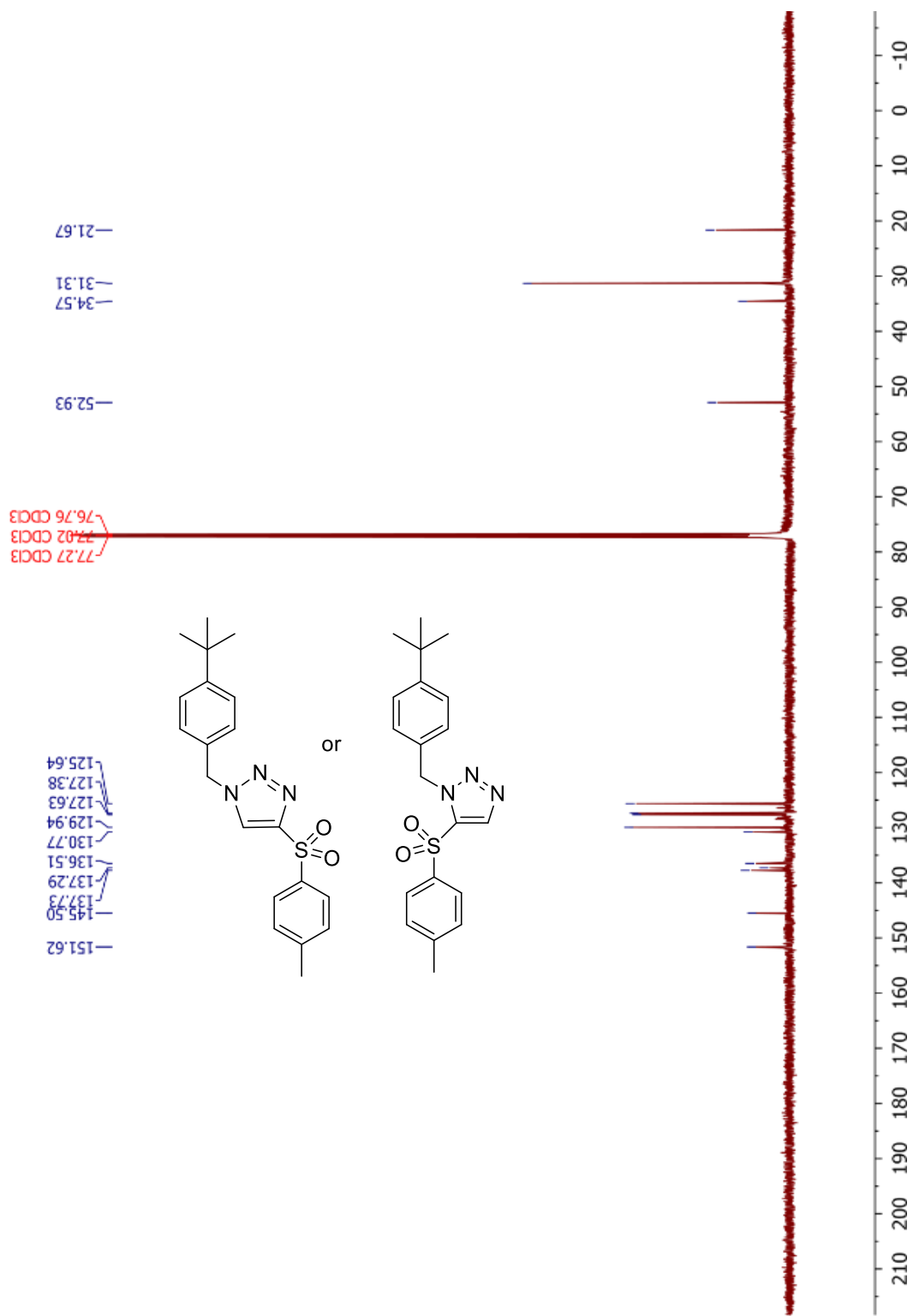


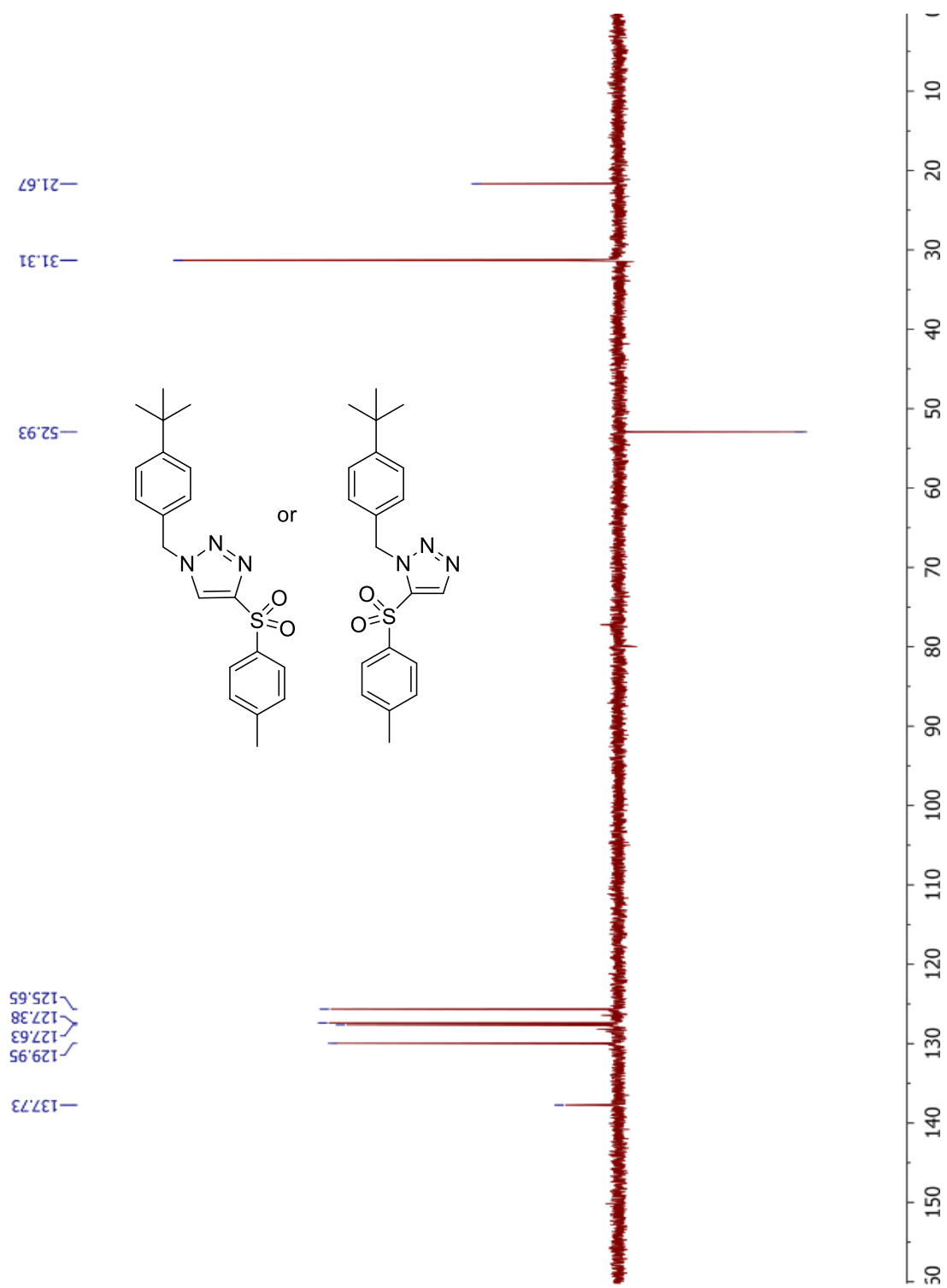




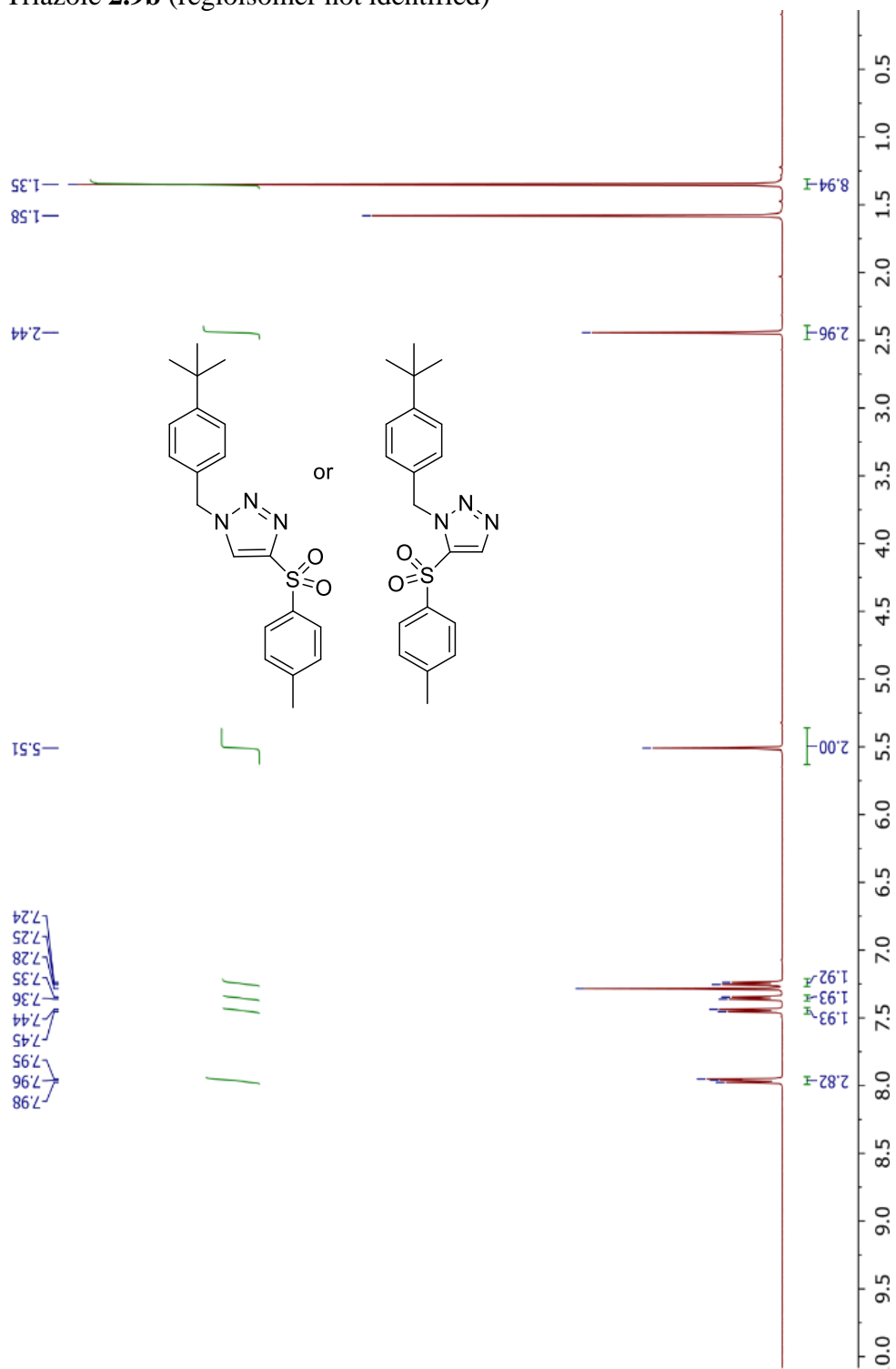
Triazole **2.9a** (regioisomer not identified)

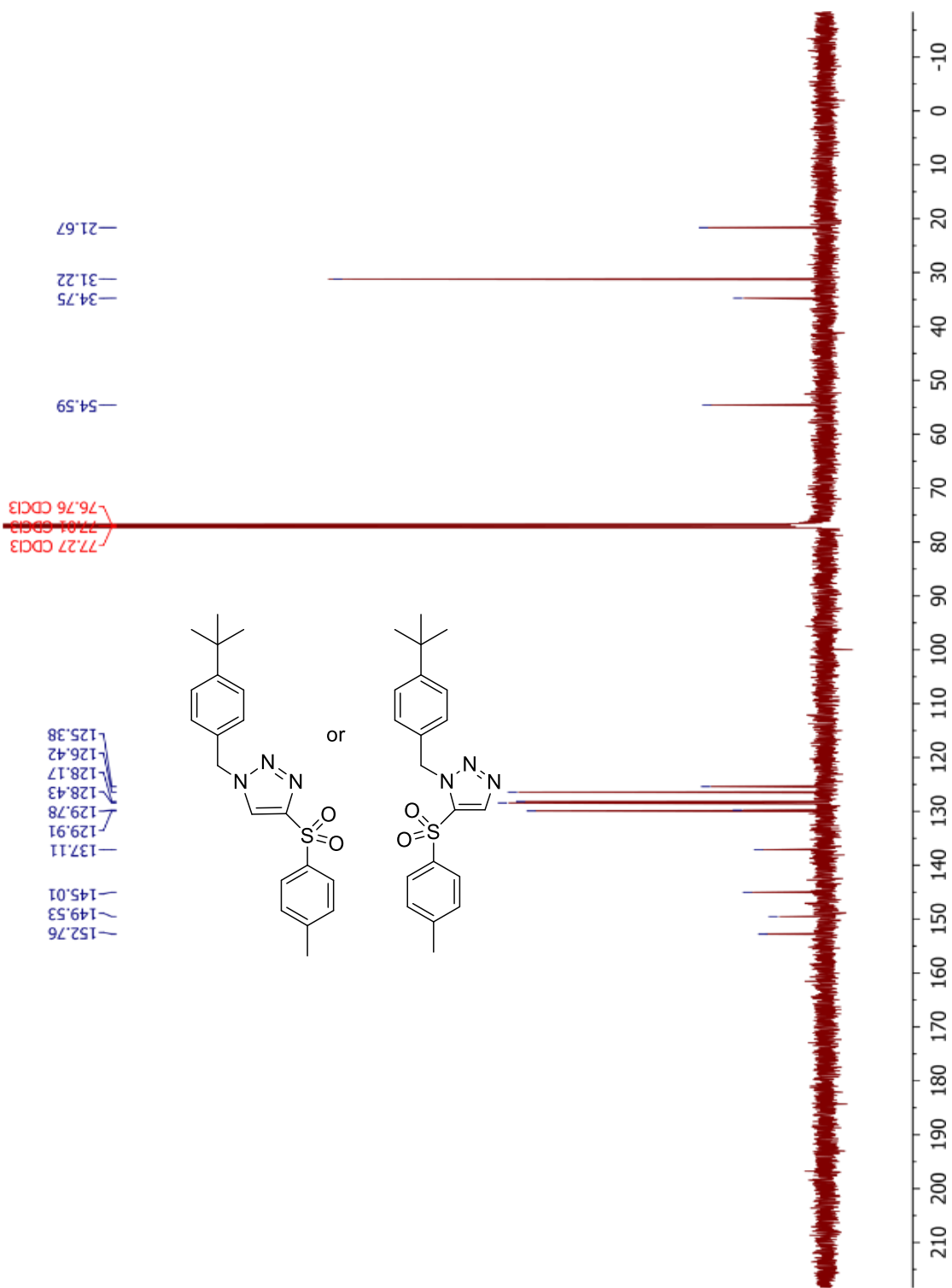




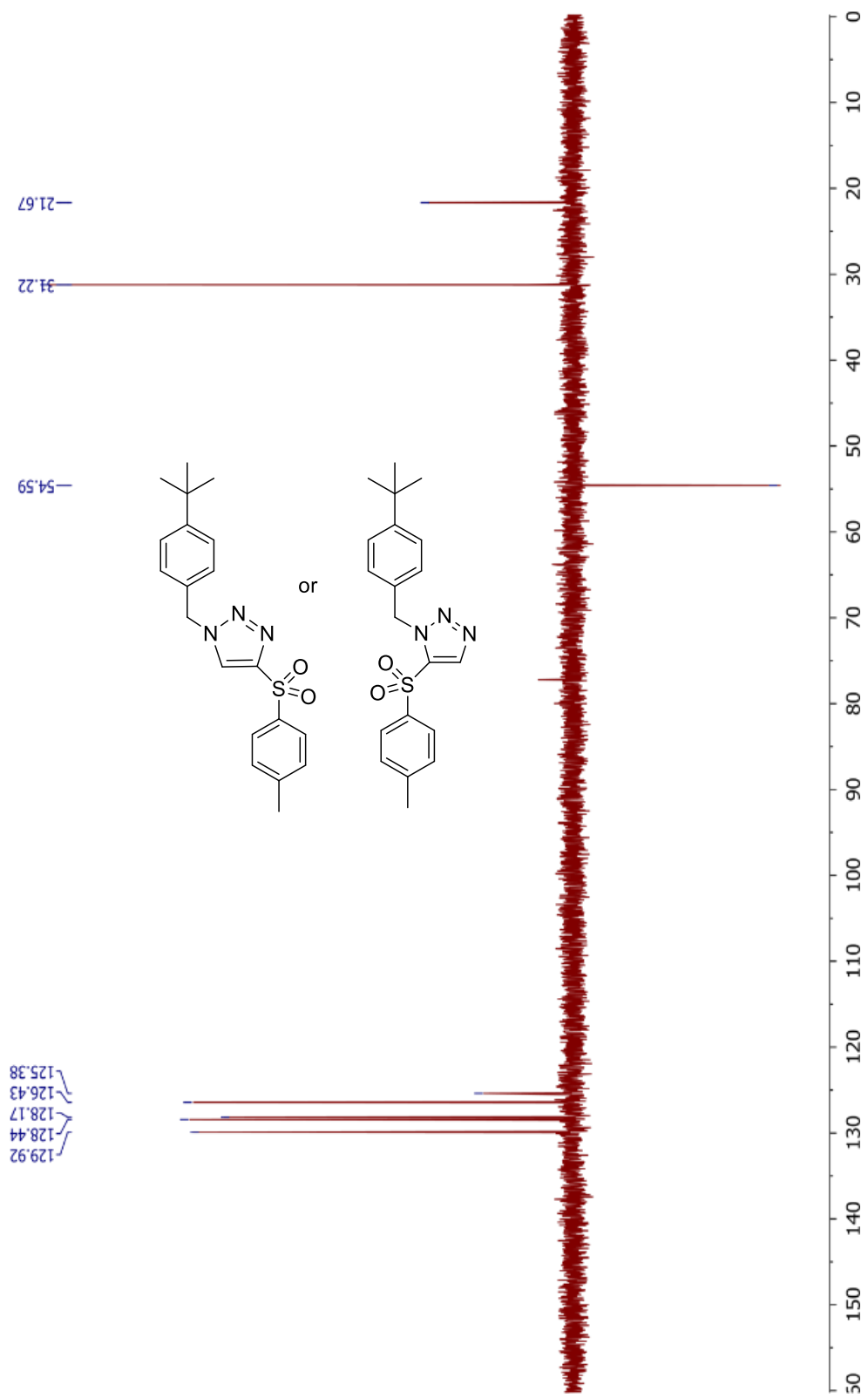


Triazole **2.9b** (regioisomer not identified)

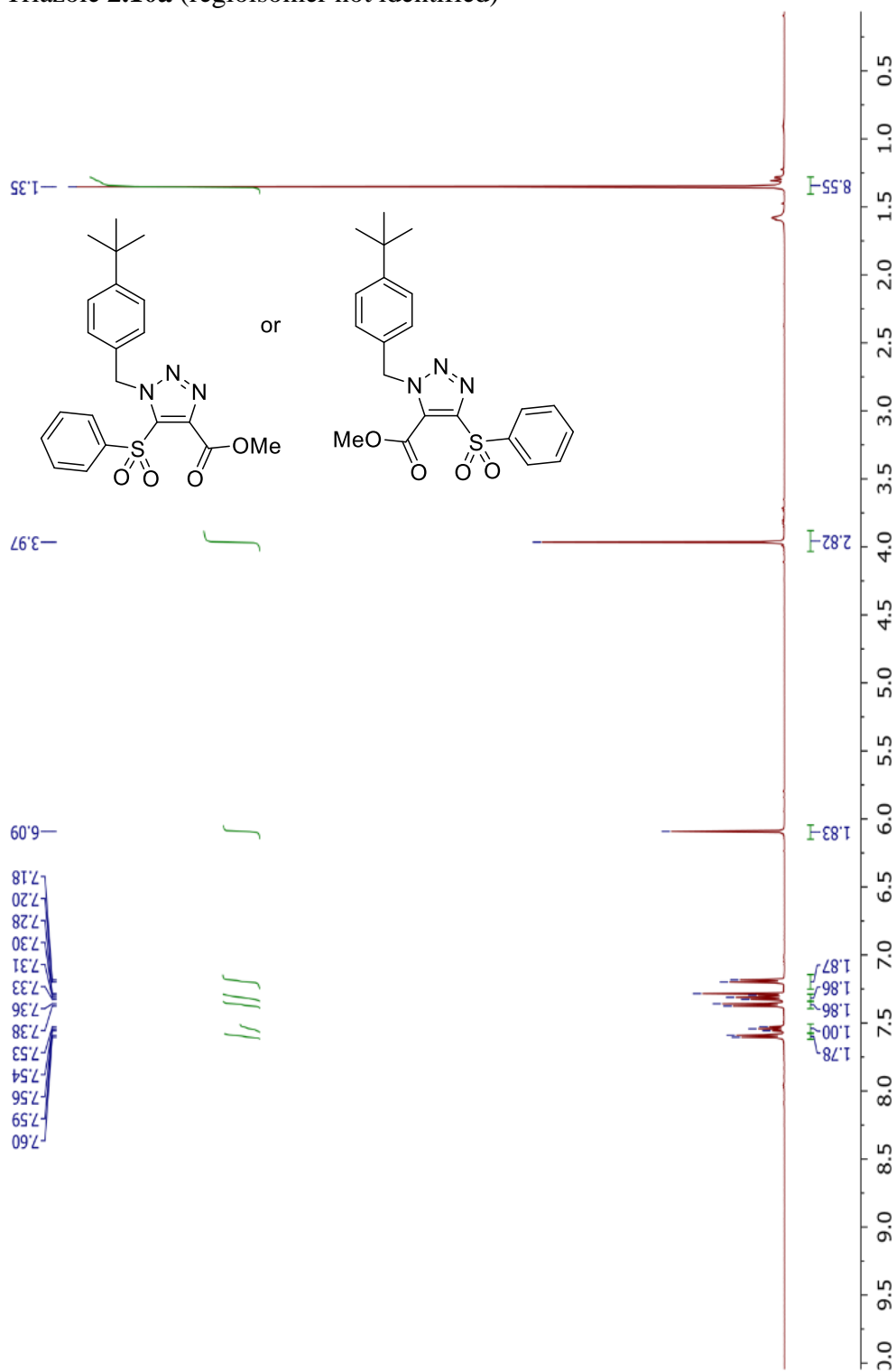


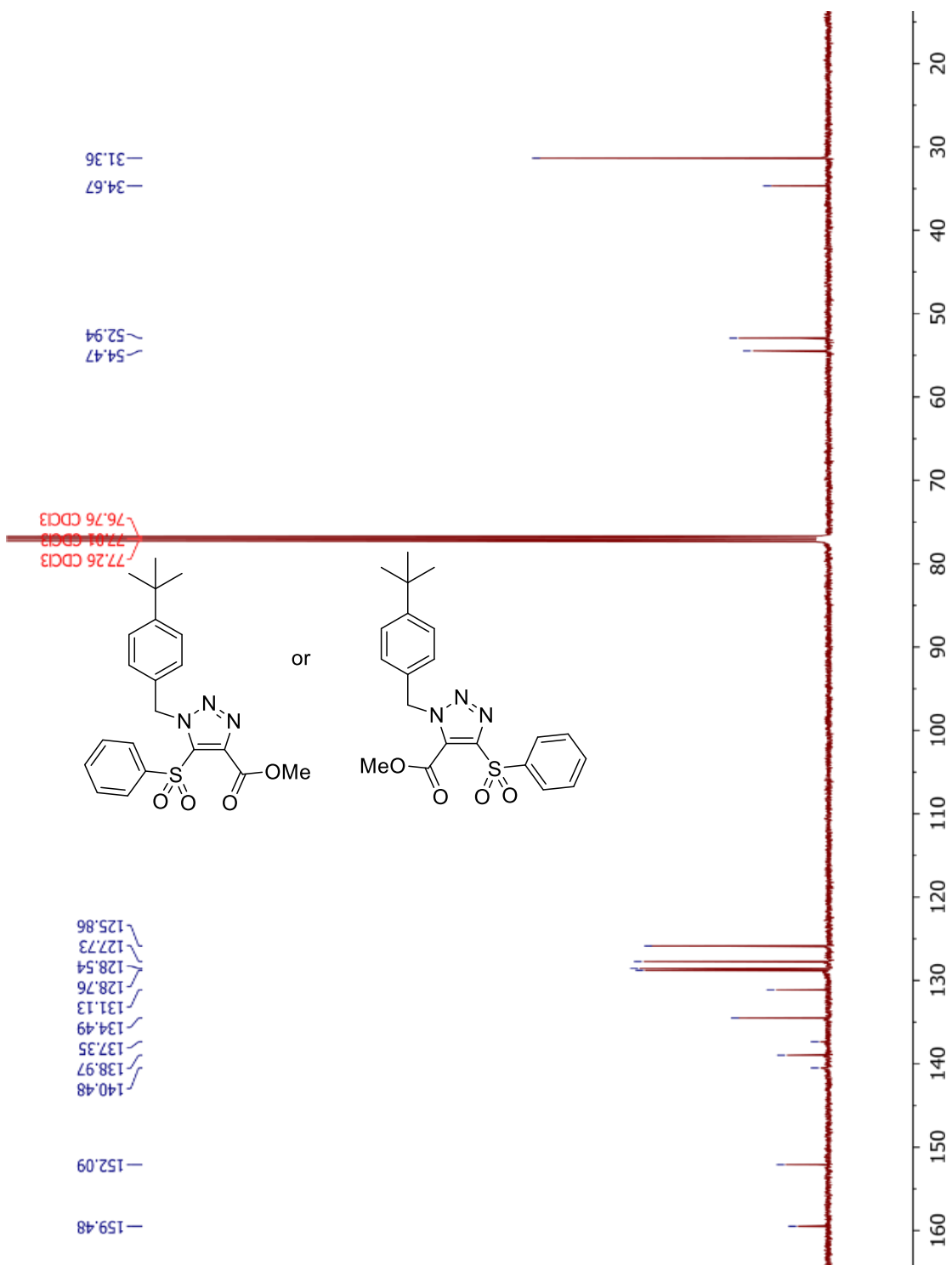


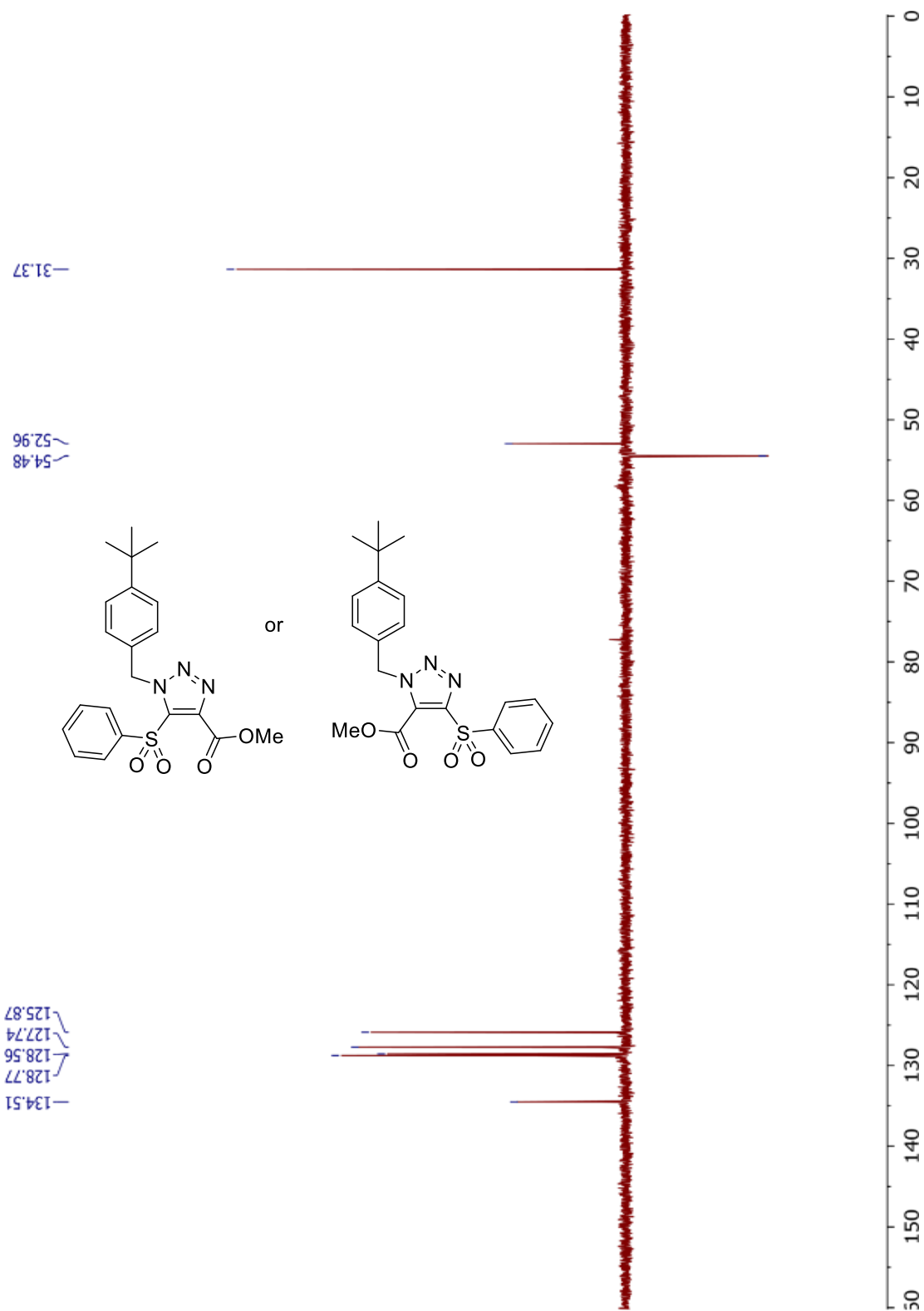




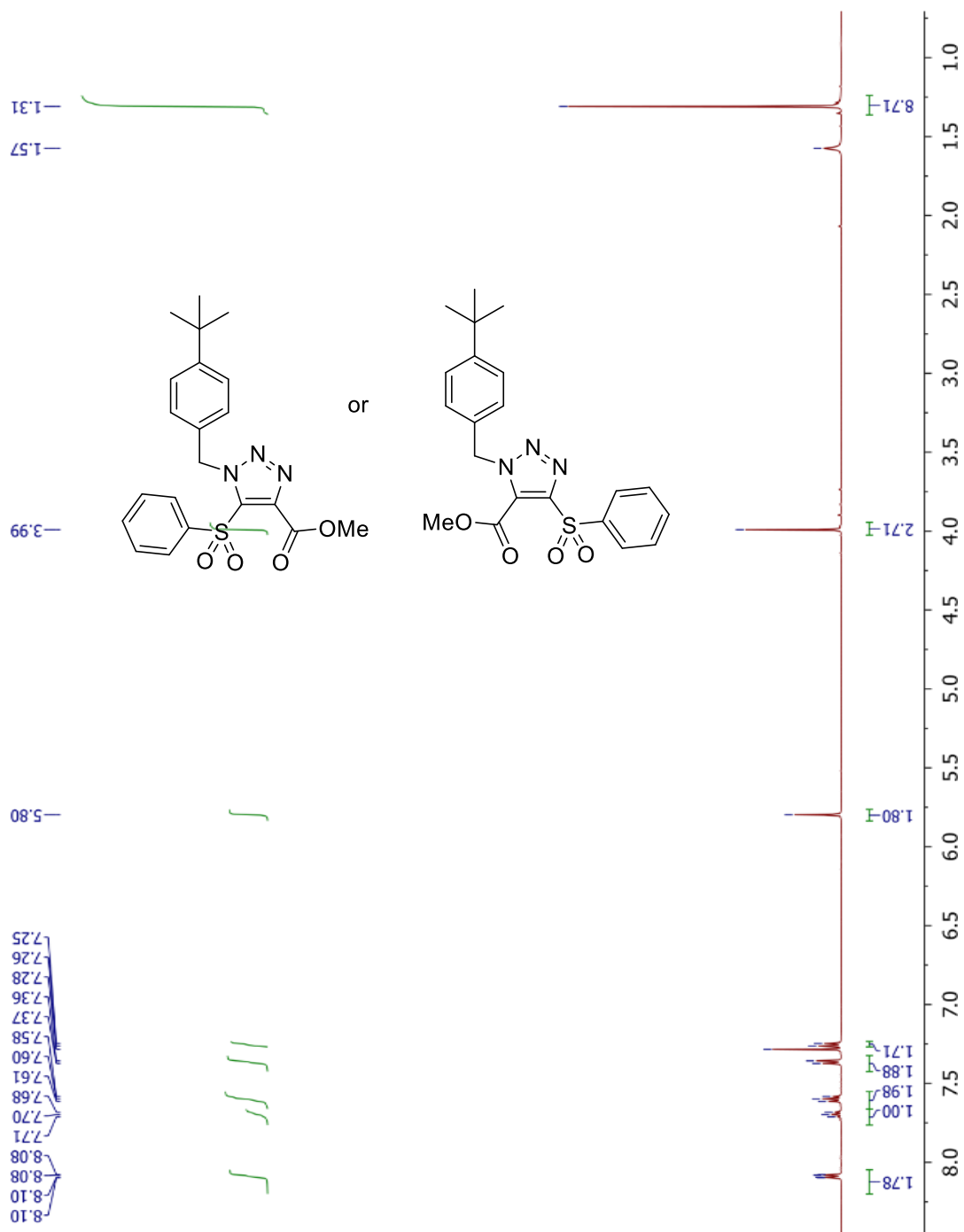
Triazole **2.10a** (regioisomer not identified)

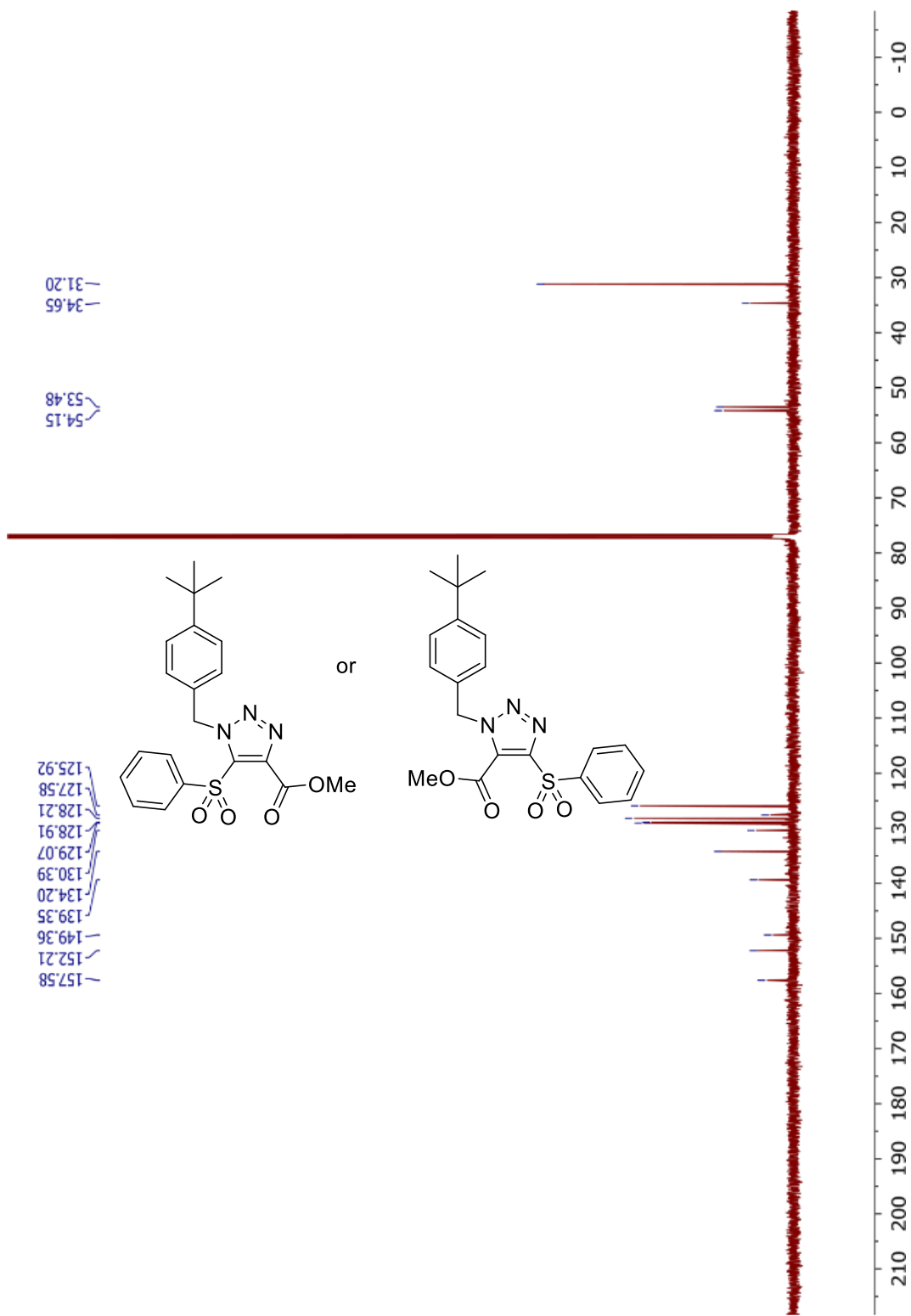


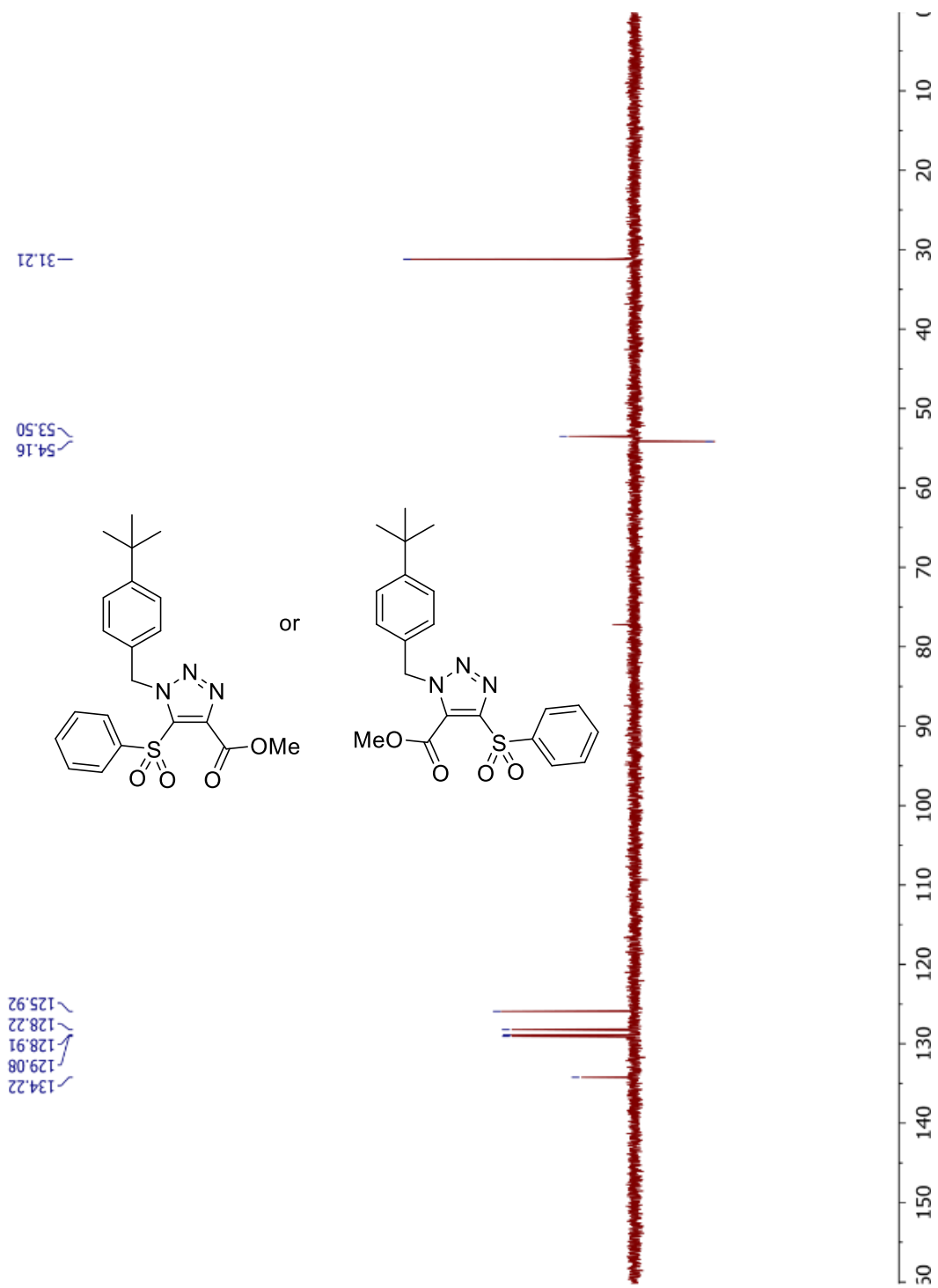




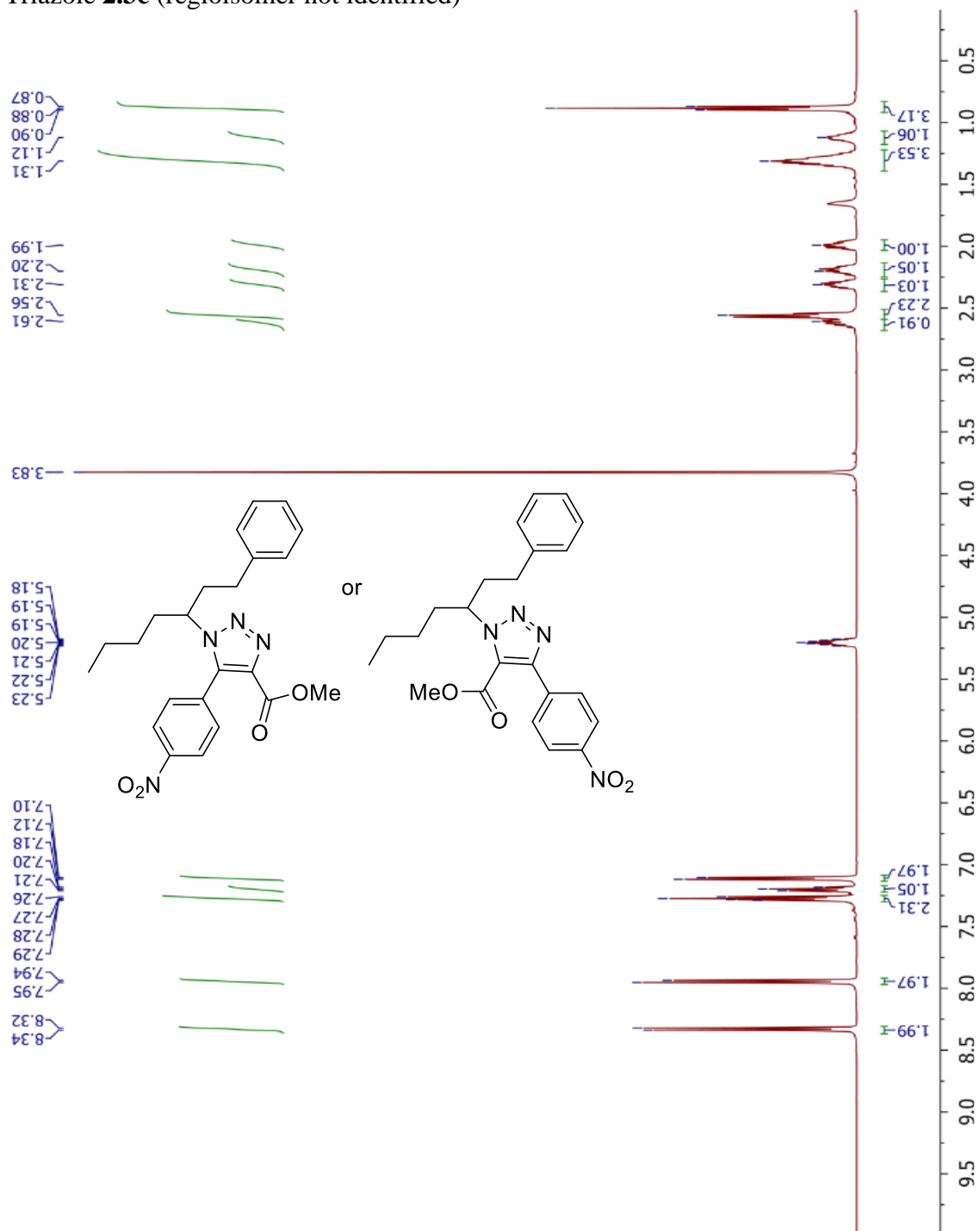
Triazole **2.10b** (regioisomer not identified)



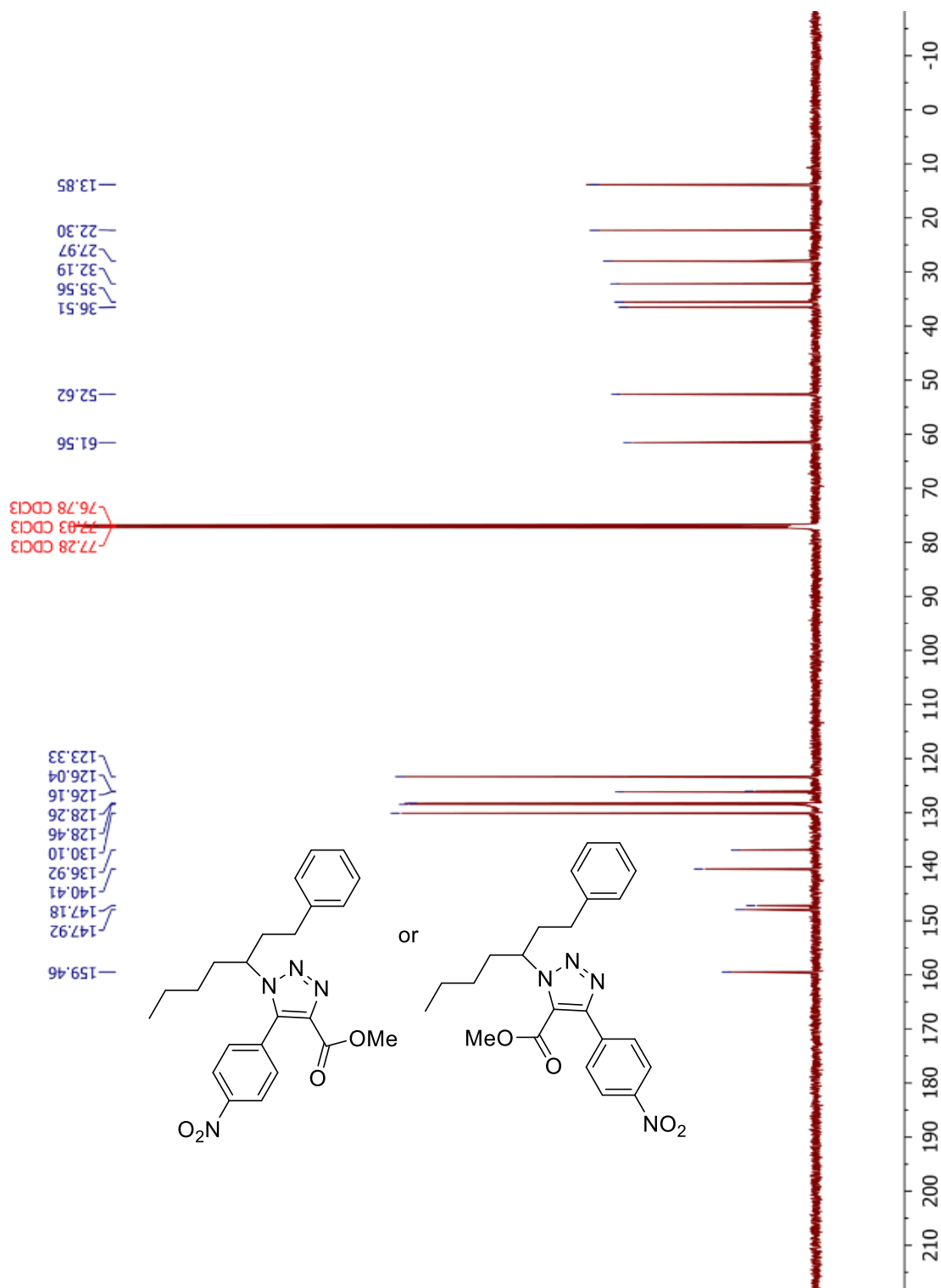


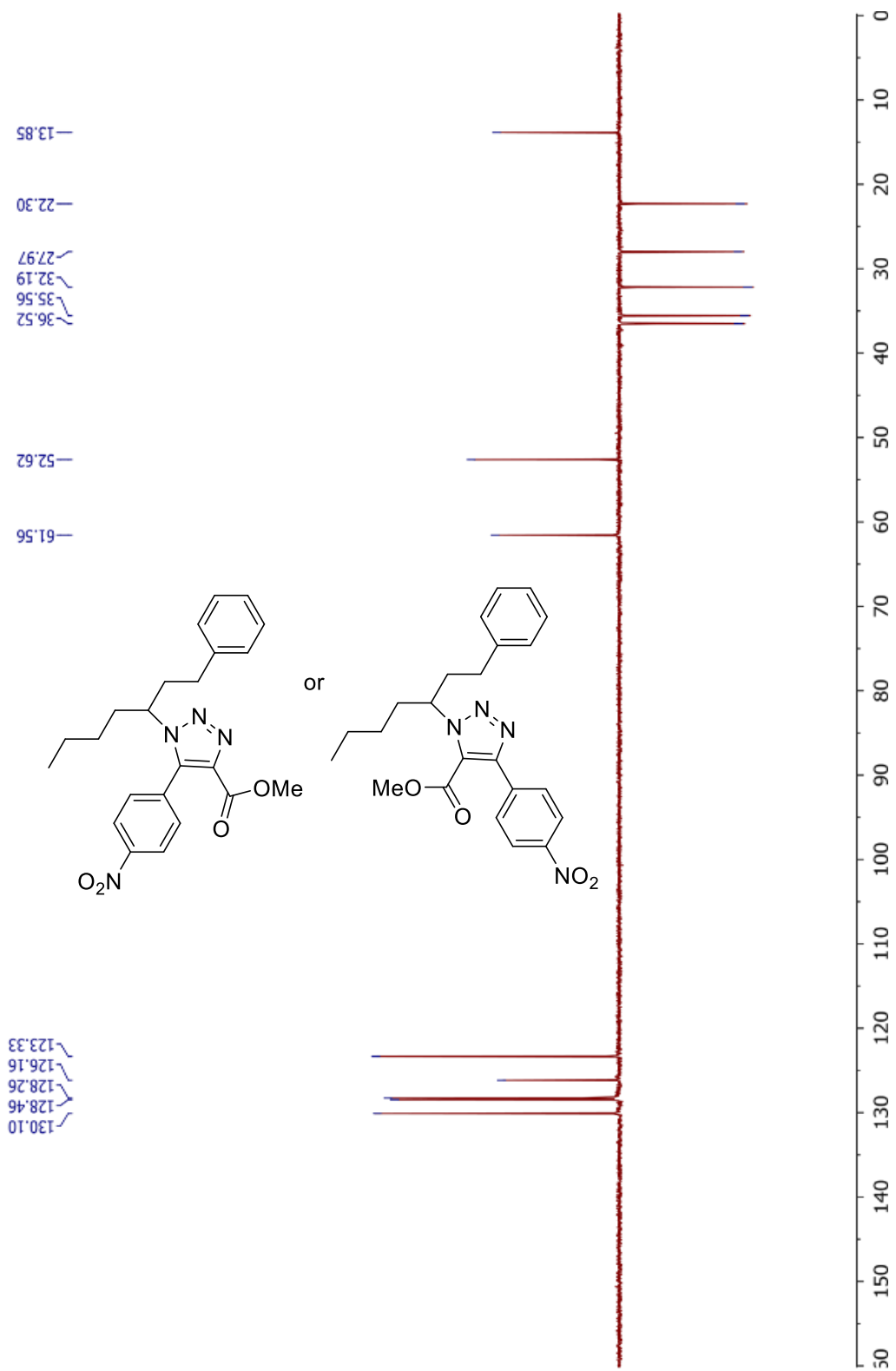


Triazole **2.3c** (regioisomer not identified)

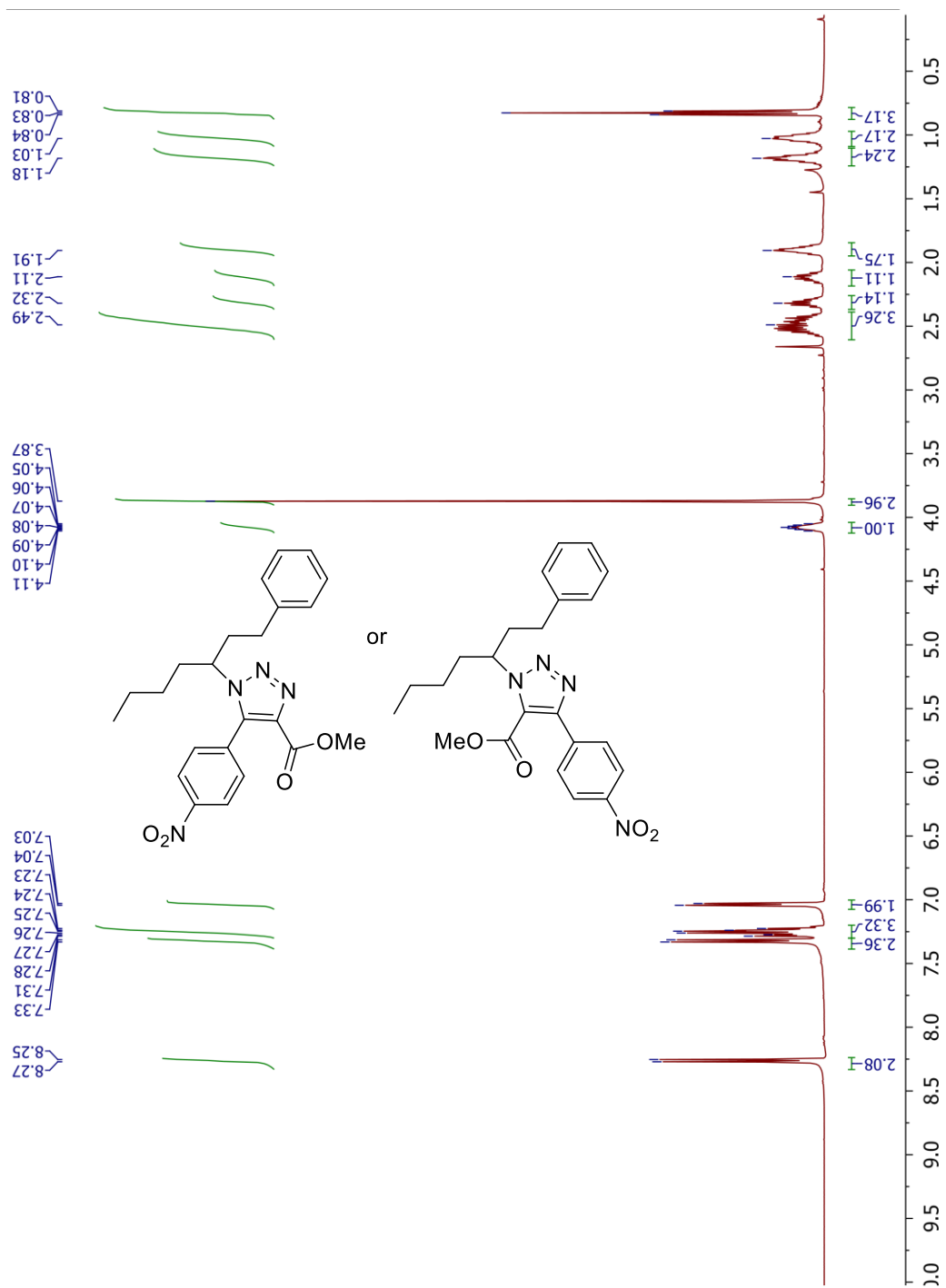


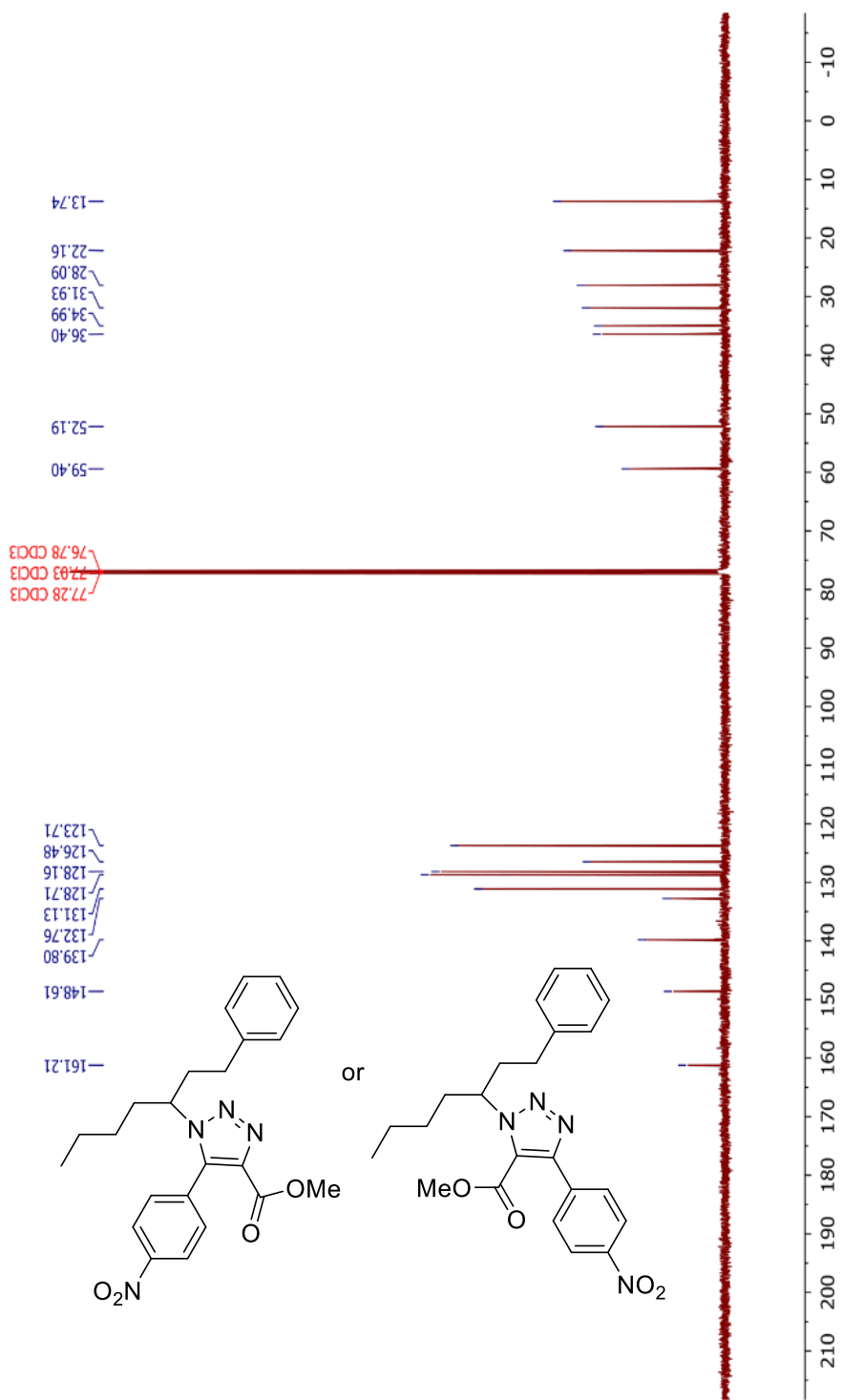


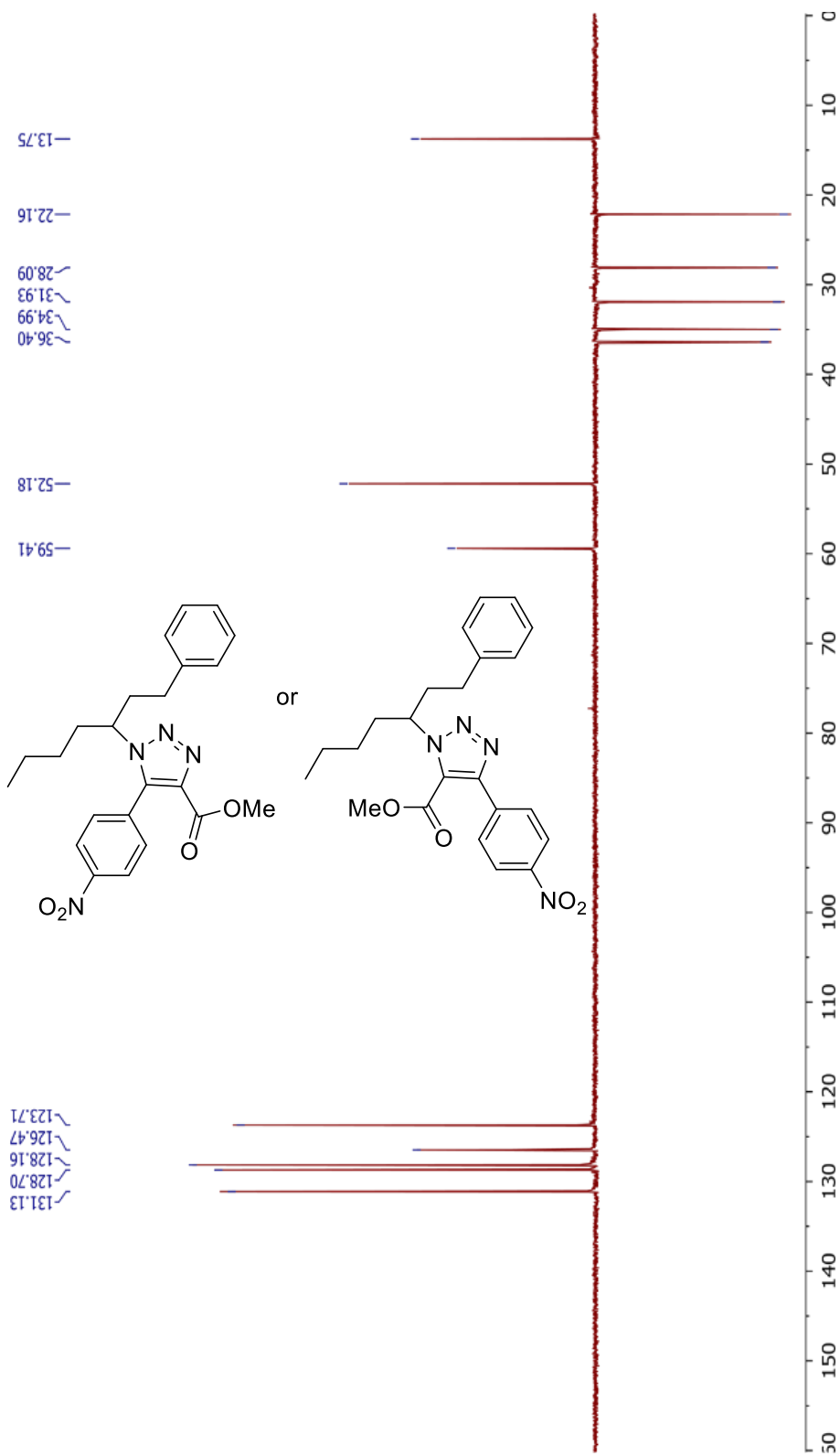




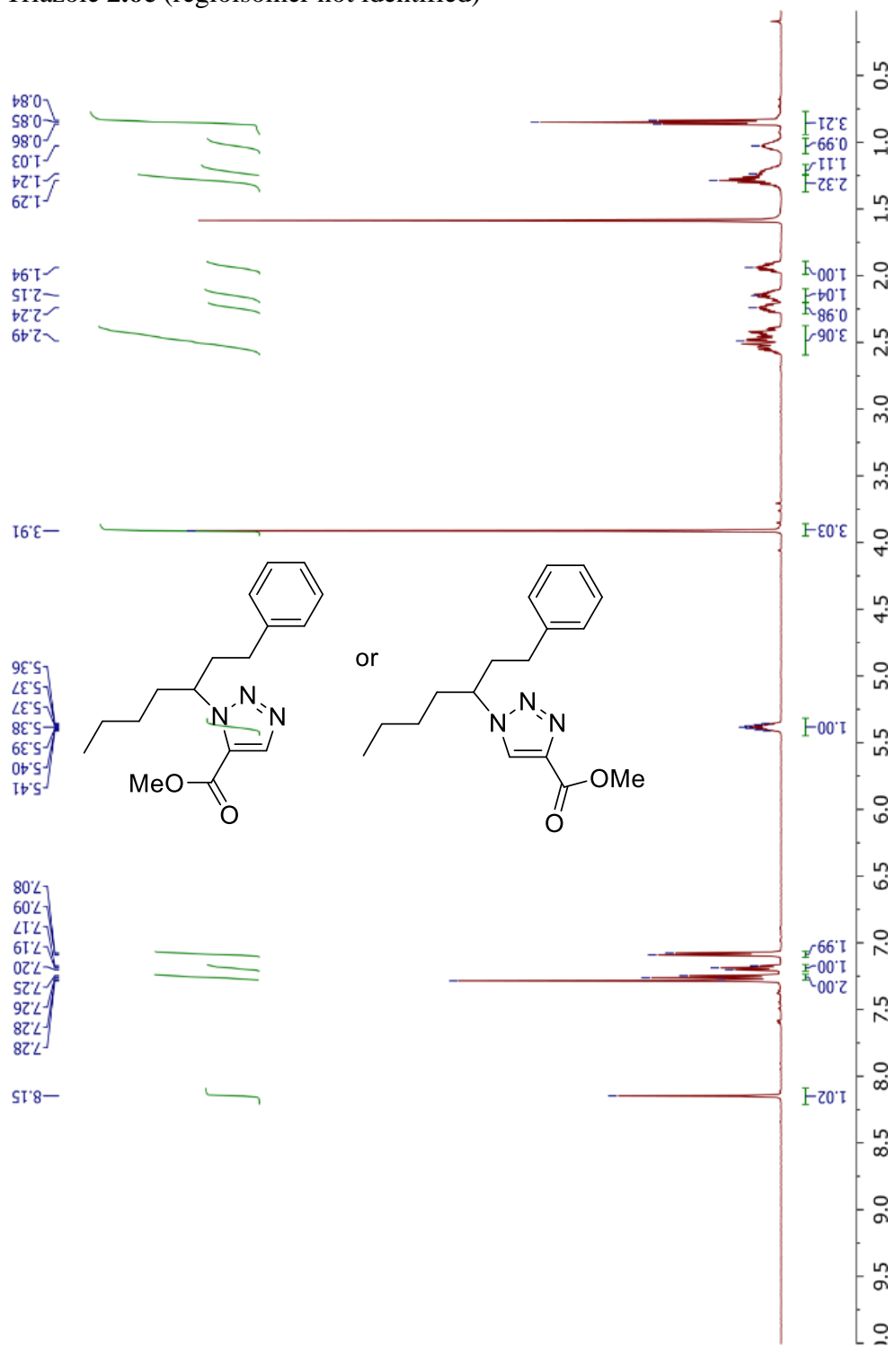
Triazole **2.3d** (regioisomer not identified)

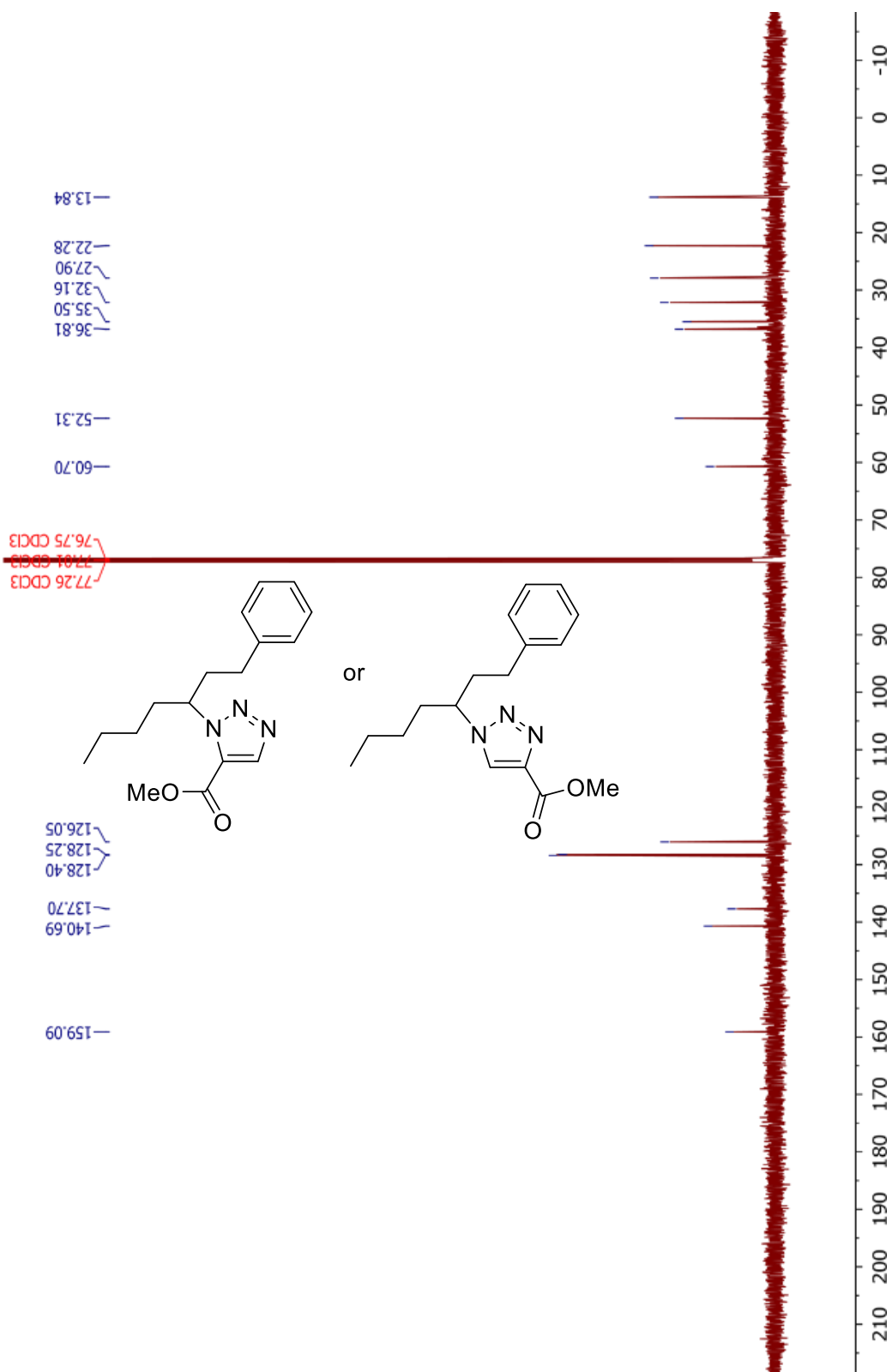


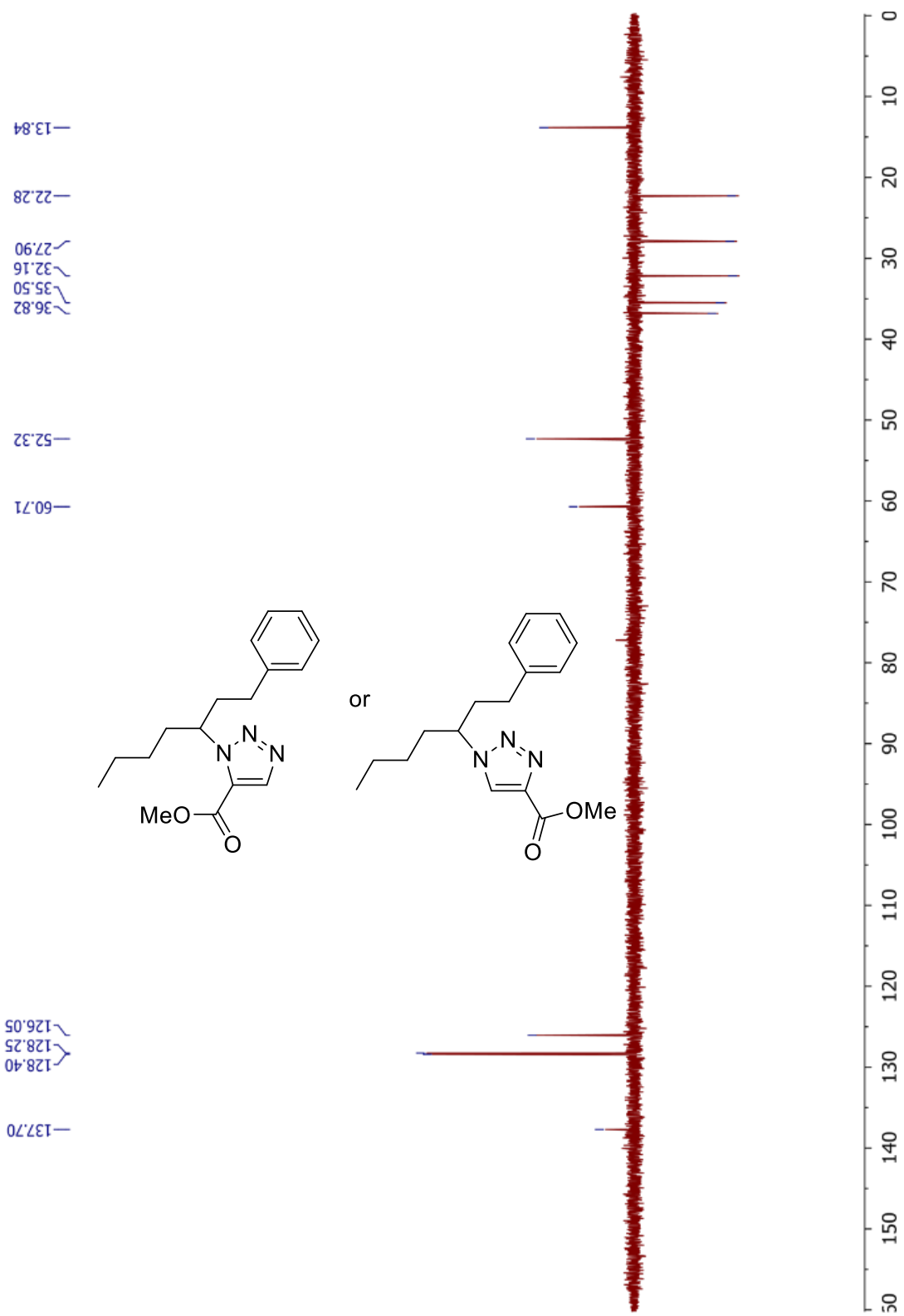




Triazole **2.6c** (regioisomer not identified)

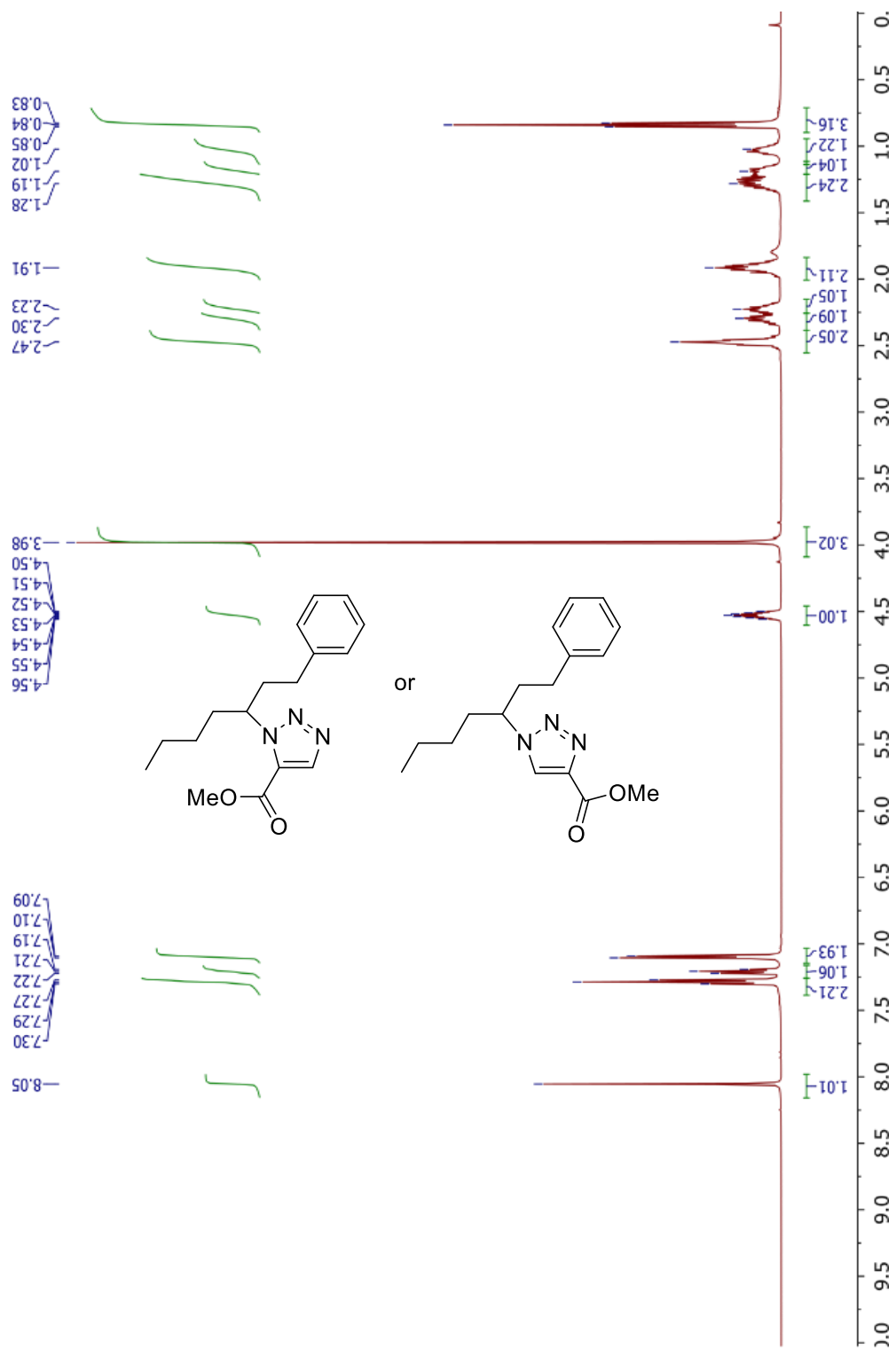


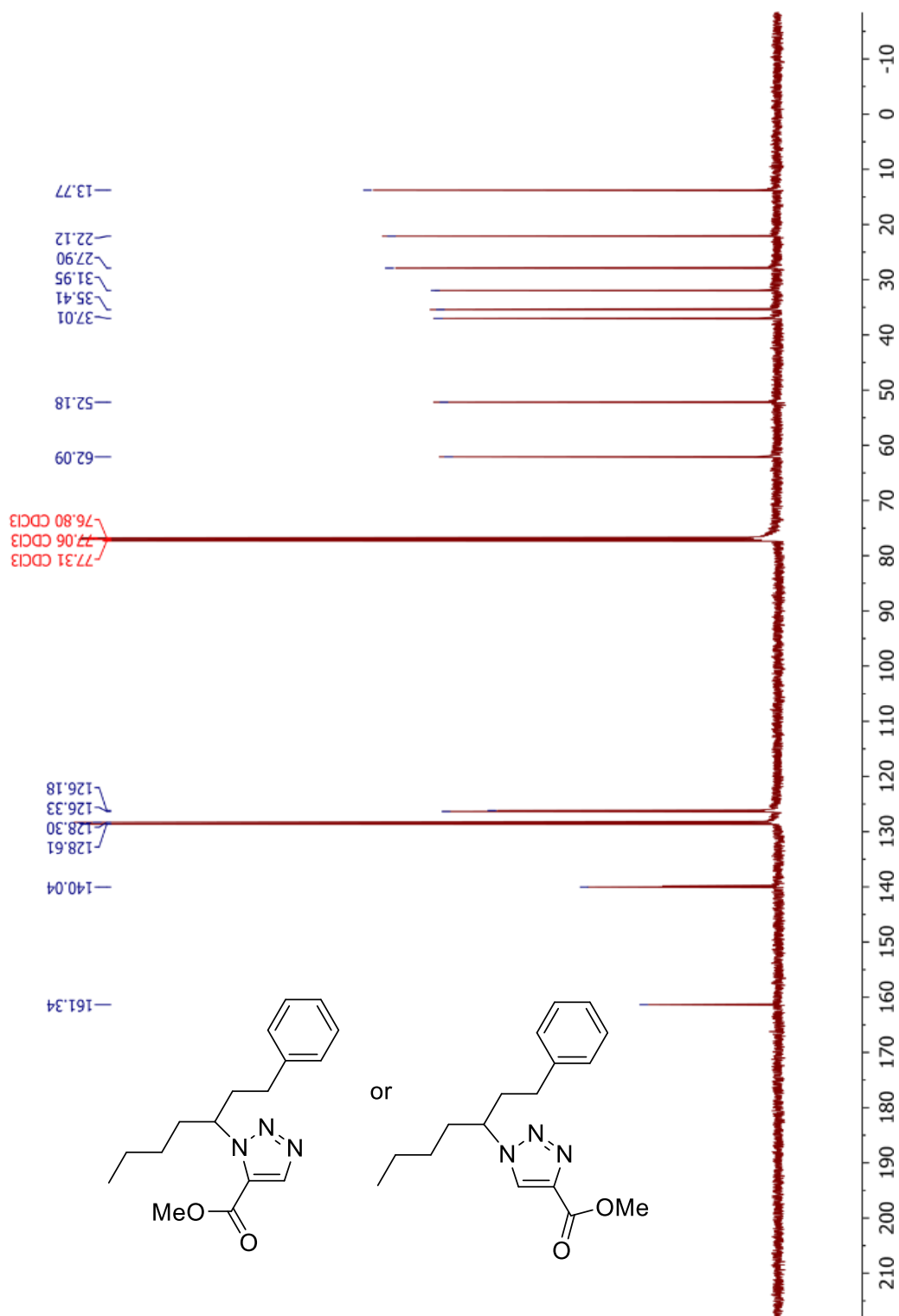


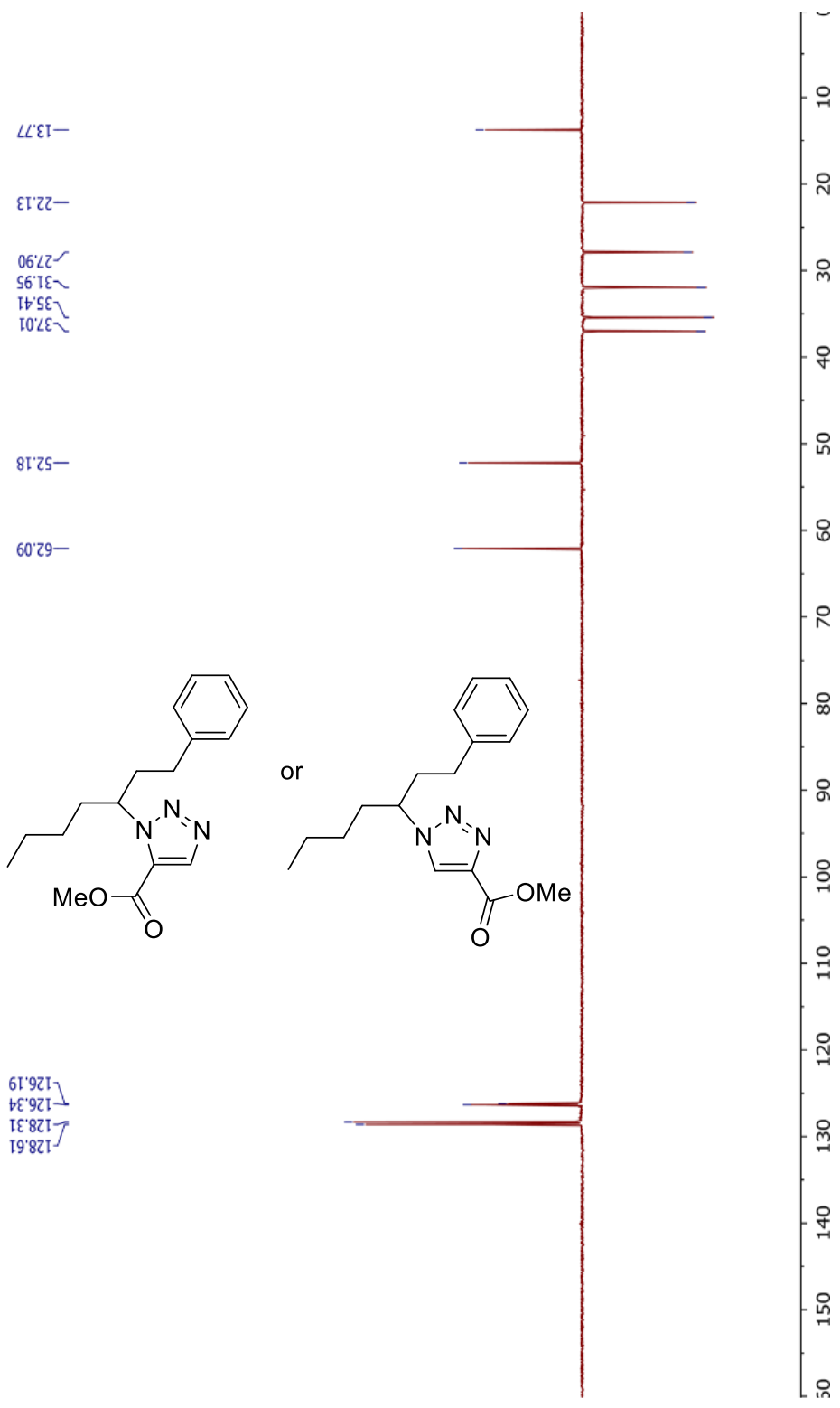




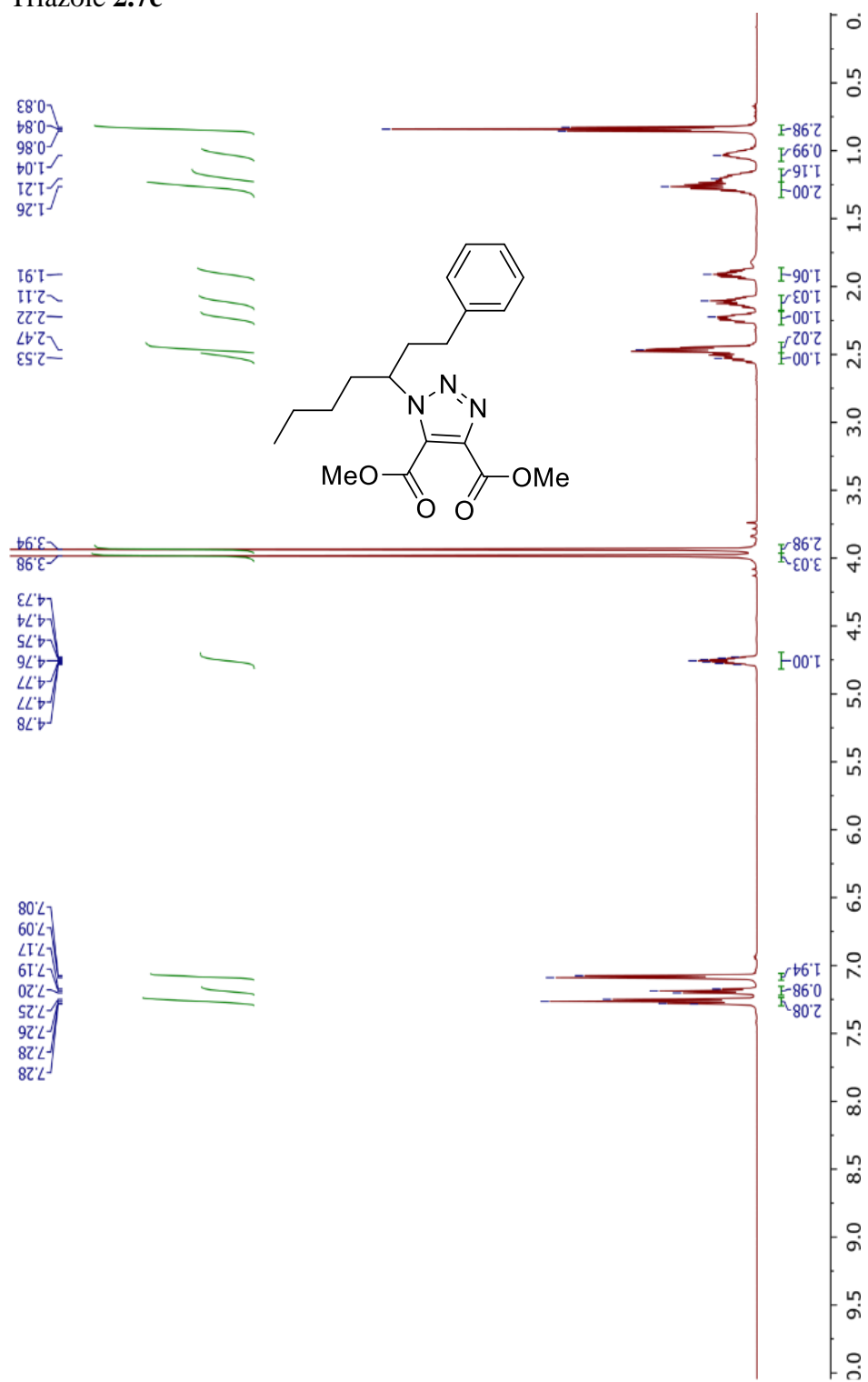
Triazole **2.6d** (regioisomer not identified)

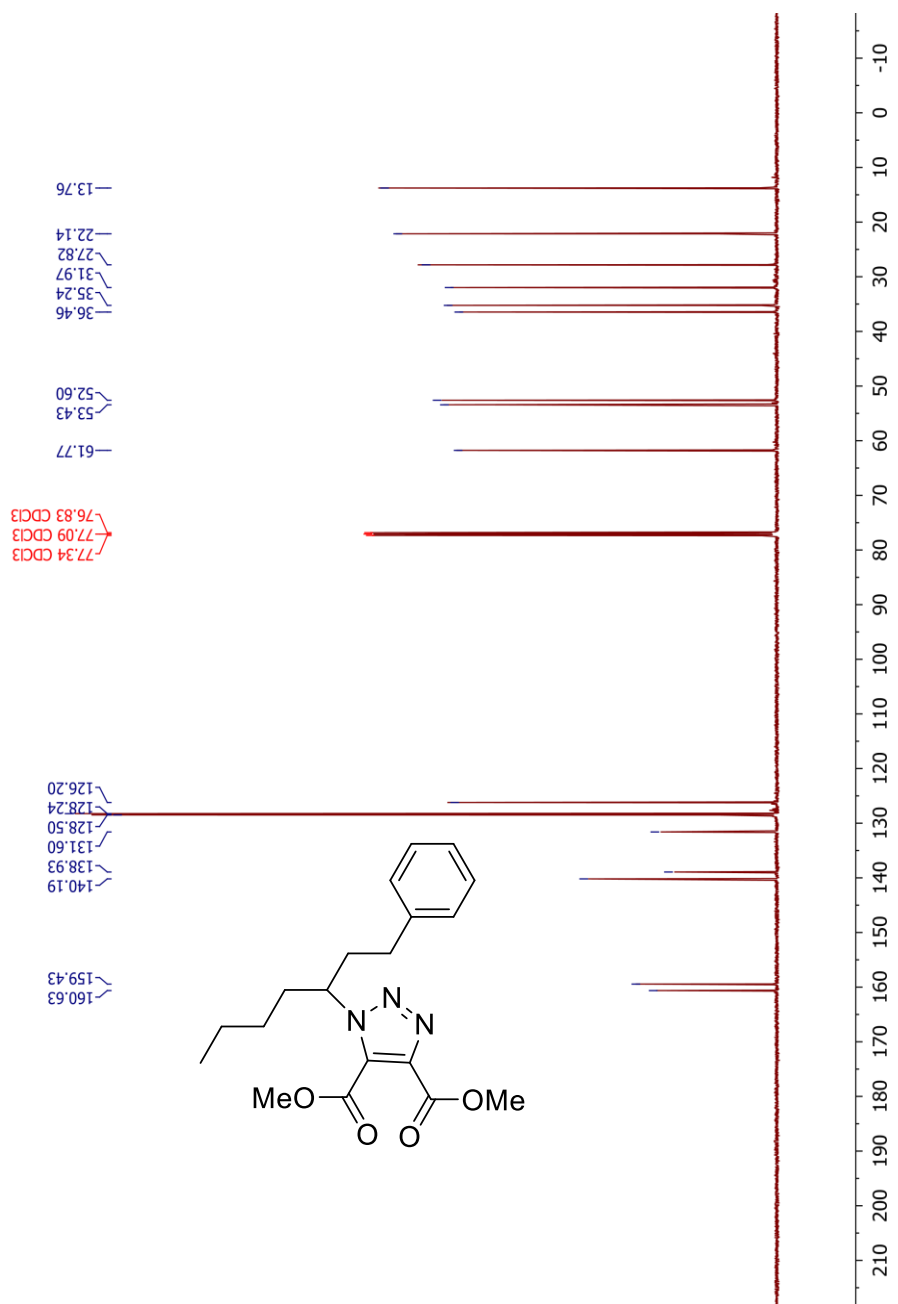


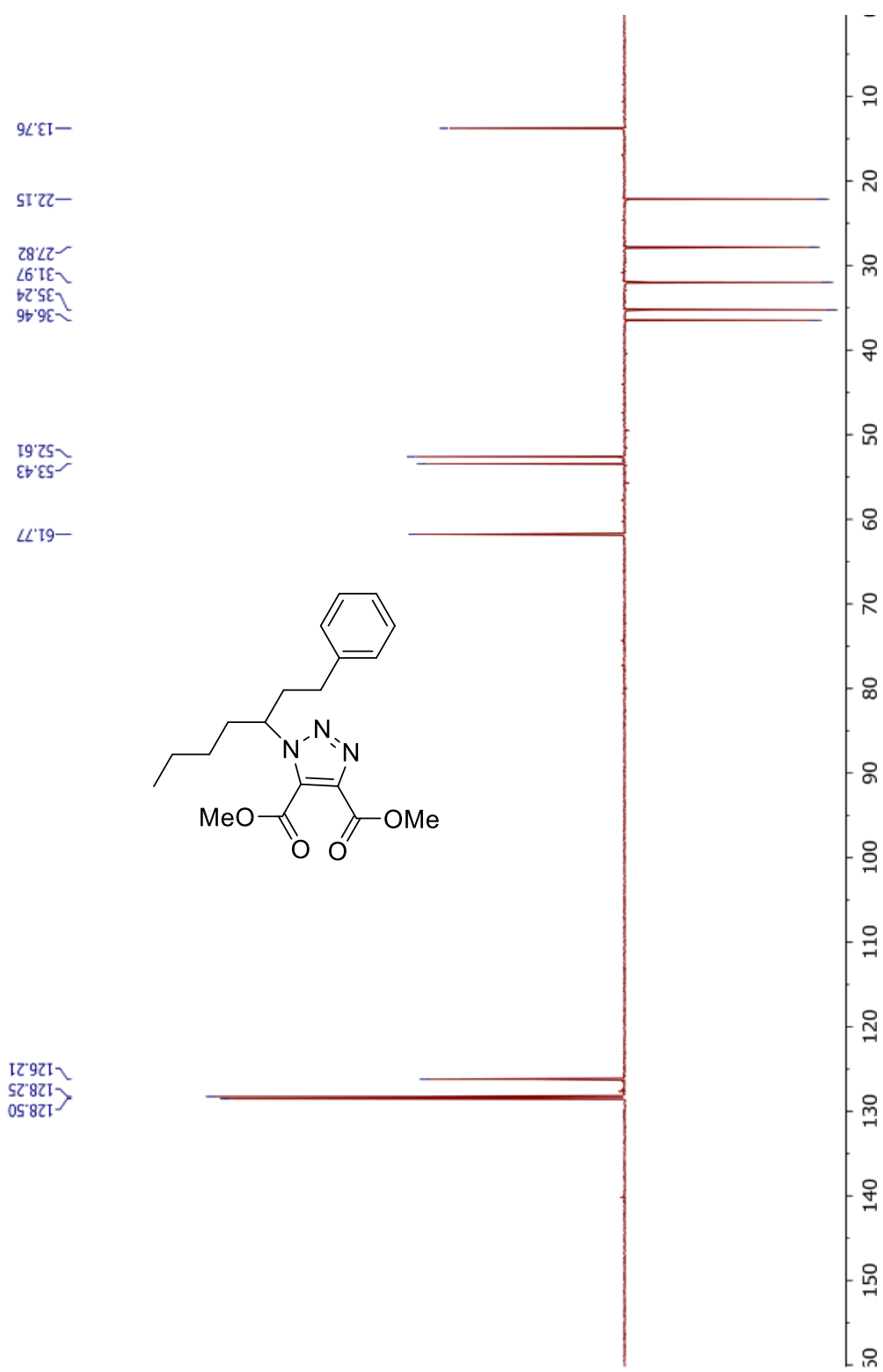




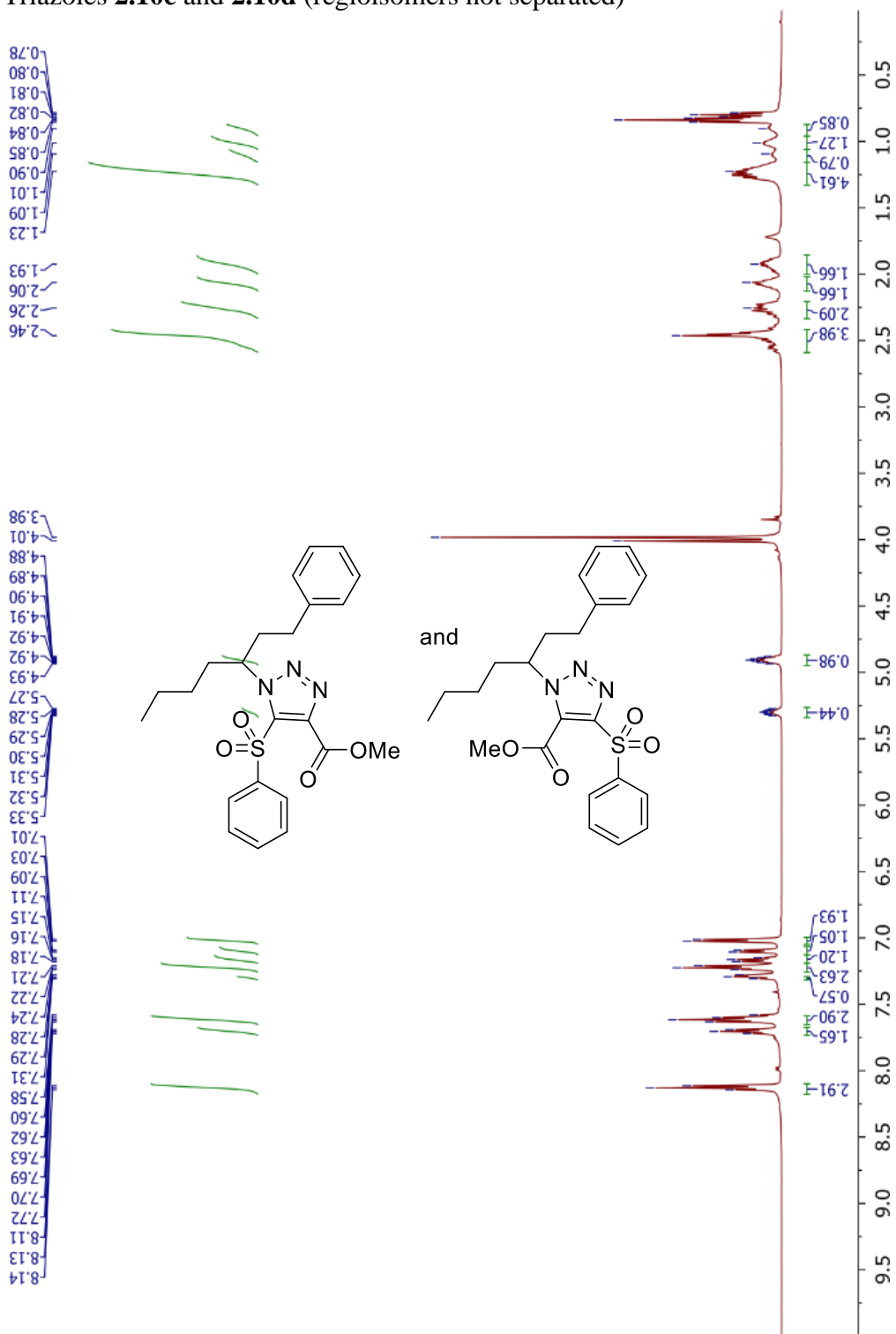
Triazole 2.7c

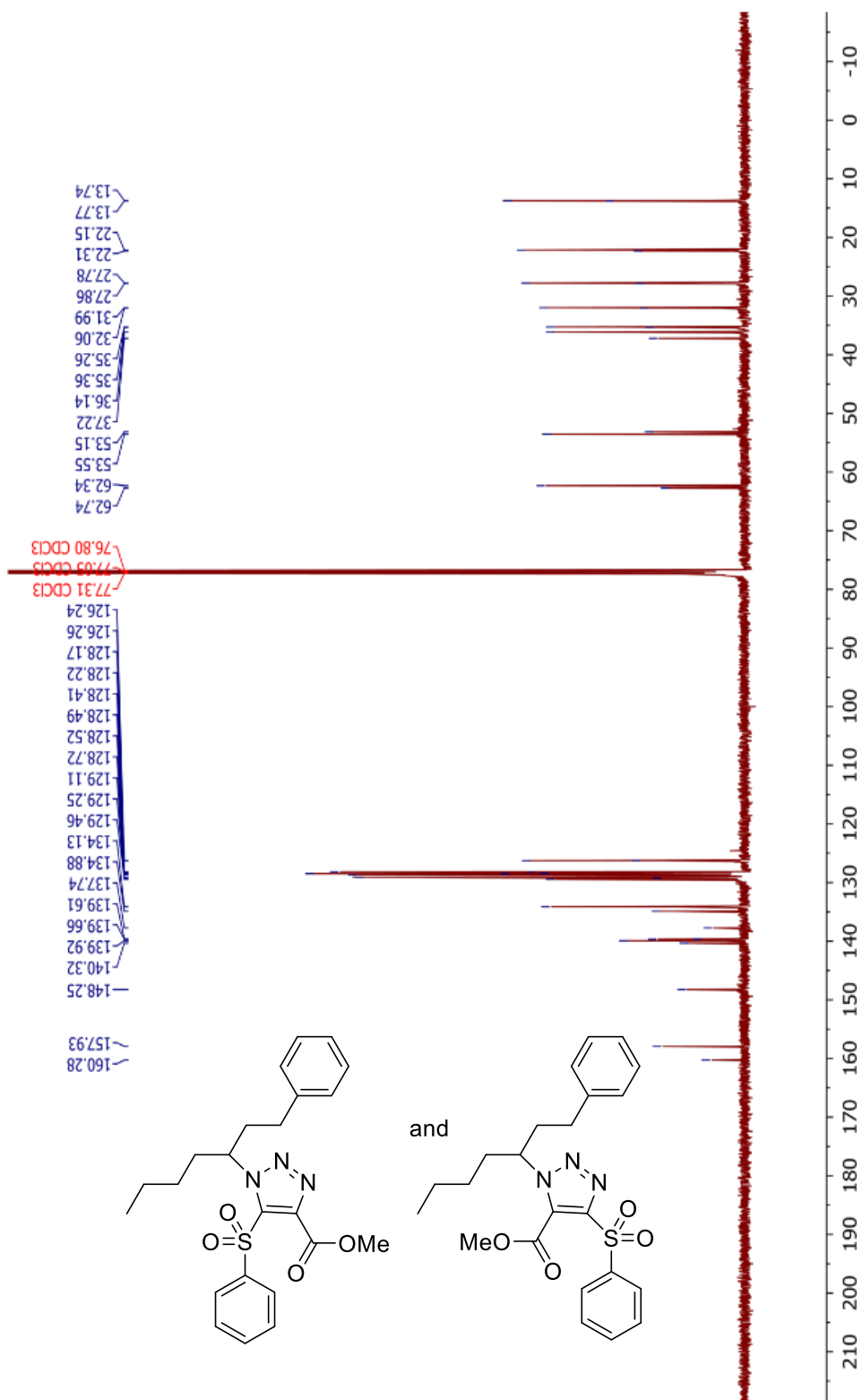




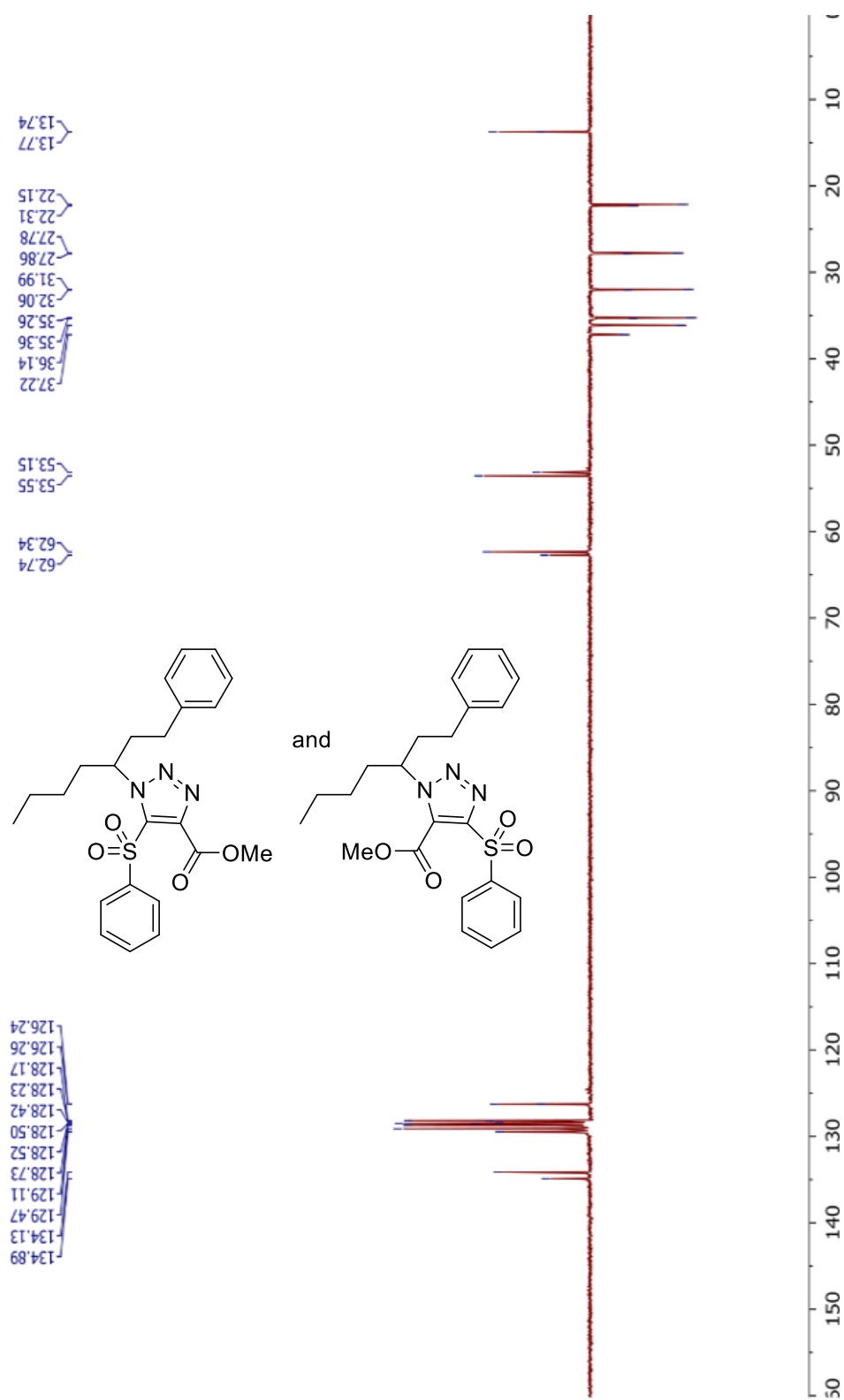


Triazoles **2.10c** and **2.10d** (regioisomers not separated)

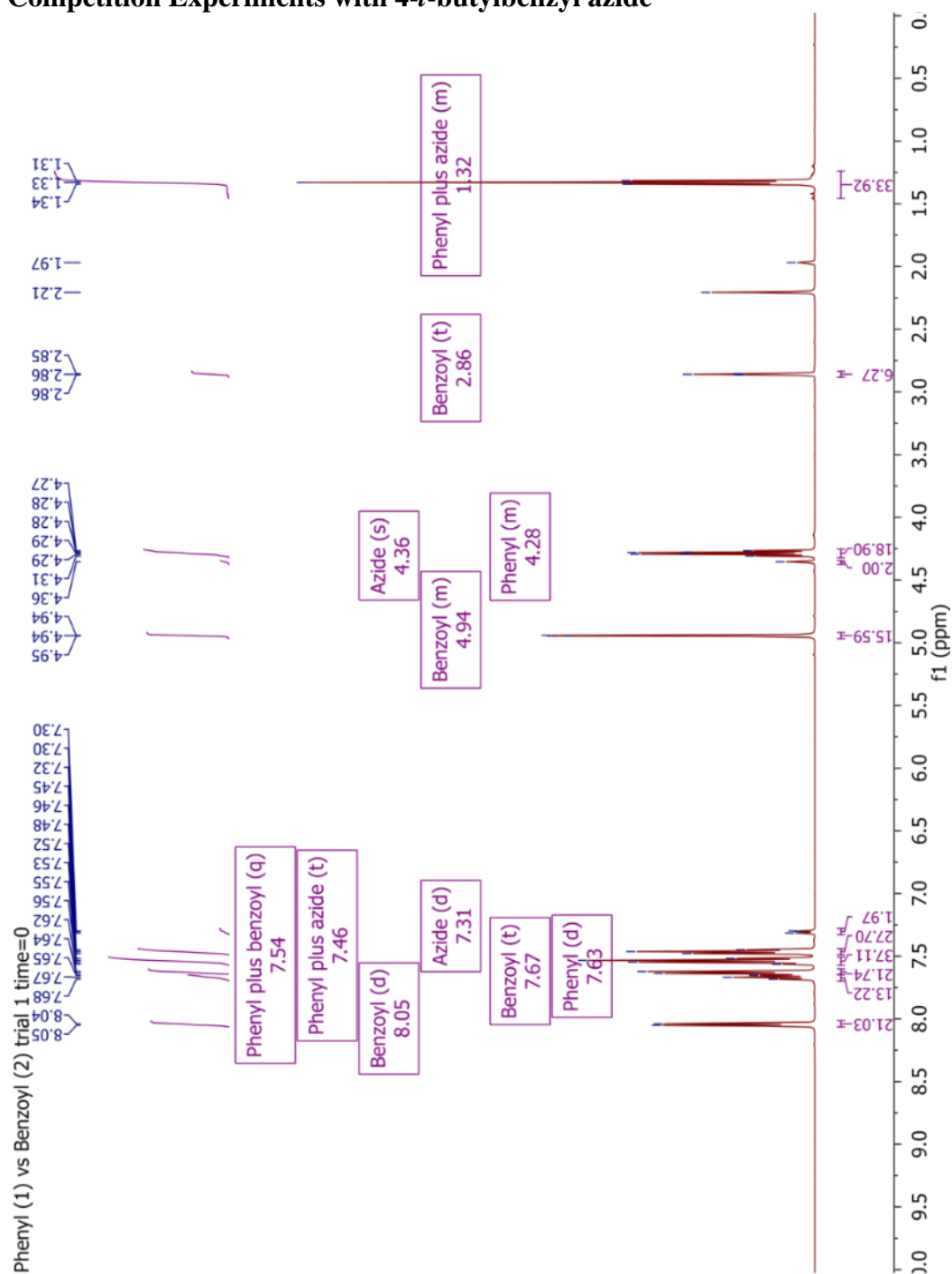




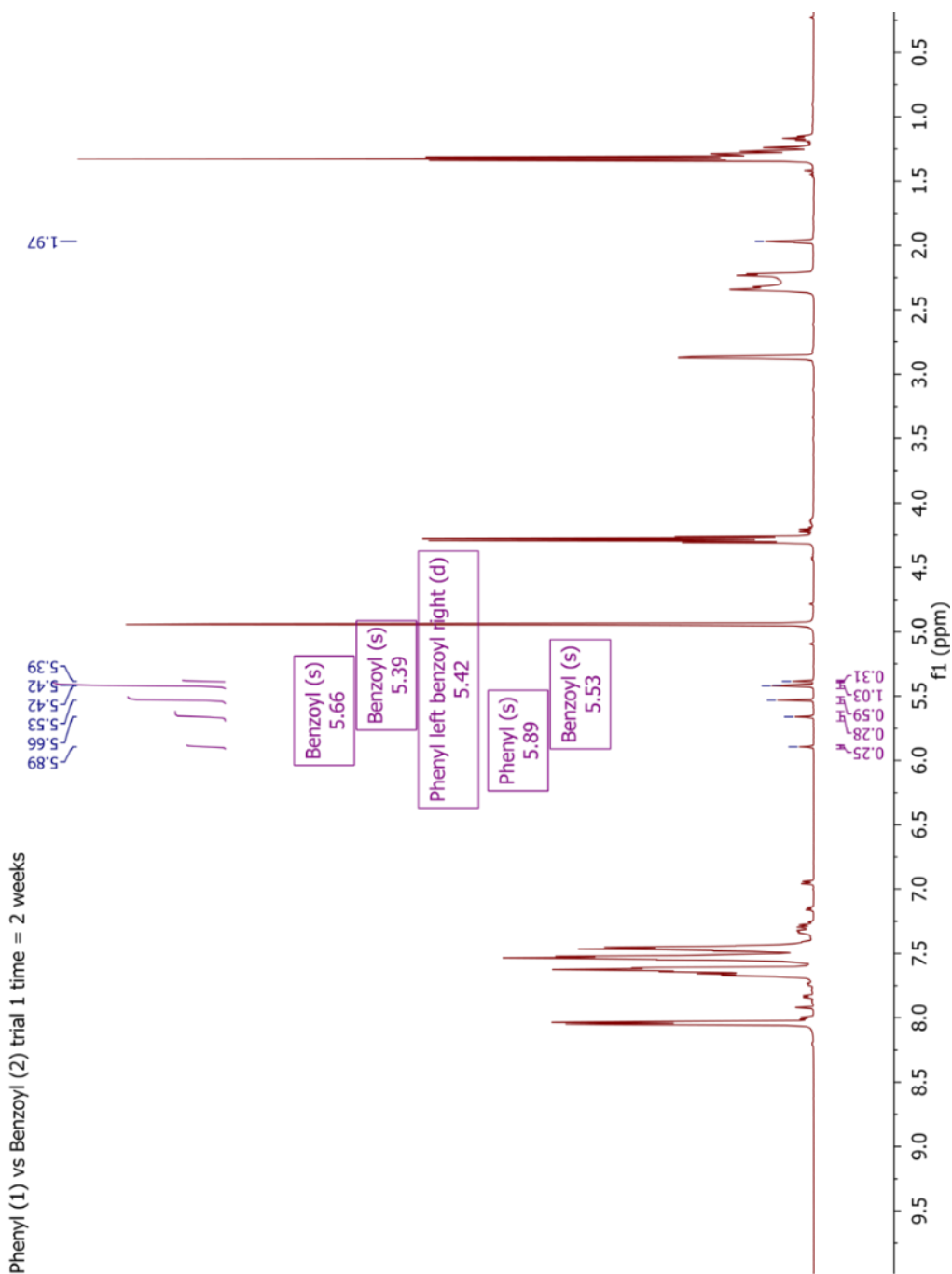




## Competition Experiments with 4-*t*-butylbenzyl azide

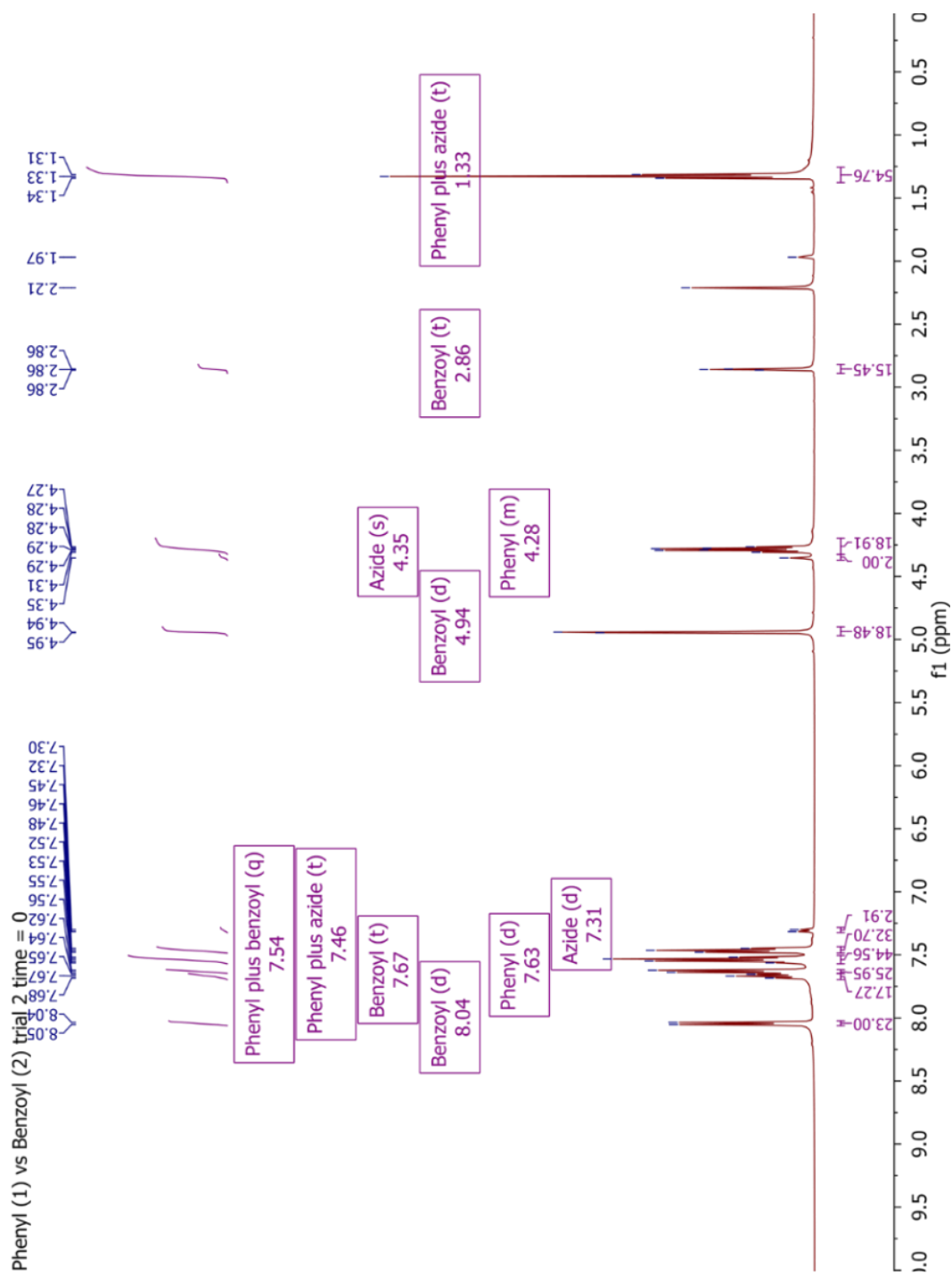


The initial ratio of azide **2.13** : benzoyl **2.2** : phenyl **2.1** was 1.0 : 7.8 : 9.5, based on integrations of azide  $\text{CH}_2\text{Ar}$  ( $\delta = 4.36$ ,  $I = 2.00$ ), benzoyl  $\text{OCH}_2$  ( $\delta = 4.94$ ,  $I = 15.59$ ), and phenyl  $\text{OCH}_2$  ( $\delta = 4.28$ ,  $I = 18.90$ ).

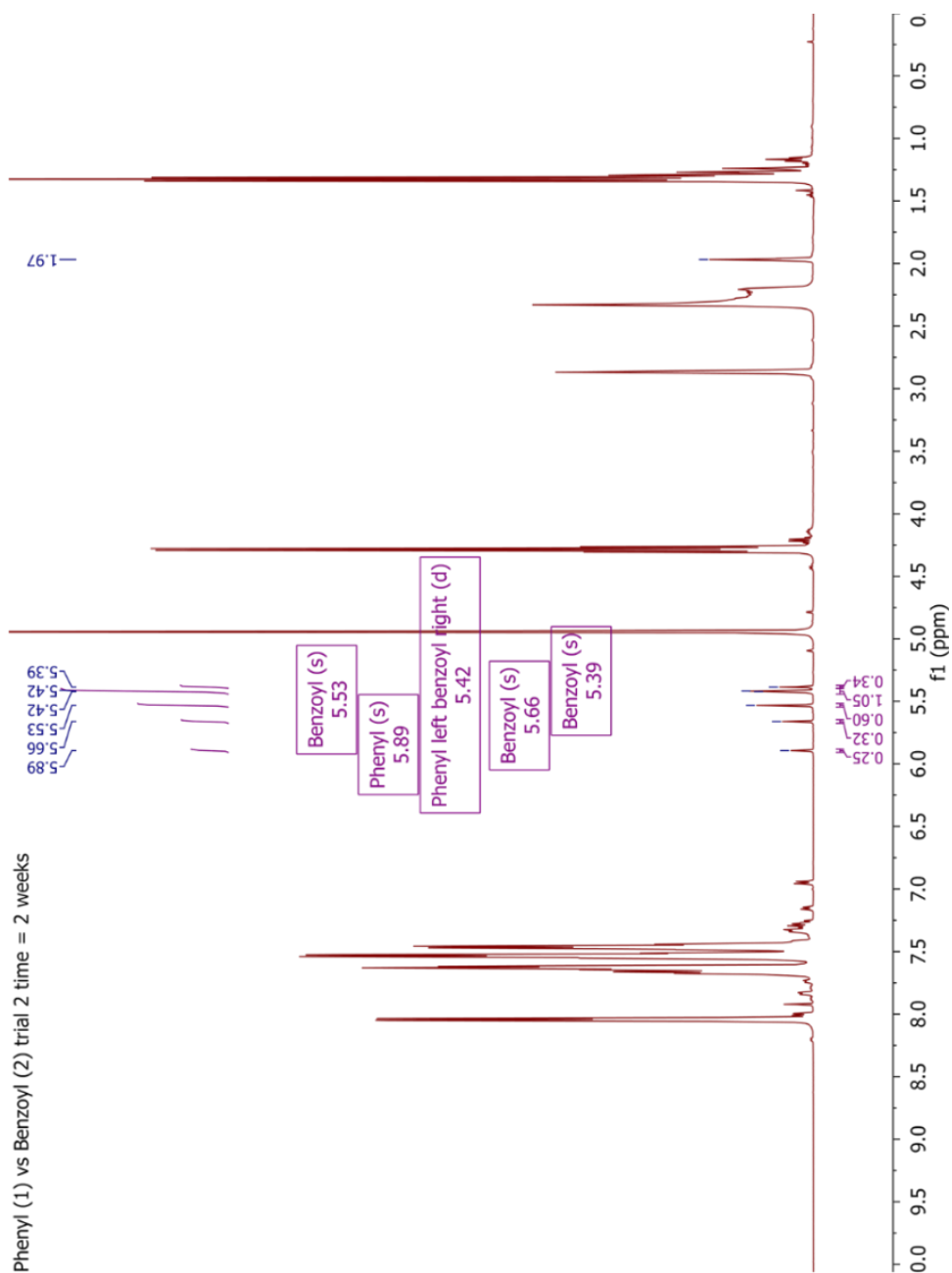


The ratio of products was benzoyl : phenyl 1.2 : 1.0, based on integrations of the benzylic protons of **2.1a** ( $\delta = 5.89$ ,  $I = 0.25$ ), **2.1b** ( $\delta = 5.42$ ,  $I = 0.50$ , overlap), **2.2b** ( $\delta = 5.66$ ,  $I = 0.28$ ,  $\delta = 5.39$ ,  $I = 0.31$ ), and **2.2a** ( $\delta = 5.53$ ,  $I = 0.59$ ,  $\delta = 5.42$ ,  $I = 0.59$ , overlap). Overlap was resolved by assuming both **2.2a** peaks were equal. After dividing by initial concentrations, the rate ratio was benzoyl : phenyl 1.4 : 1.0.

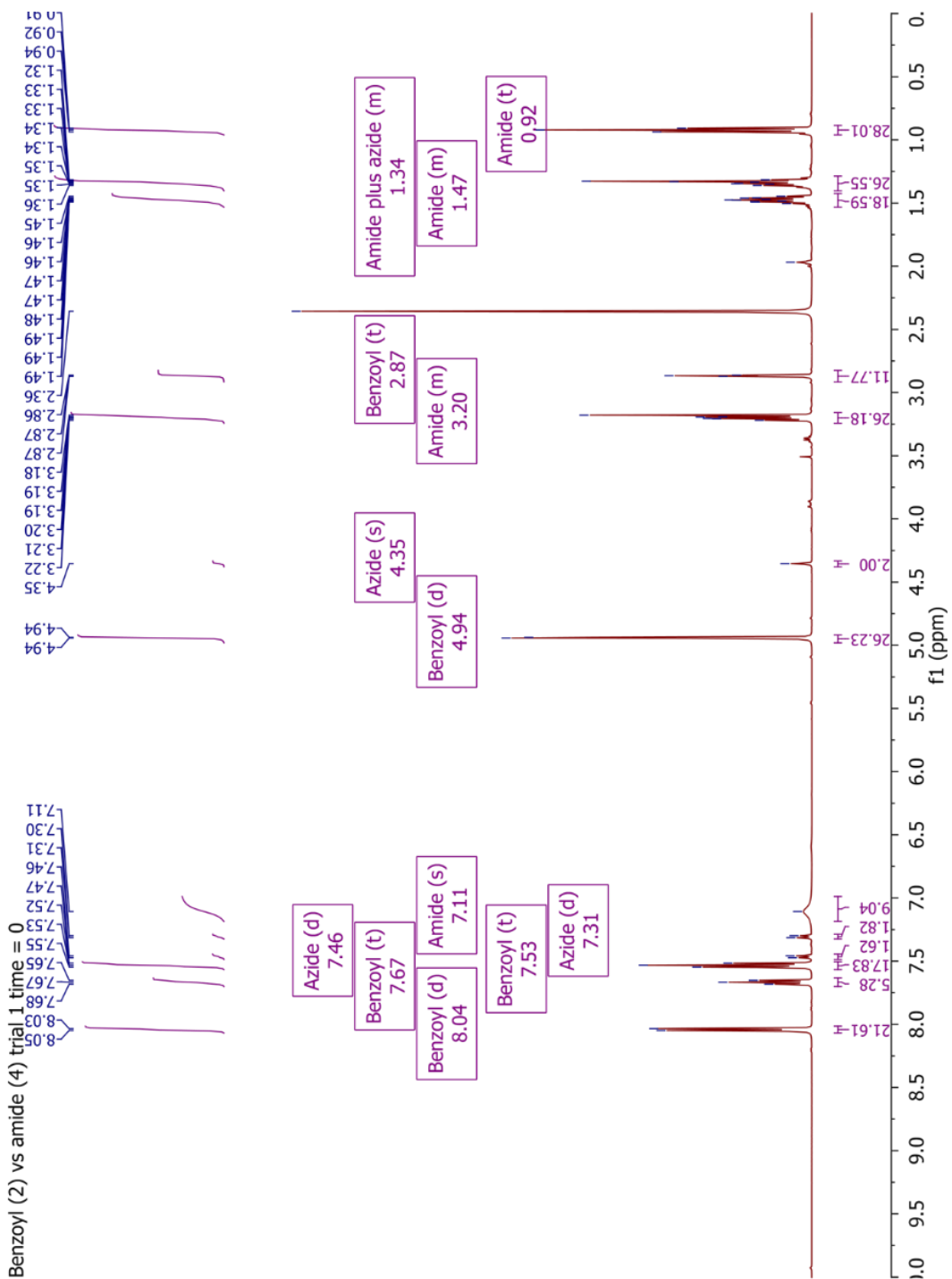
5



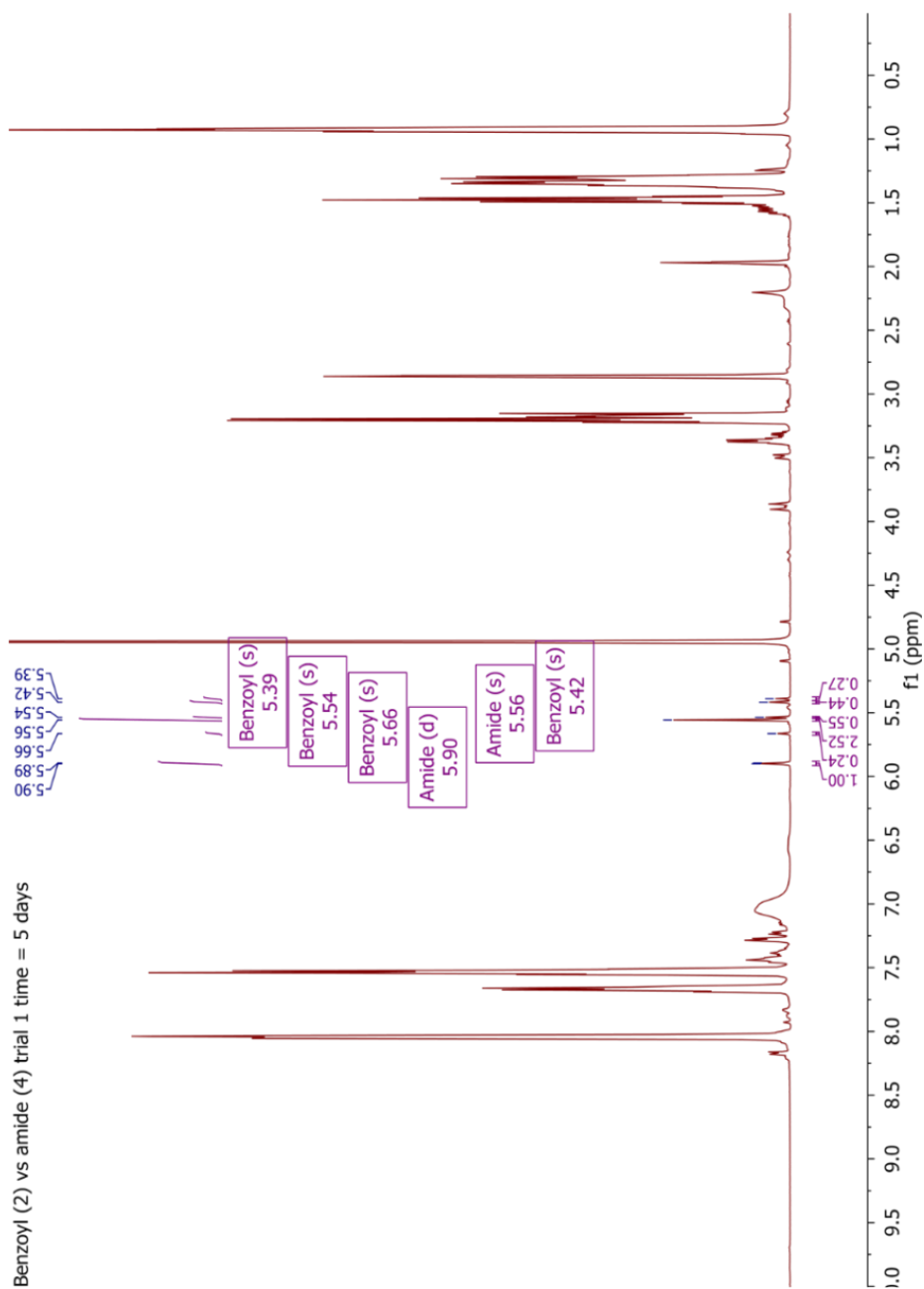
The initial ratio of azide **2.13** : benzoyl **2.2** : phenyl **2.1** was 1.0 : 9.2 : 9.5, based on integrations of azide  $\text{CH}_2\text{Ar}$  ( $\delta = 4.36$ ,  $I = 2.00$ ), benzoyl  $\text{OCH}_2$  ( $\delta = 4.94$ ,  $I = 18.48$ ), and phenyl  $\text{OCH}_2$  ( $\delta = 4.28$ ,  $I = 18.91$ ).



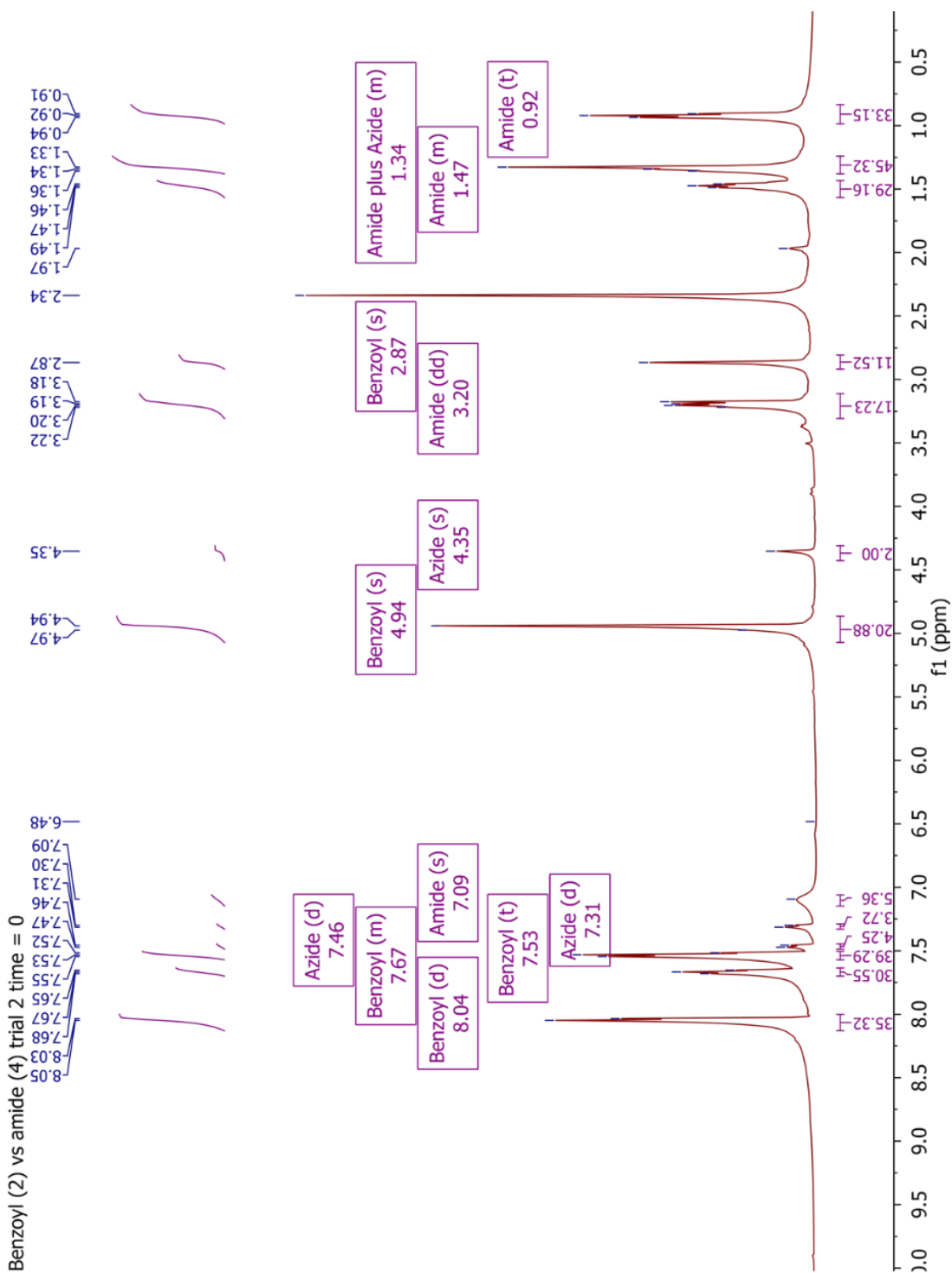
The ratio of products was benzoyl : phenyl 1.2 : 1.0, based on integrations of the benzylic protons of **2.1a** ( $\delta = 5.89$ ,  $I = 0.25$ ), **2.1b** ( $\delta = 5.42$ ,  $I = 0.55$ , overlap), **2.2b** ( $\delta = 5.66$ ,  $I = 0.32$ ,  $\delta = 5.39$ ,  $I = 0.34$ ), and **2.2a** ( $\delta = 5.53$ ,  $I = 0.60$ ,  $\delta = 5.42$ ,  $I = 0.60$ , overlap). Overlap was resolved by assuming both **2.2a** peaks were equal. After dividing by initial concentrations, the rate ratio was benzoyl : phenyl 1.3 : 1.0. Averaging the two trials gave a rate ratio of benzoyl : phenyl 1.4 ( $\pm 0.1$ ) : 1.0.



The initial ratio of azide **2.13** : amide **2.4** : benzoyl **2.2** was 1.0 : 8.7 : 13.1, based on integrations of  $\text{CH}_2\text{Ar}$  ( $\delta = 4.35$ ,  $I = 2.00$ ), amide  $\text{CH}_2\text{NH}$  plus amide  $\text{CCH}$  (overlapping,  $\delta = 3.19$ ,  $I = 26.18$ ), and benzoyl  $\text{OCH}_2$  ( $\delta = 4.94$ ,  $I = 26.23$ ).

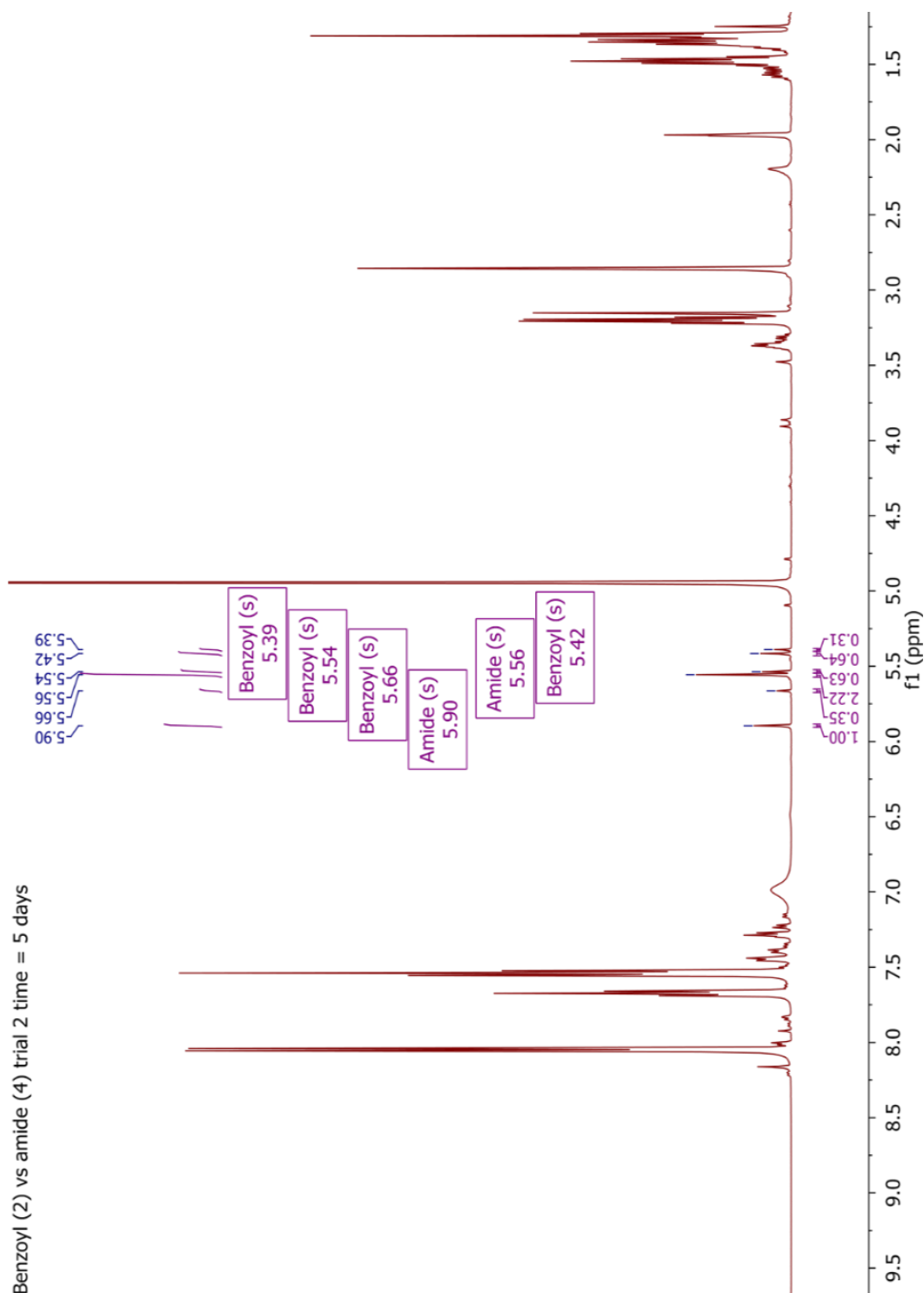


The ratio of products was amide : benzoyl 4.7 : 1, based on integrations of the benzylic protons of **2.2b** ( $\delta = 5.66$ ,  $I = 0.24$ ,  $\delta = 5.39$ ,  $I = 0.27$ ) **2.2a** ( $\delta = 5.54$ ,  $I = 0.55$ ,  $\delta = 5.42$ ,  $I = 0.44$ ), **2.4b** ( $\delta = 5.90$ ,  $I = 1.00$ ), and **2.4a** ( $\delta = 5.56$ ,  $I = 2.52$ ). After dividing by initial concentrations, the rate ratio was amide : benzoyl 7.1 : 1.0.

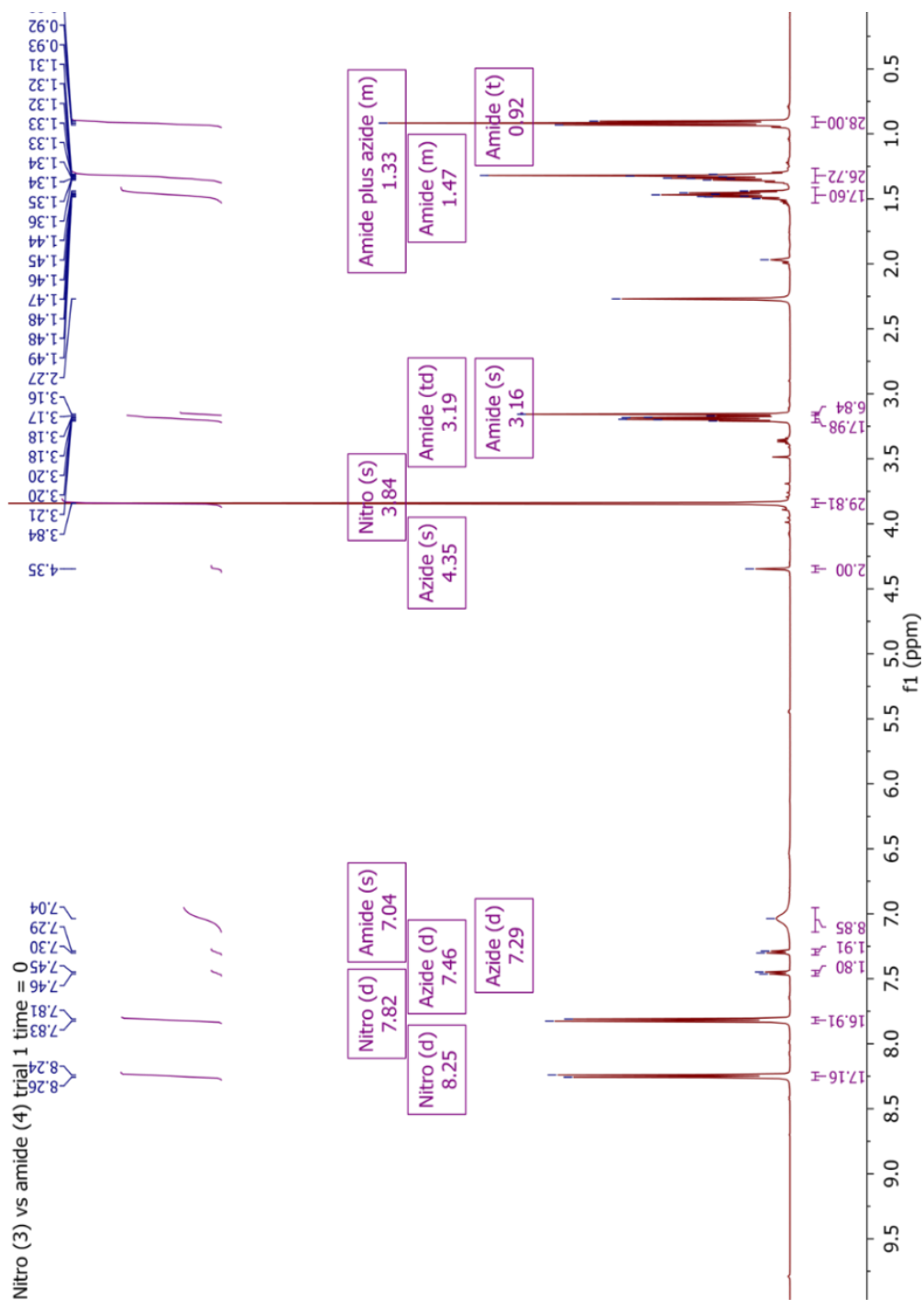


The initial ratio of azide **2.13** : amide **2.4** : benzoyl **2.2** was 1.0 : 5.7 : 10.4, based on integrations of  $\text{CH}_2\text{Ar}$  ( $\delta = 4.35$ ,  $I = 2.00$ ), amide  $\text{CH}_2\text{NH}$  plus amide  $\text{CCH}$  (overlapping,  $\delta = 3.19$ ,  $I = 17.23$ ), and benzoyl  $\text{OCH}_2$  ( $\delta = 4.94$ ,  $I = 20.88$ ).

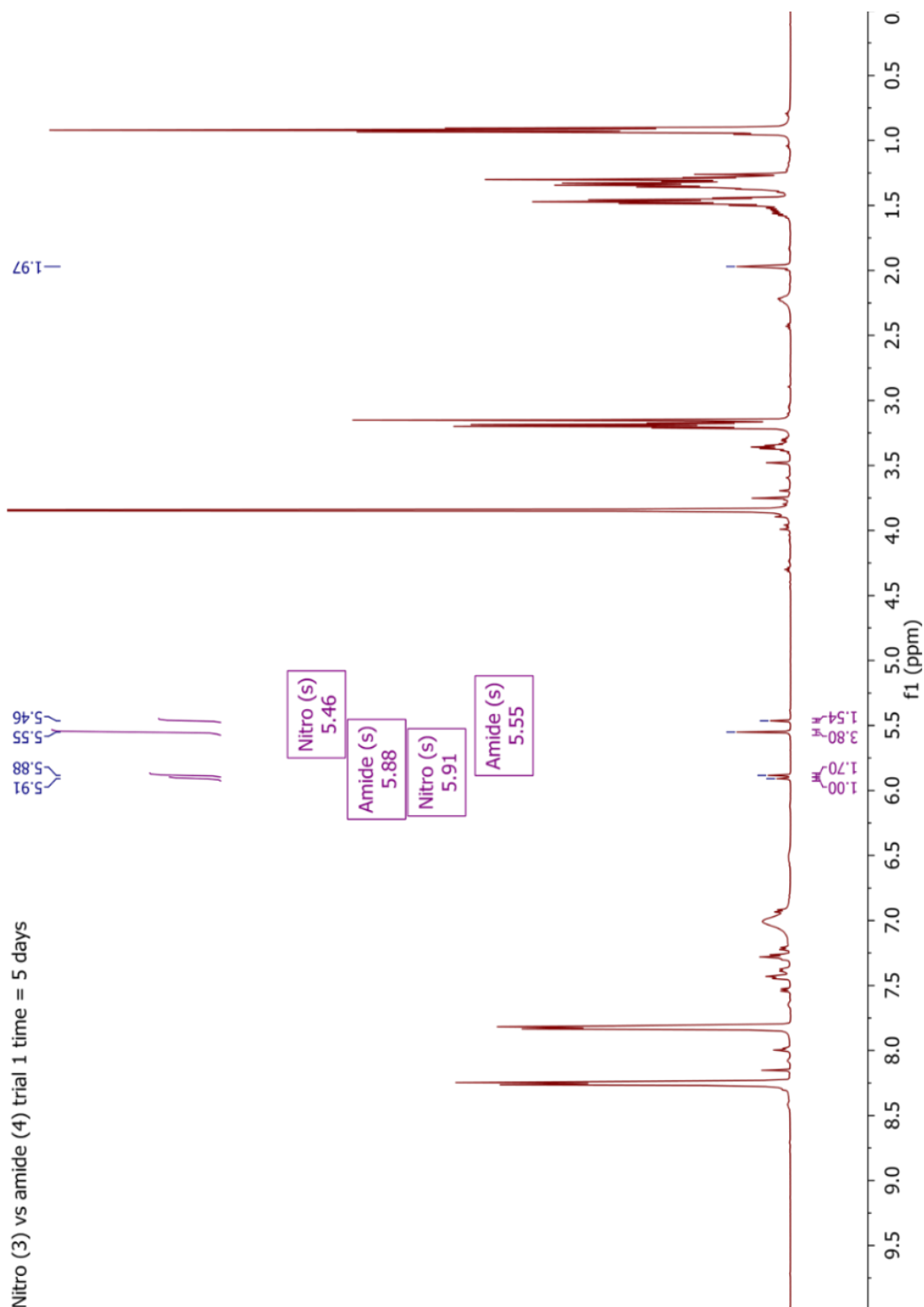




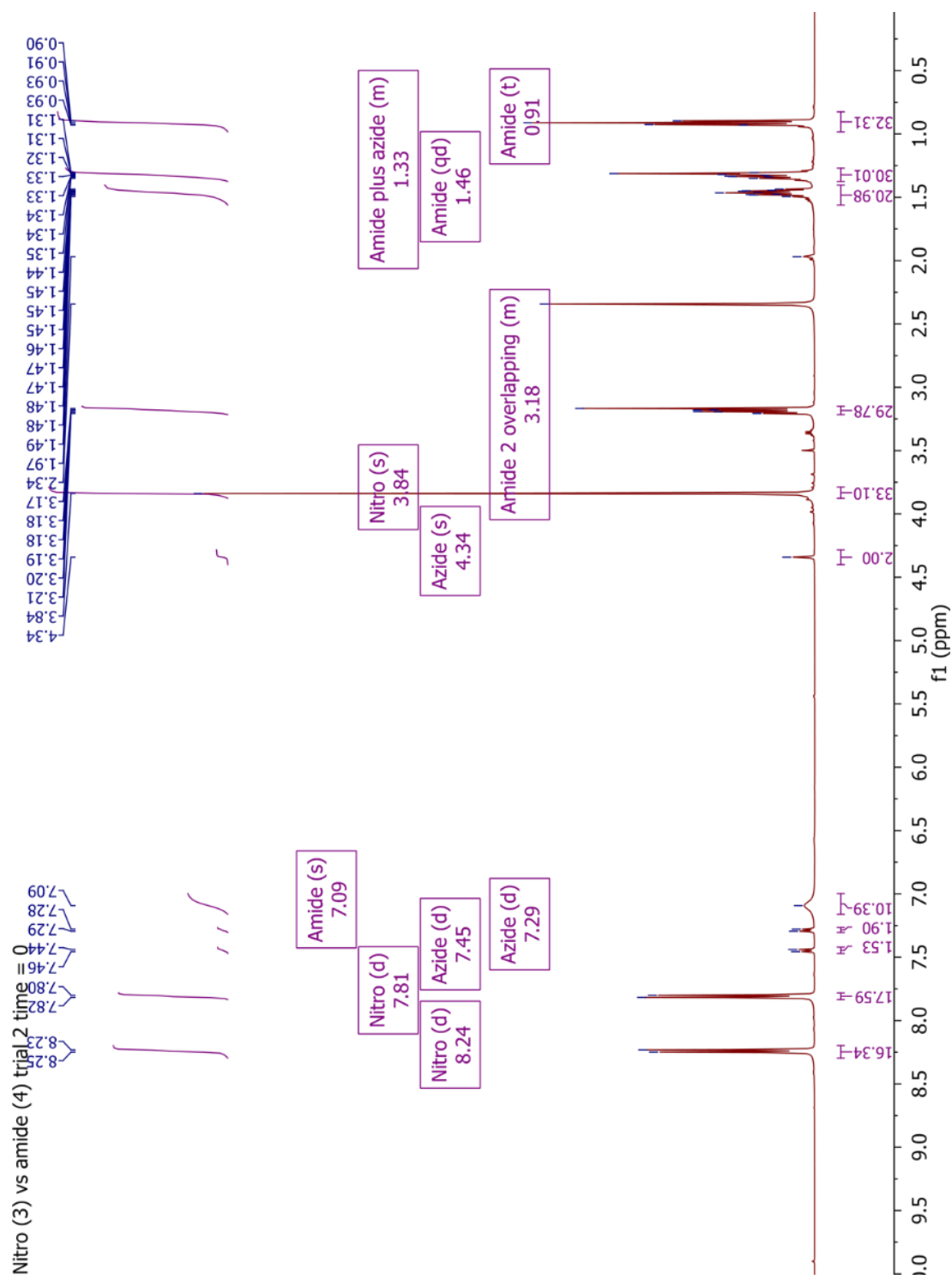
The ratio of products was amide : benzoyl 3.3 : 1, based on integrations of the benzylic protons of **2.2b** ( $\delta = 5.66$ ,  $I = 0.35$ ,  $\delta = 5.39$ ,  $I = 0.31$ ) **2.2a** ( $\delta = 5.54$ ,  $I = 0.63$ ,  $\delta = 5.42$ ,  $I = 0.64$ ), **2.4b** ( $\delta = 5.90$ ,  $I = 1.00$ ), and **2.4a** ( $\delta = 5.56$ ,  $I = 2.22$ ). After dividing by initial concentrations, the rate ratio was amide : benzoyl 6.0 : 1.0. Averaging the two trials gave amide : benzoyl 6.5 ( $\pm 0.7$ ) : 1.0.



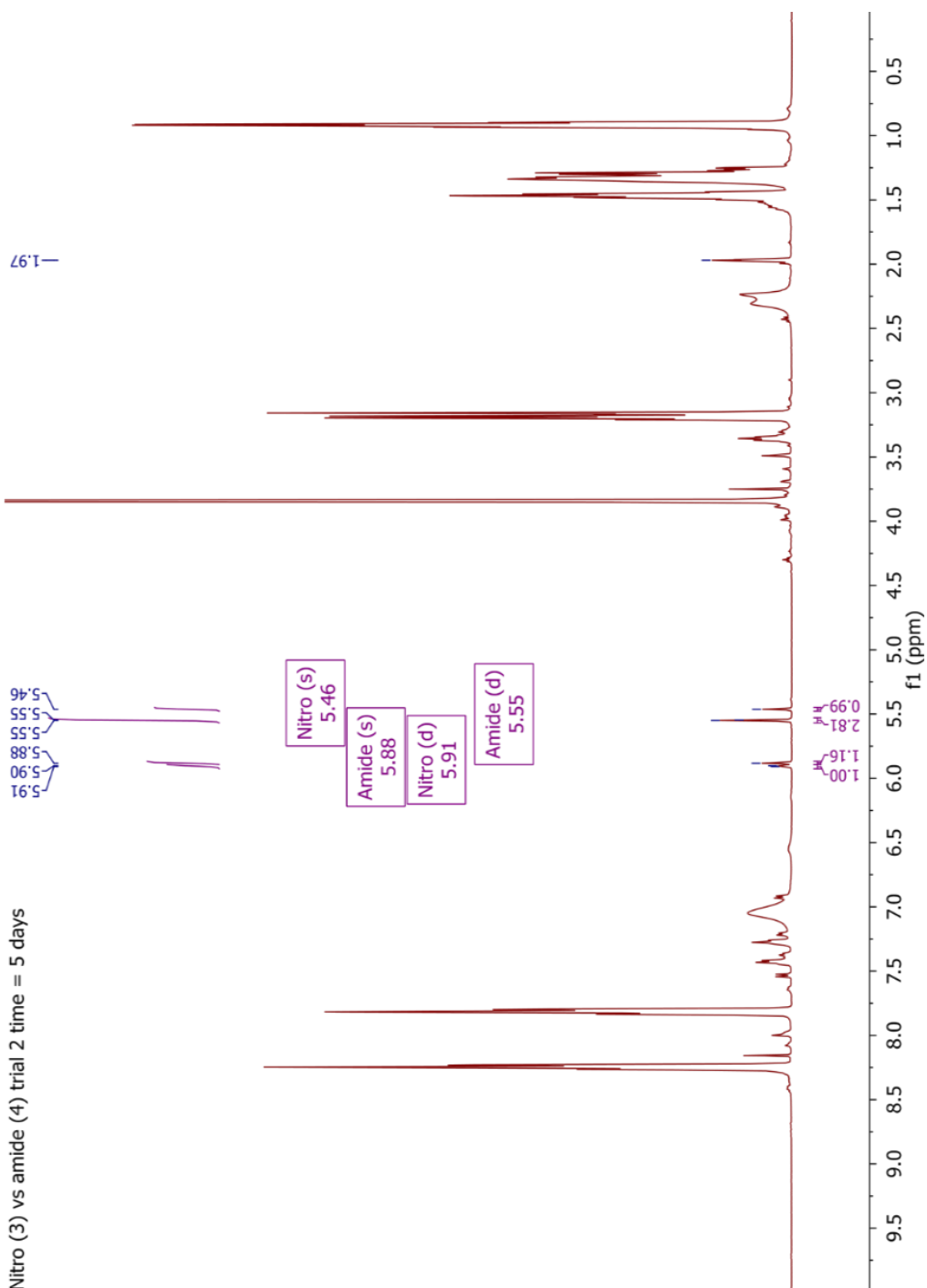
The initial ratio of azide **2.13** : amide **2.4** : nitro **2.3** was 1 : 8.3 : 9.9, based on integrations of azide  $\text{CH}_2\text{Ar}$  ( $\delta = 4.35$ ,  $I = 2.00$ ), amide  $\text{CH}_2\text{NH}$  ( $\delta = 3.19$ ,  $I = 17.98$ ), amide  $\text{CCH}$  ( $\delta = 3.16$ ,  $I = 6.84$ ), and nitro  $\text{OCH}_3$  ( $\delta = 3.84$ ,  $I = 29.81$ ).



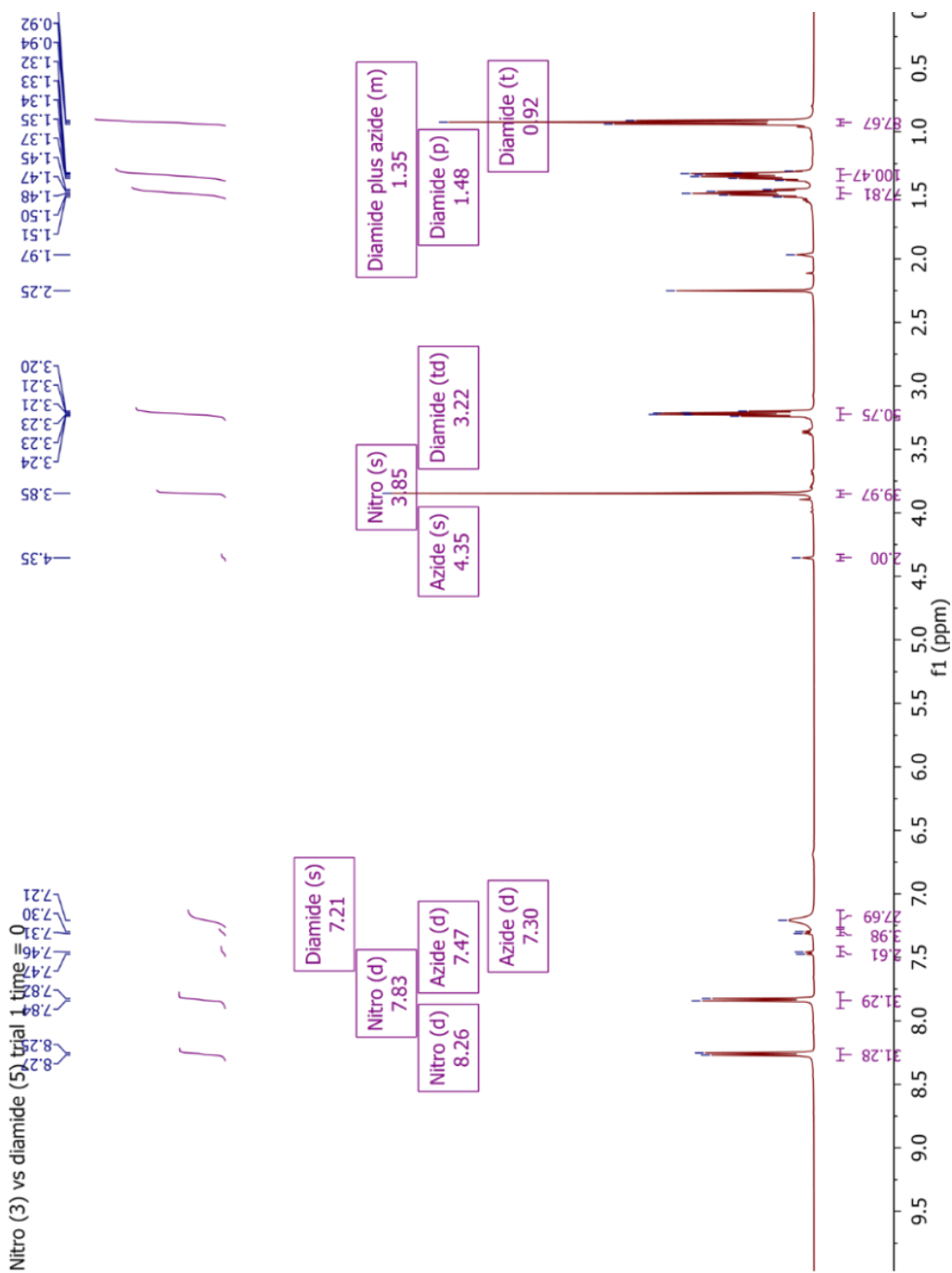
The ratio of products was amide : nitro 2.2 : 1.0, based on integrations of the benzylic protons of **2.4a** ( $\delta = 5.55$ ,  $I = 3.80$ ), **2.4b** ( $\delta = 5.88$ ,  $I = 1.70$ ), **2.3b** ( $\delta = 5.46$ ,  $I = 1.54$ ), and **2.3a** ( $\delta = 5.91$ ,  $I = 1.00$ ). After dividing by the initial concentrations, the rate ratio was amide : nitro 2.6 : 1.0.



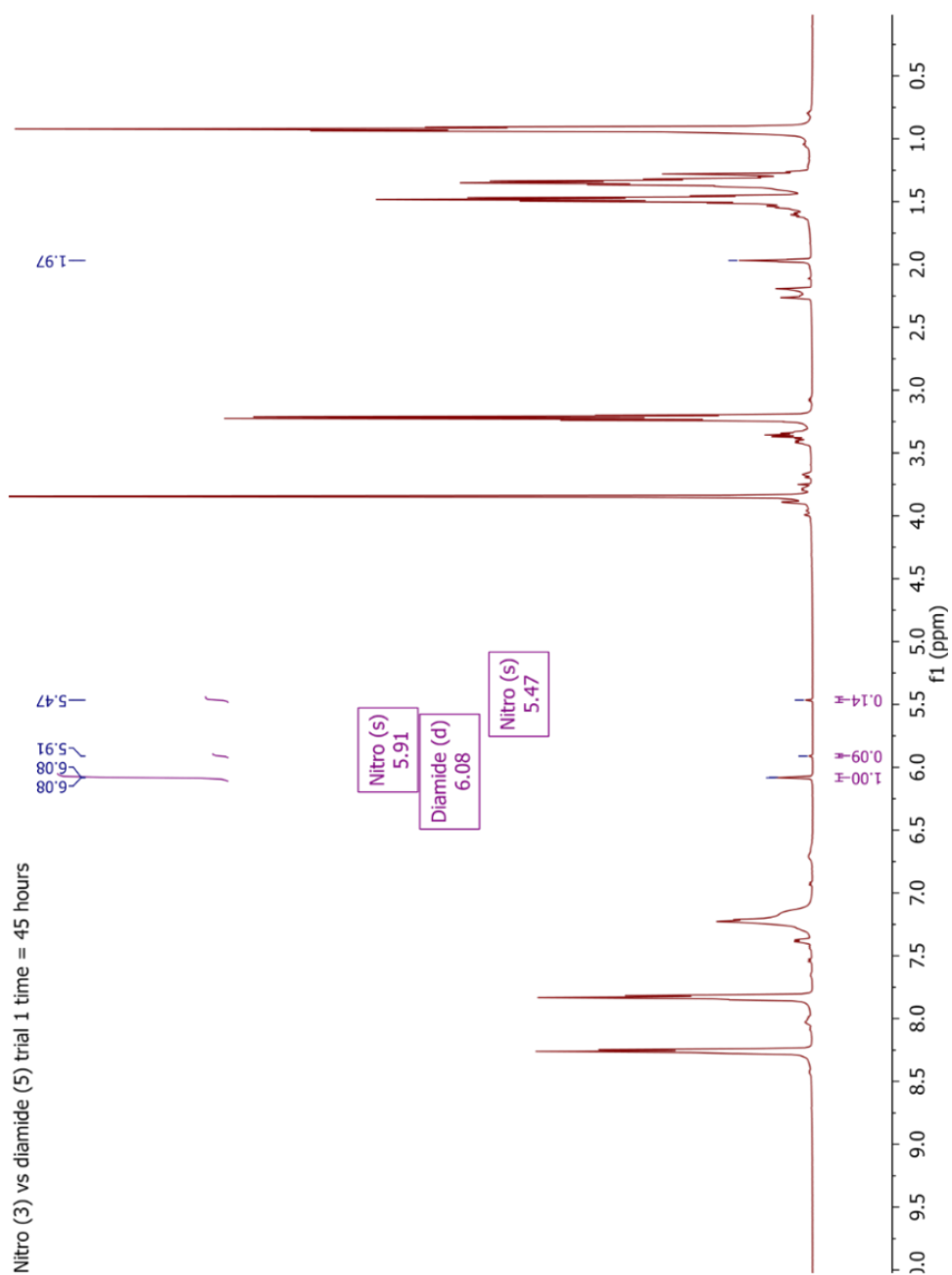
The initial ratio of azide **2.13** : amide **2.4** : nitro **2.3** was 1 : 9.9 : 11.0, based on integrations of azide  $\text{CH}_2\text{Ar}$  ( $\delta = 4.35$ ,  $I = 2.00$ ), amide  $\text{CH}_2\text{NH}$  (and  $\text{CCH}$  ( $\delta = 3.18$ ,  $I = 29.78$ , overlap), and nitro  $\text{OCH}_3$  ( $\delta = 3.84$ ,  $I = 33.10$ ).



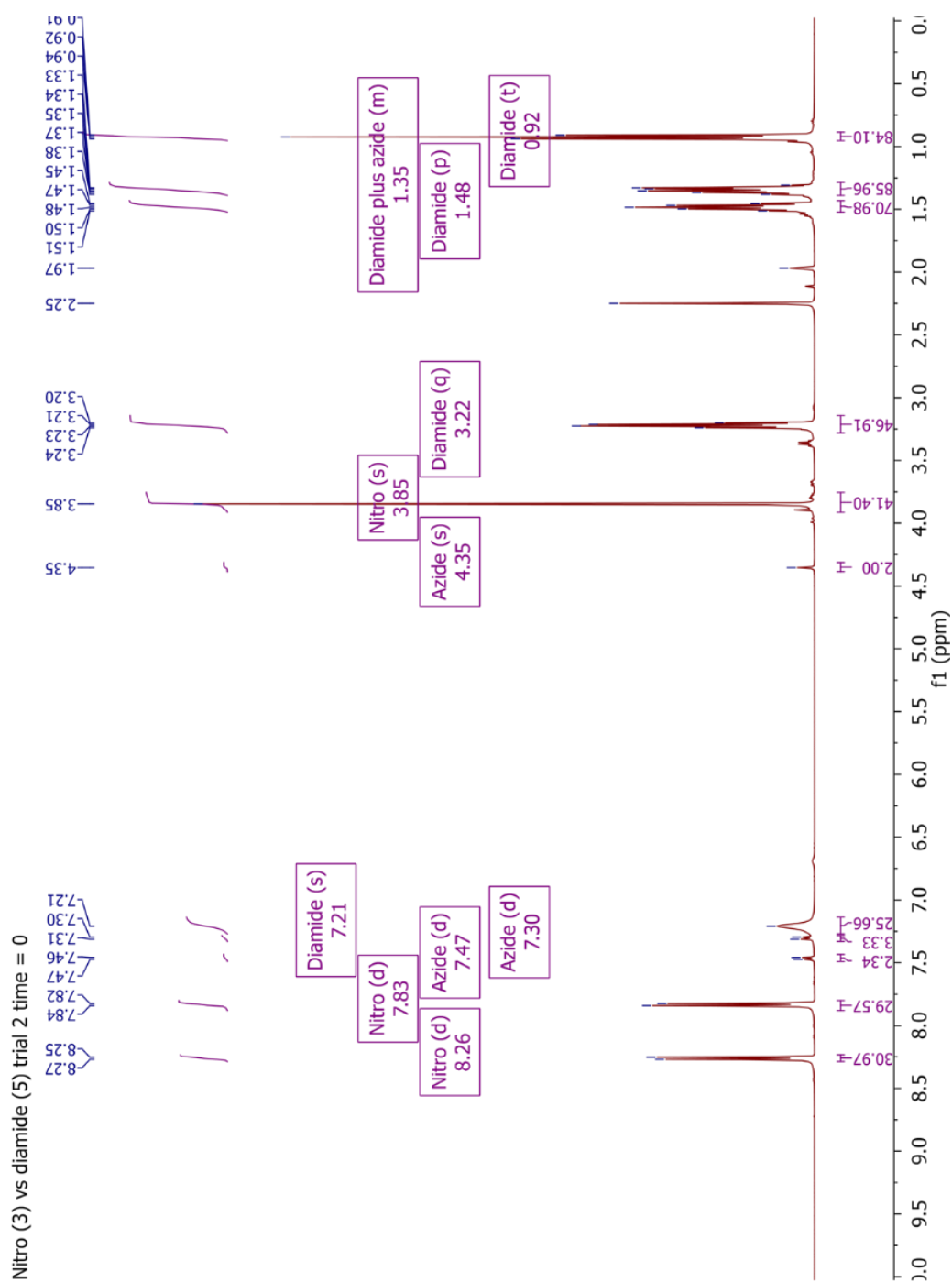
The ratio of products was amide : nitro 2.0 : 1.0, based on integrations of the benzylic protons of **2.4a** ( $\delta = 5.55$ ,  $I = 2.81$ ), **2.4b** ( $\delta = 5.88$ ,  $I = 1.16$ ), **2.3b** ( $\delta = 5.46$ ,  $I = 0.99$ ), and **2.3a** ( $\delta = 5.91$ ,  $I = 1.00$ ). After dividing by the initial concentrations, the rate ratio was amide : nitro 2.2 : 1.0. Averaging the two trials gave amide : nitro 2.4 ( $\pm 0.3$ ) : 1.0.



The initial ratio of azide **2.13** : diamide **2.5** : nitro **2.3** was 1.0 : 12.7 : 13.3, based on integrations of azide  $\text{CH}_2\text{Ar}$  ( $\delta = 4.35$ ,  $I = 2.00$ ), diamide  $\text{CH}_2\text{NH}$  ( $\delta = 3.22$ ,  $I = 50.75$ ), and nitro  $\text{OCH}_3$  ( $\delta = 3.85$ ,  $I = 39.97$ ).

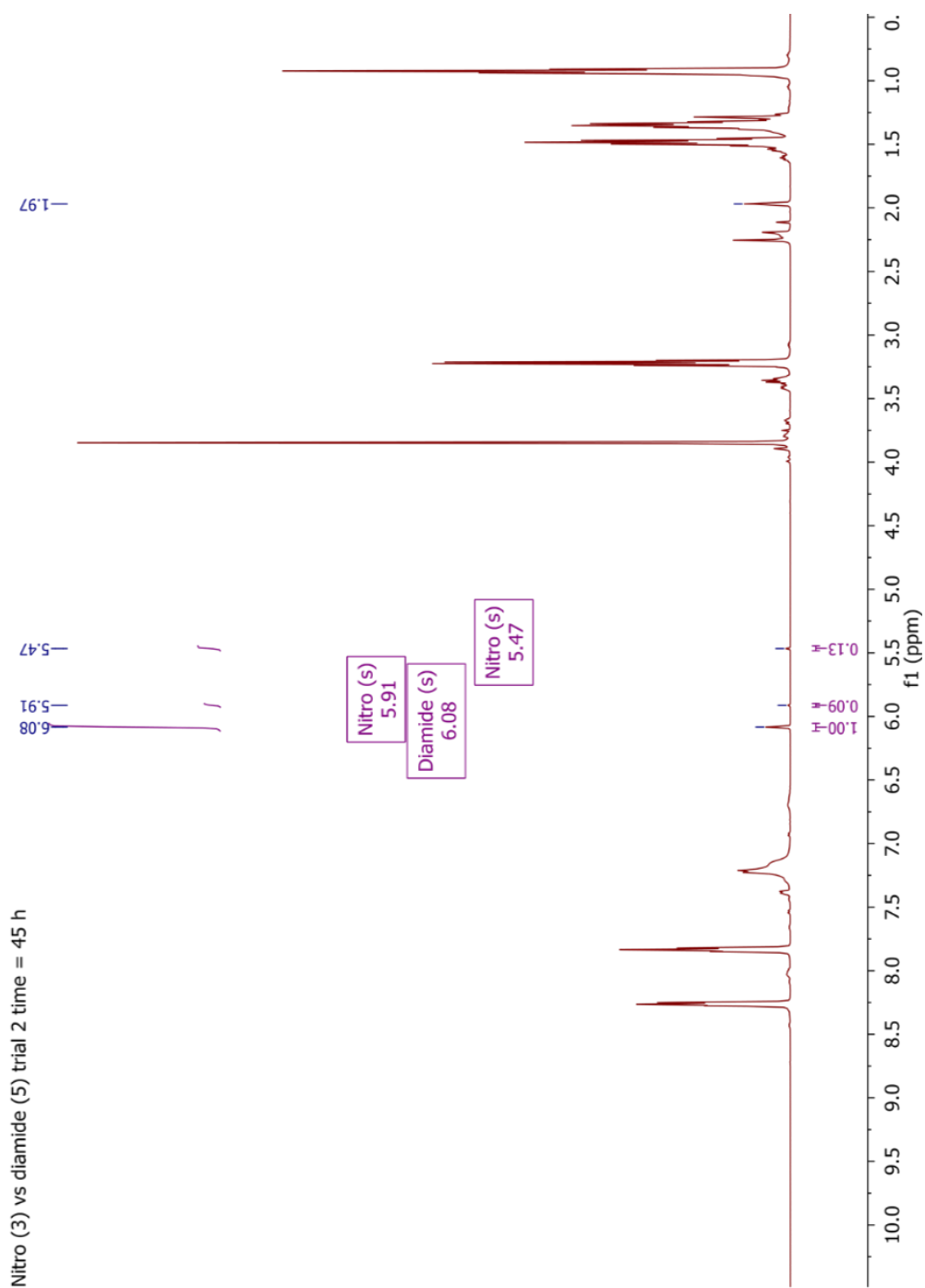


The ratio of products was diamide : nitro 4.3 : 1.0, based on integrations of the benzylic protons of **2.3a** ( $\delta = 5.91$ ,  $I = 0.09$ ), **2.3b** ( $\delta = 5.47$ ,  $I = 0.14$ ), and **2.5a** ( $\delta = 6.08$ ,  $I = 1.00$ ). After dividing by the initial concentrations, the rate ratio was diamide : nitro 4.6 : 1.0.

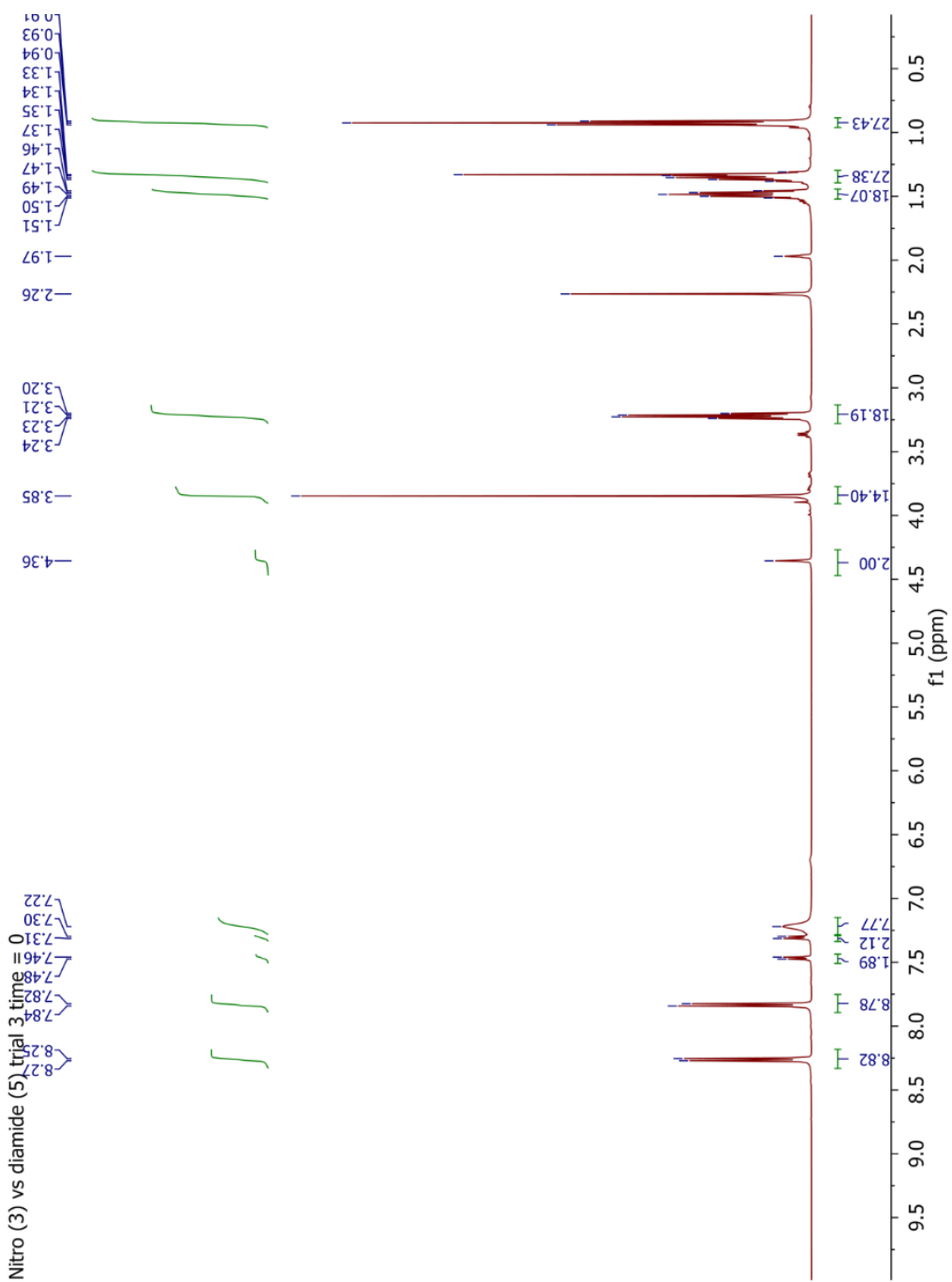


The initial ratio of azide **2.13** : diamide **2.5** : nitro **2.3** was 1.0 : 11.7 : 13.8, based on integrations of azide  $\text{CH}_2\text{Ar}$  ( $\delta = 4.35$ ,  $I = 2.00$ ), diamide  $\text{CH}_2\text{NH}$  ( $\delta = 3.22$ ,  $I = 46.91$ ), and nitro  $\text{OCH}_3$  ( $\delta = 3.85$ ,  $I = 41.40$ ).

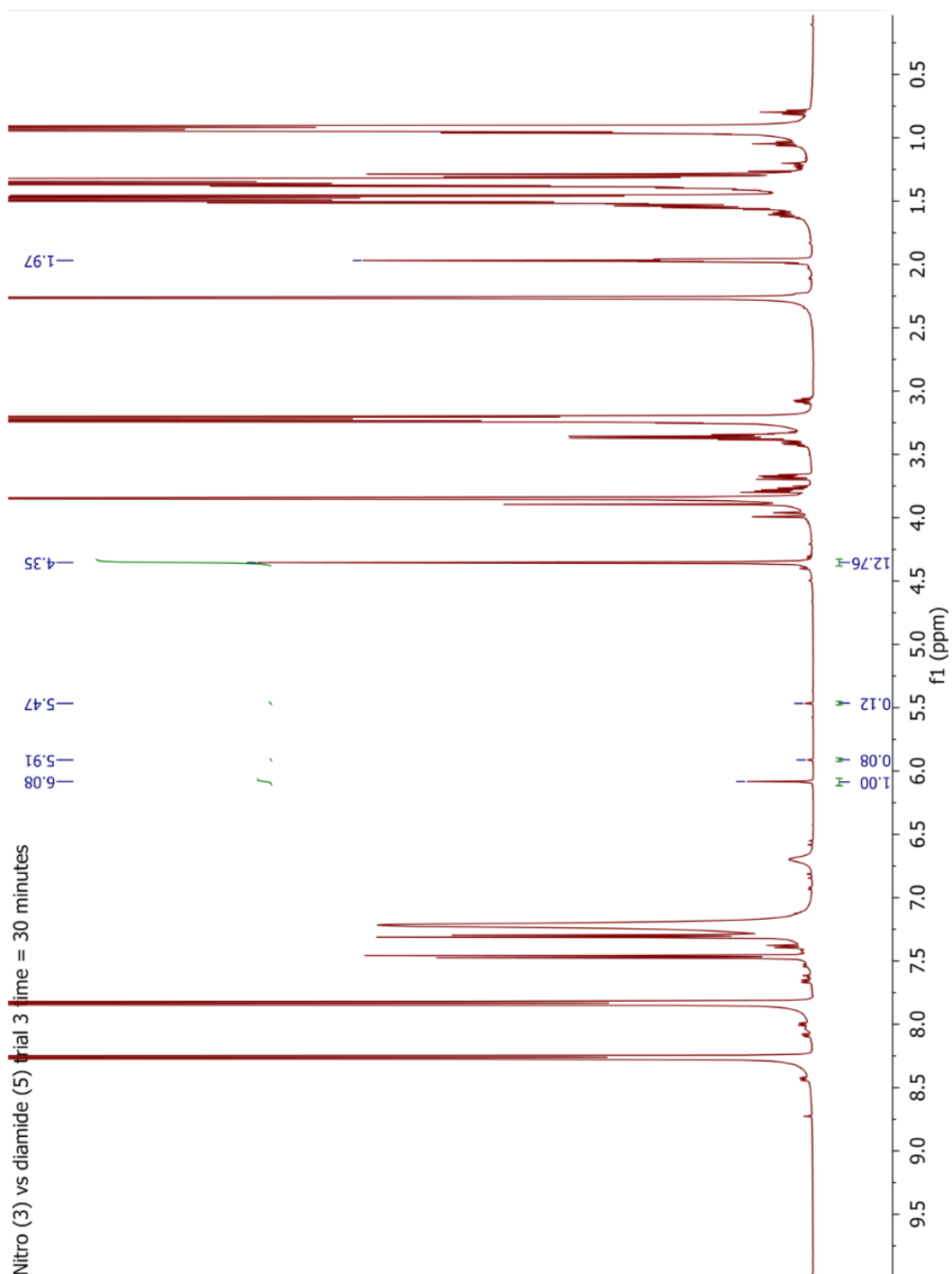




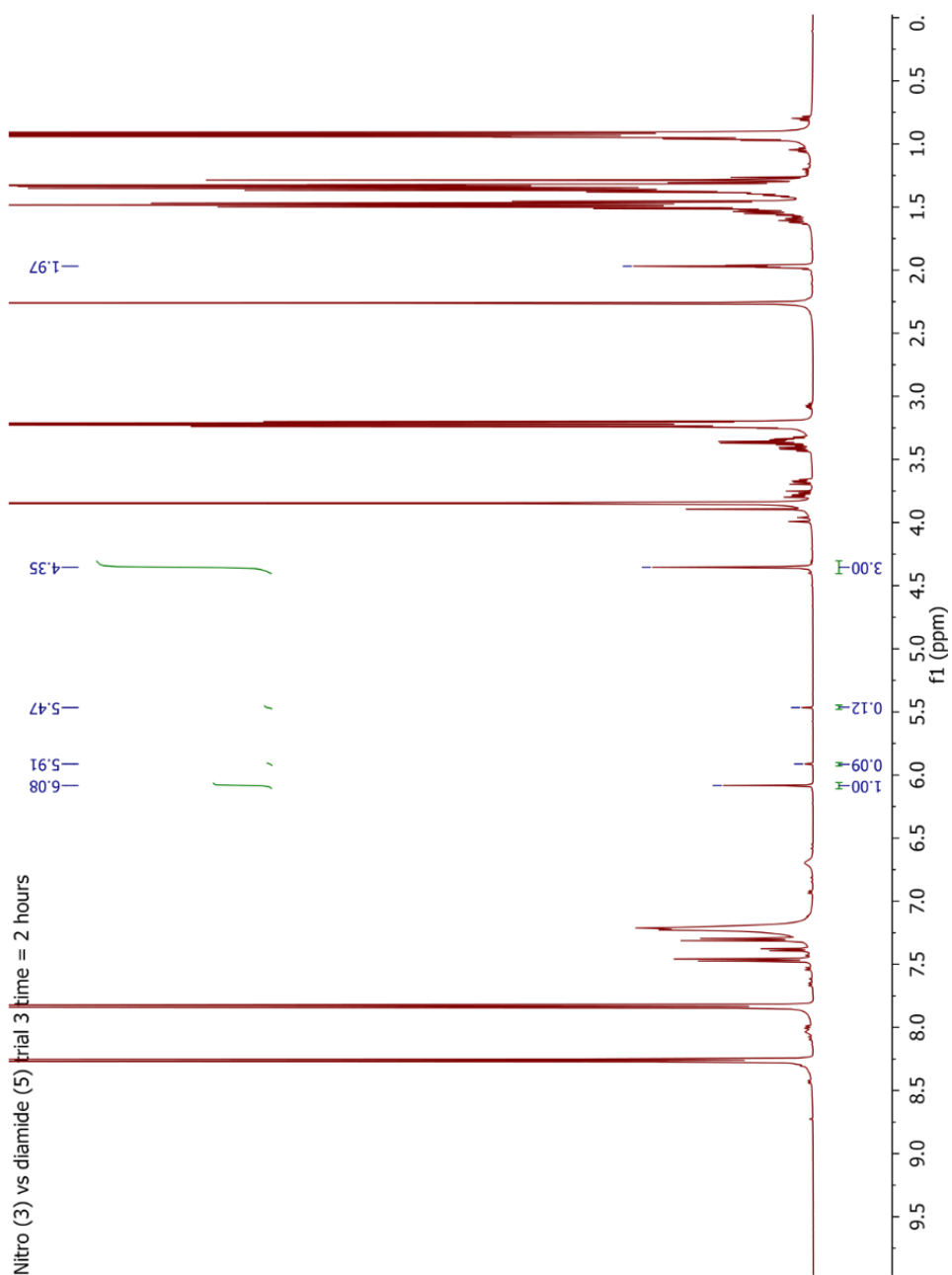
The ratio of products was diamide : nitro 4.5 : 1.0, based on integrations of the benzylic protons of **2.3a** ( $\delta = 5.91$ ,  $I = 0.09$ ), **2.3b** ( $\delta = 5.47$ ,  $I = 0.13$ ), and **2.5a** ( $\delta = 6.08$ ,  $I = 1.00$ ). After dividing by the initial concentrations, the rate ratio was diamide : nitro 5.3 : 1.0. Averaging the two trials gave diamide : nitro 5.0 ( $\pm 0.2$ ) : 1.0.



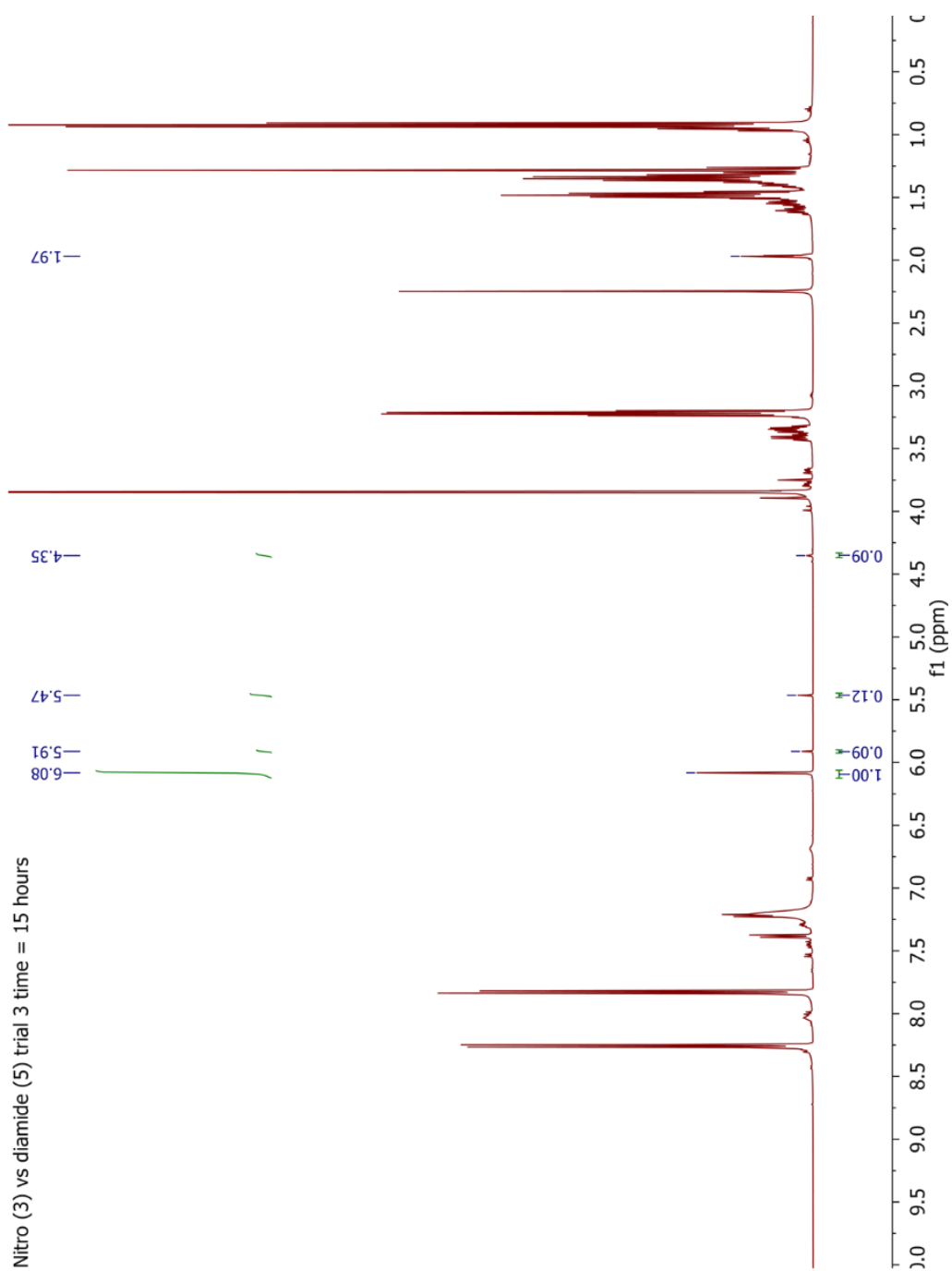
Starting ratio was azide **2.13** : diamide **2.5** : nitro **2.3** of 1.0 : 9.1 : 9.6, based on integrations of azide  $\text{CH}_2\text{Ar}$  ( $\delta = 4.36$ ,  $I = 2.00$ ), diamide  $\text{CH}_2\text{NH}$  ( $\delta = 3.23$ ,  $I = 18.19$ ), and nitro  $\text{OCH}_3$  ( $\delta = 3.85$ ,  $I = 14.40$ ).



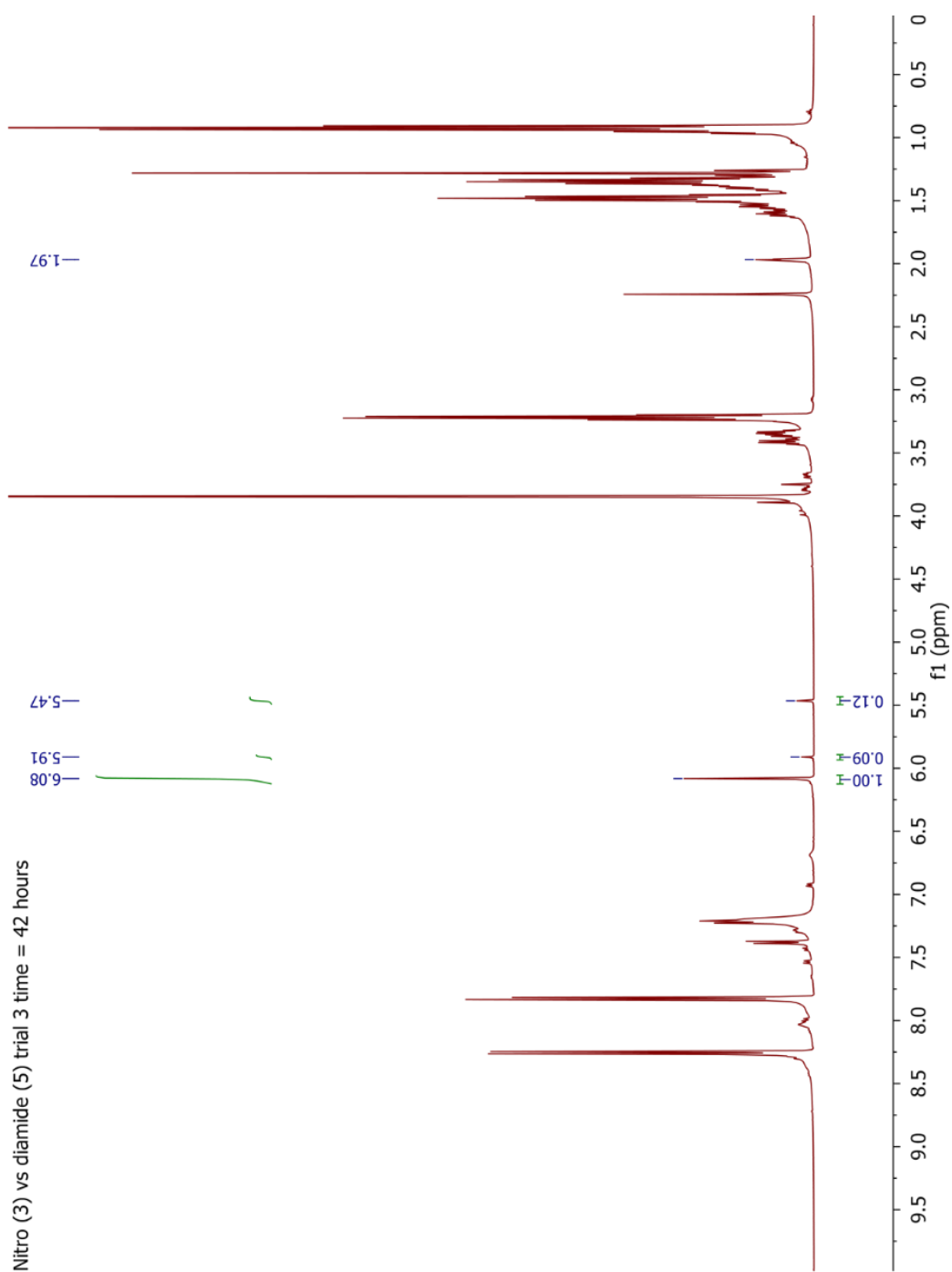
After 30 min, 8.6% of the azide had been consumed, and the product ratio was diamide : nitro 5.0 : 1.0, based on integrations of the benzylic protons of azide **2.13** ( $\delta = 4.35$ ,  $I = 12.76$ ), **2.5a** ( $\delta = 6.08$ ,  $I = 1.00$ ), **2.3a** ( $\delta = 5.91$ ,  $I = 0.08$ ), and **2.3b** ( $\delta = 5.47$ ,  $I = 0.12$ ).



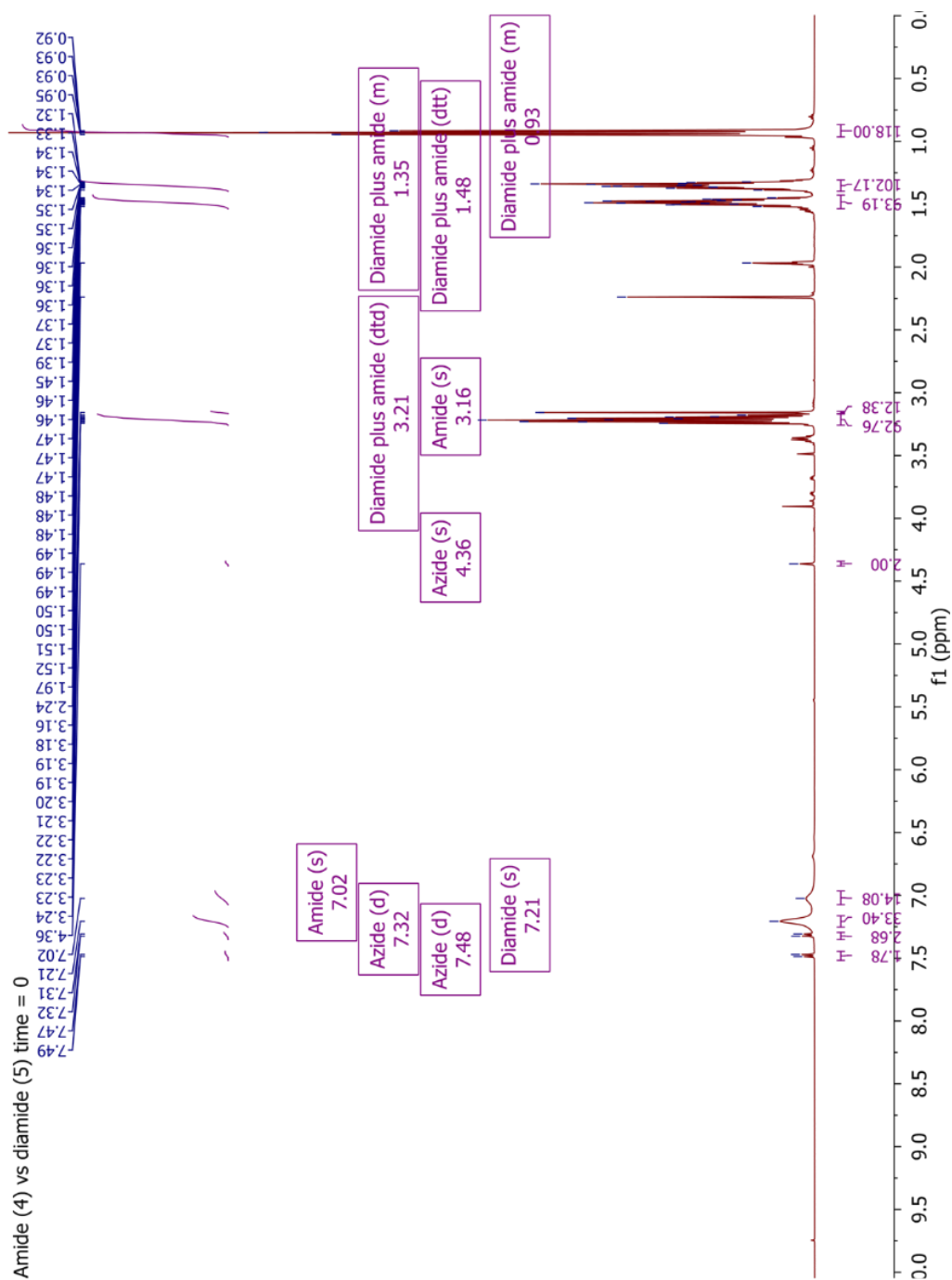
After 2 h, 29% of the azide had been consumed, and the product ratio was diamide : nitro 4.8 : 1.0, based on integrations of the benzylic protons of azide **2.13** ( $\delta = 4.35$ ,  $I = 3.00$ ), **2.5a** ( $\delta = 6.08$ ,  $I = 1.00$ ), **2.3a** ( $\delta = 5.91$ ,  $I = 0.09$ ), and **2.3b** ( $\delta = 5.47$ ,  $I = 0.12$ ).



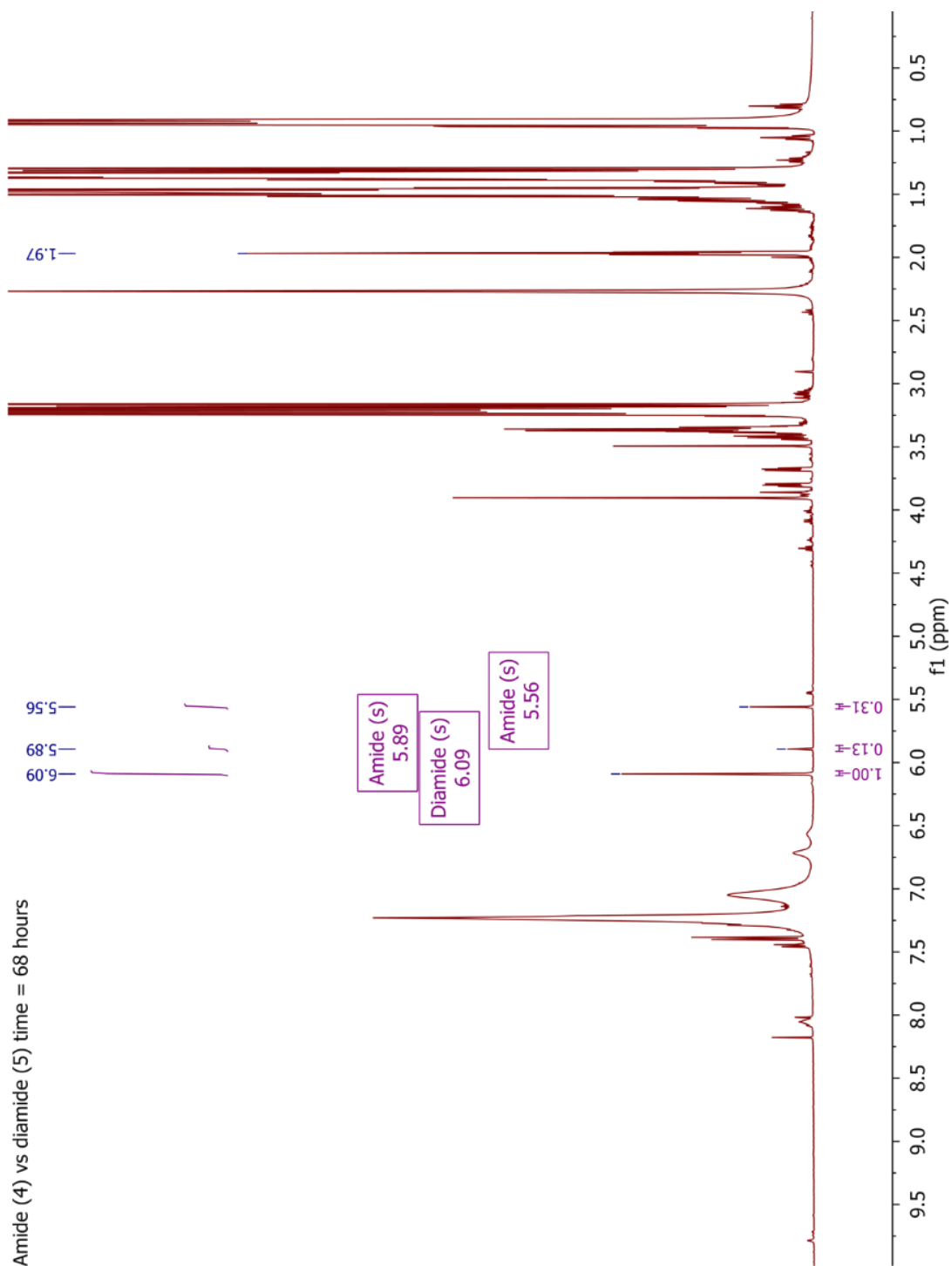
After 15 h, 93% of the azide had been consumed, and the product ratio was diamide : nitro 4.8 : 1.0, based on integrations of the benzylic protons of azide **2.13** ( $\delta = 4.35$ ,  $I = 0.09$ ), **2.5** ( $\delta = 6.08$ ,  $I = 1.00$ ), **2.3a** ( $\delta = 5.91$ ,  $I = 0.09$ ), and **2.3b** ( $\delta = 5.47$ ,  $I = 0.12$ ).



After 42 h, no azide starting material was detected, and the product ratio was diamide : nitro 4.8 : 1.0, based on integrations of the benzylic protons of **2.5a** ( $\delta = 6.08$ ,  $I = 1.00$ ), **2.3a** ( $\delta = 5.91$ ,  $I = 0.09$ ), and **2.3b** ( $\delta = 5.47$ ,  $I = 0.12$ ).

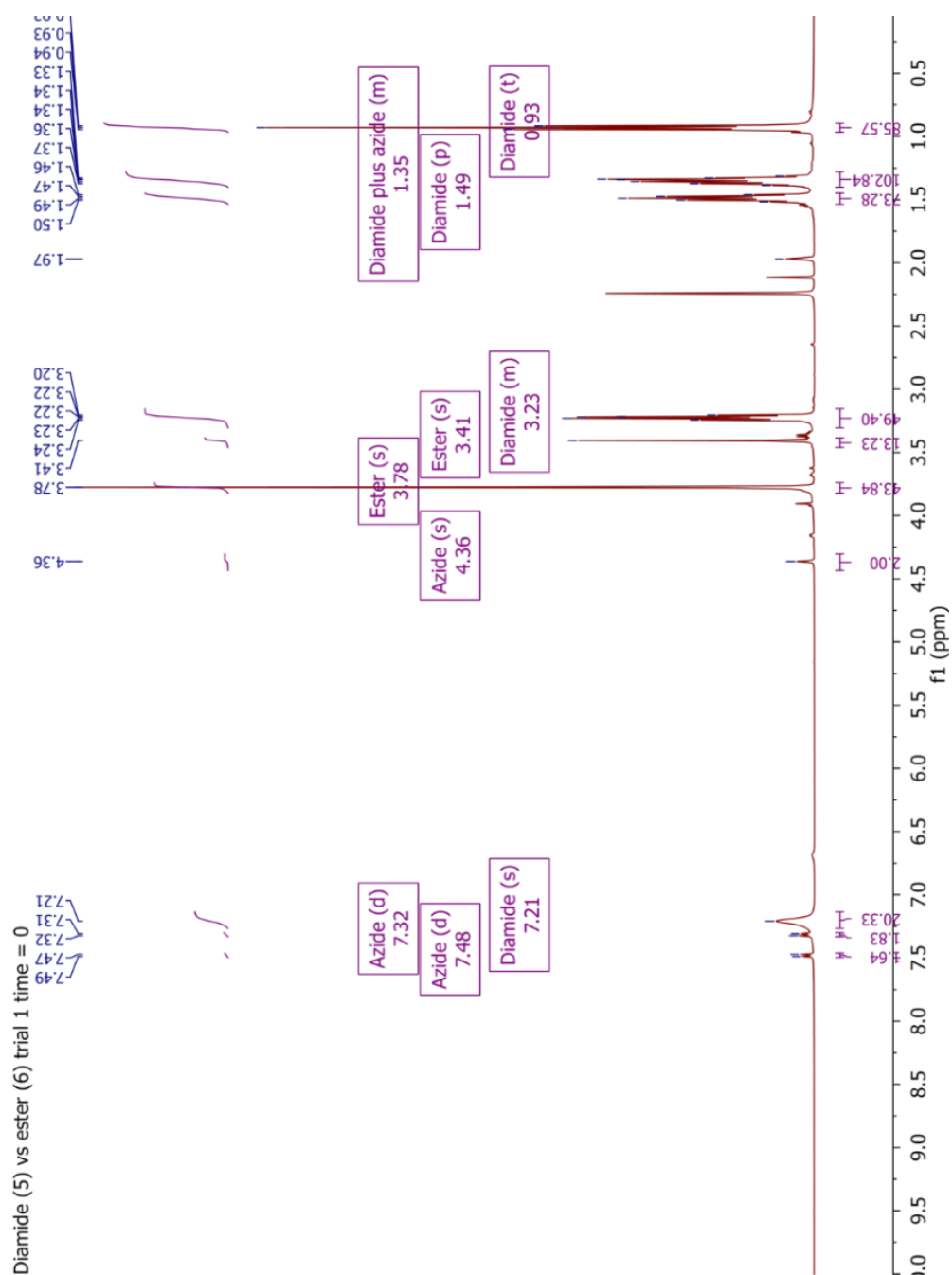


The initial ratio of azide **2.13** : diamide **2.5** : amide **2.4** was 1.0 : 17.0 : 12.4, based on integrations of azide  $\text{CH}_2\text{Ar}$  ( $\delta = 4.35$ ,  $I = 2.00$ ), diamide and amide  $\text{CH}_2\text{NH}$  ( $\delta = 3.21$ ,  $I = 92.76$ ), and amide  $\text{CCH}$  ( $\delta = 3.16$ ,  $I = 12.38$ ). Overlap was resolved by subtracting 2x the amide  $\text{CCH}$  peak from the combined  $\text{CH}_2\text{NH}$  peak.

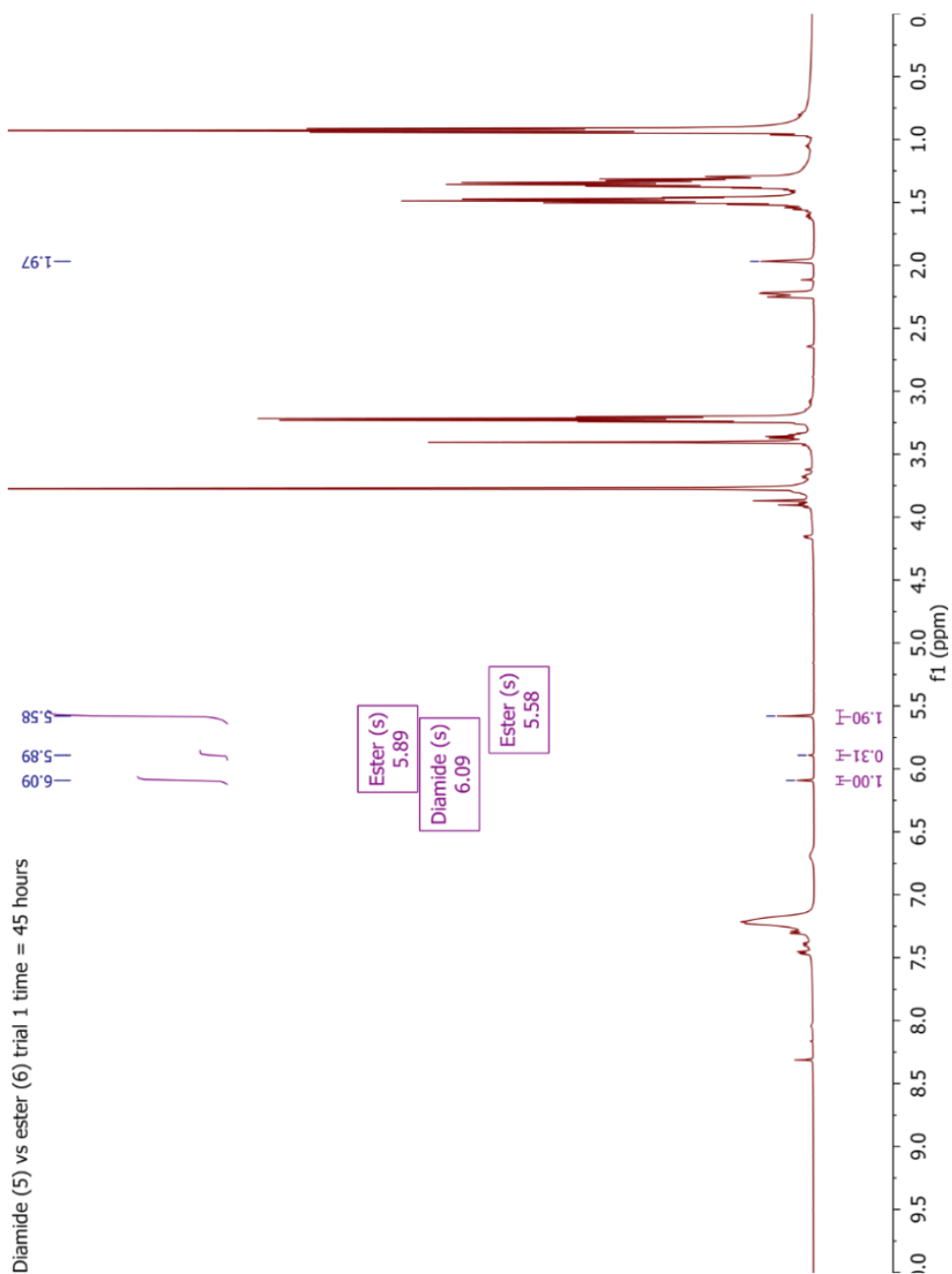


The ratio of products was diamide : amide 2.3 : 1.0, based on integrations of the benzylic protons of **2.4a** ( $\delta = 5.56$ ,  $I = 0.31$ ), **2.4b** ( $\delta = 5.89$ ,  $I = 0.13$ ), and **2.5a** ( $\delta = 6.08$ ,  $I = 1.00$ ). After dividing by the initial concentrations, the rate ratio was diamide : amide 1.7 : 1.0.

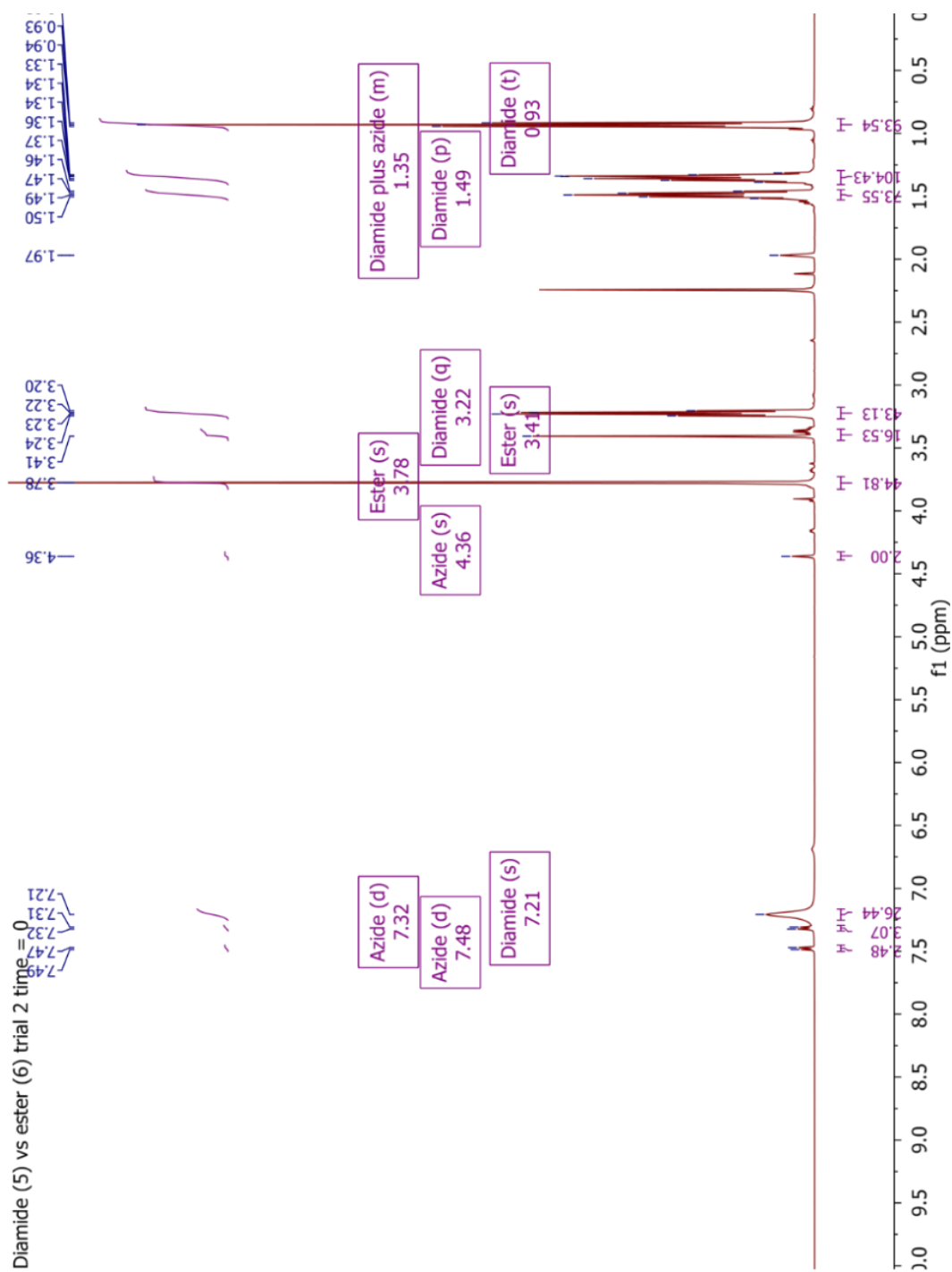




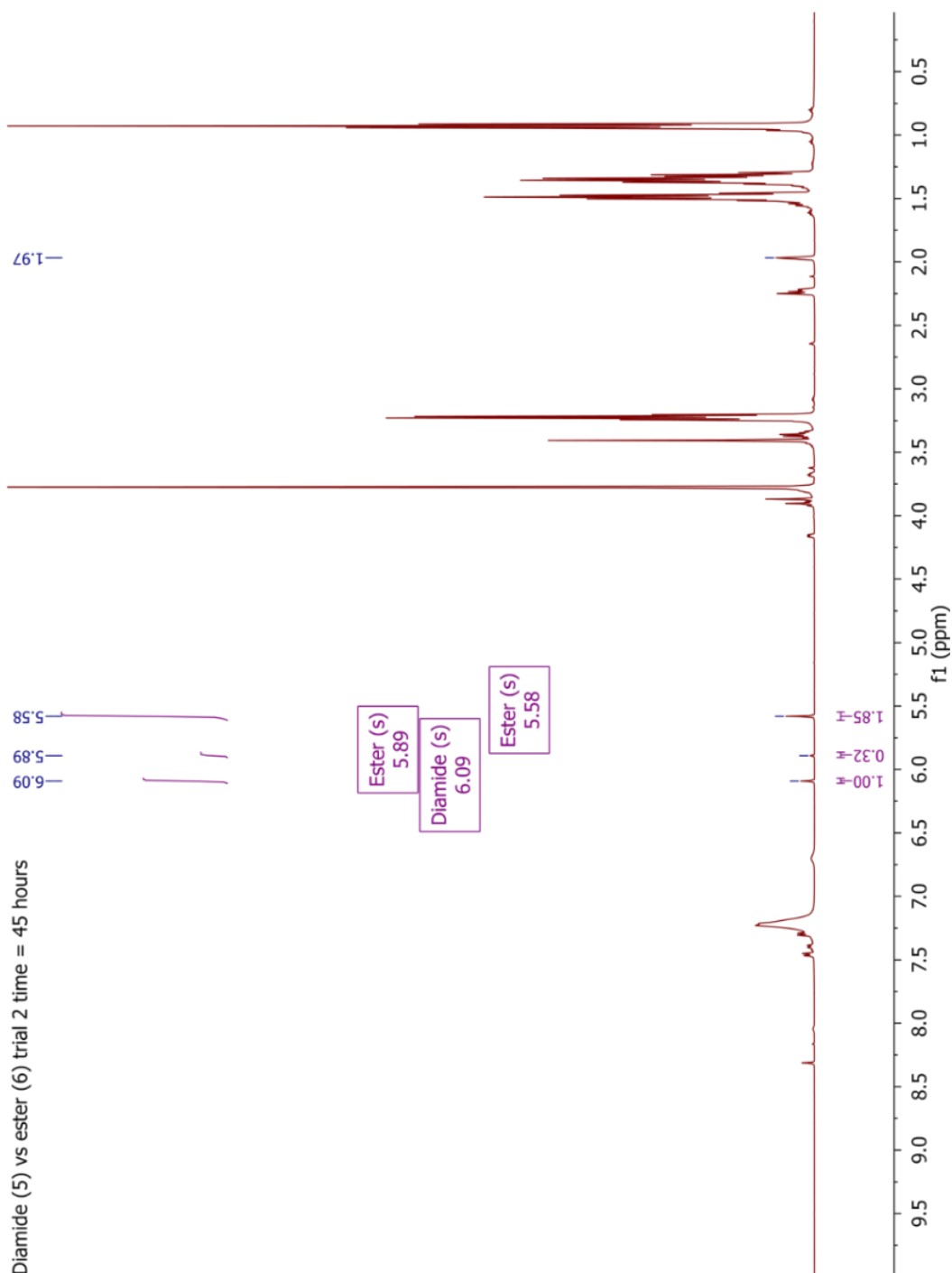
The initial ratio of azide **2.13** : ester **2.6** : diamide **2.5** was 1.0 : 14.6 : 12.4, based on integrations of azide  $\text{CH}_2\text{Ar}$  ( $\delta = 4.36$ ,  $I = 2.00$ ), ester  $\text{OCH}_3$  ( $\delta = 3.78$ ,  $I = 43.84$ ), and diamide  $\text{CH}_2\text{NH}$  ( $\delta = 3.23$ ,  $I = 49.40$ ).



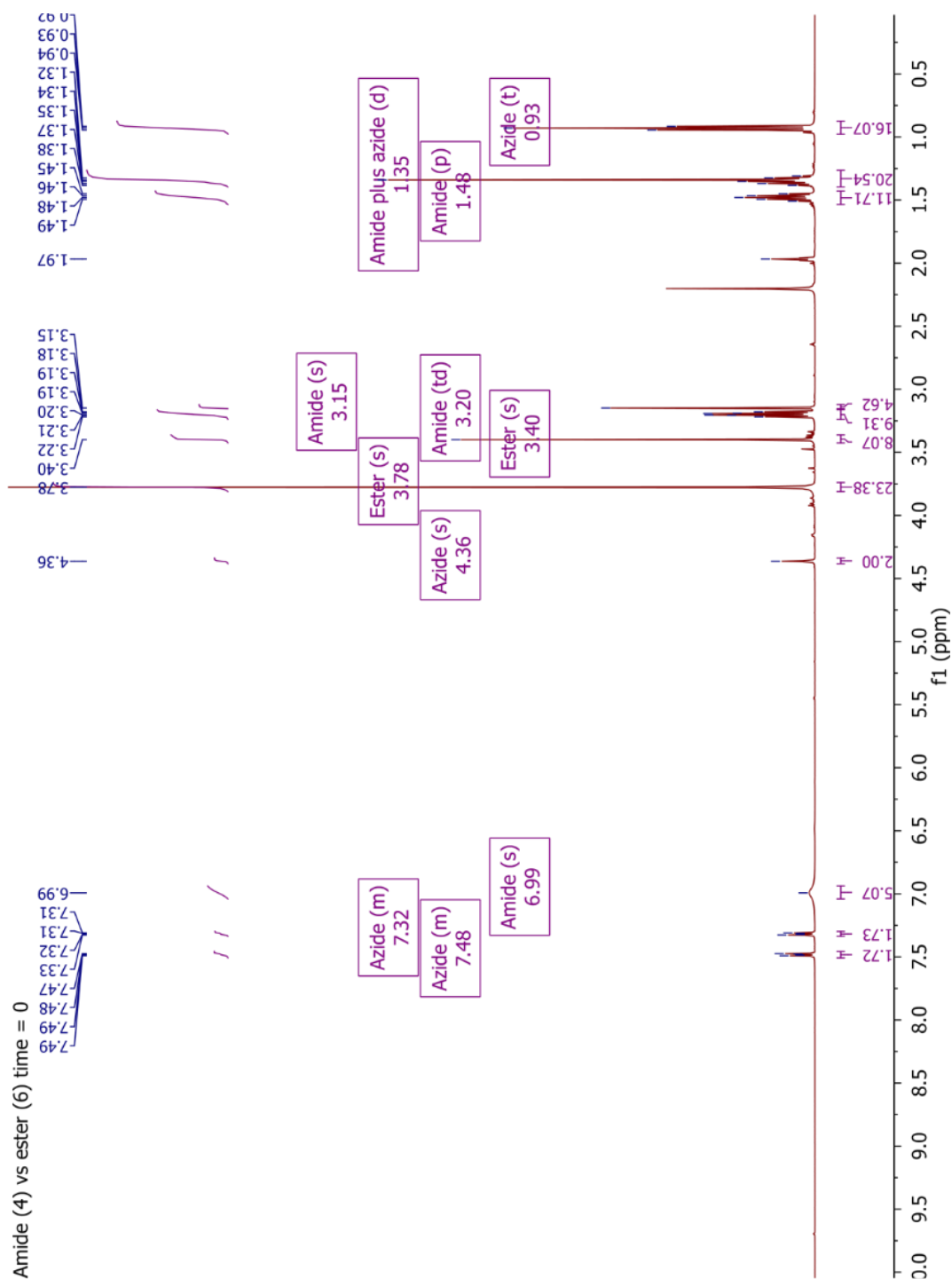
The ratio of products was ester : diamide 2.2 : 1.0, based on integrations of the benzylic protons of **2.5a** ( $\delta = 6.09$ ,  $I = 1.00$ ), **2.6a** ( $\delta = 5.89$ ,  $I = 0.31$ ), and **2.6b** ( $\delta = 5.58$ ,  $I = 1.90$ ). After dividing by the initial concentrations, the rate ratio was ester : diamide 1.9 : 1.0.



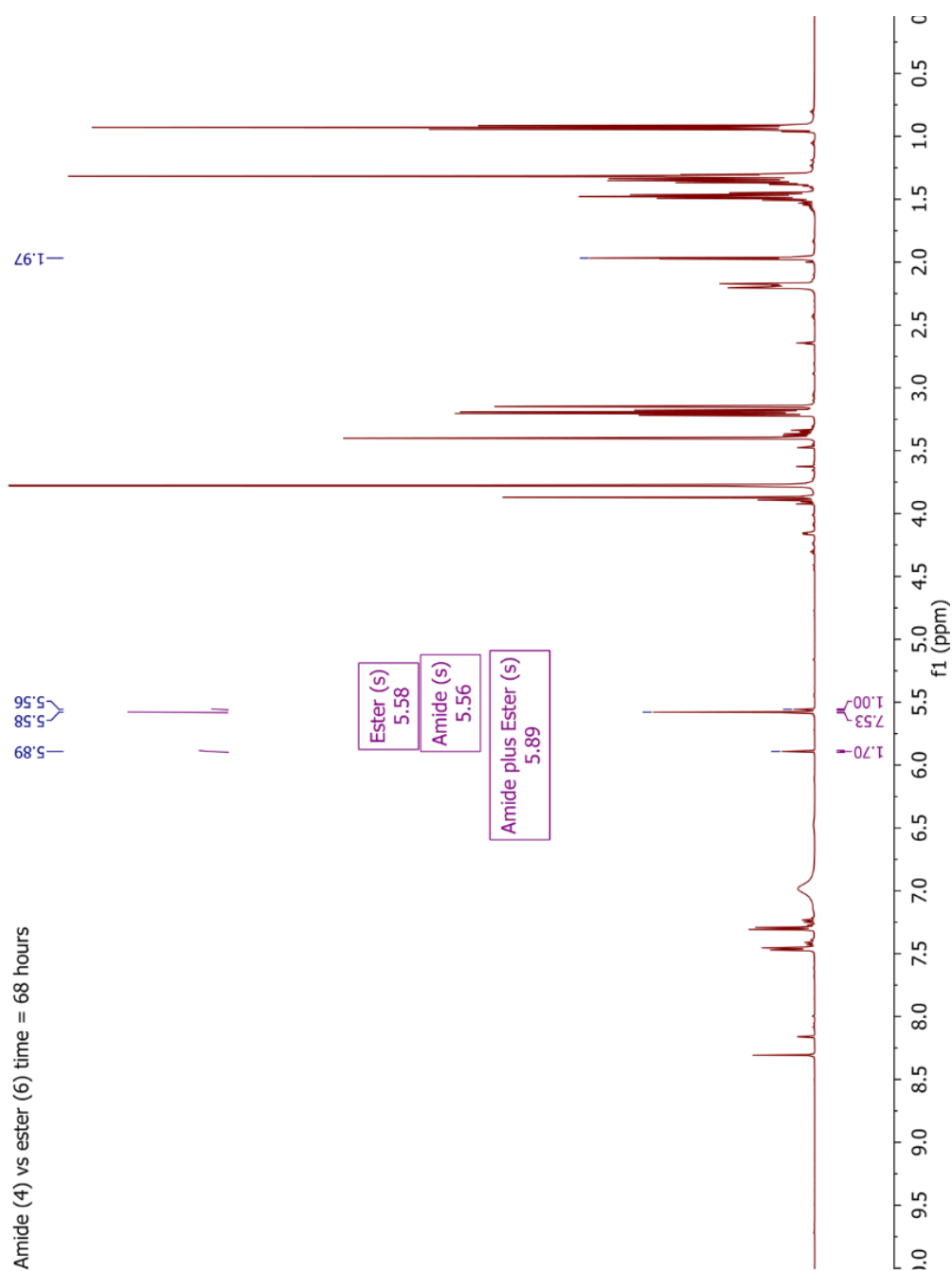
The initial ratio of azide **2.13** : ester **2.6** : diamide **2.5** was 1.0 : 14.9 : 10.8, based on integrations of azide  $\text{CH}_2\text{Ar}$  ( $\delta = 4.36$ ,  $I = 2.00$ ), ester  $\text{OCH}_3$  ( $\delta = 3.78$ ,  $I = 44.81$ ), and diamide  $\text{CH}_2\text{NH}$  ( $\delta = 3.23$ ,  $I = 43.13$ ).



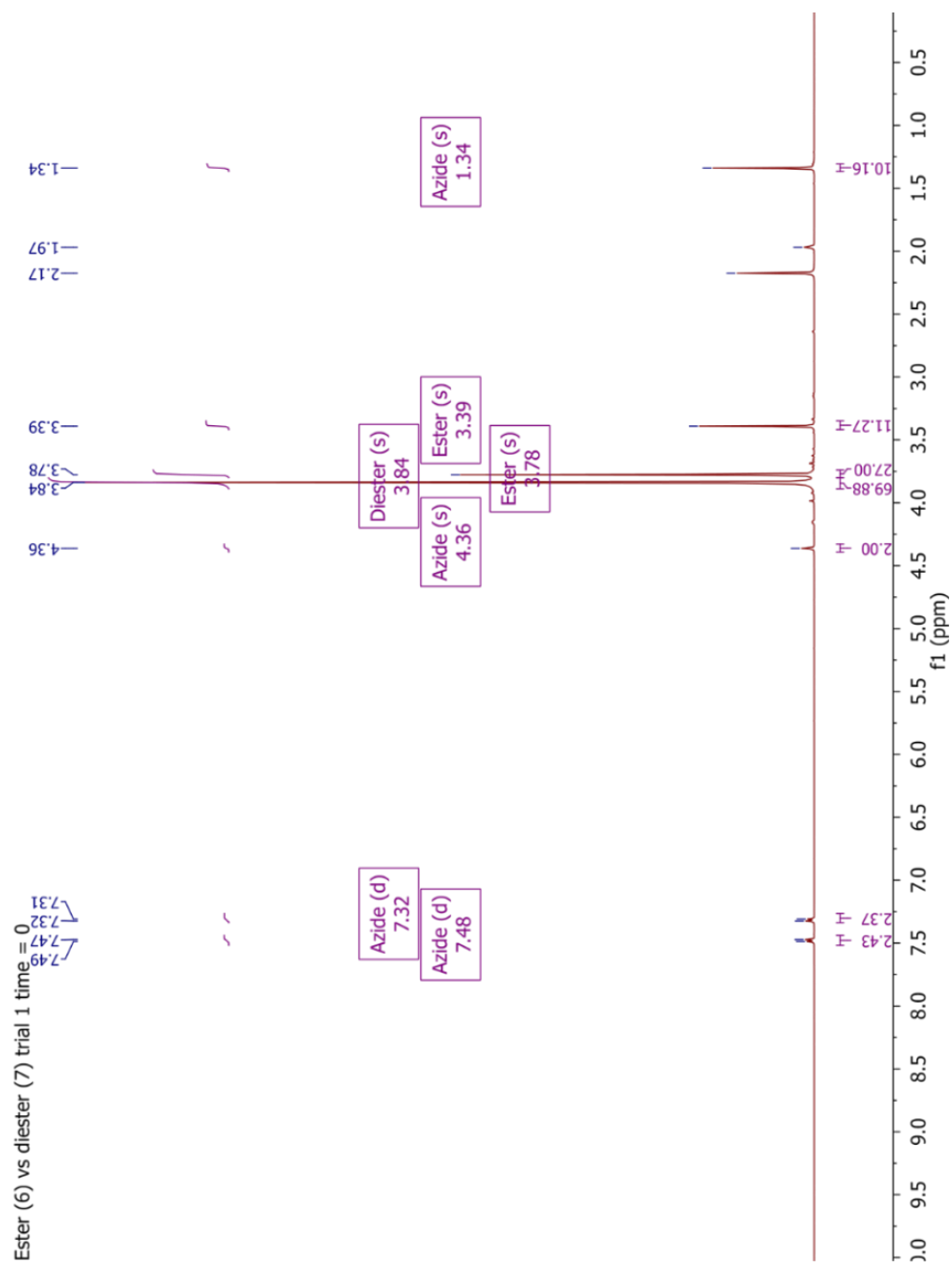
The ratio of products was ester : diamide 2.2 : 1.0, based on integrations of the benzylic protons of **2.5a** ( $\delta = 6.09$ ,  $I = 1.00$ ), **2.6a** ( $\delta = 5.89$ ,  $I = 0.32$ ), and **2.6b** ( $\delta = 5.58$ ,  $I = 1.85$ ). After dividing by the initial concentrations, the rate ratio was ester : diamide 1.6 : 1.0. Averaging the two trials gave ester : diamide 1.7 ( $\pm 0.2$ ) : 1.0.



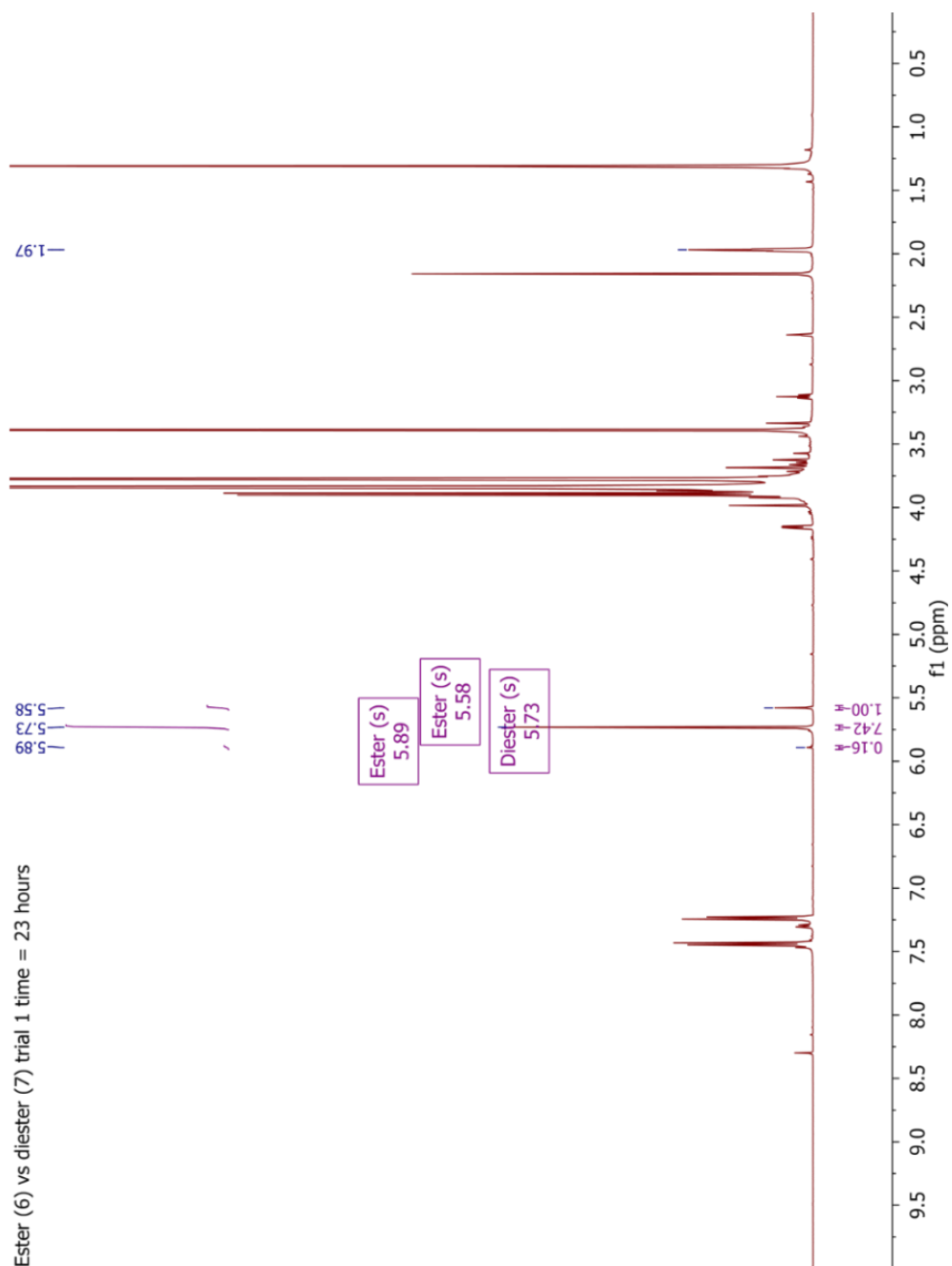
The initial ratio of azide **2.13** : ester **2.6** : amide **2.4** was 1.0 : 7.8 : 4.7, based on integrations of azide  $\text{CH}_2\text{Ar}$  ( $\delta = 4.36$ ,  $I = 2.00$ ), ester  $\text{OCH}_3$  ( $\delta = 3.78$ ,  $I = 23.38$ ), and amide  $\text{CH}_2\text{NH}$  ( $\delta = 3.23$ ,  $I = 9.31$ ).



The ratio of products was ester : diamide 5.9 : 1.0, based on integrations of the benzylic protons of **2.4a** ( $\delta = 5.56$ , I = 1.00), **2.6a** plus **2.4b** ( $\delta = 5.89$ , I = 1.70, overlap), and **2.6b** ( $\delta = 5.58$ , I = 5.89). Overlap was resolved by assuming the ratio of **2.6b** : **2.6a** 1 : 0.16 and **2.4a** : **2.4b** 0.43, which was consistently found in other competitions involving **4** or **6**. After dividing by the initial concentrations, the rate ratio was ester : diamide 3.5 : 1.0.

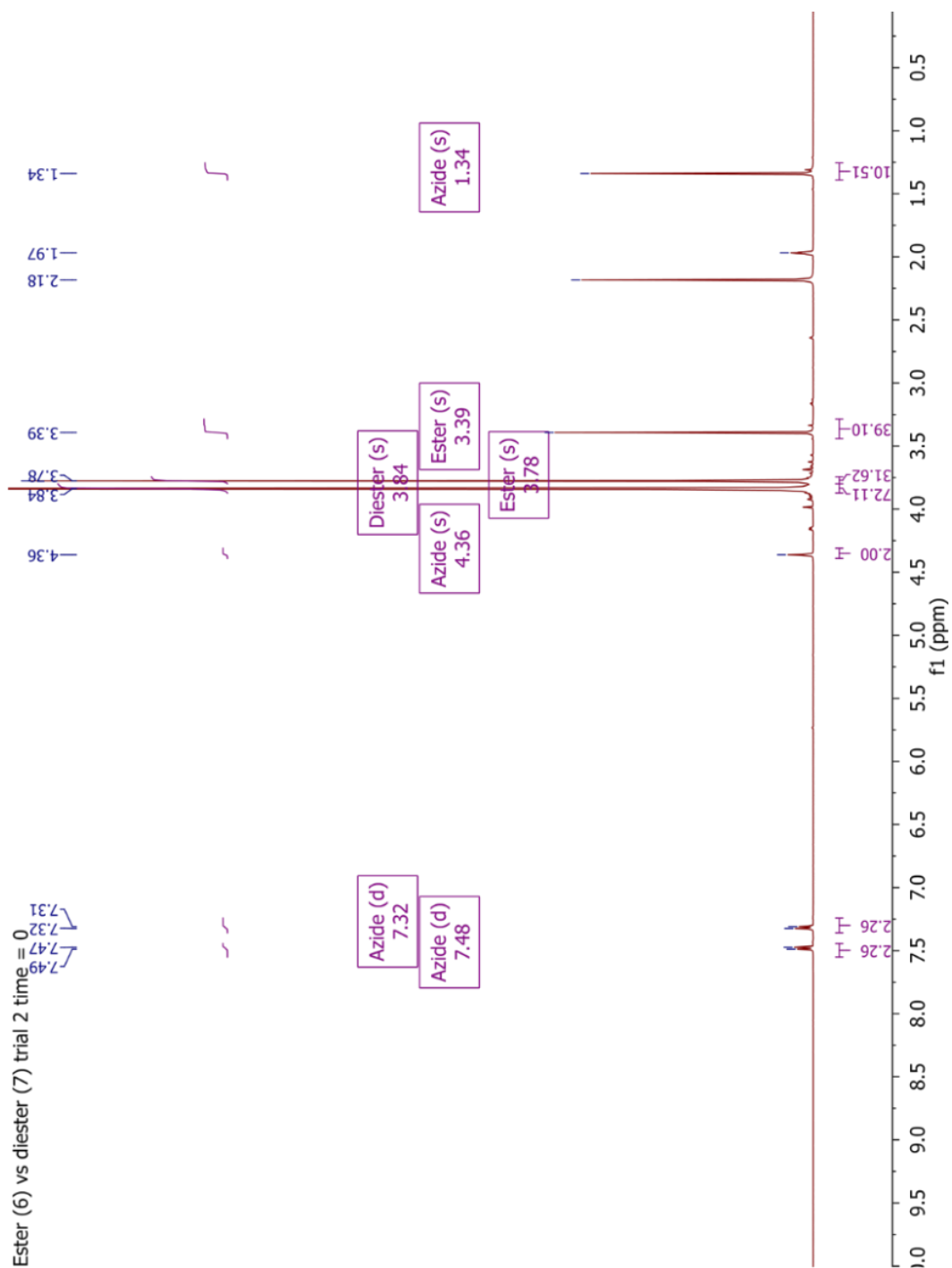


The initial ratio of azide **2.13** : diester **2.7** : ester **2.6** was 1.0 : 11.6 : 9.0, based on integrations of azide  $\text{CH}_2\text{Ar}$  ( $\delta = 4.36$ ,  $I = 2.00$ ), diester  $\text{OCH}_3$  ( $\delta = 3.84$ ,  $I = 69.88$ ), and ester  $\text{OCH}_3$  ( $\delta = 3.78$ ,  $I = 27.00$ ).

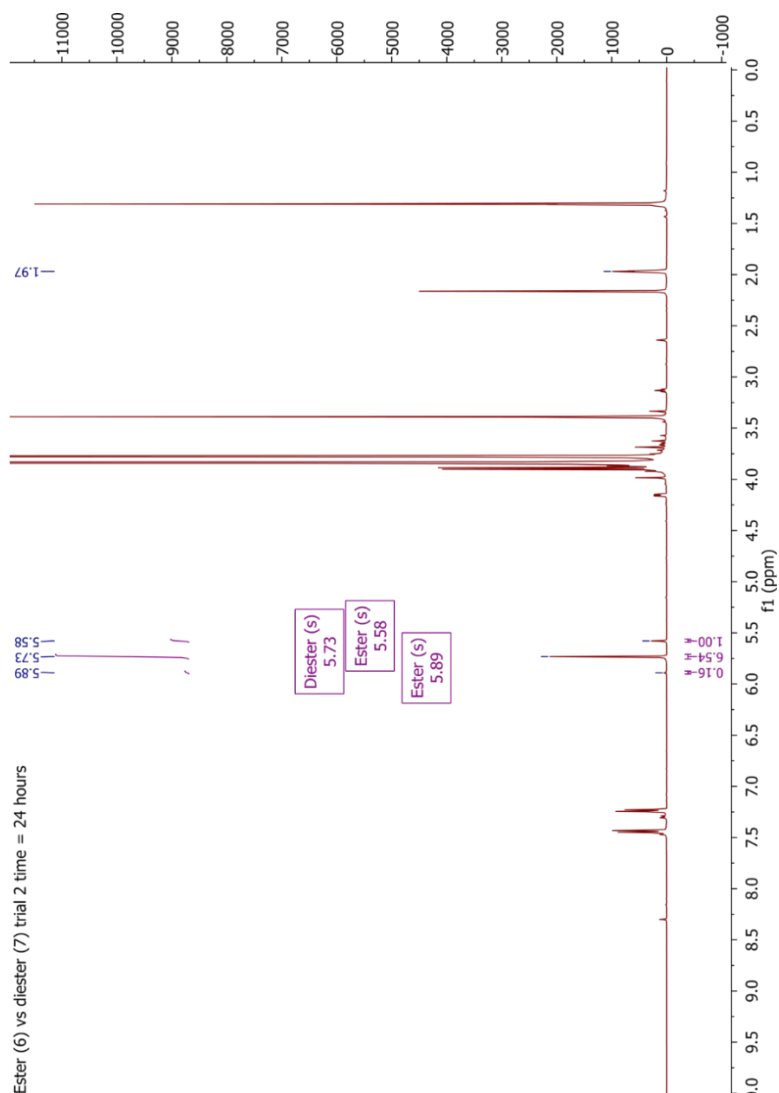


The ratio of products was diester : ester 6.4 : 1.0, based on integrations of the benzylic protons of **2.6a** ( $\delta = 5.89$ ,  $I = 0.16$ ), **2.6b** ( $\delta = 5.58$ ,  $I = 1.00$ ), and **2.7a** ( $\delta = 5.73$ ,  $I = 7.42$ ). After dividing by the starting concentrations, the rate ratio was diester : ester 4.9 : 1.0.

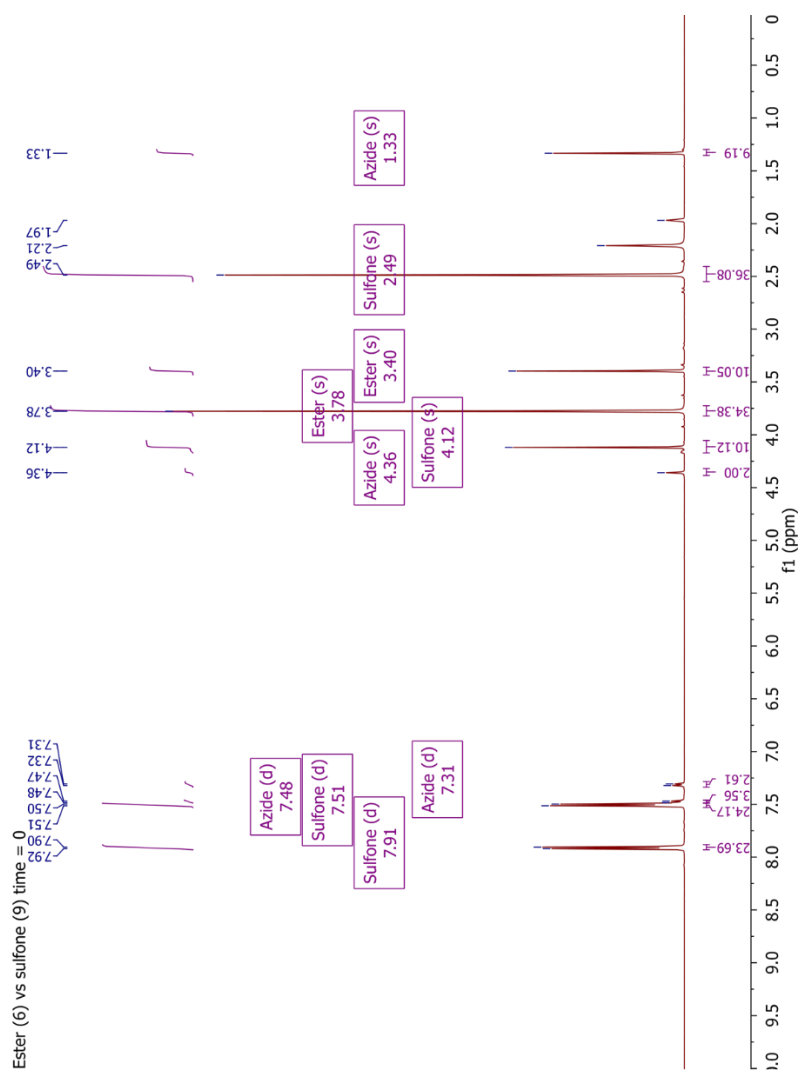




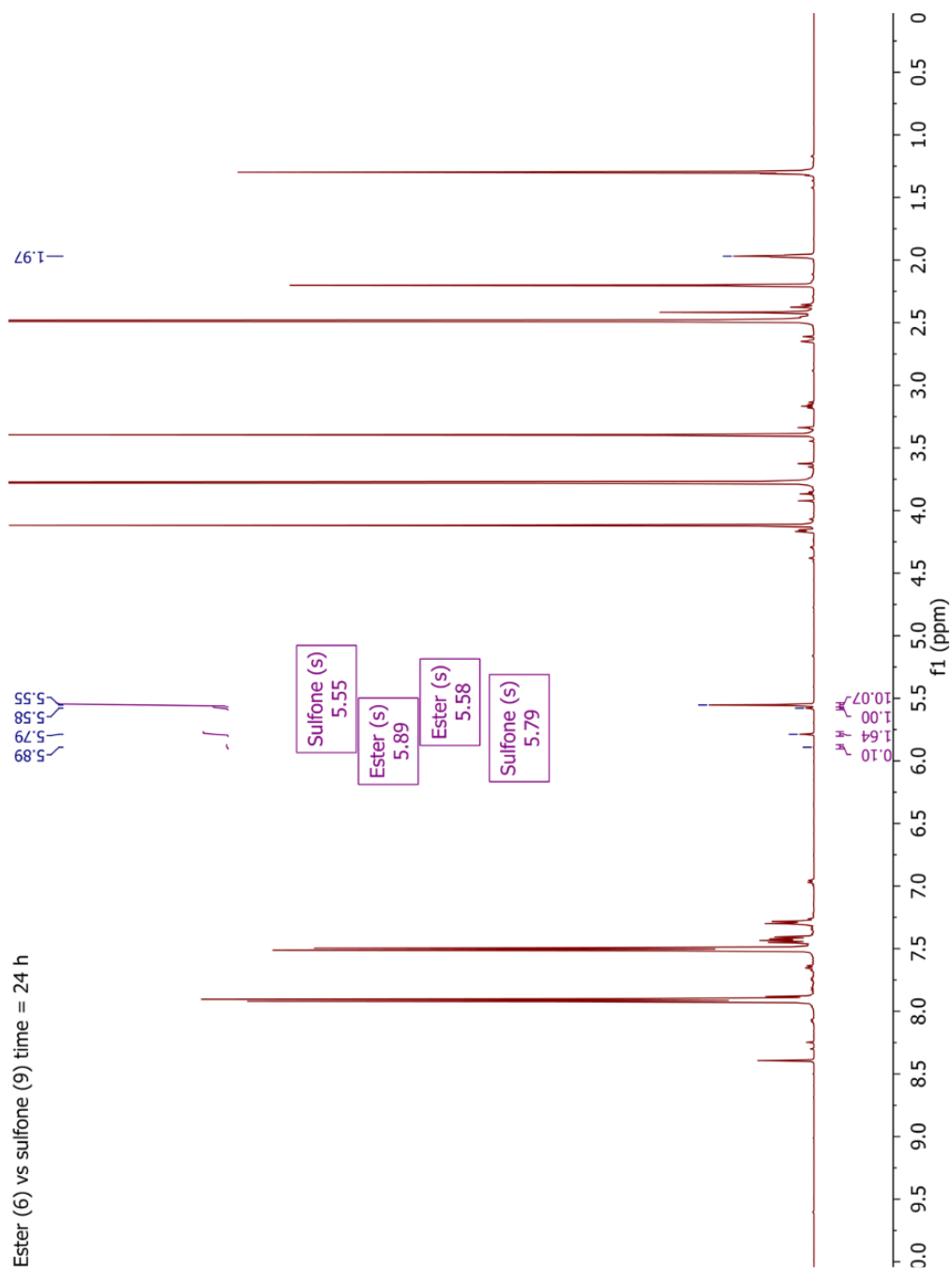
The initial ratio of azide **2.13** : diester **2.7** : ester **2.6** was 1.0 : 12.0 : 10.5, based on integrations of azide  $\text{CH}_2\text{Ar}$  ( $\delta = 4.36$ ,  $I = 2.00$ ), diester  $\text{OCH}_3$  ( $\delta = 3.84$ ,  $I = 72.11$ ), and ester  $\text{OCH}_3$  ( $\delta = 3.78$ ,  $I = 31.62$ ).



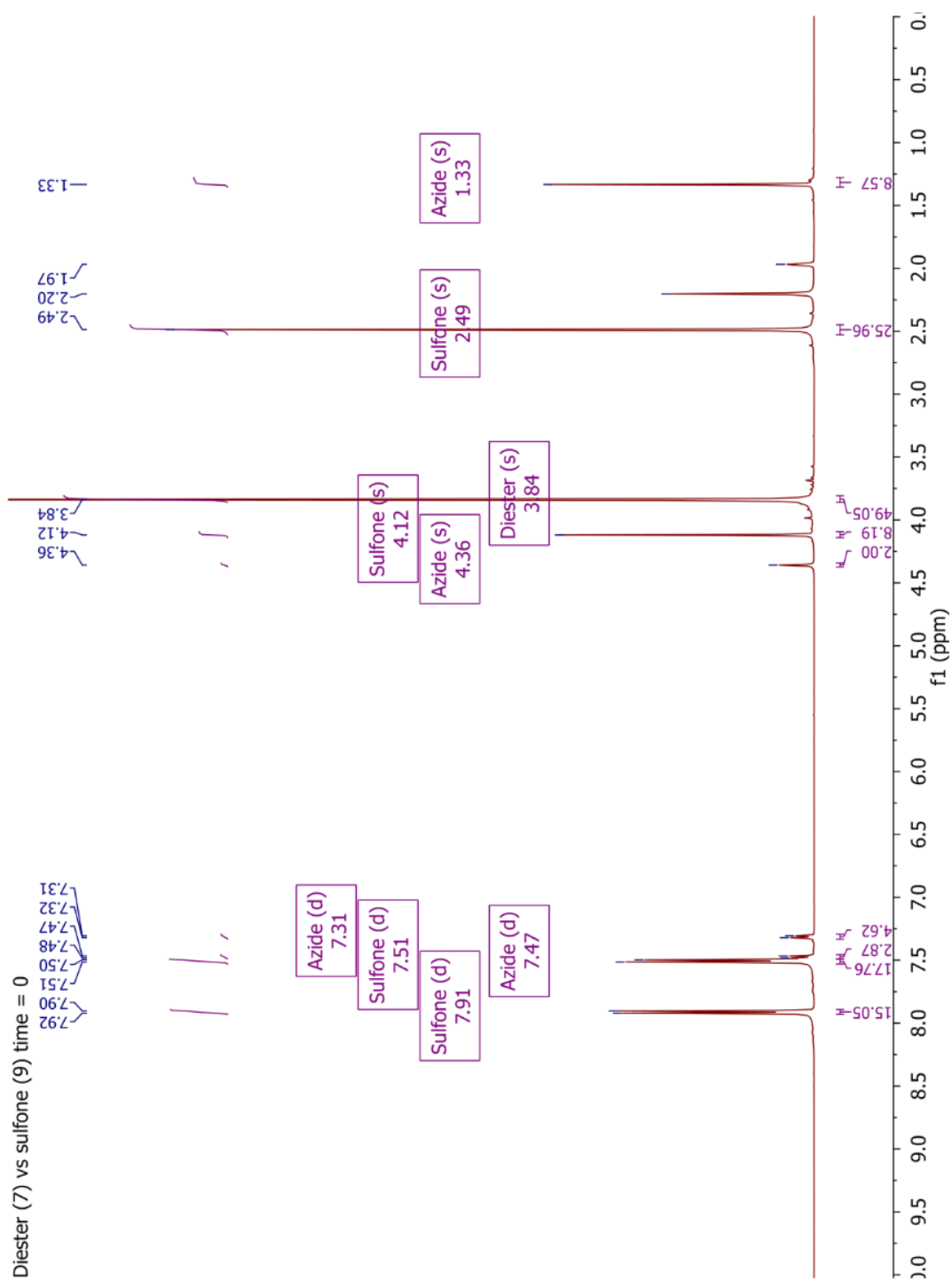
The ratio of products was diester : ester 6.3 : 1.0, based on integrations of the benzylic protons of **2.6a** ( $\delta = 5.89$ ,  $I = 0.16$ ), **2.6b** ( $\delta = 5.58$ ,  $I = 1.00$ ), and **2.7a** ( $\delta = 5.73$ ,  $I = 6.54$ ). After dividing by the starting concentrations, the rate ratio was diester : ester 5.5 : 1.0. Averaging the two trials gave diester : ester 5.2 ( $\pm 0.4$ ) : 1.0.



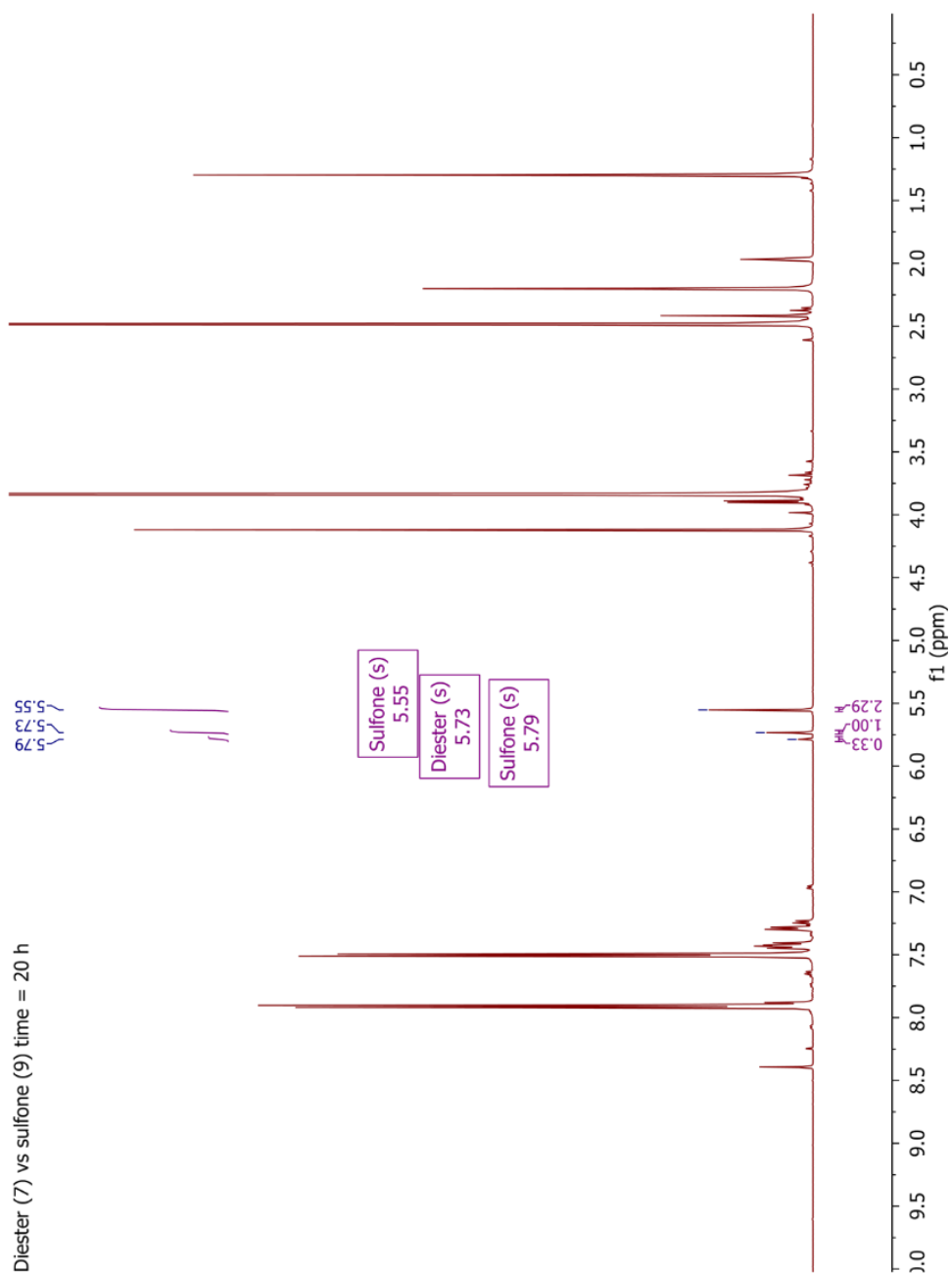
The initial ratio of azide **2.13** : sulfone **2.9** : ester **2.6** was 1.0 : 10.1 : 10.1 , based on integrations of azide  $\text{CH}_2\text{Ar}$  ( $\delta = 4.36$ , I = 2.00), sulfone  $\text{CCH}$  ( $\delta = 4.12$ , I = 10.12), and ester  $\text{CCH}$  ( $\delta = 3.40$ , I = 10.05).



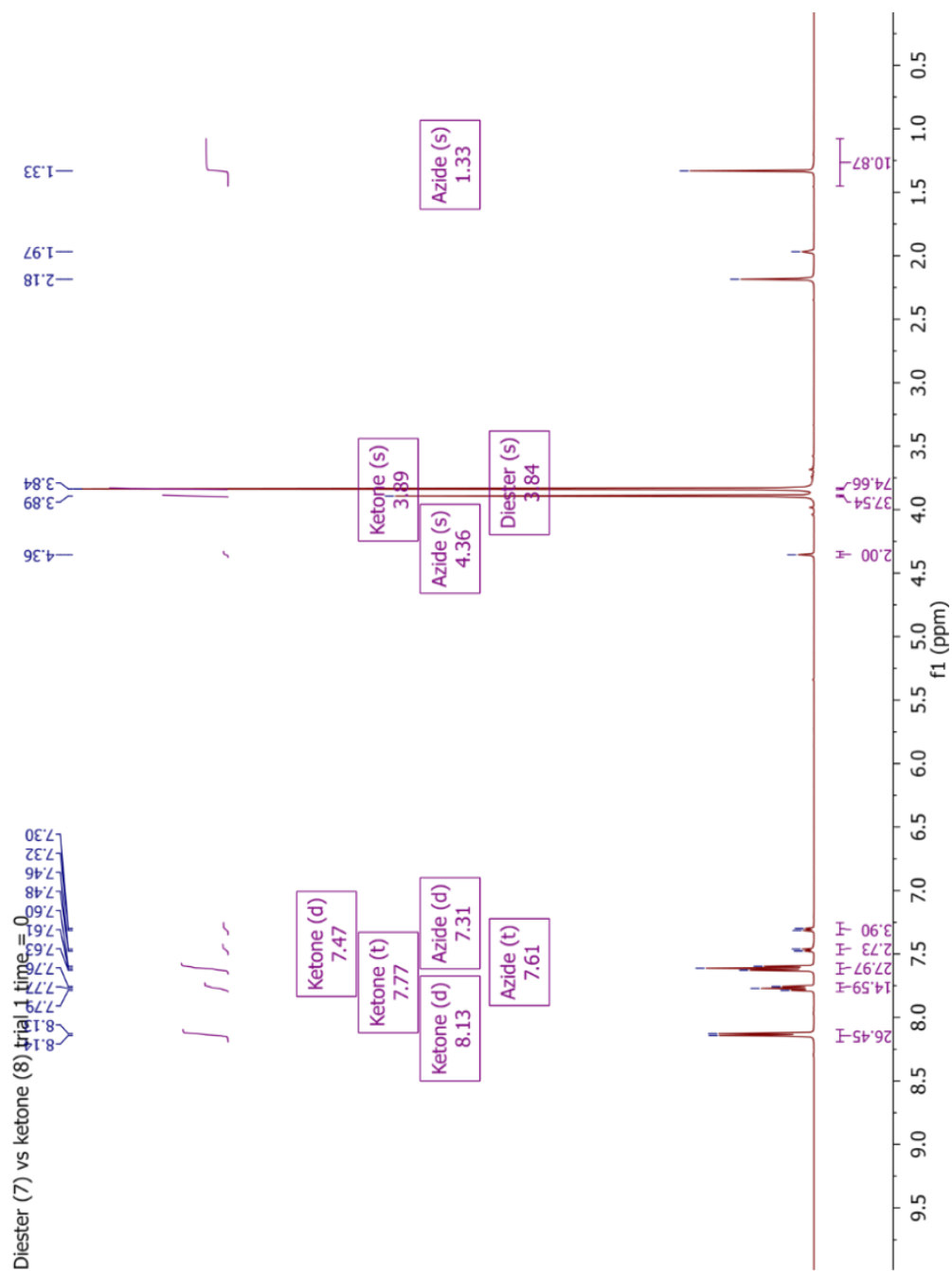
The ratio of products was sulfone : ester 10.6 : 1.0, based on integrations of the benzylic protons of **2.9a** ( $\delta = 5.79$ ,  $I = 1.64$ ), **2.9b** ( $\delta = 5.55$ ,  $I = 10.07$ ), **2.6a** ( $\delta = 5.89$ ,  $I = 0.10$ ), and **2.6b** ( $\delta = 5.58$ ,  $I = 1.00$ ). After dividing by the starting concentrations, the rate ratio was sulfone : ester = 10.6 : 1.0.



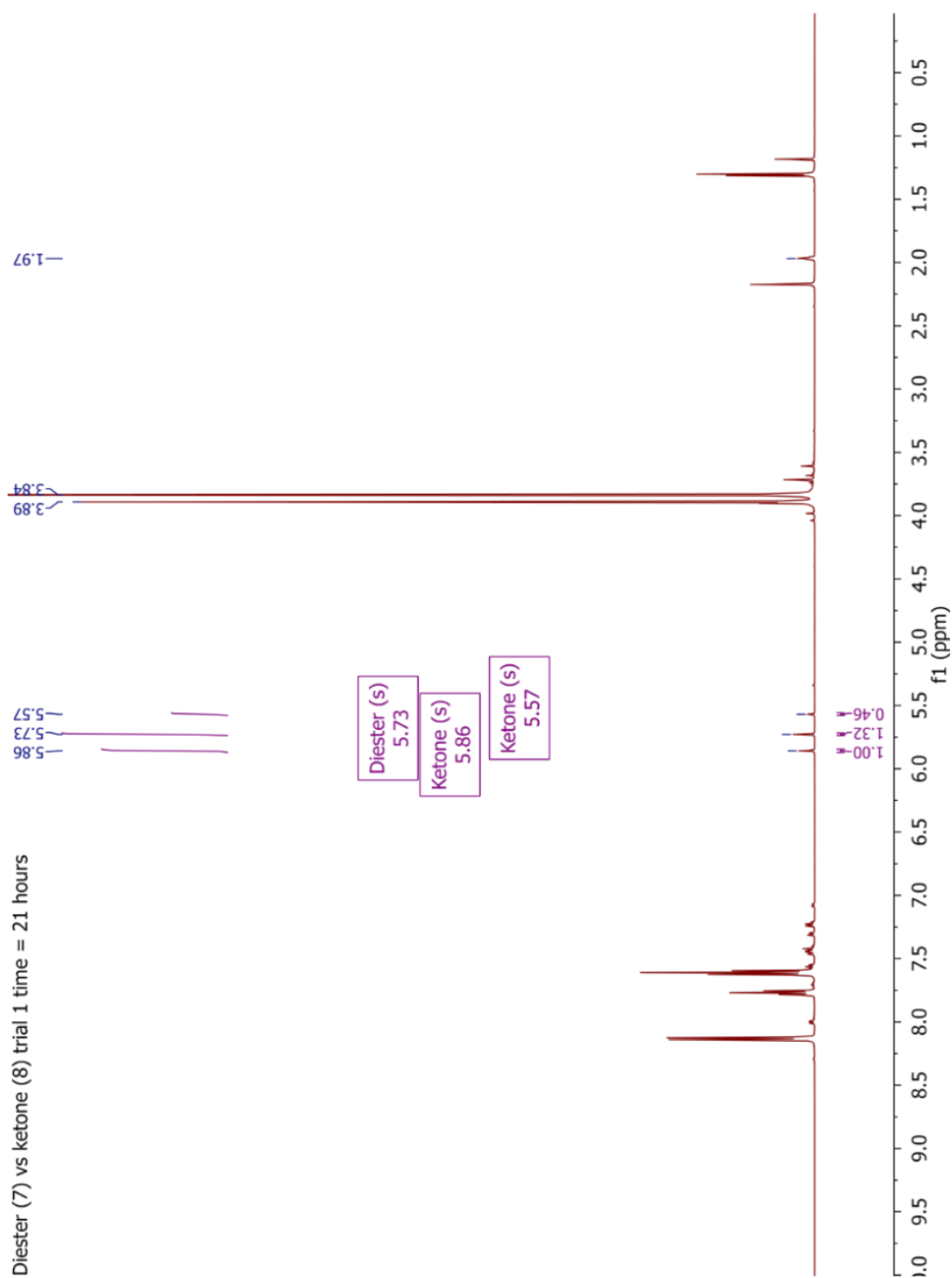
The initial ratio of azide **2.13** : sulfone **2.9** : diester **2.7** was 1 : 8.2 : 8.2, based on integrations of azide  $\text{CH}_2\text{Ar}$  ( $\delta = 4.36$ ,  $I = 2.00$ ), sulfone  $\text{CCH}$  ( $\delta = 4.12$ ,  $I = 8.19$ ), and diester  $\text{OCH}_3$  ( $\delta = 3.84$ ,  $I = 49.05$ ).



The ratio of products was sulfone : diester 2.6 : 1.0, based on integrations of the benzylic protons of **2.9a** ( $\delta = 5.79$ ,  $I = 0.33$ ), **2.9b** ( $\delta = 5.55$ ,  $I = 2.29$ ), and **2.7a** ( $\delta = 5.73$ ,  $I = 1.00$ ). After dividing by the starting concentrations, the rate ratio was sulfone : diester 2.6 : 1.0.

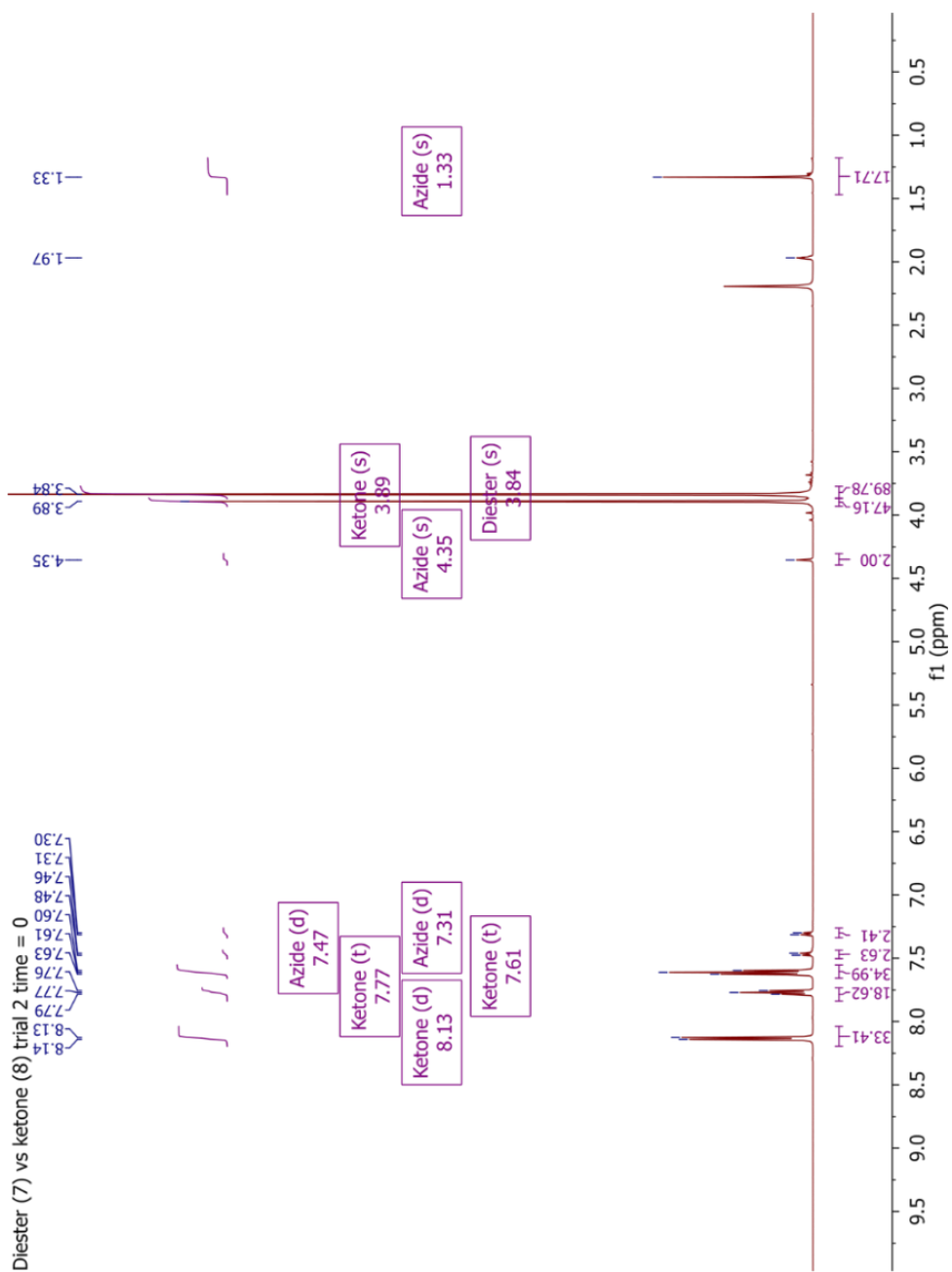


The initial ratio of azide **2.13** : ketone **2.8** : diester **2.7** was 1.0 : 12.5 : 12.4 , based on integrations of azide  $\text{CH}_2\text{Ar}$  ( $\delta = 4.36$ ,  $I = 2.00$ ), ketone  $\text{OCH}_3$  ( $\delta = 3.89$ ,  $I = 37.54$ ), and diester  $\text{OCH}_3$  ( $\delta = 3.84$ ,  $I = 74.66$ ).

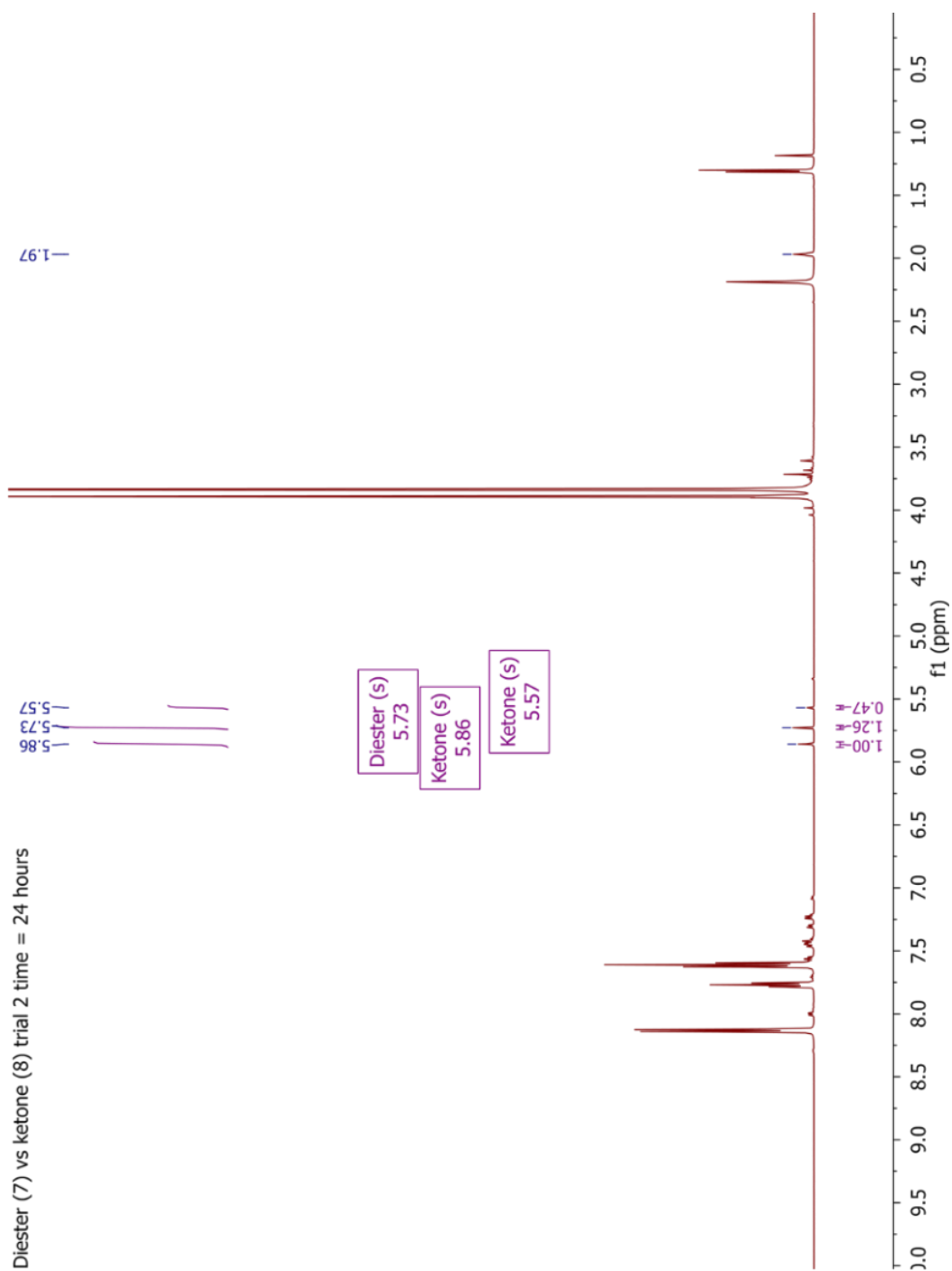


The ratio of products was ketone : diester 1.1 : 1.0, based on integrations of the benzylic protons of **2.7a** ( $\delta = 5.73$ ,  $I = 1.32$ ), **2.8b** ( $\delta = 5.86$ ,  $I = 1.00$ ), and **2.8a** ( $\delta = 5.57$ ,  $I = 0.46$ ). After dividing by the initial concentrations, the rate ratio was ketone : diester 1.1 : 1.0.

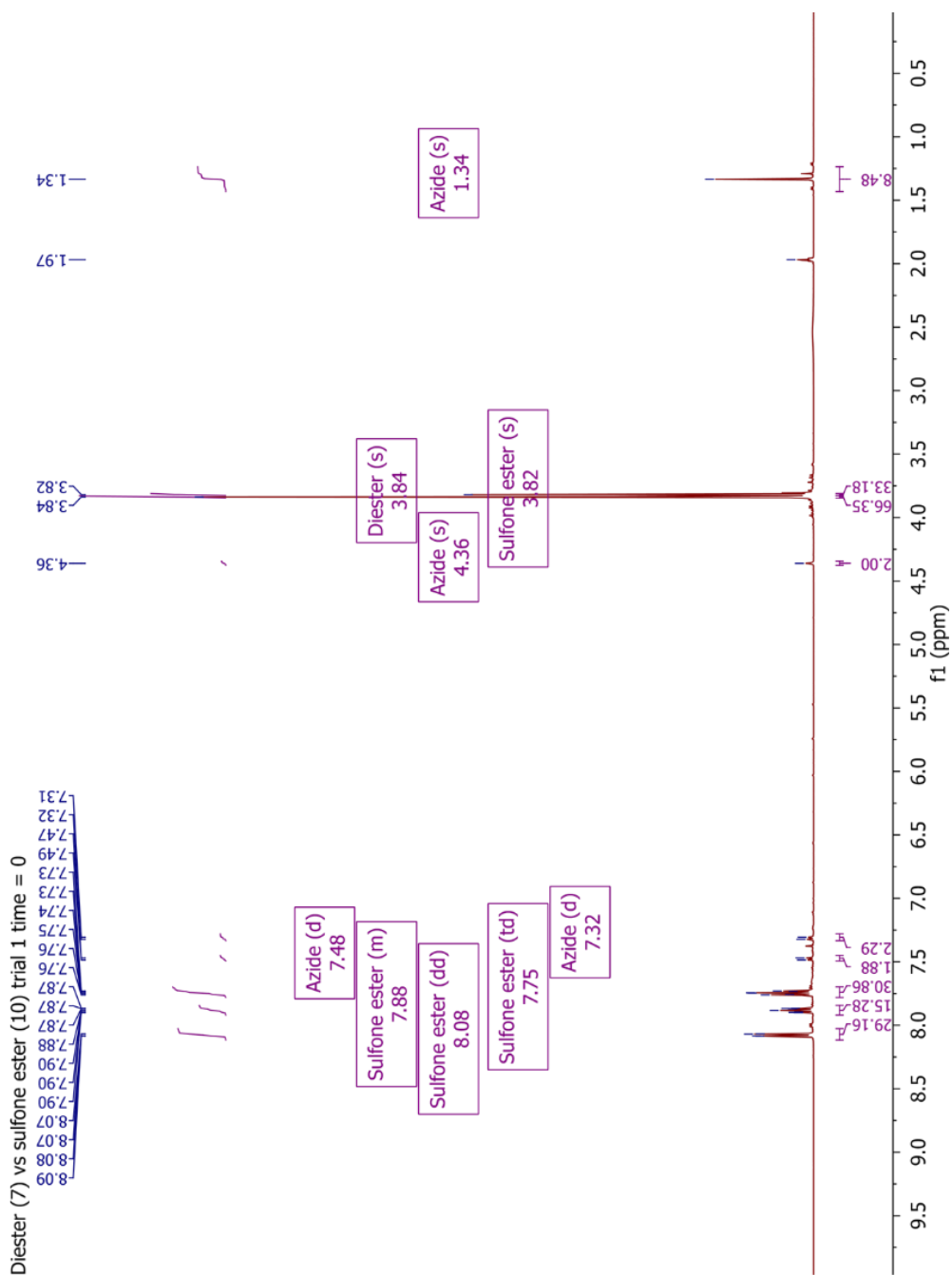




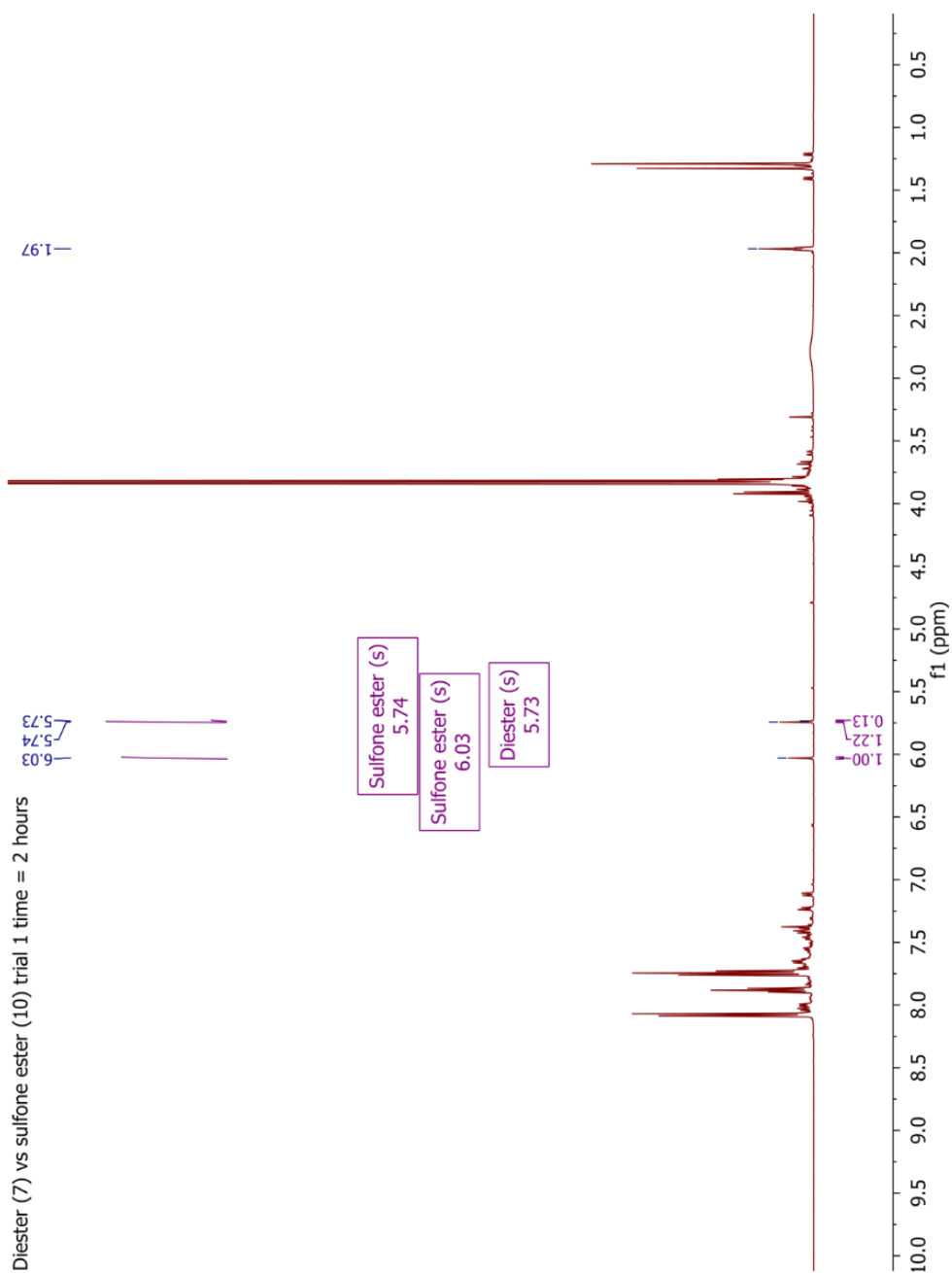
The initial ratio of azide **2.13** : ketone **2.8** : diester **2.7** was 1.0 : 15.7 : 15.0 , based on integrations of azide  $\text{CH}_2\text{Ar}$  ( $\delta = 4.36$ ,  $I = 2.00$ ), ketone  $\text{OCH}_3$  ( $\delta = 3.89$ ,  $I = 47.16$ ), and diester  $\text{OCH}_3$  ( $\delta = 3.84$ ,  $I = 89.88$ ).



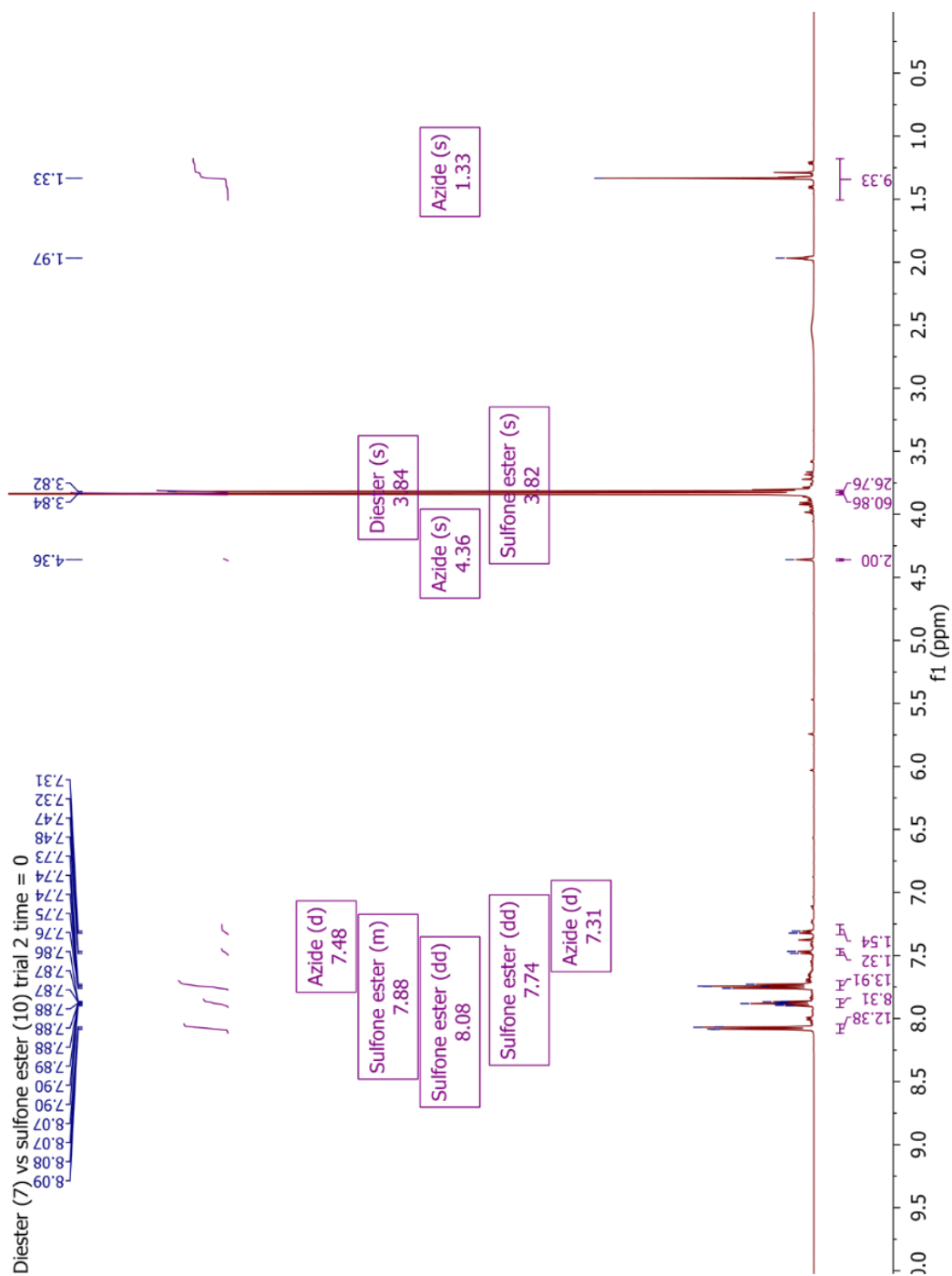
The ratio of products was ketone : diester 1.2 : 1.0, based on integrations of the benzylic protons of **2.7a** ( $\delta = 5.73$ ,  $I = 1.26$ ), **2.8b** ( $\delta = 5.86$ ,  $I = 1.00$ ), and **2.8a** ( $\delta = 5.57$ ,  $I = 0.47$ ). After dividing by the initial concentrations, the rate ratio was ketone : diester 1.1 : 1.0. Averaging the two trials gave ketone : diester 1.11 ( $\pm 0.01$ ) : 1.00.



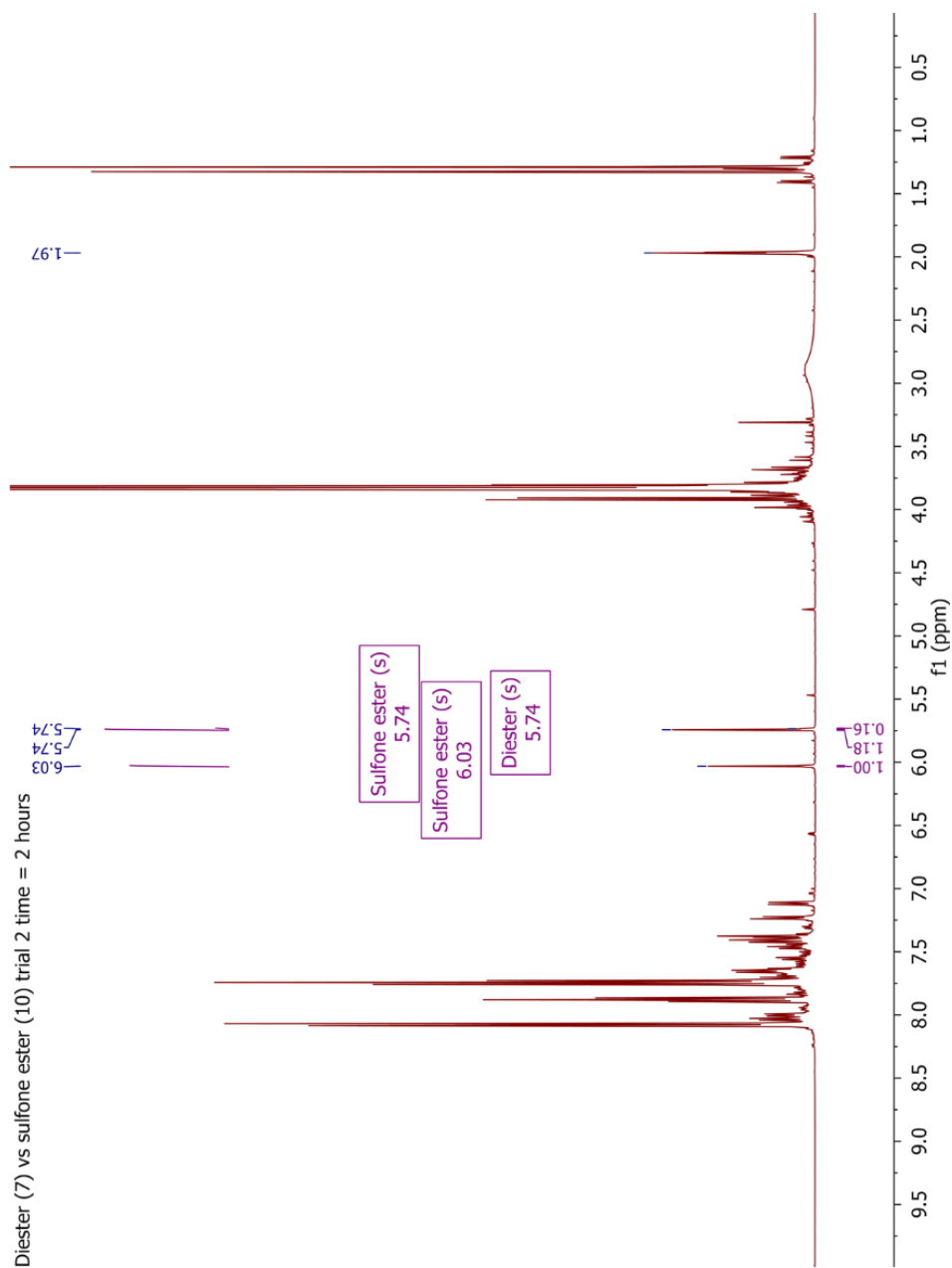
The initial ratio of azide **2.13** : sulfone ester **2.10** : diester **2.7** was 1.0 : 11.1 : 11.1, based on integrations of azide  $\text{CH}_2\text{Ar}$  ( $\delta = 4.36$ ,  $I = 2.00$ ), sulfone ester  $\text{OCH}_3$  ( $\delta = 3.89$ ,  $I = 33.18$ ), and diester  $\text{OCH}_3$  ( $\delta = 3.78$ ,  $I = 66.35$ ).



The ratio of products was sulfone ester : diester 17.2 : 1.0, based on integrations of the benzylic protons of **2.7a** ( $\delta = 5.74$ ,  $I = 0.13$ ), **2.10b** ( $\delta = 5.74$ ,  $I = 1.22$ ), and **2.10a** ( $\delta = 6.03$ ,  $I = 1.00$ ). After dividing by the initial concentrations, the rate ratio was sulfone ester : diester 17.2 : 1.0.

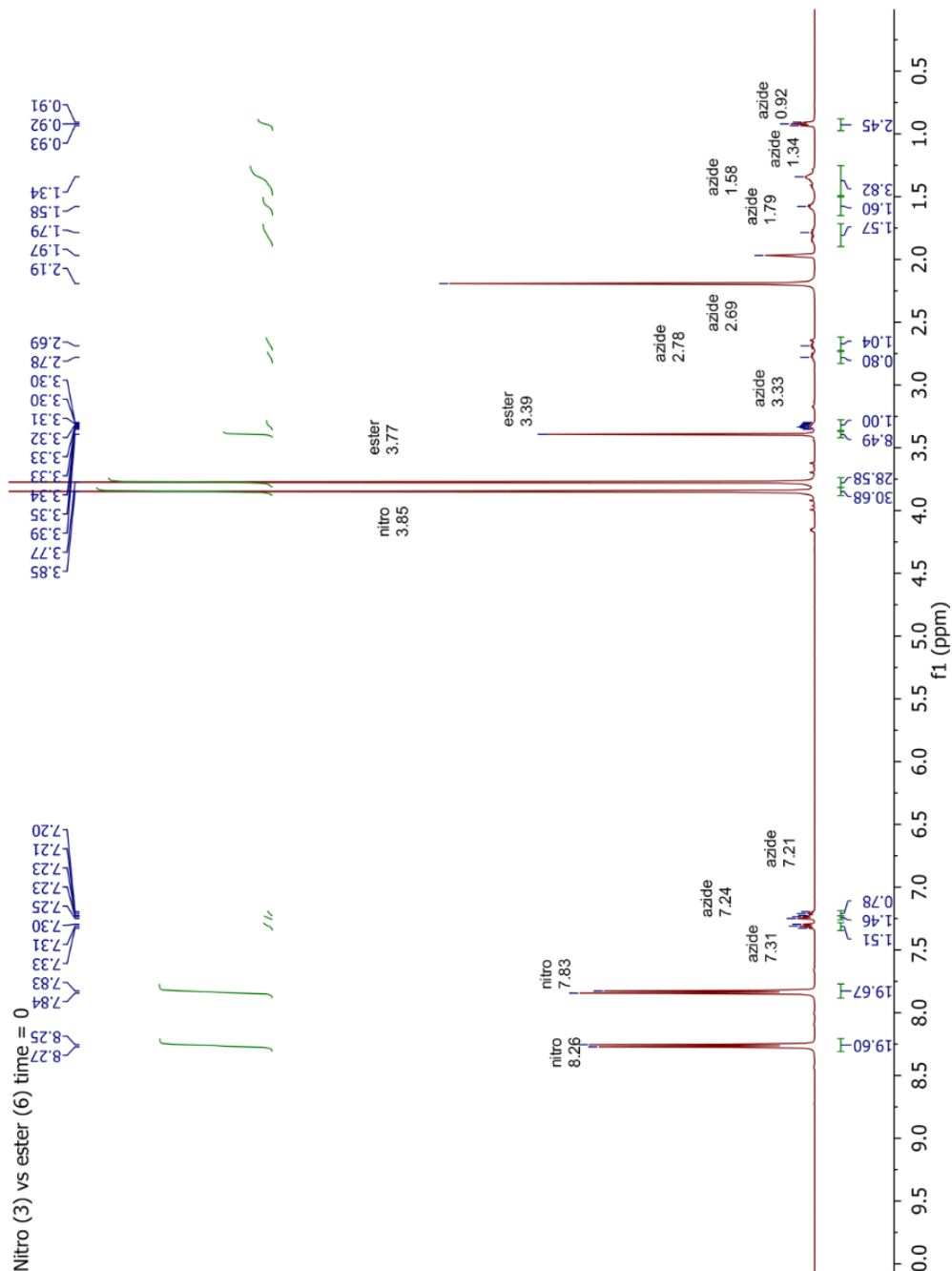


The initial ratio of azide **2.13** : sulfone ester **2.10** : diester **2.7** was 1.0 : 8.9 : 10.1, based on integrations of azide  $\text{CH}_2\text{Ar}$  ( $\delta = 4.36$ ,  $I = 2.00$ ), sulfone ester  $\text{OCH}_3$  ( $\delta = 3.89$ ,  $I = 26.76$ ), and diester  $\text{OCH}_3$  ( $\delta = 3.78$ ,  $I = 60.86$ ).

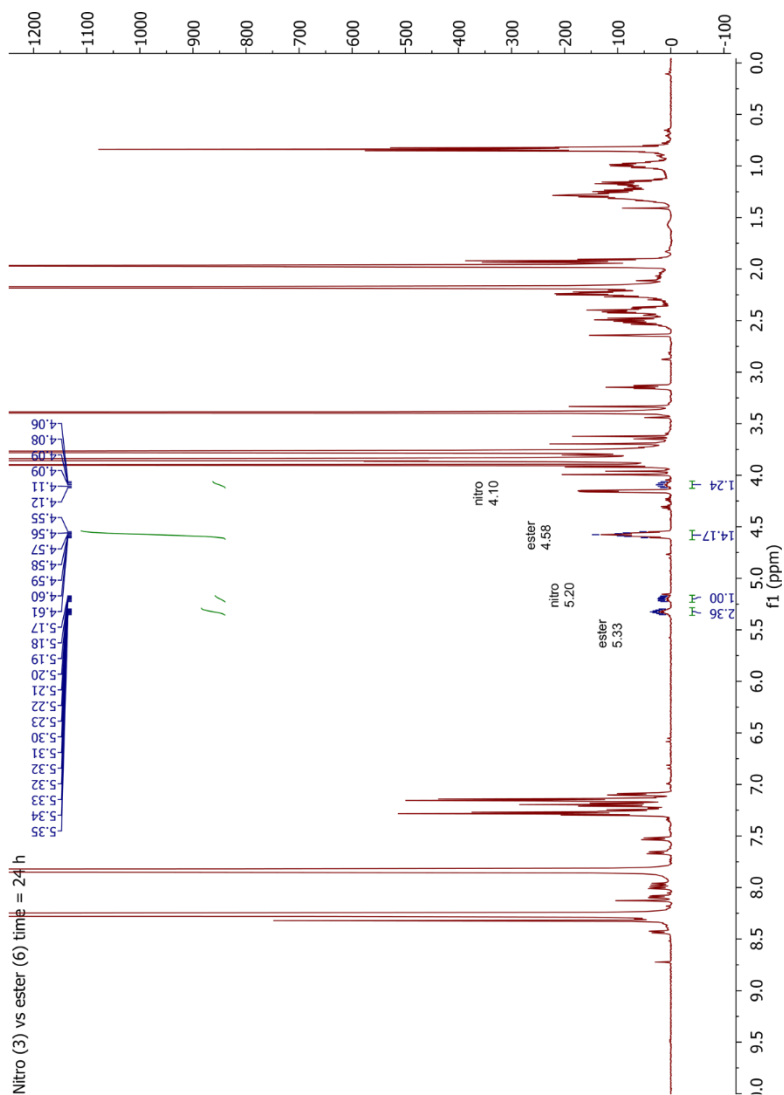


The ratio of products was sulfone ester : diester 13.6 : 1.0, based on integrations of the benzylic protons of **2.7a** ( $\delta = 5.74$ ,  $I = 0.16$ ), **2.10b** ( $\delta = 5.74$ ,  $I = 1.18$ ), and **2.10a** ( $\delta = 6.03$ ,  $I = 1.00$ ). After dividing by the initial concentrations, the rate ratio was sulfone ester : diester 15.5 : 1.0. Averaging the two trials gave sulfone ester : diester 16 ( $\pm 1$ ) : 1.0

## Competition Experiments with 3-azido-1-phenylheptane

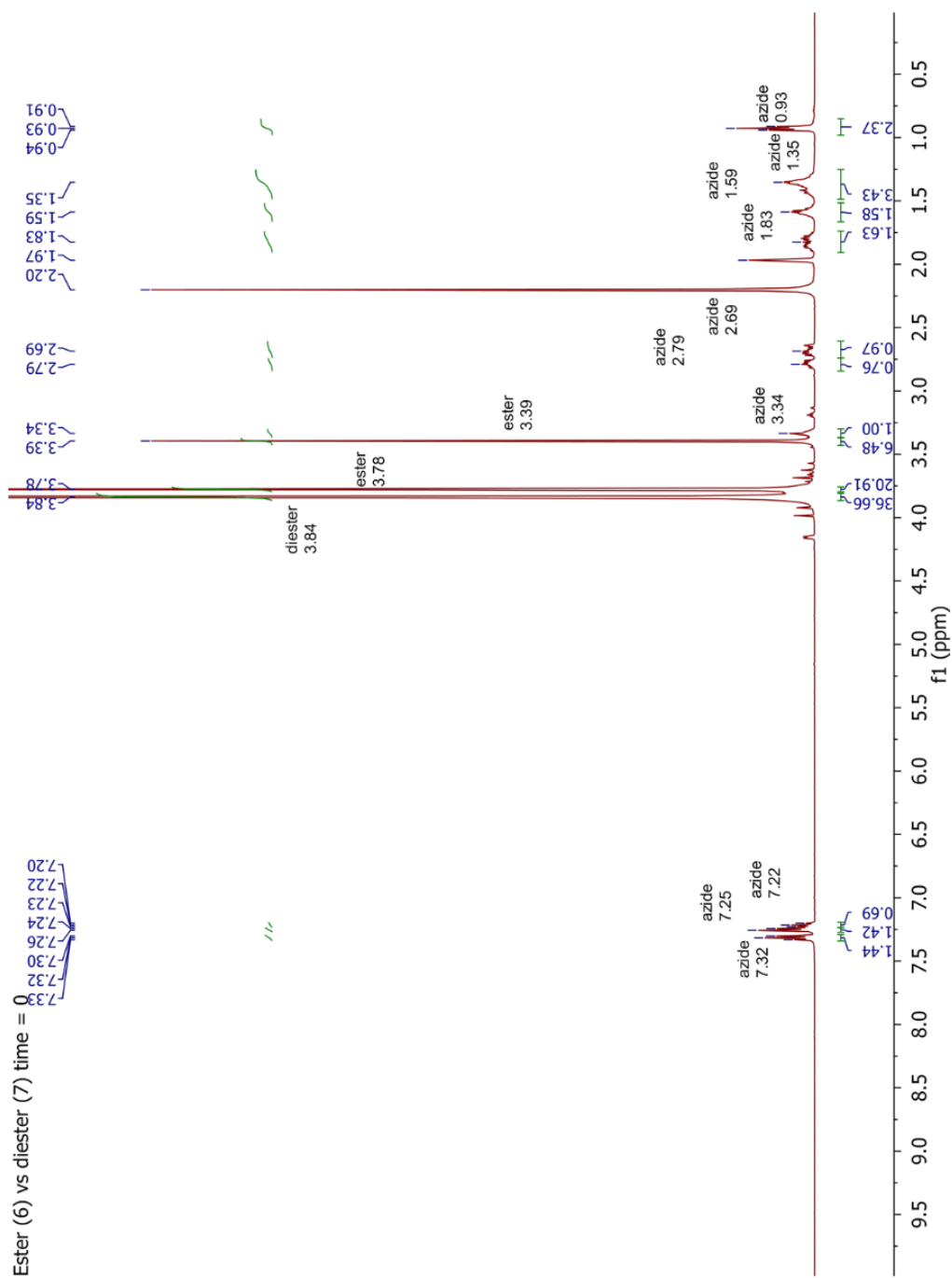


The initial ratio of azide **2.16** : ester **2.6** : nitro **2.3** was 1 : 9.5 : 10.2, based on integrations of azide  $\text{CHN}_3$  ( $\delta = 3.33$ ,  $I = 1.00$ ), ester  $\text{OCH}_3$  ( $\delta = 3.77$ ,  $I = 28.58$ ), and nitro  $\text{OCH}_3$  ( $\delta = 3.85$ ,  $I = 30.68$ ).

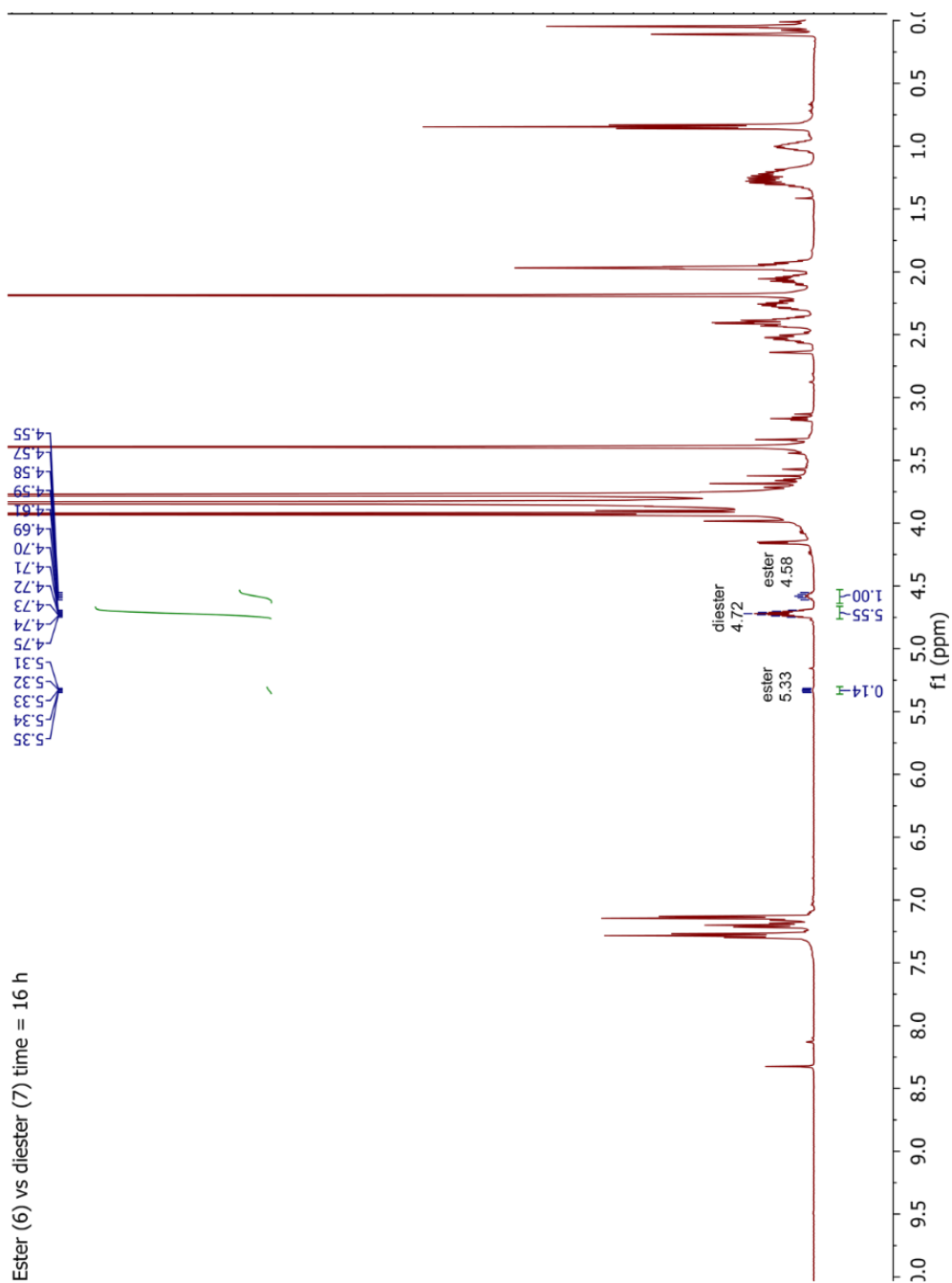


The ratio of products was ester : nitro 7.4 : 1.0, based on integrations of the protons alpha to the triazole of **2.3c** ( $\delta = 5.20$ ,  $I = 1.00$ ), **2.3d** ( $\delta = 4.10$ ,  $I = 1.24$ ), **2.6c** ( $\delta = 5.33$ ,  $I = 2.36$ ), and **2.6d** ( $\delta = 4.58$ ,  $I = 14.17$ ). After dividing by the starting concentrations, the rate ratio was ester : nitro = 7.9 : 1.0.

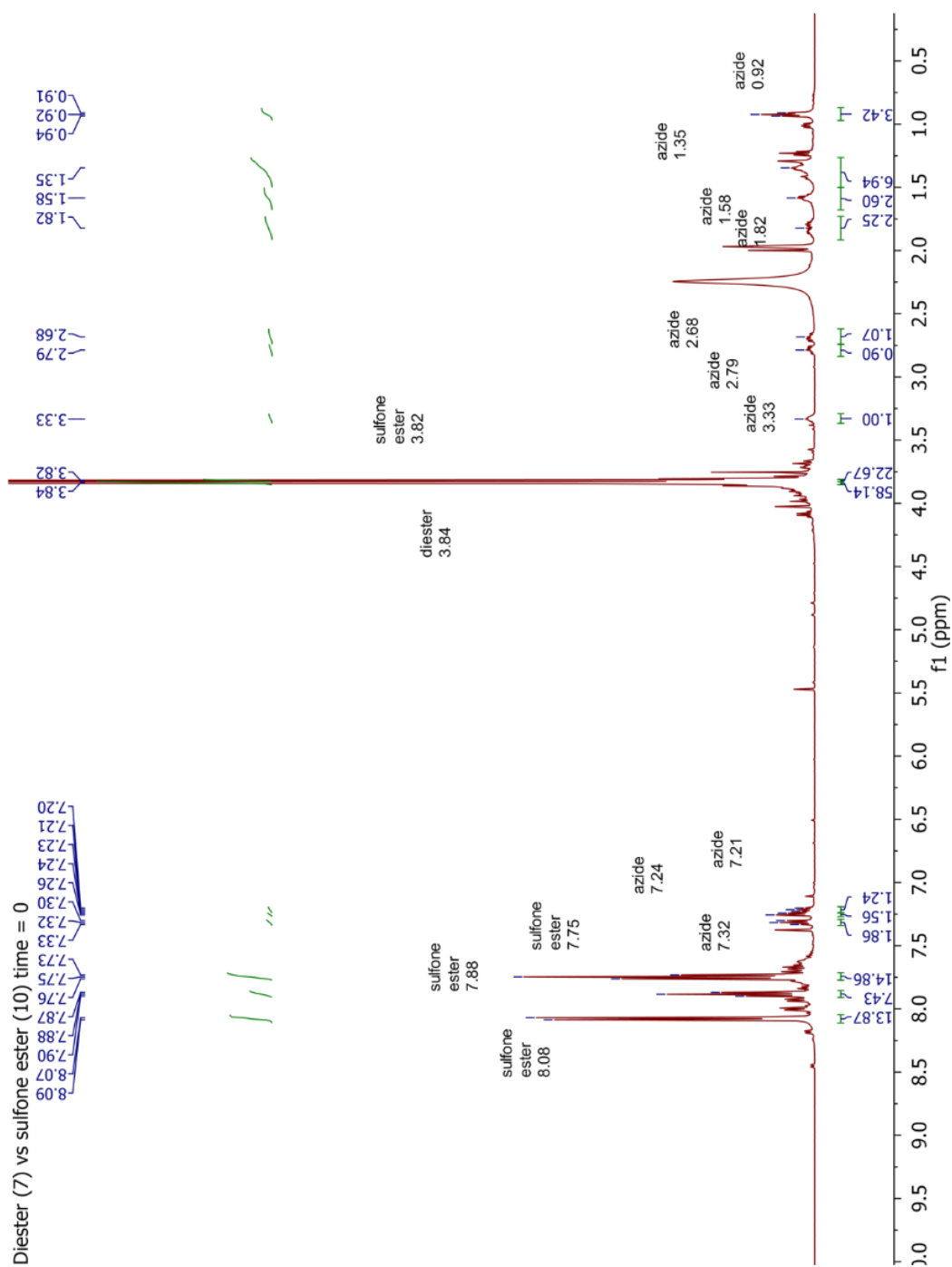




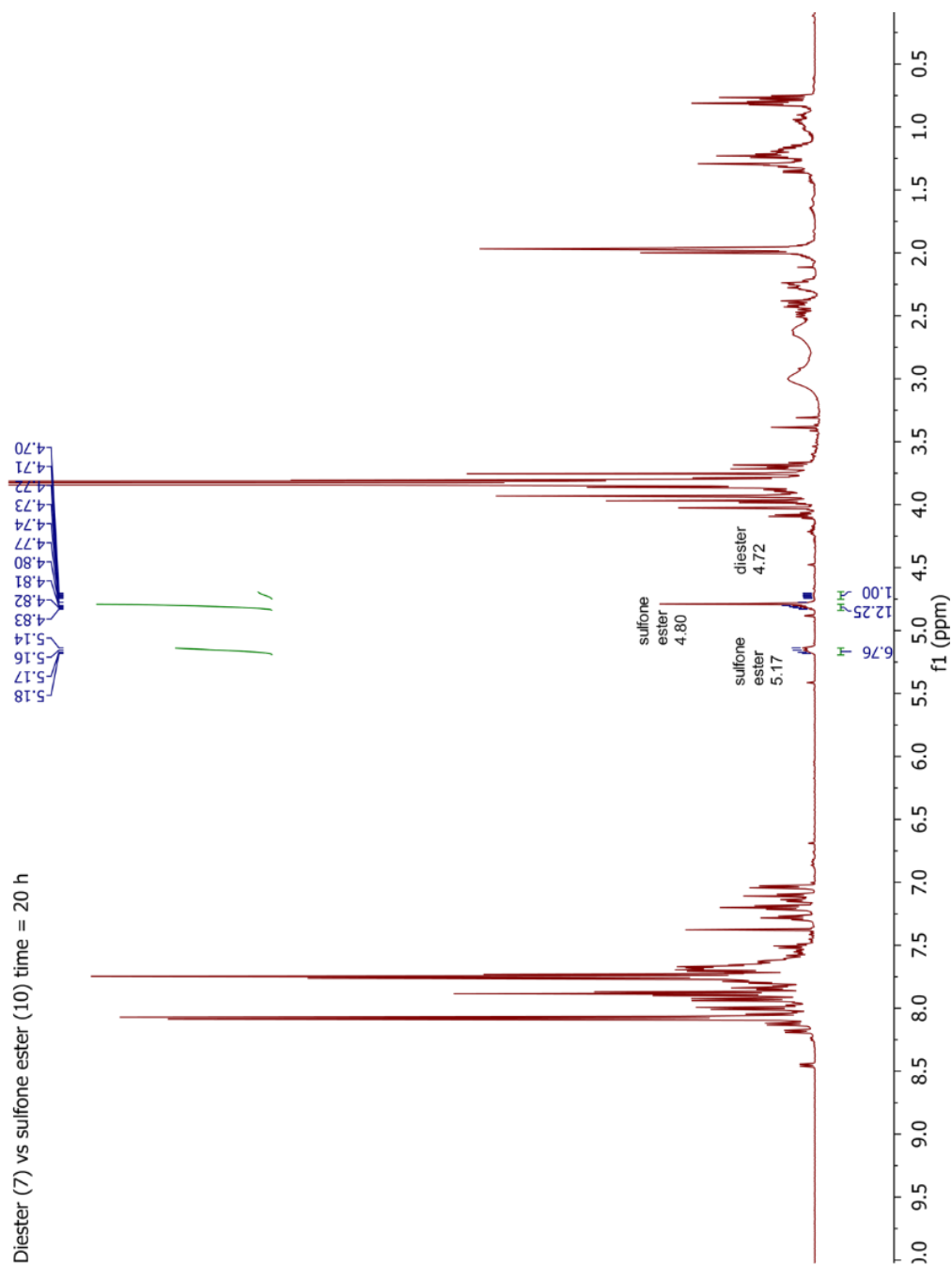
The initial ratio of azide **2.16** : diester **2.7** : ester **2.6** was 1 : 6.1 : 7.0, based on integrations of azide  $\text{CHN}_3$  ( $\delta = 3.34$ ,  $I = 1.00$ ), ester  $\text{OCH}_3$  ( $\delta = 3.77$ ,  $I = 20.91$ ), and diester  $\text{OCH}_3$  ( $\delta = 3.84$ ,  $I = 36.66$ ).



The ratio of products was diester : ester 4.9 : 1.0, based on integrations of the protons alpha to the triazole of **2.6c** ( $\delta = 5.33$ ,  $I = 0.14$ ), **2.6d** ( $\delta = 4.58$ ,  $I = 1.00$ ), and **2.7c** ( $\delta = 4.72$ ,  $I = 5.55$ ). After dividing by the starting concentrations, the rate ratio was diester : ester = 5.6 : 1.0.

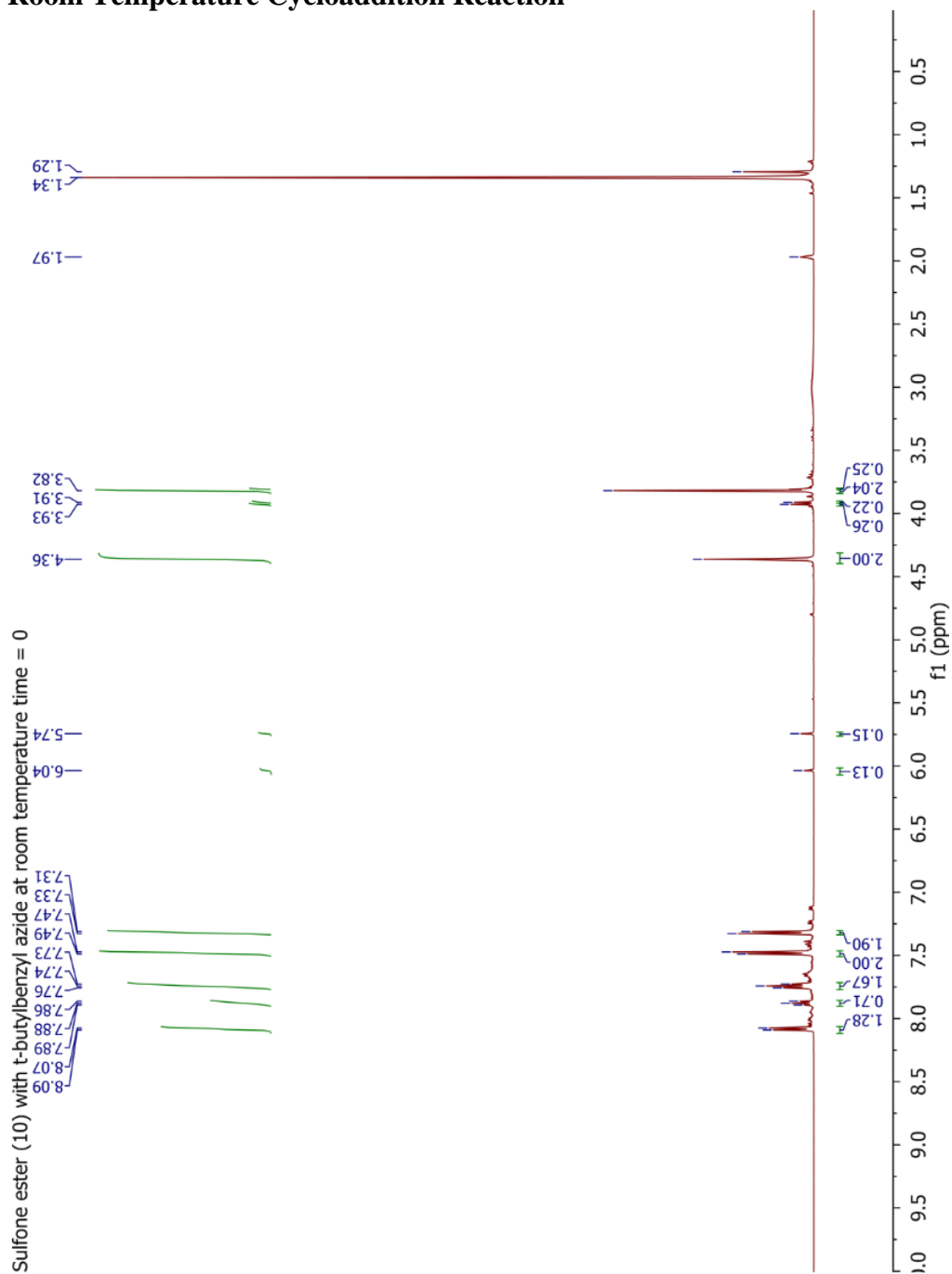


The initial ratio of azide **2.16** : sulfone ester **2.10** : diester **2.7** was 1 : 7.6 : 9.7, based on integrations of azide  $\text{CHN}_3$  ( $\delta = 3.33$ ,  $I = 1.00$ ), sulfone ester  $\text{OCH}_3$  ( $\delta = 3.82$ ,  $I = 22.67$ ), and diester  $\text{OCH}_3$  ( $\delta = 3.84$ ,  $I = 58.14$ ).

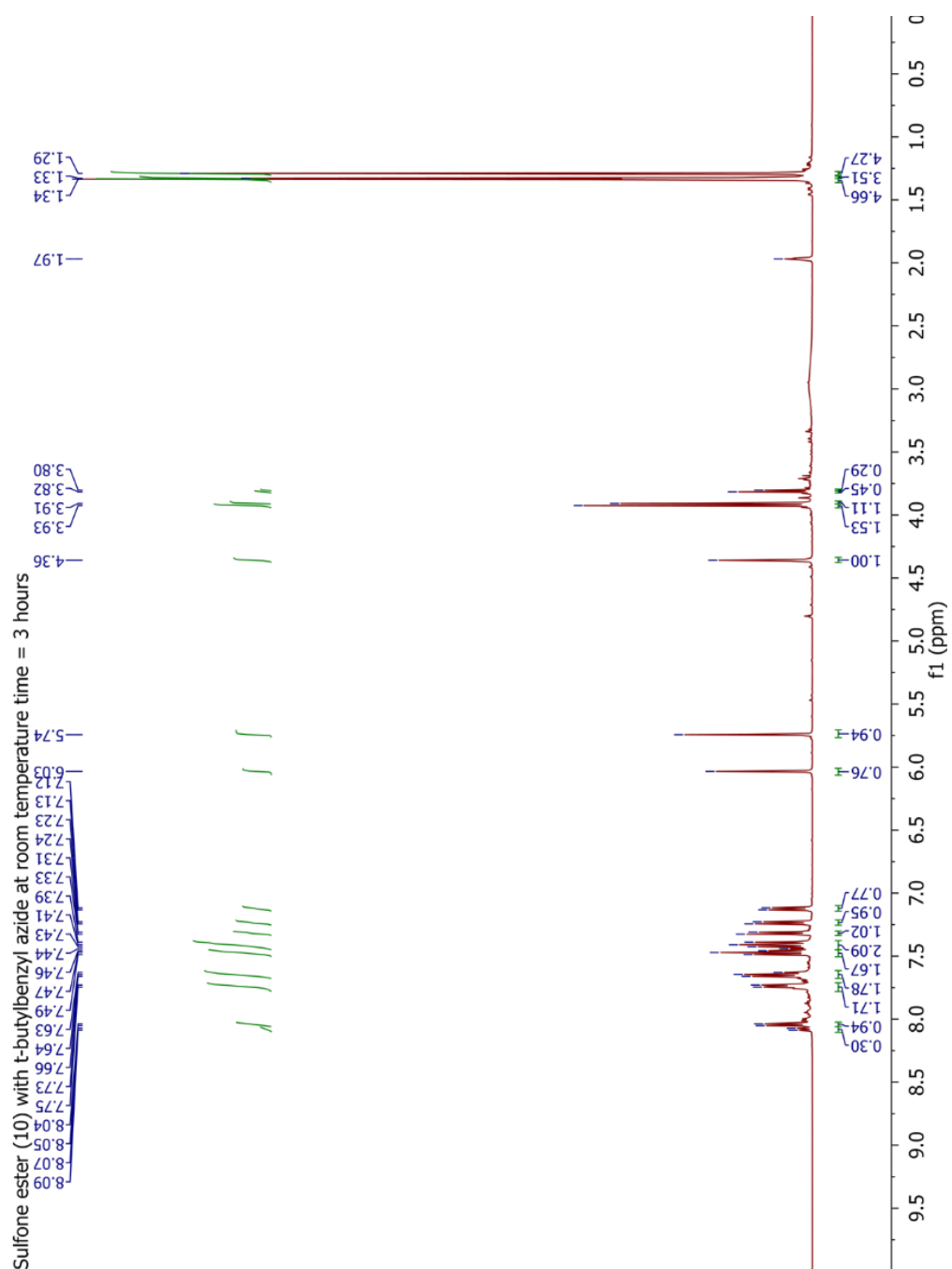


The ratio of products was sulfone ester : diester 19.0 : 1.0, based on integrations of the protons alpha to the triazole of **2.10c** ( $\delta = 5.17$ , I = 6.76), **2.10d** ( $\delta = 4.80$ , I = 12.25), and **2.7c** ( $\delta = 4.72$ , I = 1.00). After dividing by the starting concentrations, the rate ratio was sulfone ester : diester = 24.4 : 1.0.

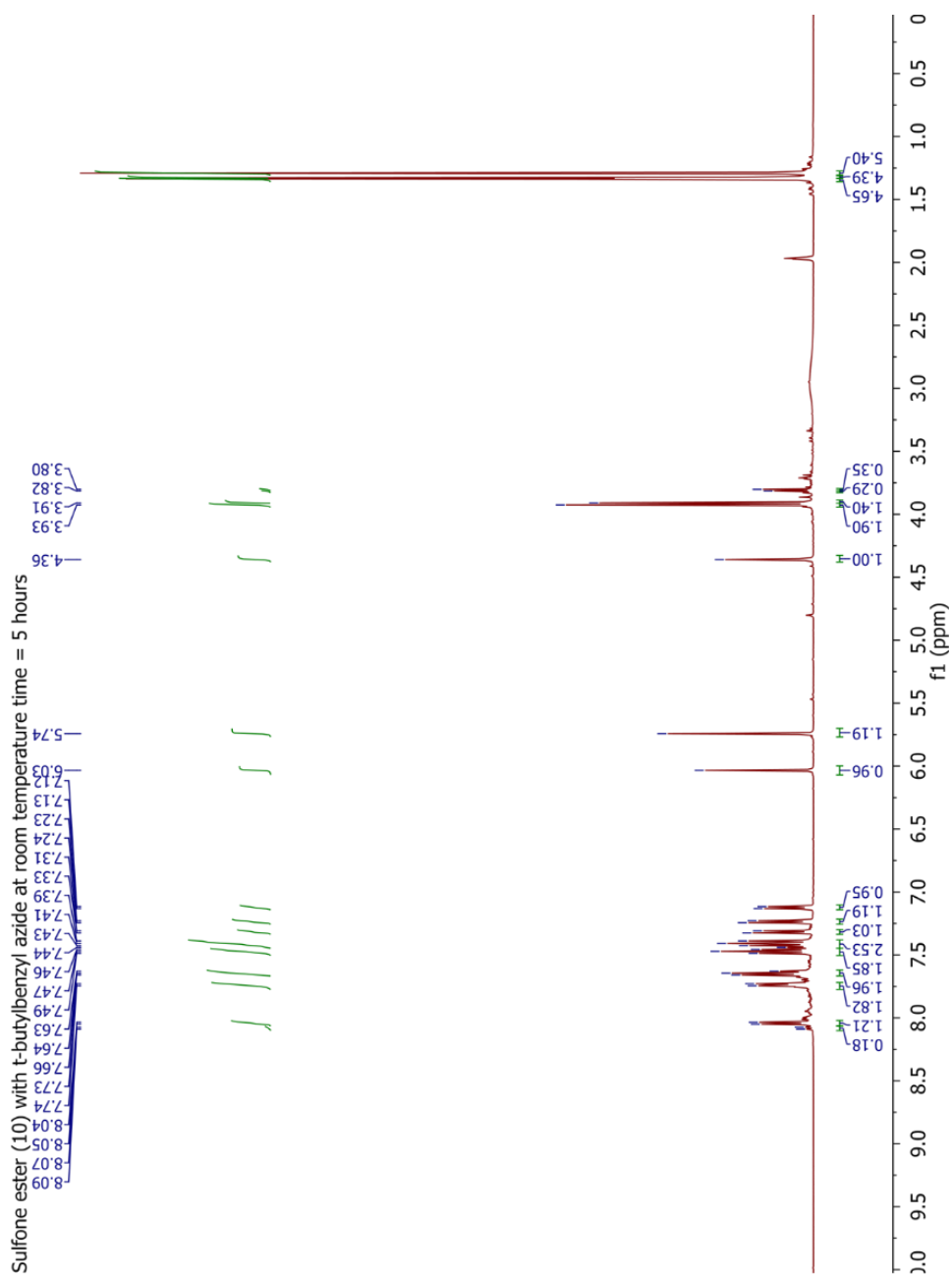
## Room Temperature Cycloaddition Reaction



At time zero, the azide **2.13** : alkyne **2.10** ratio was 1.0 : 0.68 based on integrations of azide  $\text{CH}_2\text{Ar}$  ( $\delta = 4.36$ ,  $I = 2.00$ ), sulfone ester  $\text{OCH}_3$  ( $\delta = 3.82$ ,  $I = 2.04$ ).



After 3 hours, 85% of the alkyne had been converted to triazole, based on integrations of **2.10a** OCH<sub>3</sub> ( $\delta = 3.93$ , I = 1.53), **2.10b** OCH<sub>3</sub> ( $\delta = 3.91$ , I = 1.11), and **2.10** OCH<sub>3</sub> ( $\delta = 3.82$ , I = 0.45).



After 5 hours, 92% of the alkyne had been converted to triazole, based on integrations of **2.10a** OCH<sub>3</sub> ( $\delta = 3.93$ , I = 1.90), **2.10b** OCH<sub>3</sub> ( $\delta = 3.91$ , I = 1.40), and **2.10** OCH<sub>3</sub> ( $\delta = 3.82$ , I = 0.29).

### Ratio of Regioisomers Formed from Cycloaddition Reaction

Alkyne	Ratio of products
Phenyl (1)	2.1 : 1.0
Benzoyl (2)	1.9 : 1.0
Nitro (3)	1.3 : 1.0
Amide (4)	2.4 : 1.0
vDiamide (5)	symmetric
Ester (6)	6.2 : 1.0
Diester (7)	symmetric
Ketone (8)	2.2 : 1.0
Sulfone (9)	6.5 : 1.0
Sulfone ester (10)	1.2 : 1.0

Calculated from  $^1\text{H}$ NMR integration of the competition experiments. Reaction in  $\text{CD}_3\text{CN}$  at  $75^\circ\text{C}$ .

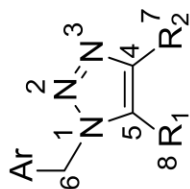
#### (Next two pages) $^1\text{H}$ NMR Integrations used to make Table 2.1

The rate ratio is determined by dividing the product ratio by the ratio of the starting materials. The reactivity scale in Table 1 is made by setting the rate of alkyne **1** to 1.0, then multiplying successively by the ratios (eg: rate of **4** =  $1.0 \times 1.4 \times 6.5 = 8.8$ ).



Azide	<b>2.13</b>	<b>2.13</b>	<b>2.13</b>	<b>2.13</b>	<b>2.13</b>	<b>2.13</b>	<b>2.13</b>	<b>2.13</b>	<b>2.13</b>	<b>2.13</b>	<b>2.13</b>	<b>2.13</b>	<b>2.13</b>
Alkyne 1	<b>2.2</b>	<b>2.2</b>	<b>2.4</b>	<b>2.4</b>	<b>2.4</b>	<b>2.4</b>	<b>2.4</b>	<b>2.4</b>	<b>2.4</b>	<b>2.4</b>	<b>2.4</b>	<b>2.4</b>	<b>2.6</b>
Peak	4.94 (t, 2H)	4.94 (t, 2H)	3.20 (m, 3H)	3.20 (m, 3H)	3.16 (s, 1H), 3.19 (q, 2H)	3.18 (m, 3H)	3.22 (td, 4H)	3.22 (td, 4H)	3.22 (td, 4H)	3.22 (td, 4H)	3.22 (td, 4H)	3.78 (s, 3H)	3.78 (s, 3H)
Integration	15.59	18.48	26.18	17.23	17.98 + 6.84	29.78	50.75	46.91	43.84	44.81	44.81	44.81	44.81
Alkyne 2	<b>2.1</b>	<b>2.1</b>	<b>2.2</b>	<b>2.2</b>	<b>2.3</b>	<b>2.3</b>	<b>2.3</b>	<b>2.3</b>	<b>2.3</b>	<b>2.3</b>	<b>2.3</b>	<b>2.3</b>	<b>2.5</b>
Peak	4.28 (q, 2H)	4.28 (q, 2H)	4.94 (d, 2H)	4.94 (d, 2H)	3.84 (s, 3H)	3.84 (s, 3H)	3.85 (s, 3H)	3.85 (s, 3H)	3.23 (td, 4H)	3.22 (td, 4H)	3.22 (td, 4H)	3.22 (td, 4H)	3.22 (td, 4H)
Integration	18.9	18.91	26.23	20.88	29.81	33.1	39.97	41.4	49.4	43.13	43.13	43.13	43.13
Product 1	<b>2.2a, 2.2b</b>	<b>2.2a, 2.2b</b>	<b>2.4a, 2.4b</b>	<b>2.4a, 2.4b</b>	<b>2.4a, 2.4b</b>	<b>2.4a, 2.4b</b>	<b>2.5a</b>	<b>2.5a</b>	<b>2.5a</b>	<b>2.5a</b>	<b>2.5a</b>	<b>2.5a</b>	<b>2.6a, 2.6b</b>
Peak	5.66 (s, 2H), 5.53 (s, 2H)	5.66 (s, 2H), 5.53 (s, 2H)	5.90 (s, 2H), 5.56 (s, 2H)	5.90 (s, 2H), 5.56 (s, 2H)	5.55 (s, 2H), 5.88 (s, 2H)	5.55 (s, 2H), 5.88 (s, 2H)	6.08 (s, 2H)	6.08 (s, 2H)	6.08 (s, 2H)	6.08 (s, 2H)	6.08 (s, 2H)	5.89 (s, 2H), 5.58 (s, 2H)	5.89 (s, 2H), 5.58 (s, 2H)
Integration	0.28 + 0.59	0.32 + 0.60	1.0 + 2.52	1.0 + 2.22	3.8 + 1.7	2.81 + 1.16	1.00	1.00	1.00	1.00	1.00	0.31 + 1.90	0.32 + 1.85
Product 2	<b>2.1a, 2.1b</b>	<b>2.1a, 2.1b</b>	<b>2.2a, 2.2b</b>	<b>2.2a, 2.2b</b>	<b>2.3a, 2.3b</b>	<b>2.3a, 2.3b</b>	<b>2.3a, 2.3b</b>	<b>2.3a, 2.3b</b>	<b>2.3a, 2.3b</b>	<b>2.3a, 2.3b</b>	<b>2.3a, 2.3b</b>	<b>2.5a</b>	<b>2.5a</b>
Peak	5.89 (s, 2H), 5.42 (s, 2H)	5.89 (s, 2H), 5.42 (s, 2H)	5.66 (s, 2H), 5.54 (s, 2H)	5.66 (s, 2H), 5.54 (s, 2H)	5.91 (s, 2H), 5.46 (s, 2H)	5.91 (s, 2H), 5.46 (s, 2H)	5.91 (s, 2H), 5.47 (s, 2H)	5.91 (s, 2H), 5.47 (s, 2H)	5.91 (s, 2H), 5.47 (s, 2H)	5.91 (s, 2H), 5.47 (s, 2H)	5.91 (s, 2H), 5.47 (s, 2H)	6.09 (s, 2H)	6.09 (s, 2H)
Integration	0.25 + 0.50	0.25 + 0.55	0.24 + 0.55	0.35 + 0.63	1.0 + 1.54	0.99 + 1.00	0.09 + 0.14	0.09 + 0.13	0.09 + 0.13	0.09 + 0.13	0.09 + 0.13	1.00	1.00
Product ratio	1.2	1.2	4.7	3.3	2.2	2.0	4.3	4.5	4.5	4.5	4.5	2.2	2.2
Rate ratio	1.4	1.3	7.1	6.0	2.6	2.2	4.6	5.3	5.3	5.3	5.3	1.9	1.6
Average	1.4 ± 0.1	1.3	6.5 ± 0.7	6.0	2.4 ± 0.3	2.2	5.0 ± 0.2	5.0 ± 0.2	5.0 ± 0.2	5.0 ± 0.2	5.0 ± 0.2	1.7 ± 0.2	1.7 ± 0.2

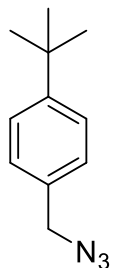
Azide	<b>2.13</b>	<b>2.13</b>	<b>2.13</b>	<b>2.13</b>	<b>2.13</b>	<b>2.13</b>	<b>2.13</b>	<b>2.13</b>	<b>2.16</b>	<b>2.16</b>	<b>2.16</b>	<b>2.16</b>
Alkyne 1	<b>2.7</b>	<b>2.8</b>	<b>2.8</b>	<b>2.9</b>	<b>2.10</b>	<b>2.10</b>	<b>2.10</b>	<b>2.6</b>	<b>2.7</b>	<b>2.7</b>	<b>2.10</b>	<b>2.10</b>
Peak	3.84 (s, 6H)	3.84 (s, 3H)	3.89 (s, 3H)	4.12 (s, 1H)	3.82 (s, 3H)	3.82 (s, 3H)	3.82 (s, 3H)	3.77 (s, 3H)	3.84 (s, 6H)	3.84 (s, 6H)	3.82 (s, 3H)	3.82 (s, 3H)
Integration	69.88	72.11	37.54	8.19	33.18	33.18	26.76	28.58	36.66	36.66	22.67	22.67
Alkyne 2	<b>2.6</b>	<b>2.6</b>	<b>2.7</b>	<b>2.7</b>	<b>2.7</b>	<b>2.7</b>	<b>2.7</b>	<b>2.3</b>	<b>2.6</b>	<b>2.6</b>	<b>2.7</b>	<b>2.7</b>
Peak	3.78 (s, 3H)	3.78 (s, 3H)	3.84 (s, 6H)	3.84 (s, 6H)	3.84 (s, 6H)	3.84 (s, 6H)	3.84 (s, 6H)	3.85 (s, 3H)	3.78 (s, 3H)	3.78 (s, 3H)	3.84 (s, 6H)	3.84 (s, 6H)
Integration	27	31.62	74.66	49.05	66.35	66.35	60.86	30.68	20.91	20.91	58.14	58.14
Product 1	<b>2.7a</b>	<b>2.8a, 2.8b</b>	<b>2.8a, 2.8b</b>	<b>2.9a, 2.9b</b>	<b>2.10a, 2.10b</b>	<b>2.10a, 2.10b</b>	<b>2.10a, 2.10b</b>	<b>2.6c, 2.6d</b>	<b>2.7c</b>	<b>2.7c</b>	<b>2.10c, 2.10d</b>	<b>2.10c, 2.10d</b>
Peak	5.73 (s, 2H)	5.73 (s, 2H), 5.57 (s, 2H)	5.86 (s, 2H), 5.57 (s, 2H)	5.79 (s, 2H), 5.55 (s, 2H)	5.74 (s, 2H), 6.03 (s, 2H)	5.74 (s, 2H), 6.03 (s, 2H)	5.74 (s, 2H), 6.03 (s, 2H)	5.33 (tt, 1H), 4.58 (tt, 1H)	4.72 (tt, 1H)	4.72 (tt, 1H)	5.17 (tt, 1H), 4.80 (tt, 1H)	5.17 (tt, 1H), 4.80 (tt, 1H)
Integration	7.42	6.54	1.00 + 0.46	0.33 + 2.29	1.22 + 1.00	1.22 + 1.00	1.18 + 1.00	2.36 + 14.17	5.55	5.55	6.76 + 12.25	6.76 + 12.25
Product 2	<b>2.6a, 2.6b</b>	<b>2.7a</b>	<b>2.7a</b>	<b>2.7a</b>	<b>2.7a</b>	<b>2.7a</b>	<b>2.7a</b>	<b>2.3c, 2.3d</b>	<b>2.6c, 2.6d</b>	<b>2.6c, 2.6d</b>	<b>2.7c</b>	<b>2.7c</b>
Peak	5.89 (s, 2H), 5.58 (s, 2H)	5.73 (s, 2H)	5.73 (s, 2H)	5.73 (s, 2H)	5.73 (s, 2H)	5.73 (s, 2H)	5.74 (s, 2H)	5.20 (tt, 1H), 4.10 (tt, 1H)	5.33 (tt, 1H), 4.58 (tt, 1H)	5.33 (tt, 1H), 4.58 (tt, 1H)	4.72 (tt, 1H)	4.72 (tt, 1H)
Integration	0.16 + 1.00	0.16 + 1.32	1.26	1	0.13	0.13	0.16	1.00 + 1.24	0.14 + 1.00	0.14 + 1.00	1	1
Product ratio	6.4	6.3	1.1	2.6	17.2	17.2	13.6	7.4	4.9	4.9	19	19
Rate ratio	4.9	5.5	1.1	2.6	17.2	17.2	15.5	7.9	5.6	5.6	24.4	24.4
Average	5.2 ± 0.4	1.11 ± 0.01	1.11 ± 0.01	2.6	16.3 ± 1.2	16.3 ± 1.2	16.3 ± 1.2	7.9	5.6	5.6	24.4	24.4



### Wiberg bond indices

R <sub>1</sub>	R <sub>2</sub>	1-5		3-4			4-5			5-8			4-7		
		TS	Prod	TS	Prod	SM	TS	Prod	SM	TS	Prod	SM	TS	Prod	SM
Ph	CO <sub>2</sub> Me	0.2893	1.2442	0.2824	1.3031	2.6661	2.3717	1.3645	1.1237	1.0914	1.0712	1.0639	1.0474	1.0487	
CO <sub>2</sub> Me	Ph	0.2652	1.1949	0.2588	1.3318	2.6661	2.3692	1.3976	1.0639	1.0501	1.0163	1.1237	1.1115	1.0573	
H	CH <sub>2</sub> Bz	0.289	1.2481	0.2664	1.3297	2.8883	2.5411	1.4744	0.919	0.8991	0.9012	1.0615	1.0568	1.0234	
CH <sub>2</sub> Bz	H	0.2415	1.2232	0.339	1.3571	2.8883	2.5329	1.4773	1.0615	1.0549	1.02	0.919	0.8923	0.9048	
NO <sub>2</sub> Ph	CO <sub>2</sub> Me	0.2909	1.2489	0.2858	1.3164	2.677	2.3691	1.397	1.1198	1.0937	1.0249	1.0525	1.0396	1.0239	
CO <sub>2</sub> Me	NO <sub>2</sub> Ph	0.2951	1.2068	0.2469	1.3297	2.677	2.3757	1.3928	1.0525	1.0274	1.0129	1.1198	1.1113	1.0641	
H	CONHBu	0.3069	1.2628	0.2485	1.3192	2.858	2.5196	1.4506	0.9177	0.8969	0.8989	1.0258	1.03	1.0085	
CONHBu	H	0.2491	1.2058	0.3222	1.382	2.858	2.5258	1.4532	1.0258	1.0163	0.9999	0.9177	0.8951	0.906	
CONHBu	CONHBu	0.27	1.2376	0.2592	1.3333	2.7294	2.4296	1.3978	1.0249	1.0107	0.9951	1.0249	1.0146	1.0133	
H	CO <sub>2</sub> Me	0.3364	1.2783	0.2219	1.311	2.8419	2.4927	1.4367	0.9168	0.8934	0.8977	1.0401	1.0691	1.0277	
CO <sub>2</sub> Me	H	0.2436	1.1979	0.3465	1.3955	2.8419	2.4974	1.4358	1.0401	1.0386	1.027	0.9168	0.8922	0.9046	
CO <sub>2</sub> Me	CO <sub>2</sub> Me	0.3148	1.2414	0.2323	1.3396	2.707	2.387	1.393	1.0344	1.0201	0.9945	1.0344	1.0526	1.0068	
COPh	CO <sub>2</sub> Me	0.3102	1.2562	0.2575	1.3228	2.695	2.3834	1.3938	1.0485	1.0303	0.9796	1.0347	1.0446	1.0204	
CO <sub>2</sub> Me	COPh	0.333	1.2408	0.2195	1.3399	2.695	2.3657	1.3896	1.0347	1.0207	0.9979	1.0485	1.08	1.0136	
H	SO <sub>2</sub> Ar	0.3064	0.2298	1.2696	1.329	2.8572	2.5216	1.4604	0.9111	0.8921	0.8928	0.8516	0.8697	0.8341	
SO <sub>2</sub> Ar	H	0.2638	0.326	1.2044	1.3833	2.8572	2.5072	1.4629	0.8516	0.8537	0.8256	0.9111	0.8898	0.9005	
SO <sub>2</sub> Ar	CO <sub>2</sub> Me	0.3209	1.2469	0.2425	1.3394	2.7376	2.4124	1.4053	0.8394	0.8292	0.7987	1.0233	1.037	1.0123	
CO <sub>2</sub> Me	SO <sub>2</sub> Ar	0.273	1.2409	0.2426	1.3633	2.7376	2.4484	1.4038	1.0233	1.0111	0.9959	0.8394	0.8417	0.8109	

## Coordinates for Optimized Structures by DFT



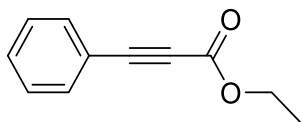
### 4-*t*-butylbenzyl azide **2.13**

No imaginary frequencies

Total energy (ZPE corrected, Hartrees): -592.159412

C	1.307595	0.373788	0.358700
C	1.163963	-0.994101	0.089321
C	-0.147300	-1.483255	-0.061966
C	-1.255588	-0.648962	0.052259
C	-1.099151	0.717282	0.321643
C	0.196577	1.214827	0.471064
C	2.361635	-1.952987	-0.037918
C	2.359467	-2.593654	-1.446560
C	-2.297905	1.623797	0.435525
N	-2.771839	1.995559	-0.938187
N	-3.799720	2.673817	-0.974192
N	-4.743405	3.300502	-1.133537
C	3.710373	-1.236069	0.161973

C	2.243544	-3.067138	1.029791
H	-0.310671	-2.537275	-0.268088
H	-2.254095	-1.063385	-0.066915
H	0.346557	2.271265	0.681958
H	2.293679	0.805592	0.486898
H	3.087884	-3.761957	0.946211
H	2.251008	-2.643705	2.040923
H	1.321735	-3.646944	0.914262
H	3.204807	-3.284853	-1.549164
H	1.441278	-3.159377	-1.636123
H	2.450463	-1.827743	-2.225516
H	4.527898	-1.958679	0.061626
H	3.869709	-0.450433	-0.585342
H	3.788866	-0.783510	1.157046
H	-3.114584	1.123886	0.969964
H	-2.040380	2.536994	0.984210



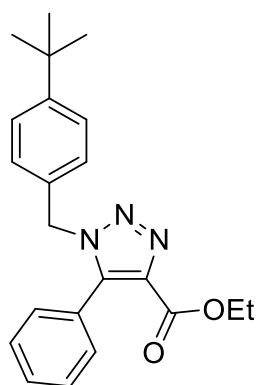
**Alkyne 2.1**

No imaginary frequencies

Total energy (ZPE corrected, Hartrees): -575.415932

C	-1.307713	1.999876	0.000000
C	-1.309424	0.590084	0.000000
C	-2.537316	-0.102309	0.000000
C	-3.736040	0.605902	0.000000
C	-3.726316	2.004156	0.000000
C	-2.512276	2.697820	0.000000
C	-0.078561	-0.127887	0.000000
C	0.977584	-0.729278	0.000000
C	2.193824	-1.503067	0.000000
O	2.227982	-2.722410	0.000000
O	3.278184	-0.708427	0.000000
C	4.566695	-1.382719	0.000000
C	5.638096	-0.310444	0.000000
H	4.623763	-2.022066	0.885871
H	4.623763	-2.022066	-0.885871
H	-2.537490	-1.187696	0.000000
H	-4.679153	0.067486	0.000000

H	-4.663875	2.552641	0.000000
H	-2.505036	3.783768	0.000000
H	-0.361576	2.531770	0.000000
H	6.625701	-0.783147	0.000000
H	5.559291	0.322917	-0.889241
H	5.559291	0.322917	0.889241



Transition state for ethyl 1-(4-t-butylbenzyl)-5-phenyl-1,2,3-triazole-4-carboxylate

1 imaginary frequency:  $-392.76\text{cm}^{-1}$

Total energy (ZPE corrected, Hartrees): -1167.542379

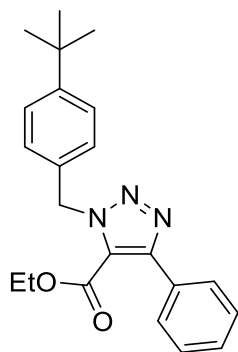
C	-2.682290	-0.848806	-1.432110
C	-1.962912	0.152832	-0.770037
C	-2.612317	0.879722	0.231635
C	-3.941722	0.612162	0.563850
C	-4.674362	-0.388856	-0.092365
C	-4.010176	-1.110759	-1.099422

C	-0.516088	0.426039	-1.122053
N	0.436720	-0.143715	-0.142477
N	0.651315	-1.380739	-0.120374
N	1.488564	-2.144599	0.165104
C	-6.142444	-0.707567	0.244556
C	-6.256495	-2.181982	0.700451
C	-6.692648	0.187665	1.371137
C	-7.016697	-0.492932	-1.014165
C	2.456871	0.497642	0.269093
C	3.025491	-0.593798	0.470132
C	4.125467	-1.432963	0.900681
O	4.316639	-1.781802	2.053138
C	2.358227	1.931047	0.130971
C	1.450507	2.682038	0.900823
C	1.408970	4.069534	0.778951
C	2.263194	4.725069	-0.112725
C	3.163930	3.985393	-0.883273
C	3.214607	2.597191	-0.765924
O	4.901546	-1.790735	-0.139454
C	6.033358	-2.647019	0.172971
H	-0.307164	1.498274	-1.093947
H	-0.280807	0.060261	-2.127551



C	6.760785	-2.928341	-1.127008
H	6.671526	-2.132054	0.897138
H	5.659002	-3.562512	0.640798
H	-2.203123	-1.427411	-2.218776
H	-4.534187	-1.893063	-1.641366
H	-4.404563	1.204117	1.345524
H	-2.078262	1.666339	0.759833
H	-8.065402	-0.723341	-0.790979
H	-6.963109	0.547289	-1.355986
H	-6.702876	-1.136264	-1.842904
H	-7.736967	-0.076256	1.571699
H	-6.133316	0.059001	2.304814
H	-6.666119	1.249073	1.099466
H	-7.299132	-2.424969	0.938272
H	-5.921077	-2.876439	-0.076936
H	-5.652547	-2.362330	1.597326
H	3.914725	2.020225	-1.362070
H	3.829363	4.488970	-1.578663
H	2.225805	5.806534	-0.206970
H	0.707856	4.640111	1.381271
H	0.788481	2.170424	1.592227
H	7.623818	-3.572834	-0.929947

H	6.106020	-3.438383	-1.840760
H	7.120839	-2.000951	-1.583767



Transition state for ethyl 1-(4-t-butylbenzyl)-4-phenyl-1,2,3-triazole-5-carboxylate

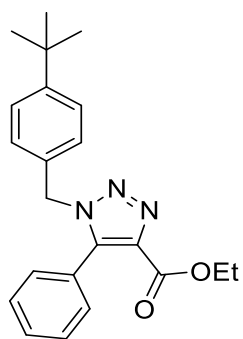
1 imaginary frequency:  $-344.649 \text{ cm}^{-1}$

Total energy (ZPE corrected, Hartrees):  $-1167.54229$

C	3.171590	-0.519501	1.651682
C	2.250824	0.284221	0.971423
C	2.645646	0.867346	-0.236558
C	3.925295	0.651675	-0.750488
C	4.859819	-0.151715	-0.077883
C	4.450192	-0.729337	1.136198
C	0.856591	0.511616	1.516139
N	-0.181204	-0.186382	0.724490
N	-0.473072	-1.379038	0.954021
N	-1.330444	-2.158069	0.813904
C	6.280420	-0.410454	-0.613359

C	7.317909	0.109419	0.410466
C	6.483623	-1.930640	-0.819129
C	6.537393	0.294197	-1.958827
C	-2.163503	0.413818	0.089633
C	-1.950194	1.833390	-0.139453
O	-3.124388	2.490193	-0.034823
C	-3.078024	3.925300	-0.260931
C	-2.842182	-0.630265	0.035975
C	-4.047182	-1.390070	-0.173877
C	-4.043444	-2.767027	-0.464308
C	-5.242213	-3.440485	-0.689828
C	-6.459734	-2.757979	-0.618855
C	-6.475794	-1.390313	-0.328222
C	-5.281817	-0.707753	-0.111925
O	-0.891795	2.381560	-0.399093
H	0.579629	1.563940	1.432111
H	0.789253	0.218084	2.568622
C	-4.483015	4.459676	-0.065450
H	-2.367774	4.365345	0.445305
H	-2.706172	4.105810	-1.273928
H	2.890221	-0.983835	2.594373
H	5.137627	-1.357313	1.695950

H	4.188485	1.125193	-1.689771
H	1.942623	1.493559	-0.780694
H	8.335701	-0.075454	0.046145
H	7.204884	1.188227	0.569112
H	7.215662	-0.386308	1.381552
H	7.555054	0.073262	-2.299557
H	5.845812	-0.048095	-2.737105
H	6.445949	1.383072	-1.874222
H	7.495467	-2.130519	-1.191966
H	6.356150	-2.489729	0.113745
H	5.768317	-2.326159	-1.549624
H	-5.284732	0.355925	0.104886
H	-7.419301	-0.854706	-0.273224
H	-7.392041	-3.288847	-0.789658
H	-5.226344	-4.502504	-0.917644
H	-3.099425	-3.296910	-0.511408
H	-4.486918	5.542587	-0.227643
H	-5.179192	4.002710	-0.775942
H	-4.839628	4.262362	0.950482



Ethyl 1-(4-t-butylbenzyl)-5-phenyl-1,2,3-triazole-4-carboxylate

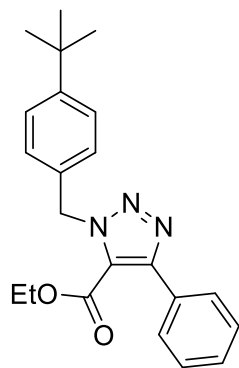
No imaginary frequencies

Total energy (Hartrees): -1168.112022

C	-1.012805	1.801134	-1.191722
C	-1.324864	1.674434	0.170331
C	-1.346375	2.819962	0.981488
C	-1.051771	4.071173	0.438154
C	-0.734128	4.189509	-0.916542
C	-0.717263	3.052791	-1.729515
C	-1.624745	0.347290	0.743285
N	-0.895281	-0.233254	1.732387
N	-1.404276	-1.447550	2.066388
N	-2.447741	-1.660592	1.322378
C	-2.626125	-0.591454	0.491401
C	0.364911	0.200473	2.356756
C	1.581928	-0.087848	1.500404
C	1.915250	-1.400874	1.140113

C	3.047594	-1.658363	0.374006
C	3.898306	-0.623858	-0.061327
C	3.553346	0.682640	0.307670
C	2.413052	0.947946	1.072704
C	5.143180	-0.955748	-0.903445
C	4.706585	-1.665928	-2.207402
C	-3.748972	-0.486683	-0.461474
O	-3.945490	0.476714	-1.183010
O	-4.530378	-1.578812	-0.437011
C	-5.666771	-1.571938	-1.339860
C	5.944406	0.303146	-1.286038
C	6.073319	-1.893503	-0.097017
H	0.288808	1.265665	2.577254
H	0.406192	-0.339272	3.306026
C	-6.407979	-2.880099	-1.145628
H	-6.293197	-0.705970	-1.106019
H	-5.298289	-1.456606	-2.363674
H	1.282637	-2.225201	1.459896
H	3.273282	-2.689010	0.115266
H	4.169991	1.519467	-0.000319
H	2.175974	1.975674	1.336929
H	6.960402	-2.147683	-0.689582

H	6.409433	-1.410759	0.827989
H	5.574081	-2.829659	0.174111
H	6.816050	0.015318	-1.884154
H	5.347977	1.000914	-1.884749
H	6.311964	0.837095	-0.402249
H	5.584936	-1.915672	-2.814573
H	4.166312	-2.596669	-2.004851
H	4.052765	-1.020305	-2.805199
H	-1.614395	2.735297	2.030855
H	-1.076503	4.951962	1.073174
H	-0.504208	5.163748	-1.338488
H	-0.472887	3.140117	-2.784245
H	-1.001709	0.918601	-1.823102
H	-7.274379	-2.911897	-1.814480
H	-5.763280	-3.734150	-1.376332
H	-6.764399	-2.979661	-0.115429



Ethyl 1-(4-t-butylbenzyl)-4-phenyl-1,2,3-triazole-5-carboxylate

No imaginary frequencies

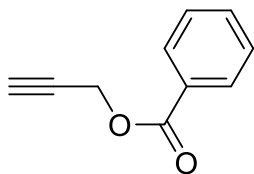
Total energy (Hartrees): -1168.110057

C	-3.727952	-0.984292	-1.444083
C	-3.781625	-0.885155	-0.043803
C	-4.977190	-1.230371	0.614415
C	-6.090885	-1.650682	-0.108952
C	-6.031083	-1.738307	-1.502761
C	-4.847254	-1.405270	-2.163673
C	-2.625053	-0.479490	0.776423
C	-1.571419	0.419711	0.574359
N	-0.870133	0.389884	1.750781
N	-1.430594	-0.474034	2.607473
N	-2.491380	-0.983689	2.040070
C	-1.260980	1.318544	-0.560916
O	-1.480833	1.048698	-1.727511
C	0.413208	1.009461	2.126681
C	1.591163	0.427155	1.371325
C	2.460590	1.253426	0.658805
C	3.565199	0.721654	-0.014530
C	3.834500	-0.652839	-0.006015
C	2.948284	-1.474458	0.717088



C	1.852274	-0.950050	1.394488
C	5.033235	-1.276338	-0.743161
C	4.518867	-2.291342	-1.791954
C	5.885915	-0.221018	-1.472418
C	5.939208	-2.008980	0.275607
O	-0.735709	2.483210	-0.149769
C	-0.397654	3.443629	-1.192967
H	0.335198	2.083974	1.967282
H	0.494699	0.821244	3.200092
C	0.032623	4.726848	-0.511733
H	0.397733	3.012722	-1.807889
H	-1.278993	3.588145	-1.822624
H	1.191433	-1.616059	1.944102
H	3.115907	-2.546909	0.757250
H	4.213154	1.403127	-0.554034
H	2.284853	2.325713	0.629297
H	6.793250	-2.465971	-0.238485
H	6.328670	-1.311861	1.026642
H	5.402358	-2.805146	0.802065
H	6.723360	-0.713122	-1.979251
H	5.308374	0.316202	-2.233349
H	6.306599	0.515487	-0.778295

H	5.363219	-2.752099	-2.318412
H	3.934840	-3.094914	-1.330921
H	3.883237	-1.797569	-2.536199
H	-5.023227	-1.162202	1.696277
H	-7.007178	-1.907184	0.415676
H	-6.899820	-2.065263	-2.067593
H	-4.788981	-1.478839	-3.246282
H	-2.811981	-0.730690	-1.961935
H	0.286274	5.471204	-1.273569
H	-0.773527	5.130378	0.108840
H	0.913824	4.568218	0.11794



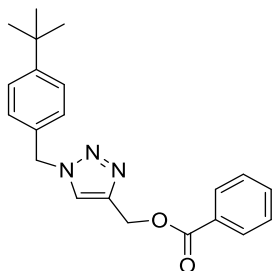
Alkyne **2.2**

No imaginary frequencies

Total energy (ZPE corrected, Hartrees): -536.117412

C	1.216461	0.029748	0.000000
O	1.185269	-1.329946	0.000000
C	0.031063	-2.197124	0.000000
C	0.520507	-3.573286	0.000000
C	0.902812	-4.717899	0.000000
O	2.335404	0.512541	0.000000
C	0.000000	0.915949	0.000000
H	1.244400	-5.730004	0.000000
H	-0.577113	-2.017003	0.892318
H	-0.577113	-2.017003	-0.892318
C	0.291673	2.295350	0.000000
C	-0.720762	3.248139	0.000000
C	-2.058999	2.846025	0.000000
C	-2.366376	1.486147	0.000000
C	-1.351526	0.527065	0.000000
H	1.331110	2.600456	0.000000

H	-0.465921	4.303918	0.000000
H	-2.854084	3.586157	0.000000
H	-3.402140	1.159941	0.000000
H	-1.653644	-0.507901	0.000000



Transition state for 1-(4-t-butylbenzyl)-1,2,3-triazol-4-ylmethyl benzoate

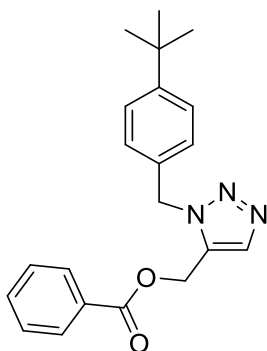
1 imaginary frequency:  $-399.086 \text{ cm}^{-1}$

Total energy (ZPE corrected, Hartrees):  $-1128.245557$

C	0.005184	0.048056	0.000460
C	0.015559	0.036576	1.403614
C	1.240359	0.061431	2.087687
C	2.438288	0.107724	1.374491
C	2.420580	0.145023	-0.021766
C	1.202461	0.117011	-0.707961
C	-1.289810	-0.116181	2.115321
O	-2.187262	-0.812933	1.681836
O	-1.469119	0.483488	3.321430
C	-0.831947	1.744118	3.675442

C	-1.857536	2.731227	4.021997
C	-2.959448	3.253216	4.223529
N	-2.526073	5.271396	4.805433
N	-1.276846	5.149476	4.857102
N	-0.432050	4.395979	4.567588
C	-3.231254	6.104928	5.804125
C	-3.068996	7.590926	5.561146
C	-3.727906	8.223020	4.502603
C	-3.568155	9.590541	4.273082
C	-2.746924	10.380446	5.092750
C	-2.090704	9.732884	6.153717
C	-2.245215	8.366679	6.384395
C	-2.553836	11.892303	4.874457
C	-3.348975	12.415557	3.663196
C	-3.030763	12.657857	6.131915
C	-1.054410	12.190394	4.633355
H	-0.213135	2.101918	2.850019
H	-4.021115	3.371964	4.276462
H	-4.279085	5.810889	5.696583
H	-2.909342	5.836642	6.816525
H	-1.722093	7.900915	7.216672
H	-1.445910	10.300261	6.819023

H	-4.101738	10.037792	3.441888
H	-4.373991	7.643345	3.847136
H	-2.891619	13.736891	5.993745
H	-4.094623	12.474259	6.322227
H	-2.472805	12.361170	7.026171
H	-3.179271	13.492110	3.550462
H	-3.037916	11.931460	2.730430
H	-4.427194	12.261919	3.785727
H	-0.901420	13.266012	4.483644
H	-0.435168	11.880618	5.481774
H	-0.689186	11.668273	3.741304
H	-0.177644	1.551794	4.530357
H	1.260461	0.017511	3.172253
H	3.383449	0.113230	1.909231
H	3.354324	0.190491	-0.575037
H	1.187469	0.141972	-1.793630
H	-0.945296	0.007180	-0.521858



Transition state for 1-(4-t-butylbenzyl)-1,2,3-triazol-5-ylmethyl benzoate

1 imaginary frequency:  $-420.201 \text{ cm}^{-1}$

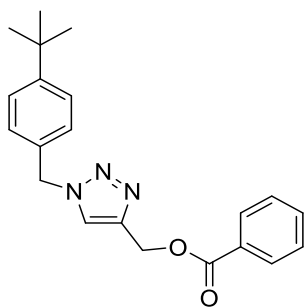
Total energy (ZPE corrected, Hartrees):  $-1128.246466$

C	-0.550634	-0.682546	0.264934
C	-0.507683	-0.422171	1.643040
C	0.709358	-0.519147	2.333570
C	1.872553	-0.872896	1.654106
C	1.826876	-1.132132	0.280854
C	0.616069	-1.036676	-0.411046
C	-1.719821	-0.040419	2.417828
O	-1.732024	0.192966	3.614700
O	-2.829249	0.023906	1.648244
C	-4.047166	0.390587	2.344558
C	-5.136280	0.389482	1.365841
C	-5.797283	0.291512	0.326479
N	-7.768622	0.815571	0.773223
N	-7.657424	1.046840	1.921614

N	-6.747888	1.124811	2.781390
C	-7.081491	1.130505	4.224000
C	-7.715823	-0.153151	4.716313
C	-6.937379	-1.203160	5.209519
C	-7.525517	-2.398046	5.632943
C	-8.913589	-2.589036	5.581205
C	-9.687773	-1.522280	5.089142
C	-9.104977	-0.330217	4.666185
C	-9.597726	-3.890432	6.038102
C	-10.385965	-4.499214	4.853560
C	-8.586513	-4.941876	6.533030
C	-10.575818	-3.578153	7.195897
H	-3.916288	1.375843	2.800660
H	-5.968235	0.089751	-0.710030
H	-6.127579	1.307529	4.726413
H	-7.724685	1.992828	4.433868
H	-9.738394	0.473058	4.296092
H	-10.768744	-1.616863	5.037208
H	-6.879447	-3.182588	6.010665
H	-5.857064	-1.091501	5.273370
H	-11.080324	-4.495233	7.523289
H	-10.042191	-3.158472	8.056680



H	-11.347584	-2.861609	6.895952
H	-9.121065	-5.847589	6.840576
H	-7.876760	-5.226727	5.747949
H	-8.015953	-4.585105	7.398027
H	-10.881993	-5.426140	5.165782
H	-11.158116	-3.816710	4.483164
H	-9.716976	-4.736896	4.018322
H	-4.227363	-0.328909	3.148531
H	0.726375	-0.314838	3.398966
H	2.812984	-0.946860	2.192354
H	2.733968	-1.408266	-0.249555
H	0.581098	-1.238047	-1.477761
H	-1.491169	-0.607048	-0.268984



1-(4-t-butylbenzyl)-1,2,3-triazol-4-ylmethyl benzoate

No imaginary frequencies

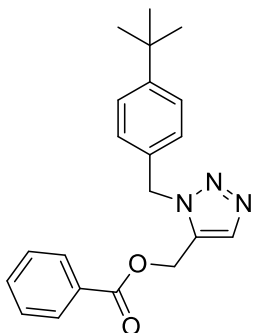
Total energy (Hartrees): -1128.779348

C	0.011199	0.077736	0.225318
C	0.305216	-0.032960	1.591662

C	1.629798	-0.256918	1.967972
C	2.639404	-0.370306	1.006488
C	2.360621	-0.259878	-0.361711
C	1.019393	-0.031816	-0.726685
C	-0.789990	0.077907	2.631237
N	-1.403166	1.412717	2.678677
N	-2.671941	1.594451	2.245452
N	-2.957923	2.862147	2.382838
C	-1.874543	3.510207	2.904583
C	-0.869267	2.583171	3.094614
C	-1.881827	4.976413	3.172942
O	-1.555925	5.677305	1.937040
C	-2.272218	6.734642	1.479737
C	3.442875	-0.380382	-1.449903
C	4.843594	-0.624433	-0.857708
C	3.100199	-1.564632	-2.385423
C	3.488883	0.926981	-2.276688
H	-2.863713	5.291057	3.529785
H	0.135541	2.664100	3.480206
H	-0.405652	-0.153266	3.628051
H	-1.617222	-0.603899	2.419251
O	-2.255844	6.962449	0.284824

C	-3.002775	7.612362	2.444979
H	-1.013563	0.253443	-0.093594
H	0.752522	0.058758	-1.775743
H	3.653758	-0.546244	1.346491
H	1.884471	-0.348719	3.021334
H	3.861498	-1.659315	-3.168961
H	3.067354	-2.507794	-1.827764
H	2.130907	-1.429662	-2.876691
H	5.575726	-0.702523	-1.669046
H	5.159573	0.197090	-0.204792
H	4.886664	-1.555974	-0.281997
H	4.250183	0.850323	-3.062340
H	2.529946	1.137920	-2.761508
H	3.741354	1.784040	-1.641607
H	-1.128582	5.235547	3.920007
C	-2.463605	7.969732	3.689765
C	-3.141071	8.869986	4.512410
C	-4.365614	9.405268	4.106180
C	-4.905469	9.054703	2.864904
C	-4.220191	8.174269	2.030881
H	-1.505590	7.569343	4.006009
H	-2.711489	9.153353	5.468756

H	-4.895989	10.098553	4.752821
H	-5.855411	9.473153	2.545384
H	-4.620598	7.910056	1.057327



1-(4-t-butylbenzyl)-1,2,3-triazol-5-ylmethyl benzoate

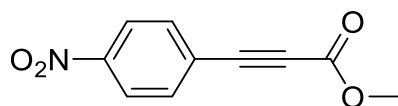
No imaginary frequencies

Total energy (Hartrees): -1128.790993

C	-0.182917	-0.014498	-0.065452
N	0.029269	-0.057006	1.277205
N	1.352611	-0.157535	1.549097
N	1.989279	-0.186197	0.407314
C	1.084183	-0.100896	-0.606071
C	-0.934118	0.036766	2.379550
C	-1.517165	1.426323	2.546552
C	-2.898265	1.625722	2.554986
C	-3.437419	2.903502	2.738703
C	-2.616414	4.024570	2.913709

C	-1.224684	3.807856	2.901026
C	-0.682857	2.539096	2.723980
C	-3.170942	5.447003	3.111694
C	-4.710756	5.482521	3.098320
C	-1.538589	0.097506	-0.683401
H	-2.190821	-0.731254	-0.385484
C	-2.686840	6.002056	4.472688
C	-2.656531	6.361222	1.973725
H	-2.040429	1.027230	-0.394148
H	1.380988	-0.109972	-1.643822
H	-1.725435	-0.699894	2.213003
H	-0.374622	-0.271703	3.266709
H	0.396725	2.409907	2.720669
H	-0.546323	4.645480	3.034714
H	-4.516233	3.009340	2.738181
H	-3.567860	0.779141	2.421265
H	-3.066184	7.019968	4.622604
H	-3.047532	5.379973	5.300067
H	-1.594164	6.042034	4.532459
H	-5.054439	6.512667	3.243077
H	-5.119376	5.128262	2.145125
H	-5.140159	4.874400	3.902732

H	-3.040360	7.380092	2.104842
H	-1.563000	6.416751	1.956264
H	-2.991274	5.995651	0.995973
O	-1.352279	0.072263	-2.107208
C	-2.489550	0.133088	-2.841504
O	-3.593780	0.199894	-2.331221
C	-2.230500	0.108980	-4.305261
C	-3.336803	0.161978	-5.166340
C	-3.150115	0.142834	-6.546260
C	-1.857515	0.070729	-7.074509
C	-0.752470	0.017850	-6.220205
C	-0.934511	0.036626	-4.838227
H	-4.332624	0.217348	-4.739481
H	-4.009117	0.184032	-7.209503
H	-1.711529	0.055907	-8.150978
H	0.251407	-0.037833	-6.630868
H	-0.078613	-0.004209	-4.174276



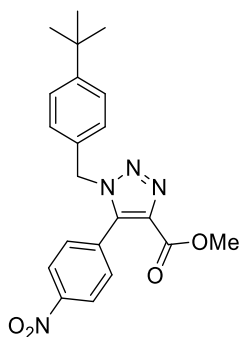
### Alkyne 2.3

No imaginary frequencies

Total energy (ZPE corrected, Hartrees): -740.624778

C	1.409646	0.211171	0.000000
C	0.000000	0.181834	0.000000
C	-0.725236	1.391053	0.000000
C	-0.056285	2.607901	0.000000
C	1.338814	2.605308	0.000000
C	2.083563	1.425479	0.000000
C	-0.692344	-1.063615	0.000000
C	-1.281962	-2.124566	0.000000
C	-2.059729	-3.342670	0.000000
O	-3.277105	-3.369354	0.000000
O	-1.268175	-4.426751	0.000000
C	-1.954157	-5.698525	0.000000
H	-1.165117	-6.449068	0.000000
H	-2.576390	-5.792748	0.892786
H	-2.576390	-5.792748	-0.892786
H	-1.809190	1.366693	0.000000
H	-0.596994	3.545535	0.000000

N	2.047969	3.890005	0.000000
H	3.165161	1.466978	0.000000
H	1.966563	-0.719131	0.000000
O	3.280281	3.871457	0.000000
O	1.375338	4.922677	0.000000



Transition state for Methyl 1-(4-t-butylbenzyl)-5-(4-nitrophenyl)-1,2,3-triazole-4-carboxylate

1 imaginary frequency:  $-389.930 \text{ cm}^{-1}$

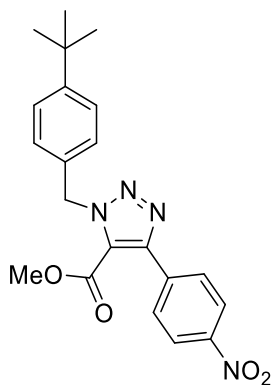
Total energy (ZPE corrected, Hartrees):  $-1332.75292$

C	-3.015219	-0.677635	-1.477896
C	-2.051116	0.016130	-0.737574
C	-2.479610	0.796432	0.340037
C	-3.833487	0.878260	0.670843
C	-4.810387	0.187627	-0.062721
C	-4.365948	-0.589743	-1.146410
C	-0.583277	-0.093284	-1.089876
N	0.167315	-0.975312	-0.162938



N	0.016643	-2.218968	-0.227318
N	0.595126	-3.214871	-0.034602
C	-6.312106	0.255387	0.270144
C	-6.834721	-1.168712	0.576519
C	-6.602825	1.147285	1.492096
C	-7.080942	0.831652	-0.942872
C	2.298993	-1.006504	0.164277
C	2.526932	-2.225717	0.287242
C	3.341842	-3.377838	0.626689
O	3.630631	-3.699637	1.764903
C	2.642183	0.391897	0.111106
C	2.023044	1.329304	0.961153
C	2.395603	2.666538	0.923723
C	3.387667	3.064472	0.026030
C	4.015285	2.159990	-0.831000
C	3.639411	0.823349	-0.786385
O	3.723504	-4.047031	-0.474767
C	4.537521	-5.216552	-0.242617
H	-0.086572	0.874642	-0.989640
H	-0.449856	-0.439098	-2.120525
H	4.745139	-5.622432	-1.231917
H	5.466604	-4.940854	0.261588

H	3.993534	-5.943869	0.364491
H	-2.709666	-1.288748	-2.324186
H	-5.083551	-1.138751	-1.749359
H	-4.119466	1.497316	1.513696
H	-1.751797	1.348872	0.929978
H	-8.154227	0.879742	-0.722851
H	-6.737070	1.845423	-1.178996
H	-6.951028	0.214570	-1.838099
H	-7.680879	1.159656	1.687816
H	-6.106631	0.776179	2.396136
H	-6.284811	2.183008	1.327181
H	-7.906276	-1.136440	0.807468
H	-6.696639	-1.845800	-0.273030
H	-6.314034	-1.600162	1.439317
H	4.115703	0.104685	-1.444089
H	4.780042	2.503609	-1.515806
N	3.779835	4.473800	-0.018459
H	1.931100	3.395601	1.575279
H	1.253797	0.999649	1.650499
O	3.211718	5.259567	0.743978
O	4.659283	4.807930	-0.816211



Transition state for Methyl 1-(4-t-butylbenzyl)-4-(4-nitrophenyl)-1,2,3-triazole-5-carboxylate

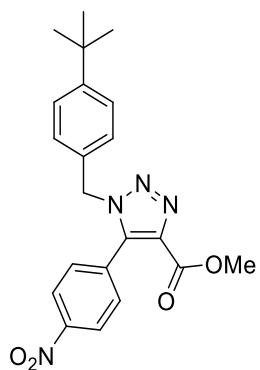
1 imaginary frequency  $-359.980 \text{ cm}^{-1}$

Total energy (ZPE corrected, Hartrees):  $-1332.752645$

C	4.100434	-0.741703	-1.143672
C	3.459072	-0.103629	-0.062378
C	4.107646	-0.047196	1.189741
C	5.365099	-0.610891	1.357204
C	5.980135	-1.226155	0.265393
C	5.362771	-1.295586	-0.985383
C	2.169441	0.503246	-0.216079
C	1.282652	1.375986	-0.163599
C	0.832383	2.733004	0.141662
O	-0.277103	3.046807	0.531976
O	1.836303	3.604482	-0.055291
C	1.528475	4.986207	0.233831

N	0.944929	-1.275174	-0.994645
N	-0.046243	-0.663673	-1.026483
N	-0.537154	0.438704	-0.698130
C	-1.720215	0.982905	-1.407992
C	-3.020263	0.416839	-0.879488
C	-3.499565	0.789355	0.379993
C	-4.692387	0.260738	0.875953
C	-5.452815	-0.656127	0.132911
C	-4.960250	-1.018911	-1.132632
C	-3.766974	-0.497055	-1.630287
C	-6.773333	-1.259152	0.645863
C	-6.644163	-2.799972	0.711013
C	-7.143608	-0.749070	2.051644
C	-7.920879	-0.883169	-0.321839
H	-1.661794	2.055631	-1.218427
H	-1.620958	0.813352	-2.484697
H	2.440906	5.535767	0.006576
H	0.704124	5.329961	-0.394975
H	1.260435	5.102488	1.286289
H	-3.416932	-0.801916	-2.614089
H	-5.513180	-1.722892	-1.748102
H	-5.026524	0.578791	1.857290

H	-2.932867	1.498148	0.979177
H	-8.866576	-1.316288	0.025876
H	-8.045686	0.204541	-0.377619
H	-7.737199	-1.253368	-1.335879
H	-8.084165	-1.210349	2.372681
H	-6.378730	-1.006157	2.793215
H	-7.285528	0.337521	2.067881
H	-7.583321	-3.243743	1.062785
H	-6.417479	-3.232858	-0.268935
H	-5.847680	-3.097552	1.402971
H	3.617877	0.440602	2.025292
H	5.870970	-0.573942	2.313654
N	7.305257	-1.815556	0.436502
H	5.866604	-1.783260	-1.810182
H	3.599756	-0.799456	-2.103308
O	7.835043	-2.353434	-0.540117
O	7.834317	-1.748245	1.549764



Methyl 1-(4-t-butylbenzyl)-5-(4-nitrophenyl)-1,2,3-triazole-4-carboxylate

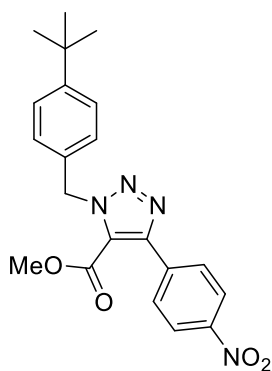
No imaginary frequencies

Total energy (Hartrees): -1333.295956

C	1.465565	0.950640	0.848801
C	1.723545	0.430633	-0.429794
C	2.040030	1.303387	-1.483849
C	2.087909	2.677694	-1.271588
C	1.817314	3.165121	0.005502
C	1.508959	2.321574	1.072681
C	1.664414	-1.025729	-0.661722
N	0.806412	-1.623917	-1.528955
N	0.991692	-2.968192	-1.541578
N	1.954261	-3.248261	-0.715034
C	2.399693	-2.091528	-0.144585
C	-0.312193	-1.056863	-2.302238
C	-1.554718	-0.827584	-1.465565
C	-2.202255	-1.897005	-0.831536
C	-3.356299	-1.682113	-0.085269
C	-3.918006	-0.398579	0.057668
C	-3.261226	0.659608	-0.583386
C	-2.097253	0.450733	-1.330098
C	-5.200207	-0.208660	0.888114

C	-4.946219	-0.676764	2.341154
C	3.516313	-2.033451	0.819640
O	3.928242	-1.001915	1.321517
O	4.022748	-3.249877	1.075271
C	5.118876	-3.284168	2.011387
C	-5.658126	1.261450	0.929420
C	-6.341092	-1.052949	0.271228
H	0.025186	-0.127642	-2.762742
H	-0.492621	-1.781579	-3.099789
H	5.391697	-4.335266	2.096801
H	5.960399	-2.698496	1.633985
H	4.804939	-2.888885	2.980304
H	-1.799006	-2.902570	-0.921616
H	-3.830113	-2.535958	0.390465
H	-3.646994	1.669945	-0.508066
H	-1.614979	1.297796	-1.812066
H	-7.259039	-0.934447	0.859341
H	-6.552661	-0.734886	-0.756267
H	-6.094295	-2.119568	0.249521
H	-6.570825	1.343787	1.529910
H	-4.902460	1.911787	1.384644
H	-5.884101	1.646788	-0.071309

H	-5.855993	-0.554445	2.941042
H	-4.656404	-1.731781	2.385720
H	-4.149072	-0.087645	2.809264
H	2.269980	0.908243	-2.468002
H	2.334911	3.361226	-2.073671
N	1.863258	4.613228	0.235984
H	1.307347	2.737189	2.051615
H	1.229201	0.279107	1.666123
O	1.625183	5.027263	1.372170
O	2.137001	5.343854	-0.718196



Methyl 1-(4-t-butylbenzyl)-4-(4-nitrophenyl)-1,2,3-triazole-5-carboxylate

No imaginary frequencies

Total energy (Hartrees): -1333.296329

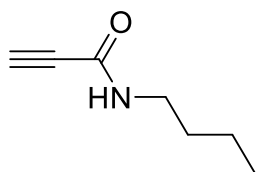
C	-3.142655	0.714982	0.504408
C	-3.001749	-0.274574	-0.484748
C	-4.123687	-0.626172	-1.262799
C	-5.354633	-0.019894	-1.055385



C	-5.463994	0.951917	-0.059431
C	-4.372318	1.327551	0.721766
C	-1.721192	-0.940188	-0.779852
C	-0.594519	-1.254870	-0.010054
N	0.219735	-1.938325	-0.870760
N	-0.346297	-2.023993	-2.083635
N	-1.514565	-1.446746	-2.031722
C	-0.288062	-1.027637	1.422144
O	-0.676325	-0.069689	2.063812
C	1.593856	-2.451200	-0.709090
C	2.621589	-1.350022	-0.545943
C	3.503810	-1.354931	0.534994
C	4.479511	-0.361867	0.668989
C	4.601822	0.673884	-0.266142
C	3.703013	0.666807	-1.350194
C	2.735855	-0.322878	-1.493094
C	5.657088	1.788361	-0.150951
C	4.946992	3.160256	-0.058464
C	6.548801	1.623633	1.094351
C	6.565989	1.766228	-1.403269
O	0.453784	-2.018523	1.935664
C	0.829629	-1.872452	3.324955

H	1.607268	-3.132926	0.140341
H	1.767187	-3.027851	-1.621005
H	1.421494	-2.756917	3.554361
H	1.420648	-0.964375	3.459512
H	-0.063405	-1.830778	3.951259
H	2.063574	-0.296142	-2.347349
H	3.758404	1.446630	-2.104321
H	5.143062	-0.409034	1.525143
H	3.438924	-2.141947	1.281948
H	7.319760	2.559955	-1.337035
H	7.089259	0.806999	-1.490785
H	5.995725	1.924351	-2.324708
H	7.281366	2.437524	1.129627
H	5.966178	1.662538	2.021788
H	7.103928	0.678838	1.077499
H	5.688017	3.965257	0.015610
H	4.325803	3.358920	-0.938096
H	4.302895	3.208997	0.827215
H	-4.019857	-1.383390	-2.030940
H	-6.220428	-0.291642	-1.645731
N	-6.758472	1.594202	0.168591
H	-4.487397	2.091815	1.479934

H	-2.287540	1.001826	1.101380
O	-6.835969	2.452984	1.051206
O	-7.712561	1.246951	-0.532695



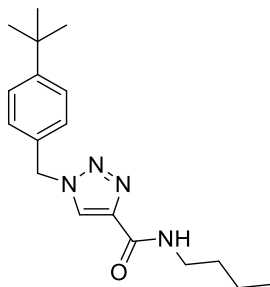
#### Alkyne 2.4

No imaginary frequencies

Total energy (ZPE corrected, Hartrees): -403.124843

C	0.132243	4.148408	-0.006818
C	-0.129727	2.992781	0.232630
C	-0.461494	1.614728	0.589268
O	-0.869690	1.323838	1.716615
N	-0.293127	0.723565	-0.418723
C	-0.523053	-0.708994	-0.256798
C	0.747179	-1.490830	0.105271
C	0.485017	-2.995400	0.247882
C	1.744002	-3.787416	0.615287
H	-1.277376	-0.827123	0.525398
H	-0.948862	-1.085607	-1.193191
H	0.364630	5.169398	-0.220783
H	0.096758	1.056865	-1.290930
H	1.510051	-1.318982	-0.666569
H	1.151961	-1.091569	1.044605
H	-0.286914	-3.157976	1.013010

H	0.070172	-3.382427	-0.693439
H	1.526524	-4.857232	0.711054
H	2.521629	-3.671227	-0.149575
H	2.162593	-3.444334	1.569342



Transition state for N-butyl 1-(4-t-butylbenzyl)-1,2,3-triazole-4-carboxamide

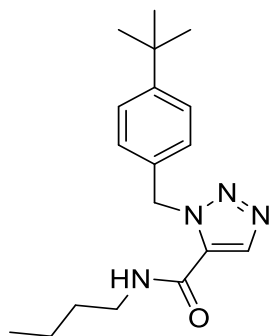
1 imaginary frequency:  $-409.252 \text{ cm}^{-1}$

Total energy (ZPE corrected, Hartrees):  $-995.256322$

C	0.021352	-0.017185	0.007876
C	-0.000822	-0.007940	1.411282
C	1.177264	0.025822	2.159270
C	2.425634	0.048595	1.530538
C	2.462003	0.038797	0.131762
C	1.283008	0.008416	-0.611367
C	3.706269	0.070197	2.337599
N	4.008956	-1.228106	2.983544
N	4.402822	-2.196997	2.287625
N	5.054790	-3.160928	2.352910
C	-1.257455	-0.050291	-0.848749

C	-2.536466	-0.080850	0.009465
C	-1.307668	1.209698	-1.745744
C	-1.244554	-1.314026	-1.741737
C	5.276568	-1.530800	4.636853
C	5.852971	-2.609843	4.443143
C	6.665128	-3.795531	4.719091
N	7.779437	-3.912835	3.951203
C	8.690782	-5.047554	4.052477
C	8.324380	-6.212873	3.122753
C	9.306054	-7.385306	3.239043
C	8.950184	-8.556882	2.317962
O	6.353005	-4.598628	5.603838
H	4.992666	-0.633415	5.147435
H	3.621890	0.765851	3.176845
H	4.553359	0.388137	1.719658
H	9.700083	-4.684855	3.828484
H	8.679932	-5.379237	5.094281
H	3.419754	0.058826	-0.383414
H	1.355812	0.006107	-1.695348
H	-0.945798	-0.022288	1.942817
H	1.120112	0.033263	3.245366
H	-2.208629	1.194387	-2.370844

H	-1.331414	2.121953	-1.138270
H	-0.440449	1.271036	-2.411518
H	-3.415783	-0.107097	-0.643766
H	-2.575531	-0.967187	0.652874
H	-2.623253	0.807794	0.645023
H	-2.146968	-1.347531	-2.364009
H	-0.377544	-1.332421	-2.410330
H	-1.218959	-2.224494	-1.131708
H	7.889095	-3.271221	3.177035
H	7.308240	-6.550414	3.366160
H	8.298280	-5.852398	2.084985
H	10.321401	-7.033330	3.007622
H	9.332928	-7.733939	4.281021
H	9.669951	-9.376862	2.421478
H	7.954642	-8.954594	2.550183
H	8.946386	-8.246042	1.266002



Transition state for N-butyl 1-(4-t-butylbenzyl)-1,2,3-triazole-5-carboxamide

1 imaginary frequency: -431.708 cm<sup>-1</sup>

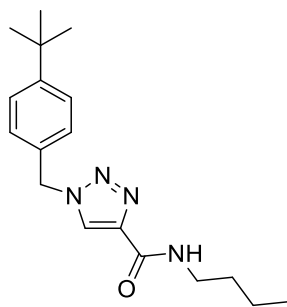
Total energy (ZPE corrected, Hartrees): -995.255368

C	0.000000	0.000000	0.000000
C	0.000000	0.000000	1.406023
C	1.250086	0.000000	2.043332
C	2.440702	-0.001304	1.313579
C	2.427274	-0.004243	-0.083954
C	1.186199	-0.003349	-0.731522
C	-1.332916	0.004685	2.176662
C	-2.148693	-1.254651	1.798489
C	3.716410	-0.029995	-0.877191
N	4.321415	-1.378965	-0.949209
N	3.895755	-2.225449	-1.768864
N	4.269394	-3.155555	-2.378443
C	-1.127512	0.003708	3.703442
C	-2.140954	1.269332	1.798857
C	6.345124	-2.971354	-1.929811
C	6.450467	-2.000607	-1.168850
C	7.044996	-0.976561	-0.300794
O	6.995836	0.227743	-0.569365
N	7.664246	-1.483050	0.795315
C	8.270921	-0.643860	1.824295



C	7.328197	-0.348895	2.999174
C	7.991451	0.516355	4.078094
C	7.058441	0.821661	5.254371
H	6.668223	-3.800700	-2.523765
H	4.490339	0.570893	-0.394443
H	3.564624	0.365994	-1.887296
H	9.174772	-1.151015	2.179576
H	8.577830	0.286815	1.340478
H	1.145042	-0.002224	-1.818624
H	-0.941975	0.003451	-0.541410
H	1.311266	0.006014	3.125904
H	3.391155	0.000055	1.842950
H	-3.097803	1.281613	2.334577
H	-1.591137	2.179601	2.065031
H	-2.358857	1.308914	0.726341
H	-2.101997	0.005907	4.204325
H	-0.583785	-0.885534	4.042333
H	-0.579435	0.890199	4.042321
H	-3.107423	-1.259403	2.331021
H	-2.362735	-1.294589	0.725319
H	-1.605857	-2.168175	2.067935
H	7.611972	-2.480964	0.952060

H	6.431874	0.156152	2.614517
H	6.992032	-1.297758	3.439681
H	8.892926	0.007715	4.447729
H	8.333842	1.458586	3.627792
H	7.558955	1.439355	6.008654
H	6.164119	1.361355	4.919674
H	6.725468	-0.101217	5.744904



N-butyl 1-(4-t-butylbenzyl)-1,2,3-triazole-4-carboxamide

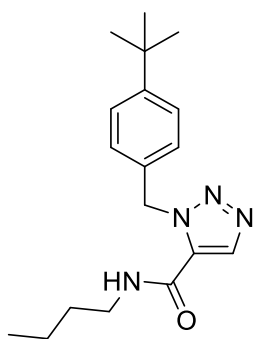
No imaginary frequencies

Total energy (Hartrees): -995.823576

C	0.069086	0.476162	0.376710
C	0.066406	-0.152772	1.629678
C	1.256847	-0.714154	2.091642
C	2.424426	-0.653140	1.323676
C	2.443285	-0.024576	0.072147
C	1.234300	0.539085	-0.380196
C	-1.200583	-0.232281	2.455475
N	-1.704905	1.088651	2.857808

N	-2.781773	1.621857	2.230882
N	-2.988459	2.803020	2.746242
C	-2.047794	3.042559	3.706298
C	-1.215445	1.942781	3.781370
C	-1.980579	4.293392	4.503836
N	-2.932818	5.205382	4.205266
C	-3.018259	6.500948	4.870593
C	3.707324	0.070246	-0.800716
C	4.924822	-0.607623	-0.143983
C	3.446310	-0.618380	-2.161932
C	4.054414	1.559335	-1.039751
O	-1.111707	4.462455	5.367246
H	-0.356979	1.722157	4.395573
H	-1.040221	-0.819852	3.362669
H	-2.019743	-0.688956	1.894580
C	-4.251472	7.273030	4.401932
H	-3.054010	6.341549	5.955479
H	-2.106282	7.077958	4.666136
H	-0.845949	0.921708	-0.006428
H	1.196933	1.035394	-1.345686
H	3.324918	-1.104748	1.724518
H	1.281183	-1.208889	3.059777

H	4.337530	-0.548624	-2.797006
H	3.208366	-1.679687	-2.025353
H	2.615020	-0.153535	-2.702449
H	5.795127	-0.513985	-0.802889
H	5.183643	-0.142302	0.813890
H	4.753836	-1.676229	0.029216
H	4.949940	1.642483	-1.667273
H	3.242257	2.091969	-1.545497
H	4.254976	2.071837	-0.091724
H	-3.591609	4.978920	3.470145
C	-4.378470	8.644878	5.075629
H	-4.203485	7.404694	3.311535
H	-5.151276	6.676880	4.608678
C	-5.609928	9.425043	4.604890
H	-4.423024	8.511099	6.165236
H	-3.472544	9.233075	4.874178
H	-5.674475	10.400128	5.100591
H	-5.576608	9.601186	3.522778
H	-6.533913	8.876251	4.824166



N-butyl 1-(4-t-butylbenzyl)-1,2,3-triazole-5-carboxamide

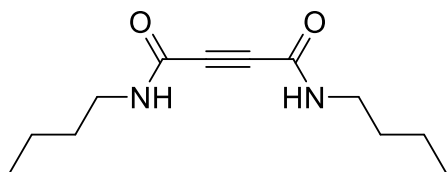
No imaginary frequencies

Total energy (Hartrees): -995.814556

C	0.586374	-0.049524	0.115091
N	0.364497	-0.025267	1.464078
N	1.536850	-0.003767	2.132545
N	2.507973	-0.003063	1.250934
C	1.965713	-0.042659	0.009951
C	-0.878779	-0.063904	2.244493
C	-1.536762	1.293813	2.415010
C	-2.920178	1.429449	2.270392
C	-3.544905	2.664771	2.473136
C	-2.812000	3.805491	2.823268
C	-1.419210	3.652690	2.965287
C	-0.790882	2.427487	2.768226
C	-3.462081	5.181437	3.053080
C	-4.986801	5.151612	2.837561

C	-0.384716	-0.122767	-1.016304
N	-1.606480	0.431332	-0.829800
C	-2.636559	0.412272	-1.868234
C	-3.186688	5.639582	4.505499
C	-2.853750	6.208486	2.067830
O	-0.032020	-0.659200	-2.070315
H	2.567191	-0.060500	-0.886728
H	-1.559210	-0.772101	1.766128
H	-0.589353	-0.482796	3.212008
H	-3.225189	1.329010	-1.761927
H	-2.131740	0.447058	-2.837808
C	-3.546697	-0.820633	-1.788684
H	0.285977	2.349239	2.890393
H	-0.807123	4.507466	3.237798
H	-4.620213	2.720437	2.348445
H	-3.525032	0.565074	2.004705
H	-3.633283	6.625408	4.681571
H	-3.619746	4.936657	5.226609
H	-2.114296	5.717241	4.712974
H	-5.400757	6.150698	3.012820
H	-5.248597	4.859360	1.814239
H	-5.483452	4.461958	3.529465

H	-3.303636	7.195819	2.226425
H	-1.771504	6.310737	2.199687
H	-3.040589	5.913206	1.028803
H	-1.794876	0.959809	0.012985
C	-4.622454	-0.825481	-2.881906
H	-2.925980	-1.722299	-1.872930
H	-4.022156	-0.854078	-0.798823
C	-5.534832	-2.054488	-2.813301
H	-5.229536	0.087002	-2.799092
H	-4.138019	-0.783207	-3.867438
H	-6.290663	-2.033275	-3.606540
H	-4.958338	-2.980898	-2.924836
H	-6.060287	-2.103753	-1.851697



Alkyne **2.5**

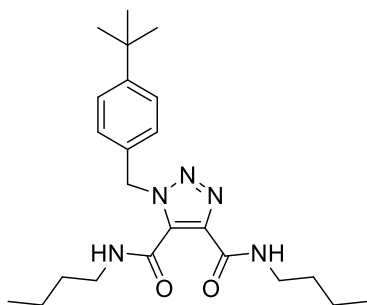
No imaginary frequencies

Total energy (ZPE corrected, Hartrees): -728.947501

C	0.039085	-0.728006	0.247996
C	0.128172	0.026608	1.578369
C	1.496247	-0.120198	2.256513
C	1.571104	0.641289	3.586898
N	2.871420	0.529542	4.242582
C	3.137482	-0.394358	5.196110
O	2.318767	-1.199370	5.646180
C	4.511851	-0.368305	5.694543
C	5.627511	-0.401814	6.168605
C	7.005236	-0.483670	6.651476
O	7.866191	-1.082323	6.002421
N	7.224329	0.153571	7.826023
C	8.521237	0.155966	8.497753
C	8.650372	-0.935534	9.568876
C	10.013153	-0.902025	10.272278
C	10.155990	-1.986003	11.345526



H	9.282574	0.023181	7.724988
H	8.664032	1.146656	8.942723
H	0.824842	0.258151	4.287446
H	1.368073	1.706101	3.429537
H	3.633446	1.106153	3.909170
H	6.432364	0.568884	8.299992
H	2.284311	0.247019	1.584719
H	1.708821	-1.181009	2.443635
H	-0.654672	-0.336189	2.258994
H	-0.081190	1.092288	1.410051
H	-0.948244	-0.606853	-0.211839
H	0.787680	-0.361833	-0.465226
H	0.212638	-1.801663	0.389972
H	7.847955	-0.812524	10.309289
H	8.497555	-1.914764	9.096341
H	10.810042	-1.018855	9.524593
H	10.162399	0.086880	10.727940
H	11.138420	-1.939178	11.828832
H	9.393399	-1.872850	12.125792
H	10.043087	-2.987736	10.913320



Transition state for N,N'-Bis-(n-butyl) 1-(4-t-butylbenzyl)-1,2,3-triazole-4,5-dicarboxamide **2.5a**

1 imaginary frequency:  $-344.053 \text{ cm}^{-1}$

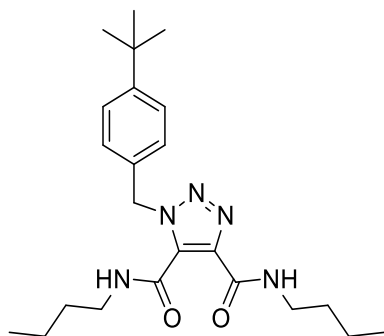
Total energy (ZPE corrected, Hartrees):  $-1321.078916$

C	-5.444902	-0.871222	-0.075798
C	-4.604500	-0.104949	0.747744
C	-3.329915	0.282461	0.331085
C	-2.846875	-0.086847	-0.928217
C	-3.671367	-0.853577	-1.757799
C	-4.945358	-1.234773	-1.338115
C	-1.461043	0.330600	-1.372819
N	-0.390734	-0.354772	-0.619200
N	0.008454	-1.497990	-0.911994
N	0.887560	-2.240908	-0.708541
C	-6.858896	-1.310143	0.347247
C	-7.226255	-0.821705	1.761425
C	-7.894593	-0.732669	-0.647243
C	-6.944690	-2.855231	0.333125

C	1.365953	0.269449	0.465162
C	2.073089	-0.751932	0.508629
C	3.225234	-1.549537	0.959876
N	3.810019	-2.306163	0.001425
C	5.016494	-3.094964	0.224209
C	6.271598	-2.462949	-0.392122
C	7.524164	-3.321311	-0.175493
C	8.785514	-2.700248	-0.784162
C	1.001613	1.667632	0.762351
N	2.077257	2.494225	0.789041
C	1.972782	3.929611	1.037144
C	1.947289	4.763784	-0.250650
C	1.859047	6.269227	0.030057
C	1.838870	7.113172	-1.248501
O	-0.153514	2.037151	0.988125
O	3.606932	-1.487188	2.131845
H	-1.291264	1.386546	-1.155554
H	-1.322692	0.169870	-2.446714
H	2.821639	4.222950	1.664798
H	1.058662	4.090107	1.613710
H	5.132394	-3.199924	1.305608
H	4.853179	-4.095642	-0.193321

H	-3.318720	-1.153240	-2.742328
H	-5.556942	-1.826629	-2.013295
H	-4.939978	0.205036	1.731278
H	-2.698735	0.875109	0.988723
H	-8.906982	-1.046065	-0.365074
H	-7.866641	0.363225	-0.649601
H	-7.712238	-1.076153	-1.670979
H	-8.237121	-1.160147	2.014746
H	-6.543894	-1.219794	2.521047
H	-7.216269	0.271949	1.831418
H	-7.951071	-3.181712	0.621932
H	-6.733109	-3.266234	-0.659543
H	-6.229706	-3.294074	1.038780
H	6.109298	-2.311287	-1.468467
H	6.419835	-1.467239	0.047142
H	7.675287	-3.476926	0.901907
H	7.360529	-4.317912	-0.609056
H	9.662808	-3.334501	-0.613686
H	8.676430	-2.564293	-1.867153
H	8.993247	-1.716758	-0.345168
H	2.850578	4.549142	-0.838282
H	1.090803	4.446569	-0.860393

H	0.955522	6.475727	0.620501
H	2.710351	6.572292	0.655643
H	1.776239	8.182604	-1.017577
H	2.746510	6.951637	-1.842809
H	0.978745	6.855975	-1.878700
H	2.982786	2.109143	0.554639
H	3.375762	-2.323081	-0.911856



N,N'-Bis-(n-butyl) 1-(4-t-butylbenzyl)-1,2,3-triazole-4,5-dicarboxamide **2.5a**

No imaginary frequencies

Total energy (Hartrees): -1321.791654

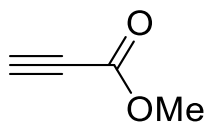
C	-1.597100	-0.597137	1.221238
N	-1.102010	-1.499391	2.111478
N	0.040678	-1.073277	2.568517
N	0.301447	0.111744	1.990363
C	-0.693094	0.469363	1.125771
C	1.601839	0.747197	2.310271

C	2.712814	0.289044	1.387416
C	3.099657	1.055899	0.285429
C	4.128263	0.625881	-0.557955
C	4.803734	-0.582236	-0.335652
C	4.402400	-1.344062	0.777566
C	3.381246	-0.919757	1.623208
C	5.936624	-1.089174	-1.246074
C	7.225562	-1.275916	-0.410324
C	-0.671443	1.784646	0.393738
O	0.191003	2.638377	0.649424
C	-2.903350	-0.882068	0.558751
O	-3.384427	-0.160499	-0.333784
C	5.526397	-2.447638	-1.863676
C	6.246029	-0.111655	-2.395767
N	-3.517331	-1.991333	1.013530
C	-4.764027	-2.505477	0.456793
N	-1.628846	1.943422	-0.534284
C	-1.768052	3.184308	-1.289346
H	1.448636	1.820716	2.251648
H	1.804736	0.454804	3.342166
H	-2.219279	2.928723	-2.254018
C	-2.618357	4.240885	-0.568803

H	-0.765361	3.577350	-1.481699
C	-4.545531	-3.581149	-0.616283
H	-5.356371	-2.909416	1.285024
H	-5.308669	-1.655278	0.038687
H	3.099681	-1.534448	2.474792
H	4.896209	-2.286810	0.995907
H	4.396781	1.255280	-1.399271
H	2.589054	1.992135	0.080660
H	8.039198	-1.644050	-1.046830
H	7.545482	-0.326447	0.034583
H	7.085360	-1.997417	0.401396
H	7.058092	-0.514524	-3.011222
H	5.378858	0.037456	-3.048988
H	6.567064	0.867781	-2.023297
H	6.329127	-2.830003	-2.505708
H	5.325654	-3.201289	-1.094949
H	4.623039	-2.342137	-2.475719
H	-3.020941	-2.537461	1.708127
H	-2.351453	1.217041	-0.617766
C	-5.866000	-4.130386	-1.170426
H	-3.948214	-3.151375	-1.431370
H	-3.953114	-4.401984	-0.188992

C	-5.659487	-5.203727	-2.244072
H	-6.461052	-4.546740	-0.345466
H	-6.456832	-3.303001	-1.587768
H	-6.617961	-5.577601	-2.621577
H	-5.095876	-4.806280	-3.096930
H	-5.100151	-6.058927	-1.845523
C	-2.767281	5.529726	-1.386449
H	-3.610084	3.819410	-0.354767
H	-2.152860	4.465580	0.399559
C	-3.610928	6.592833	-0.675277
H	-1.770442	5.938467	-1.603819
H	-3.220341	5.292806	-2.359425
H	-3.697158	7.502556	-1.280313
H	-4.625332	6.225427	-0.477200
H	-3.165144	6.872084	0.287260



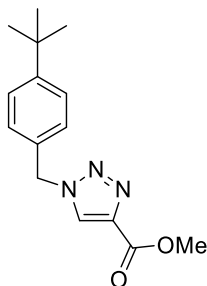


Alkyne **2.6**

No imaginary frequencies

Total energy (ZPE corrected, Hartrees): -305.136176

C	0.000000	0.314943	0.000000
C	1.447395	0.241783	0.000000
O	-0.546588	-0.909451	0.000000
O	-0.625566	1.358160	0.000000
C	-1.991510	-0.947294	0.000000
H	-2.249956	-2.005141	0.000000
H	-2.382330	-0.454470	0.892899
H	-2.382330	-0.454470	-0.892899
C	2.655331	0.238952	0.000000
H	3.724552	0.234107	0.000000



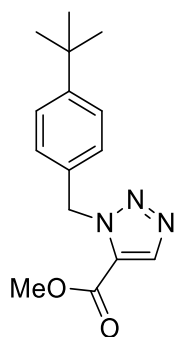
Transition state for methyl 1-(4-t-butylbenzyl)-1,2,3-triazole-4-carboxylate

1 imaginary frequency: -406.250 cm<sup>-1</sup>

Total energy (ZPE corrected, Hartrees): -897.269852

C	-0.070380	0.153489	-0.190743
C	0.211273	0.248495	1.175151
C	1.499755	0.635222	1.560737
C	2.473420	0.918534	0.604532
C	2.204688	0.824901	-0.772056
C	0.908910	0.435042	-1.144870
C	-0.841823	-0.071814	2.213741
N	-1.103714	-1.525998	2.341914
N	-0.256318	-2.269561	2.894532
N	-0.151253	-3.249077	3.512135
C	3.308988	1.149498	-1.795049
C	4.513008	0.203928	-1.569400
C	2.830169	0.978450	-3.249109
C	3.767654	2.615348	-1.606167
C	-2.819371	-2.385229	3.170233
C	-2.445724	-3.388184	3.791899
C	-2.459426	-4.630542	4.528428
O	-2.242600	-4.424687	5.842084
C	-2.236070	-5.610613	6.663131
H	-3.510862	-1.676229	2.762225
O	-2.638166	-5.726771	4.026497
H	-1.810888	0.342963	1.924457

H	-0.572072	0.346379	3.189574
H	-2.054756	-5.256776	7.677470
H	-3.198863	-6.123581	6.602984
H	-1.440718	-6.289660	6.346604
H	1.744491	0.719944	2.617169
H	3.460344	1.219370	0.944068
H	0.644448	0.349725	-2.192797
H	-1.064373	-0.143972	-0.516997
H	4.560243	2.859604	-2.323697
H	2.935722	3.310232	-1.769684
H	4.161823	2.792644	-0.600014
H	3.650348	1.217856	-3.935007
H	2.514675	-0.050423	-3.456533
H	1.995040	1.647456	-3.486079
H	5.311033	0.429771	-2.286921
H	4.931091	0.307777	-0.562689
H	4.219695	-0.843395	-1.706117



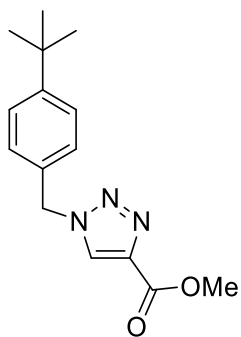
Transition state for methyl 1-(4-t-butylbenzyl)-1,2,3-triazole-5-carboxylate

1 imaginary frequency: -439.311 cm<sup>-1</sup>

Total energy (ZPE corrected, Hartrees): -897.267323

C	0.174236	0.107645	0.165708
C	0.336835	0.124637	1.551991
C	1.609566	0.054076	2.126016
C	2.716178	-0.031381	1.274031
C	2.549655	-0.042340	-0.109948
C	1.275851	0.024352	-0.700165
C	1.788540	0.055118	3.629279
N	1.358996	-1.215245	4.259592
N	2.112676	-2.215138	4.234050
N	2.385737	-3.157167	4.878376
C	1.137044	0.007090	-2.233464
C	1.885876	1.222666	-2.830781
C	1.754861	-1.297466	-2.791465
C	-0.332778	0.075228	-2.689846
C	1.364747	-2.655444	6.621996
C	0.783164	-1.584509	6.402444
C	-0.004191	-0.376986	6.567809
O	0.466261	0.723827	6.795169
O	-1.316986	-0.629403	6.434366

C	-2.188393	0.514239	6.572156
H	1.658989	-3.504319	7.204508
H	1.150052	0.807925	4.098868
H	2.825566	0.277562	3.902058
H	-3.195500	0.126271	6.425647
H	-2.085959	0.952115	7.567577
H	-1.951525	1.265717	5.815441
H	3.718029	-0.085449	1.694179
H	3.434082	-0.103844	-0.737576
H	-0.831808	0.164692	-0.234391
H	-0.539933	0.191606	2.192163
H	1.801607	1.218902	-3.924208
H	1.463584	2.164249	-2.460859
H	2.951449	1.209580	-2.578092
H	-0.377745	0.055818	-3.784461
H	-0.914856	-0.776422	-2.319617
H	-0.823101	0.996495	-2.355189
H	1.666726	-1.320409	-3.884339
H	2.817160	-1.386110	-2.540866
H	1.239346	-2.177931	-2.390640



Methyl 1-(4-t-butylbenzyl)-1,2,3-triazole-4-carboxylate

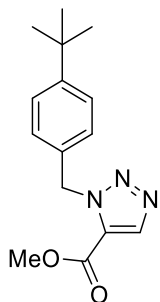
No imaginary frequencies

Total energy (Hartrees): -897.737154

C	0.123178	0.074245	0.193140
N	0.377219	0.992148	1.174011
N	1.663012	1.050131	1.370487
N	2.253088	0.171758	0.516533
C	1.328235	-0.458117	-0.230990
C	3.713511	-0.004693	0.534651
C	4.139757	-1.321963	1.147001
C	4.779856	-2.294014	0.377620
C	5.184446	-3.506239	0.946033
C	4.958615	-3.789865	2.299041
C	4.309787	-2.799844	3.062407
C	3.909785	-1.590586	2.503543
C	5.385711	-5.112784	2.960316
C	6.370440	-4.814730	4.116380

H	1.571266	-1.201037	-0.974251
C	-1.212685	-0.276632	-0.320593
O	-1.393800	-1.103366	-1.198495
C	4.136665	-5.831295	3.524328
C	6.081175	-6.064911	1.969091
O	-2.193476	0.412207	0.283877
C	-3.530764	0.120631	-0.169147
H	4.074370	0.083948	-0.492861
H	4.092050	0.847627	1.103947
H	-4.181946	0.765663	0.419527
H	-3.629851	0.344378	-1.233993
H	-3.771829	-0.930494	0.006307
H	3.412468	-0.849130	3.124451
H	4.114557	-2.972010	4.116934
H	5.680706	-4.230321	0.309823
H	4.972201	-2.108899	-0.676695
H	6.681688	-5.749388	4.598135
H	7.268971	-4.308329	3.745166
H	5.918212	-4.178494	4.884389
H	6.364444	-6.988391	2.486189
H	5.422822	-6.340326	1.137316
H	6.994390	-5.625173	1.552347

H	4.427523	-6.773656	4.003943
H	3.617643	-5.222446	4.272049
H	3.423870	-6.063717	2.724571



Methyl 1-(4-t-butylbenzyl)-1,2,3-triazole-5-carboxylate

No imaginary frequencies

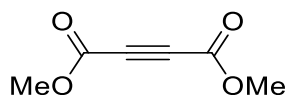
Total energy (Hartrees): -897.732842

C	-1.923531	1.127717	-0.756932
C	-0.629801	0.912246	-1.241969
C	-0.033413	-0.345999	-1.154593
C	-0.761993	-1.387563	-0.564190
C	-2.045700	-1.165336	-0.075495
C	-2.662297	0.097571	-0.160521
C	1.349814	-0.587245	-1.726928
N	2.284087	-1.180167	-0.754367
N	2.464031	-2.510432	-0.776336
N	3.278879	-2.836380	0.204201
C	-4.086190	0.297102	0.388834



C	-5.060341	-0.650208	-0.352054
C	-4.105309	-0.031913	1.900996
C	-4.587568	1.741907	0.204170
C	3.622740	-1.709212	0.867106
C	2.995992	-0.626299	0.273660
C	3.123021	0.788168	0.670414
O	3.752871	1.131595	1.653530
O	2.492961	1.631626	-0.159964
C	2.586358	3.034019	0.176284
H	4.294049	-1.712691	1.713068
H	1.789451	0.338813	-2.094362
H	1.318023	-1.308042	-2.547825
H	2.020599	3.552747	-0.595863
H	2.150824	3.213986	1.161246
H	3.630560	3.353240	0.170345
H	-0.320635	-2.377861	-0.484314
H	-2.577064	-1.997781	0.376850
H	-2.346316	2.121835	-0.848903
H	-0.085492	1.737136	-1.694241
H	-6.078329	-0.524791	0.036129
H	-5.077339	-0.432925	-1.426400
H	-4.782826	-1.701901	-0.225486

H	-5.602091	1.832337	0.608056
H	-3.955380	2.464359	0.732841
H	-4.625384	2.028752	-0.852915
H	-5.116820	0.100324	2.303453
H	-3.799916	-1.064946	2.097864
H	-3.430073	0.630519	2.455053

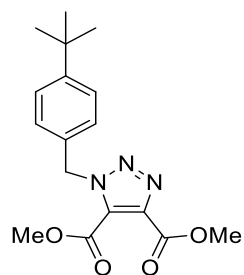


Alkyne **2.7**

No imaginary frequencies

Total energy (ZPE corrected, Hartrees): -532.968994

C	0.000000	0.000000	0.000000
C	0.000000	0.000000	1.451711
O	1.246808	0.000000	1.932261
O	-1.018375	-0.000651	2.114529
C	1.362156	0.002348	3.375207
H	2.432347	0.003588	3.574679
H	0.890116	0.896415	3.787746
H	0.891291	-0.890953	3.790621
C	-0.079024	-0.009106	-1.208381
C	-0.157642	0.068747	-2.655890
O	-0.182200	-1.150628	-3.201877
O	-0.193601	1.120843	-3.262879
C	-0.259252	-1.188504	-4.647006
H	-0.268073	-2.246448	-4.903443
H	-1.174699	-0.699712	-4.986677
H	0.610056	-0.691244	-5.082085



Transition state for dimethyl 1-(4-t-butylbenzyl)-1,2,3-triazole-4,5-dicarboxylate

### 2.7a

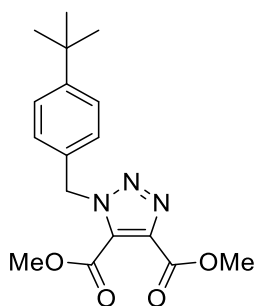
1 imaginary frequency:  $-344.444 \text{ cm}^{-1}$

Total energy (ZPE corrected, Hartrees):  $-1125.103195$

C	-0.008054	0.129577	-0.059701
N	0.333120	0.338523	1.371522
N	1.469962	0.742210	1.700024
N	2.059864	1.300777	2.531198
C	-0.752228	1.303856	2.862841
C	-2.133380	0.938724	2.533714
O	-2.477686	-0.039738	1.898495
C	0.080963	1.832418	3.619522
C	0.652449	2.487837	4.775638
O	0.789055	1.948017	5.858690
O	1.010557	3.751100	4.495338
C	1.590764	4.491830	5.591225
O	-2.977371	1.842962	3.052425
C	-4.382020	1.591048	2.820835

H	-1.097571	0.170459	-0.071313
H	0.379554	0.960208	-0.657495
C	0.485892	-1.202741	-0.578325
H	-4.902397	2.420628	3.297100
H	-4.589575	1.568752	1.748783
H	-4.675269	0.640939	3.272580
H	1.814391	5.476812	5.183726
H	0.879621	4.570196	6.416627
H	2.503871	4.002912	5.938255
C	1.568829	-1.275961	-1.460742
C	2.021285	-2.508672	-1.929139
C	1.417299	-3.714680	-1.533652
C	0.333169	-3.626021	-0.646021
C	-0.126208	-2.394217	-0.177564
H	2.061498	-0.363342	-1.788841
H	2.862641	-2.524293	-2.616059
C	1.950688	-5.054904	-2.072615
H	-0.172245	-4.524462	-0.310130
H	-0.968988	-2.357909	0.508633
C	1.160524	-6.261543	-1.531710
C	1.849549	-5.065237	-3.616760
C	3.431723	-5.222031	-1.655921

H	2.231042	-6.013202	-4.014926
H	0.808495	-4.955116	-3.942019
H	2.431194	-4.255478	-4.069733
H	1.577087	-7.186801	-1.945033
H	1.218559	-6.331767	-0.439541
H	0.103157	-6.218528	-1.816783
H	3.828654	-6.169552	-2.039817
H	4.059361	-4.414545	-2.047345
H	3.533061	-5.228796	-0.564424



Dimethyl 1-(4-t-butylbenzyl)-1,2,3-triazole-4,5-dicarboxylate **2.7a**

No imaginary frequencies

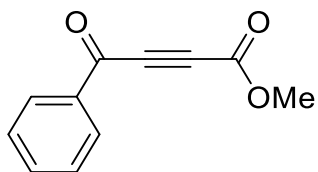
Total energy (Hartrees): -1125.607074

C	-0.004323	-0.007560	0.011293
C	-0.002960	0.003985	1.409222
C	1.228099	0.010292	2.074985
C	2.422386	0.005928	1.357909
C	2.438504	-0.007947	-0.048009

C	1.196727	-0.014790	-0.701302
C	-1.299070	0.013435	2.191345
N	-1.910156	-1.331339	2.290367
N	-1.338415	-2.244873	3.096658
N	-2.040369	-3.343629	3.030725
C	3.781617	-0.010950	-0.800395
C	4.598656	-1.258851	-0.388126
C	3.597764	-0.040875	-2.329638
C	4.577290	1.264946	-0.434225
C	-3.017876	-1.845463	1.694851
C	-3.086786	-3.148539	2.182731
C	-4.026098	-4.234161	1.811290
O	-4.047029	-5.201815	2.740048
C	-4.894286	-6.331154	2.443250
C	-3.875472	-1.061812	0.767908
O	-5.161646	-1.365441	0.925079
C	-6.084468	-0.698381	0.033354
O	-3.444544	-0.232836	-0.014208
O	-4.678878	-4.250591	0.785366
H	-2.042818	0.658007	1.725703
H	-1.134851	0.346721	3.217817
H	-7.065911	-1.090136	0.294570

H	-6.043607	0.381330	0.190609
H	-5.837628	-0.931479	-1.004438
H	-4.779159	-7.007592	3.289122
H	-5.933878	-6.009941	2.346241
H	-4.573125	-6.814177	1.517495
H	1.254517	0.021477	3.161874
H	3.357565	0.014695	1.910317
H	1.149878	-0.021777	-1.784533
H	-0.950338	-0.011913	-0.522863
H	5.540968	1.272964	-0.957597
H	4.026072	2.167033	-0.724200
H	4.780471	1.324895	0.640167
H	4.579621	-0.047159	-2.815691
H	3.059628	-0.937097	-2.658881
H	3.054141	0.838335	-2.693692
H	5.562463	-1.269476	-0.911160
H	4.803278	-1.275839	0.687399
H	4.063010	-2.180306	-0.644174





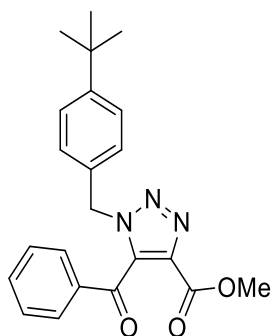
Alkyne **2.8**

No imaginary frequencies

Total energy (ZPE corrected, Hartrees): -649.435726

C	0.008279	0.007777	-0.003712
C	0.002282	-0.004004	1.400237
C	1.218709	-0.008296	2.104451
C	2.423843	-0.001035	1.410893
C	2.424656	0.010935	0.010712
C	1.218406	0.015413	-0.694862
C	-1.261491	-0.011619	2.173695
O	-1.307162	-0.014126	3.401284
C	-2.519699	-0.017728	1.432002
C	-3.608066	-0.036481	0.895850
C	-4.902243	0.035466	0.244849
O	-5.434764	1.084688	-0.060419
O	-5.406538	-1.185098	0.036662
C	-6.700284	-1.226241	-0.611073
H	-6.943725	-2.284213	-0.692372
H	-7.441614	-0.703786	-0.002984

H	-6.640442	-0.765416	-1.599218
H	1.196881	-0.017483	3.189106
H	3.363339	-0.004482	1.955460
H	3.367238	0.016681	-0.529238
H	1.221230	0.024621	-1.780564
H	-0.929848	0.011256	-0.550373



Transition state for Methyl 1-(4-t-butylbenzyl)-5-phenyloxomethyl-1,2,3-triazole-4-carboxylate **2.8a**

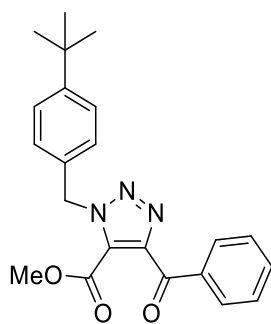
1 imaginary frequency:  $-358.940 \text{ cm}^{-1}$

Total energy (ZPE corrected, Hartrees): -1241.568149

C	2.598371	-1.085904	-0.219528
C	2.248372	-0.006089	-1.034980
C	3.213676	0.977227	-1.281726
C	4.488093	0.878572	-0.726753
C	4.852414	-0.200839	0.097383
C	3.875858	-1.179829	0.336149
C	0.859299	0.108577	-1.622397

N	-0.133002	0.624065	-0.644312
N	-0.095013	1.815461	-0.264600
N	-0.759105	2.663956	0.180028
C	6.271189	-0.271208	0.690774
C	6.520426	0.976127	1.572361
C	6.480910	-1.525007	1.560762
C	7.308529	-0.301413	-0.456912
C	-2.224649	0.374660	-0.513306
C	-2.640604	1.452340	-0.048205
C	-3.586738	2.361191	0.567148
O	-3.977633	3.323257	-0.280735
C	-4.936794	4.267622	0.244545
C	-2.426708	-0.991682	-1.026541
C	-3.353276	-1.877756	-0.265889
O	-1.864877	-1.365883	-2.051770
O	-3.967132	2.252128	1.720317
H	0.461699	-0.866373	-1.903139
H	0.855768	0.745318	-2.513582
H	-5.139008	4.955453	-0.575258
H	-5.850496	3.752090	0.548538
H	-4.513675	4.800534	1.098910
H	2.969861	1.826244	-1.916505

H	5.209692	1.660492	-0.945865
H	4.102421	-2.037183	0.960151
H	1.867624	-1.864594	-0.013140
H	8.324807	-0.344381	-0.047075
H	7.161810	-1.181339	-1.093944
H	7.242293	0.588796	-1.091236
H	7.501163	-1.527006	1.960309
H	5.792101	-1.551744	2.412835
H	6.349352	-2.448192	0.984873
H	7.530920	0.943533	1.997341
H	6.429165	1.905075	0.999681
H	5.804737	1.019976	2.401615
C	-3.593138	-3.165137	-0.779579
C	-4.443204	-4.040087	-0.112129
C	-5.063090	-3.640285	1.077320
C	-4.829123	-2.363941	1.594656
C	-3.977570	-1.482809	0.929260
H	-3.103940	-3.458195	-1.702271
H	-4.624584	-5.032451	-0.514453
H	-5.726769	-4.323925	1.599256
H	-5.309054	-2.054132	2.518228
H	-3.802380	-0.494387	1.339914



Transition state for Methyl 1-(4-t-butylbenzyl)-4-phenyloxomethyl-1,2,3-triazole-5-carboxylate **2.8b**

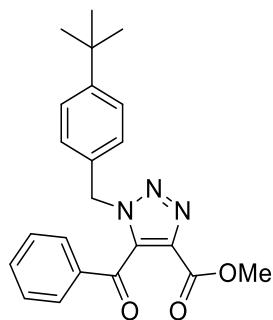
1 imaginary frequency:  $-338.774 \text{ cm}^{-1}$

Total energy (ZPE corrected, Hartrees):  $-1241.569799$

C	-2.752441	0.794228	0.518487
C	-2.407144	0.782077	-0.836522
C	-3.275894	0.158135	-1.737963
C	-4.457872	-0.432476	-1.292878
C	-4.817205	-0.429942	0.065883
C	-3.934312	0.197292	0.959463
C	-1.121608	1.423229	-1.309744
N	0.079882	0.654680	-0.886170
N	0.468231	-0.325886	-1.560190
N	1.392292	-0.977792	-1.822703
C	-6.132909	-1.091786	0.515601
C	-6.116073	-2.588698	0.123516
C	-6.346729	-0.995464	2.037960

C	-7.323183	-0.393662	-0.185052
C	1.905551	1.342780	-0.252565
C	2.773266	0.545162	-0.658898
C	4.045675	-0.060178	-1.001884
O	4.652812	0.326791	-2.000848
C	1.555110	2.505578	0.570712
O	2.640979	3.270446	0.760298
C	2.442879	4.442161	1.583133
O	0.455965	2.749189	1.032130
C	4.567651	-1.136264	-0.112784
H	-0.979432	2.398253	-0.843741
H	-1.114016	1.549597	-2.396475
H	3.414803	4.931947	1.619977
H	1.696051	5.098969	1.131690
H	2.119244	4.150721	2.584760
H	-3.031048	0.136206	-2.797561
H	-5.108478	-0.902888	-2.024698
H	-4.163076	0.231658	2.018795
H	-2.089192	1.273718	1.234217
H	-8.268413	-0.857803	0.121172
H	-7.365231	0.669199	0.080008
H	-7.253610	-0.466370	-1.275547

H	-7.291661	-1.480680	2.306662
H	-5.547065	-1.496377	2.595449
H	-6.400796	0.045211	2.377141
H	-7.051103	-3.071567	0.432252
H	-6.010906	-2.725841	-0.957780
H	-5.286152	-3.112353	0.612134
C	5.814883	-1.705288	-0.416169
C	6.340542	-2.708822	0.392381
C	5.625177	-3.152686	1.510235
C	4.383046	-2.590704	1.817128
C	3.854440	-1.585281	1.008802
H	6.354530	-1.347528	-1.286823
H	7.305707	-3.146833	0.154925
H	6.036187	-3.936213	2.140672
H	3.827302	-2.935719	2.684036
H	2.888364	-1.150070	1.246476



Methyl 1-(4-t-butylbenzyl)-5-phenyloxomethyl-1,2,3-triazole-4-carboxylate **2.8a**

No imaginary frequencies

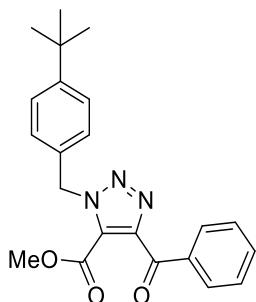
Total energy (Hartrees): -1242.117554

C	1.885910	1.579675	0.263661
N	1.056750	2.338744	1.034728
N	0.132643	1.574036	1.539945
N	0.339903	0.314890	1.090499
C	1.436842	0.261493	0.295790
C	-0.579583	-0.761002	1.513631
C	-1.977626	-0.580844	0.961736
C	-2.243875	-0.758569	-0.399432
C	-3.538440	-0.598986	-0.896651
C	-4.612211	-0.262405	-0.057512
C	-4.327754	-0.090283	1.308181
C	-3.036857	-0.243102	1.810526
C	-6.051808	-0.081125	-0.572561
C	-6.984055	-1.090665	0.139272
C	1.878698	-0.988693	-0.413027
O	1.066469	-1.556079	-1.138708
C	3.003479	2.120690	-0.535166
O	3.613156	1.463721	-1.361311
C	-6.528405	1.358847	-0.265782
C	-6.164677	-0.311391	-2.091379



O	3.256023	3.405380	-0.250061
C	4.318728	4.016217	-1.011241
C	3.245266	-1.511901	-0.187369
H	-0.135427	-1.697979	1.176492
H	-0.587410	-0.757659	2.605636
H	4.373155	5.044154	-0.655410
H	5.262182	3.496112	-0.830579
H	4.085063	3.990176	-2.078075
H	-2.853764	-0.100008	2.872772
H	-5.124165	0.170194	1.999390
H	-3.701151	-0.746521	-1.958363
H	-1.433119	-1.020666	-1.074140
H	-8.014765	-0.967723	-0.214670
H	-6.675288	-2.122198	-0.066551
H	-6.985333	-0.949756	1.225194
H	-7.204428	-0.168907	-2.406272
H	-5.547664	0.394651	-2.658637
H	-5.869526	-1.328456	-2.373307
H	-7.555968	1.501250	-0.621678
H	-6.514488	1.573150	0.807966
H	-5.890725	2.097415	-0.765327
C	3.699830	-2.556765	-1.011584

C	4.962186	-3.104814	-0.813527
C	5.778256	-2.624976	0.217644
C	5.329221	-1.594828	1.048049
C	4.068833	-1.035616	0.846008
H	3.052090	-2.920730	-1.802093
H	5.312969	-3.905527	-1.457777
H	6.763041	-3.056072	0.373850
H	5.959973	-1.228000	1.852110
H	3.722756	-0.240516	1.498311



Methyl 1-(4-t-butylbenzyl)-4-phenyloxomethyl-1,2,3-triazole-5-carboxylate **2.8b**

No imaginary frequencies

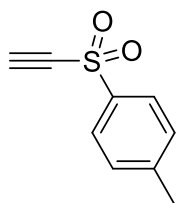
Total energy (Hartrees): -1242.117141

C	2.054371	-0.059032	-0.193148
N	1.606537	-1.193669	-0.799778
N	0.488711	-0.932845	-1.425123
N	0.192385	0.364372	-1.228351
C	1.143157	0.961275	-0.463625
C	-1.032931	0.917829	-1.846717

C	-2.294732	0.440419	-1.159811
C	-2.708700	0.996154	0.054519
C	-3.875785	0.551648	0.678848
C	-4.672192	-0.457154	0.115568
C	-4.242959	-1.004383	-1.106289
C	-3.077675	-0.567920	-1.733065
C	-5.966092	-0.967728	0.775820
C	-7.156838	-0.750772	-0.188467
C	1.107696	2.397950	-0.092002
O	0.081665	3.019438	0.122853
C	3.222649	-0.030487	0.733708
O	3.176845	0.707666	1.714729
C	-5.823763	-2.478202	1.081024
C	-6.277968	-0.237995	2.096069
C	4.399277	-0.906393	0.473254
O	2.334186	2.916371	-0.049066
C	2.422737	4.300410	0.359764
H	-0.938505	2.001717	-1.801589
H	-1.013145	0.604043	-2.892040
H	3.485908	4.534005	0.346416
H	1.877755	4.934789	-0.342165
H	2.012291	4.421645	1.364431

H	-2.777135	-1.014225	-2.677917
H	-4.825812	-1.786390	-1.584324
H	-4.161433	1.011073	1.618374
H	-2.114661	1.781427	0.513683
H	-8.085060	-1.112351	0.270084
H	-7.284986	0.312891	-0.420548
H	-7.020766	-1.287616	-1.133156
H	-7.206393	-0.634007	2.522327
H	-5.485479	-0.380970	2.839401
H	-6.416103	0.838661	1.944802
H	-6.740492	-2.857813	1.548173
H	-5.645035	-3.063306	0.172759
H	-4.990786	-2.661714	1.769613
C	5.310616	-1.104853	1.525850
C	6.446561	-1.884959	1.337416
C	6.694597	-2.466299	0.088766
C	5.801783	-2.265103	-0.966305
C	4.655981	-1.492429	-0.777584
H	5.106830	-0.641530	2.485546
H	7.140109	-2.040913	2.158672
H	7.583249	-3.073317	-0.060394
H	5.997526	-2.709220	-1.937938

H 3.968382 -1.341531 -1.601122



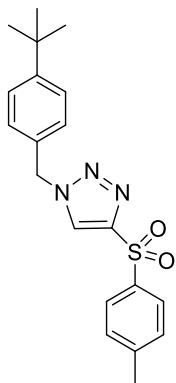
Alkyne **2.9**

No imaginary frequencies

Total Energy (ZPE corrected, Hartrees): -896.1207434

C	2.157215	0.309960	0.023531
C	0.927489	0.141362	-0.608041
C	-0.173937	-0.251018	0.157201
C	-0.062646	-0.478005	1.532093
C	1.176260	-0.303228	2.142384
C	2.302520	0.091077	1.402267
S	-1.752799	-0.467567	-0.636293
O	-2.570774	-1.390612	0.165012
C	3.644990	0.249639	2.071693
C	-2.488479	1.096511	-0.519956
C	-3.045938	2.167999	-0.465965
O	-1.538850	-0.739204	-2.065849
H	-0.926518	-0.790226	2.108872
H	1.270952	-0.477550	3.210654
H	3.018348	0.614863	-0.564567
H	0.824518	0.305176	-1.675272

H	-3.530185	3.120448	-0.412745
H	4.285190	0.947430	1.523808
H	3.537994	0.609208	3.099878
H	4.170519	-0.713186	2.116198



Transition state for 1-(4-*t*-Butylbenzyl)-4-(4-methylphenylsulfonyl)-1,2,3-triazole

1 Imaginary frequency:  $-378.576 \text{ cm}^{-1}$

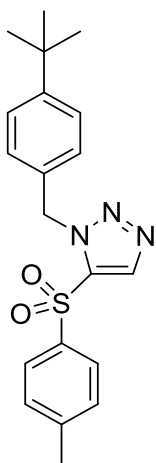
Total Energy (ZPE corrected, Hartrees):  $-1488.257004$

C	-0.035184	-0.018132	0.009619
C	0.034595	-0.000736	1.404769
C	1.262138	-0.052429	2.069261
C	2.433245	-0.116583	1.317394
C	2.396995	-0.127177	-0.085513
C	1.147523	-0.082659	-0.723404
S	-1.477560	0.081387	2.357632
O	-2.568938	-0.466931	1.534161
C	3.672652	-0.165895	-0.890842

C	-1.777003	1.768451	2.572677
C	-1.538184	2.977427	2.443714
O	-1.217016	-0.499923	3.686086
N	-3.084847	3.957703	3.494902
N	-3.768257	2.942346	3.764383
N	-3.771083	1.782450	3.780457
C	-3.759287	5.186041	2.999300
C	-4.543879	5.901857	4.076539
C	-3.896163	6.641979	5.069887
C	-4.625193	7.291430	6.067626
C	-6.026783	7.228884	6.109351
C	-6.664651	6.481753	5.103917
C	-5.941118	5.828996	4.107693
C	-6.865367	7.939183	7.187791
C	-5.992035	8.691052	8.210054
C	-7.807832	8.963208	6.510963
C	-7.711901	6.893868	7.953225
H	-1.031241	3.876173	2.155520
H	-2.935414	5.807482	2.640085
H	-4.397672	4.938474	2.144570
H	-6.469369	5.261558	3.344874
H	-7.747978	6.405145	5.091425



H	-4.081443	7.856328	6.816223
H	-2.810977	6.714416	5.067310
H	-8.417314	9.473901	7.266171
H	-7.234875	9.722943	5.966741
H	-8.489423	8.482788	5.801180
H	-6.634325	9.174178	8.954685
H	-5.315614	8.014964	8.745467
H	-5.389244	9.474058	7.736061
H	-8.317659	7.388021	8.722321
H	-8.394177	6.354278	7.288061
H	-7.070020	6.156160	8.448547
H	1.298260	-0.056475	3.153351
H	3.390669	-0.165542	1.829101
H	1.099237	-0.105112	-1.808812
H	-0.997355	0.004204	-0.490629
H	3.526084	-0.677679	-1.847059
H	4.020572	0.851035	-1.114971
H	4.474971	-0.672249	-0.345475



Transition state for 1-(4-*t*-butylbenzyl)-5-(4-methylphenylsulfonyl)-1,2,3-triazole

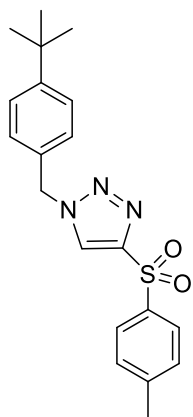
1 imaginary frequency: -416.254

Total Energy (ZPE corrected, Hartrees): -1488.256107

C	0.862712	-0.263162	2.253953
C	-0.406794	-0.610907	1.781814
C	-0.511018	-1.144027	0.490931
C	0.621930	-1.320715	-0.300583
C	1.904172	-0.973298	0.160100
C	1.994725	-0.441684	1.455513
C	-1.641239	-0.402955	2.629949
N	-2.162261	0.989273	2.632045
N	-2.305776	1.610629	1.558431
N	-2.315019	2.693663	1.115279
C	3.130673	-1.184708	-0.746326
C	2.959668	-0.356448	-2.042405

C	4.443173	-0.749168	-0.067463
C	3.250242	-2.683962	-1.110662
C	-1.643115	3.717850	2.866294
C	-1.519875	2.820020	3.710738
S	-1.272767	2.212939	5.320196
O	-2.593680	1.885978	5.883320
C	-0.601154	3.611438	6.206445
C	0.784272	3.772013	6.284967
C	1.295722	4.863908	6.982655
C	0.446384	5.796340	7.598047
C	-0.940991	5.601517	7.507866
C	-1.473663	4.517030	6.815659
C	1.010678	6.992608	8.324072
O	-0.241809	1.160271	5.262334
H	-1.630609	4.695780	2.431363
H	-1.439941	-0.606441	3.682552
H	-2.454695	-1.063646	2.310294
H	-1.485860	-1.429697	0.101646
H	0.498585	-1.741706	-1.294339
H	2.959429	-0.160817	1.863292
H	0.966646	0.151067	3.253292
H	4.116674	-2.846641	-1.762992

H	3.382526	-3.296950	-0.211521
H	2.362530	-3.048022	-1.638546
H	5.283049	-0.921165	-0.749778
H	4.437055	0.316588	0.187973
H	4.638307	-1.319792	0.847637
H	3.823256	-0.503081	-2.702293
H	2.062019	-0.648237	-2.597623
H	2.882911	0.713431	-1.816193
H	-2.546576	4.367426	6.760169
H	-1.613355	6.305169	7.991076
H	2.372479	4.990691	7.054590
H	1.446947	3.049511	5.821129
H	2.000734	6.778807	8.738235
H	1.119090	7.844402	7.639929
H	0.354204	7.311446	9.139531



1-(4-*t*-Butylbenzyl)-4-(4-methylphenylsulfonyl)-1,2,3-triazole

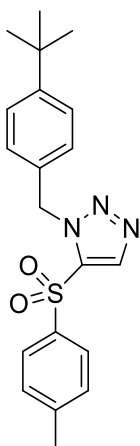
No imaginary frequencies

Total Energy (Hartrees): -1488.798894

C	-0.418792	4.228885	0.305198
N	-0.737608	3.255257	1.182269
N	-2.066630	2.988805	1.148606
N	-2.609955	3.778118	0.262863
C	-1.629372	4.551095	-0.273770
C	0.147208	2.480590	2.070416
C	0.992646	1.472285	1.322641
C	0.400286	0.374402	0.683112
C	1.181838	-0.552591	0.001722
C	2.583349	-0.430449	-0.067866
C	3.161049	0.670060	0.578015
C	2.379828	1.608311	1.260401
C	3.408092	-1.483655	-0.829285
C	2.954346	-1.518530	-2.308560
S	-1.940737	5.763341	-1.534486
O	-0.619796	6.314146	-1.894062
O	-2.784010	5.135702	-2.567707
C	4.918176	-1.181977	-0.795879
C	3.178135	-2.874690	-0.191052
H	0.582880	4.600458	0.159953

H	0.771702	3.191119	2.616744
H	-0.525698	1.997697	2.782785
H	-0.679063	0.246270	0.717279
H	0.687313	-1.390188	-0.481566
H	4.235150	0.815132	0.557855
H	2.863613	2.450131	1.750237
H	3.750620	-3.637839	-0.731801
H	3.503418	-2.884534	0.855753
H	2.123280	-3.167501	-0.218669
H	5.458925	-1.958173	-1.348650
H	5.152785	-0.218901	-1.263434
H	5.310094	-1.170858	0.227527
H	3.528775	-2.270699	-2.862372
H	1.893403	-1.772148	-2.404136
H	3.113509	-0.546819	-2.790271
C	-2.897043	7.042975	-0.732479
C	-2.236076	8.123656	-0.143628
C	-2.989387	9.114835	0.481609
C	-4.389787	9.039354	0.532646
C	-5.024832	7.943784	-0.073220
C	-4.290607	6.942892	-0.704764
H	-1.154435	8.192444	-0.186952

H	-2.481489	9.962637	0.933255
C	-5.195307	10.101011	1.240382
H	-6.109172	7.875719	-0.054783
H	-4.789729	6.106112	-1.181183
H	-6.174968	10.237701	0.771893
H	-5.370917	9.819793	2.286996
H	-4.674511	11.063359	1.243578



1-(4-*t*-butylbenzyl)-5-(4-methylphenylsulfonyl)-1,2,3-triazole

No imaginary frequencies

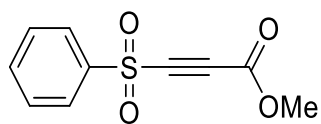
Total Energy (Hartrees): -1488.79111266

C	-3.419622	-1.528212	0.472213
C	-3.478189	-0.140370	0.606078
C	-4.615784	0.580089	0.223138
C	-5.699326	-0.109510	-0.308760
C	-5.668921	-1.506777	-0.463428
C	-4.519453	-2.199986	-0.061530

S	-2.083623	0.735802	1.297888
O	-2.583513	1.858710	2.107245
C	-6.852834	-2.234301	-1.050626
C	-1.260309	1.503358	-0.083933
N	-0.394661	0.930984	-0.969384
N	-0.016073	1.836919	-1.882415
N	-0.617441	2.974527	-1.614270
C	-1.392989	2.809663	-0.515916
C	0.185471	-0.430212	-1.026764
C	1.658267	-0.451058	-0.678344
C	2.085714	-0.409633	0.652010
C	3.447226	-0.427045	0.962512
C	4.428159	-0.491633	-0.038487
C	3.981628	-0.538635	-1.370874
C	2.625343	-0.517452	-1.687884
C	5.936682	-0.517379	0.267259
C	6.620409	0.690713	-0.417007
C	6.230864	-0.443841	1.777663
C	6.548115	-1.829005	-0.281438
O	-1.159177	-0.252444	1.885057
H	-1.988172	3.605690	-0.094710
H	-0.392907	-1.045439	-0.339195



H	0.016899	-0.790460	-2.043419
H	2.316770	-0.554382	-2.729785
H	4.702003	-0.593864	-2.181957
H	3.735232	-0.393900	2.007277
H	1.351631	-0.363551	1.451980
H	7.625879	-1.856733	-0.081085
H	6.091408	-2.703881	0.195796
H	6.407119	-1.923464	-1.363310
H	7.314154	-0.460827	1.940833
H	5.843359	0.478748	2.224704
H	5.801737	-1.294117	2.319826
H	7.698323	0.678341	-0.215870
H	6.483973	0.676445	-1.503433
H	6.215066	1.636444	-0.038962
H	-4.656067	1.657019	0.348423
H	-6.586406	0.443264	-0.605874
H	-4.481793	-3.280868	-0.162804
H	-2.540385	-2.074602	0.795119
H	-6.702241	-3.317227	-1.042647
H	-7.768856	-2.011320	-0.491418
H	-7.026779	-1.923447	-2.087945



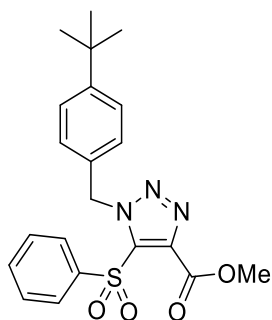
Alkyne **2.10**

No imaginary frequencies

Total energy (ZPE corrected, Hartrees): -1084.660586

C	0.631888	-0.637107	-0.421958
C	0.638827	-1.277934	0.816315
C	1.252838	-0.636605	1.896292
C	1.859842	0.616556	1.770723
C	1.843224	1.242364	0.524875
C	1.229946	0.618244	-0.565291
S	1.272284	-1.448673	3.483329
C	-0.187145	-0.893867	4.248987
C	-1.180077	-0.560699	4.858142
C	-2.400587	-0.099013	5.503212
O	-2.525445	-0.629469	6.720445
C	-3.709328	-0.237679	7.458062
O	2.387856	-0.925352	4.282757
O	-3.177043	0.667705	4.971036
H	-3.636970	-0.762354	8.408903
H	-3.714042	0.843467	7.610198
H	-4.606021	-0.541056	6.914064

H	2.339256	1.082594	2.624539
H	2.311994	2.214106	0.405726
H	1.221039	1.111365	-1.532754
H	0.163280	-1.119769	-1.273820
H	0.187564	-2.255904	0.942669
O	1.117540	-2.896432	3.289772



Transition state for Methyl 1-(4-t-butylbenzyl)-5-phenylsulfonyl-1,2,3-triazole-4-carboxylate

1 imaginary frequency:  $-341.508 \text{ cm}^{-1}$

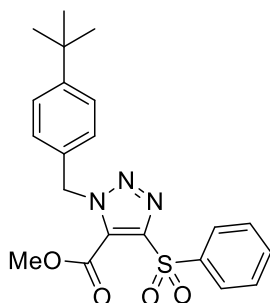
Total energy (ZPE corrected, Hartrees):  $-1676.798436$

C	3.606241	1.106695	-1.295239
C	2.573067	0.203638	-1.021914
C	2.847524	-0.890040	-0.195329
C	4.121944	-1.075561	0.342645
C	5.168843	-0.179352	0.075692
C	4.877625	0.915391	-0.756925
C	1.189837	0.408342	-1.596101

N	0.228780	0.915772	-0.577011
N	0.119035	2.138910	-0.348441
N	-0.606631	2.953391	0.054507
C	6.585940	-0.354851	0.651293
C	6.710914	-1.617294	1.525068
C	7.603180	-0.469231	-0.509239
C	6.940669	0.873906	1.522681
C	-1.764660	0.430891	-0.228258
C	-2.342723	1.455146	0.173332
C	-3.355851	2.318970	0.751045
O	-3.929149	3.087955	-0.184593
C	-4.960366	3.983296	0.289457
S	-1.786331	-1.292119	-0.558714
O	-1.646286	-1.468743	-2.014370
C	-3.435171	-1.782656	-0.069418
C	-3.669894	-2.134244	1.262916
C	-4.957059	-2.522649	1.632431
C	-5.980435	-2.556013	0.680464
C	-5.725710	-2.205609	-0.648289
C	-4.444320	-1.813472	-1.035319
O	-0.808402	-1.931267	0.336993
O	-3.630162	2.331406	1.936008

H	0.754103	-0.536734	-1.923903
H	1.203567	1.088468	-2.452577
H	-5.303564	4.516916	-0.595567
H	-5.778431	3.415675	0.738282
H	-4.548228	4.679126	1.023533
H	3.419437	1.965154	-1.936597
H	5.653561	1.637208	-0.995928
H	4.290923	-1.939596	0.975639
H	2.057024	-1.600655	0.034448
H	8.618331	-0.588948	-0.111981
H	7.381015	-1.337535	-1.140387
H	7.598003	0.420909	-1.146934
H	7.733722	-1.696478	1.909797
H	6.034689	-1.586607	2.386912
H	6.499620	-2.529740	0.955985
H	7.953068	0.768763	1.930972
H	6.907812	1.804883	0.946979
H	6.244101	0.972467	2.363413
H	-4.226949	-1.546335	-2.063576
H	-6.522119	-2.240061	-1.385164
H	-6.980380	-2.860200	0.975234
H	-5.158685	-2.802646	2.661666

H -2.863180 -2.113282 1.987537



Transition state for Methyl 1-(4-t-butylbenzyl)-4-phenylsulfonyl-1,2,3-triazole-5-carboxylate

1 imaginary frequency:  $-319.578 \text{ cm}^{-1}$

Total energy (ZPE corrected, Hartrees): -1676.795902

C 4.217442 -2.558418 0.463463

C 4.460466 -1.211462 0.183069

C 5.183772 -0.808910 -0.943768

C 5.664534 -1.786133 -1.814595

C 5.426804 -3.138268 -1.550810

C 4.709418 -3.523704 -0.414945

S 3.862097 0.034809 1.315198

O 3.564151 -0.591013 2.613445

C 2.347249 0.543652 0.615247

C 1.585661 1.433694 0.202881

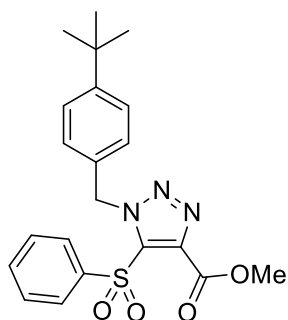
C 1.191498 2.803376 -0.144707

O 0.079464 3.272495 -0.004988

O 2.249509 3.466565 -0.627661

C	2.009062	4.845731	-0.993923
O	4.783397	1.183661	1.269032
N	-0.278852	0.385825	-0.148933
N	0.174491	-0.750500	0.089865
N	1.074983	-1.344566	0.520327
C	-1.246742	0.596615	-1.257823
C	-2.661419	0.243000	-0.856576
C	-3.256371	-0.945908	-1.292595
C	-4.557292	-1.270099	-0.911657
C	-5.313805	-0.426759	-0.079301
C	-4.703161	0.760917	0.352723
C	-3.401878	1.091735	-0.028701
C	-6.749020	-0.820391	0.315254
C	-6.725181	-2.176703	1.060077
C	-7.410986	0.221469	1.237190
C	-7.613542	-0.953990	-0.961393
H	-1.159649	1.662827	-1.471812
H	-0.927390	0.034623	-2.140861
H	2.963129	5.210373	-1.370876
H	1.239802	4.900147	-1.767174
H	1.694290	5.417211	-0.118343
H	-2.701849	-1.622627	-1.938814

H	-4.985996	-2.199919	-1.274431
H	-5.241897	1.449552	0.993699
H	-2.957654	2.020121	0.322753
H	-8.638392	-1.240266	-0.696256
H	-7.657049	-0.003930	-1.506608
H	-7.220051	-1.715601	-1.642823
H	-8.425409	-0.106284	1.490149
H	-6.859467	0.345204	2.176155
H	-7.491120	1.202314	0.754932
H	-7.743524	-2.471289	1.340831
H	-6.305821	-2.976210	0.440433
H	-6.126306	-2.110754	1.975870
H	3.663046	-2.839152	1.351523
H	4.533884	-4.575379	-0.210553
H	5.806174	-3.894876	-2.231278
H	6.228914	-1.491743	-2.693982
H	5.373202	0.243095	-1.127785





Methyl 1-(4-t-butylbenzyl)-5-phenylsulfonyl-1,2,3-triazole-4-carboxylate

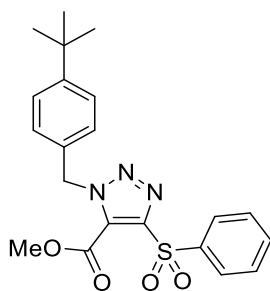
No imaginary frequencies

Total energy (Hartrees): -1677.345335

C	3.441826	-2.245554	0.866015
C	3.267315	-1.467612	-0.284484
C	4.339140	-1.107877	-1.103966
C	5.620348	-1.534515	-0.752191
C	5.815300	-2.298247	0.400760
C	4.729793	-2.653297	1.207807
S	1.606428	-0.999980	-0.760398
O	0.715346	-2.126897	-0.426963
C	1.152075	0.354338	0.352306
C	1.640712	1.659424	0.448329
N	0.970218	2.289353	1.448253
N	0.107848	1.462969	1.967554
N	0.198271	0.283446	1.321802
C	2.704258	2.334200	-0.330916
O	2.805107	3.628913	-0.005476
C	3.823242	4.370772	-0.709892
C	-0.765323	-0.773079	1.729928
C	-2.132794	-0.587029	1.105198
C	-2.513317	-1.306753	-0.029929

C	-3.783502	-1.138267	-0.588726
C	-4.715872	-0.248888	-0.037123
C	-4.318131	0.468045	1.106806
C	-3.055751	0.304121	1.669341
C	-6.124259	-0.040673	-0.622243
C	-6.373820	-0.906982	-1.871303
C	-7.182559	-0.413085	0.443773
C	-6.299945	1.444352	-1.020959
O	3.397763	1.777561	-1.161219
H	-0.328482	-1.730756	1.463304
H	-0.816012	-0.688092	2.816750
H	3.762738	5.384555	-0.316792
H	4.808267	3.940227	-0.516170
H	3.623743	4.361334	-1.783810
H	-2.784135	0.873437	2.554521
H	-5.006657	1.165599	1.575074
H	-4.036519	-1.720064	-1.467965
H	-1.814927	-2.003766	-0.483111
H	-8.192208	-0.261130	0.043580
H	-7.088781	-1.464830	0.738351
H	-7.085702	0.199127	1.346524
H	-7.385369	-0.721465	-2.249175

H	-5.670498	-0.672049	-2.678196
H	-6.295177	-1.977051	-1.648263
H	-7.304107	1.609677	-1.429499
H	-6.173385	2.115228	-0.164737
H	-5.570020	1.733397	-1.786042
H	4.168880	-0.507964	-1.988092
H	6.464532	-1.268071	-1.380585
H	6.815842	-2.623580	0.670016
H	4.883399	-3.254877	2.098215
H	2.593150	-2.537808	1.475349
O	1.604509	-0.464844	-2.126008



Methyl 1-(4-t-butylbenzyl)-4-phenylsulfonyl-1,2,3-triazole-5-carboxylate

No imaginary frequencies

Total energy (Hartrees): -1677.349343

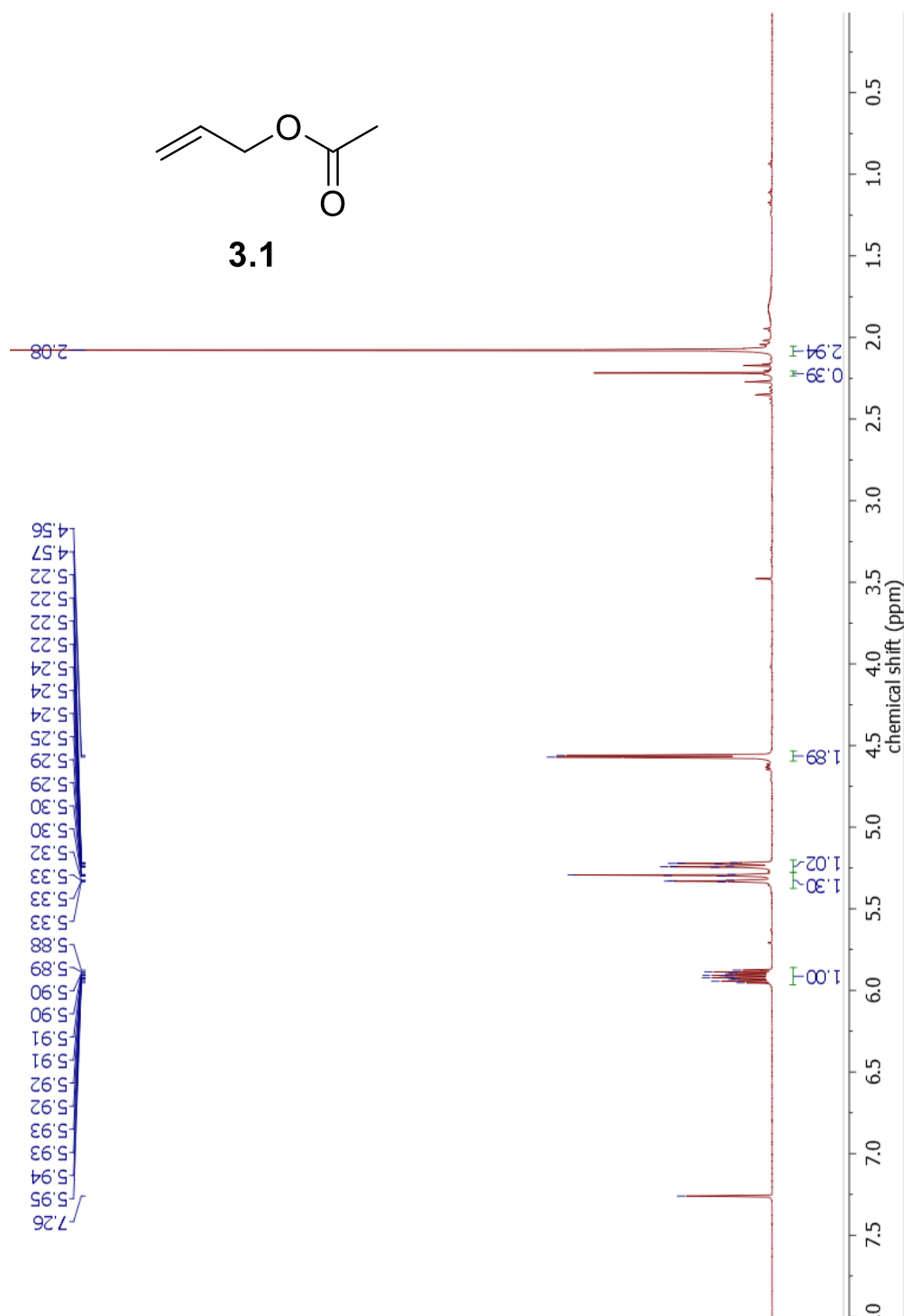
C	5.156577	0.507980	0.455161
C	4.399358	-0.660882	0.365470
C	4.780458	-1.727824	-0.454801
C	5.946303	-1.608794	-1.209461

C	6.715987	-0.443590	-1.132088
C	6.325862	0.608745	-0.300438
S	2.915211	-0.823230	1.355323
O	2.814856	0.325741	2.269370
C	1.558537	-0.712027	0.183802
N	0.994080	-1.853402	-0.273905
N	-0.008262	-1.538161	-1.052800
N	-0.106371	-0.199309	-1.091098
C	0.866402	0.378804	-0.336357
C	-1.189976	0.408050	-1.902544
C	-2.551442	0.241189	-1.263229
C	-2.986689	1.107178	-0.255957
C	-4.244638	0.943509	0.327950
C	-5.111958	-0.084770	-0.070761
C	-4.659959	-0.945556	-1.086790
C	-3.405872	-0.789169	-1.672522
C	1.022822	1.850029	-0.199871
O	2.297428	2.178739	-0.005008
C	2.566454	3.586951	0.196093
C	-6.504146	-0.292589	0.552154
C	-6.824958	0.757025	1.633053
C	-7.583302	-0.193303	-0.552496

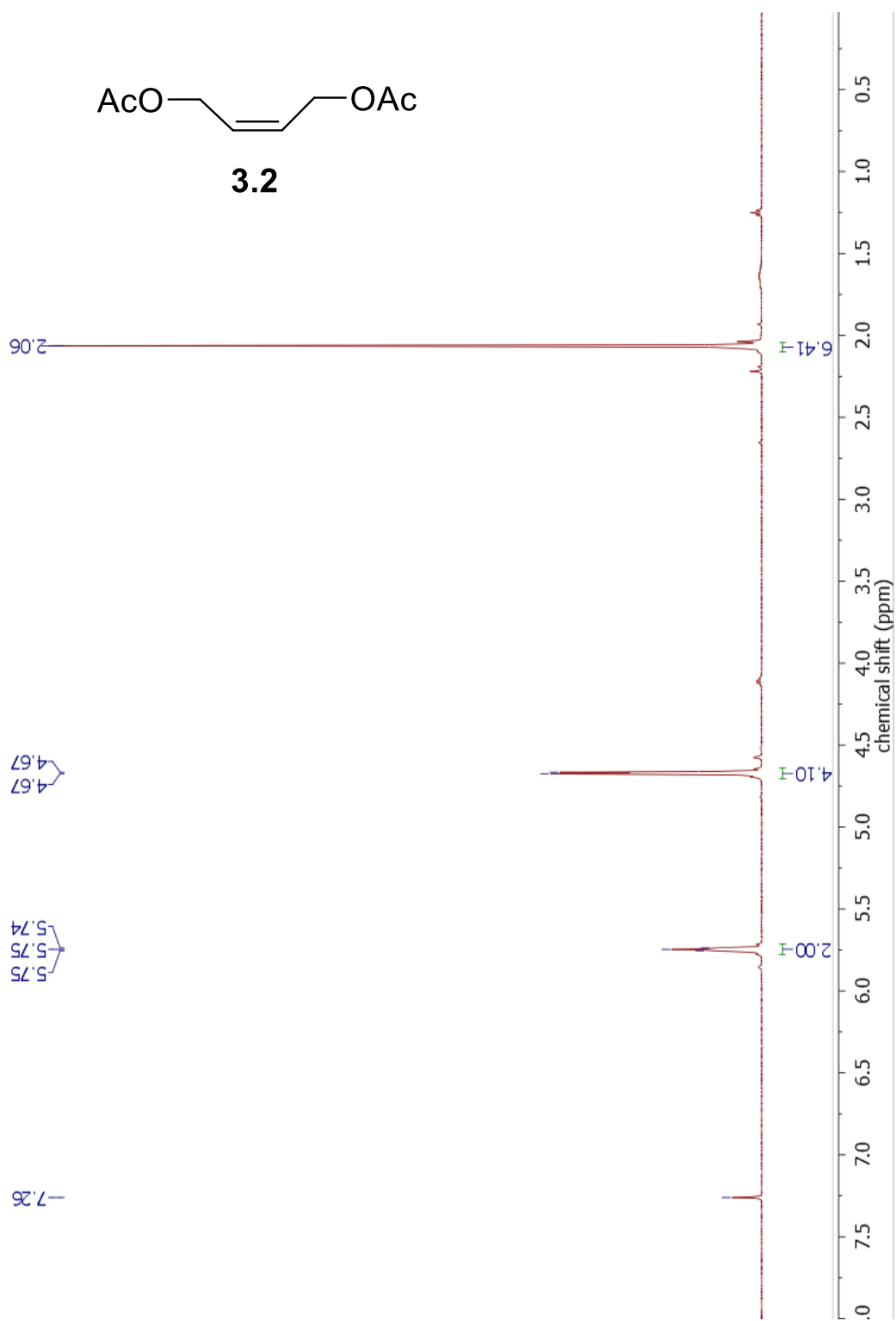
C	-6.567983	-1.694307	1.205066
O	0.100364	2.640585	-0.276203
H	-0.929855	1.457199	-2.028156
H	-1.146433	-0.089567	-2.872946
H	3.643763	3.653933	0.334889
H	2.252466	4.155216	-0.681333
H	2.037259	3.944496	1.081489
H	-3.090769	-1.473445	-2.456342
H	-5.294756	-1.755426	-1.434769
H	-4.543168	1.639336	1.104050
H	-2.338544	1.913606	0.075100
H	-8.580162	-0.344924	-0.121414
H	-7.566305	0.793605	-1.029387
H	-7.440368	-0.947331	-1.333613
H	-7.822905	0.566661	2.043281
H	-6.112406	0.717767	2.464734
H	-6.822606	1.774979	1.227084
H	-7.558639	-1.862093	1.644528
H	-6.386047	-2.491921	0.477187
H	-5.822175	-1.789198	2.002854
H	4.182054	-2.631968	-0.497801
H	6.255949	-2.426664	-1.852718

H	7.624904	-0.358197	-1.720294
H	6.930005	1.508612	-0.237750
H	4.838641	1.310560	1.110084
O	2.867797	-2.192235	1.893353

### NMR Spectra from Chapter 3

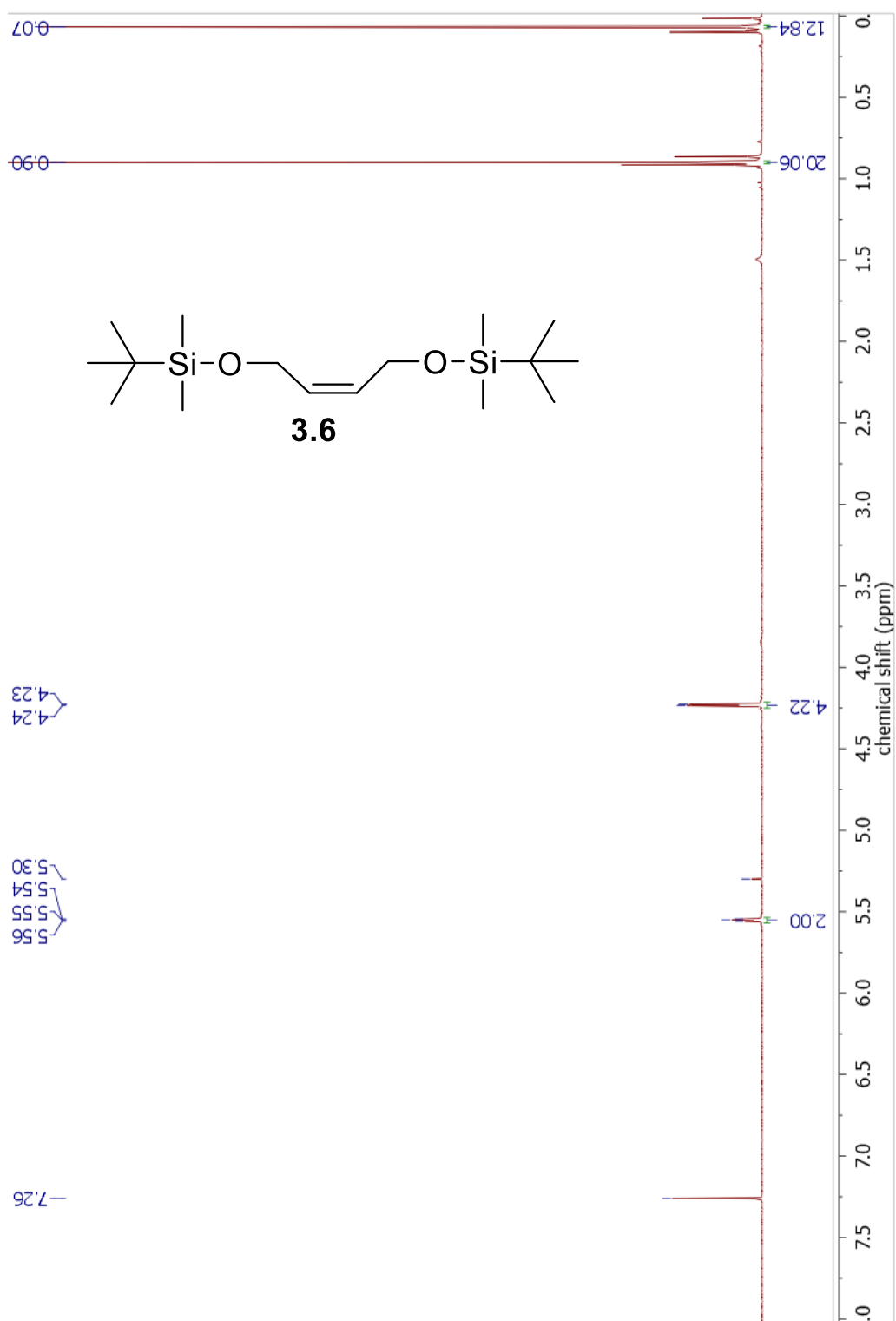


$^1\text{H}$  NMR of allyl acetate (**3.1**) in  $\text{CDCl}_3$

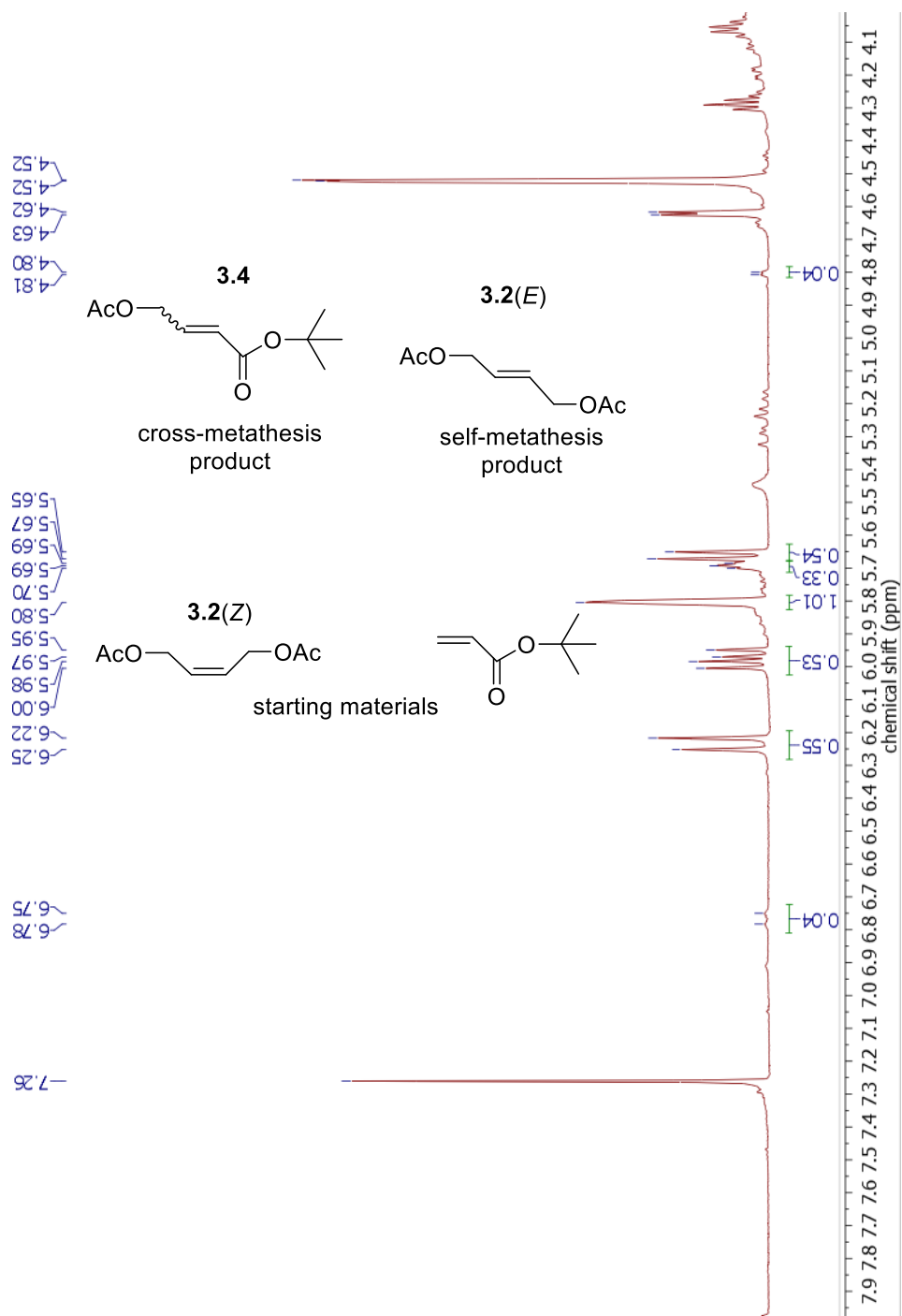


$^1\text{H}$  NMR of Z-1,4-diacetoxy-2-butene (**3.2**) in  $\text{CDCl}_3$

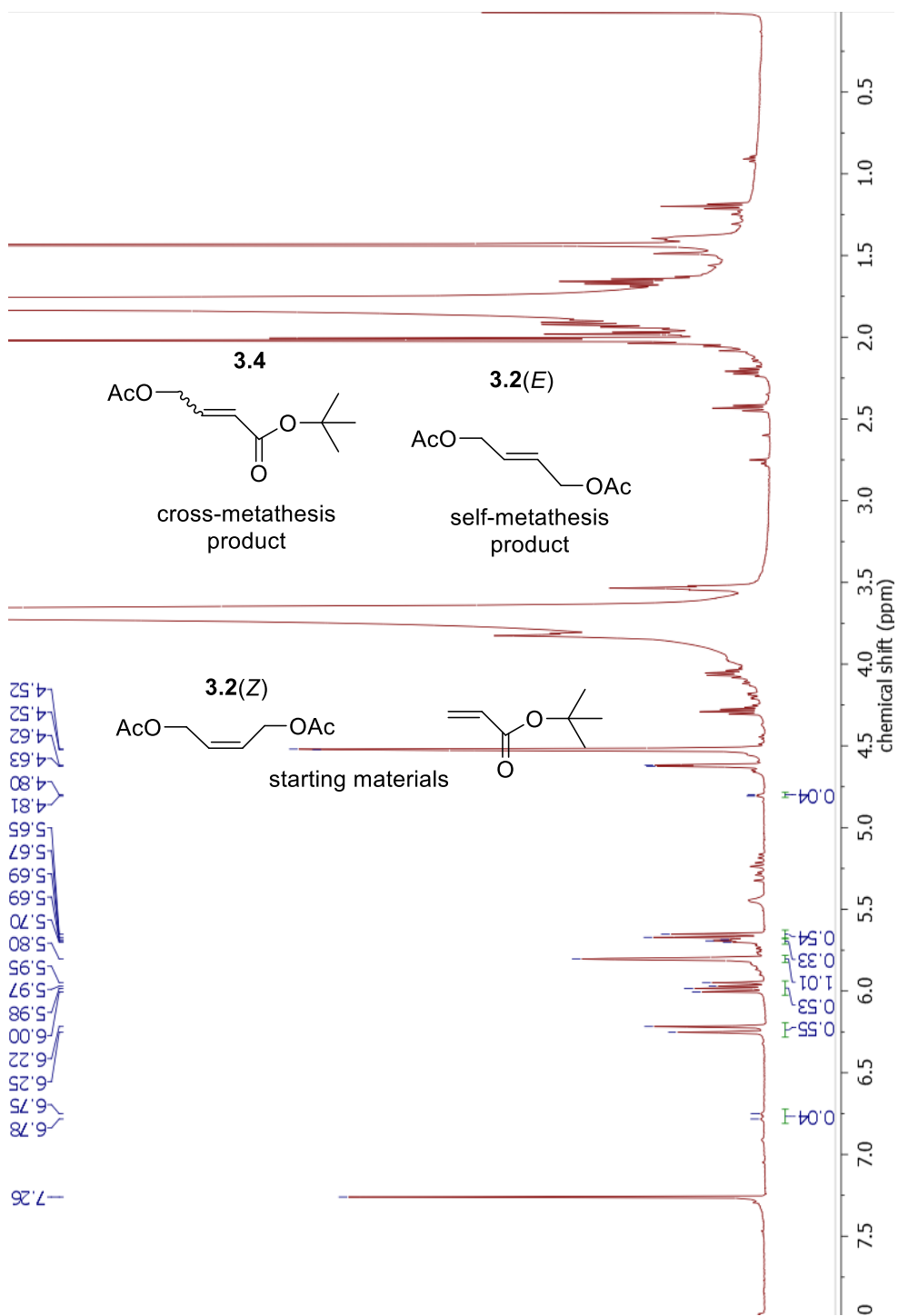




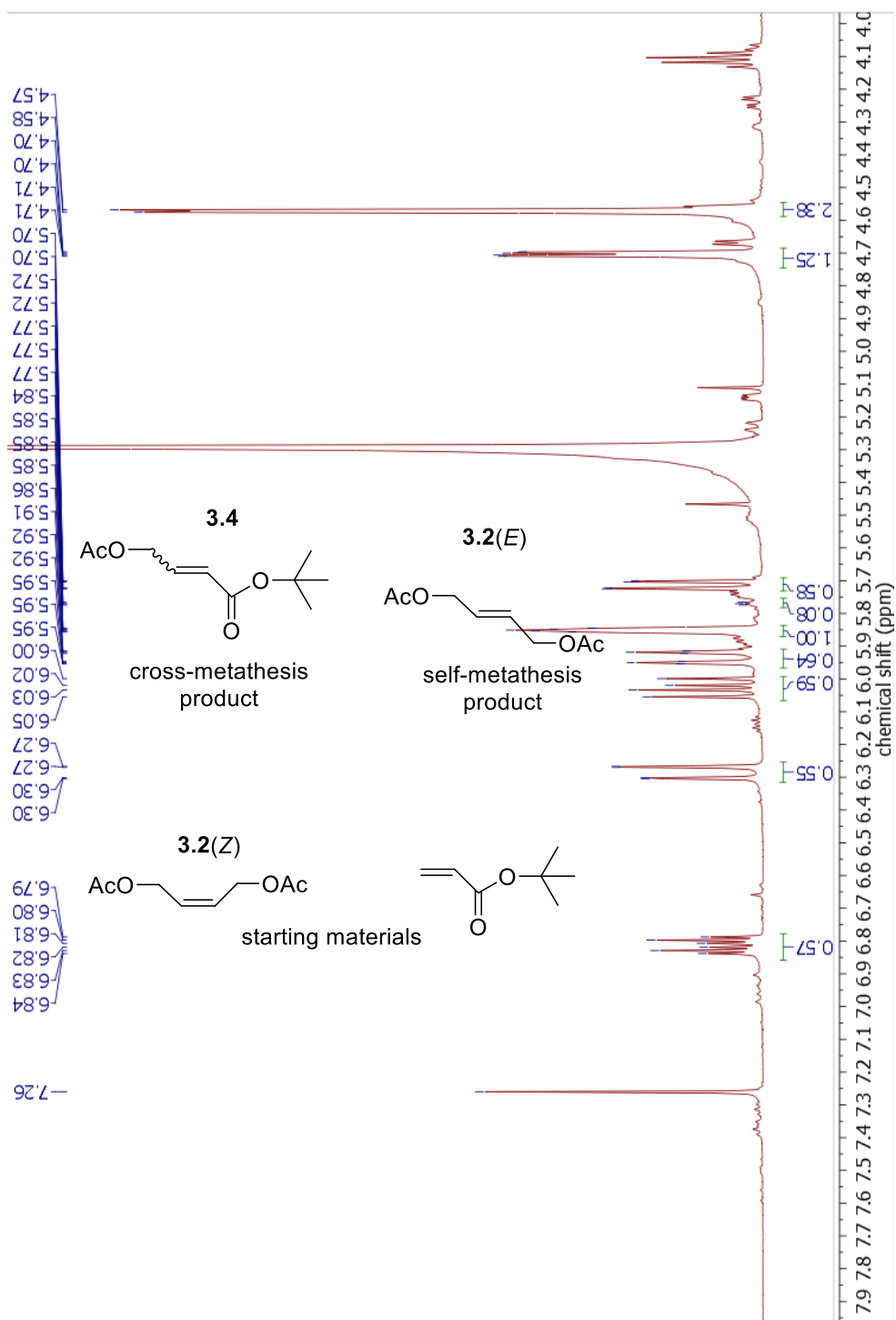
$^1\text{H}$  NMR of Z-1,4-bis-TBSO-2-butene (**3.6**) in  $\text{CDCl}_3$



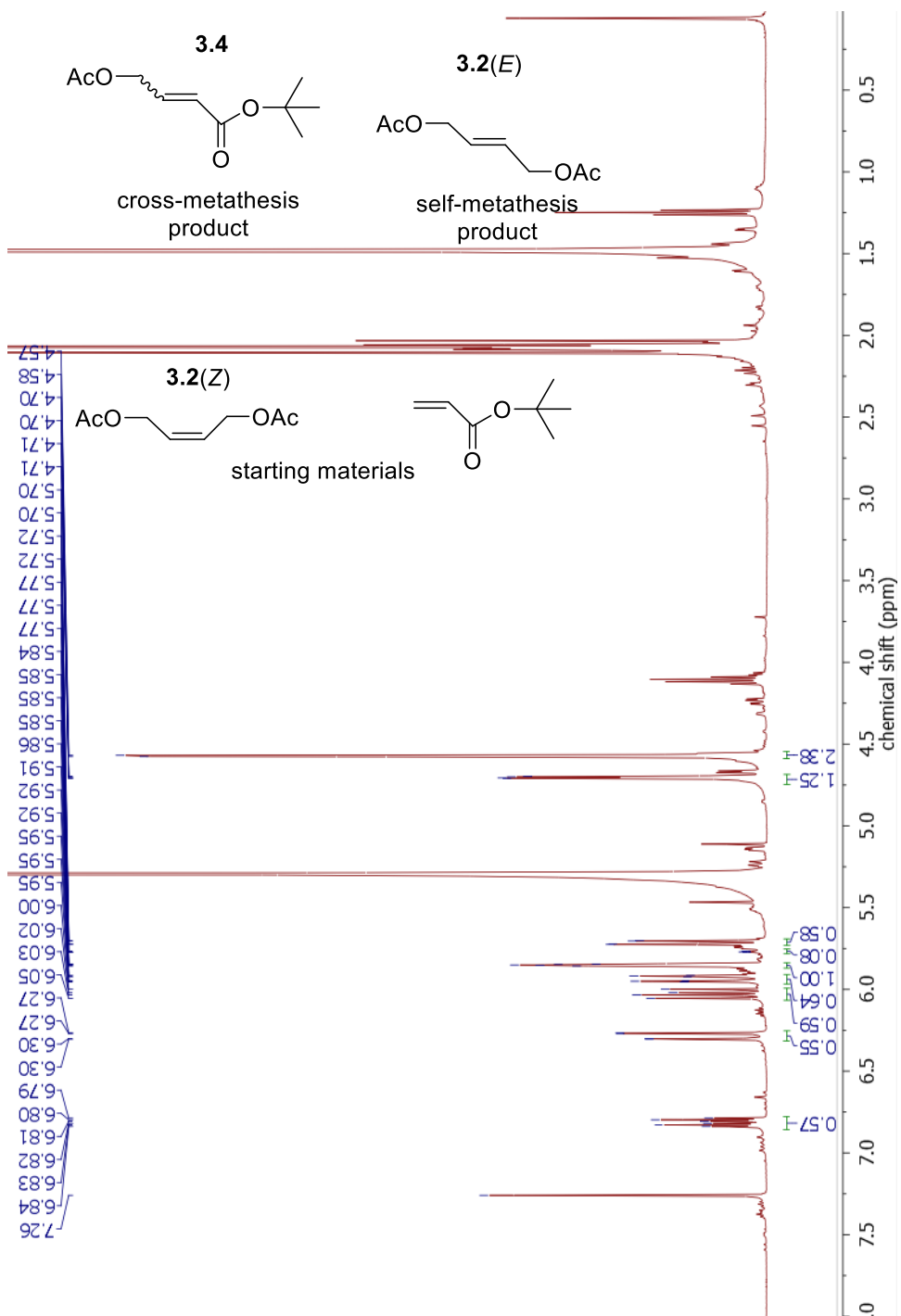
Cross Metathesis control reaction in THF (Table 3.2, entry 1), crude reaction mixture without evaporating solvent. (Relevant peaks)



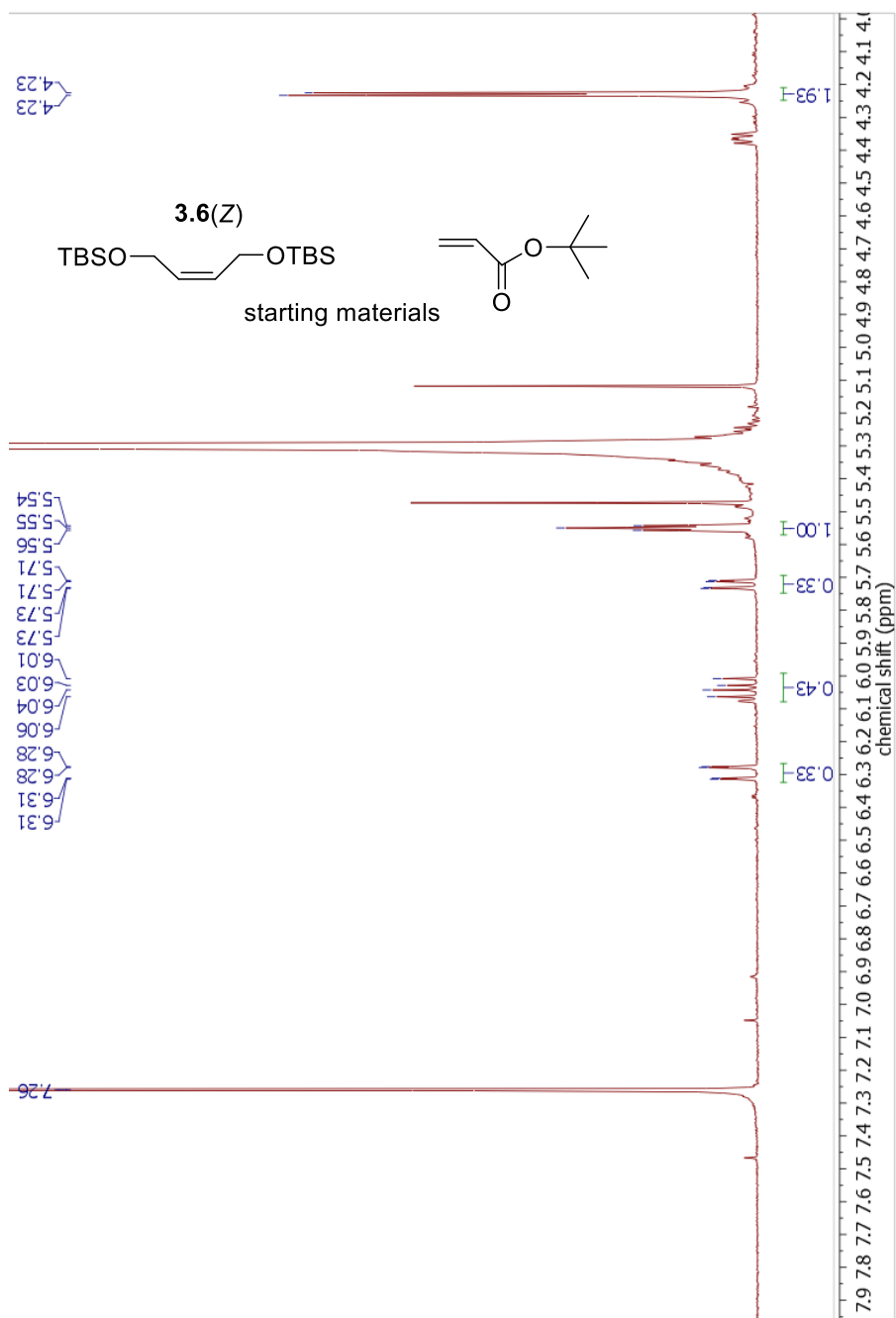
Cross Metathesis control reaction in THF (Table 3.2, entry 1), crude reaction mixture without evaporating solvent (Full spectrum)



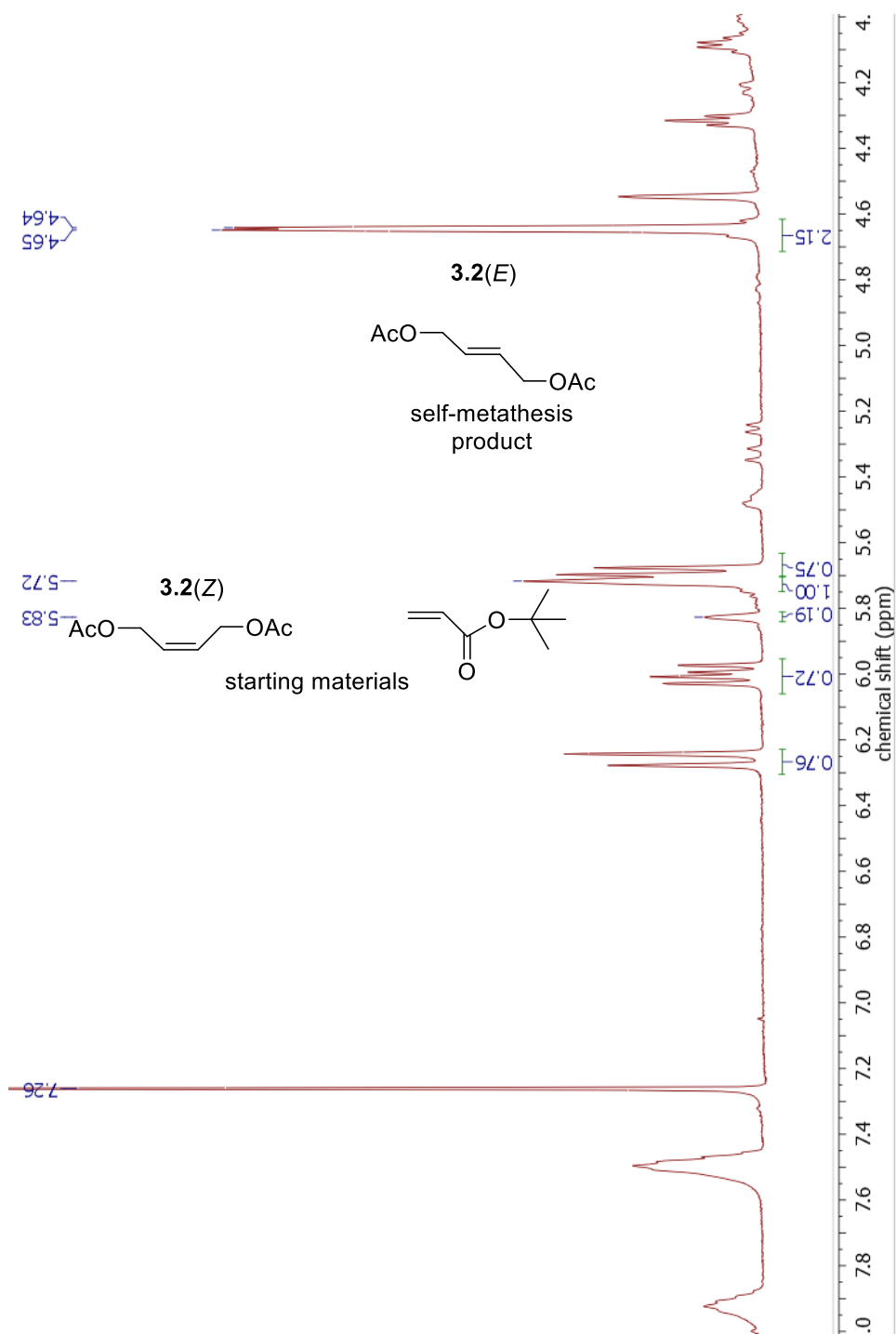
Cross Metathesis control reaction in DCM (Table 3.2, entry 2), crude reaction mixture without evaporating solvent. (Relevant peaks)



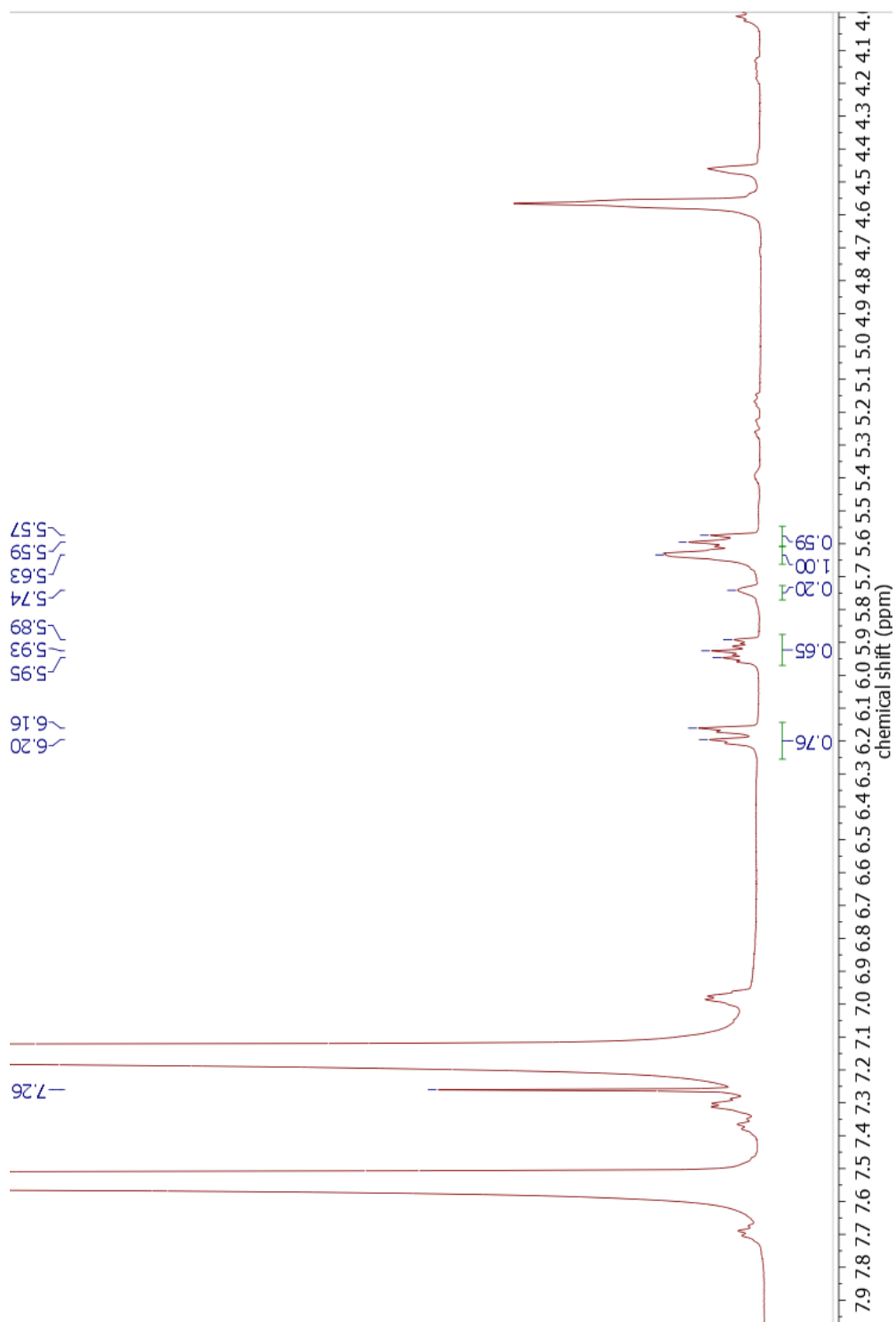
Cross Metathesis control reaction in DCM (Table 3.2, entry 2), crude reaction mixture without evaporating solvent. (Full spectrum)



Cross metathesis reaction in the presence of KO-*t*Bu (Table 3.2, entry 3). Crude  $^1\text{H}$  NMR without evaporating solvent.



Cross metathesis reaction in the presence of pyridine in THF (Table 3.2, entry 4). Crude  $^1\text{H}$  NMR without evaporating solvent.



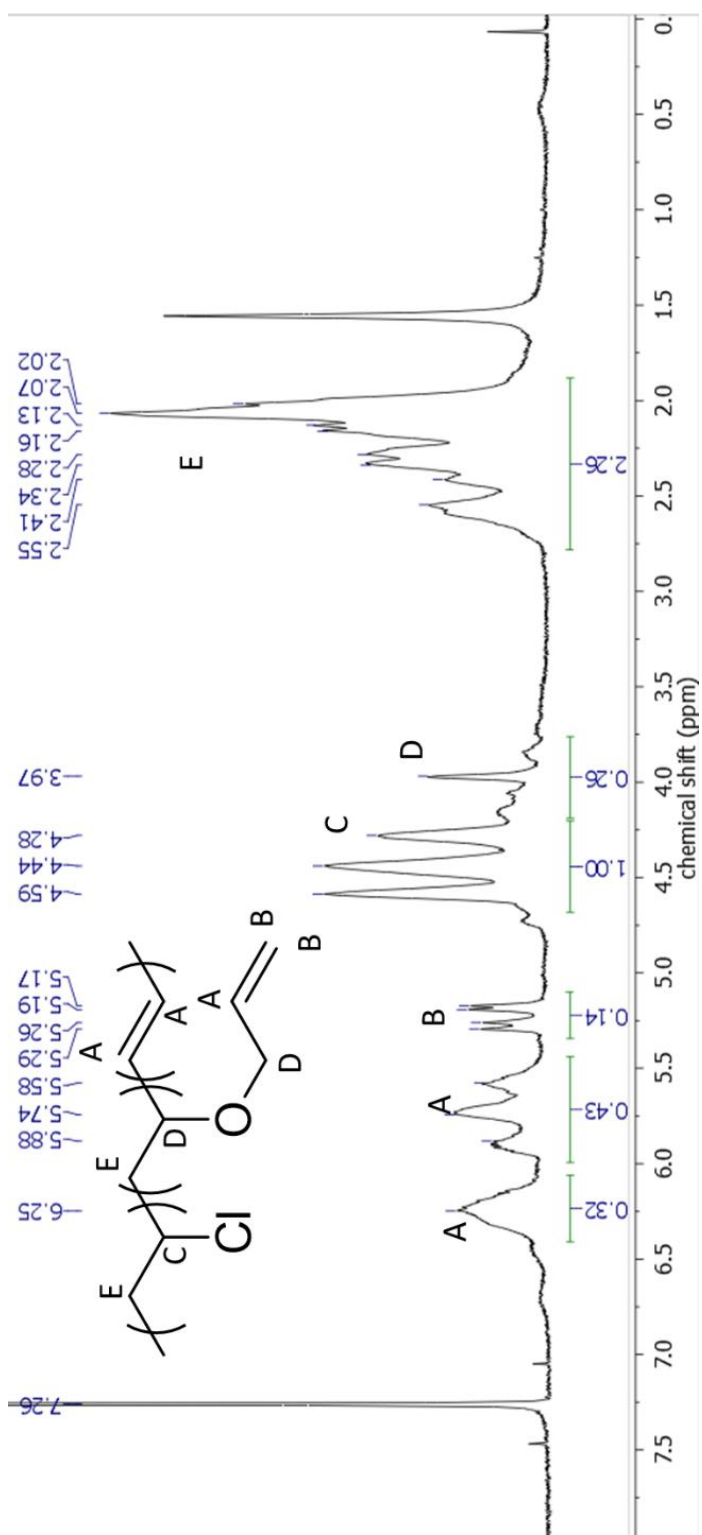
Cross metathesis reaction in the presence of pyridine as solvent (Table 3.2, entry 5).

Crude <sup>1</sup>H NMR without evaporating solvent.

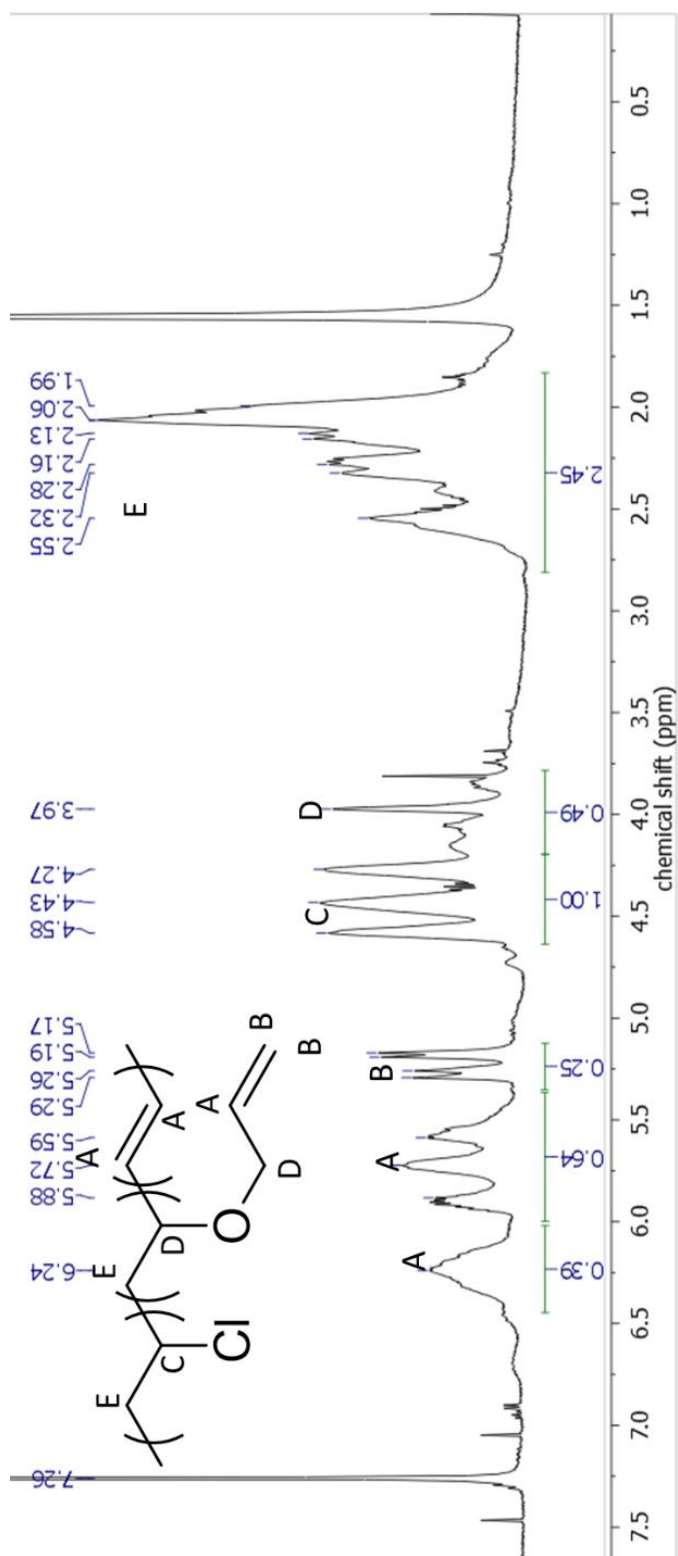




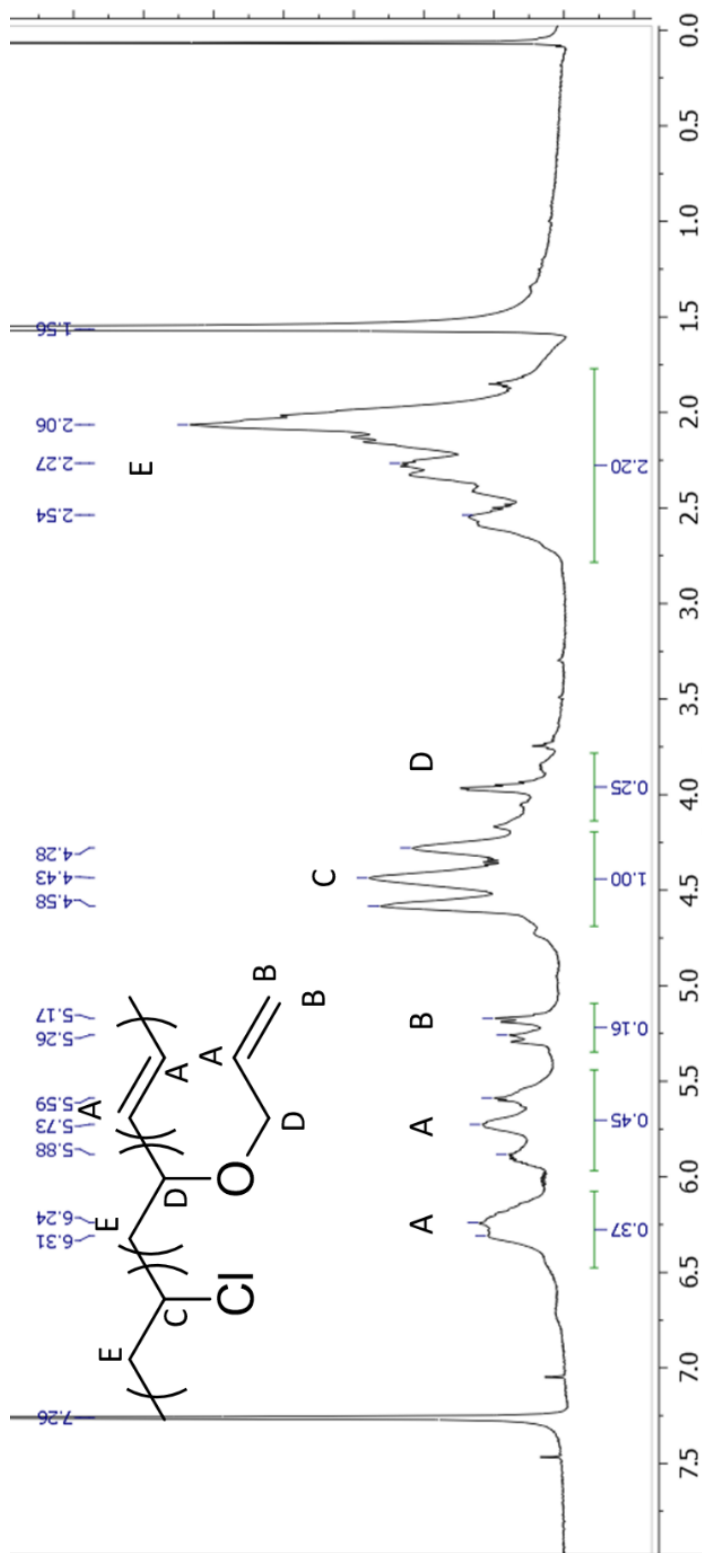




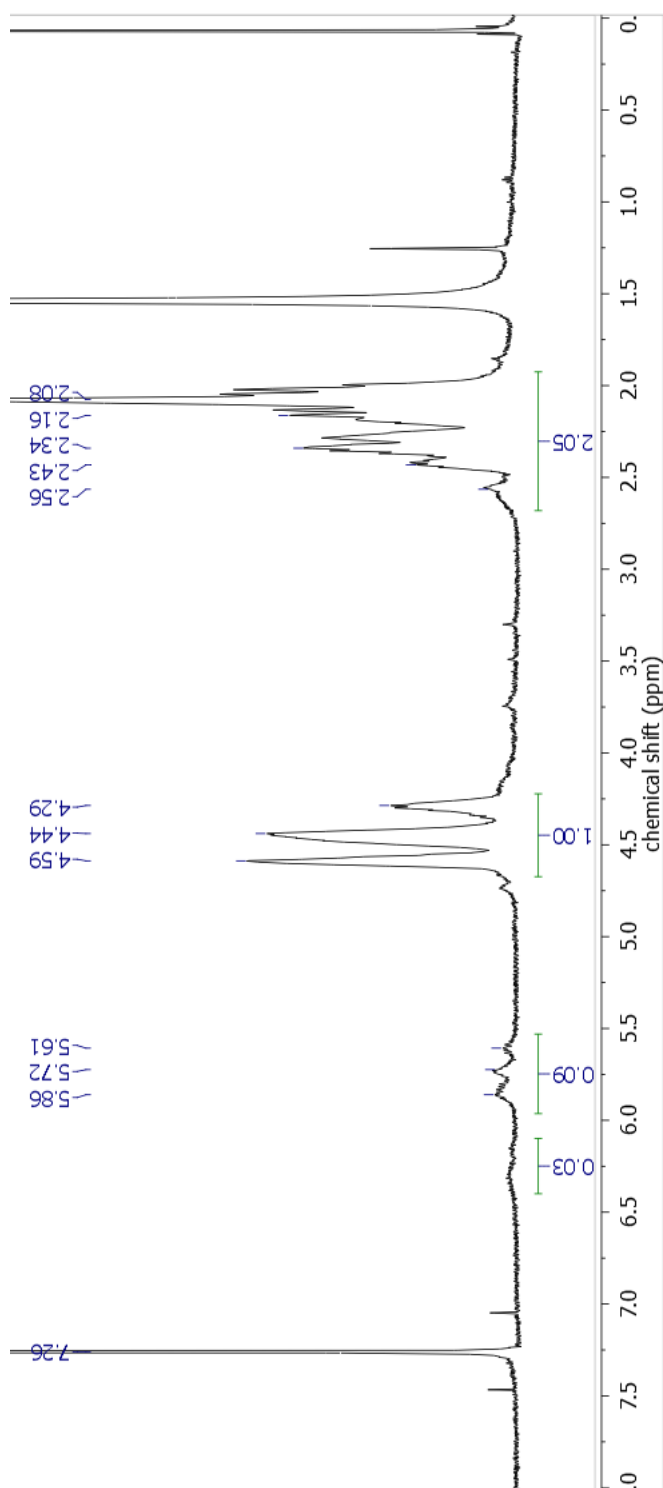
$^1\text{H}$  NMR of DPVC3 in  $\text{CDCl}_3$



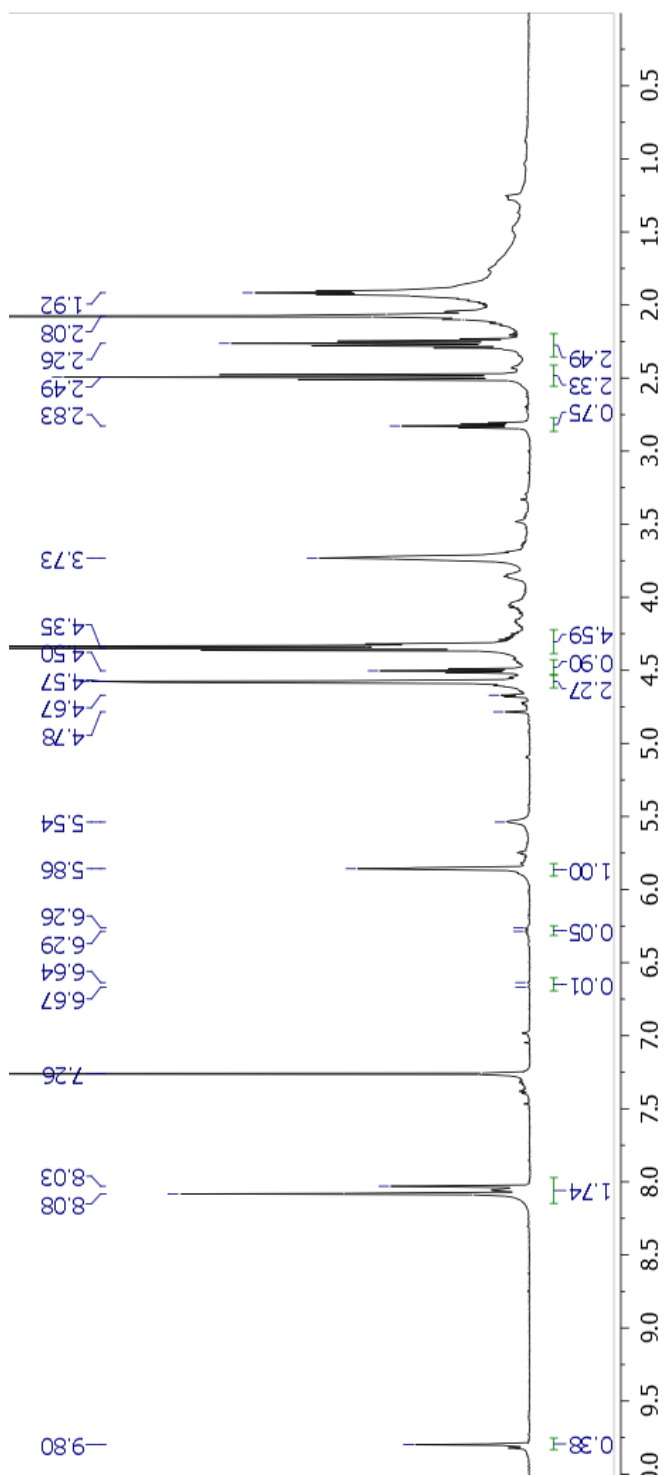
<sup>1</sup>H NMR of DPVC4 in CDCl<sub>3</sub>



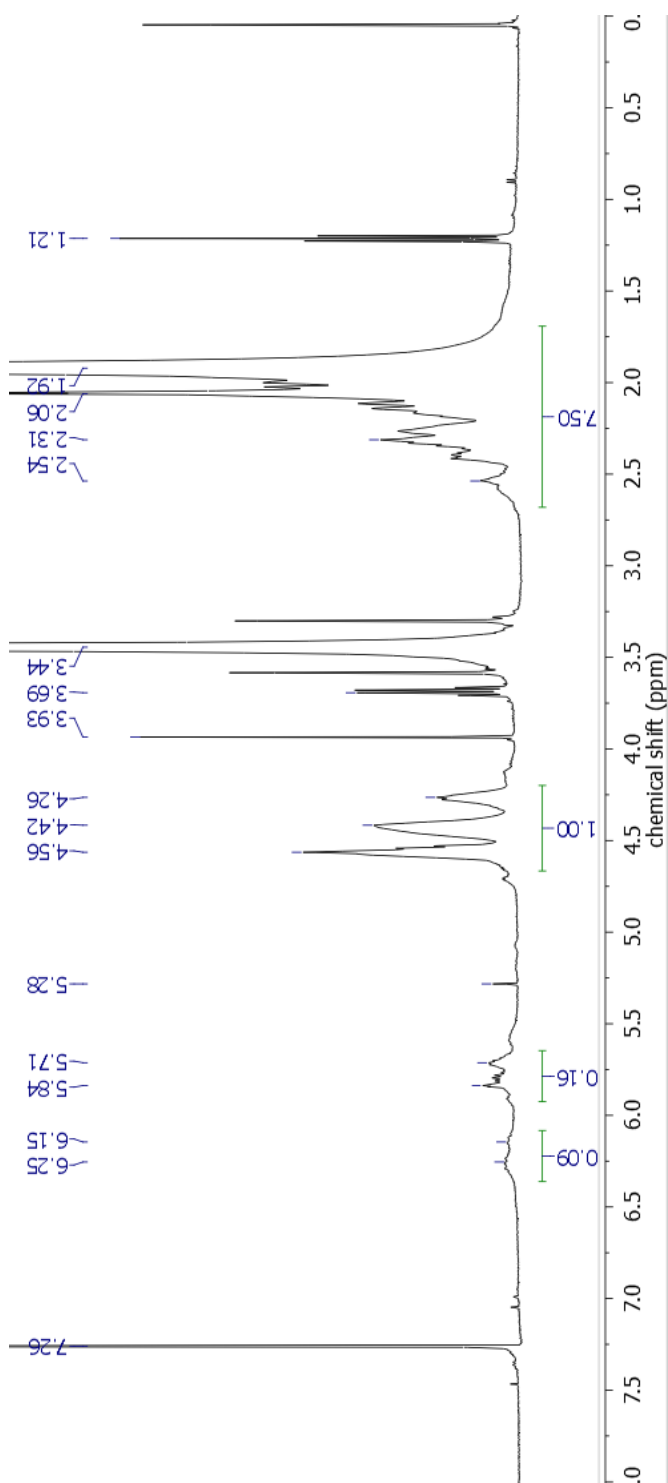
$^1\text{H}$  NMR of DPVC5 in  $\text{CDCl}_3$



<sup>1</sup>H NMR in CDCl<sub>3</sub> of Table 3.4, entry 1 (DPVC 1 with 1.0eq DAB and 6% Grubbs 2, DCM reflux, 44 h), precipitated in methanol.

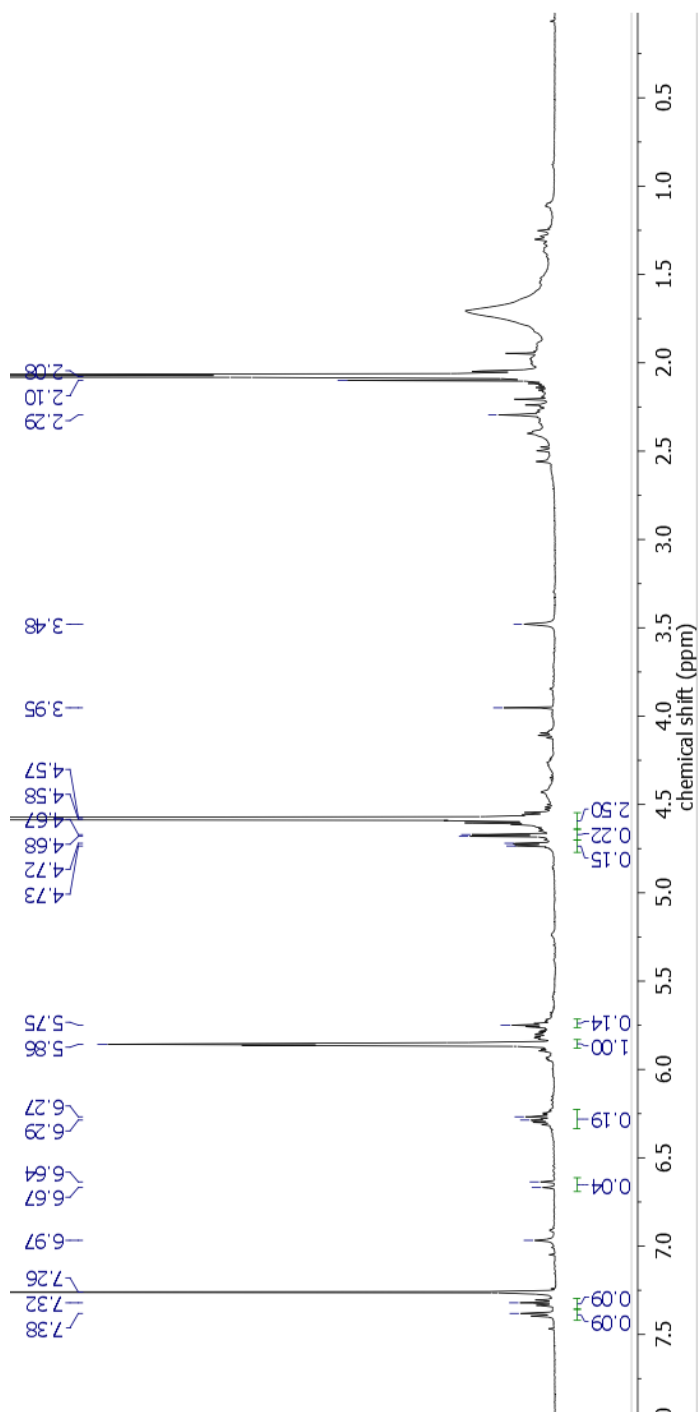


<sup>1</sup>H NMR in CDCl<sub>3</sub> of Table 3.4, entry 1, methanol-soluble fraction, concentrated by rotavap

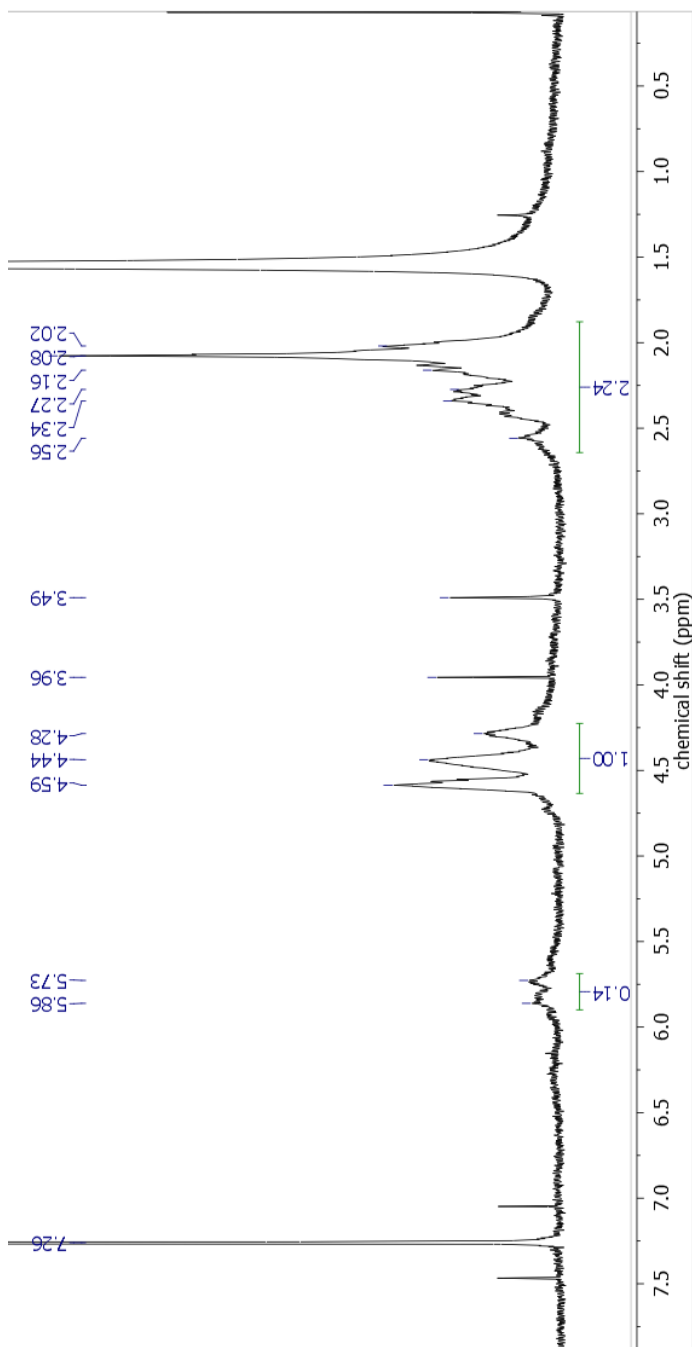


<sup>1</sup>H NMR in CDCl<sub>3</sub> of Table 3.4, entry 2 (DPVC 2 with 1.15eq DAB and 7% Grubbs 2, DCM reflux, 30 h), precipitated in methanol

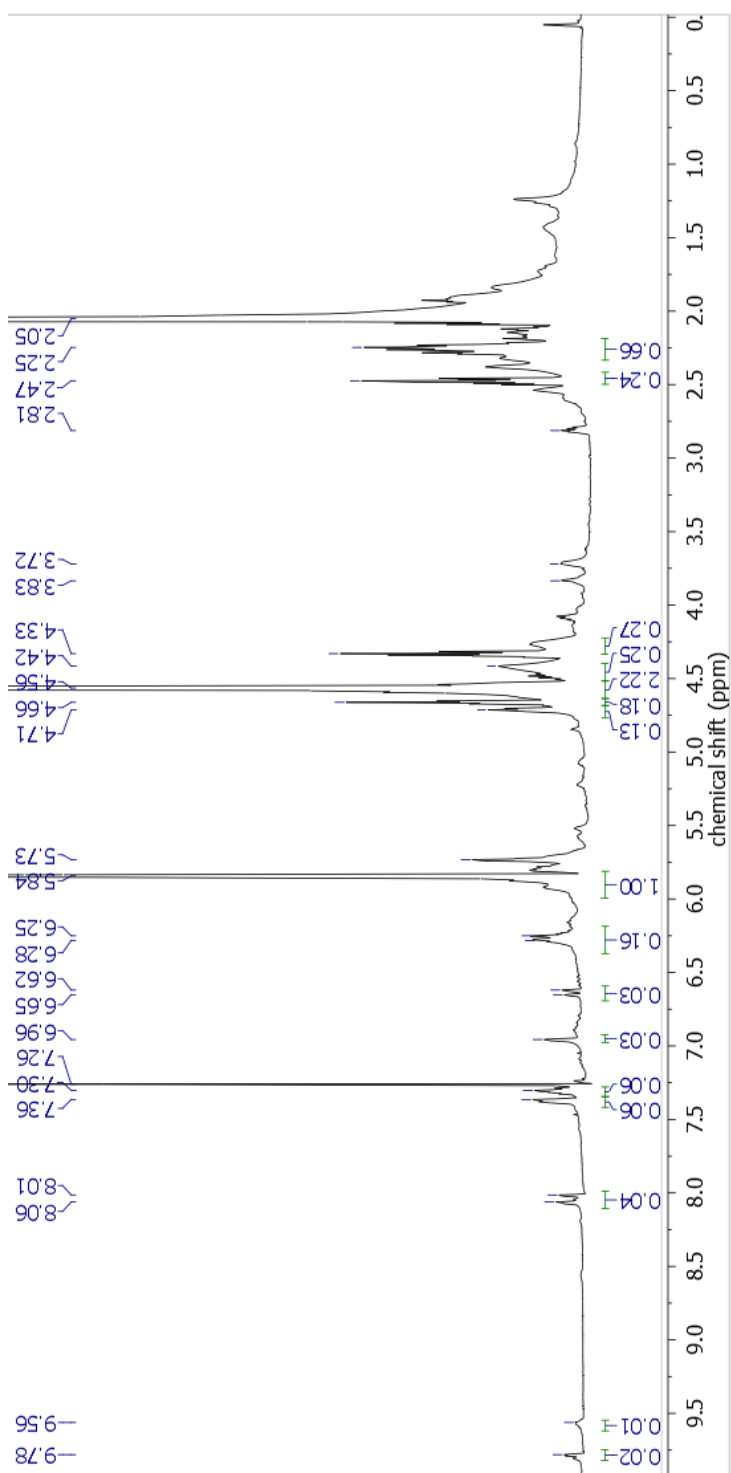




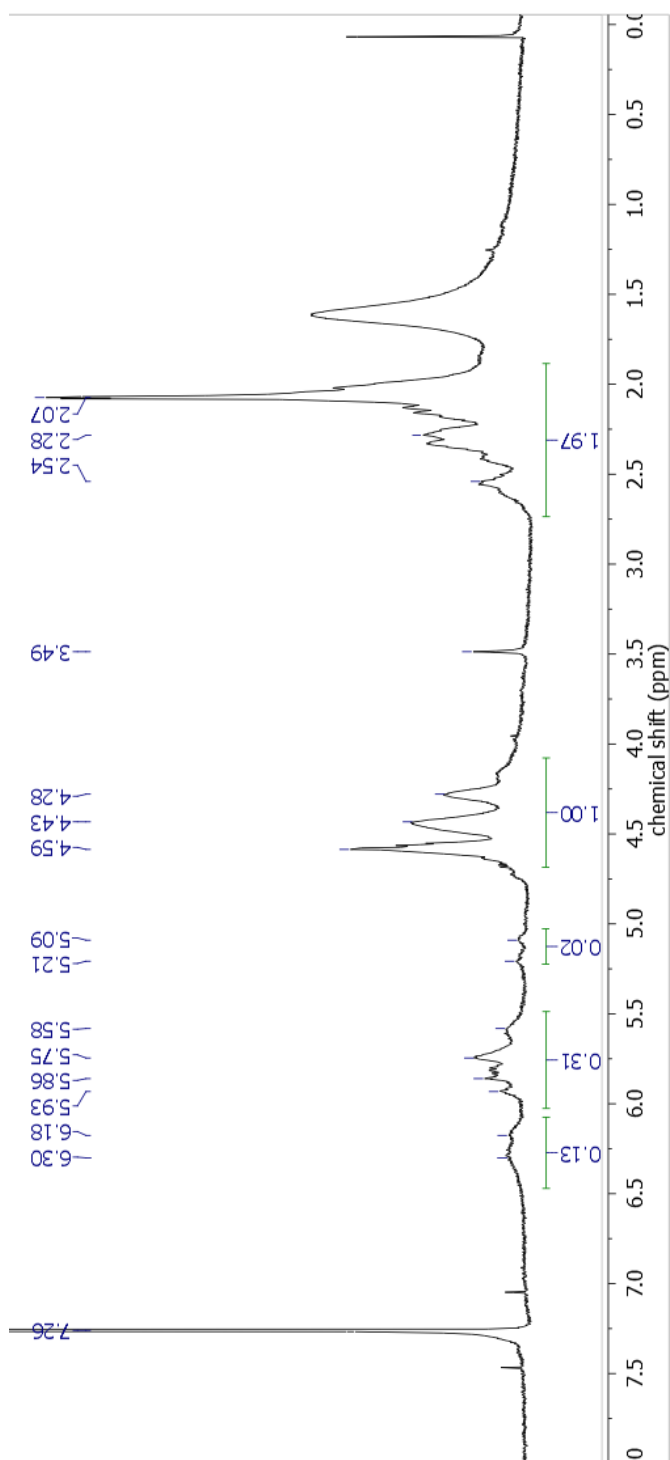
<sup>1</sup>H NMR in CDCl<sub>3</sub> of Table 3.4, entry 2, methanol-soluble fraction, concentrated by rotavap



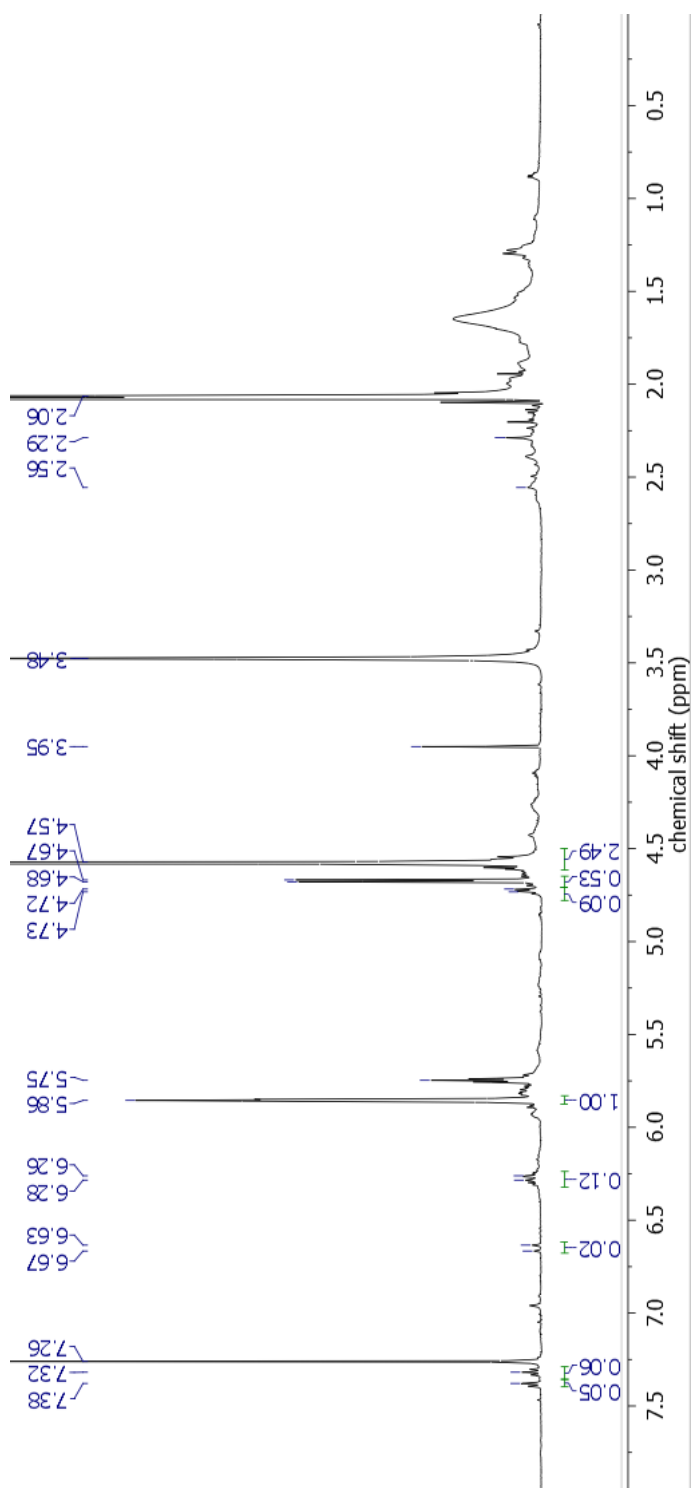
$^1\text{H}$  NMR in  $\text{CDCl}_3$  of Table 3.4, entry 3 (DPVC 3 with 1.12eq DAB and 6% Grubbs 2, DCM reflux, 4 d), precipitated in methanol



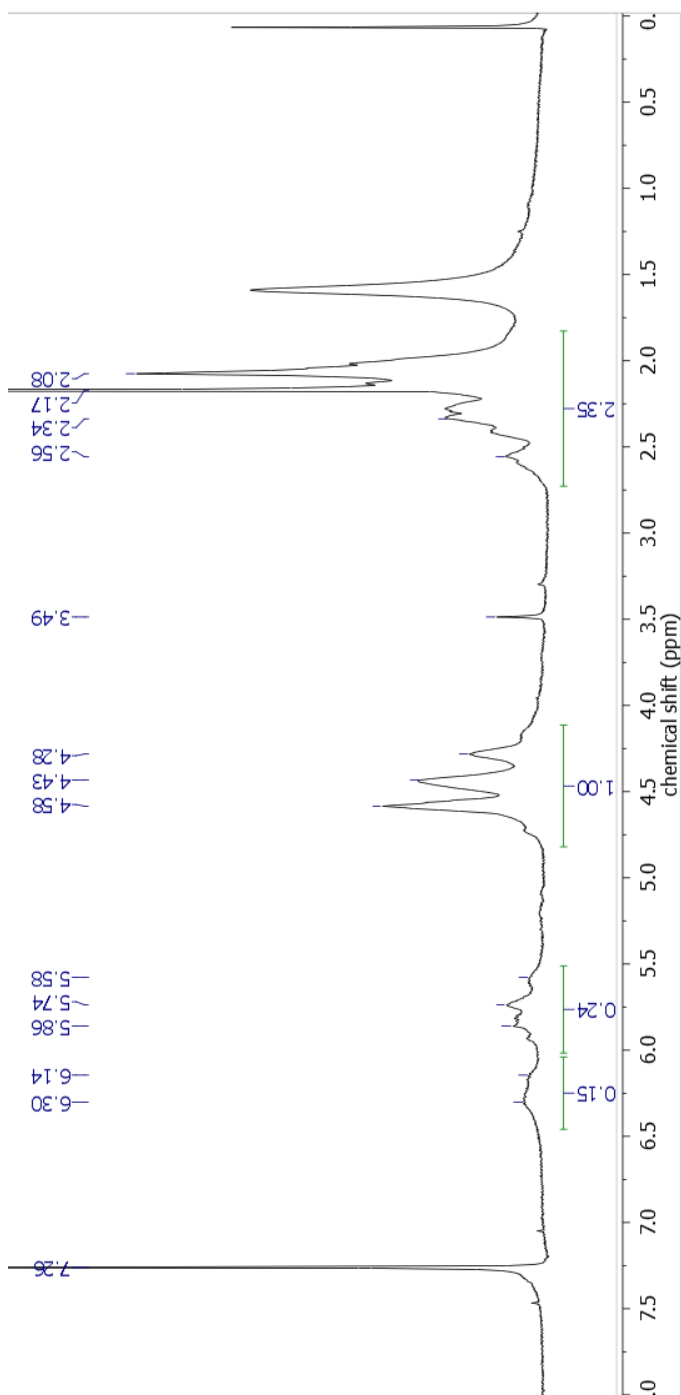
<sup>1</sup>H NMR in CDCl<sub>3</sub> of Table 3.4, entry 3, methanol-soluble fraction, concentrated by rotavap



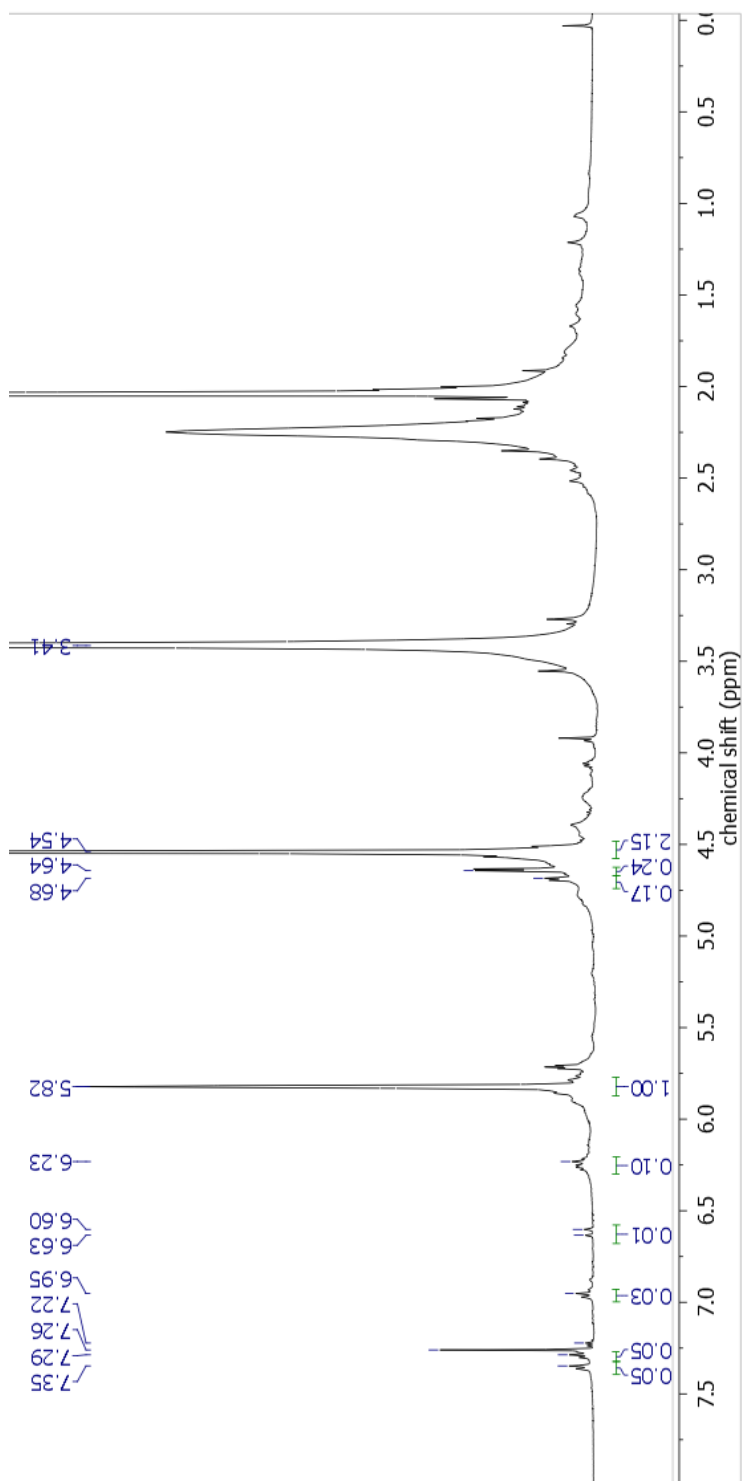
$^1\text{H}$  NMR in  $\text{CDCl}_3$  of Table 3.4, entry 4 (DPVC 4 with 1.14eq DAB and 5% Grubbs 2, DCM reflux, 30 h), precipitated in methanol



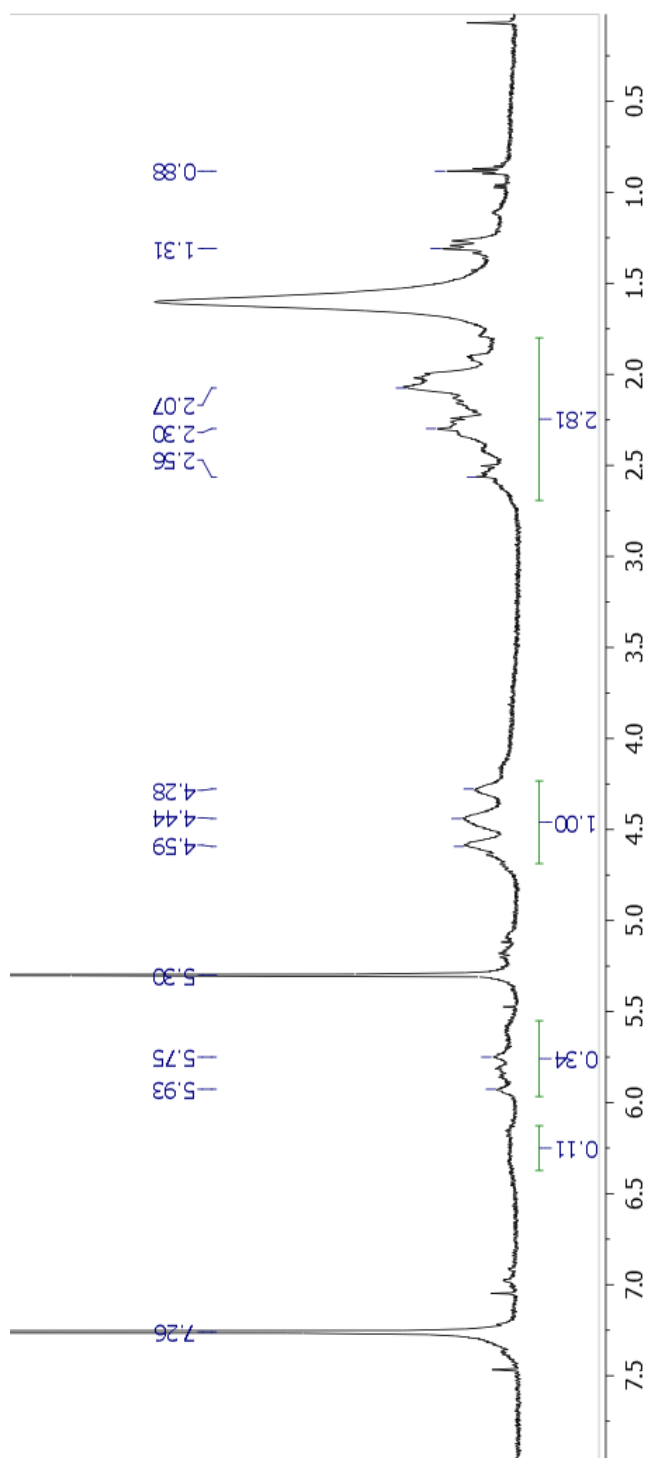
<sup>1</sup>H NMR in CDCl<sub>3</sub> of Table 3.4, entry 4, methanol-soluble fraction, concentrated by rotavap



<sup>1</sup>H NMR in CDCl<sub>3</sub> of Table 3.10, entry 2 (DPVC 5 with 0.96eq DAB and 4% Grubbs 2, degassed by bubbling N<sub>2</sub>, DCM reflux, 18 h), precipitated in methanol

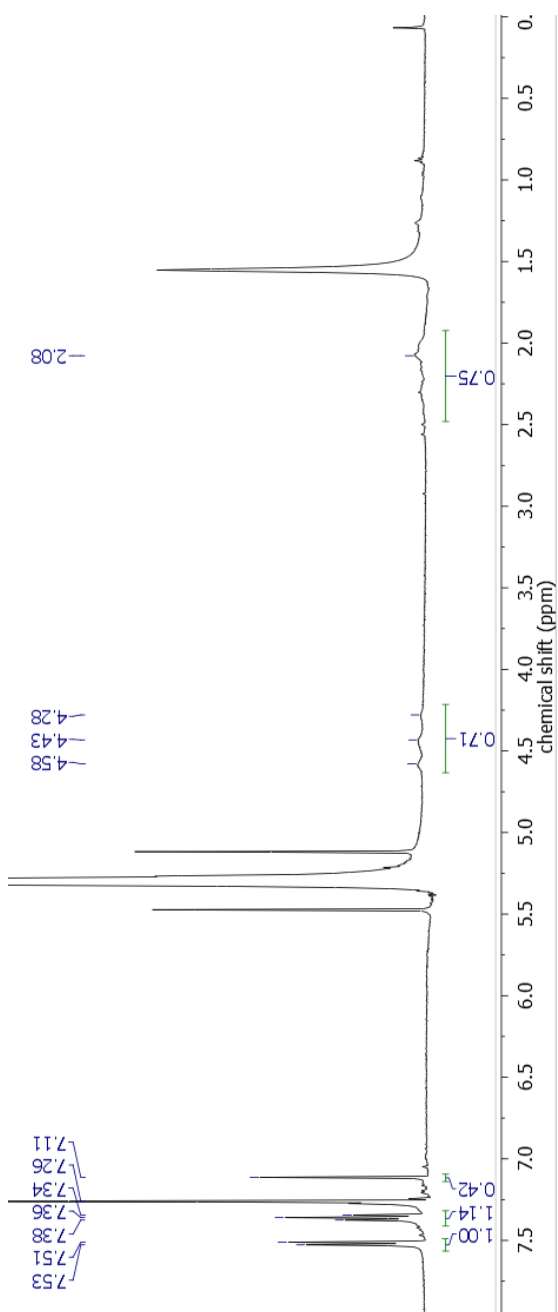


<sup>1</sup>H NMR in CDCl<sub>3</sub> of Table 3.10, entry 2, methanol-soluble fraction, concentrated by rotavap

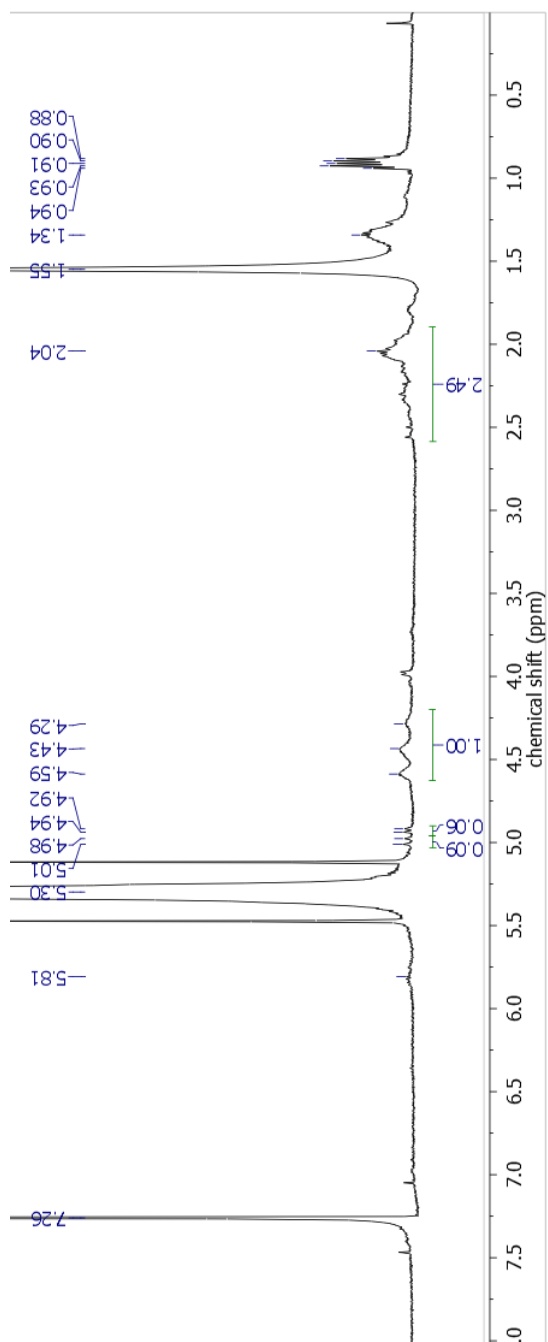


$^1\text{H}$  NMR in  $\text{CDCl}_3$  of Table 3.5, entry 1 (DPVC 4 with no partner alkene and 5% Grubbs 2, degassed by bubbling Ar, DCM reflux, 17 h), crude product

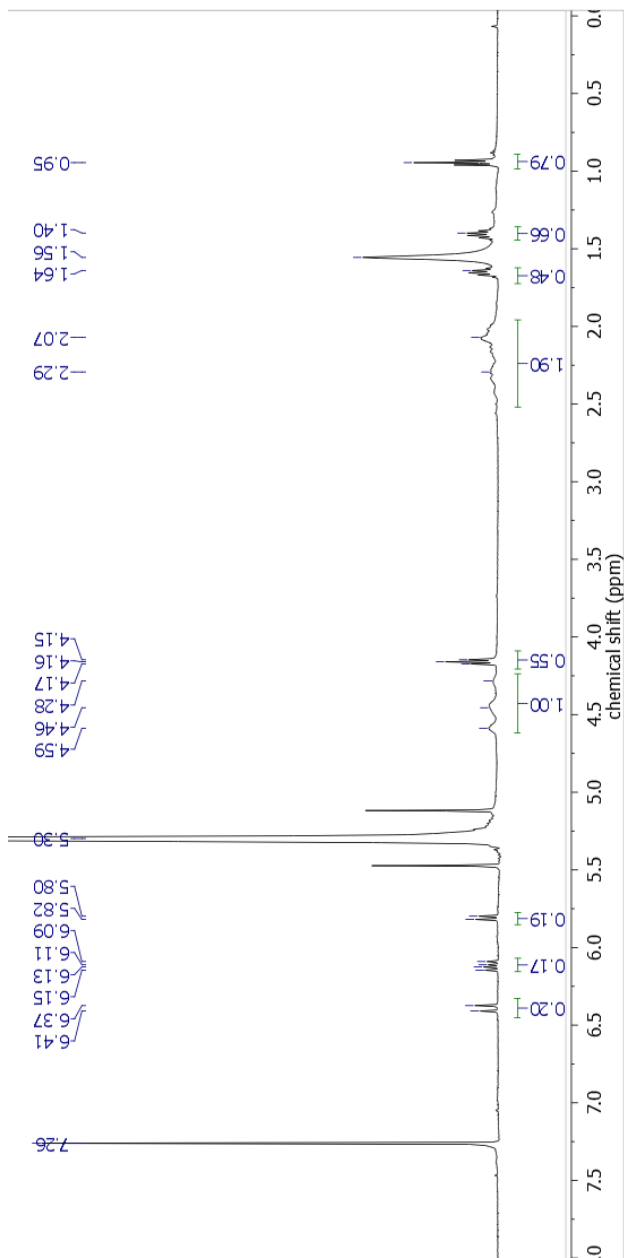




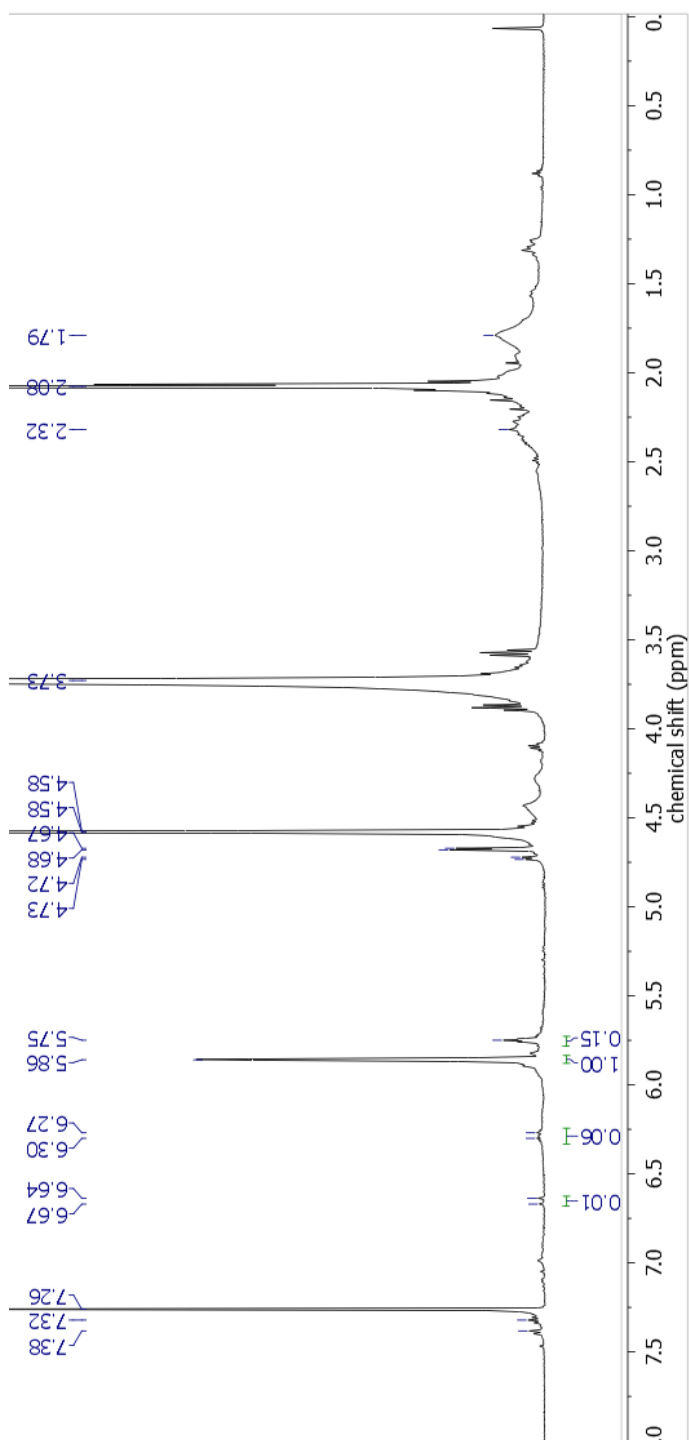
$^1\text{H}$  NMR in  $\text{CDCl}_3$  of Table 3.7, entry 3 (DPVC 3 with 1.13eq trans-stilbene and 5% Grubbs 2, degassed by bubbling Ar, DCM reflux, 17 h), crude product. The stilbene starting material is seen at 7.11, 7.37, and 7.52. The diene (1,4-diphenyl-1,3-butadiene) would be expected at 6.54-6.74 and 6.95-7.02 but is not seen.



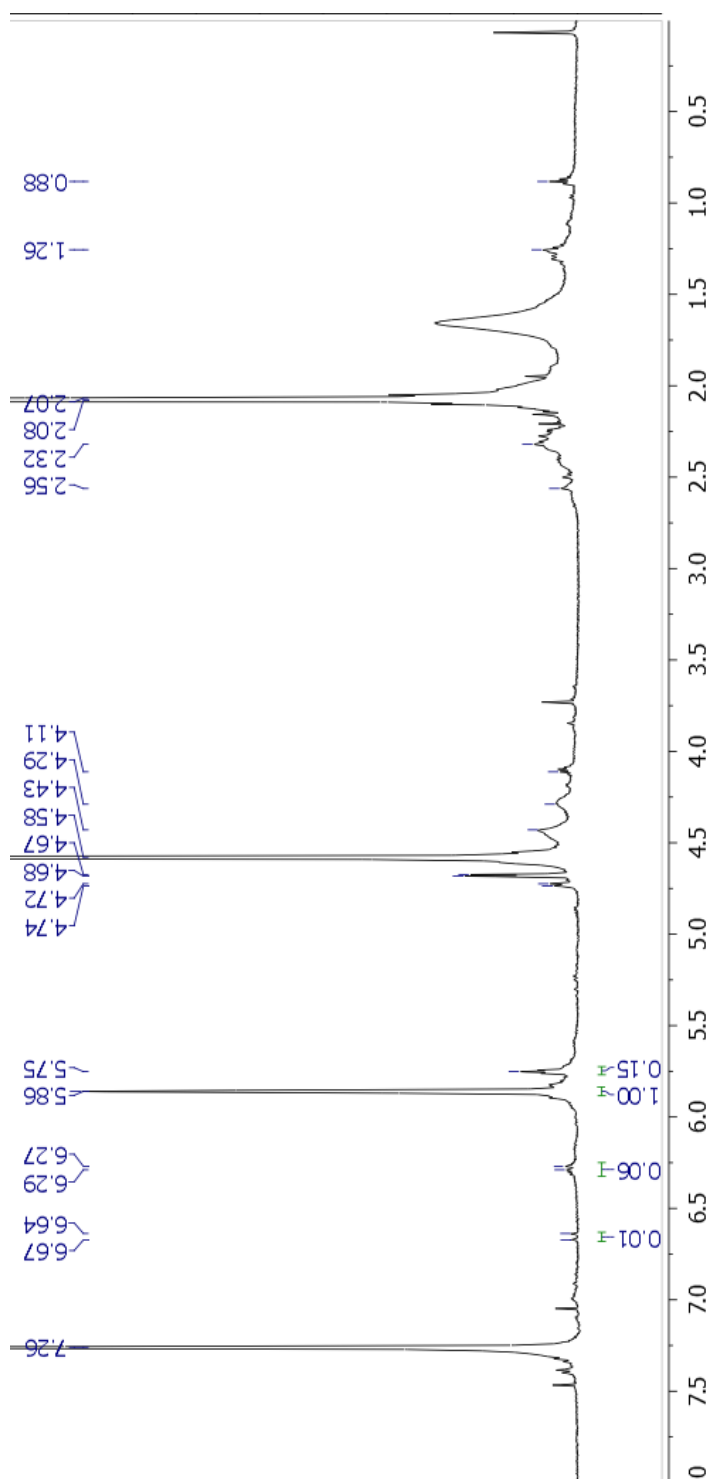
$^1\text{H}$  NMR in  $\text{CDCl}_3$  of Table 3.7, entry 4 (DPVC 1 with 1.0eq 1-hexene and 5% Grubbs 2, degassed by bubbling Ar, DCM reflux, 17 h), crude product. The 1-hexene starting material is visible at 4.93, 5.00, and 5.81. The diene product (5,7-dodecadiene) would be expected at 5.56 and 6.00 but is not seen.



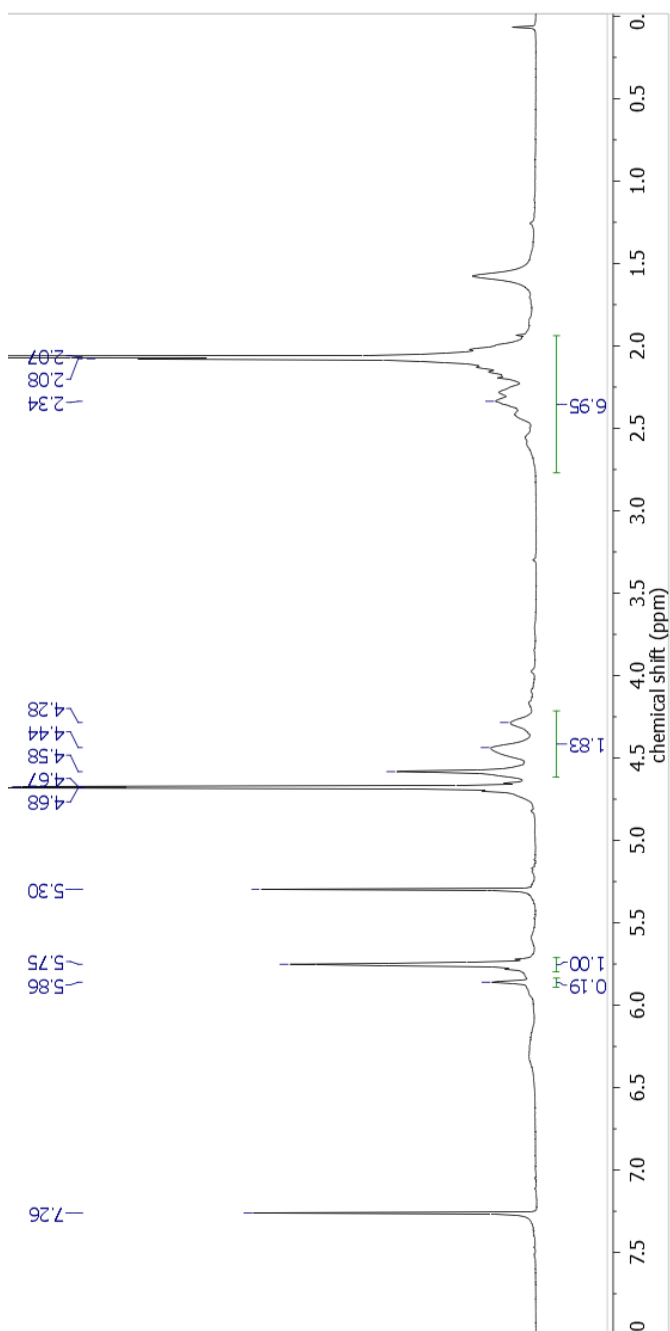
$^1\text{H}$  NMR in  $\text{CDCl}_3$  of Table 3.7, entry 5 (DPVC 2 with 1.0eq butyl acrylate and 5% Grubbs 2, degassed by bubbling Ar, DCM reflux, 17 h), crude product. Butyl acrylate starting material is present at 5.81, 6.12, and 6.39. The diene product (dibutyl muconate) would be expected at 7.32-7.26 and 6.21-6.12, but was not seen.



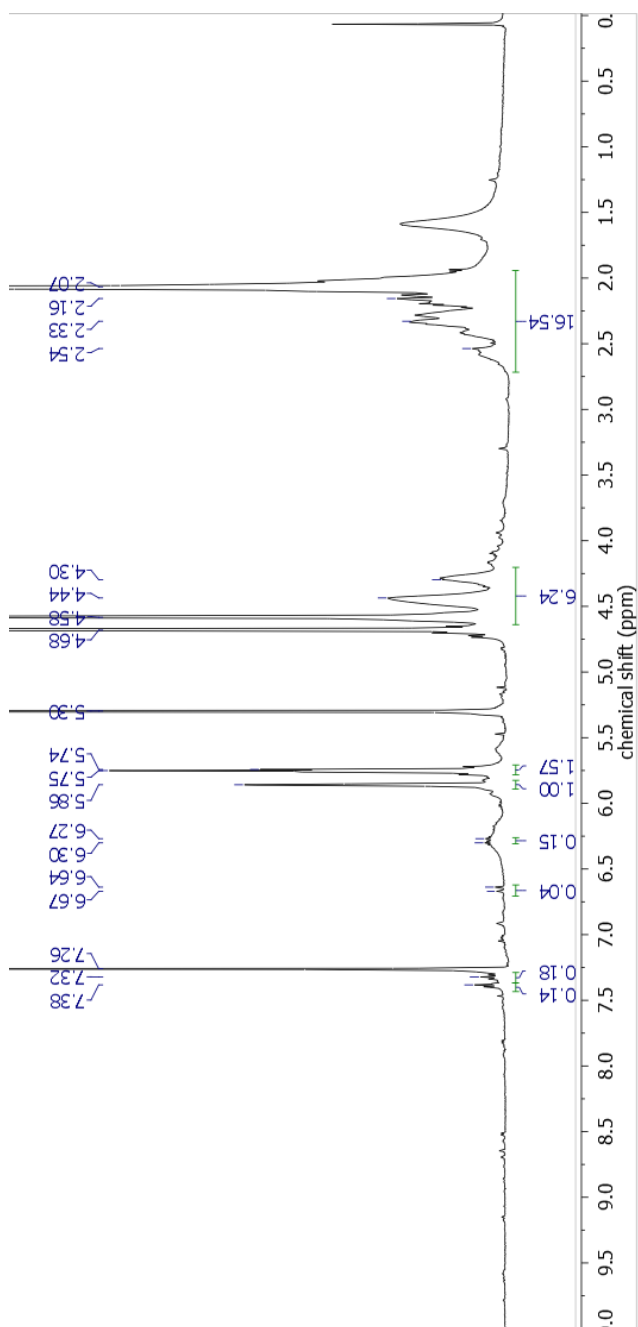
$^1\text{H}$  NMR in  $\text{CDCl}_3$  of Table 3.8, entry 2 (DPVC 5 with 1.02eq DAB and 4% Grubbs 2, degassed by bubbling Ar, 1,2-dichloroethane, 55 °C, 17 h), crude product



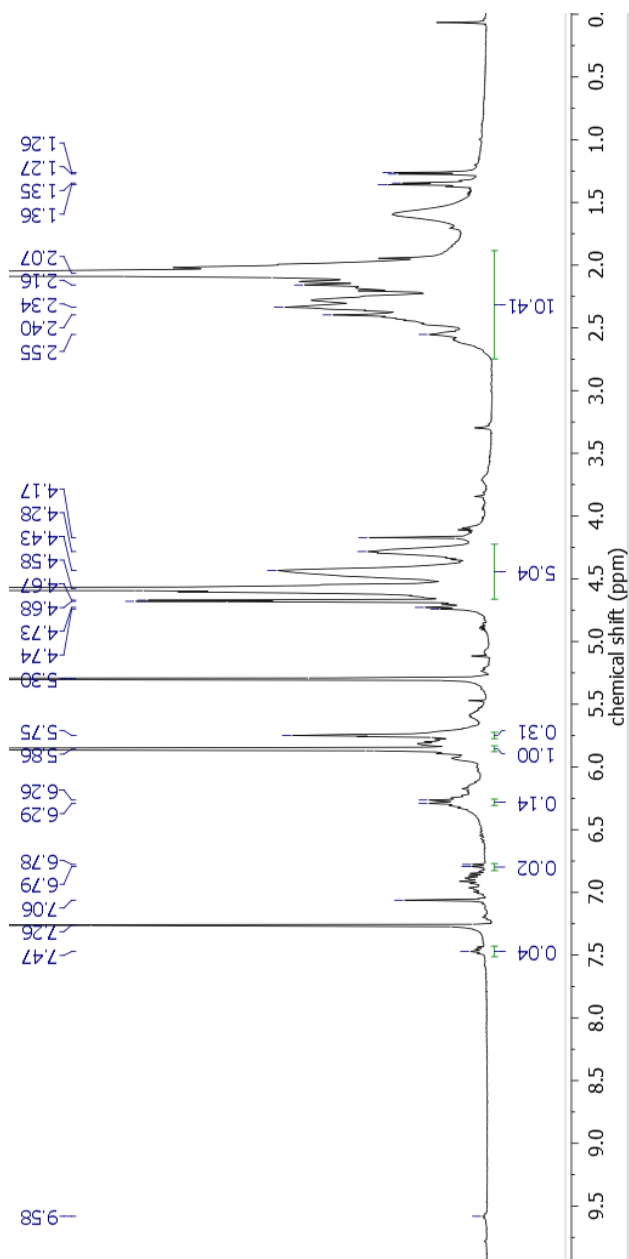
$^1\text{H}$  NMR in  $\text{CDCl}_3$  of Table 3.8, entry 3 (DPVC 5 with 0.96eq DAB and 3% Grubbs 2, degassed by bubbling Ar, chloroform, 55 °C, 17 h), crude product



<sup>1</sup>H NMR in CDCl<sub>3</sub> of Table 3.9, entry 4 (DPVC2 with 1.05eq DAB and 1% Grubbs 2, degassed by bubbling Ar, DCM reflux, 17 h), crude product. The ratio of *Z*-DAB (5.75) to *E*-DAB (5.86) is much higher than in other reactions, indicating incomplete self-metathesis.

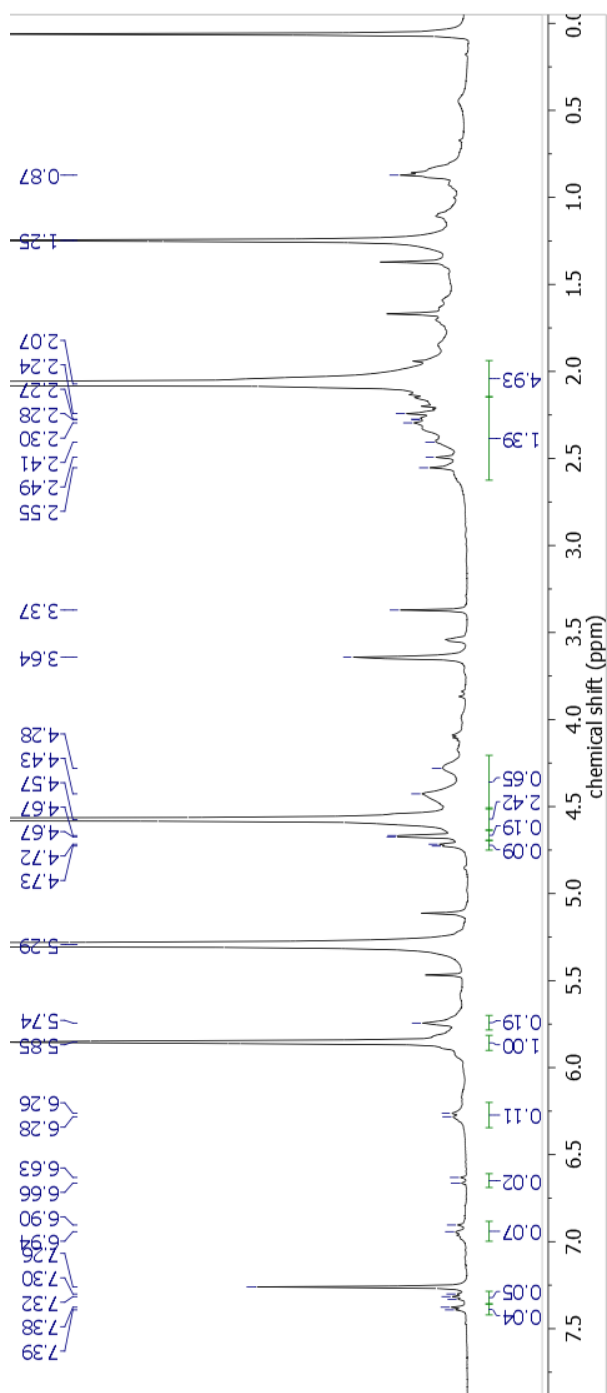


$^1\text{H}$  NMR in  $\text{CDCl}_3$  of Table 3.9, entry 3 (DPVC2 with 1.08eq DAB and 5% Grubbs 3, degassed by bubbling Ar, DCM reflux, 17 h), crude product. The ratio of *Z*-DAB (5.75) to *E*-DAB (5.86) is much higher than in other reactions, indicating incomplete self-metathesis.

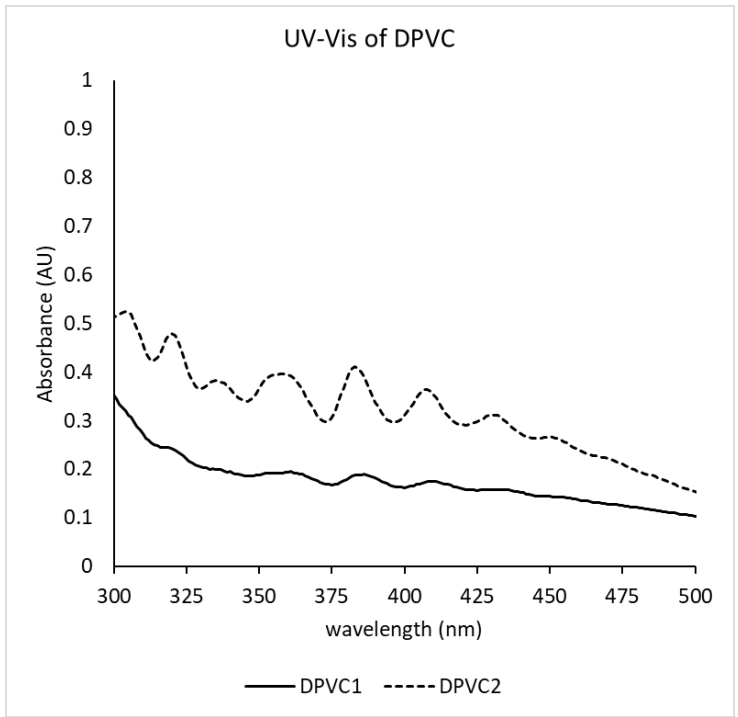


$^1\text{H}$ NMR in  $\text{CDCl}_3$  of Table 3.9, entry 2 (DPVC2 with 1.07eq DAB and 6% Hoveyda-Grubbs 2, degassed by bubbling Ar, DCM reflux, 17 h), crude product. The ratio of *Z*-DAB (5.75) to *E*-DAB (5.86) is higher than in other reactions, possibly indicating incomplete self-metathesis.

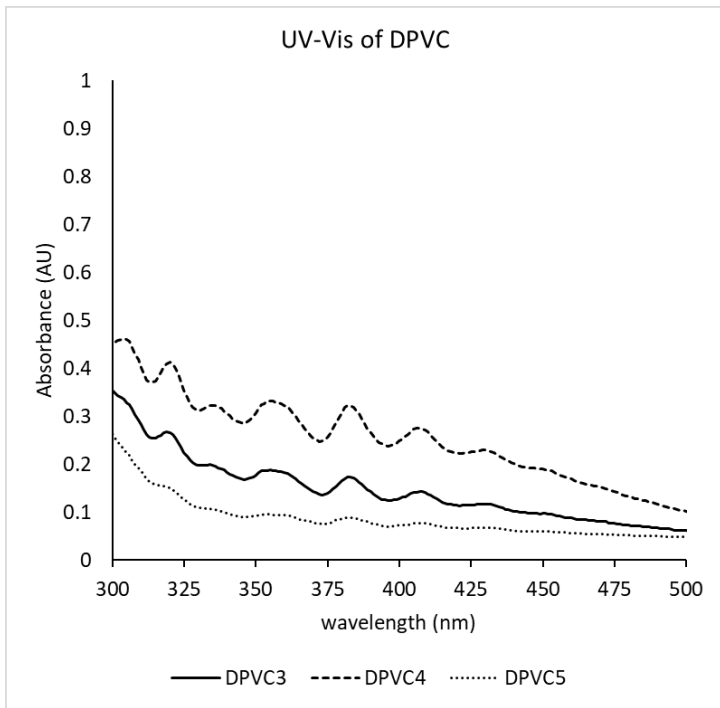




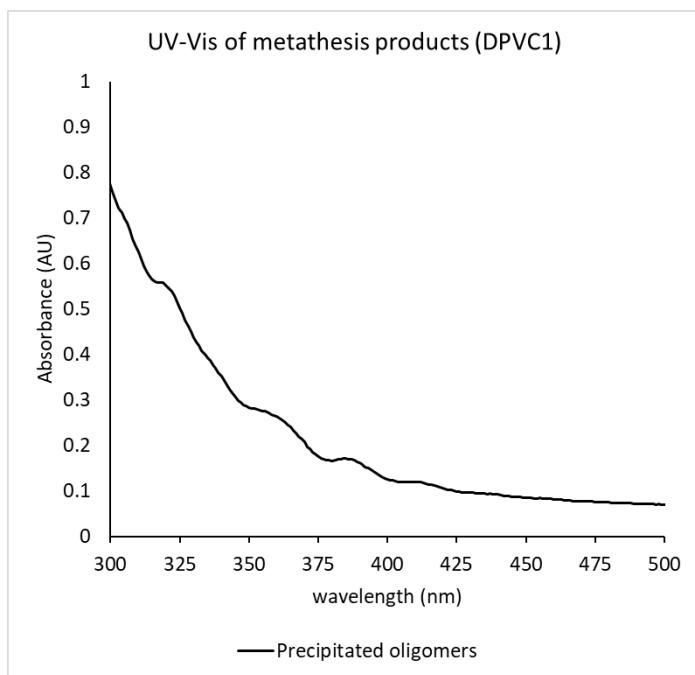
$^1\text{H}$  NMR in  $\text{CDCl}_3$  of Table 3.10, entry 3 (freshly-prepared DPVC5 with 0.95eq DAB and 3% Grubbs 2, freeze-pump-thaw degassed, DCM reflux in the dark, 17 h), crude product



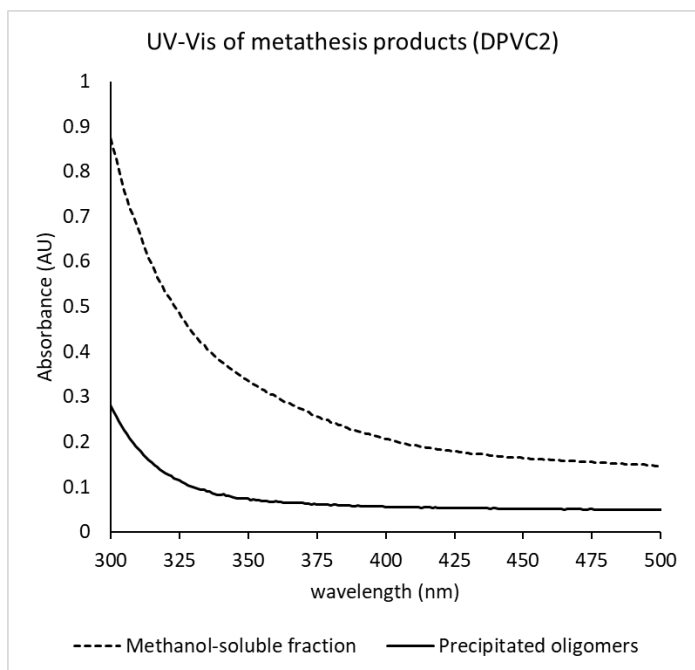
UV-Vis spectrum of DPVC1 and DPVC2



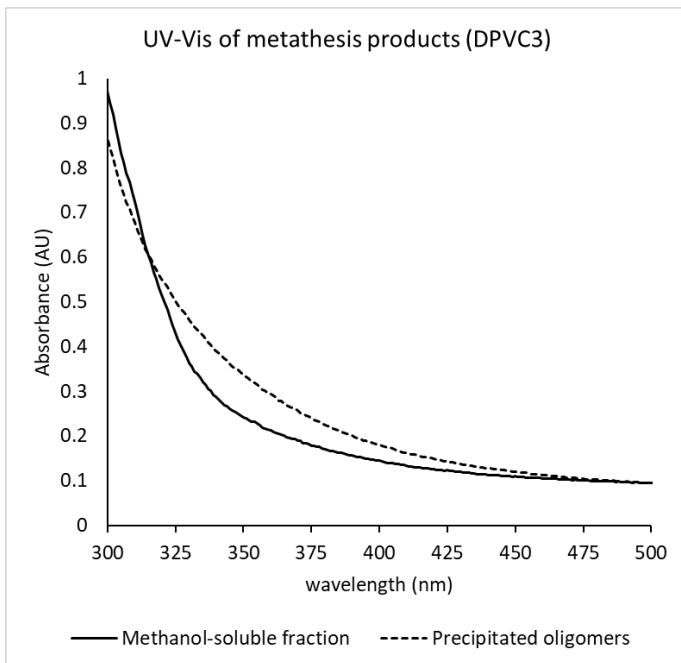
UV-Vis spectrum of DPVC3-5



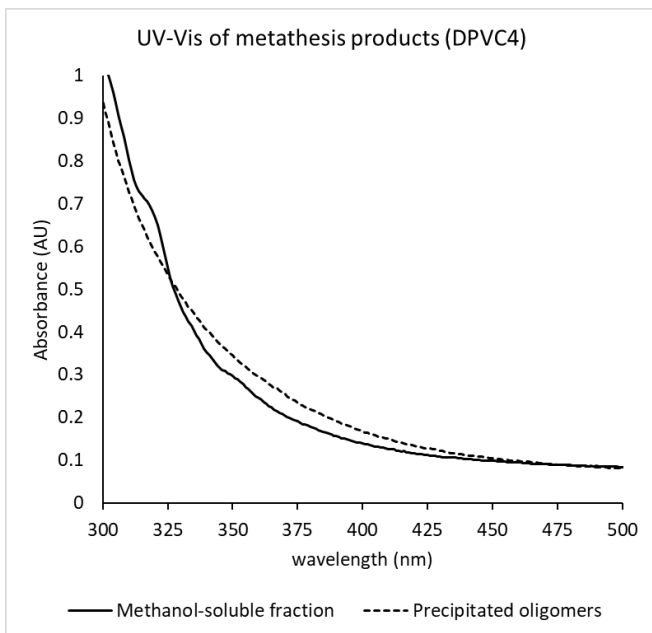
UV Visible spectrum of metathesis products of DPVC1 (Table 3.4, entry 1)



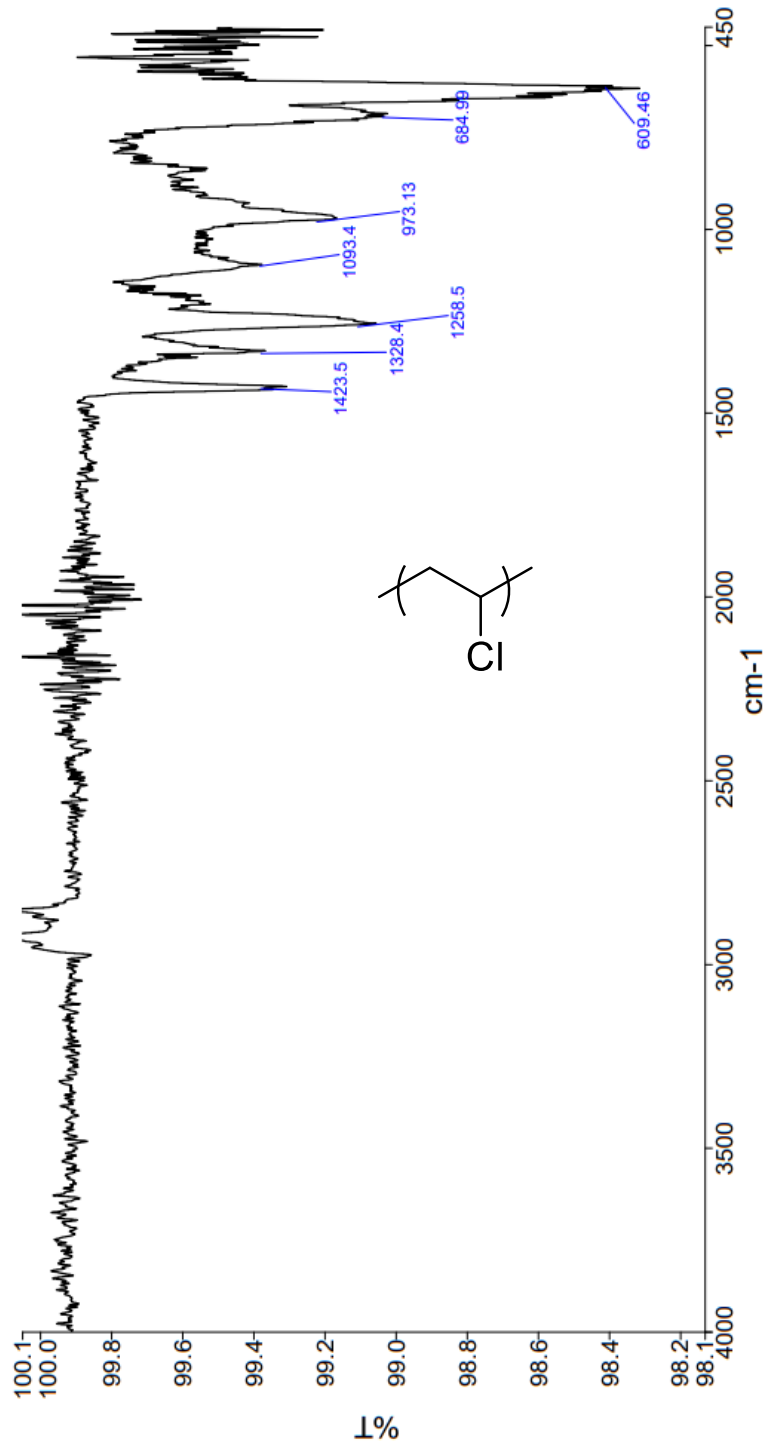
UV Visible spectrum of metathesis products of DPVC2 (Table 3.4, entry 2)



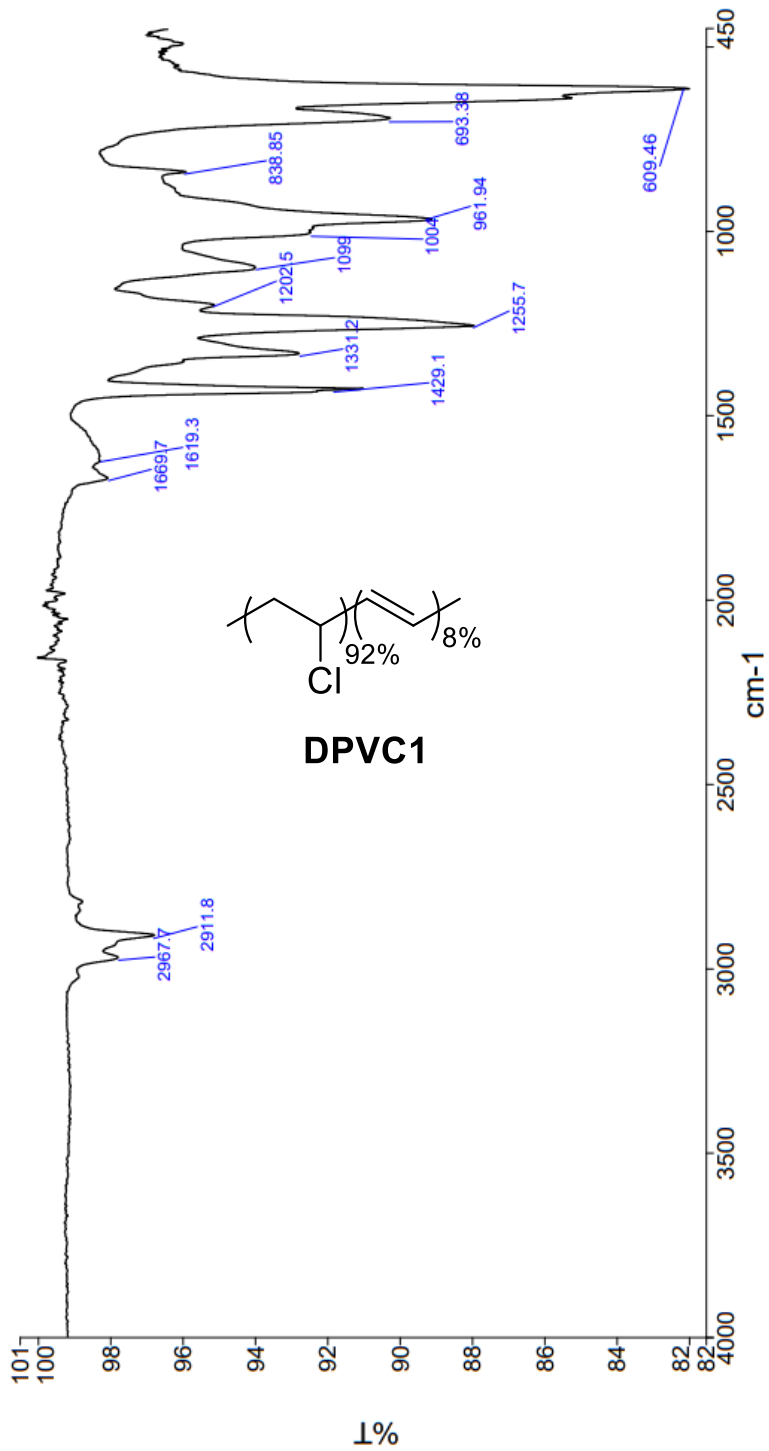
UV Visible spectrum of metathesis products of DPVC3 (Table 3.4, entry 3)



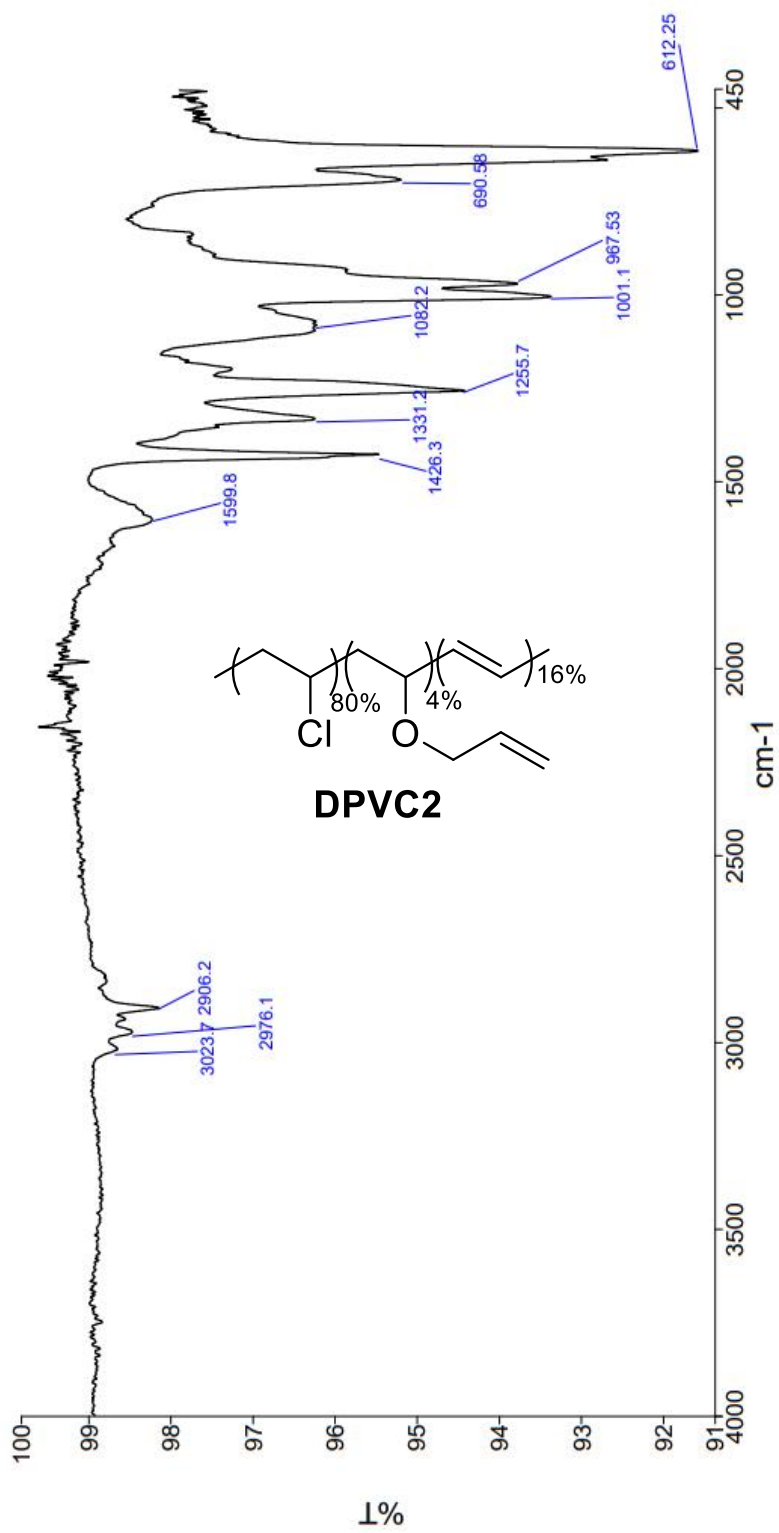
UV Visible spectrum of metathesis products of DPVC4 (Table 3.4, entry 4)



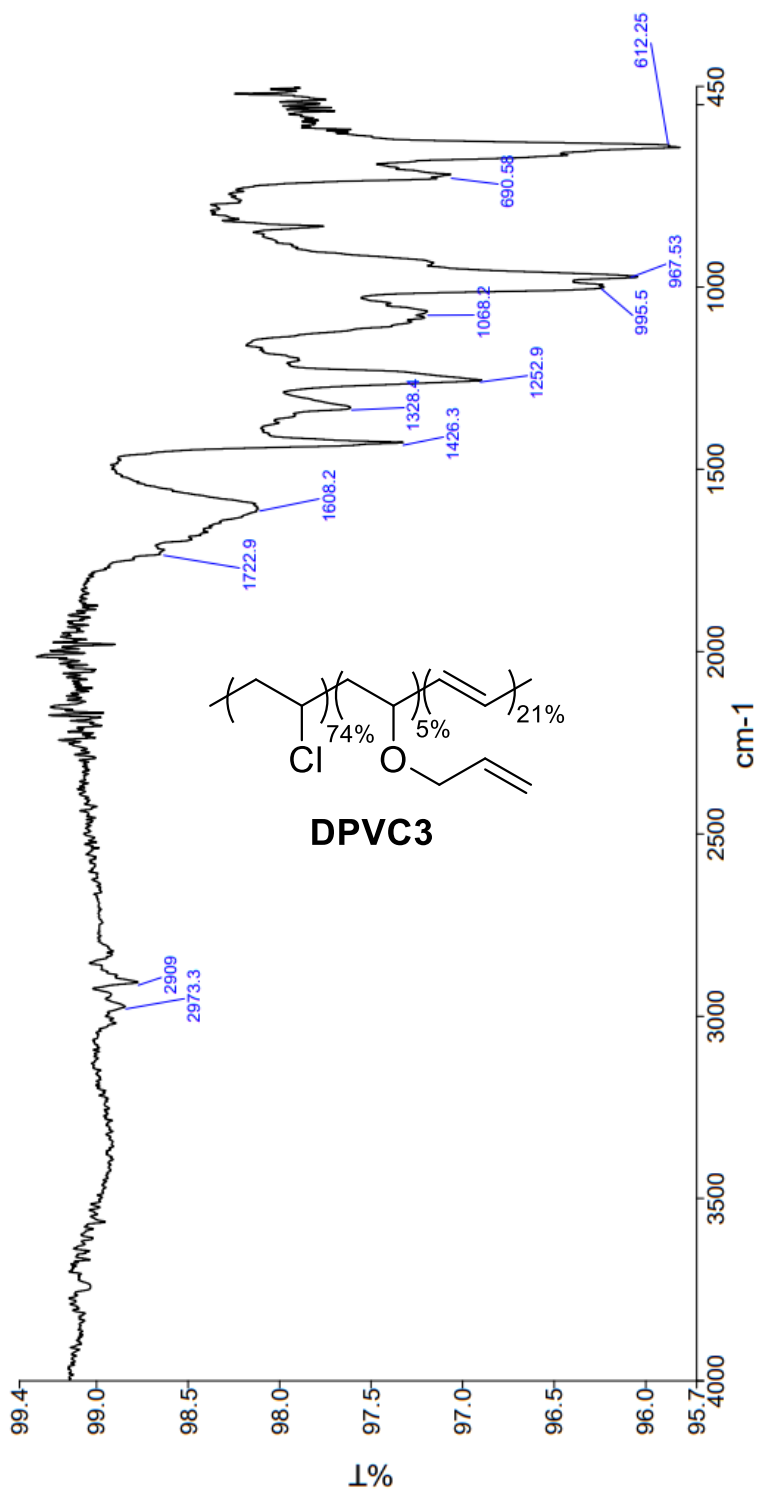
ATR-FTIR of PVC



ATR-FTIR of DPVC1

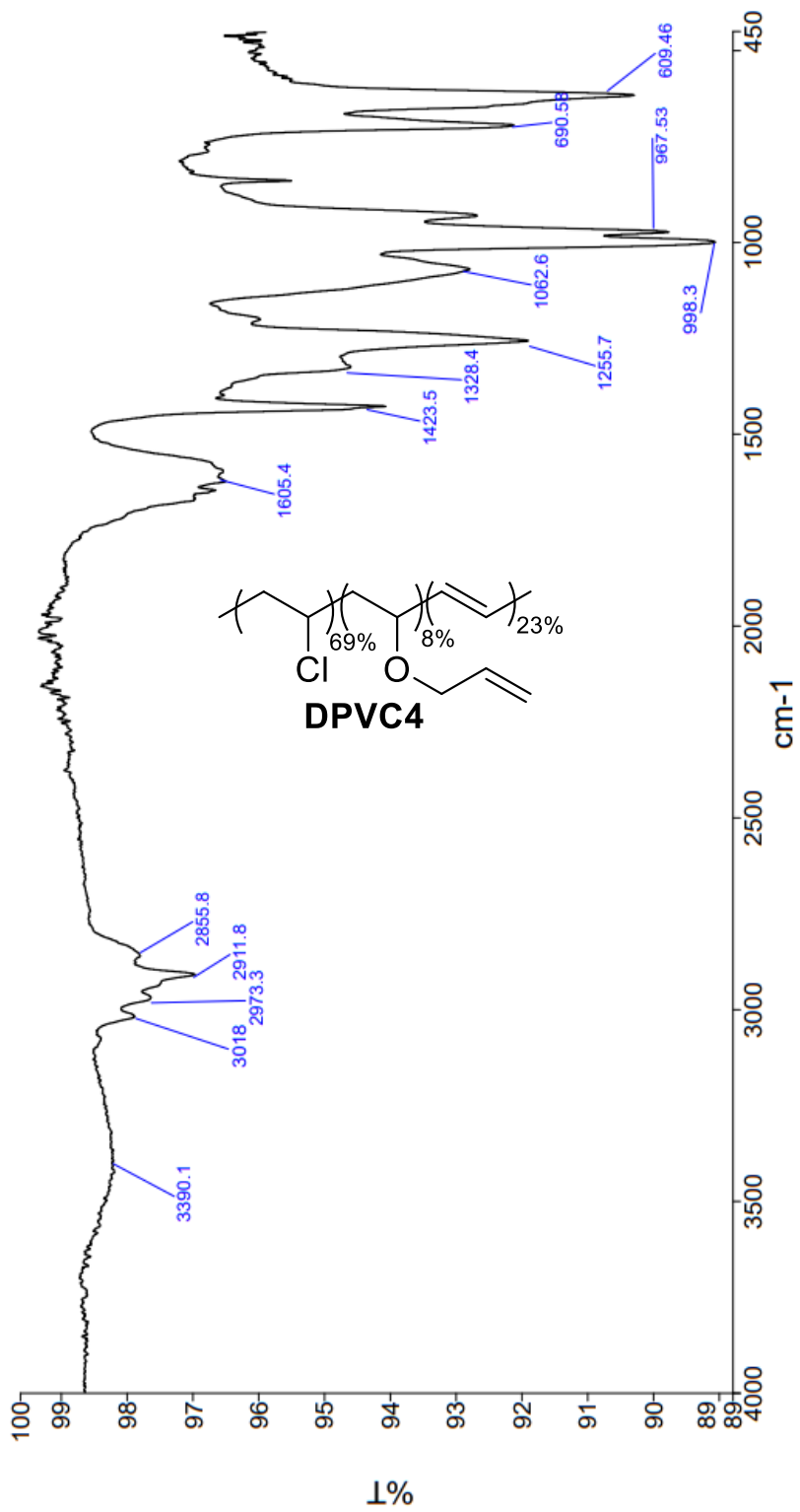


ATR-FTIR of DPVC2

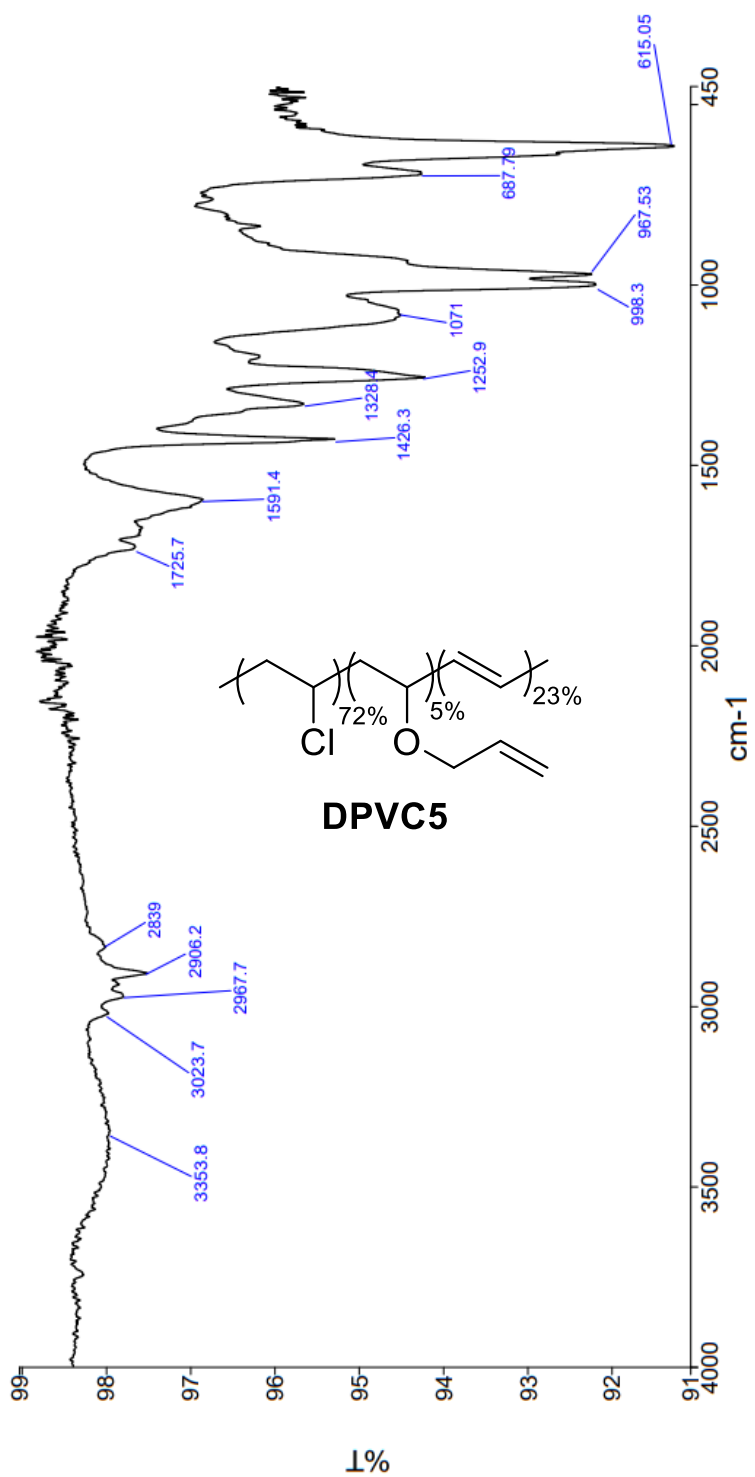


ATR-FTIR of DPVC3





ATR-FTIR of DPVC4



ATR-FTIR of DPVC5

GPC Retention Times

PS Standards	Retention time (min)	Samples	Retention time (min)	Calculated MW (kDa)
68 kDa	36.9	PVC	37.5	61.1
34.5 kDa	39.2	DPVC1	38.1	49.8
20.4 kDa	40.9	DPVC2	39.2	34.2
9 kDa	43.6	DPVC3	41.8	14.1
2 kDa	47.2	DPVC4	41.5	15.6
		DPVC5	42.6	10.7

PS Standards	Retention time (min)	Samples	Retention time (min)	Calculated MW (kDa)
68 kDa	36.5	PVC	36.8	68.1
34.5 kDa	38.8	DPVC1	38.5	38.1
20.4 kDa	40.4	DPVC2	39.9	23.7
9 kDa	43.3	DPVC3	42.2	10.8
2 kDa	46.8	DPVC4	41.7	12.8
		DPVC5	42.1	11.2

PS Standards	Retention time (min)	Samples	Retention time (min)	Calculated MW (kDa)
68 kDa	36.6	Table 3.4, entry 1	41.4	15.2
34.5 kDa	38.9			
20.4 kDa	40.7			
9 kDa	43.6			
2 kDa	47.0			

PS Standards	Retention time (min)	Samples	Retention time (min)	Calculated MW (kDa)
68 kDa	36.7	Table 3.4, entry 2	45.2	4.4
34.5 kDa	39.0	Table 3.4, entry 3	45.4	4.1
20.4 kDa	40.6	Table 3.4, entry 4	43.5	3.1
9 kDa	43.5	Table 3.10, entry 2	47.2	4.2
2 kDa	47.2			

PS Standards	Retention time (min)	Samples	Retention time (min)	Calculated MW (kDa)
68 kDa	36.7	Table 3.5, entry 1	47.6	2.1
34.5 kDa	39.2	Table 3.8, entry 2	47.0	2.5
20.4 kDa	40.9	Table 3.8, entry 3	47.4	2.2
9 kDa	43.7			
2 kDa	47.3			

PS Standards	Retention time (min)	Samples	Retention time (min)	Calculated MW (kDa)
68 kDa	37.1	Table 3.7, entry 3	46.6	3.1
34.5 kDa	39.5	Table 3.7, entry 4	47.6	2.2
20.4 kDa	41.1	Table 3.7, entry 5	44.9	5.5
9 kDa	43.9			
2 kDa	47.6			

PS Standards	Retention time (min)	Samples	Retention time (min)	Calculated MW (kDa)
68 kDa	37.0	Table 3.9, entry 3	42.6	11.8
34.5 kDa	39.5	Table 3.9, entry 2	43.7	8.2
20.4 kDa	41.1	Table 3.9, entry 1	45.2	5.0
9 kDa	43.9			
2 kDa	47.6			

PS Standards	Retention time (min)	Samples	Retention time (min)	Calculated MW (kDa)
68 kDa	37.0	Table 2, entry 15	46.5	3.0
34.5 kDa	39.3			
20.4 kDa	40.9			
9 kDa	43.8			
2 kDa	47.4			

PS Standards	Retention time (min)	Samples	Retention time (min)	Calculated MW (kDa)
68 kDa	37.9	Table 3.4, entry 3 duplicate reaction	49.0	1.7
34.5 kDa	40.2	Table 3.5, entry 1 duplicate reaction	49.3	1.5
20.4 kDa	41.8			

9 kDa	44.5			
2 kDa	48.2			

PS Standards	Retention time (min)	Samples	Retention time (min)	Calculated MW (kDa)
68 kDa	36.6	Table 3.4, entry 2 duplicate reaction	46.4	2.6
34.5 kDa	38.8	Table 3.4, entry 4 duplicate reaction	47.0	2.1
20.4 kDa	40.5			
9 kDa	43.2			
2 kDa	46.9			

PS Standards	Retention time (min)	Samples	Retention time (min)	Calculated MW (kDa)
68 kDa	36.4	Table 3.8, entry 2 duplicate reaction	46.9	1.7
34.5 kDa	38.7	Table 3.8, entry 3 duplicate reaction	47.2	1.5
20.4 kDa	40.5			
2 kDa	46.3			

## Bibliography

- Abbasian, M.; Entezami, A. A. Metal-Catalyzed Living Radical Graft Copolymerization of Styrene Initiated from Arylated Poly(Vinyl Chloride). *Iran. Polym. J. (English Ed.)* **2006**, *15* (5), 395–404.
- Abbasian, M.; Entezami, A. A. Nitroxide Mediated Living Radical Polymerization of Styrene onto Poly (Vinyl Chloride). *Polym. Adv. Technol.* **2007**, *18* (4), 306–312. <https://doi.org/10.1002/pat.886>.
- Ahn, S. H.; Park, J. T.; Kim, J. H.; Ko, Y.; Hong, S. U. Nanocomposite Membranes Consisting of Poly(Vinyl Chloride) Graft Copolymer and Surface-Modified Silica Nanoparticles. *Macromol. Res.* **2011**, *19* (11), 1195–1201. <https://doi.org/10.1007/s13233-011-1116-1>.
- Ahn, S. H.; Seo, J. A.; Kim, J. H.; Ko, Y.; Hong, S. U. Synthesis and Gas Permeation Properties of Amphiphilic Graft Copolymer Membranes. *J. Memb. Sci.* **2009**, *345* (1–2), 128–133. <https://doi.org/10.1016/j.memsci.2009.08.037>.
- Anderson, N. A.; Campbell, I. B.; Fallon, B. J.; Lynn, S. M.; Macdonald, S. J. F.; Pritchard, J. M.; Procopiou, P. A.; Sollis, S. L.; Thorp, L. R. Synthesis and Determination of Absolute Configuration of a Non-Peptidic Av $\beta$ 6 Integrin Antagonist for the Treatment of Idiopathic Pulmonary Fibrosis. *Org. Biomol. Chem.* **2016**, *14* (25), 5992–6009. <https://doi.org/10.1039/c6ob00496b>.
- Balakrishnan, B.; Kumar, D. S.; Yoshida, Y.; Jayakrishnan, A. Chemical Modification of Poly (Vinyl Chloride) Resin Using Poly (Ethylene Glycol) to Improve Blood Compatibility. *Biomaterials* **2005**, *26*, 3495–3502. <https://doi.org/10.1016/j.biomaterials.2004.09.032>.
- Balla, Á.; Al-Hashimi, M.; Hlil, A.; Bazzi, H. S.; Tuba, R. Ruthenium-Catalyzed Metathesis of Conjugated Polyenes. *ChemCatChem* **2016**, *8* (18), 2865–2875. <https://doi.org/10.1002/cctc.201600479>
- Barnard, D.; Bateman, L.; Cunneen, J. I. *Oxidation of Organic Sulfides*; Pergamon Press Inc., **1961**. <https://doi.org/10.1016/b978-1-4831-9982-5.50024-5>.
- Bengough, W. I.; Varma, I. K. The Thermal Degradation of Polyvinylchloride in Solution - IV Changes in Absorption Spectra During Degradation. *Eur. Polym. J.* **1966**, *2*, 61–77. [https://doi.org/10.1016/0014-3057\(66\)90061-9](https://doi.org/10.1016/0014-3057(66)90061-9).

- Bicak, N.; Karagoz, B.; Emre, D. Atom Transfer Graft Copolymerization of 2-Ethyl Hexylacrylate from Labile Chlorines of Poly(Vinyl Chloride) in an Aqueous Suspension. *J. Polym. Sci. Part A Polym. Chem.* **2006**, *44* (6), 1900–1907. <https://doi.org/10.1002/pola.21298>.
- Bicak, N.; Ozlem, M. Graft Copolymerization of Butyl Acrylate and 2-Ethyl Hexyl Acrylate from Labile Chlorines of Poly(Vinyl Chloride) by Atom Transfer Radical Polymerization. *J. Polym. Sci. Part A Polym. Chem.* **2003**, *41* (21), 3457–3462. <https://doi.org/10.1002/pola.10944>.
- Bickelhaupt, F. M.; Houk, K. N. Analyzing Reaction Rates with the Distortion/Interaction-Activation Strain Model. *Angew. Chemie - Int. Ed.* **2017**, *56* (34), 10070–10086. <https://doi.org/10.1002/anie.201701486>.
- Bodaghi, A. An Overview on the Recent Developments in Reactive Plasticizers in Polymers. *Polym. Adv. Technol.* **2020**, *31* (3), 355–367. <https://doi.org/10.1002/pat.4790>.
- Bolton, S. L.; Schuehler, D. E.; Niu, X.; Gopal, L.; Sponsler, M. B. Olefin Metathesis for Metal Incorporation: Preparation of Conjugated Ruthenium-Containing Complexes and Polymers. *J. Organomet. Chem.* **2006**, *691* (24–25), 5298–5306. <https://doi.org/10.1016/j.jorganchem.2006.08.085>.
- Boone, M.A. and Hembre, R.T., Eastman Chemical Co, **2015**. *Low-pressure synthesis of cyclohexanedimethanol and derivatives*. U.S. Patent 9,115,155.
- Bräse, S.; Gil, C.; Knepper, K.; Zimmermann, V. Organic Azides: An Exploding Diversity of a Unique Class of Compounds. *Angew. Chem. Int. Ed.* **2005**, *44* (33), 5188–5240. <https://doi.org/10.1002/anie.200400657>.
- Braun, D. Recycling of PVC. *Prog. Polym. Sci.* **2002**, *27* (10), 2171–2195. [https://doi.org/10.1016/S0079-6700\(02\)00036-9](https://doi.org/10.1016/S0079-6700(02)00036-9).
- Bui, T. T.; Giovanoulis, G.; Cousins, A. P.; Magnér, J.; Cousins, I. T.; de Wit, C. A. Human Exposure, Hazard and Risk of Alternative Plasticizers to Phthalate Esters. *Sci. Total Environ.* **2016**, *541* (Supplement C), 451–467. <https://doi.org/10.1016/j.scitotenv.2015.09.036>.
- Bunz, U. H. F.; Mäker, D.; Porz, M. Alkene Metathesis - A Tool for the Synthesis of Conjugated Polymers. *Macromol. Rapid Commun.* **2012**, *33* (10), 886–910. <https://doi.org/10.1002/marc.201200001>.

- Chatterjee, A. K.; Choi, T. L.; Sanders, D. P.; Grubbs, R. H. A General Model for Selectivity in Olefin Cross Metathesis. *J. Am. Chem. Soc.* **2003**, *125* (37), 11360–11370. <https://doi.org/10.1021/ja0214882>.
- Chi, W. S.; Hong, S. U.; Jung, B.; Kang, S. W.; Kang, Y. S.; Kim, J. H. Synthesis, Structure and Gas Permeation of Polymerized Ionic Liquid Graft Copolymer Membranes. *J. Memb. Sci.* **2013**, *443*, 54–61. <https://doi.org/10.1016/j.memsci.2013.04.049>.
- Chi, W. S.; Kim, S. J.; Lee, S. J.; Bae, Y. S.; Kim, J. H. Enhanced Performance of Mixed-Matrix Membranes through a Graft Copolymer-Directed Interface and Interaction Tuning Approach. *ChemSusChem* **2015**, *8* (4), 650–658. <https://doi.org/10.1002/cssc.201402677>.
- Chiellini, F.; Ferri, M.; Morelli, A.; Dipaola, L.; Latini, G. Perspectives on Alternatives to Phthalate Plasticized Poly(Vinyl Chloride) in Medical Devices Applications. *Prog. Polym. Sci.* **2013**, *38* (7), 1067–1088. <https://doi.org/10.1016/j.progpolymsci.2013.03.001>.
- Clark, M.; Kiser, P. In Situ Crosslinked Hydrogels Formed Using Cu(I)-Free Huisgen Cycloaddition Reaction. *Polym. Int.* **2009**, *58* (10), 1190–1195. <https://doi.org/10.1002/pi.2650>.
- Conn, C.; Lloyd-Jones, D.; Kannangara, G. S. K.; Baker, A. T. Reductive Coupling of Alkynes by Oxobis(Diethyldithiocarbamate)Molybdenum(IV)-Sodium Borohydride. *J. Organomet. Chem.* **1999**, *585* (1), 134–140. [https://doi.org/10.1016/S0022-328X\(99\)00205-3](https://doi.org/10.1016/S0022-328X(99)00205-3).
- Coşkun, M.; Barim, G.; Demirelli, K. A Grafting Study on Partially Dehydrochlorinated Poly(Vinyl Chloride) by Atom Transfer Radical Polymerization. *J. Macromol. Sci. Part A Pure Appl. Chem.* **2007**, *44* (5), 475–481. <https://doi.org/10.1080/10601320701229068>.
- Coşkun, M.; Seven, P. Synthesis, Characterization and Investigation of Dielectric Properties of Two-Armed Graft Copolymers Prepared with Methyl Methacrylate and Styrene onto PVC Using Atom Transfer Radical Polymerization. *React. Funct. Polym.* **2011**, *71* (4), 395–401. <https://doi.org/10.1016/j.reactfunctpolym.2010.12.012>.
- CPSC Prohibits Certain Phthalates in Children's Toys and Child Care Products <https://www.cpsc.gov/Newsroom/News-Releases/2018/CPSC-Prohibits-Certain-Phthalates-in-Childrens-Toys-and-Child-Care-Products>, accessed Dec 16, 2022.



- Czogała, J.; Pankalla, E.; Turczyn, R. Recent Attempts in the Design of Efficient PVC Plasticizers with Reduced Migration. *Materials (Basel)*. **2021**, *14* (4), 844. <https://doi.org/10.3390/ma14040844>.
- Dow, M.; Marchetti, F.; Abrahams, K. A.; Vaz, L.; Besra, G. S.; Warriner, S.; Nelson, A. Modular Synthesis of Diverse Natural Product-Like Macrocycles: Discovery of Hits with Antimycobacterial Activity. *Chem. - A Eur. J.* **2017**, *23* (30), 7207–7211. <https://doi.org/10.1002/chem.201701150>.
- Earla, A.; Braslau, R. Covalently Linked Plasticizers: Triazole Analogues of Phthalate Plasticizers Prepared by Mild Copper-Free “Click” Reactions with Azide-Functionalized PVC. *Macromol. Rapid Commun.* **2014**, *35* (6), 666–671. <https://doi.org/10.1002/marc.201300865>.
- Earla, A.; Li, L.; Costanzo, P.; Braslau, R. Phthalate Plasticizers Covalently Linked to PVC via Copper-Free or Copper Catalyzed Azide-Alkyne Cycloadditions. *Polymer (Guildf)*. **2017**, *109*, 1–12. <https://doi.org/10.1016/j.polymer.2016.12.014>.
- Eaton, P. E.; Steele, I.; Gilardi, R. Nitroacetylene: HC≡CNO<sub>2</sub>. *Synthesis (Stuttg)*. **2002**, No. 14, 2013–2018. <https://doi.org/10.1055/s-2002-34387>.
- EliceGUI, A.; del Val, J. J.; Bellenger, V.; J, V. A Study of Plasticization Effects in Poly (Vinyl Chloride). **1997**, *38* (7), 1647–1657. [https://doi.org/10.1016/S0032-3861\(96\)00671-4](https://doi.org/10.1016/S0032-3861(96)00671-4).
- Ellis, L. D.; Orski, S. V.; Kenlaw, G. A.; Norman, A. G.; Beers, K. L.; Román-Leshkov, Y.; Beckham, G. T. Tandem Heterogeneous Catalysis for Polyethylene Depolymerization via an Olefin-Intermediate Process. *ACS Sustain. Chem. Eng.* **2021**, *9* (2), 623–628. <https://doi.org/10.1021/acssuschemeng.0c07612>.
- Ess, D. H.; Houk, K. N. Theory of 1,3-Dipolar Cycloadditions: Distortion/Interaction and Frontier Molecular Orbital Models. *J. Am. Chem. Soc.* 2008, *130* (31), 10187–10198. <https://doi.org/10.1021/ja800009z>.
- Fang, L.; Wang, N.; Zhou, M.; Zhu, B.; Zhu, L.; John, A. E. Poly(N,N-Dimethylaminoethyl Methacrylate) Grafted Poly(Vinyl Chloride)s Synthesized via ATRP Process and Their Membranes for Dye Separation. *Chinese J. Polym. Sci.* **2015**, *33* (11), 1491–1502. <https://doi.org/10.1007/s10118-015-1701-4>.
- Francová, D.; Kickelbick, G. Synthesis of Methacrylate-Functionalized Phosphonates and Phosphates with Long Alkyl-Chain Spacers and Their Self-Aggregation in Aqueous

Solutions. *Monatshefte für Chemie* **2009**, *140* (4), 413–422.  
<https://doi.org/10.1007/s00706-008-0045-y>.

Frisch, M. J.; Trucks, G. W.; Schlegel, H. B.; Scuseria, G. E.; Robb, M. A.; Cheeseman, J. R.; Scalmani, G.; Barone, V.; Mennucci, B.; Petersson, G. A.; Nakatsuji, H.; Caricato, M.; Li, X.; Hratchian, H. P.; Izmaylov, A. F.; Bloino, J.; Zheng, G.; Sonnenberg, J. L.; Hada, M.; Ehara, M.; Toyota, K.; Fukuda, R.; Hasegawa, J.; Ishida, M.; Nakajima, T.; Honda, Y.; Kitao, O.; Nakai, H.; Vreven, T.; Montgomery, J. A., Jr.; Peralta, J. E.; Ogliaro, F.; Bearpark, M.; Heyd, J. J.; Brothers, E.; Kudin, K. N.; Staroverov, V. N.; Kobayashi, R.; Normand, J.; Raghavachari, K.; Rendell, A.; Burant, J. C.; Iyengar, S. S.; Tomasi, J.; Cossi, M.; Rega, N.; Millam, J. M.; Klene, M.; Knox, J. E.; Cross, J. B.; Bakken, V.; Adamo, C.; Jaramillo, J.; Gomperts, R.; Stratmann, R. E.; Yazyev, O.; Austin, A. J.; Cammi, R.; Pomelli, C.; Ochterski, J. W.; Martin, R. L.; Morokuma, K.; Zakrzewski, V. G.; Voth, G. A.; Salvador, P.; Dannenberg, J. J.; Dapprich, S.; Daniels, A. D.; Farkas, O.; Foresman, J. B.; Ortiz, J. V.; Cioslowski, J.; Fox, D. J.. Gaussian 09, revision A.02; Gaussian, Inc.: Wallingford, CT, 2009

Gao, P.; Song, X. R.; Liu, X. Y.; Liang, Y. M. Recent Developments in the Trifluoromethylation of Alkynes. *Chem. - A Eur. J.* **2015**, *21* (21), 7649–7661.  
<https://doi.org/10.1002/chem.201406432>.

Geyer, R.; Jambeck, J. R.; Law, K. L. Production, Use, and Fate of All Plastics Ever Made. *Sci. Adv.* **2017**, *3* (7), 25–29. <https://doi.org/10.1126/sciadv.1700782>.

Glas, D.; Hulsbosch, J.; Dubois, P.; Binnemans, K.; Vos, D. E. De. End-of-Life Treatment of Poly (Vinyl Chloride) and Chlorinated Polyethylene by Dehydrochlorination in Ionic Liquids. **2014**, 610–617. <https://doi.org/10.1002/cssc.201300970>.

Guarrotxena, N.; Martinez, G.; Gomez-Elvira, J. M.; Millan, J. L. Effect of Some Tacticity-Depending Local Chain Conformations on the Behaviour of Poly(Vinyl Chloride). Changes of Glass Transition Temperature through Stereoselective Substitution in Solution. *Macromol. Rapid Commun.* **1994**, *15*, 189–196.  
<https://doi.org/10.1002/marc.1994.030150302>.

Guarrotxena, N.; Martinez, J. M.; Gomez-Elvira, J. M.; Millan, J. Solvent Dependence of Stereoselective Substitution Reaction on Poly(Vinyl Chloride). A Useful Tool to Investigate the Tacticity Effect on Tg. *Eur. Polym. J.* **1993**, *29* (5), 685–688.  
[https://doi.org/10.1016/0014-3057\(93\)90129-4](https://doi.org/10.1016/0014-3057(93)90129-4).

- Guo, L.; Shi, G.; Liang, Y. Poly (Ethylene Glycol) s Catalyzed Homogeneous Dehydrochlorination of Poly (Vinyl Chloride) with Potassium Hydroxide. *Polymer (Guildf)*. **2001**, *42*, 5581–5587. [https://doi.org/10.1016/S0032-3861\(01\)00037-4](https://doi.org/10.1016/S0032-3861(01)00037-4).
- Gutiérrez, S.; Tlenkopatchev, M. A. Metathesis of Renewable Products: Degradation of Natural Rubber via Cross-Metathesis with  $\beta$ -Pinene Using Ru-Alkylidene Catalysts. *Polym. Bull.* **2011**, *66* (8), 1029–1038. <https://doi.org/10.1007/s00289-010-0330-x>.
- Hansch, C.; Leo, A.; Taft, R. W. A Survey of Hammett Substituent Constants and Resonance and Field Parameters. *Chem. Rev.* **1991**, *91* (2), 165–195. <https://doi.org/10.1021/cr00002a004>.
- Hassner, A.; Stern, M. Synthesis of Alkyl Azides with a Polymeric Reagent. *Angew. Chem. Int. Ed. Engl.* 1986, *25* (5), 478–479. <https://doi.org/10.1002/anie.198604781>
- Herrero, M.; Tiemblo, P.; Reyes-Labarta, J.; Mijangos, C.; Reinecke, H. PVC Modification with New Functional Groups. Influence of Hydrogen Bonds on Reactivity, Stiffness and Specific Volume. *Polymer (Guildf)*. **2002**, *43*, 2631–2636. [https://doi.org/10.1016/S0032-3861\(02\)00064-2](https://doi.org/10.1016/S0032-3861(02)00064-2).
- Heyl, D.; Fessner, W. D. Facile Direct Synthesis of Acetylenedicarboxamides. *Synth.* **2014**, *46* (11), 1463–1468. <https://doi.org/10.1055/s-0033-1341101>.
- Higa, C. M.; Tek, A. T.; Wojtecki, R. J.; Braslau, R. Nonmigratory Internal Plasticization of Poly(Vinyl Chloride) via Pendant Triazoles Bearing Alkyl or Polyether Esters. *J. Polym. Sci. Part A Polym. Chem.* **2018**, *56* (21), 2397–2411. <https://doi.org/10.1002/pola.29205>.
- Hong, S. H.; Day, M. W.; Grubbs, R. H. Decomposition of a Key Intermediate in Ruthenium-Catalyzed Olefin Metathesis Reactions. *J. Am. Chem. Soc.* **2004**, *126* (24), 7414–7415. <https://doi.org/10.1021/ja0488380>.
- Hong, S. H.; Sanders, D. P.; Lee, C. W.; Grubbs, R. H. Prevention of Undesirable Isomerization during Olefin Metathesis. *J. Am. Chem. Soc.* **2005**, *127* (49), 17160–17161. <https://doi.org/10.1021/ja052939w>.
- Hou, Q.; Zhen, M.; Qian, H.; Nie, Y.; Bai, X.; Xia, T. Upcycling and Catalytic Degradation of Plastic Wastes. *Cell Reports Phys. Sci.* **2021**, *2* (8), 1–30. <https://doi.org/10.1016/j.xcrp.2021.100514>.

- Huy, P. H.; Filbrich, I. A General Catalytic Method for Highly Cost- and Atom-Efficient Nucleophilic Substitutions. *Chem. - A Eur. J.* **2018**, *24* (29), 7410–7416. <https://doi.org/10.1002/chem.201800588>.
- IHS Markit. Plasticizers <https://Ihsmarkit.com/Products/Plasticizers-Chemical-Economics-Handbook.Html>, (Accessed April 2023)
- IHS Markit. Population Growth and Materials Demand Study Prepared for: American Chemistry Council <https://www.americanchemistry.com/content/download/8057/file/Population-Growth-and-Materials-Demand-Study-IHS-Markit.pdf> (Accessed April 2023).
- Impact of lead restrictions on the recycling of PVC [https://vinylplus.eu/wp-content/uploads/2021/06/2013\\_07\\_13-impact\\_lead-restrictions\\_pvc\\_recycling-tauw.pdf](https://vinylplus.eu/wp-content/uploads/2021/06/2013_07_13-impact_lead-restrictions_pvc_recycling-tauw.pdf), accessed Dec 16, 2022.
- Jewett, J. C.; Bertozzi, C. R. Cu-Free Click Cycloaddition Reactions in Chemical Biology. *Chemical Society Reviews*. 2010, pp 1272–1279. <https://doi.org/10.1039/b901970g>.
- Jia, P.; Hu, L.; Zhang, M.; Feng, G.; Zhou, Y. Phosphorus Containing Castor Oil Based Derivatives: Potential Non-Migratory Flame Retardant Plasticizer. *Eur. Polym. J.* **2017**, *87*, 209–220. <https://doi.org/10.1016/j.eurpolymj.2016.12.023>.
- Jia, P.; Ma, Y.; Song, F.; Hu, Y.; Zhang, C.; Zhou, Y. Toxic Phthalate-Free and Highly Plasticized Polyvinyl Chloride Materials from Non-Timber Forest Resources in Plantation. *React. Funct. Polym.* **2019**, *144*, 104363. <https://doi.org/10.1016/j.reactfunctpolym.2019.104363>.
- Jia, P.; Ma, Y.; Zhang, M.; Hu, L.; Li, Q.; Yang, X.; Zhou, Y. Flexible PVC Materials Grafted with Castor Oil Derivative Containing Synergistic Flame Retardant Groups of Nitrogen and Phosphorus. *Sci. Rep.* **2019**, *9* (1766), 1–8. <https://doi.org/10.1038/s41598-018-38407-4>.
- Jia, P.; Wang, R.; Hu, L.; Zhang, M.; Zhou, Y. Self-Plasticization of PVC via Click Reaction of a Monoctyl Phthalate Derivative. *Polish J. Chem. Technol.* **2017**, *19* (3), 16–19. <https://doi.org/10.1515/pjct-2017-0042>.
- Jia, P.; Zhang, M.; Hu, L.; Song, F.; Feng, G.; Zhou, Y. A Strategy for Nonmigrating Plasticized PVC Modified with Mannich Base of Waste Cooking Oil Methyl Ester. *Sci. Rep.* **2018**, *8* (1589). <https://doi.org/10.1038/s41598-018-19958-y>.

- Jia, P.; Zhang, M.; Hu, L.; Wang, R.; Sun, C.; Zhou, Y. Cardanol Groups Grafted on Poly(Vinyl Chloride)-Synthesis, Performance and Plasticization Mechanism. *Polymers (Basel)*. **2017**, *9* (621), 1–12. <https://doi.org/10.3390/polym9110621>.
- Jia, X.; Qin, C.; Friedberger, T.; Guan, Z.; Huang, Z. Efficient and Selective Degradation of Polyethylenes into Liquid Fuels and Waxes under Mild Conditions. *Sci. Adv.* **2016**, *2* (6), 1–8. <https://doi.org/10.1126/sciadv.1501591>.
- Khunsriya, P.; Wootthikanokkhan, J.; Seeponkai, N.; Luangchaisri, C. Preparation of Dehydrochlorinated Poly (Vinyl Chloride) (DHPVC) and DHPVC Nanofibres : Effects of Reaction Time on Conductivity , Electrospinnability , and Fibre Morphology. *Polym. Polym. Compos.* **2014**, *22* (7), 581–591. <https://doi.org/10.1177/096739111402200701>.
- Klavetter, F. L.; Grubbs, R. H. Polycyclooctatetraene (Polyacetylene): Synthesis and Properties. *J. Am. Chem. Soc.* **1988**, *110* (23), 7807–7813. <https://doi.org/10.1021/ja00231a036>.
- Koh, J. H.; Lee, K. J.; Seo, J. A.; Kim, J. H. Amphiphilic Polymer Electrolytes Consisting of PVC-g-POEM Comb-Like Copolymer and LiCF<sub>3</sub>SO<sub>3</sub>. *J. Polym. Sci. Part B Polym. Phys.* **2009**, *47* (15), 1443–1451. <https://doi.org/10.1002/polb.21745>.
- Koh, J. H.; Seo, J. A.; Koh, J. K.; Kim, J. H. Self-Assembled Structures of Hydrogen-Bonded Poly(Vinyl Chloride-g-4-Vinyl Pyridine) Graft Copolymers. *Nanotechnology* **2010**, *21* (35). <https://doi.org/10.1088/0957-4484/21/35/355604>.
- Krasovskiy, A.; Tishkov, A.; Del Amo, V.; Mayr, H.; Knochel, P. Transition-Metal-Free Homocoupling of Organomagnesium Compounds. *Angew. Chemie - Int. Ed.* **2006**, *45* (30), 5010–5014. <https://doi.org/10.1002/anie.200600772>.
- Kunishima, M.; Kawachi, C.; Morita, J.; Terao, K.; Iwasaki, F.; Tani, S. 4-(4,6-Dimethoxy-1,3,5-Triazin-2-Yl)-4-Methylmorpholinium Chloride: An Efficient Condensing Agent Leading to the Formation of Amides and Esters. *Tetrahedron* **1999**, *55* (46), 13159–13170. [https://doi.org/10.1016/S0040-4020\(99\)00809-1](https://doi.org/10.1016/S0040-4020(99)00809-1).
- Kurashima, K.; Kumagai, S.; Kameda, T.; Saito, Y.; Yoshioka, T. Heavy Metal Removal from Municipal Solid Waste Fly Ash through Chloride Volatilization Using Poly (Vinyl Chloride) as Chlorinating Agent. *J. Mater. Cycles Waste Manag.* **2020**, *22* (4), 1270–1283. <https://doi.org/10.1007/s10163-020-01021-6>.

- Lanzalaco, S.; Galia, A.; Lazzano, F.; Mauro, R. R.; Scialdone, O. Utilization of Poly(Vinylchloride) and Poly(Vinylidene fluoride) as Macroinitiators for ATRP Polymerization of Hydroxyethyl Methacrylate: Electroanalytical and Graft-Copolymerization Studies. *J. Polym. Sci. Part A Polym. Chem.* **2015**, *53* (21), 2524–2536. <https://doi.org/10.1002/pola.27717>.
- Lewandowski, K.; Skórczewska, K. A Brief Review of Poly(Vinyl Chloride) (PVC) Recycling. *Polymers (Basel)*. **2022**, *14* (15), 3035. <https://doi.org/10.3390/polym14153035>.
- Li, L.; Schneider, Y.; Hoeglund, A. B.; Braslau, R. Advances in Internal Plasticization of PVC: Copper-Mediated Atom-Transfer Radical Polymerization from PVC Defect Sites To Form Acrylate Graft Copolymers. *Synlett* **2021**, No. Scheme 1, 497–501. <https://doi.org/10.1055/s-0037-1610764>.
- Li, L.; Schneider, Y.; Hoeglund, A. B.; Braslau, R. Internal Plasticization of Poly(Vinyl Chloride) by Grafting Acrylate Copolymers via Copper-Mediated Atom Transfer Radical Polymerization. *J. Appl. Polym. Sci.* **2021**, *138* (31), 1–11. <https://doi.org/10.1002/app.50747>.
- Li, L.; Tek, A. T.; Wojtecki, R. J.; Braslau, R. Internal Plasticization of Poly(Vinyl Chloride) Using Glutamic Acid as a Branched Linker to Incorporate Four Plasticizers per Anchor Point. *J. Polym. Sci. Part A Polym. Chem.* **2019**, *57* (17), 1821–1835. <https://doi.org/10.1002/pola.29455>.
- Li, Z.; Seo, T. S.; Ju, J. 1,3-Dipolar Cycloaddition of Azides with Electron-Deficient Alkynes under Mild Condition in Water. *Tetrahedron Lett.* **2004**, *45* (15), 3143–3146. <https://doi.org/10.1016/j.tetlet.2004.02.089>.
- Liu, K.; Bao, Y. Synthesis of Poly(Vinyl Chloride)- Butyl Acrylate Graft Copolymer by ARGET ATRP Method. *CIESC J.* **2014**, *65* (8).
- Liu, Y.; Cheng, P. Structure and Thermal Properties of PVC Grafted with Crystallizable Side Chains. *Hecheng Shuzhi Ji Suliao/China Synth. Resin Plast.* **2013**, *30* (2), 67–70.
- Lopez, D.; Mijangos, C. Effect of Solvent on Glass Transition Temperature in Chemically Modified Polyvinyl Chloride (PVC). *Colloid Polym. Sci.* **1994**, *272*, 159–167. <https://doi.org/10.1007/BF00658842>.

- Lu, L.; Kumagai, S.; Kameda, T.; Luo, L.; Yoshioka, T. Degradation of PVC Waste into a Flexible Polymer by Chemical Modification Using DINP Moieties. *RSC Adv.* **2019**, *9* (49), 28870–28875. <https://doi.org/10.1039/c9ra05081g>.
- Lu, L.; Zhong, H.; Wang, T.; Wu, J.; Jin, F.; Yoshioka, T. A New Strategy for CO<sub>2</sub> Utilization with Waste Plastics: Conversion of Hydrogen Carbonate into Formate Using Polyvinyl Chloride in Water. *Green Chem.* **2020**, *22* (2), 352–358. <https://doi.org/10.1039/c9gc02484k>.
- Lv, B.; Zhao, G.; Li, D.; Liang, C. Dechlorination and Oxidation for Waste Poly (Vinylidene Chloride) by Hydrothermal Catalytic Oxidation on Pd / AC Catalyst. *Polym. Degrad. Stab.* **2009**, *94*, 1047–1052. <https://doi.org/10.1016/j.polymdegradstab.2009.04.004>.
- Ma, Y.; Liao, S.; Li, Q.; Guan, Q.; Jia, P.; Zhou, Y. Physical and Chemical Modifications of Poly(Vinyl Chloride) Materials to Prevent Plasticizer Migration - Still on the Run. *React. Funct. Polym.* **2020**, *147* (December 2019), 104458. <https://doi.org/10.1016/j.reactfunctpolym.2019.104458>
- Maiti, A. K.; Choudhary, M. S. Melt Grafting of *N*-Butyl Methacrylate onto Poly(Vinyl Chloride): Synthesis and Characterization. *J. Appl. Polym. Sci.* **2004**, *92* (4), 2442–2449. <https://doi.org/10.1002/app.20234>.
- Marian, S.; Levin, G. Modification of Polyvinylchloride in Solution or Suspension by Nucleophilic Substitution. *J. Appl. Polym. Sci.* **1981**, *26*, 3295–3304. <https://doi.org/10.1002/app.1981.070261009>.
- Martin, A. J.; Mondelli, C.; Jaydev, S. D.; Perez Ramirez, J. Catalytic Processing of Plastic Waste on the Rise. *Chem* **2021**, *7* (6), 1487–1533. <https://doi.org/10.1016/j.chempr.2020.12.006>.
- Martínez, A.; Gutiérrez, S.; Tlenkopatchev, M. A. Citrus Oils as Chain Transfer Agents in the Cross-Metathesis Degradation of Polybutadiene in Block Copolymers Using Ru-Alkylidene Catalysts. *Nat. Sci.* **2013**, *05* (07), 857–864. <https://doi.org/10.4236/ns.2013.57103>.
- Matyjaszewski, K. Atom Transfer Radical Polymerization (ATRP): Current Status and Future Perspectives. *Macromolecules* **2012**, *45* (10), 4015–4039. <https://doi.org/10.1021/ma3001719>.

- Miao, F.; Liu, Y.; Gao, M.; Yu, X.; Xiao, P.; Wang, M.; Wang, S.; Wang, X. Degradation of Polyvinyl Chloride Microplastics via an Electro-Fenton-like System with a TiO<sub>2</sub>/Graphite Cathode. *J. Hazard. Mater.* **2020**, *399* (May), 1–9. <https://doi.org/10.1016/j.jhazmat.2020.123023>.
- Najafi, V.; Abdollahi, H. Internally Plasticized PVC by Four Different Green Plasticizer Compounds. *Eur. Polym. J.* **2020**, *128* (109620). <https://doi.org/10.1016/j.eurpolymj.2020.109620>.
- Navarro, R.; Bierbrauer, K.; Mijangos, C.; Goiti, E.; Reinecke, H. Modification of Poly (Vinyl Chloride) with New Aromatic Thiol Compounds. Synthesis and Characterization. *Polym. Degrad. Stab.* **2008**, *93*, 585–591. <https://doi.org/10.1016/j.polymdegradstab.2008.01.015>.
- Okuda, K.; Yanagisawa, K.; Moritaka, S.; Onda, A. Solubilization of Dechlorinated Poly (Vinyl Chloride) in Water by Wet Oxidation. *Polym. Degrad. Stab.* **2003**, *79*, 105–110. [https://doi.org/10.1016/S0141-3910\(02\)00262-8](https://doi.org/10.1016/S0141-3910(02)00262-8).
- Okumura, S.; Takeda, Y.; Kiyokawa, K.; Minakata, S. Hypervalent Iodine(III)-Induced Oxidative [4+2] Annulation of o-Phenylenediamines and Electron-Deficient Alkynes: Direct Synthesis of Quinoxalines from Alkyne Substrates under Metal-Free Conditions. *Chem. Commun.* **2013**, *49* (81), 9266–9268. <https://doi.org/10.1039/c3cc45469j>
- Ouardad, S.; Peruch, F. Metathetic Degradation of Trans-1,4-Polyisoprene with Ruthenium Catalysts. *Polym. Degrad. Stab.* **2014**, *99* (1), 249–253. <https://doi.org/10.1016/j.polymdegradstab.2013.10.022>.
- Paik, H. J.; Gaynor, S. G.; Matyjaszewski, K. Synthesis and Characterization of Graft Copolymers of Poly(Vinyl Chloride) with Styrene and (Meth)Acrylates by Atom Transfer Radical Polymerization. *Macromol. Rapid Commun.* **1998**, *19* (1), 47–52. [https://doi.org/10.1002/\(SICI\)1521-3927\(19980101\)19:1<47::AID-MARC47>3.0.CO;2-Q](https://doi.org/10.1002/(SICI)1521-3927(19980101)19:1<47::AID-MARC47>3.0.CO;2-Q).
- Park, E. J.; Park, B. C.; Kim, Y. J.; Canlier, A.; Hwang, T. S. Elimination and Substitution Compete During Amination of Poly(Vinyl Chloride) with Ethylenediamine: XPS Analysis and Approach of Active Site Index. *Macromol. Res.* **2018**, *26* (10), 913–923. <https://doi.org/10.1007/s13233-018-6123-z>.



- Partenheimer, W. Valuable Oxygenates by Aerobic Oxidation of Polymers Using Metal / Bromide Homogeneous Catalysts. *Catal. Today* **2003**, *81*, 117–135. [https://doi.org/10.1016/S0920-5861\(03\)00124-X](https://doi.org/10.1016/S0920-5861(03)00124-X).
- Pascoal, M.; Brook, M. A.; Gonzaga, F.; Zepeda-Velazquez, L. Thermally Controlled Silicone Functionalization Using Selective Huisgen Reactions. *Eur. Polym. J.* **2015**, *69*, 429–437. <https://doi.org/10.1016/j.eurpolymj.2015.06.026>.
- Pasquato, L.; De Lucchi, O.; Krotz, L. Bis(Arylsulphonyl)Acetylenes. *Tetrahedron Lett.* **1991**, *32* (19), 2177–2178. [https://doi.org/10.1016/S0040-4039\(00\)71269-X](https://doi.org/10.1016/S0040-4039(00)71269-X).
- Patel, R.; Chi, W. S.; Ahn, S. H.; Park, C. H.; Lee, H. K.; Kim, J. H. Synthesis of Poly(Vinyl Chloride)-g-Poly(3-Sulfopropyl Methacrylate) Graft Copolymers and Their Use in Pressure Retarded Osmosis (PRO) Membranes. *Chem. Eng. J.* **2014**, *247*, 1–8. <https://doi.org/10.1016/j.cej.2014.02.106>.
- Percec, V.; Asgarzadeh, F. Metal-Catalyzed Living Radical Graft Copolymerization of Olefins Initiated from the Structural Defects of Poly(Vinyl Chloride). *J. Polym. Sci. Part A Polym. Chem.* **2001**, *39* (7), 1120–1135. [https://doi.org/10.1002/1099-0518\(20010401\)39:7<1120::AID-POLA1089>3.0.CO;2-Z](https://doi.org/10.1002/1099-0518(20010401)39:7<1120::AID-POLA1089>3.0.CO;2-Z).
- Qi, Y.; He, J.; Xiu, F. R.; Nie, W.; Chen, M. Partial Oxidation Treatment of Waste Polyvinyl Chloride in Critical Water: Preparation of Benzaldehyde/Acetophenone and Dechlorination. *J. Clean. Prod.* **2018**, *196*, 331–339. <https://doi.org/10.1016/j.jclepro.2018.06.074>.
- Qin, A.; Jim, C. K. W.; Lu, W.; Lam, J. W. Y.; Häussler, M.; Dong, Y.; Sung, H. H. Y.; Williams, I. D.; Wong, G. K. L.; Tang, B. Z. Click Polymerization: Facile Synthesis of Functional Poly(Aroyltriazole)s by Metal-Free, Regioselective 1,3-Dipolar Polycycloaddition. *Macromolecules* **2007**, *40* (7), 2308–2317. <https://doi.org/10.1021/ma062859s>.
- Qin, A.; Lam, J. W. Y.; Tang, B. Z. Click Polymerization. *Chem. Soc. Rev.* **2010**, *39* (7), 2522–2544. <https://doi.org/10.1039/b909064a>.
- Roh, D. K.; Park, J. T.; Ahn, S. H.; Ahn, H.; Ryu, D. Y.; Kim, J. H. Amphiphilic Poly(Vinyl Chloride)-g-Poly(Oxyethylene Methacrylate) Graft Polymer Electrolytes: Interactions, Nanostructures and Applications to Dye-Sensitized Solar Cells. *Electrochim. Acta* **2010**, *55* (17), 4976–4981. <https://doi.org/10.1016/j.electacta.2010.03.106>.

- Rowdhwal, S. S. S.; Chen, J. Toxic Effects of Di-2-Ethylhexyl Phthalate: An Overview. *Biomed Res. Int.* **2018**, *2018* (Figure 1). <https://doi.org/10.1155/2018/1750368>.
- Sadat-Shojai, M.; Bakhshandeh, G. R. Recycling of PVC Wastes. *Polym. Degrad. Stab.* **2011**, *96* (4), 404–415. <https://doi.org/10.1016/j.polymdegradstab.2010.12.001>.
- Salazar Avalos, A.; Hakkarainen, M.; Odelius, K. Superiorly Plasticized PVC/PBSA Blends through Crotonic and Acrylic Acid Functionalization of PVC. *Polymers (Basel)*. **2017**, *9* (12), 84. <https://doi.org/10.3390/polym9030084>.
- Saxman, A. M.; Liepins, R.; Aldissi, M. Polyacetylene: Its Synthesis, Doping and Structure. *Prog. Polym. Sci.* **1985**, *11* (1–2), 57–89. [https://doi.org/10.1016/0079-6700\(85\)90008-5](https://doi.org/10.1016/0079-6700(85)90008-5).
- Scherman, O. A.; Rutenberg, I. M.; Grubbs, R. H. Direct Synthesis of Soluble, End-Functionalized Polyenes and Polyacetylene Block Copolymers. *J. Am. Chem. Soc.* **2003**, *125* (28), 8515–8522. <https://doi.org/10.1021/ja0301166>
- Schultz-Simonton, W.; Skelly, P.; Chakraborty, I.; Mascharak, P.; Braslau, R. Synthesis, Structure, and Fluorescence Behavior of Profluorescent 8-Amino BODIPY Nitroxides. *European J. Org. Chem.* **2019**, *2019* (7). <https://doi.org/10.1002/ejoc.201801758>.
- Schulz, M. D.; Ford, R. R.; Wagener, K. B. Insertion Metathesis Depolymerization. *Polym. Chem.* **2013**, *4* (13), 3656–3658. <https://doi.org/10.1039/c3py00531c>.
- Seo, J. A.; Koh, J. K.; Koh, J. H.; Kim, J. H. Preparation and Characterization of Plasticized Poly(Vinyl Chloride)-g-Poly(Oxyethylene Methacrylate) Graft Copolymer Electrolyte Membranes. *Membr. J.* **2011**, *21* (3), 222–228. [https://doi.org/10.14579/membrane\\_journal.2011.21.3.222](https://doi.org/10.14579/membrane_journal.2011.21.3.222).
- Sherwood, J. Closed-loop recycling of polymers using solvents; remaking plastics for a circular economy *Johnson Matthey Technol. Rev.*, **2020**, *64*, 4-15. <https://doi.org/10.1595/205651319X15574756736831>
- Shin, N.; Kwon, S.; Moon, S.; Hong, C. H.; Kim, Y. G. Ionic Liquid-Mediated Deoxydehydration Reactions: Green Synthetic Process for Bio-Based Adipic Acid. *Tetrahedron* **2017**, *73* (32), 4758–4765. <https://doi.org/10.1016/j.tet.2017.06.053>.
- Shin, S.; Yoon, K. Y.; Choi, T. L. Simple Preparation of Various Nanostructures via in Situ Nanoparticlization of Polyacetylene Blocklike Copolymers by One-Shot

- Polymerization. *Macromolecules* **2015**, *48* (5), 1390–1397. <https://doi.org/10.1021/ma502530x>.
- Singh, K.; Staig, S. J.; Weaver, J. D. Facile Synthesis of Z -Alkenes via Uphill Catalysis. *J. Am. Chem. Soc.* **2014**, *136* (14), 5275–5278. <https://doi.org/10.1021/ja5019749>.
- Skelly, P. W.; Fuentes Chang, C.; Braslau, R. Degradation of Polyvinyl Chloride by Sequential Dehydrochlorination and Olefin Metathesis. *Chempluschem* **2023**, *88* (e202300184). <https://doi.org/10.1002/cplu.202300184>. Smith, R. F.; Boothroyd, S. C.; Thompson, R. L.; Khosravi, E. A Facile Route for Rubber Breakdown via Cross Metathesis Reactions. *Green Chem.* **2016**, *18* (11), 3448–3455. <https://doi.org/10.1039/c5gc03075g>.
- Skelly, P. W.; Li, L.; Braslau, R. Internal Plasticization of PVC. *Polym. Rev.* **2022**, *62* (3), 485–528. <https://doi.org/10.1080/15583724.2021.1986066>.
- Skelly, P. W.; Sae-Jew, J.; Kitos Vasconcelos, A. P.; Tasnim, J.; Li, L.; Raskatov, J. A.; Braslau, R. Relative Rates of Metal-Free Azide–Alkyne Cycloadditions: Tunability over 3 Orders of Magnitude. *J. Org. Chem.* **2019**, *84* (21), 13615–13623. <https://doi.org/10.1021/acs.joc.9b01887>.
- Solanky, S. S.; Campistrone, I.; Laguerre, A.; Pilard, J. F. Metathetic Selective Degradation of Polyisoprene: Low-Molecular-Weight Telechelic Oligomer Obtained from Both Synthetic and Natural Rubber. *Macromol. Chem. Phys.* **2005**, *206* (10), 1057–1063. <https://doi.org/10.1002/macp.200400416>.
- Sorensen, E.; Bjerre, A. B. Combined Wet Oxidation and Alkaline Hydrolysis of Polyvinylchloride. *Waste Manag.* **1992**, *12*, 349–354. [https://doi.org/10.1016/0956-053X\(92\)90037-J](https://doi.org/10.1016/0956-053X(92)90037-J).
- Statista. PVC Production Worldwide in 2018 and 2025. <https://www.statista.com/statistics/720296/global-polyvinyl-chloride-market-size-in-tons/#:~:text=Global%20PVC%20production%20volume%202018%20%26%202025&text=The%20total%20global%20production%20volume,to%2044.3%20million%20metric%20tons>, (Accessed April 2023).
- Tanaka, R.; Miller, S. I. Nucleophilic Substitution at an Acetylenic Carbon. Kinetics of the Reaction between Bromoacetylene and Triethylamine in Dimethylformamide. *J. Org. Chem.* **1971**, *36* (25), 3856–3861. <https://doi.org/10.1021/jo00824a003>.

Tikhomirov, D. A.; Shubina, Y. V.; Ereemeev, A. V. Ynaziradines. Methods of Synthesis of a New Type of Ynamines. *Chem. Heterocycl. Compd.* **1984**, *20*, 1231–1235. <https://doi.org/10.1007/BF00505713>.

Timeline on European Regulations on DEHP [https://pvcmed.org/wp-content/uploads/2020/08/DEHP\\_Timeline\\_5.pdf](https://pvcmed.org/wp-content/uploads/2020/08/DEHP_Timeline_5.pdf), accessed Oct 10, 2022.

Toma, M. A.; Najim, T. S.; Abdulhameed, Q. F. Synthesis and Characterization of Poly (Vinyl Chloride)-Graft-Poly (Ethyl Acrylate) and Its Membrane. *Al-Mustansiriyah J. Sci.* **2016**, *27* (1), 15–20.

Tsarevsky, N. V.; Bernaerts, K. V.; Dufour, B.; Du Prez, F. E.; Matyjaszewski, K. Well-Defined (Co)Polymers with 5-Vinyltetrazole Units via Combination of Atom Transfer Radical (Co)Polymerization of Acrylonitrile and “Click Chemistry”-Type Postpolymerization Modification. *Macromolecules* **2004**, *37* (25), 9308–9313. <https://doi.org/10.1021/ma048207q>.

Turczel, G.; Kovács, E.; Csizmadia, E.; Nagy, T.; Tóth, I.; Tuba, R. One-Pot Synthesis of 1,3-Butadiene and 1,6-Hexanediol Derivatives from Cyclopentadiene (CPD) via Tandem Olefin Metathesis Reactions. *ChemCatChem* **2018**, *10* (21), 4884–4891. <https://doi.org/10.1002/cctc.201801088>.

#### Vinyloop

[https://www.plasteurope.com/news/Closure\\_of\\_operation\\_in\\_Italy\\_Phthalates\\_issue\\_und%20er\\_REACH\\_brings\\_do\\_t240095/](https://www.plasteurope.com/news/Closure_of_operation_in_Italy_Phthalates_issue_und%20er_REACH_brings_do_t240095/), accessed Oct 10, 2022.

von Czapiewski, M.; Kreye, O.; Mutlu, H.; Meier, M. A. R. Cross-Metathesis versus Palladium-Catalyzed C-H Activation: Acetoxy Ester Functionalization of Unsaturated Fatty Acid Methyl Esters. *Eur. J. Lipid Sci. Technol.* **2013**, *115* (1), 76–85. <https://doi.org/10.1002/ejlt.201200196>.

Wang, M.; Kong, X.; Song, X.; Chen, Y.; Bu, Q. Construction of Enhanced Self-Plasticized PVC via Grafting with a Bio-Derived Mannich Base. *New J. Chem.* **2021**, 3441–3447. <https://doi.org/10.1039/d0nj05714b>.

Watson, M. D.; Wagener, K. B. Acyclic Diene Metathesis (ADMET) Depolymerization: Ethenolysis of 1,4-Polybutadiene Using a Ruthenium Complex. *J. Polym. Sci. Part A Polym. Chem.* **1999**, *37* (12), 1857–1861. [https://doi.org/10.1002/\(SICI\)1099-0518\(19990615\)37:12<1857::AID-POLA15>3.0.CO;2-C](https://doi.org/10.1002/(SICI)1099-0518(19990615)37:12<1857::AID-POLA15>3.0.CO;2-C).

- Wiberg, K. B. Application of the Pople-Santry-Segal CNDO Method to the Cyclopropylcarbinyl and Cyclobutyl Cation and to Bicyclobutane. *Tetrahedron* **1968**, *24* (3), 1083–1096. [https://doi.org/10.1016/0040-4020\(68\)88057-3](https://doi.org/10.1016/0040-4020(68)88057-3).
- Yoon, K. Y.; Lee, I. H.; Kim, K. O.; Jang, J.; Lee, E.; Choi, T. L. One-Pot in Situ Fabrication of Stable Nanocaterpillars Directly from Polyacetylene Diblock Copolymers Synthesized by Mild Ring-Opening Metathesis Polymerization. *J. Am. Chem. Soc.* **2012**, *134* (35), 14291–14294. <https://doi.org/10.1021/ja305150c>.
- Yoshida, S.; Shiraishi, A.; Kanno, K.; Matsushita, T.; Johmoto, K.; Uekusa, H.; Hosoya, T. Enhanced Clickability of Doubly Sterically-Hindered Aryl Azides. *Sci. Rep.* **2011**, *1*, 4–7. <https://doi.org/10.1038/srep00082>.
- Yoshioka, T.; Furukawa, K.; Okuwaki, A. Chemical Recycling of Rigid-PVC by Oxygen Oxidation in NaOH Solutions at Elevated Temperatures. *Polym. Degrad. Stab.* **2000**, *67*, 285–290. [https://doi.org/10.1016/S0141-3910\(99\)00128-7](https://doi.org/10.1016/S0141-3910(99)00128-7).
- Yoshioka, T.; Furukawa, K.; Sato, T.; Okuwaki, A. Chemical Recycling of Flexible PVC by Oxygen Oxidation in NaOH Solutions at Elevated Temperatures. *J. Appl. Polym. Sci.* **1998**, *70*, 129–135. [https://doi.org/10.1002/\(SICI\)1097-4628\(19981003\)70:1%3C129::AID-APP13%3E3.0.CO;2-2](https://doi.org/10.1002/(SICI)1097-4628(19981003)70:1%3C129::AID-APP13%3E3.0.CO;2-2).
- Zakharyan, E. M.; Petrukhina, N. N.; Dzhabarov, E. G.; Maksimov, A. L. Pathways of Chemical Recycling of Polyvinyl Chloride. Part 2. *Russ. J. Appl. Chem.* **2020**, *93* (10), 1445–1490. <https://doi.org/10.1134/S1070427220100018>.
- Zakharyan, E. M.; Petrukhina, N. N.; Maksimov, A. L. Pathways of Chemical Recycling of Polyvinyl Chloride: Part 1. *Russ. J. Appl. Chem.* **2020**, *93* (9), 1271–1313. <https://doi.org/10.1134/S1070427220090013>.
- Zeng, M.; Lee, Y. H.; Strong, G.; Lapointe, A. M.; Kocen, A. L.; Qu, Z.; Coates, G. W.; Scott, S. L.; Abu-Omar, M. M. Chemical Upcycling of Polyethylene to Value-Added  $\alpha,\omega$ -Divinyl-Functionalized Oligomers. *ACS Sustain. Chem. Eng.* **2021**, *9* (41), 13926–13936. <https://doi.org/10.1021/acssuschemeng.1c05272>.
- Zhang, H. P.; Dai, Y. Z.; Zhou, X.; Yu, H. Efficient Pyrimidone-Promoted Palladium-Catalyzed Suzuki-Miyaura Cross-Coupling Reaction. *Synlett* **2012**, *23* (8), 1221–1224. <https://doi.org/10.1055/s-0031-1290885>.